QUATERNARY SEDIMENTS OF A TROPICAL ESTUARY AND BAY: PHANGNGA BAY, SOUTH THAILAND

by

Deborah Jacqueline Carr

Submitted for the degree of

Doctor of Philosophy

at The University of Edinburgh

January, 1992

I declare that this thesis has been composed by myself and all work is my own unless otherwise acknowledged.

Deborah Jacqueline Carr

To,

the people of the Phuket Marine Biological Centre, Thailand

as a key to the past and a reference for the future.

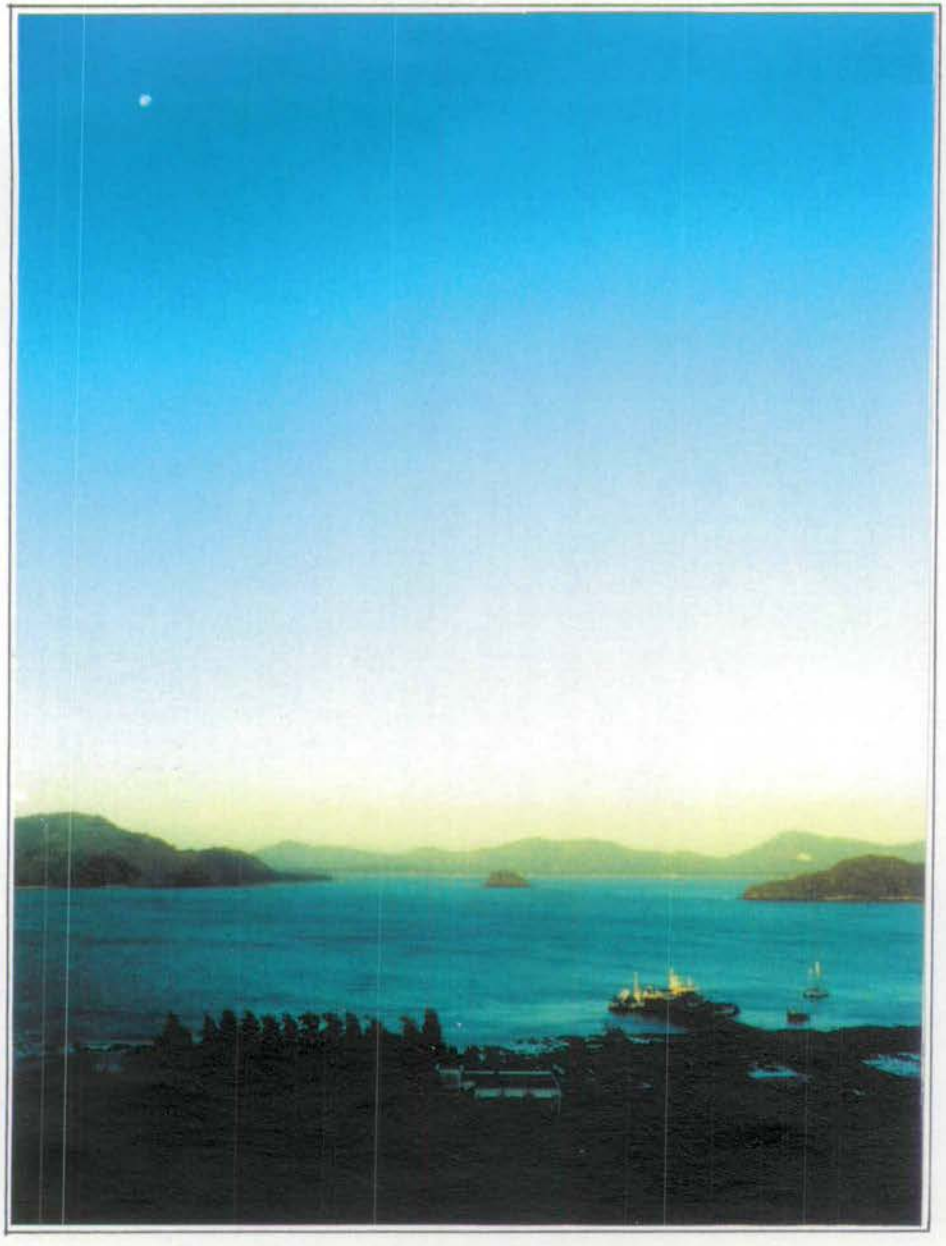

The Phuket Marine Biological Centre's Lab. and Pier

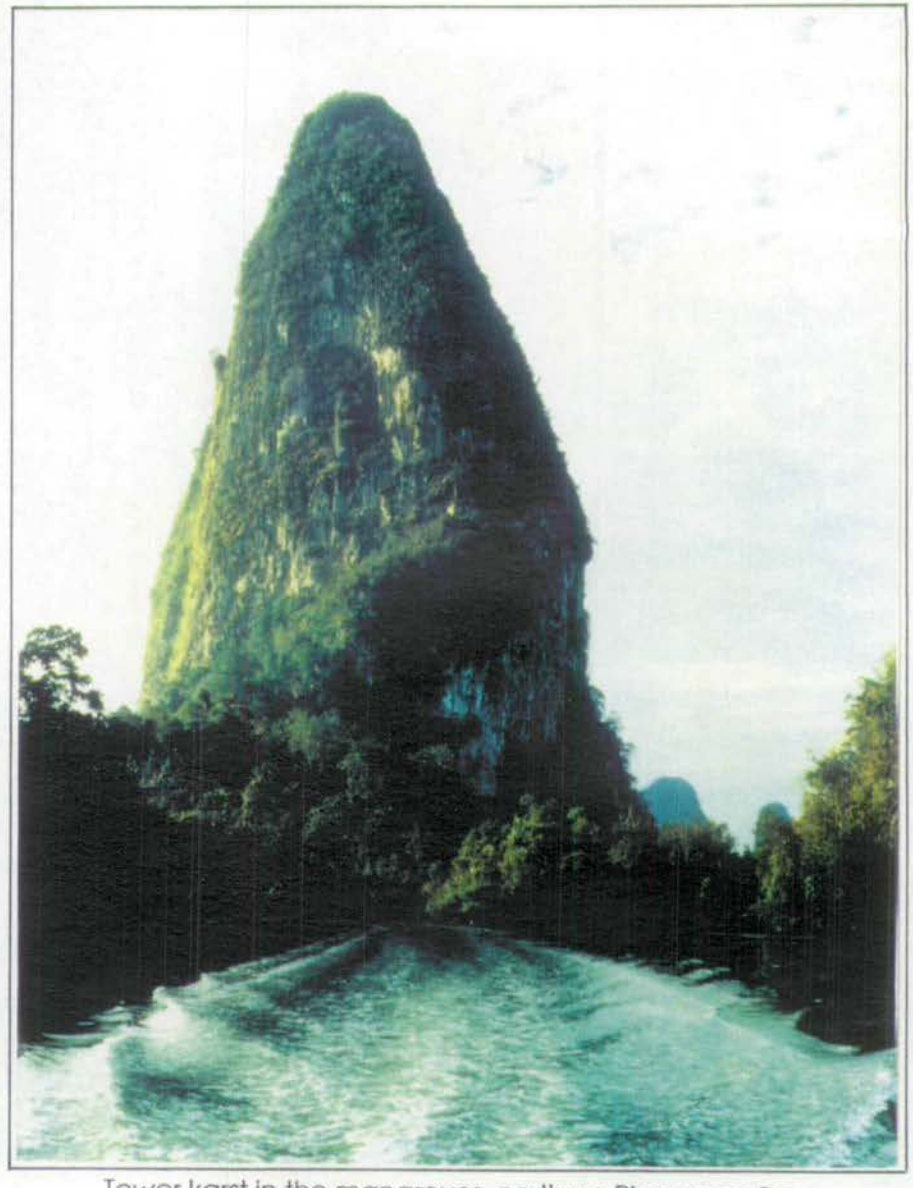

Tower karst in the mangroves, northern Phangnga Bay

LIST OF CONTENTS

LIST OF FIGURES

Chapter 7

Chapter 8

Chapter 9

LIST OF TABLES

LIST OF PLATES

ABSTRACT

Phangnga Bay is a 2000km^2 shallow marine tropical embayment on the peninsula coast of South Thailand. The surrounding catchment area consists of Sn-bearing granites, Permian and Mesozoic sediments and Sn-rich pegmatites intruded in NE-SW trending fault systems.

Grain size analysis of surface sediments reveals that mean grain size and sediment sorting show an overall increase southwards towards the more open marine environment. This is thought to reflect the transition from fine grained recent sediments presently settling out in the low energy sheltered conditions in the north to coarse relict sands in the south deposited during Pleistocene low sea-level stands and not covered by recent sedimentation.

Geochemical analysis of the sediments reveals that the majority of elements studied (namely, Fe, Mn, Al P_2O_5, K, Rb, Nb, Y, Th, Pb, V, Cr, Zr, Ni, La, Ce, Nb and Organic Carbon) are closely associated with clays through adsorption and cation exchange processes. These elements show concentration distributions which mirror that of the clay content. Sn, Zr and Ti when ratioed to Al, show highest values in the south of the area which is thought to reflect the concentration of these elements in heavy minerals which themselves are concentrated in the relict sands of the south. Both Sn and Rb show distributions strongly controlled by the distribution of cassiterite and lepidolite respectively in the catchment area. Both Mg and Sr show distributions partly controlled by clays and partly by carbonates.

$CaCO_3$ shows a general increase southwards reflecting improved conditions for carbonate-secreting organisms and a decrease in the diluting effect of terrigenous material. The carbonate mineralogy varies in relation to the biogenic content of the sediments. Kaolinite is the dominant clay mineral due to the intense chemical weathering of granites in the catchment area, however, clay mineral proportions change from north to south as a result of the variations in settling velocities of different clay minerals.

The sediments of 8 depositional environments which have been distinguished on the basis of geomorphology and water depth are compared. Different techniques for

distinguishing populations from the data are discussed particularly in relation to the 8 depositional environments mentioned above.

From radiocarbon dates of core material sediment accumulation rates in the north of the Bay have been calculated and vary between 0.3 and 1.5mm/year. Progradation rates of the main mangrove development in the north of the Bay have been estimated at approximately 1.5m/year. From the study of cored material and the distribution of surface sediments it is concluded that Holocene sedimentation in Phangnga Bay represents a regressive, fining-upward sequence. Comparisons are made between this model of sedimentation in Phangnga Bay and possible analogues in the geological record.

CHAPTER 1

INTRODUCTION

CHAPTER 1 - INTRODUCTION

1.1 THE OBJECTIVES

The study of recent sediments has long been recognised as an integral part of geological studies in that knowledge of a recent sediment's characteristics and mode of deposition contributes to an understanding of ancient sedimentation and makes it possible to reconstruct sedimentary processes throughout the Earth's history. The concept of 'the present is the key to the past' is still a major impetus to studies of recent sediments whether terrestrial or marine, particularly considering the economic value of some ancient sediments and the need to pin-point the most prospective area once the palaeoenvironmental position is known.

However, there is now another major objective in studying recent sediments particularly those of marine environments. This is due to environmental concerns and the realisation that Man's activities can have a significant impact on sedimentary processes. Estuaries and sheltered bays are of great importance to Man and many major cities are located on them. They are used for shipping and transportation, for their biological and mineralogical resources, for waste disposal, and for recreational activities. Channels are dredged to preserve shipping lanes and areas are reclaimed to provide building land. Such demands are often in sharp conflict and many bays and estuaries have been deleteriously affected by such activities.

Phangnga Bay is a shallow, sheltered bay and estuary on the west coast of peninsula South Thailand. An increasing number of human activities are impinging on the Bay either in the catchment area (deforestation, tin-mining, urbanisation, agriculture) or in the Bay itself (mariculture, tin-dredging, charcoal production, port construction and tourism). The effects of any one of these activities on natural processes operating in the Bay may significantly affect any of the other activities (eg, sediment stirred up from tin-dredging may smother shell beds or wash up on sandy tourist beaches whilst untreated sewage entering the sea from hotel developments may kill off marine organisms) and so conflicts of interests are likely to occur.

This study forms part of a larger research programme which aims to formulate an effective coastal management plan to prevent deterioration of the Bay's resources which may be brought about by the combined effects of these activities. The specific objectives of this study are summarised below:

1. to describe the surface sediment characteristics of the Bay using grain size parameters, geochemistry and mineralogy and to account for these by consideration of depositional environments, sediment supply and processes of transport and deposition.

2. to compare techniques for classifying the sediments into units which may reflect the prevailing sedimentary processes.

3. to assess the influence of drainage basin geochemistry on the geochemistry of Bay sediments.

4. to describe the distribution of sediment macrofauna in geological terms and how such distributions may be of use in determining the landward position of ancient environments.

5. to determine sediment accumulation and progradation rates and to ascertain as far as possible the Late Quaternary and Holocene depositional history of the Bay.

6. to provide a model of a modern depositional environment to help identify analogues in the geological record. This may also help in pin-pointing deposits of economic significance eg, hydrocarbons and heavy minerals.

1.2 THE STUDY AREA

Phangnga Bay is situated on the west coast of Peninsula South Thailand (Fig 1.1a and 1.1b), 8°N and 98°30'E in the tropical monsoonal area of South East Asia. The Bay encompasses approximately 2000km^2 and is partly surrounded by a relatively small catchment area of approximately 2500km^2. Water depth increases from the intertidal area to 65m in the southern limit of the study area. Much of the area north

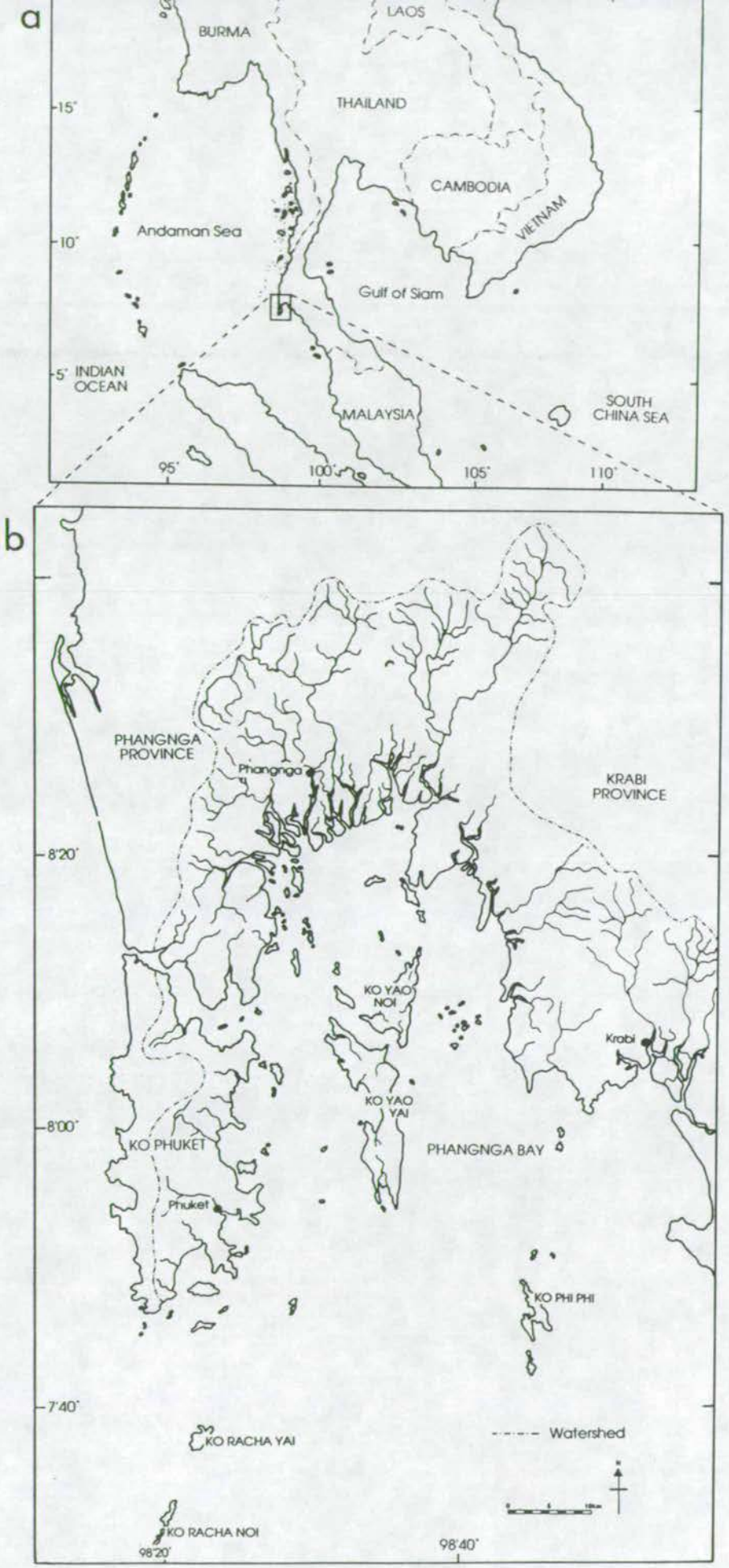

Figure 1.1 a. Location of the study area in a regional context
b. .Detail of the study area with catchment basin and location of main towns, provinces and islands

of Ko Yao Noi (Fig 1.1b and Fig 1.4) is less than 5m in water depth. Land surrounds the bay on 3 sides with the southern side being open to the Andaman Sea.

The dry north easterly monsoon occurs from November to April whilst the wet south westerly monsoon extends from May to October with strong westerly winds and peak rainfall in July. Rainfall is highly seasonal with an average of 300mm/month in the wet season and an average of 2300mm/year. Coastal waters vary in temperature between 26°C and 31°C.

The Bay was formed by the drowning, during the Holocene transgression, of 2 ancient river systems (Hummel and Phawandon, 1967) which run north-south and lie on either side of the central Ko Yao islands[1]. The submerged basin lying in the west channel is called the Ancient Phangnga River and the one on the east the Ancient Marui River. These basins are not thought to have been connected during low sea-level stands and even at present are only connected by a narrow channel to the north of Ko Yao Noi.

At the northern end of the Bay is a large area of mangrove swamps dissected by tidal creeks and channels draining rivers and streams of the northern catchment area. Smaller areas of mangroves are found in small bays down either side of the Bay, however, there is a gradual transition from mud-dominated mangrove coastlines to fringing coral reefs in clearer waters, fronting sandy and shelly beaches. The location of mangrove swamps and coral reefs are illustrated in Figure 1.2. The fringing reefs are 30-150 metres in width and are confined laterally by rocky headlands. Many of the small islands in the north of the Bay and within the mangroves themselves are steep-sided limestone outcrops typical of tower karst topography (see frontispiece).

Most of the terrigenous material is brought into the Bay through the mangrove swamps in the north and the shallow waters in front of this area are sediment-laden whilst the waters in the south are much clearer (see Plate 18 - Chapter 9). There is thus a transition from terrigenous-dominated sedimentation in the north to carbonate accretion in relatively sediment-free water in the south.

[1] Place-names mentioned in the text throughout this work are illustrated on Figure 1b which is also included in the enclosures as an overlay for use with maps presented throughout the thesis.

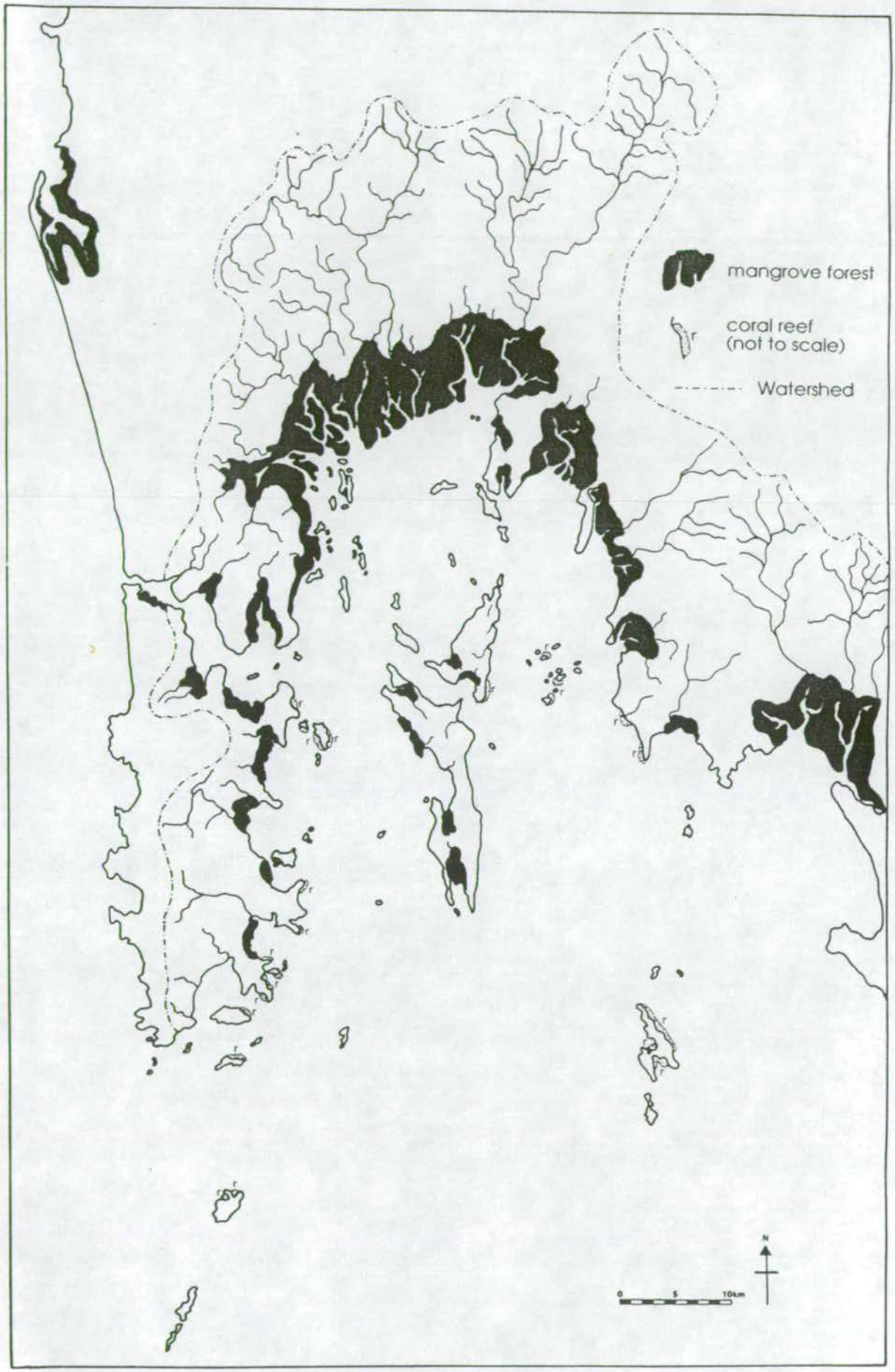

Figure 1.2 Location of mangrove swamps and coral reefs around Phangnga Bay (from Siripong et al (1980) and the Royal Thai Navy bathymetric map)

Around the northern part of the bay estuarine conditions prevail. Pritchard (1967) describes an estuary as a "semi-enclosed coastal body of water which has free connection with the open sea and within which sea water is measurably diluted with fresh water derived from land drainage". Although the area in Phangnga Bay which is "measurably diluted with fresh water" cannot really be described as semi-enclosed and thus not conform to Pritchard's definition, there is an input of fresh water into a marine environment which is protected to a large extent from open marine conditions.

1.3 THE GEOLOGY

1.3.1 **Regional tectonics**

Although Indo-china is part of the Eurasian plate, the tectonics of the Peninsula Thailand region have been controlled by the collision of the Indian plate with the Eurasian plate and the formers subduction around the Sunda Arc. Subduction events have taken place in the region since the Late Carboniferous (Mitchell, 1977) accounting for the calc-alkaline, tin-bearing granite belts running approximately N-S along the Peninsula. One of these belts to the West has been offset by a large sinistral fault system thought to be a continental extension of a transform fault in the Andaman Sea basin which has displaced the Western tin-belt by approximately 200km. This fault system runs through Phangnga bay and its catchment area and is expressed by 2 large faults (Phangnga fault and Khlong Marui fault - see figure 3) along which parallel swarms of tin and tungsten rich pegmatites have been intruded (Garson & Mitchell, 1970). At present the area around Phangnga is tectonically inactive therefore there is no major uplift or subsidence to affect patterns of sedimentation.

1.3.2 **Catchment area geology**

The geology and stratigraphy of the catchment area and Bay islands has been described by Garson et al (1975) and is illustrated in figure 1.3. A sequence of clastic sediments of the Ordovician to Lower Permian Phuket Group outcrop in the west of the area and are overlain by a thick limestone succession, the Rat Buri formation of Permian age. The formation outcrops sporadically in spectacular tower karst either as islands or on-shore surrounded by flat alluvial plains. A period of uplift and erosion

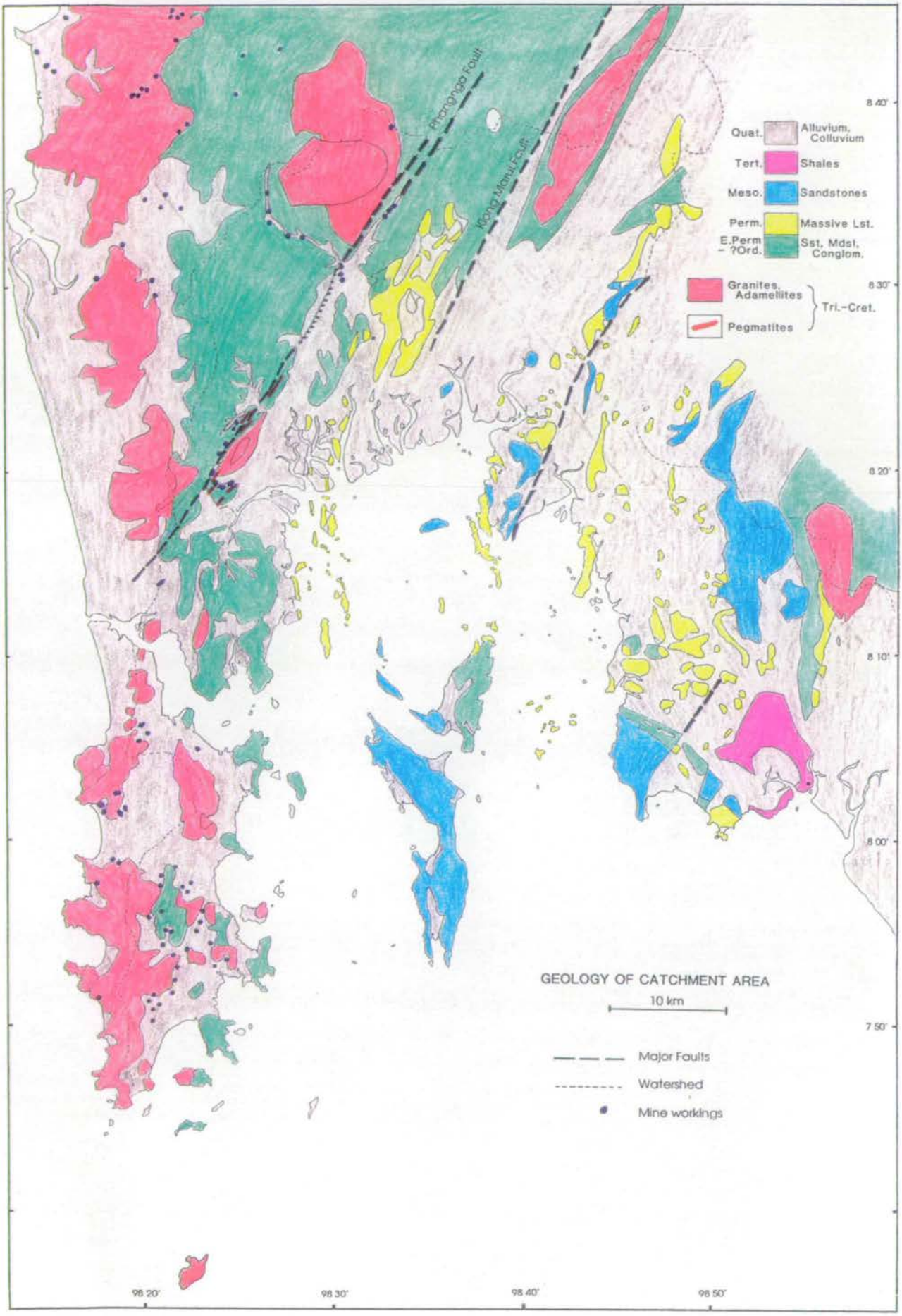

Fig 1.3 Geological map of the catchment area of Phangnga Bay (from the IGS, Overseas Memoir No.1, Garson et al, 1975)

preceded deposition of the Jurassic-Cretaceous Ko Yao formation consisting of cross-bedded sandstones and siltstones. Intrusion of tin-rich granites in the Cretaceous was associated with subduction which began in the Carboniferous. These granites were affected by major NNE-SSW faulting along which pegmatites were intruded. Thermal metamorphism has locally hornfelsed Phuket Group sediments and vertical movements on the major faults have formed a graben in the eastern half of the area in which younger sediments are exposed. The Tertiary Krabi formation was deposited in localised basins after much of the tectonic movement. Erosion and deep weathering during the Quaternary has led to the accumulation of thick alluvium and colluvium deposits which are rich in tin. With the Holocene sea-level rise the sea has transgressed over the alluvial plain drowning the 2 river valleys and forming the Bay.

The tin-rich granites and pegmatites have been deeply weathered in the humid tropical climate and have sourced tin-rich alluvial deposits. These are mined along with the pegmatites themselves using water jets and sluice boxes (palongs) from which the heavy minerals including cassiterite are collected. Tin-rich sediments are also currently being dredged off-shore to the west of Ko Phuket and Phangnga Province, within the mangroves in the north and in a small area to the south east of Ko Phuket. Past dredging activity is known to have been restricted to these areas.

1.4 HYDRODYNAMICS

Oceanographic variations in Phangnga Bay are temporally and spatially highly variable and complex. They are influenced by the interaction of run-off, tidal currents, monsoonal airflow and the topography and bathymetry of the Bay. Figure 1.4 illustrates the bathymetry of Phangnga Bay. The Ko Yao islands effectively divide the Bay along a north-south line with relatively deep channels (> 20m) on either side. These channels are thought to be remnants of the low sea-level stand topography of the area and represent 2 ancient river systems (Hummel and Phawandon, 1967). Most of the northern area of the Bay is < 5m water depth whilst the southern part of the study area (not actually part of the Bay proper but considered as such here) extends to 65m depth. Work on the oceanography of Phangnga Bay by Siripong et al (1987) and Khokiattiwong et al (1991) has shown that much of the variation in the hydrodynamics is due to the two monsoonal seasons which affect this region. Although storms are frequent in the south west monsoon they rarely cause wave

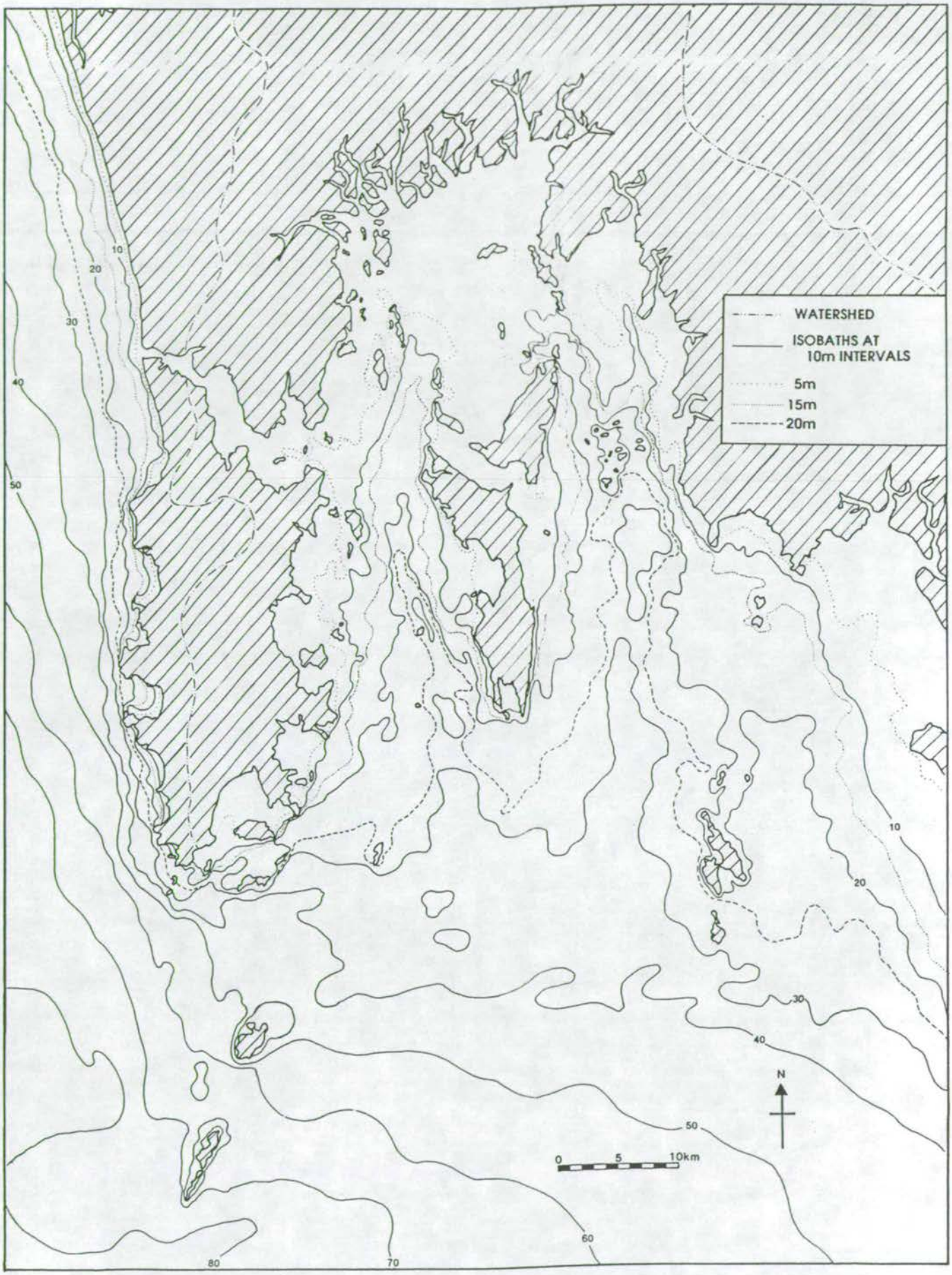

Figure 1.4 Bathymetric map of Phangnga Bay (from information on the Royal Thai Navy bathymetric map of Phangnga Bay)

heights >1m (in the south of the area) and very rarely cause wave disturbance in the northern sheltered area.

1.4.1 South west monsoon

During the SW monsoon (May-Oct, the wet season) monsoonal airflow from the south west causes net surface currents to flow northwards with bottom currents directed southwards out of the Bay through both the eastern and western channels (Siripong et al, 1987). High variabilities in salinity gradients and mixing were found during this season particularly in the shallower, north of the Bay. An increase in run-off results in lower salinities in the north of the Bay in front of the main mangrove development (near-shore water is diluted to approximately 25ppt during highest river discharges in July, (Siripong et al, 1987)). With greater vertical salinity gradients it would be expected that there would be less mixing of waters, however, high tidal currents (1m/second) have been measured in the western channel in the SW monsoon and these currents result in vigorous mixing hence there is very little stratification in the water column particularly in the shallower areas.

Siripong et al (1987) note that tidal mixing is efficient throughout the year and so salinity stratification through the water column is slight. Well mixed waters are also a result of the Bay's topography. Numerous islands create turbulent water movement particularly on the leeward side of islands. This phenomenon can be seen in a satellite image of the Bay (Plate 18 - Chapter 9) where an incoming tide creates eddies of turbulent water on the leeward side of islands.

1.4.2 North east monsoon

From November to April, winds are generally from the north east causing the net surface flow to be directed southwards. Bottom inflow of oceanic water into the Bay occurs through both channels (Khokiattiwong et al, 1991). Undiluted sea water tends to reach all coastal areas in the dry season.

Khokiattiwong et al (1991) have also reported that there is a slight eastwards movement of water in the inner Bay which may be a result of the Coriolis force. However, the dominant north-south (and vice versa) movements of surface and bottom waters are controlled by tidal currents and monsoonal airflow.

1.4.3 Tides

The tidal range is greater in the north of the Bay than the south due to funnelling of the northward moving rising tide. The maximum range in the north is 4.4m during spring tide with a mean annual range of 2.4m. In the south the mean annual range is 1.7m (Siripong et al, 1987).. The tidal currents are semi-diurnal with zero velocity at high and low tides and maximum velocity at mid-tide.

1.4.4 Localised currents

Strong localised currents are noted on the bathymetric map produced by the Royal Thai Navy and were also evident during fieldwork. Strong currents sweep around Ko Racha Yai in the south (Fig 1.1b) and around the northern tip of Ko Yao Noi (Fig 1.1b).

1.5 SAMPLING PROCEDURE AND INITIAL TREATMENT

Three types of sample were required for this study: surface sediment samples (for grain size analysis, geochemistry and mineralogy); cored sub-surface samples (for dating to calculate accumulation rates and to assess grain size and geochemical changes through time) and samples of the biogenic fraction (to assess macrofaunal distributions)

1.5.1 Sample sites

Sediment samples were collected using the Phuket Marine Biological Centre (PMBC) research vessel No 14 (Plate C) in 2 field seasons. The distribution of the sample sites is illustrated in figure 1.5. Sites 1-63 were sampled between 17th and 20th January 1989 and sites 64-139 (including transects) were sampled between 5th and 9th January 1990. The distribution of sampling sites reflects an attempt to gain a good areal coverage of the area as well as to assess the degree of local variation at a few selected sites. In the north, 2 transects cross mangrove channel mouths and one runs from the mangrove front over the intertidal flat. At the south east tip of Ko Phuket, one transect crosses the beach and reef at Tang Khen and another runs from the Aquarium beach across to Ko Lon (these samples are labelled T.K.1-6 and

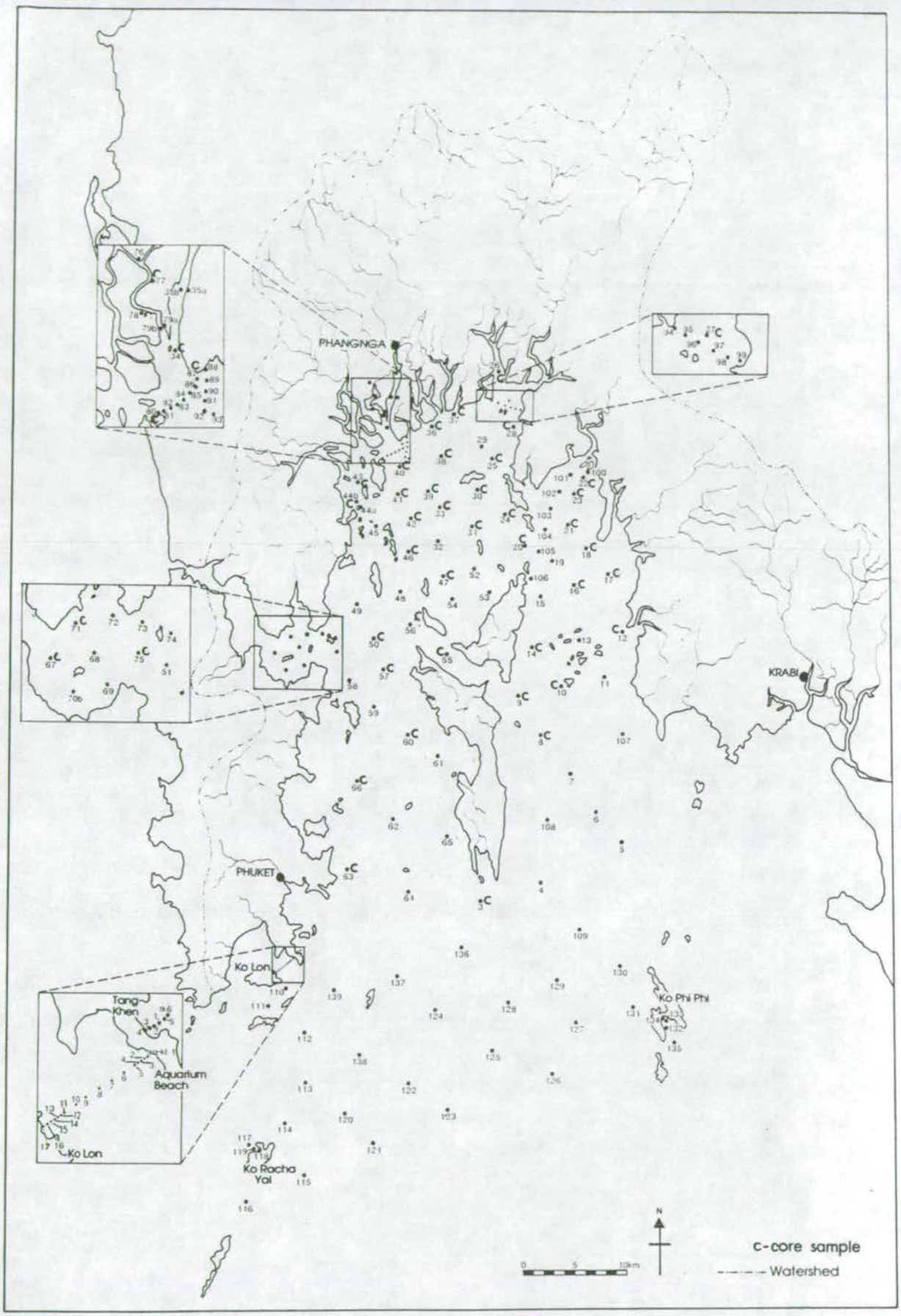

Figure 1.5 The distribution of sample sites throughout the Bay. Sites 1-63 were sampled in January 1989 and 64-139 (including transects) were sampled in January 1990.

Plate A
Gravity corer used for subsurface sediment sampling

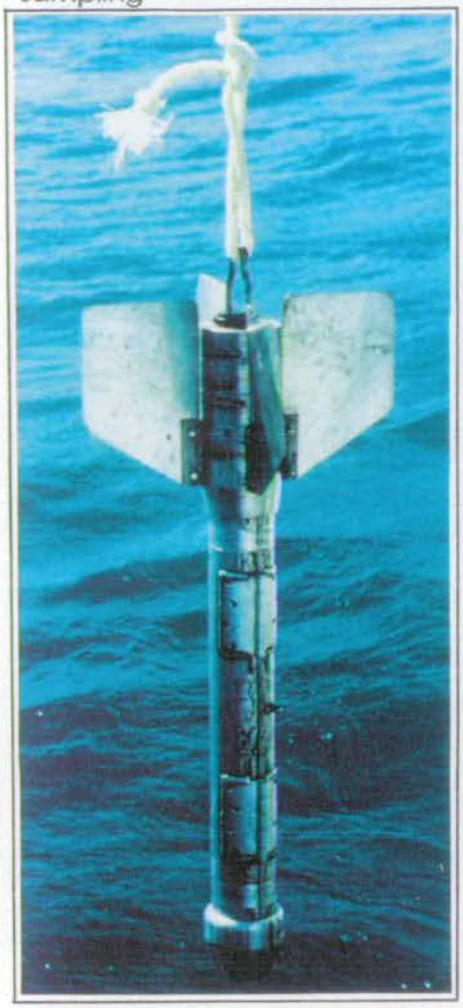

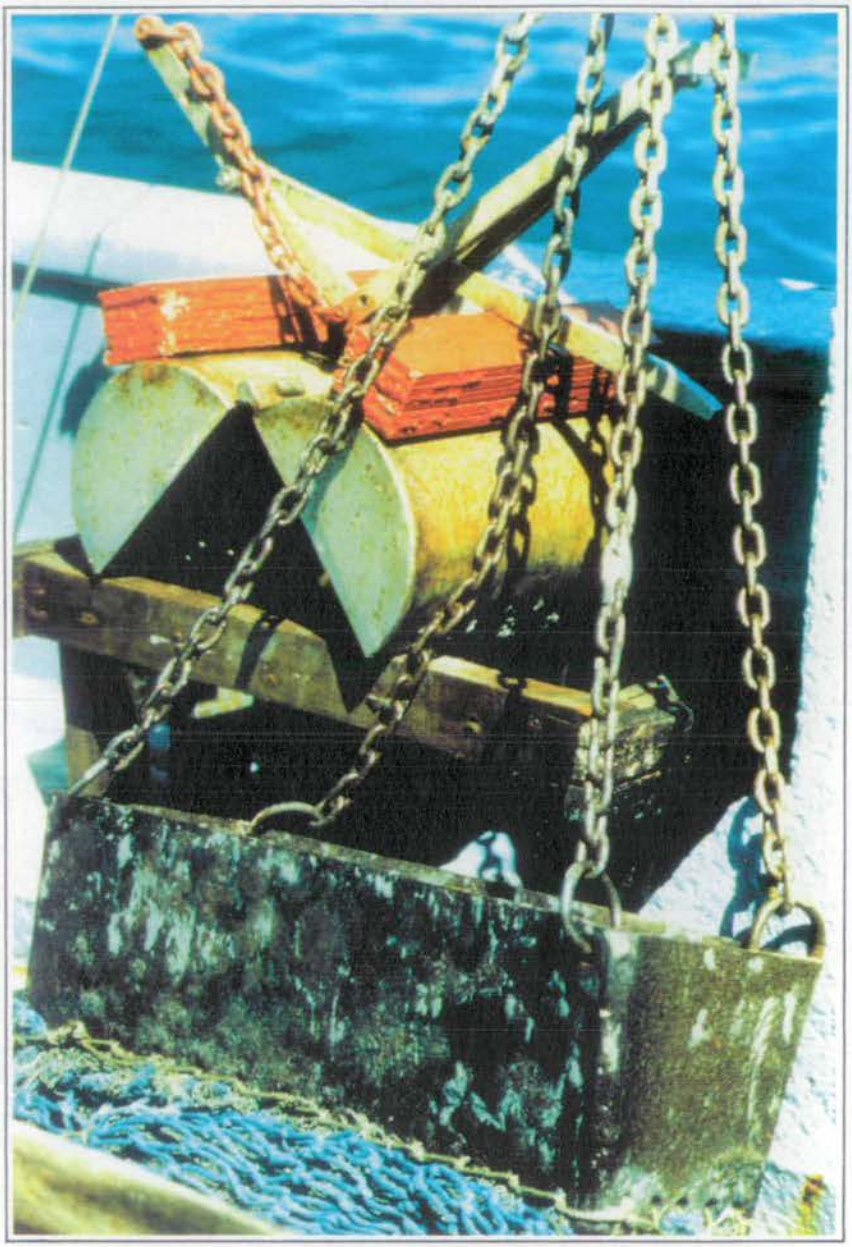

Plate B Van Veen grab and rectangular bucket dredge used for surface sediment sampling

Plate C
The *Pramong 14* - the sampling survey ship

Aq-Kl.1-17 respectively - see figure 1.5). Details of sample sites and the samples collected from them are given in Appendix A.

1.5.2 **Sampling procedure**

1.5.2.1 Grabs

Surface sediment samples were collected by 2 methods depending on the water depth. For water depths greater than approximately 5m a Van Veen type grab (Plate B) was used from the research vessel. For shallower sites SCUBA equipment was used from a small boat to collect the surface sediment with a hand held scoop. The Van Veen grab collected the top 15-20cm of sediment. Since it was not possible to open the top of the grab bucket to collect the surface material, the whole sample was gently emptied into a tray (taking care not to disturb the surface) and the top 5cm was collected for further analysis.

Two sub-samples of sediment were collected from each grab sample. One sub-sample for grain size analysis was sealed in a plastic bottle and stored on ice until returning to the laboratory. Sediment which was to be dried for chemical and mineralogical analysis was stored wet in sealed polythene bags and kept on ice until ready for drying at the laboratory. The remains of the grab sample were then washed through 5mm and 1mm mesh sieves and the 1-5mm fraction collected for analysis of the biogenic component along with the dredge sample.

1.5.2.2 Cores

Cores were taken from a selection of sites (marked "C" on Fig 1.5) using either a gravity corer operated from the research vessel or manually with a length of 4cm diameter PVC piping. Although it would have been preferable to use just one method this was not possible as a large part of the study area was too shallow for the research vessel so manual coring had to be employed. The rest of the area was too deep for manual coring.

Gravity corer - The success of the gravity corer (Fig 1.6 and Plate A) used from the research vessel depended on the sediment type. If it was of sand or gravel grain size then there was virtually no core penetration whilst if the sediment was muddy then recovery was good (30-60cm). The core sites illustrated on figure 1.5 show the northern bias thus obtained in the distribution of cored samples. Of the 35 cores

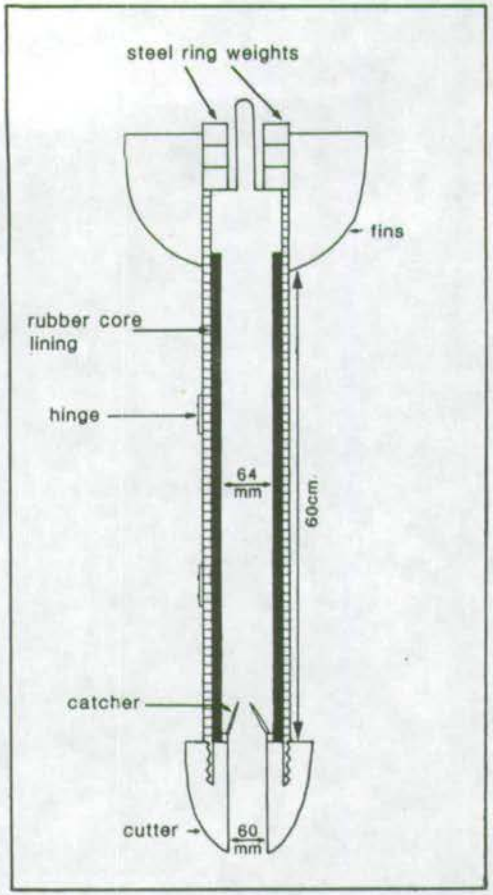

Figure 1.6

Dimensions of the gravity corer used for sub-surface sediment sampling (see also Plate A)

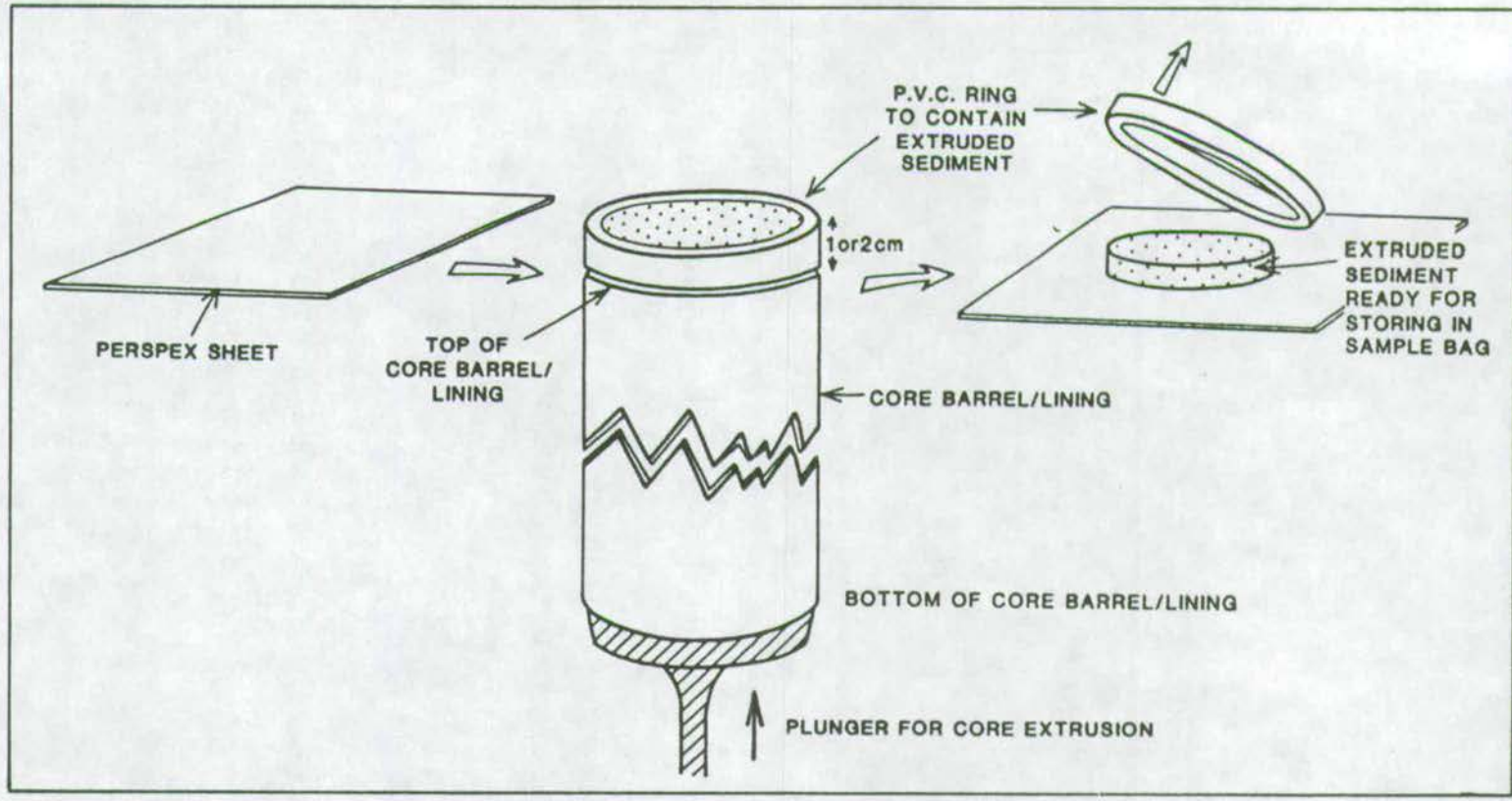

Figure 1.7 Method of core extrusion (1cm sections for the top 10cm and 2cm sections thereafter, however, for cores longer than 1m, 2cm sections were taken for the top 20cm and 5cm sections thereafter).

obtained using this method the average length was 36cm with a maximum length of 56cm.

One problem with this corer was that the internal diameter of the rubber hosing inside the core barrel was greater than that of the bottom end of the corer (Fig 1.6), therefore, there was a gap between the sediment and the sides of the rubber tube. Whether this had a notable effect on the water content of the sediment is not known. Another problem is that the core cutter which is screwed on to the core barrel tapers upward to a significant thickness which causes a large amount of sediment around the corer to be displaced thereby creating resistance to the downward penetration of the corer. However, this latter problem only reduced the effectiveness of the corer rather than affecting the cored material itself.

Manual coring - This method involved using various lengths of 4cm diameter PVC pipe (1m, 2m and 3m lengths) which were manually pushed in and retrieved from the sediment in shallow areas. A hammer was generally required for pushing the pipe past the soft surface layer and a tight-fitting rubber bung provided the suction for retrieving the cored sediment when the pipe was pulled out. A cap fitted over the base of the core to prevent sediment falling out. This method of coring proved very successful and cores of up to 2.5m in length were retrieved. 23 cores were obtained by this method

Core extrusion and sub-sampling - It was not possible to split the cores vertically and observe sediment structures downcore, therefore the cored sediments were extruded (see Fig 1.7) and sliced at 1cm intervals for the top 10cm and at 2cm intervals thereafter (cores greater than 1m in length were sectioned at 2cm intervals for the top 20cm and 5cm intervals thereafter). Each sub-sample was stored in a sealed plastic bag on ice.

1.5.2.3 Dredge samples

In order to collect biogenic material, a rectangular dredge with a 1cm mesh bag (Plate B) was dragged along the bottom for 5 minutes at 1 knot (approximately 150m). The material collected was then washed on a large sieve table (with a 1cm mesh size) and the contents stored in polythene bags.

1.5.3 Initial treatment

On return to the PMBC lab in Thailand initial treatment of the samples before transport back to Britain was as follows:

Grab samples:
To enable accurate grain size determination it was essential to preserve a sub-sample of the sediments wet to prevent any aggregation of clays through drying. The sub-samples to be used for grain size analysis were thus treated with 30% hydrogen peroxide (H_2O_2) to remove organic matter thus preventing deterioration of the sample by organic matter degradation and algal growth during transit back to Britain. When reaction with H_2O_2 had ceased the samples were then kept sealed in polythene bottles until opened for analysis. The sub-samples of sediment for chemical analysis were dried in an oven at 55°C and stored in sealed polythene bags.

Core samples: each core sub-sample was weighed wet, then dried to a constant weight at 55°C (the time for this varied depending on the mud content) and then weighed again. These measurements allowed the calculation of water content and amount of compaction downcore.

Dredge samples: these were kept sealed as collected in polythene bags until opened for analysis in Britain (consequently this was a rather smelly job!).

1.5.4 Limitations on sampling

Because of the remoteness of the area from a source of geological technical back-up and the limit on the amount of sampling equipment that could be taken out to the area, there was a restriction on the type of data that could be acquired. For instance, long cores (> 60cm) are unobtainable from deep water areas and no cores could be obtained from coarse sediments in deep water areas. For diagenetic work on sub-surface sediments, the splitting of the cores has to take place in an oxygen-free atmosphere. There were no facilities for such work available. Also, it would have been logistically very difficult to preserve whole cores (for analysis of sedimentary structures) by freezing and keep them frozen for the journey back to Britain. Thus core material had to be split and dried soon after

collection in Thailand. Seismic profiles of the sub-surface sediments are not available.

However, with a bit of thought and innovation and searching of local stores, various bits of sampling equipment (such as PVC pipe lengths) could be put together to work effectively. The coring methods, the grab and the dredge all worked well and more than enough material was collected to work on. Much use was made of equipment that was available in the PMBC lab for preparing samples for transit back to Britain, such as a freezer for storing samples until ready for drying, a set of scales and an oven.

1.6 PREVIOUS WORK

1.6.1 **Previous work in the study area**

Previous investigations of Phangnga Bay have focused on aspects of hydrodynamics (Siripong, 1980 and 1987, and Khokiattiwong et al, 1991), on resources and resource utilization (Limpsaichol, 1989) and on faunal distributions on mangrove shores (Frith et al, 1976), reef flats (Nielsen, 1976, Brown and Holley, 1984 and Ditlev, 1978) and selected areas of the Peninsula west coast including southern regions of Phangnga Bay (Chatananthawej and Bussarawit, 1987 and Tantanasiriwong, 1978). On sediments, Limpsaichol (1978) investigated the redox potential of mangrove muds from the east coast of Phuket Island (south west Phangnga Bay) and Hylleberg et al, (1985) described the effects of tin dredging on sediments on the west coast of Phuket Island. A detailed description of the geology of the catchment area of the Bay is given by Garson et al (1975).

1.6.2 **Similar studies in other areas**

There have been numerous studies of the sediments of estuarine, bay and shallow shelf areas particularly in temperate regions. The North Sea coast has been studied by van Straaten (1950), Evans (1965), Reineck (1967), Terwindt (1971), McManus et al (1980), Grant and Middleton (1990) and others. Allen (1971) has carried out extensive studies of the sedimentation in the Gironde Estuary (western France) and the estuaries of the eastern seaboard of the United States have received attention from Duane (1964), Loring (1978), Ashley (1988) and others. Reinson (1975 and 1977)

described the sediments of Mallacoota Inlet, Australia. In Korea, Alexander et al (1991) have studied the intertidal mudflats of Nam Yang Bay and Park et al (1991) have examined the shallow seismic stratigraphy and distribution of Late Quaternary sediments in Gunhung Bay.

It is probably because most of these areas are close to densely urbanised and industrialised regions that they have been subject to a great deal of research. Nowadays it is realised that the marine sediments of these near-shore areas are the largest repository and potential source of metallic contaminants in the marine environment hence knowledge of their sedimentology and geochemistry is of increasing interest.

Until comparatively recently, the coasts of tropical regions have been virtually ignored. Exceptions were the thorough studies by Van Andel and Postma (1954) and Hirst (1962a and 1962b) on the sediments (former) and geochemistry of the sediments (latter) of the Gulf of Paria, west of Trinidad. Also Coleman et al (1970) studied the sediments of the Klang river delta on the west coast of Malaysia (just south of the Phangnga Bay region). Although many of the basic processes of sedimentation are the same in both temperate and tropical coastlines (particularly the formation of large areas of intertidal mudflats in sheltered areas), there are differences in the type of sediment supplied to tropical coasts. Terwindt (1988) noted that humid tropical tidal sedimentary basins contain greater amounts of silt and clay-bearing facies than do the more arid and colder counter-parts. Also, tropical coastal areas have not been subjected to glacial processes such as scouring, and sedimentation from glacier retreat. There are also significant differences in the vegetational regimes of tropical areas compared to temperate. An obvious example of this is the presence of mangroves in calm, intertidal areas of the tropics as opposed to salt marshes in temperate regions.

More recently, studies have started to focus on tropical estuary and bay environments, particularly in Australia. Cook and Mayo (1978) described in detail the sedimentation of Broad Sound, Queensland, Risk and Rhodes (1985) studied the sediments of Missionary Bay, Queensland and Woodroffe et al (1989) described the sediments of the South Alligator River estuary in northern Australia. Allen et al (1982) described the sediments of the mud-dominated tropical tidal Mahakam delta on the east coast of Kalimantan. Attention has also been focused on the geochemistry of such sediments. Cook and Mayo (1980) studied the geochemistry of the above-

mentioned sediments of Broad Sound, De Luca Rebello et al (1986) studied the heavy metals in Guanabara Bay, Brazil and Windom et al (1988) studied trace metal transport in Bang Pakong estuary, Gulf of Thailand.

The study of the sediments of Broad Sound (Cook and Mayo, 1978 and 1980) provides a useful comparison to the sediments of Phangnga Bay. Although Broad Sound is similar in size and shape to Phangnga Bay and there are similar developments of mangroves, the climate of the Broad Sound area is more arid and there are no significant ore deposits in the catchment area. Hence, there are likely to be differences in sedimentary patterns and these will be commented on throughout the text.

1.7 USAGE OF PLACE NAMES

All place names used are as written on the Royal Thai Navy bathymetric map of Phangnga Bay which was used as a base map for this study. Occasionally, some Thai nouns are used in the text and on maps (such as *Ko* (island) and *Ao* (bay)) however on the whole English equivalents are used. The words *Yai* and *Noi* are frequently attached to 2 islands with the same name - *Yai* means large and *Noi* means small.

General areas of the Bay are often referred to as *north* (the region of the Bay north of Ko Yao Noi), *central* (the channels on either side of the Ko Yao islands) and *south* (the area south of the Ko Yao islands). The surrounding land areas are referred to as *Ko Phuket* (Phuket island), *Phangnga Province* (the mainland area around the north of the Bay) and *Krabi Province* (the mainland area down the east side of the Bay). All names used throughout the text are illustrated on figure 1.1b.

CHAPTER 2

GRAIN SIZE VARIATIONS IN THE SURFACE SEDIMENTS

CHAPTER 2 - GRAIN SIZE VARIATIONS IN SURFACE SEDIMENTS

2.1 INTRODUCTION

The objective of this chapter is to firstly describe the observational features of the surface sediments of Phangnga Bay and then illustrate and describe variations in sediment grain size across the study area and account for these variations by consideration of sediment supply and processes of transport and deposition.

Mean grain size, sorting, skewness, and percent gravel, sand and mud are the most common descriptive grain size parameters used in sedimentological studies (Folk and Ward, 1957; Allen, 1971; Spencer, 1963; Thomas et al, 1972; Tucker, 1973; Cook and Mayo, 1978; Ogorelec et al 1991 and others) and these parameters are all used in this study to aid in description and interpretation. The Kurtosis (the fourth moment) of sediment distributions has not been studied as it has only rarely been found to be useful in sedimentary studies (eg, Moiola and Weiser, 1968) - the first 3 moments are considered the most useful descriptive parameters. The use of mean, sorting and skewness parameters in distinguishing distinct depositional groups, as is commonly attempted in many sedimentological studies, is discussed and attempted later in this study (Chapter 6).

Therefore, this chapter simply attempts to provide a basic observational and textural description of the sediments and pin-point the main underlying controls on the patterns which will be referred to in following chapters.

2.2 OBSERVATIONAL DESCRIPTION OF THE SEDIMENTS

A basic description of each sediment grab sample made on collection is given in the sample data tables in Appendix A. The majority of the sediments are grey-green in colour although there are some orange-brown oxidised sediments, white carbonate sands and black reducing sediments. A thin (1-2mm) orange-brown oxidised surface layer was noted for most sediment samples with dark, reducing sediment beneath.

Although it was not possible to visually observe the sediment surface in the majority of sample sites (because of water depth and/or turbidity) it was possible to view a few sample areas as well as make deductions on the character of the sea-floor by the material sampled in the grab/dredge.

It is thought that the sediments of the Bay are on the whole not deeply bioturbated. Although it was not possible to look for evidence of bioturbation structures downcore, the lack of deep burrowing organisms in grab and dredge samples and the lack of burrow structures on the sediment surface, where observed, indicated that bioturbation of the surface sediments is not great. Additionally the very thin oxidised surface layer above reducing sediments in the majority of sample sites indicates little sediment mixing is taking place. Although polychaete worms were found in tubes at 10-15cm depth, they were not abundant. One area of sediments which appears to be an exception to the general lack of bioturbation is the area between Aquarium beach and Ko Lon (SE Phuket) sampled in the Aq-KL transect (Fig 1.5). Here, *Callianassa* shrimp burrows are common especially near coral reefs. Elsewhere across the transect, smaller burrow holes and mounds were evident over the sediment surface indicating some degree of sediment reworking and mixing. The sediments are orange-brown from the surface down to approximately 10cm depth indicating mixing is taking place.

No algal mats were found on the sediment surface of any of the sites and on the whole there is very little sea-grass cover (sea-grass was found in only 2 sites - 74G and Aq-KL 1). Therefore, the trapping and binding effects of these plants are not significant in Phangnga Bay.

2.3 METHODS OF GRAIN SIZE ANALYSIS

Grain size analysis was performed on wet sediment samples which had been treated with H_2O_2 to remove organic matter. Large whole shells were removed from the sample before analysis especially for samples where clumps of barnacles and mussels were common. The method of grain size analysis is described in Appendix B.

Results are presented as ϕ units where:

$$\phi = -\log_2 \frac{d}{d_o}$$

where d is the diameter of the grain (in mm) and d_o is the diameter of a 1mm grain, hence ϕ is dimensionless. Table 2.1 lists grain sizes with the corresponding ϕ scale and the Udden-Wentworth textural nomenclature of the size divisions which is used in this study.

Metric Size	phi	Udden – Wentworth (1922) Nomenclature	
4 mm	-2	Pebble	GRAVEL
		Granule	
2	-1		
		Very coarse	SAND
1	0		
		Coarse	
500 µm	1		
		Medium	
250	2		
		Fine	
125	3		
		Very fine	
62	4		
		Coarse silt	MUD
31	5		
		Medium silt	
16	6		
		Fine silt	
8	7		
		Very fine silt	
4	8		
		Clay	CLAY
2	9	⬇	

Table 2.1 Phi scale of grain size divisions and the Udden-Wentworth nomenclature as used in this study.

Since the grain size analysis method provides the full size distribution of the sediment rather than an open ended distribution, the moments method of statistical analysis of the grain size population was used. This method uses the entire grain population which provides more representative parameters than the graphically derived values (McManus, 1988). The formulae for the first (mean), second (standard deviation or sorting in grain size terms) and third (skewness) moments are as follows:

$$\text{Mean (first moment):} \quad \chi = \frac{\Sigma f m\phi}{100}$$

$$\text{Sorting (second moment)} \quad \sigma^2 = \frac{\Sigma f(m\phi - \chi)^2}{100}$$

$$\text{Skewness (third moment)} \quad \alpha^3 = \frac{\Sigma f(m\phi - \chi)^3}{100}$$

where f is the percentage fraction in each class interval of the total weight of sediment and $m\phi$ is the mid-point interval of each class interval in ϕ units. To check the reproducibility of the whole grain size method, the first moment was calculated for 10 replicate runs of one sample through the whole process. A precision of 0.2ϕ (1σ) was obtained.

In order to assess the effect of biogenic carbonate on grain size distributions and to study the purely terrigenous sediment distribution, the carbonate fraction of the sediment was removed (by a method described in Appendix B) and the percent gravel, sand and mud calculated. No detailed grain size analysis was carried out on the non-carbonate fraction as acidulation is likely to affect the clay fraction (it tends to cause agglomeration of clay particles) which would affect the overall distribution making comparisons with the untreated sediment invalid. Comparison of the 3 size fractions is considered adequate in order to examine shell debris contributions and the terrigenous component.

All of the individual grain size parameters described above are plotted on geographical distribution maps of the study area. Using this method, patterns related to hydrodynamics and/or sediment supply may be evident through systematic variations in these parameters.

Unfortunately, little information on sedimentary structures or bedforms is available for these sediments. This is due to the inability to observe surface sediments in situ due to poor water visibility or water depth and also the inability to observe cores in full due to the opaque core barrels and the extruding and sectioning method. Although such structures would aid interpretation, significant deductions on sedimentary processes operating in the Bay can be made on grain size data alone.

2.4 RESULTS

2.4.1 Mean Grain Size

The areal distribution of mean grain size is illustrated in Figure 2.1. It is evident that there is a general trend of increasing mean grain size from the north of Phangnga Bay to the south. The northern area of the bay is dominated by coarse silts (4-6 ϕ) and areas of medium to fine silts (>6 ϕ). The central and southern area is dominated by fine sands (2-4 ϕ) and the extreme southern area around Ko Racha Yai is dominated by medium to coarse sands and gravels (2 to -2 ϕ).

In the northern half of the Bay there are patches of coarser sediments within the dominantly silty and muddy area. Across the front of the main northern mangrove system is a belt of fine sands (2-4 ϕ) and coarse silts. Medium sands (0-2 ϕ) are coincident with the mangrove channels. The small area of coarse sediments on the north eastern tip of Ko Yao Noi (sampled at site 106) and other patches of coarse sediments are coincident with areas of high $CaCO_3$ content (see Fig 4.4). This is due to shell debris which contributes to the coarse sediment fraction. The samples from beaches and reefs on Ko Racha Yai, Ko Phi Phi (pronounced as pee pee) and South East Phuket show a coarser mean grain size than the surrounding shallow marine sediment.

2.4.2 Sorting

Figure 2.2 illustrates the areal distribution of sorting values for the surface sediments of Phangnga Bay. Like the mean grain size distribution, a general trend can be seen. This is an increase in sorting (decrease in standard deviation ϕ values) from north to south. The pattern in the northern part of the Bay is, like mean grain size, more complicated than in the southern area. Patches of poorly sorted sediments (>2.5 ϕ)

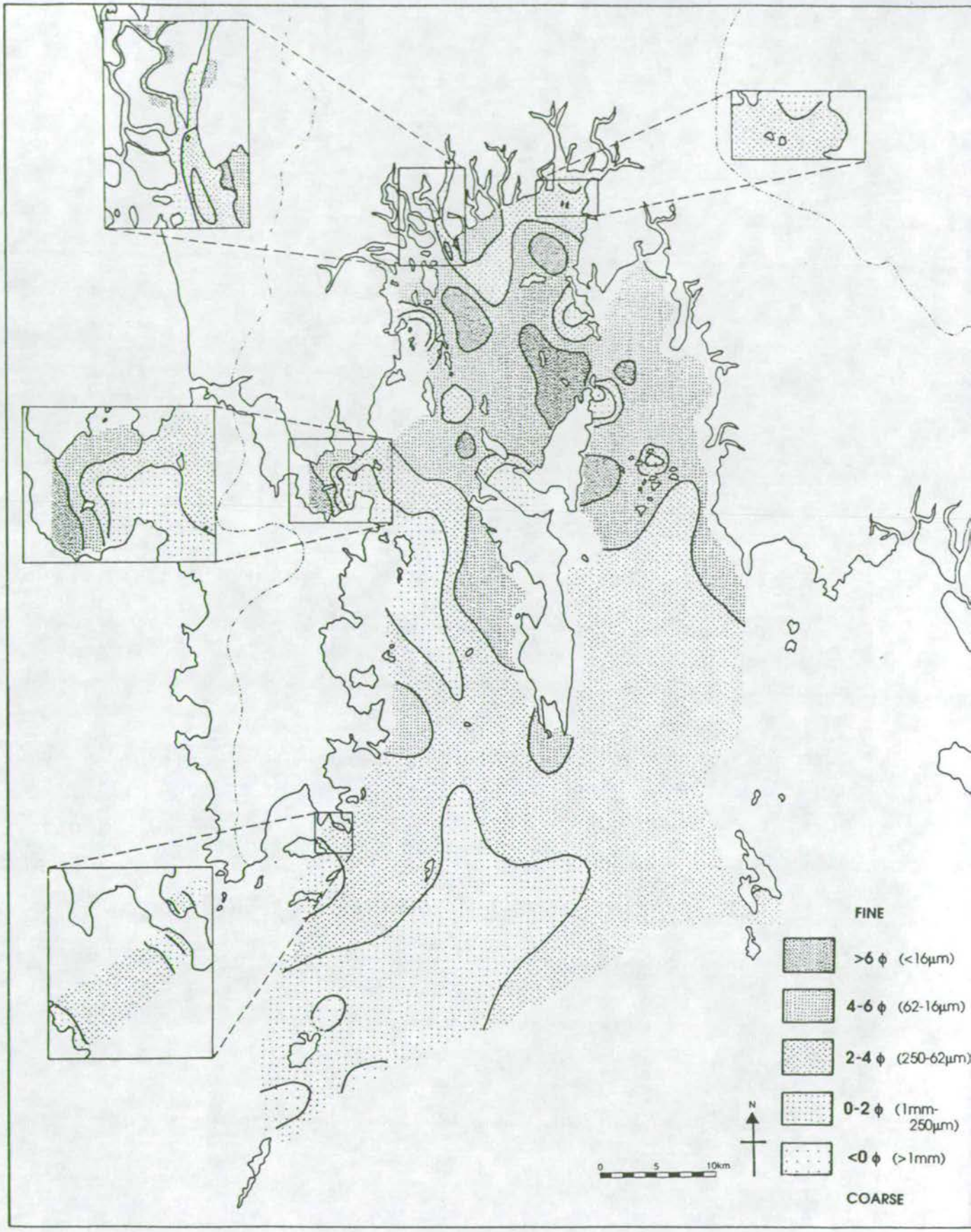

Figure 2.1 Areal distribution of mean grain size (first moment) of surface sediments.

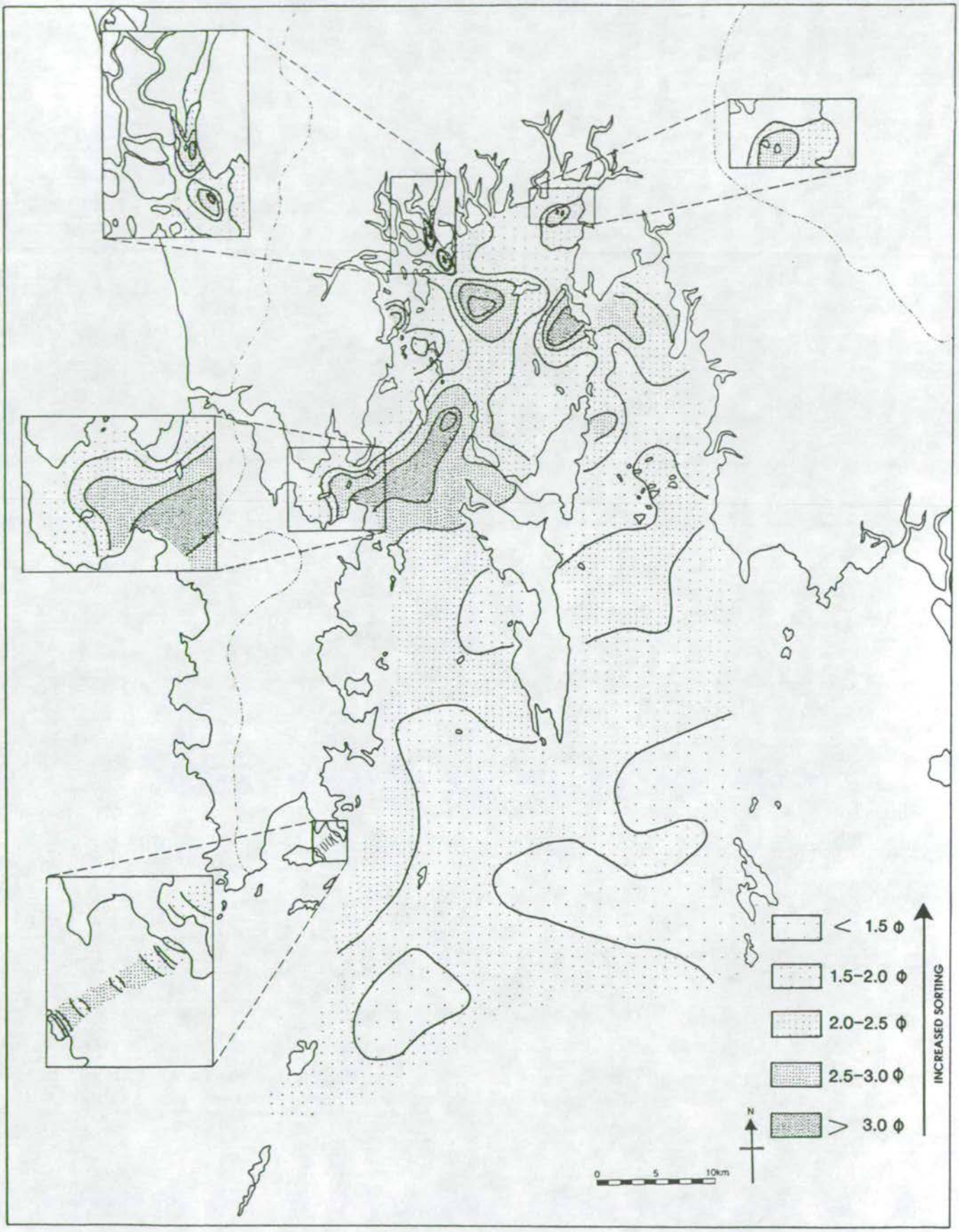

Figure 2.2 Areal distribution of sorting values (second moment) of surface sediments.

coincide with the areas of coarse mean grain size and with areas of high $CaCO_3$ content. The exceptions to this are the mangrove channels where coarse mean grain size and poor sorting do not relate to high $CaCO_3$ content.

2.4.3 Skewness

Figure 2.3 illustrates the variation in skewness values for surface sediments. Again, a general north-south trend is evident with dominantly negatively-skewed sediments in the north and positively-skewed sediments in the south.[1]

The pattern is generally similar to that of mean grain size with the negatively-skewed sediments corresponding to fine mean grain size and vice versa. Figure 2.4 illustrates the skewness of grain size distributions from 2 sites (42G and 124G) from the north and south of the Bay respectively.

2.4.4 Percent Gravel

2.4.4.1 Whole Sediment

A distribution map of percent gravel (> 2mm) in the whole sediment is illustrated in Figure 2.5. The areas of high gravel content are irregular and patchy but tend to be concentrated in the northern half of the Bay, however, there are particularly high values in the extreme south west of the area near to Ko Racha Yai. Much of the southern half has gravel values of < 10% but it is clear that most of the surface sediment in the Bay contains some gravel sized material.

2.4.4.2 Carbonate-free sediment

Figure 2.6 illustrates the carbonate-free gravel content and the difference from the previous diagram is quite striking. Most of the sediments have no terrigenous gravel content. Areas of highest terrigenous gravel content are in mangrove channels in the north, to the east of Ko Yao Noi in the eastern channel and to the north and east of Ko Racha Yai in the south west of the area. Sediments with low (0-4%) gravel content extend up the western channel up to the NE tip of Ko Phuket.

[1] In this work, the terms positive and negative skew are used whereby positive skewness refers to the bulk of the sediment being of a coarser size fraction (median is coarser than the mean) compared to negative skewness where the bulk of the sediment is of a finer size fraction (median is finer than the mean). Terms of "coarse-skew" and "fine-skew" as defined by Folk (1974) are not used here as there is sometimes confusion in the interpretation of these terms.

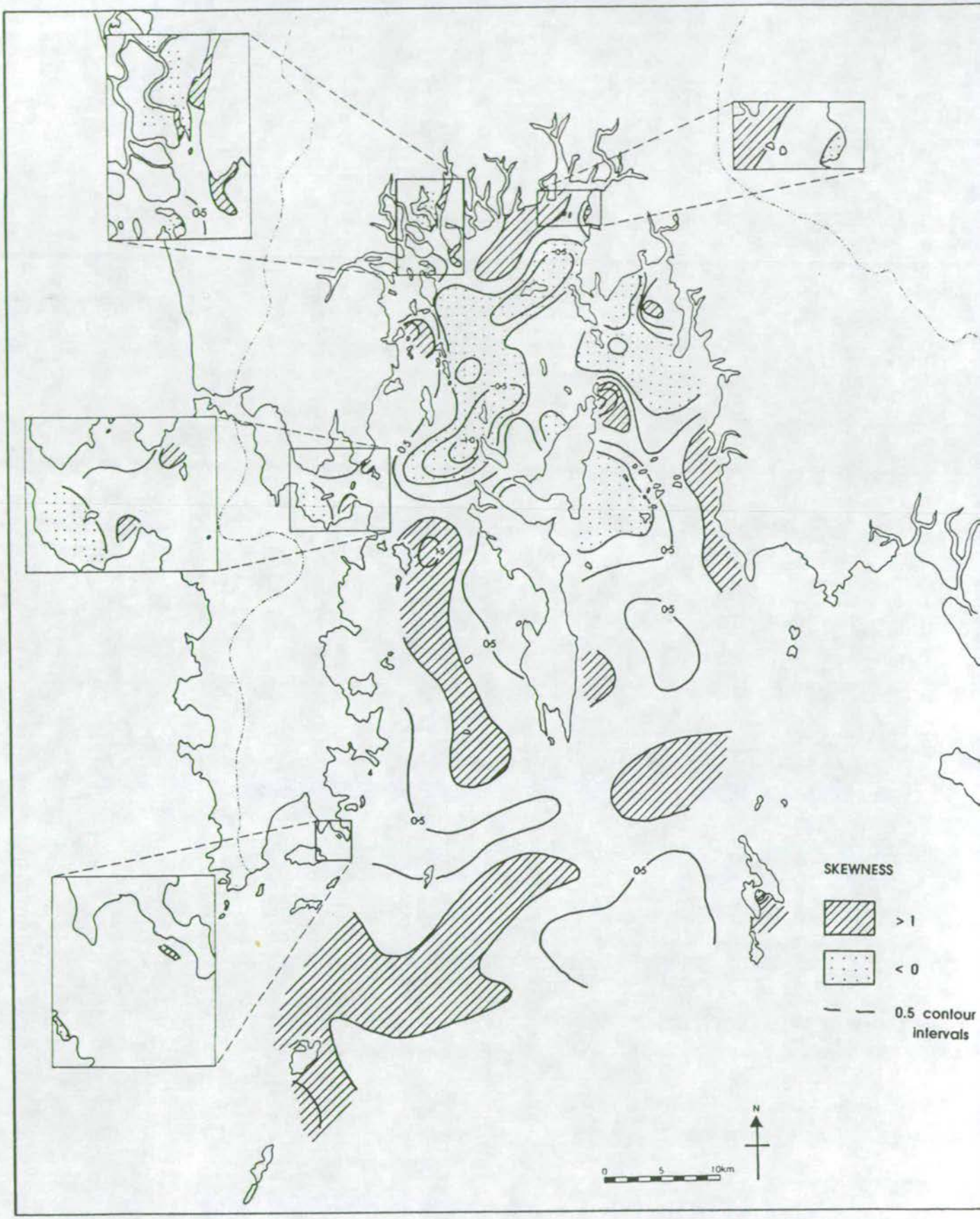

Figure 2.3 Areal distribution of skewness values (third moment) of surface sediments.

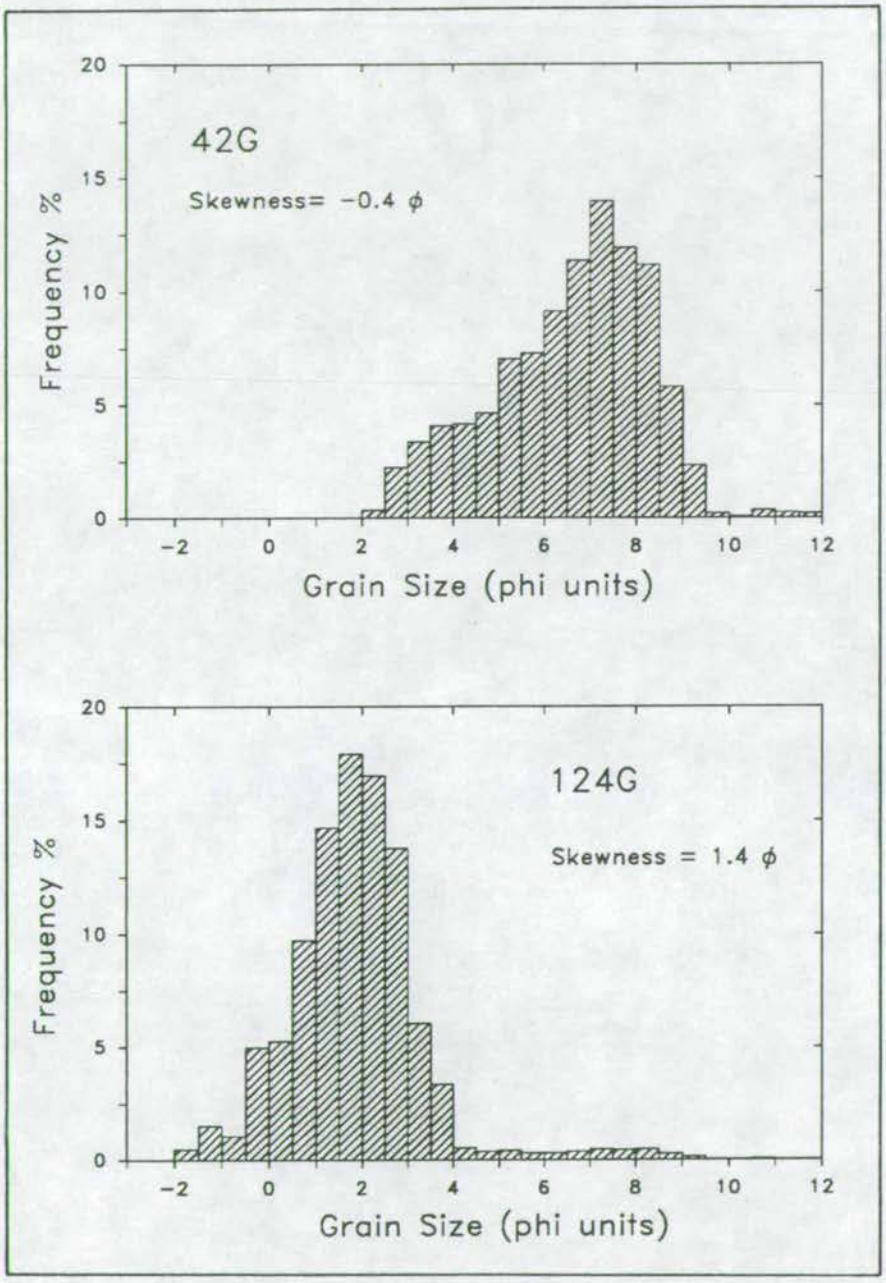

Figure 2.4 Frequency histograms of the grain size distribution of 2 samples exhibiting negative (42G) and positive (124G) skewness values.

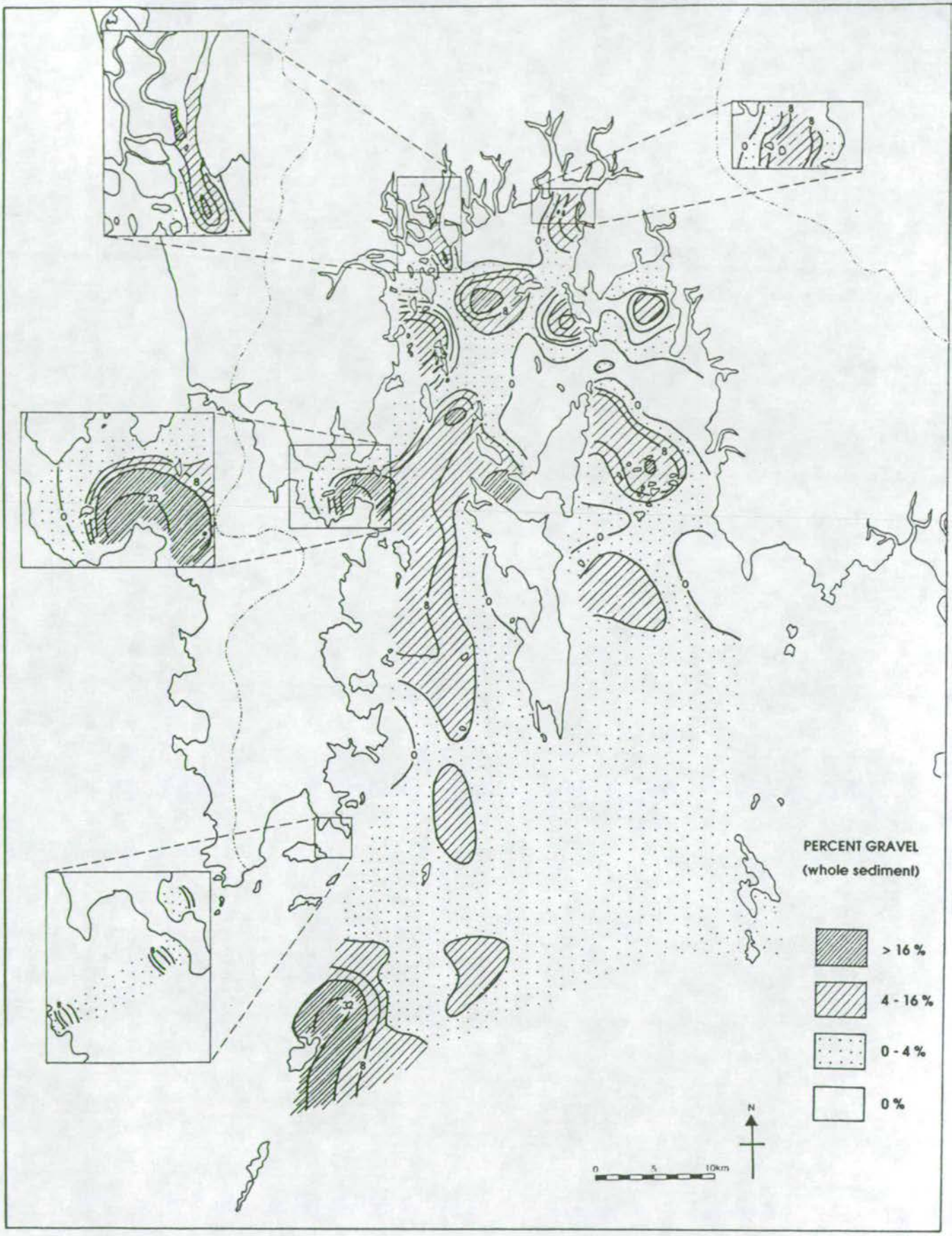

Figure 2.5 Areal distribution map of the percent gravel in the whole sediment for surface sediments.

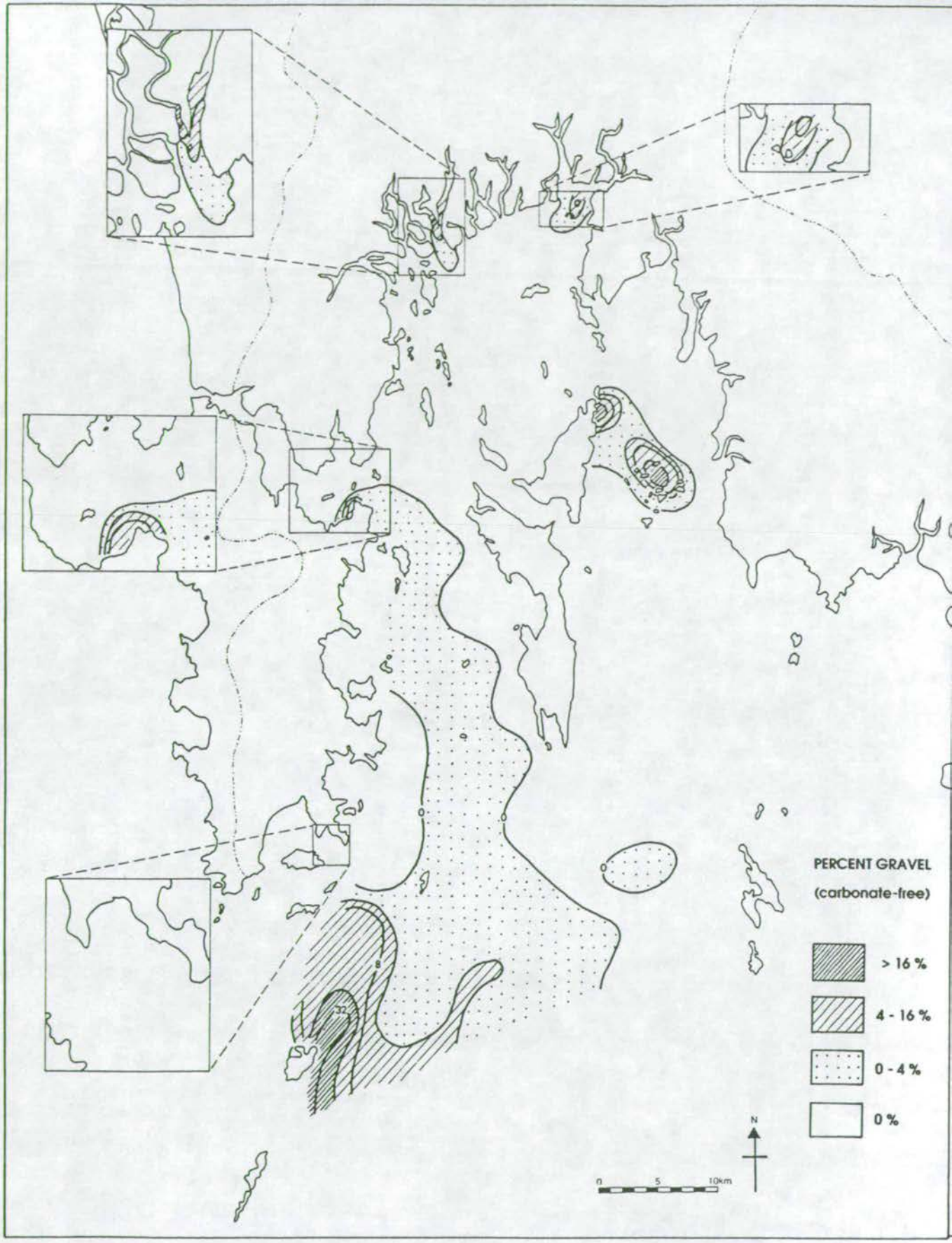

Figure 2.6 Areal distribution map of the percent gravel in the carbonate-free fraction of the surface sediments.

Figures 2.7a and b plot the 3 sediment size fractions in triangular diagrams for the whole sediment and for carbonate-free sediment respectively. Figure 2.7c illustrates the nomenclature of sediment grain sizes as devised by Folk (1954). It is clear that carbonate material adds a gravel fraction to most sediments, sometimes constituting up to 80% of the sediment. The terrigenous component of the sediment falls dominantly between the sand and mud categories. Several sediment samples retain a gravel component when carbonate is removed and these samples correspond to those plotted as > 16% gravel in Figure 2.6.

2.4.5 **Percent Sand**

2.4.5.1 Whole Sediment

Figure 2.8 plots percent sand in the whole sediment and the overall trend is roughly opposite to that of mean grain size (in ϕ units) as would be expected. Lowest sand values are found in the north where the finest mean grain size sediments are located and highest values are in the south where the coarsest sediments are found.

2.4.5.2 Carbonate-free Sediment

Distribution patterns of percent terrigenous sand (Fig. 2.9) are similar to whole sediment patterns reflecting the lack of carbonate material in the sand sized fraction. The terrigenous sand fraction is highest in mangrove channels, in the front of the mangroves in the north east of the Bay and in a large area covering the southern part of the study area.

2.4.6 **Percent Mud**

2.4.6.1 Whole Sediment

The percent mud distribution map for the whole sediment (Fig. 2.10) shows a similar pattern to the mean grain size map with high values in the north and < 10% in the south.

2.4.6.2 Carbonate-free Sediment

The carbonate-free distribution map of percent mud (Fig. 2.11) shows a similar pattern to the above map again indicating that carbonate forms an insignificant part of the mud fraction.

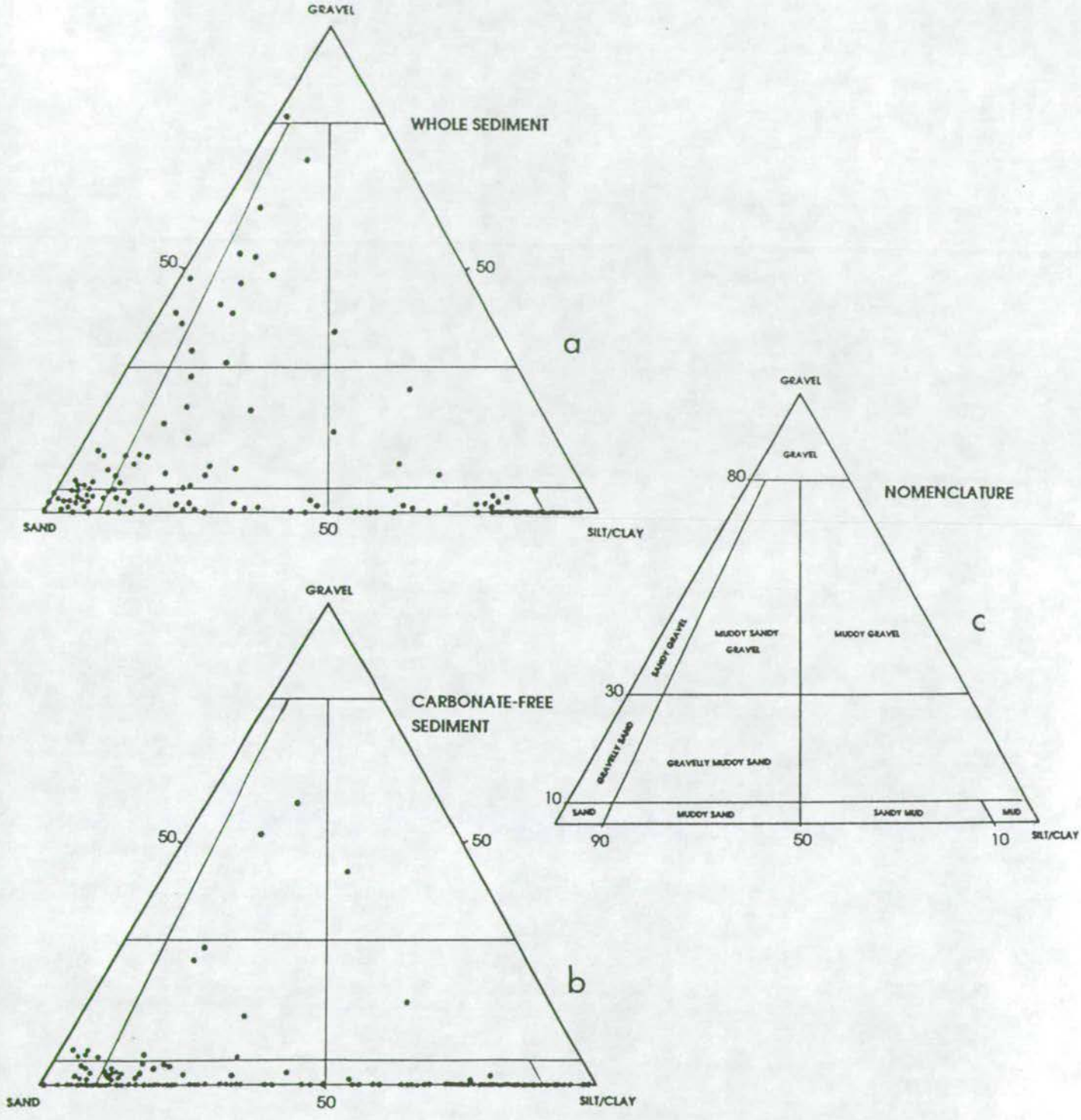

Figure 2.7 a. textural classification of the whole surface sediment samples plotted on a triangular plot of gravel v. sand v. silt/clay.
b. textural classification of the carbonate-free surface sediment samples.
c. nomenclature of Folk (1954) for the gravel v. sand v. silt/clay plot of sediment grain size fractions

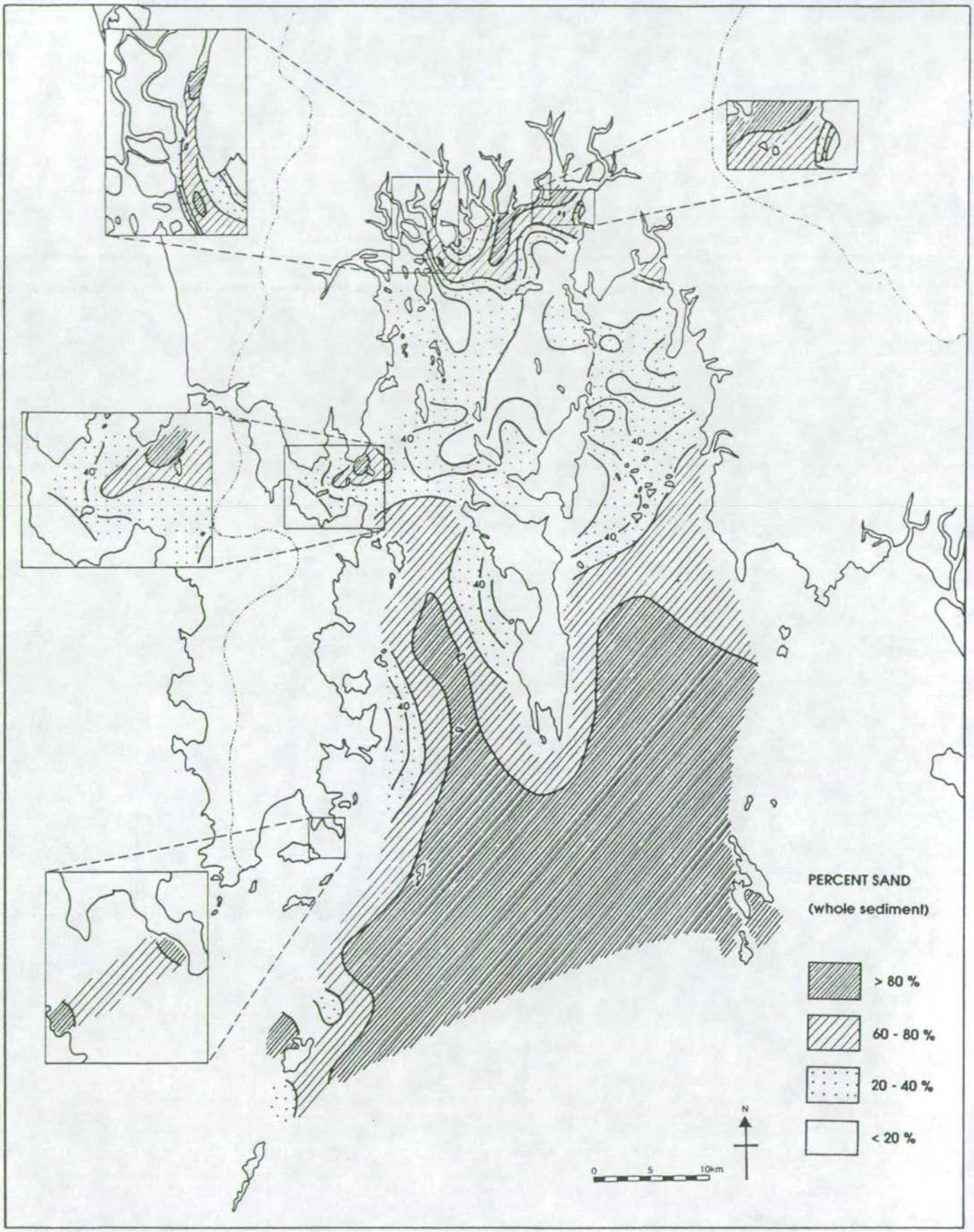

Figure 2.8 Areal distribution map of percent sand for the whole sediment for surface samples.

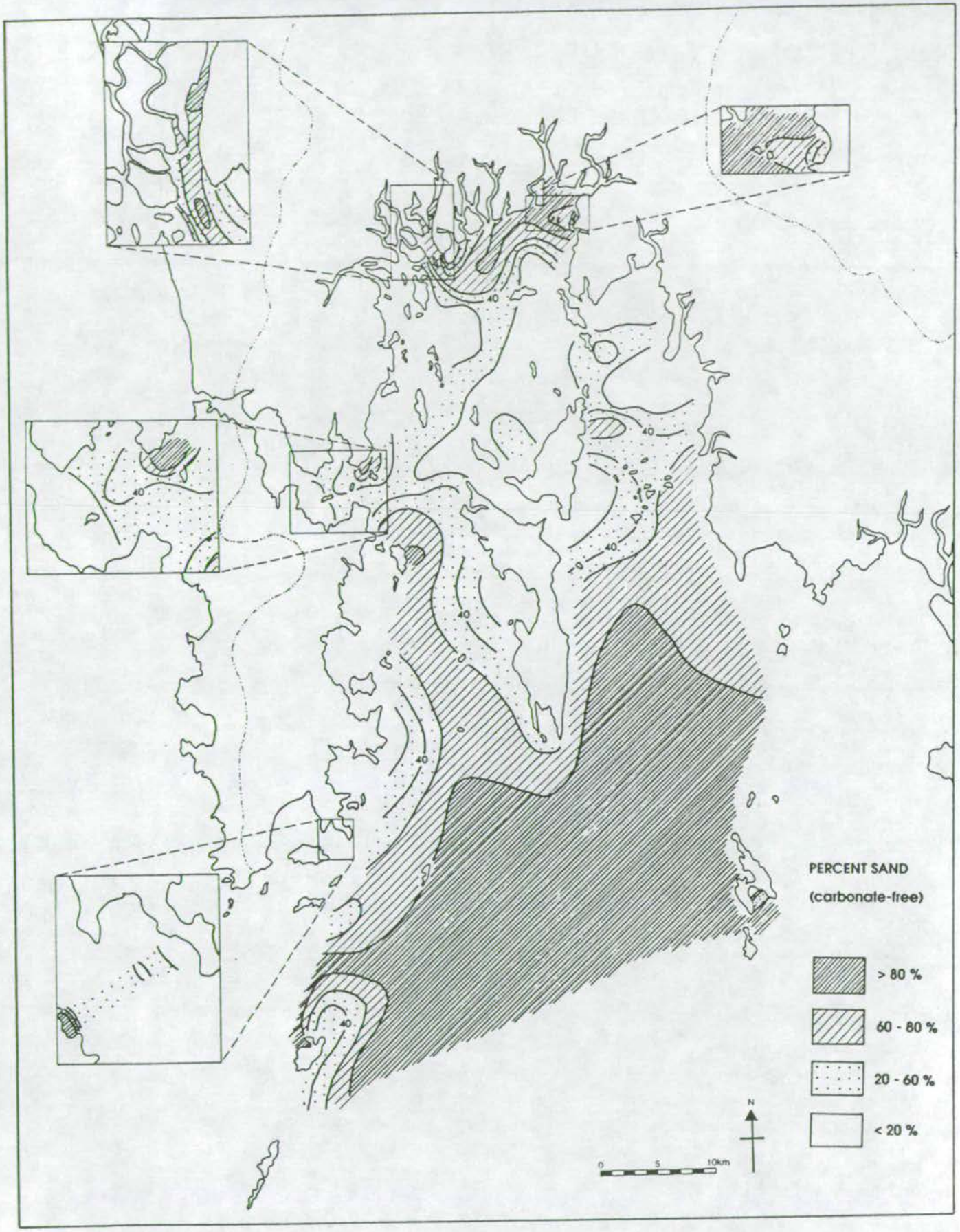

Figure 2.9 Areal distribution map of percent sand for the carbonate-free sediments for surface samples.

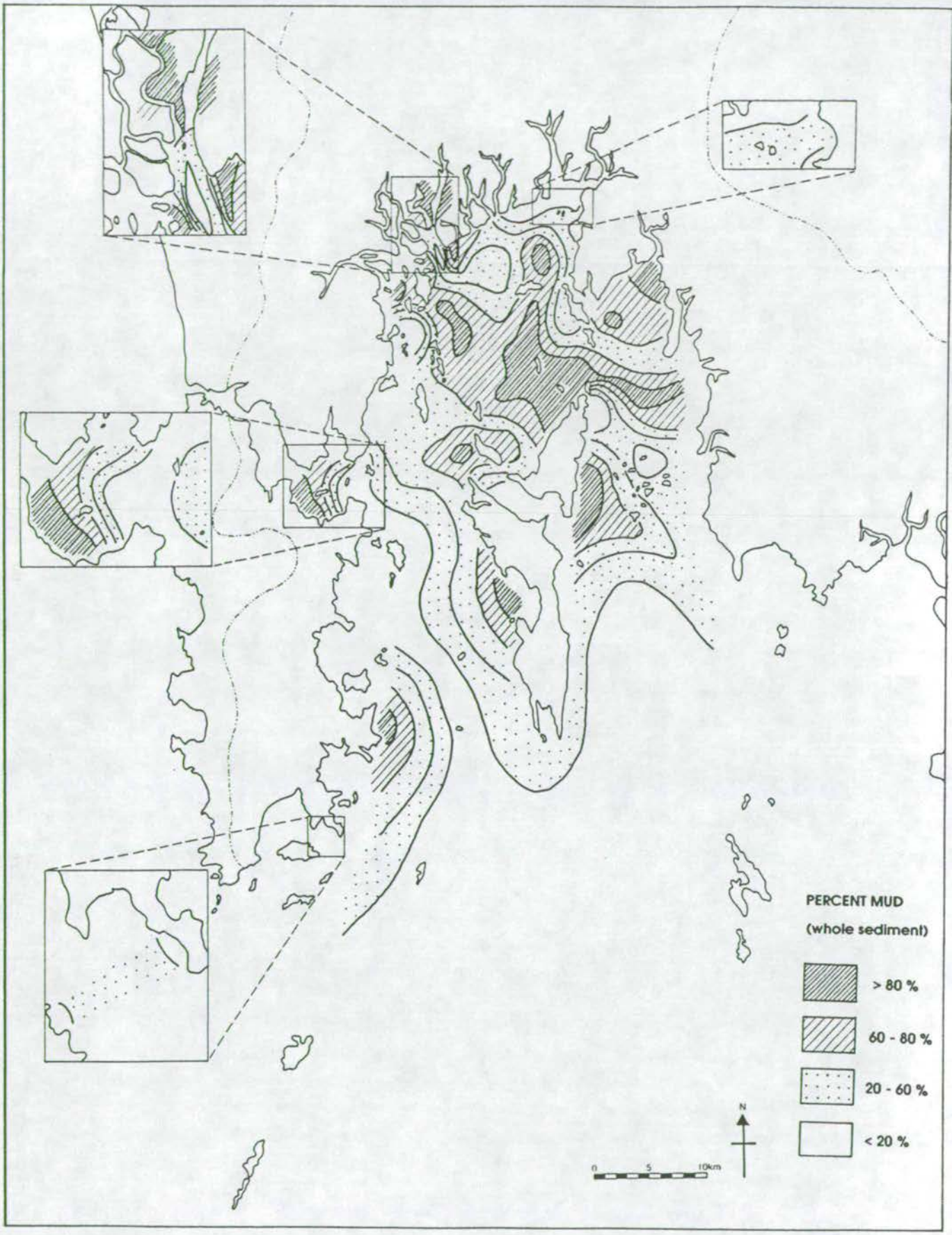

Figure 2.10 Areal distribution map of percent mud (< 62 µm) for the whole sediment for surface samples.

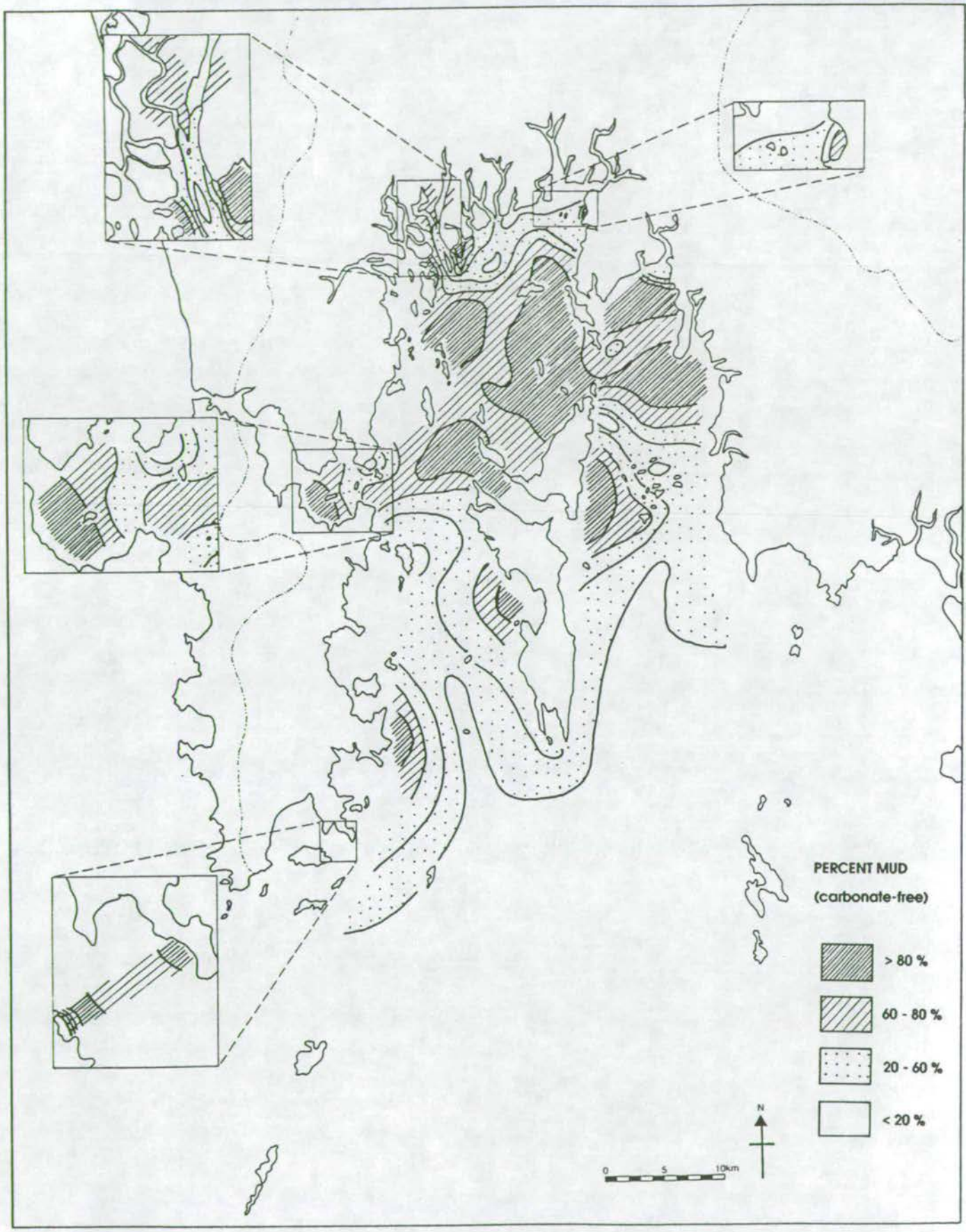

Figure 2.11 Areal distribution map of percent mud (< 62 µm) for the carbonate-free sediment for surface samples.

2.5 DISCUSSION

2.5.1 Large scale controls on sediment patterns

The generalised view of coastal sediment deposition especially in the geological record is that coarse material represents onshore/coastal environments (coastal plain, beaches etc) whilst fine sediments represent quieter off-shore depositional environments. In the case of Phangnga Bay and many other present-day shallow, sheltered bays and estuaries, the opposite is the case. Fine sediments settle in salt marsh and mangrove swamp environments whilst coarse sediment lies off-shore on the continental shelf. The reasons for this pattern will be discussed in this section.

2.5.1.1 Inshore fine sediment

Most of the recent material deposited in Phangnga Bay enters in the northern part of the Bay where the largest rivers meet the Bay. Considering the extreme chemical weathering of the rocks in the hinterland in the tropical climate and the consequent fine grained nature of tropical soils (Mohr and Van Baren, 1954), most of the material entering the Bay will be of fine grain size (fine silts and clays). There is therefore an abundant supply of fine grained material available for deposition.

Since most of Phangnga Bay is enclosed by land on 3 sides, it is protected from the influence of major currents sweeping along the Andaman Sea coast of peninsular Thailand. It is also sheltered from most strong wave action - only southerly winds would develop large waves able to sweep right into the north of the Bay and even then, the region is so shallow that any such waves from the south would be spent before reaching the northern-most part of the area. Since the dominant onshore winds are from the south west during the April to August monsoon, most of Phangnga Bay would be sheltered from these waves by Ko Phuket. Therefore, low energy conditions prevail in northern Phangnga Bay allowing deposition of the finer grain size sediments.

Most of the coarse terrigenous sand and gravel material brought into the Bay from fluvial transport settles out early on in these low energy conditions and is thus concentrated in mangrove channels and channel mouths. Tidal currents are focussed in channels allowing the transport of sand and gravel and the winnowing

of fines. In the fine grained muddy areas, because of the lack of coarse material reaching these areas the sediments are comparatively well sorted.

Settling out of the fine material is helped by the changes in equilibria between dissolved and solid chemical species at the estuarine (freshwater-seawater) interface. Flocculation of colloids occurs as freshwater containing these colloids meets with sea-water (ie, an electrolyte bearing medium). Once flocculation occurs the originally dispersed particles are capable of settling out of the dispersion medium. Additionally, organisms which use the suspended sediments as a food source (eg, epifaunal filter feeders) bind the sediment in their faecal pellets thus contributing to the settling out of fine particles.

As well as flocculation and biogenic sediment binding, the action of tides in shallow sheltered areas allows the settling out of fines. As tidal currents decrease at high slack tide, fines settle out and, in shallow areas, reach the sea bed. Some of this material may be resuspended as tidal currents increase again but some remains and so fine grained sediments accumulate. Since the highest tidal velocities are in the middle of the tidal cycle, areas only covered by high tides are not affected by these high velocities and so material that drops out of suspension at high water slack tide can accumulate. Additionally, since higher current velocities are required to resuspend fine grained sediment (particularly clay) than are required for the material to fall out of suspension the potential for the accumulation of this fine material is increased. The mangrove vegetation acts as a baffle to tidal currents thus increasing the possibility of fines settling out in the mangrove environment and reducing the likelihood of resuspension as the tide turns.

2.5.1.2 Off-shore coarse sediment

The occurrence of coarse material off-shore on the continental shelf has been recognised in many studies of coastal and shelf sedimentation (Shepard 1932; Emery 1952 and 1968; Bird, 1964; Curray 1965; ; Swift 1969 and 1970; Kulm et al 1975; McManus, 1975; Batchelor, 1979; Diaz et al, 1990; Demirpolat 1991 and others). It is thought to have been deposited during low sea-level stands (during glacial periods) in depositional environments very different from those prevalent today and is hence termed "relict" sediment. Such environments may have been sub-aerial, lacustrine or shoreline. With a rise in sea-level, sediments deposited in such environments have been preserved unreworked (true "relict" sediments) or reworked thus possessing

aspects of both its present and former environments (termed 'palimpsest' sediment, Swift et al, 1971).

Is this a suitable explanation for the sand deposits found in the off-shore southern part of Phangnga Bay? The position of fine silts and clays in the north of the Bay (with the only coarse terrigenous deposits evident in mangrove channels) suggests that there is some sort of low energy fence in this calm, sheltered area preventing coarse material presently being brought into the Bay from being transported any further than the mangrove front.

However, there is the possibility that all the surface sediment present today is of recent origin and a winnowing process in the southern area has effectively removed all the fine fraction (carrying it further off-shore) leaving only coarse material to accumulate as well sorted sediment. The SW-NE trend of the coarse deposits follows the direction of the south west monsoonal winds. Waves generated by monsoonal air flow would be strong enough to affect sediment deposition in the southern area effectively removing fines and/or preventing their settling out. The key to this theory is whether any coarse material sourced from the north could be transported far enough south in the sediment load.

Plotting frequency histograms of grain size data from a series of low carbonate samples (so shell fragments do not affect the grains size distribution) from the north of the Bay (Fig. 2.12) and comparing these to sediments from the southern area (Fig. 2.13) allows a comparison of sediment types between the two areas. The mode of sediments from the southern area ranges between 2 and 3 ϕ (medium to fine sands). This size fraction constitutes < 2% of the sediments in the north. This means that for the above theory to be correct, a huge volume of material has to pass through the low energy area in the north to be winnowed in the south for only the sand fraction to be left. The volume of sediment required to pass through the Bay to account for the large area of sand in the south, seems incompatible with the comparatively small size of the drainage basin. Additionally, although the mode of these sands is between 2 and 3 ϕ, 30-40% of the sediment is coarser than this and such a fraction is not represented in the sediments to the north (apart from in mangrove channels).

Thus it is improbable that these sands are presently accumulating via a source in the north due to the low energy fence in the northern part of the Bay which is preventing coarse material from being transported further south. Equally, there is no large

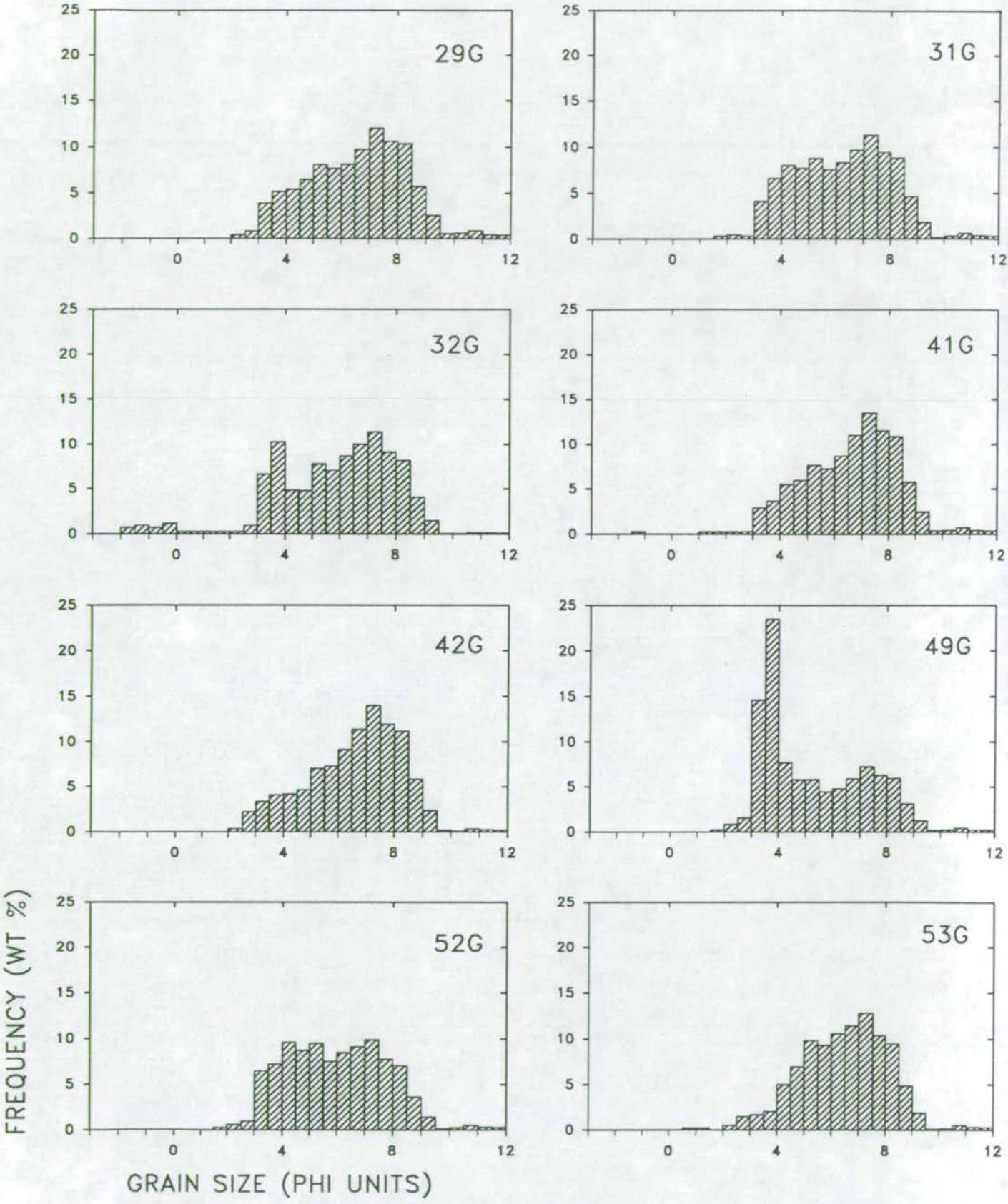

Figure 2.12 Frequency histograms of grain size distributions for low carbonate samples from the north of Phangnga Bay.

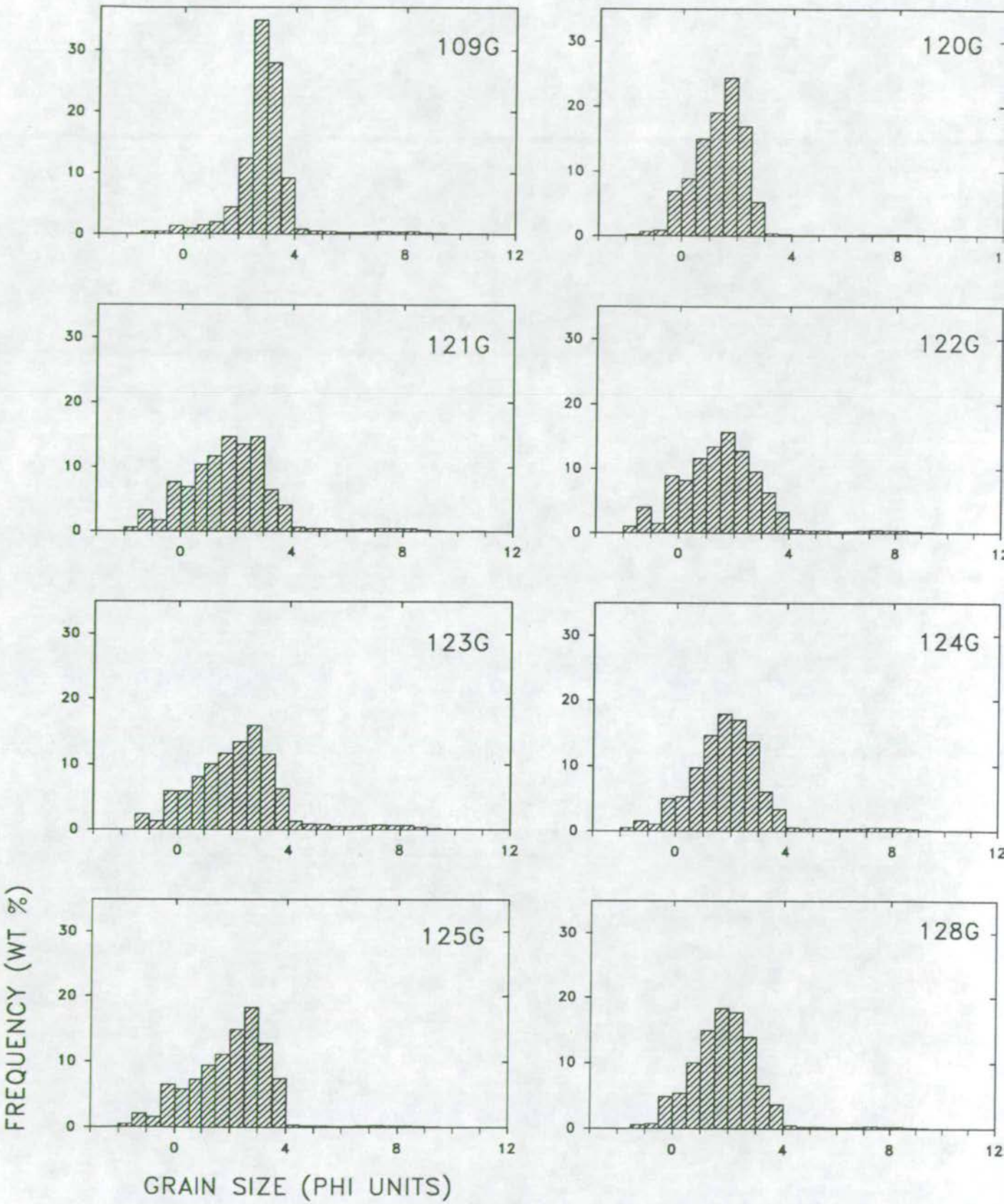

Figure 2.13 Frequency histograms of grain size distributions for samples from the south of Phangnga Bay.

terrigenous source to the south east which may provide the sand. Thus the only explanation for the origin of this terrigenous sediment is that it is relict. The higher energy conditions in the south provide a mechanism for preserving the coarse sands by preventing fines from settling.

Quaternary eustatic sea-level curves presented by Chappell (1974), and Shackleton (1987) show that sea-level hovers around a level of 40-60m lower than present between 100,000 and 40,000 years ago and Geyh et al (1979) states that between 36,000 and 10,000 year B.P. sea-level in the Straits of Malacca (just south of Phangnga Bay) hovered around 40-60 m below the present level. Since these sands are presently 40-60m below sea-level, it is likely that they represent shallow coastal and alluvial deposits which have been subject to reworking during transgressions thus accounting for the dominance of coarse material.

Further evidence will be put forward in following chapters supporting this theory of relict sediments although the most conclusive evidence from radiocarbon dating of relict carbonate material in the sediment is not available.

2.5.2 Local controls on sediment patterns

2.5.2.1 Shell material

It is clear from studying the variations in gravel contents between whole sediment and carbonate-free sediment (and comparing these maps with the $CaCO_3$ distribution map - Figure 4.4) that shell material accounts for many of the smaller patches of coarse sediment in the north of the Bay. These shell accumulations are formed either from the *in situ* growth of carbonate-secreting organisms eg, mussels (site 28G), or from development of lag deposits in beach environments (site 44a) or possibly from concentration through storm reworking. The latter feature has been recognised as an important evolutionary process in the Ord River/Cambridge Gulf area, Western Australia (Thom et al, 1975). Tidal flats accrete laterally and vertically, however this general pattern is interspersed with short erosional episodes with coarse shelly debris transported across the mudflats.

2.5.2.2 Localised currents

High terrigenous gravel concentrations in the north of the Bay result from the enhancement of currents in tidal channels and around headlands which winnow fine material leaving coarse lag deposits. Carbonate debris also forms part of these

sediments but the presence of coarse terrigenous material attests to an influence other than *in situ* carbonate accumulation.

2.6 CONCLUSIONS

From both detailed grain size analysis of the whole sediment and from measuring grain size fractions of the carbonate-free sediment a picture of sedimentation in Phangnga Bay has been established. In the calm, sheltered, shallow area in the north of the Bay, fine grained sediments (muds and clays) sourced from the surrounding catchment area and transported into the Bay through streams and rivers have accumulated. Coarse terrigenous material has been trapped in fluvial and tidal mangrove channels and at channel mouths. The low energy conditions have prevented this material from being transported any further south into the Bay. In the south, surface sediments are dominated by coarser sand and gravel sized terrigenous material which is thought to represent relict sediments deposited during low sea-level stands in glacial periods and since covered by the Holocene transgression. The area is open to oceanic influences such as waves and currents particularly during the south west monsoon and these higher energy conditions prevent fine sediment transported southwards in suspension from the north of the Bay to settle out in the south and cover the relict sediments in a veneer of recent sediments.

The present day surface sediments of Phangnga Bay therefore represent a diachronous surface with recent fine-grained sediments in the north and Pleistocene coarse sediments in the south.

Carbonate shell material adds a gravel component to the sediments as a result of either *in situ* growth of carbonate-secreting organisms or from development of shell lag deposits through sediment reworking. Localised strong currents have resulted in a winnowed lag surface with coarse sediment.

CHAPTER 3

THE MINERALOGY OF THE SURFACE SEDIMENTS

CHAPTER 3 - MINERALOGY OF SURFACE SEDIMENTS

3.1 INTRODUCTION AND METHODS

A simple classification of shallow marine sediments based on a compositional description of the sediment results in 3 basic components ie, **terrigenous** (including detrital, residual, volcanic and relict), **biogenic** and **authigenic** (Emery, 1968). In Phangnga Bay, two of these components dominate namely terrigenous and biogenic. No authigenic minerals such as glauconite have been conclusively identified. The following chapter discusses the petrology and mineralogy of the terrigenous and biogenic components and discusses the likely type and source of the terrigenous material.

Binocular microscope examination of the sediment components and thin sections of such components have been used to describe the petrology of the sediments. The mineralogy has been ascertained using X-ray diffraction (XRD) the method of which is described in Appendix B. Although all of the surface sediments were analysed by XRD as bulk samples to give a qualitative survey of the sediments' mineralogy, only a selection of samples were analysed in detail for semi-quantitative data on clay and carbonate mineralogy. An attempt was made at semi-quantitative determination of bulk sediment minerals, however, errors of 10-30% on the resulting figures were too large compared to the estimation of mineral variations made by X-ray fluorescence analysis of elements.

3.2 TERRIGENOUS COMPONENT

The terrigenous component of the sediments is effectively the non-carbonate fraction ie, that which is originally derived from continental erosion and has not been formed by biogenic secretion or by diagenetic processes within the sediment. In Phangnga Bay, this fraction is dominated by quartz sand and silt and by aluminosilicate clays. Feldspars, micas, lithic fragments and "heavy" resistate minerals are additional minor components of the sand and silt sized fractions and iron-oxide minerals occasionally form coatings on coarser grains. A variety of techniques have been used to identify and examine these components including

XRD, thin-sections, and binocular microscopy. Light minerals (quartz, mica and feldspar), heavy minerals, iron-oxides and then clays will be discussed in turn.

3.2.1 Light Minerals

3.2.1.1 Mineralogy

Quartz - identified on XRD by a pronounced sharp (101) peak at 3.34Å (26.27° 2θ) and a less intense (100) peak and 4.26Å (20.85° 2θ).

Alkali Feldspar - identified by a (002) peak at 3.24Å (27.53° 2θ) and a (130) peak at 3.77Å (23.6° 2θ).

Lepidolite Mica - $K_2 (Li,Al)_{5-6} (Si_{6-7} Al_{2-1} O_{20})(OH, F)_4$ - identified by the characteristic basal spacings: (001) at 10Å (8.84° 2θ); (002) at 4.99Å (17.74° 2θ); (003) at 3.34Å (26.68° 2θ) and (004) at 2.47Å (36.36° 2θ).

A typical X-ray diffractogram for feldspar and quartz is illustrated in Figure 3.1 and for lepidolite in Fig 3.2.

No quantitative survey of quartz versus feldspar was attempted as feldspar was only found in 3 of the 169 surface samples qualitatively analysed. Also, peak intensities were comparatively low which suggests that feldspar is present in very low quantities. The samples in which feldspar was found were 35b, 79b and 85 which are all mangrove channel samples from the north west of Phangnga Bay. Therefore, feldspar does not form a major constituent of Phangnga Bay sediments as it is chemically weathered and removed from the incoming terrigenous fraction before being transported any distance into the bay.

3.2.1.2 Petrology

Quartz dominates the > 4μm light terrigenous fraction of the sediments (ie, non-clay, non-carbonate fraction). From visual examination of surface sediments with carbonate and clays removed quartz forms 95-100% of this fraction in all sediments (see plate 1).

The quartz in these sediments was originally derived from sub-aerial weathering of rocks, however, from other studies (listed in Chapter 2, section 2.5.1.2) it is known that most of the terrigenous fraction in outer parts of modern day estuaries (ie, on the

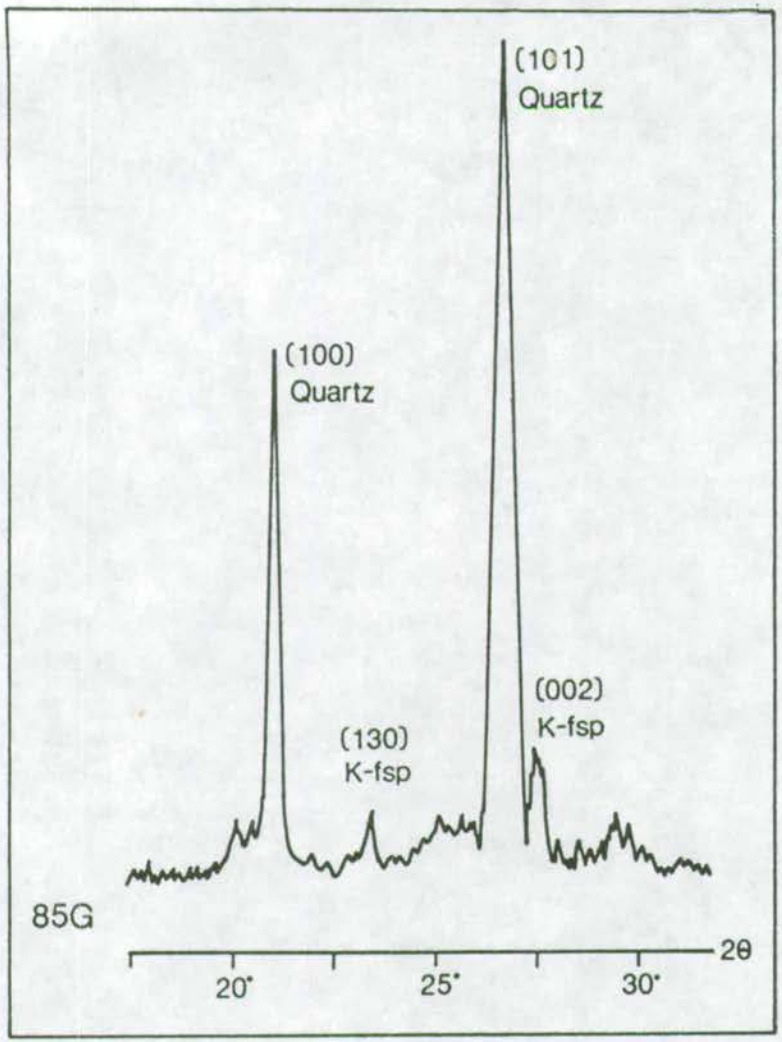

Figure 3.1 Typical XRD trace of quartz and feldspar

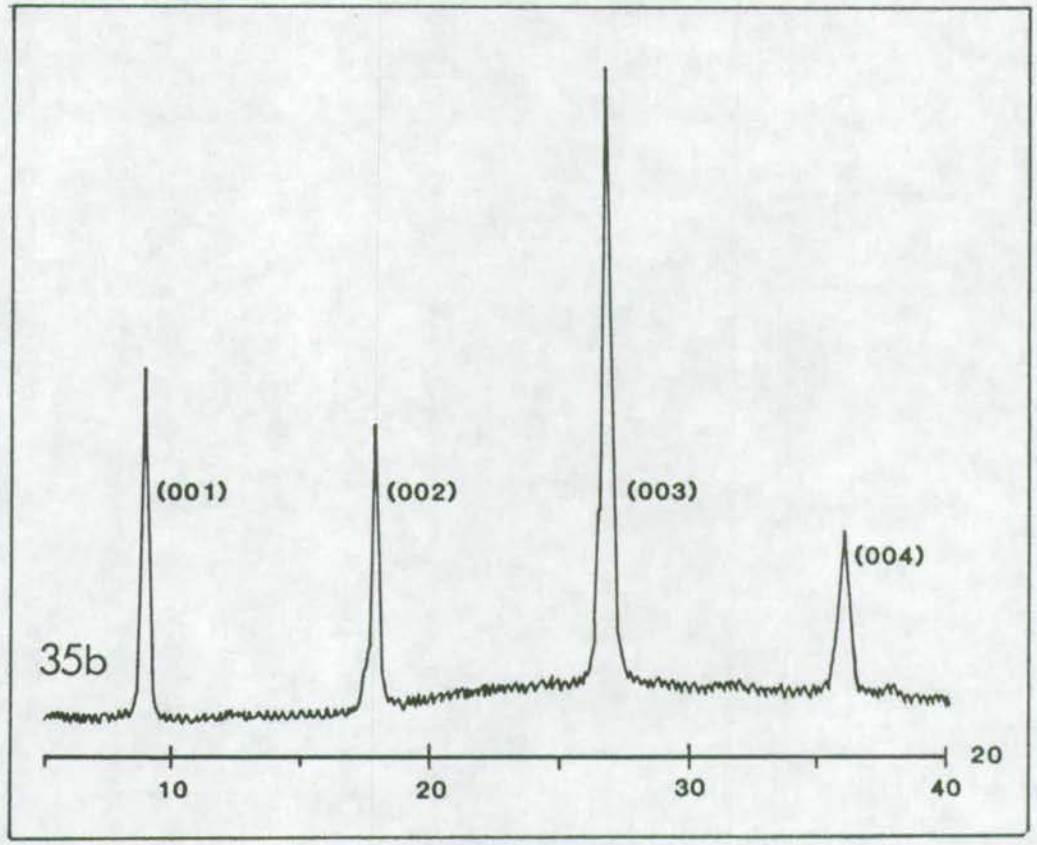

Figure 3.2 Typical XRD trace of lepidolite mica (basal spacings of an oriented section)

Plate 1

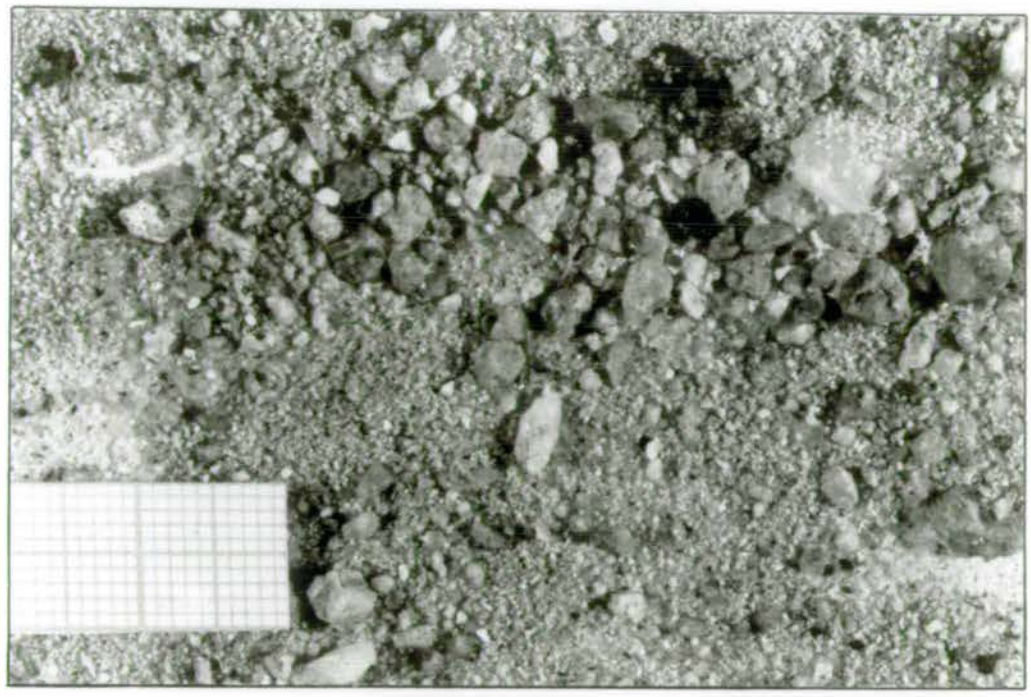

mm grids on scale bar

79bG Quartz fraction
(clay and $CaCO_3$ free)

Plate 2

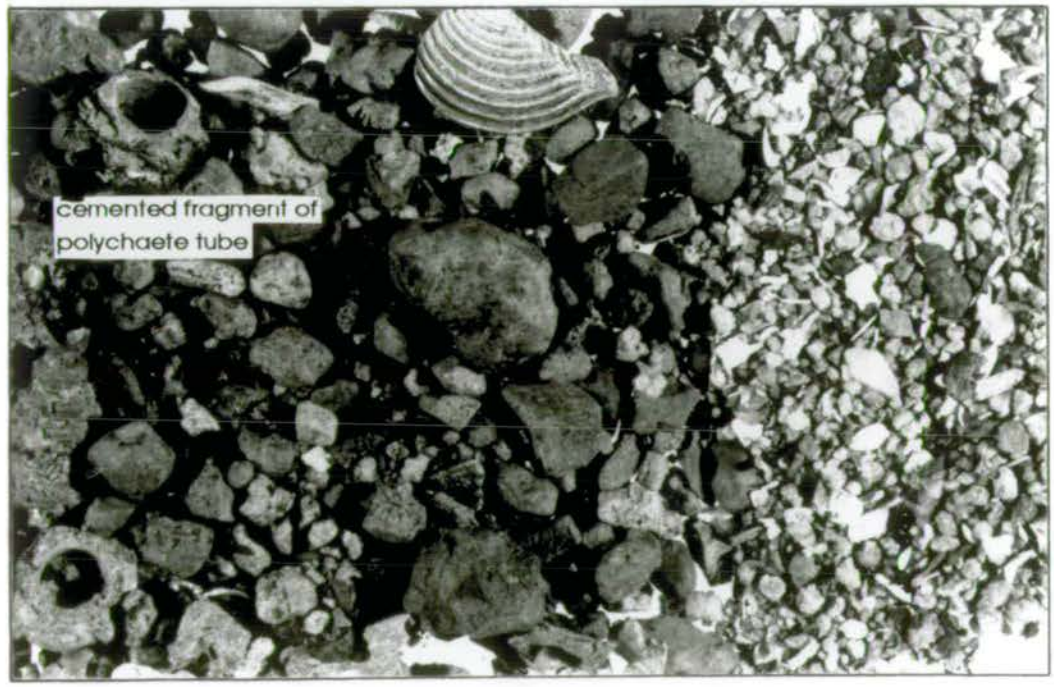

34G Quartz and carbonate grains with Fe-oxide coatings
(note dusty appearance compared with above sample)

continental shelf) are relict sediments derived from continental erosion and deposited during low sea-level stands in conditions very different from those prevalent now. The quartz material in the upper reaches of the bay in mangrove channels and the silt sized material in the muddy sediment of the northern part of the bay is thought to have been derived from recent fluvial deposition and is therefore in equilibrium with the present conditions. To test this theory, 2 surface sediment samples (35bG in a mangrove channel and 122G in southern area) were examined for mineralogy, roundness and sphericity by thin section.

Thin sections of the >62μm, carbonate-free fraction of both sediment samples were made by setting the grains in resin then cutting a thin section. 250 grains in each slide were then studied by placing the slide on a mechanical point-counting stage on a petrological microscope and recording the mineralogy, roundness and sphericity of the grains present. The grain fabric of quartz grains (single or composite grains and type of extinction) was also noted.

Crystal optics were used to ascertain the mineralogy. The Powers scale of roundness and sphericity (Powers, 1953) was used to visually estimate the grain shape characteristics. Observation of the grain fabric was made by rotating the stage and observing the quartz grains under crossed polars.

Table 3.1 gives the results for each sample which have been recalculated to percentages of either the total sample (for mineralogy) or of the particular mineral for which each feature is observed. Photomicrographs of these thin sections are illustrated in plates 3 and 4.

Clear differences in the samples are picked out by this simple study. The mangrove channel sediments contain more feldspar (microcline and orthoclase) and mica (lepidolite and some biotite) than the open marine sands. Of the quartz grains, mangrove channel grains have more angularity, less grains show high sphericity and there are more composite quartz grains (ie, one distinct grain is composed of more than one quartz crystal) than the open marine sediment grains. The extinction properties of either single or composite grains do not show any particular difference between samples. Feldspars in the mangrove channel sample are more abundant, more angular and more grains show low sphericity compared to the open marine sample. Mica is not present in the open marine sample and that which is present in the mangrove channel is dominantly angular and of low sphericity.

MINERAL	35bG Mangrove Channel %	122G Open Marine %
QUARTZ	72	98
Roundness:		
very angular	17	10
angular	44	23
sub-angular	23	19.5
sub-rounded	13	21
rounded	3	19.5
well rounded	0	7
Sphericity:		
High	54	77
Low	46	23
Grain Fabric:		
Single Grain	39	87
with straight extinction	(58)	(69)
with undulose extinction	(42)	(31)
Composite grain	61	13
with straight extinction	(63)	(53)
with undulose extinction	(12)	(7)
with both types of extinction	(25)	(40)
FELDSPAR	12	2
Roundness:		
very angular	0	0
angular	29	0
sub-angular	57	0
sub-rounded	14	50
rounded	0	50
well rounded	0	0
Sphericity:		
High	71	100
Low	29	0
MICA	16	0
Roundness:		
very angular	11	-
angular	32	-
sub-angular	47	-
sub-rounded	10	-
rounded	0	-
well rounded	0	-
Sphericity:		
High	10	-
Low	90	-

Figures in bold type refer to percent of the whole number of grains in point count.

Figures in normal type refer to percent of the mineral in question.

Figures in brackets refer to percent of the total number of Single or Composite quartz grains showing either type of extinction properties.

Table 3.1 Comparison of mineralogy, texture and fabric of the carbonate-free fraction of 2 sediments from the north and south of the Bay.

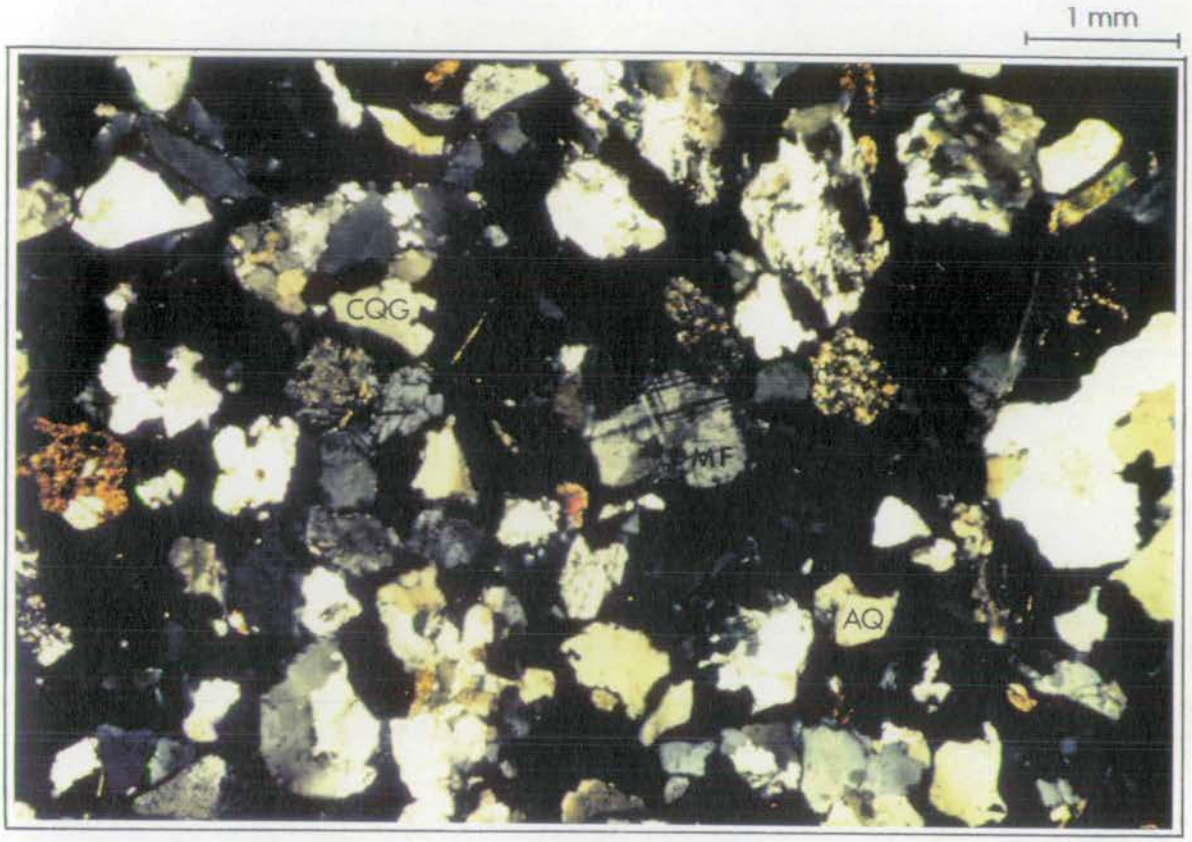

Plate 3 35bG thin-section of carbonate-free mangrove channel sand

CQG = composite quartz grain MF = microcline feldspar
AQ = angular quartz grain

Plate 4 122G thin-section of carbonate-free relict sand

RQ = rounded quartz grain

The results from thin section analysis indicate that the terrigenous coarse fraction of the open marine sediment is both compositionally and texturally more mature than that of the mangrove channel sediment. The greater degree of rounding and sphericity of both quartz and feldspar grains of the open marine sediment suggest the grains have been subjected to a longer transport history or at least a transport history of higher energy environments. The lower percent of composite quartz grains also indicates this as such grains are susceptible to breakage through transport processes resulting in single grains. Lack of feldspar and mica in the open marine sample similarly indicates a longer transport history as these minerals are more unstable both chemically and mechanically than quartz and would eventually be removed through transportation. The similarity of extinction properties between quartz grains of both samples however, indicates that the quartz grains may be derived from the same source. Straight extinction suggests a reworked sedimentary origin for the grains (although not if the grains were originally igneous) and/or an originally recrystallised metamorphic origin. The slightly undulose extinction properties suggest an igneous source (Folk, 1974). The catchment area geology of Phangnga Bay contains sedimentary rocks, recrystallised metamorphic rocks (in the form of hornfels) and igneous rocks (emplaced during a period of faulting and therefore likely to show some strain features in the grain fabric).

The greater compositional and textural maturity of sample 122G from the southern open marine area compared to the mangrove channel sample indicates that the sands in the south have undergone a greater degree of erosional reworking through longer transportation histories and/or from reworking in a higher energy environment. The suggestion that the southern sands are relict deposits from low sea-level stands is supported by this textural evidence - both sands are from a similar source area however in the case of sample 122G they have travelled further possibly along a fluvial system developed north-south along the exposed part of Phangnga Bay during low sea-levels. The present depth below datum of these sediments (-40 to -60m) coincides with the projected sea-level during a large part of the Pleistocene Epoch (see Chapter 2) and so it is likely that reworking of these sands in a coastal shallow marine beach environment occurred.

Lepidolite Mica was found in surface sediment samples 35b, 79b, 34, 85, 38, 113, 114, and 115 as < 2mm platey, whitish yellow grains. Figure 3.3 illustrates the location of the northern sample sites listed above and the location of lepidolite pegmatites in Phangnga Province which are the likely source of these grains. These pegmatites

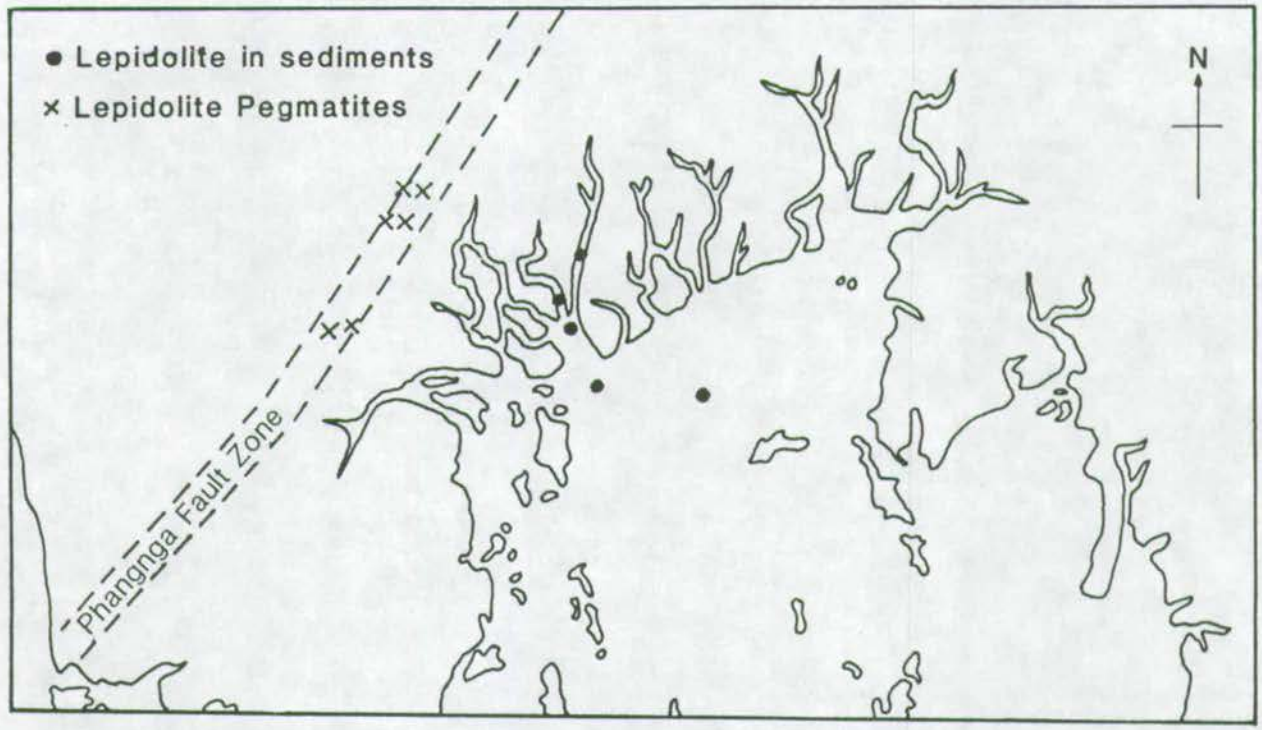

Figure 3.3 Location of samples containing lepidolite mica in the northern part of the Bay and the associated lepidolite pegmatite veins in the drainage basin.

have been described in detail by Garson et al (1975) and carry economic amounts of cassiterite - for this reason the pegmatites are mined with lepidolite being the main gangue mineral. The pegmatites were formed along the Phangnga fault zone (described in Chapter 1) and are generally unzoned with lepidolite distributed evenly throughout the veins. In the World context, such pegmatites are rare and Garson et al (1975) describes these Thai examples as "possibly the largest unzoned pegmatites yet discovered".

The precise origin of the lepidolite in the sediments from the 3 sites in the south of the Bay (to the NE of Ko Racha Yai) is not known, however, this topic is considered further in Chapter 4 (section 4.5.1.1) when discussing Rb anomalies in the surface sediments as lepidolite is one of the few minerals which contains significant amounts of Rb in its structure.

3.2.2 Heavy Minerals

No areal survey of heavy mineral concentrations has been carried out for this study. However, some information has been gained from XRD analysis of panned samples, a detailed petrological study of the heavy minerals present in one sample (124G) and from a report by the Thai Department of Mineral Resources (Phuket Division).

3.2.2.1 XRD Analysis

Excess grab sediment from 16 sites in the southern area of Phangnga Bay was panned in order to collect a concentrated sample of the heavy mineral fraction. Visual examination of the panned concentrates revealed a dark metallic fraction and a light pinky brown fraction which was preliminarily identified as garnet. XRD analysis of these samples revealed hematite (Fe_2O_3), ilmenite ($FeTiO_3$), magnetite (Fe_3O_4), rutile (TiO_2), tourmaline ($(Na,Mg_3\ Al_6\ (BO_3)_3\ (Si_6O_{18})(OH_4)$), garnet ($(Fe,Mg)_3\ Al_2\ (SiO_4)_3$) and cassiterite ($SnO_2$).

3.2.2.2. Reflected Light Microscopy

Approximately 25 grams of wet sediment from 124G was sieved to remove the mud fraction then treated with HCl to remove the calcareous fraction. The heavy minerals were then separated using Tetrabromoethane and mounted in an epoxy resin disc. This was then ground and polished to achieve a suitable surface to enable identification of the minerals present by reflected light microscopy.

Hematite (medium reflectance, no birefringence, hard), ilmenite (pinkish brown birefringence), and rutile (low reflectance, yellow brown internal reflections) were present in the greatest quantities followed by leucoxene and anatase. These latter two minerals are alteration products of ilmenite and rutile respectively. Most ilmenite and rutile grains showed some degree of alteration to these secondary minerals. A few grains of zircon ($Zr(SiO_4)$) were identified by their distinctive tetragonal form. A few cassiterite grains were also identified by their hardness, low reflectance and yellowish internal reflections.

3.2.2.3 Government Report Findings

A detailed study of the mineral content of a surface sediment from a site off the south east coast of Phuket island was made by the Thai Department of Mineral Resources (Phuket Division) in 1988. No precise location is available for this site but it is known to be within a dredging concession area off Phuket town (Fig 3.4). Also, no information is available on whether this is a whole sediment analysis or a panned concentrate analysis. However, the information which is listed in Table 3.2 is useful in that it gives some idea of the heavy minerals present and their relative proportions to each other in this area.

3.2.2.4. Discussion

The IGS study on the stream sediment and panned concentrate samples by Garson et al (1975) recorded the following heavy mineral assemblage from mined areas in Phuket and Phangnga Districts:

Major minerals-
topaz; garnet; ilmenite; ilmenorutile; rutile; cassiterite; fergusonite; zircon; tourmaline.
Minor minerals-
xenotime; monazite; altered pyrite; epidote; hornblende; chromite; secondary manganese oxides.

The garnet and dark coloured minerals are contained in the fine sand fraction of the samples. The garnet is described as 'pale pink to pale orange' almandine ($Fe_3 Al_2 (SiO_4)_3$) - pyrope ($Mg_3 Al_2 (SiO_4)_3$) garnet (Garson et al, 1975 pg 104) which fits the description of the garnet recorded in this study's off-shore panned sample. Most of the above minerals are associated with the tin-bearing granites and pegmatites of the drainage basin.

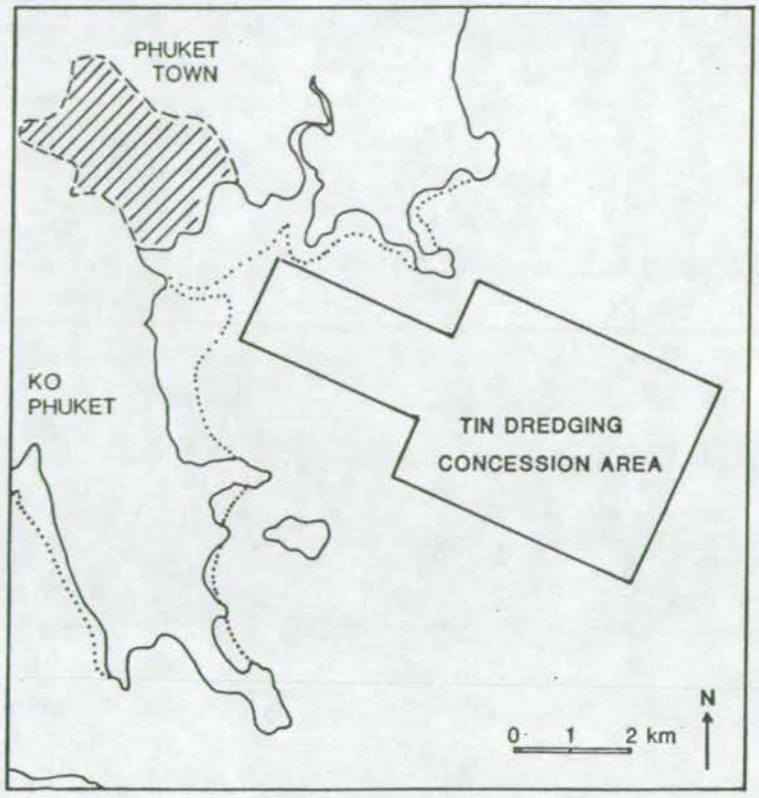

Figure 3.4 Location of dredging concession area off the south east coast of Ko Phuket from which samples recorded in the Government Report (see text) were taken.

Mineral and Composition	% by weight
Cassiterite (SnO_2)	trace
Monazite ($(Ce,La,Y,Th)\ PO_4$)	0.16
Zircon ($ZrSiO_4$)	0.78
Rutile (TiO_2)	0.50
Leucoxene (TiO_2)	0.45
Ilmenite ($FeTiO_3$)	14.04
Garnet ($(Mg_3,Fe_3,Mn_3)\ Al_2\ (SiO_4)_3$)	1.40
Tourmaline ($XY_3\ Al_6\ (BO_3)_3\ (Si_6O_{18})(OH)_4$)	9.38
Hydroilmenite ($FeTiO_3.nH_2O$)	6.57
Sand (SiO_2)	66.01
Pyrite (Fe_3O_4)	0.36
Siderite ($FeCO_3$)	0.35

Data from the Department of Mineral Resources (Phuket Division) Report

Table 3.2 Sediment analysis recorded in Government Report from dredging area offshore from Phuket town (see above for location).

The heavy mineral assemblage present in the sediments of the Bay is dominated by altered opaque minerals showing varying signs of degradation to amorphous alteration products and by stable non-opaque minerals such as zircon, rutile and tourmaline. Unstable non-opaques present in the drainage basin but not in the Bay sediments are epidote and hornblende. The heavy mineral assemblage in the sediments of the south of the Bay can therefore by described as reasonably mature. Unstable minerals have been removed through chemical alteration and abrasion, opaque non-silicates are being altered and resistant minerals are abundant.

3.2.3 Altered Iron-Oxide Minerals

Orange coatings on quartz grains are found in sands from mangrove channels and from sites in the south of the Bay (Fig 3.5). These sands were analysed by XRD for their mineralogical composition. The following minerals were identified:

Hematite - (Fe_2O_3), recognised by the characteristic (104), (116), (110) and (024) d-spacings of 2.69Å (33.31° 2θ), 1.69Å (54.28° 2θ), 2.51Å (35.77° 2θ) and 1.84Å (49.6° 2θ) respectively.

Goethite - (FeO.OH) recognised by the characteristic (110), (111) and (130) d-spacings of 4.18 (21.25° 2θ), 2.45 (36.65° 2θ) and 2.69 (33.31° 2θ) respectively.

A typical X-ray diffractogram of these minerals is illustrated in Figure 3.6 from a sample of thick orange coating on a quartz grain in sediment from site 34G - Plate 2 illustrates this sediment (with clays removed).

Hematite and goethite form under oxidising conditions from the weathering of iron-bearing minerals such as magnetite and pyrite. In the case of the mangrove channel sands, the original minerals may have been part of the quartz dominated lithic structure and have since oxidised and formed a cement and coating to the quartz crystals. The iron-coatings on the quartz sands in the south of the Bay may have formed in a similar manner when these sands were deposited in alluvial or coastal environments during low sea-level stands. An oxidising environment is required to prevent goethite and hematite from being reduced. Strong currents have been noted around Ko Racha Yai and such active water is likely in the southern part of the Bay which is not sheltered by Ko Phuket or the mainland.

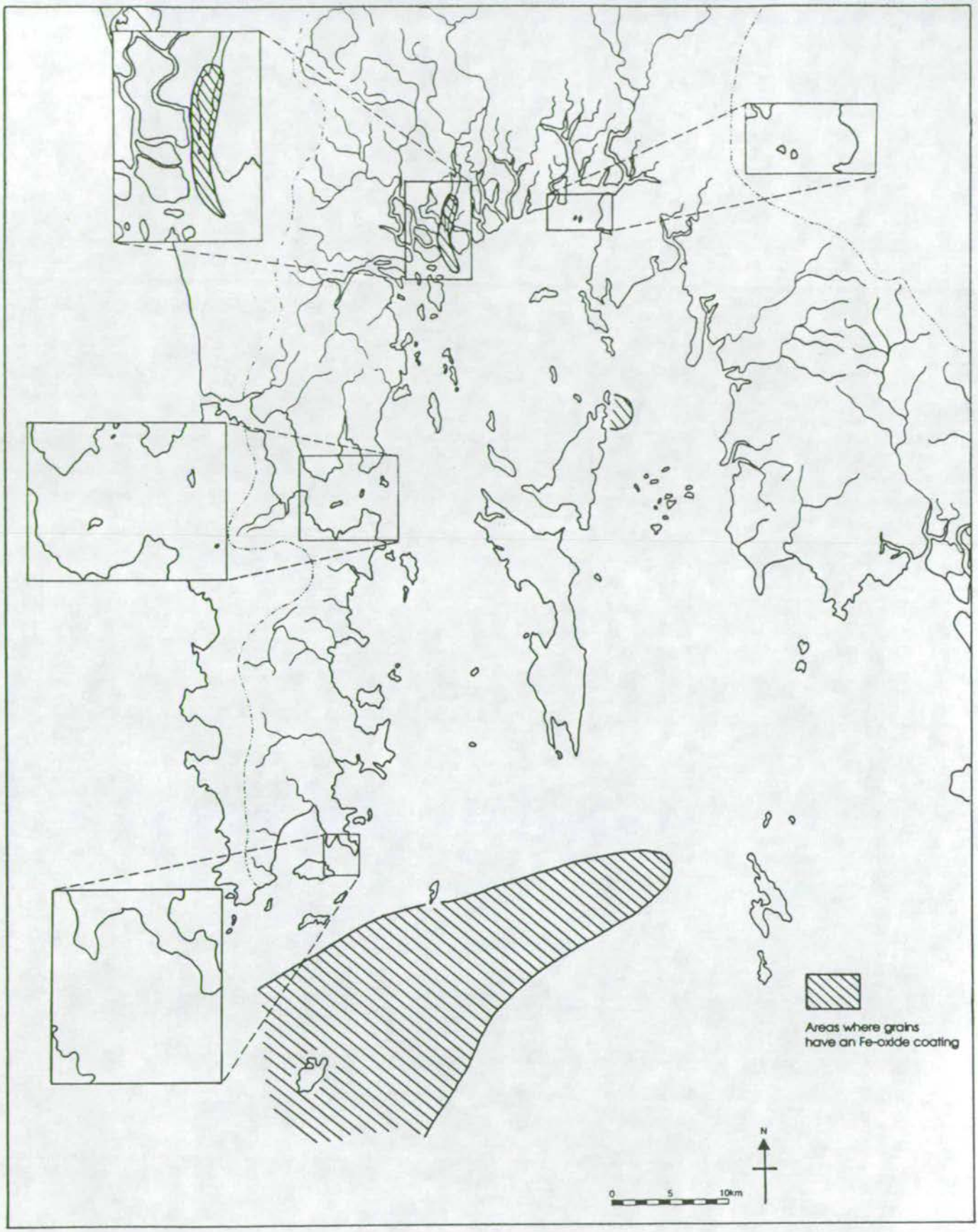

Figure 3.5 Distribution of orange Fe-oxide coated quartz sand grains in surface sediments.

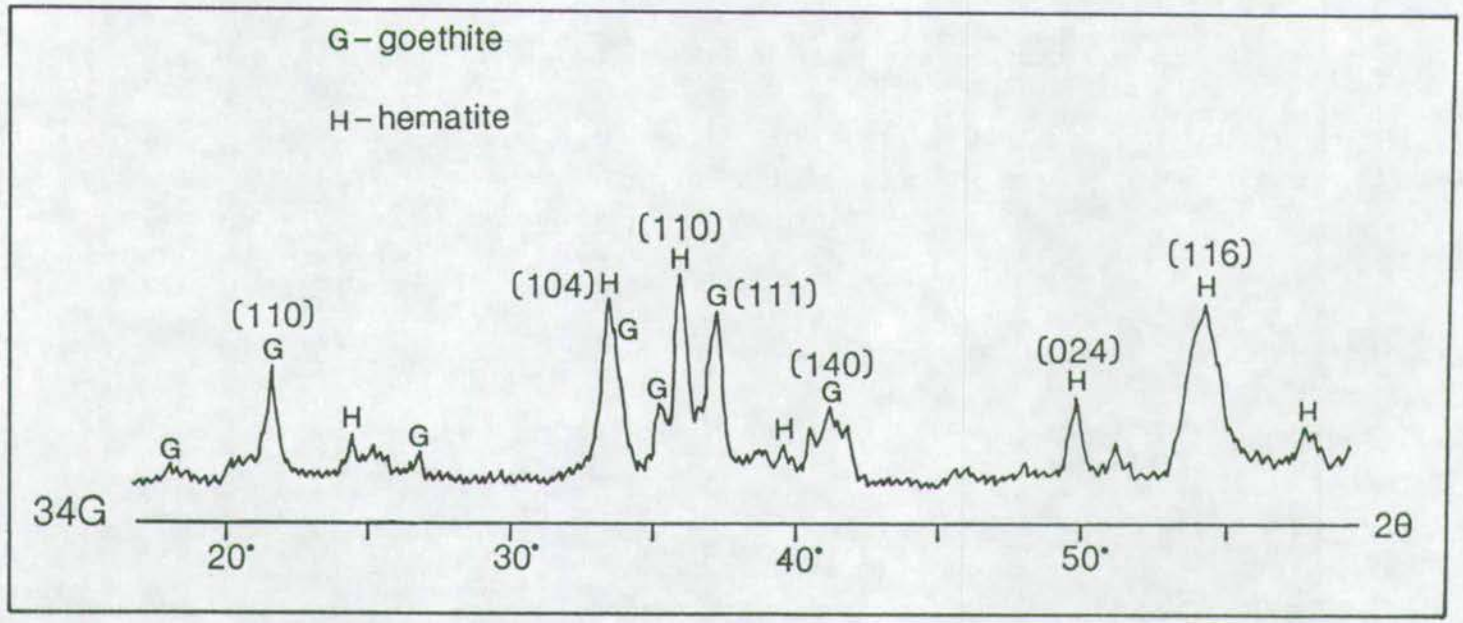

Figure 3.6 Typical XRD trace of Fe-oxide minerals.

Therefore, oxygenated sediment surface conditions are prevalent in this area thus preserving the oxidised iron coatings.

An alternative theory is that oxidised Fe and Mn in terrigenous minerals was trapped in the sediments during burial and on reaching the anoxic zone the Fe and Mn were reduced and migrated in this mobile form back to the oxic zone where they precipitated as coatings on the grains. Maiklem (1967) suggested this origin for the limonite stains on relict foraminiferans from the Great Barrier Reef.

3.2.4 Lithic Fragments

Very few lithic fragments were observed in the surface sediments of Phangnga Bay. Lumps of quartz crystals "cemented" together with haematite and goethite formed approximately 20% of the mangrove channel sands. < 1mm grains of dark, non-crystalline fragments were observed in a few samples from the sandy sediments of the southern area but these have not been closely studied due to their rarity. Due to the intense chemical weathering of the rocks in the hinterland it is thought that very little lithic material is transported into the Bay.

3.2.5 Clay Minerals

3.2.5.1 Mineralogy

Clay mineral determination was carried out on the clay fraction (< 4μm) of the whole sediment of selected samples by X-ray diffractometry. The method is detailed in Appendix B. 15 surface samples (see Figure 3.8 for distribution) were treated identically in this way and one sample was run in triplicate to check reproducibility of results.

The minerals identified are as follows:

Kaolinite - $Al_4(Si_4O_{10})(OH)_8$ - untreated basal spacing of 7Å (001) with no change after glycolation or heating to 400°C but which is mostly destroyed after 550°C (small peak still visible).

Illite - $K_{1-15}\,Al_4(Si_{7-6.5}\,Al_{1-1.5}\,O_{20})(OH)_4$ - untreated basal spacing of 10Å (001) and 5Å (002) which does not change after glycolation or heating to 550°C.

Montmorillonite - $(1/2Ca,Na)_{0.7}(Al,Mg,Fe)_4((Si,Al)_8\ O_{20})(OH)_4.nH_2O$ - untreated basal spacing of 14Å which expands to 17Å after glycolation, collapses to 10Å after heating to 400°C and 550°C.

No mixed-layer illite-montmorillonite clays are thought to be present in significant amounts as the main basal reflections of illite and montmorillonite do not shift towards each other nor does the illite 5Å spacing increase as would be expected with any illite-smectite layering (Reynolds and Hower, 1970). No chlorite is present either as no 14Å peak was visible after heating to 400°.

Gypsum - $CaSO_4.2H_2O$ - identified by its characteristic (020) spacing of 7.6Å and its collapse on heating due to the removal of water from the structure. It was thought unlikely that gypsum forms a true component of the sediment clay fraction and on testing of the water with which the sediments had been diluted during the clay separation process it was found that gypsum is present in the tap water supply (distiled water was not available in large enough quantities to use in the clay separation process).

Quartz - SiO_2 - identified by its (101) 3.34Å reflection. Present in very low quantities, sometimes the 3.34Å peak is only just visible above the background.

Figures 3.7 a and b illustrate the typical 2°-20° 2θ X-ray diffractogram obtained from 2 clay fraction samples (76G and 8G). The charts illustrate the 3 clay minerals identified and their reaction to glycolation and heating as described above. The main difference in charts of the 2 samples is the absence of the montmorillonite peak in 76G and its obvious presence in 8G. The charts for the other samples also show variations in montmorillonite peak intensity. This variation was considered important and needed in some way to be quantified.

3.2.5.2 Semi-quantitative Aspects

A method of semi-quantitative evaluation of clay mineral mixtures suggested by Biscaye (1965) was used. This method entails measuring basal peak intensity areas and weighting them to make direct comparison of their peak areas more meaningful. The peaks and weighting factors used are : Montmorillonite 17Å (glycolated) peak; 4x the Illite 10Å (glycolated) peak; 2x the Kaolinite 7Å peak (unchanged with glycolation). An assumption has to be made that these 3 minerals constitute 100% of the clay (< 4μm) fraction. As mentioned earlier, gypsum and

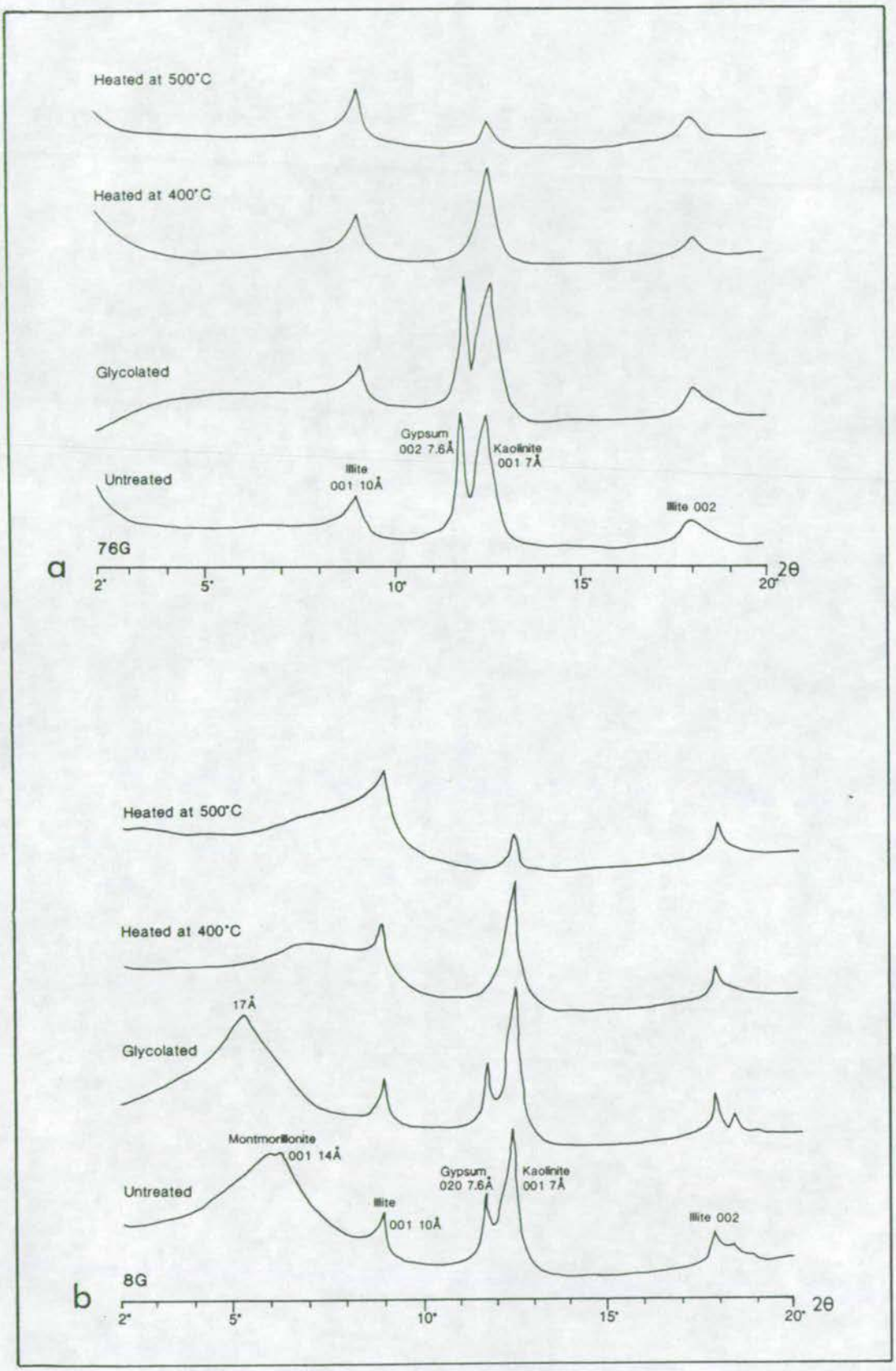

Figure 3.7 a. XRD trace obtained from the clay fraction (< 4 μm) of 76G.
b. XRD trace obtained from the clay fraction of 8G.

small amounts of quartz are present in this fraction in these samples and so some error may be introduced by these minerals affecting recorded intensities of the 3 clay minerals. However, because of the small peak intensities of quartz and gypsum compared to the clay peaks this error is thought to be negligible and is ignored. There are many other sources of error in such calculations, for example, difficulty in pin-pointing the background level especially in the 2° to 7° 2θ section and precise calculation of the area under the curve. These errors serve to make such determinations semi-quantitative. However, for the purpose of comparing areal clay mineral variations in this study, the method is considered adequate. The triplicate run of one sample provided a check on the relative accuracy of the method and gave consistent results (1-3% variation) for each clay mineral percentage.

Figure 3.8 illustrates the variation in the proportions of montmorillonite, illite and kaolinite as percentages of the clay fraction throughout Phangnga Bay. The main feature which is illustrated here is that montmorillonite increases in sites furthest away from land with a corresponding relative decrease in kaolinite. Illite does not appear to show any trend in its variation and constitutes between 10-30% of the clay mineral fraction.

3.2.5.3. Discussion

When discussing the distribution of clays in the marine setting, Keller (1956) concluded that both the source area of the clays and the depositional environments of the resulting marine sediments affect the clay distributions. The increasing montmorillonite and decreasing kaolinite trend away from source is also recorded in other areas. Prior and Glass (1961) studied the clay distributions of the upper Mississippi embayment and found that clays deposited in the fluvial environment are dominantly kaolinitic, those in the outer neritic environment are dominantly montmorillonite and those in the inner neritic environment are an equal mix of kaolinite, illite and montmorillonite. Their explanation for this is that montmorillonite is prevented from settling out in the fluvial environment because of its finer grain size compared to illite and kaolinite. It therefore dominates in the outer neritic zone where depositing currents are weaker and much of the illite and kaolinite have already settled out. Griffin and Ingram (1955) observed a decrease in kaolinite downstream in the Neuse River estuary and a corresponding increase in vermiculitic chlorite. Similarly, Nelson (1960) found a decrease in kaolinite downstream from the Rappahannock River estuary in Virginia and Hirst (1962a)

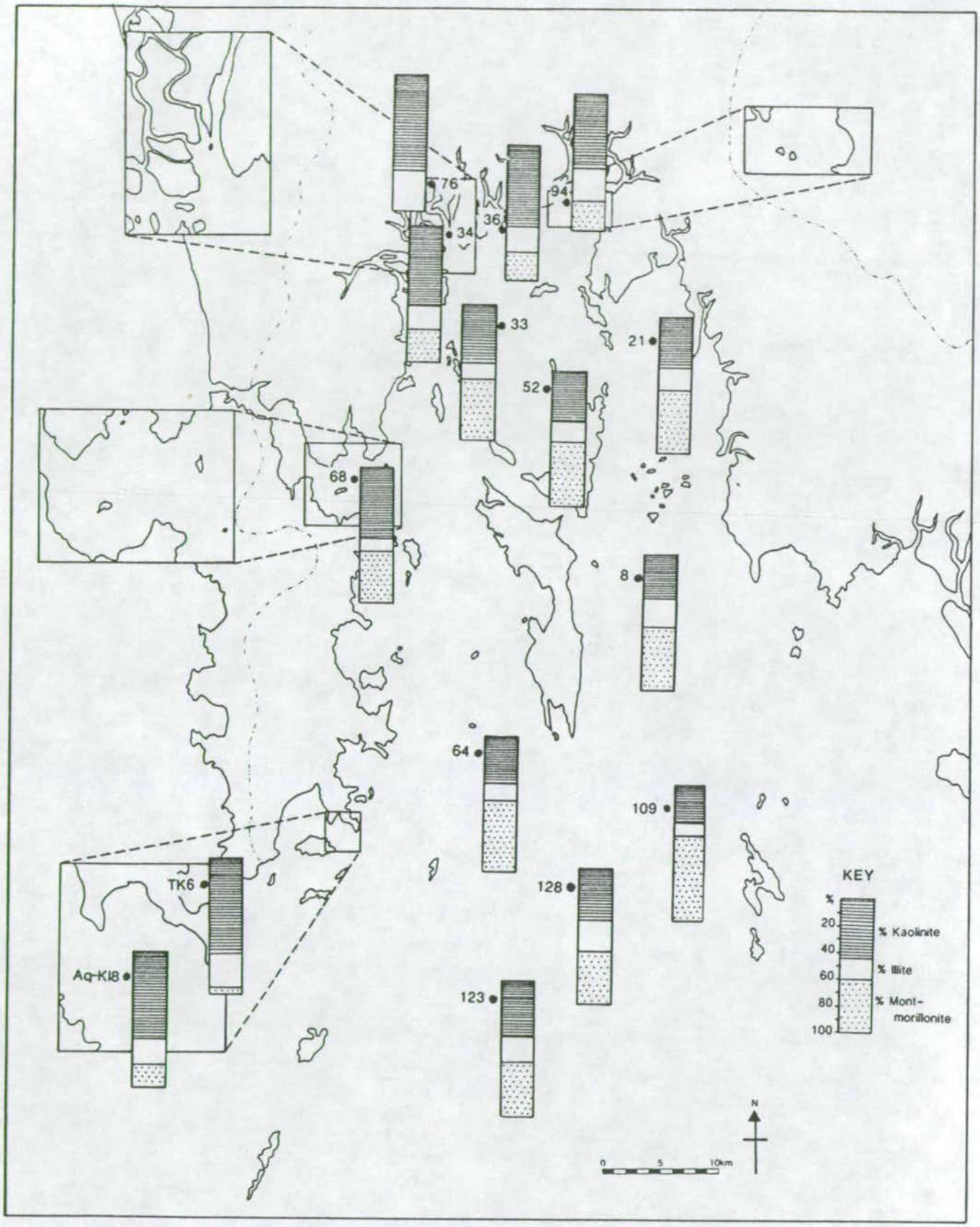

Figure 3.8 Variation in proportion of montmorillonite, illite and kaolinite as percentages of the clay fraction (< 4 μm) of selected surface samples (numbered)

recorded an increase in montmorillonite from estuary to open gulf in the Gulf of Paria. Cook and Mayo (1978), working in Broad Sound, Australia, recorded an increase in montmorillonite from the supratidal flat environment into the shallow marine environment with a corresponding decrease in kaolinite and a slight decrease in illite . Their explanation for this was two-fold. Firstly, the slow settling rate of montmorillonite increases its proportion of the total clay fraction further away from source, compared to illite and kaolinite. Secondly, montmorillonite converts to illite in the high saline environment of the supratidal flats and some of this material is eroded into the mangrove inlets thus effectively reducing the montmorillonite proportion in the supratidal flats and increasing it seawards.

Laboratory experiments by Whitehouse et al (1960) illustrated the varying settling velocities of montmorillonite compared to illite and kaolinite. At salinities of 0-3 ppt the clays flocculated - at this point the settling rate of kaolinite was 12×10^{-3} cm/second, illite, 15×10^{-3} cm/second and montmorillonite 0 cm/second. At 18 ppt, illite and kaolinite settling velocities remained the same and montmorillonite reached 1×10^{-3} cm/second. Montmorillonite has a slower settling velocity because of its finer overall grain size and its smaller floccule size compared to illite and kaolinite. This variation in settling rate is the proposed explanation for the variation in montmorillonite concentration away from land sources in Phangnga Bay. The greenish colour of the sediments especially in the south of the Bay may be due to the presence of ferric silicate which according to Keller (1953) is green in colour. Ferric silicate results from the substitution of Fe^{3+} in Al^{3+} sites in illite and montmorillonite.

The world wide distribution of clays in marine sediments has been studied by Rateev et al (1969). For the area of the Indian Ocean abutting the Peninsula west coast of Thailand, they record the following average clay contents (as percentage of the total clay fraction):

Kaolinite 20-40%; Montmorillonite 10-20%; Chlorite <10%; Illite 40-60%

This differs from the values recorded in Phangnga Bay which are:

Kaolinite 30-70%; Montmorillonite 0-64%; Chlorite 0%; Illite 10-30%

Rateev et al (1969) explain the world wide variation in clay mineralogy in terms of the nature of the catchment basins of the surrounding continents (including climate, type of weathering, geology etc), the sedimentary conditions in the oceans (current velocities, directions and water depth) and the influence of vulcanism. High kaolinite values occur in 0-30°S belt and values decrease symmetrically about this belt towards the poles. Montmorillonite shows a similar "equatorial type" trend. Chlorite and illite however show a "bipolar type" trend. They tend to be concentrated in mid to high latitudinal areas. Therefore, all clay minerals show a distinct latitudinal zonal character which is controlled dominantly by climatic zones in the catchment areas. Tropical humid climates allow intense chemical weathering of rocks and both montmorillonite and kaolinite are typical chemical weathering alteration products in such environments. Kaolinite is generally formed from the weathering of feldspars and other silicates characteristic of acidic igneous rocks. Montmorillonite tends to be a weathering product of basic igneous rocks but is also produced by the hydrothermal alteration of metalliferous veins (Deer, Howie and Zussman, 1966). In temperate and cold climates where physical weathering is dominant over chemical weathering, chloritic and illitic clays tend to be produced. Chlorite is unstable and would be rapidly destroyed in a warm humid environment. Illite tends to be produced from the mechanical grinding of primary minerals rather than as an alteration product.

Deviations to the general pattern of clay mineral distributions as described by Rateev et al (1969), do occur and Phangnga Bay is an example of this. Higher kaolinite and montmorillonite values and lower illite values compared to the average for the latitude are explained by the distinctive local catchment area geology of Phangnga Bay (which is described in Chapter 1) and also the Bays' close proximity to the land sources of the clays. Most of Rateev et al's samples are from open ocean environments as opposed to coastal settings. The intense chemical weathering of the granites will produce large quantities of kaolinite. The metalliferous deposits are likely to produce montmorillonite as a weathering product. The surrounding sedimentary rocks are dominantly limestones and sandstones and are unlikely to produce large quantities of clay material. Because of the profusion of metalliferous granitic material in the catchment area and the humid tropical climate, there are high rates of kaolinite and montmorillonite production. These clays will swamp any illite produced and thus effectively reduce its proportion of the total clay fraction compared to the latitudinal norm. In the more open oceanic

environments, a mixing of clays from a wider variety of sources will produce the typical latitudinal clay assemblages.

3.3 BIOGENIC COMPONENT

3.3.1 Petrology

The biogenic component of the surface sediments of Phangnga Bay is dominantly carbonate. Siliceous diatoms may provide an exception to this generality, however, these form only a small part of the sediment as a whole. Plates 5-10 illustrate the typical biogenic component of various sediments taken from 1-5mm sieved grab samples and > 5mm sieved dredge samples. The biogenic fragments identified in the surface samples include; bivalves, gastropods, scaphopods (*Dentalium sp.*), pteropods, echinoderms, ophiurids, barnacles, crabs, foraminifera, coral, bryozoa and calcareous algae. Discussion of the distribution of these individual biogenic components follows in Chapter 7. Plates 9, 11 and 12 illustrate the calcareous algal material found in sediments from site 114. Some of the apparently algal fragments illustrated in Plate 9 are in fact quartz grains covered in an algal coating (Plate 11). Shell material from this area to the north and east of Ko Racha Yai is abraded, bored and encrusted (see also Plate 9 & 10). No limestone fragments are evident in any of the surface samples and therefore it is assumed that all the carbonate material in the sediments is biogenic.

As detailed in Chapter 2 the carbonate material forms the coarsest fraction in most of the sediments. Very little of the macrofauna material collected in the grabs and dredges was living, but the occurrence of this coarse carbonate fraction suggests that most of the material may be close to its 'life position'. However, it cannot be ruled out that due to the hydraulic equivalence of lighter, flatter carbonate fragments against heavier, rounded terrigenous grains, a measure of sorting has produced this mixture of compositionally controlled grain size distribution. Details of the distribution of $CaCO_3$ content of the surface sediments are discussed in Chapter 4 along with geochemical components of the sediments.

>5 mm

1-5 mm

Plate 5

1 cm

12G

polychaete tubes
echiniod spines
and plates,
bivalve fragments

Plate 6

1 cm

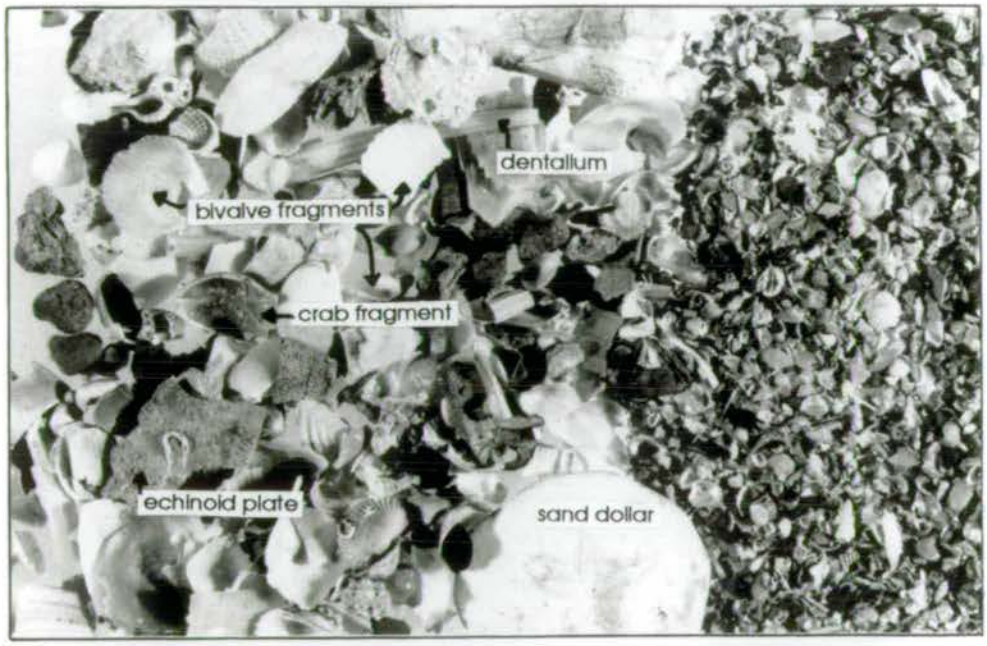

7G

sand dollar,
dentalium, crab,
echinoid and
bivalve fragments

Plate 7

1 cm

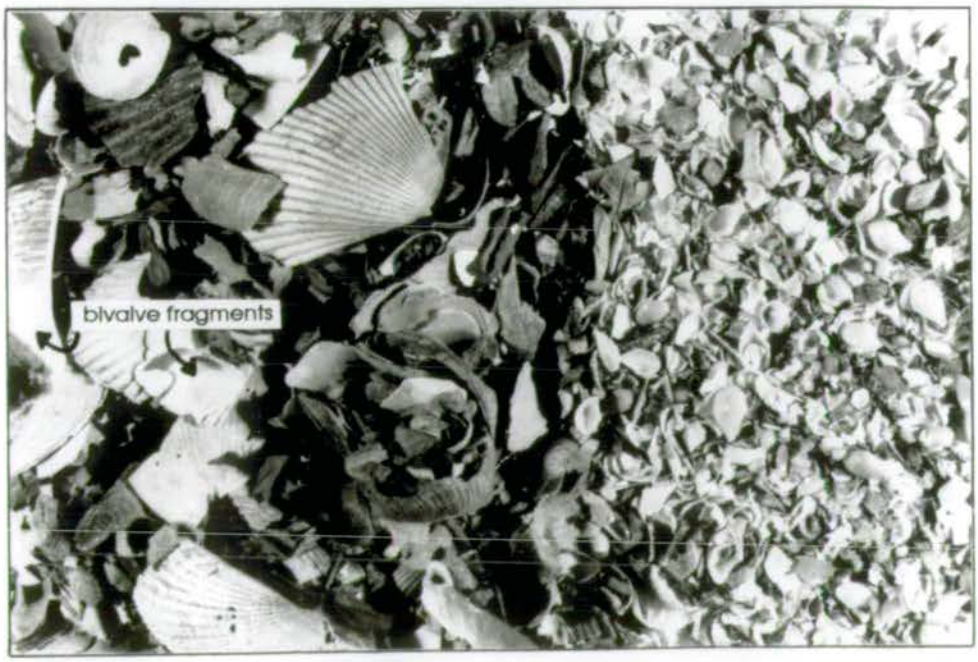

56G

crab, gastropod,
dentalium, bryozoa
and bivalve
fragments

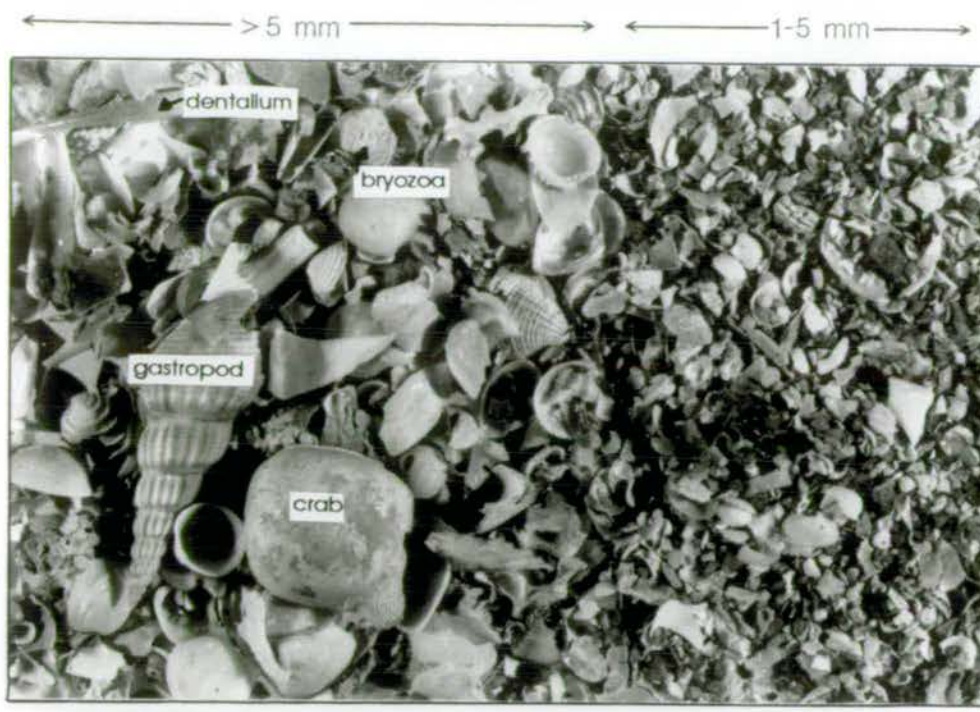

Plate 8

1 cm

128G

crab, gastropod, dentalium, bivalve, bryozoa fragments

Plate 9

1 cm

114G

calcareous algae, solitary corals, bryozoa fragments

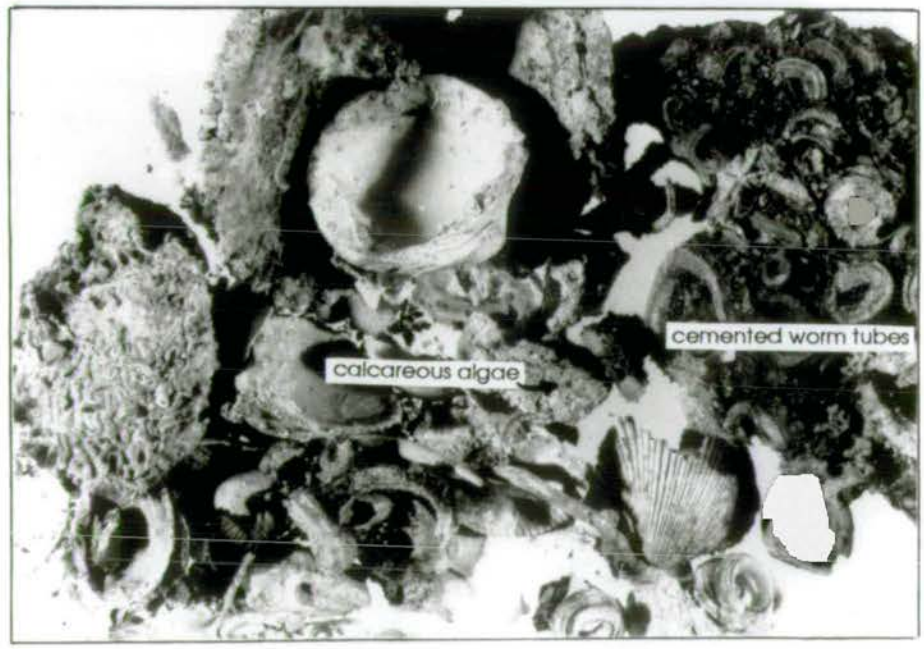

Plate 10

1 cm

116G

cemented worm tubes, calcareous algae, encrusted and bored bivalves

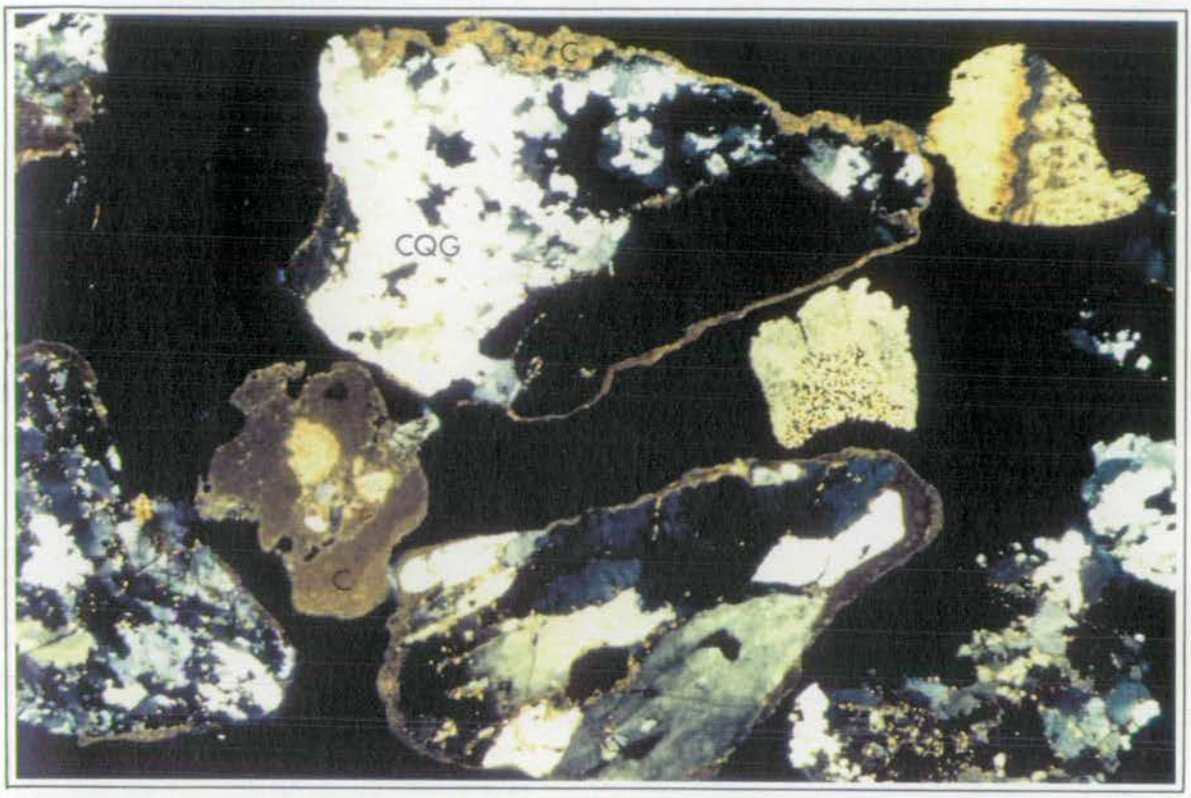

Plate 11 114G > 5mm fraction

CQG = composite quartz grain

C = calcareous algal coatings

Plate 12 114G > 5mm fraction

CA = calcareous algae

B = bivalve fragments

3.3.2. Mineralogy

3.3.2.1. Carbonate Minerals

The carbonate mineralogy of Phangnga Bay surface sediments has been determined by XRD. The carbonate material is essentially a 3 component system of aragonite, low magnesium calcite (LMC) and high magnesium calcite (HMC). No dolomitic or sideritic material was detected on XRD traces of the samples run for qualitative or quantitative analyses. Aragonite is detected by its characteristic (111) and (021) reflections at 26.24° (3.39Å) and 27.25° (3.27Å) on either side of the main quartz (101) peak. The calcite peak may vary according to whether Mg^{2+} ions are present in the calcite structure. LMC is classified as 0-4 mole % $MgCO_3$ whereas HMC contains >4 mole % $MgCO_3$ but there is commonly a gap in the solid solution series at approximately 10 mole % hence HMC has generally 10-19 mole % $MgCO_3$ (Hardy and Tucker, 1988). The effect of Mg^{2+} ions in the calcite structure is a decrease in the (104) lattice spacing (Goldsmith and Graf, 1958). Goldsmith et al (1961) produced a graph of mole % $MgCO_3$ against (104) lattice spacing and this has provided the basis for determining the Mg content of both calcites from the twin calcite peaks. To ensure accurate measurement of the calcite peaks and to account for machine shift, the quartz (101) peak was used as an internal standard.

Of the samples analysed quantitatively the LMC (if present) varies between 0.5 and 3.4 mole % $MgCO_3$ and the HMC (if present) varies between 13.3 and 18.7 mole % $MgCO_3$.

Individual biogenic components have also been analysed for their carbonate composition to aid in interpretation of the whole sediment carbonate composition.

3.3.2.2. Semi-Quantitative Aspects

Because carbonate mineralogy is controlled by the organism secreting the carbonate it would be expected that variations in carbonate mineralogy throughout Phangnga Bay are reflections of variations in biotic distributions (assuming no diagenetic changes). To examine this, quantitative methods were employed to calculate aragonite, LMC and HMC proportions from XRD peak areas. All samples were ground for 1 minute to a size able to pass through a 62μm sieve mesh. Because the (111) aragonite peak may form a shoulder to the quartz (101) peak and because the LMC and HMC peaks are not usually separated at the background level, the areas of the free half of these peaks were calculated and

their values doubled to obtain the whole peak area (Fig. 3.9). The background level is taken as just above the minor peak heights between major peaks and this is used as a base level to calculate peak area. In order to determine the amounts of each mineral present the aragonite ratio was calculated from the equation in Figure 3.9. As the XRD response of similar amounts of aragonite and calcite is different, Milliman (1974) constructed a graph of aragonite ratio (calculated from peak areas) versus percent aragonite of the total carbonate fraction and this is used to obtain the aragonite percentage. Hence, once the percent aragonite is known the percent HMC and LMC can be calculated from their relative peak heights.

Typical XRD traces from 4 different samples illustrating varying proportions of aragonite, LMC and HMC are illustrated in Figure 3.10. This technique was applied to 33 samples and the areal distribution of these results is illustrated in Figure 3.11. The ratios of HMC to LMC and of aragonite to total calcite are also illustrated on these diagrams. The main points to pick out from Figure 3.11 are:

1. aragonite is the dominant carbonate mineral constituting between 55 to 70% of most samples. There are no obvious trends in the variation of aragonite ratios although there may be an ill-defined decrease in the aragonite proportion seawards.

2. LMC constitutes on average, 10-30% of most samples however at sites 34 and 97, LMC forms approximately 50% of the carbonate fraction and HMC is not present.

3. HMC forms 0-30% of the carbonate fraction with a general trend of increasing HMC:LMC ratios southwards into the open marine environment.

The carbonate compositions of 10 biogenic components are illustrated in Table 3.3. Clearly, benthic foraminifera, echinoderm fragments, calcareous red algae and crab fragments have a HMC composition. Barnacles and Oysters have an unusual composition in that the Mg content lies between that of the usual definitions of LMC and HMC. Scaphopods (*Dentalium sp.*), gastropods (*Murex trapa*) and bivalves (*Paphia gallus*) all have aragonitic exo-skeletons.

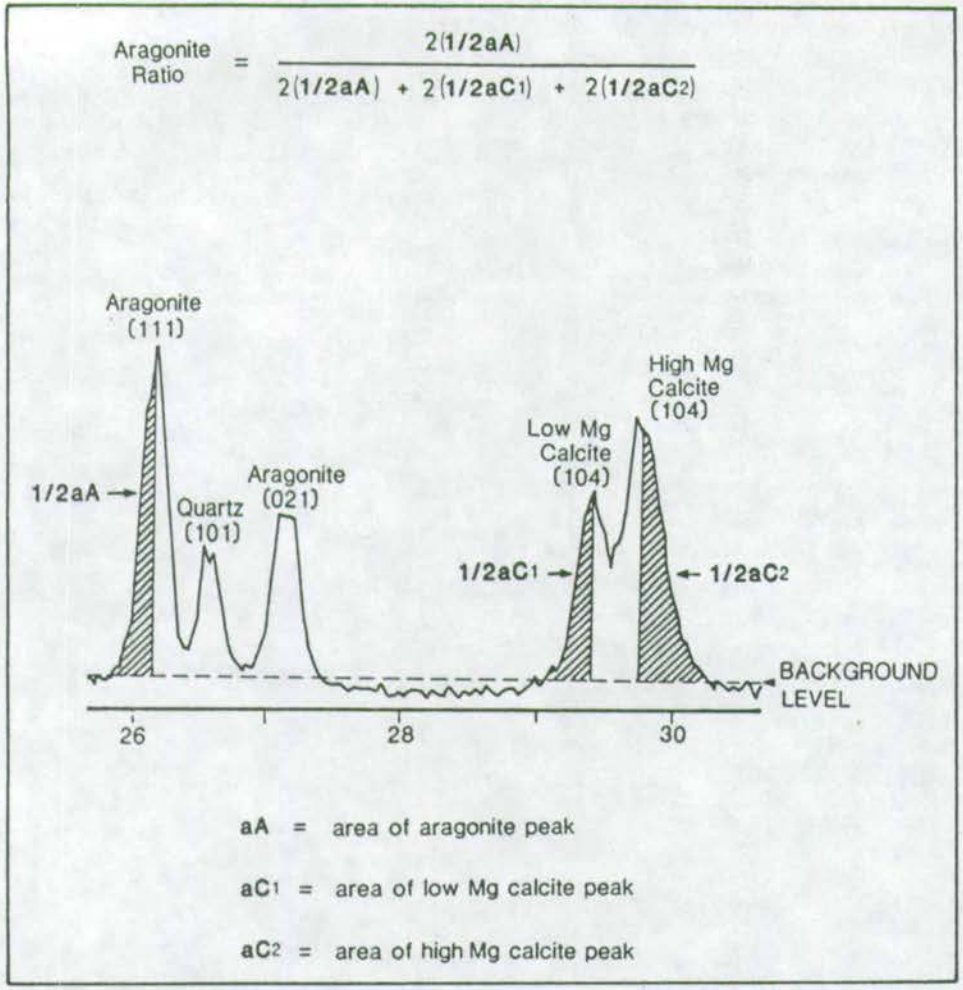

Figure 3.9 Method of calculation of proportions of aragonite, low magnesium calcite (LMC) and high magnesium calcite (HMC) from XRD trace peak areas (see text for explanation).

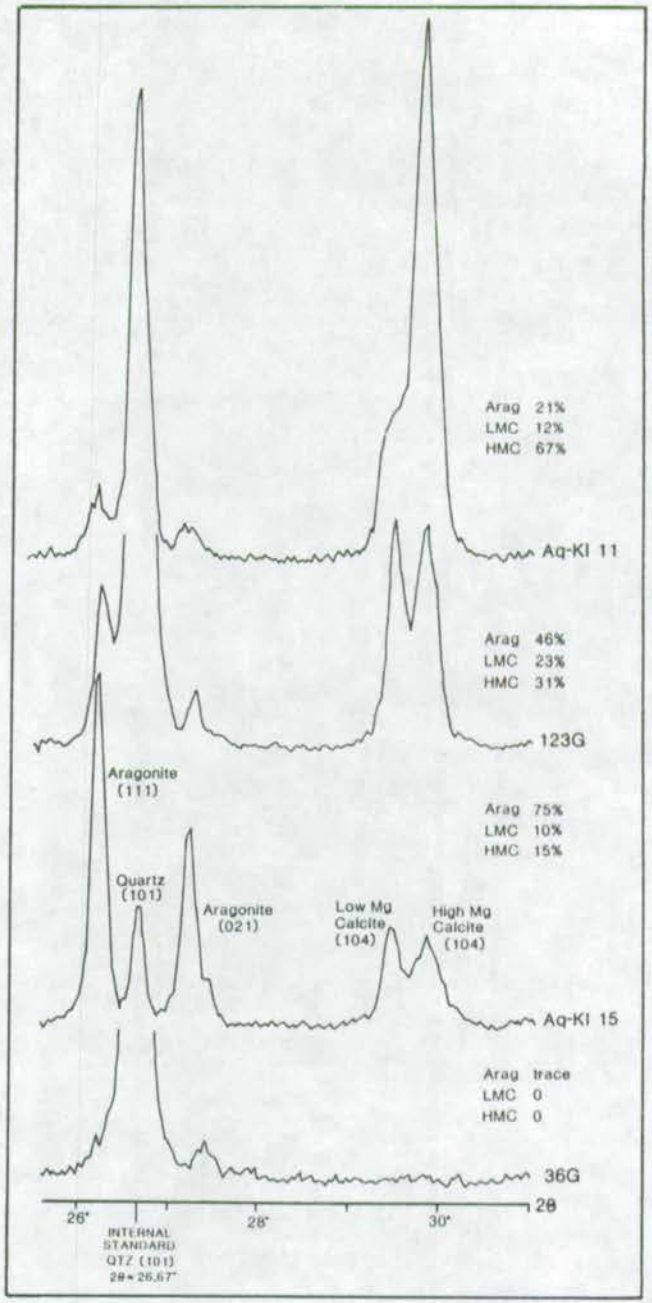

Figure 3.10 XRD traces from 4 samples exhibiting varying proportions or aragonite, LMC and HMC.

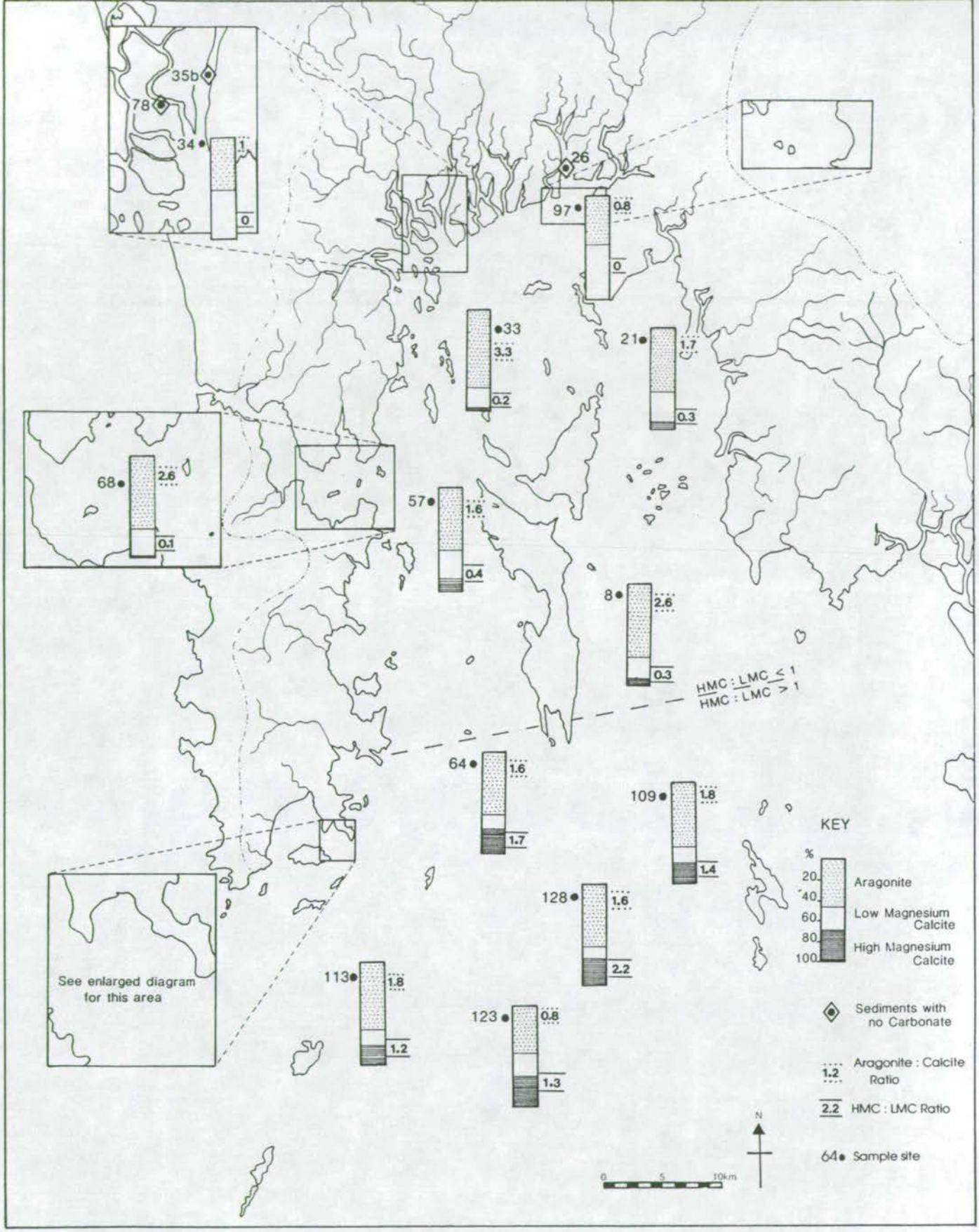

Figure 3.11 Variation in proportions of aragonite, LMC and HMC as percentages of the carbonate fraction of selected surface samples.

BIOGENIC COMPONENT	CALCITE	ARAGONITE
Paphia gallus (Bivalve)		•
Murex trapa (Gastropod)		•
Dentalium sp. (Scaphopod)		•
Coral fragment		•
Benthic Foraminifera	• 18	
Echinoderm fragments	• 16	
Calcareous Red Algae	• 21	
Crab fragment	Chitinous	
Barnacle	• 7	
Ostrea sp.	• 7	

Numbers in Calcite column refer to the mole % $MgCO_3$ in structure. (calculated from position of main calcite peak on XRD trace)

Table 3.3 Carbonate composition of 10 biogenic components calculated from XRD peak areas.

3.3.3. Discussion

Although detailed discussions on macrofauna distributions follow later (Chapter 7) it is pertinent here to consider some of the results from that part of the study in the discussion of carbonate mineralogy variations.

Bivalves form the highest proportion of carbonate material and have the widest distribution in the sediments of the Bay. Their shells can be mineralogically composed of either aragonite or calcite but aragonitic shells are most common (as illustrated in the genera analysed here - Table 3.3), thus explaining the high aragonite proportion throughout the Bay. Only in the northern mangrove channel area does the aragonite proportion vary significantly where it drops to approximately 50%. In both these cases (sites 34 and 97) the actual carbonate content of the sediments are low and XRD peaks are barely distinguishable. Therefore, error in peak area calculation is likely and these values may not be a true reflection of the carbonate mineralogy. Bivalve and gastropod species assemblages do not show any particularly different characteristics in these areas compared to the rest of the bay, apart from low abundance. However, the calcitic structures of barnacles and oysters are prevalent and in some sites abundant only in these northern areas (which includes samples 21, 26 and 33 - see Chapter 7). Therefore, their presence effectively dilutes the proportion of aragonite. Other organisms which secrete an aragonite skeleton include scaphopods, pteropods, gastropods and coral. Fragments of these organisms are found in small quantities in the open marine sites (see Chapter 7) and are rare in the northern sites.

The effect of coral on carbonate mineralogy is discussed later but in general a slight increase in aragonite may be expected southwards corresponding with the increase in these fragments. However, other truly marine biogenic fragments occur in these southern sites and their non-aragonitic composition may explain the increase in the HMC proportion southwards thus over-riding a possible proportional increase in aragonite. The most predominant organisms with an entirely HMC skeleton are echinoderms, calcareous red algae, benthic foraminiferans and bryozoa. In general, fragments of echinoderm spines and plates increase in quantity southwards as do foraminifera and bryozoa fragments. LMC seems to show no great variability in proportion which is probably because some of the bivalve, foraminifera and bryozoa species present in the assemblages are likely to have a LMC structure and this keeps the LMC proportion level with the aragonite proportion.

Figure 3.12a illustrates the contribution of reefal carbonate to nearby shallow marine sediments in the area between south east Phuket island and Ko Lon (referred to as "Aq-Kl" transect) and in Tang Khen Bay ("TK" transect). The 2 transects cut across beach, reef top, reef front and shallow marine environments and significant variations in the proportions of aragonite, LMC and HMC are evident. Figure 3.12b schematically illustrates the scale of the fringing reefs in this area.

The reef top sediments, (Aq-Kl 16, Aq-Kl "r" and TK 1) which were collected from between clumps of coral, show the high proportion of aragonite (70-80%) (see Plates 13 and 14) . This aragonite is contributed by coral fragments and also from non-framework builder organisms such as bivalves and calcareous green algae. LMC and HMC are contributed by calcareous red algae indigenous to coral reefs and also probably molluscs. The beach sands (TK 2,3,4 and Aq-Kl"b") show similar mineralogical compositions to the reef sediment.

The reef front sediments (Aq-Kl 2, 15 and TK 5) start to show a decrease in aragonite and increase in HMC. Further out from the reefs (TK 6, Aq-Kl 3, 5, 6, 7, 8, 9, 10, 11, 13) the coralline aragonite influence decreases rapidly in proportion to the HMC. LMC shows no significant change. The increase in HMC comes from benthic foraminifera which are particularly predominant in the Aq-Kl transect compared to other sampled areas around Phangnga Bay. Therefore, the aragonitic reef debris does not have a significant impact on the carbonate mineralogy once the shallow marine environment is reached due to the abundance of other carbonate secreting organisms.

Comparing these results with other similar studies of carbonate mineralogy in marine environments, it is clear that Phangnga Bay shows some differences to other areas. Cook and Mayo (1978) reported aragonite values dominantly less than 50% in Broad Sound (Australia) with an overall trend of decreasing aragonite seawards. There is also a seaward increase in the relative abundance of LMC compared to HMC. They suggested that diagenetic sub-aerial weathering changes have affected the shelf sediments during low sea-level stands hence altering HMC and aragonite to LMC. Siesser (1971) working on South African dune, beach coastal bay, continental shelf and upper slope sediments also suggested that diagenetic alteration of HMC to LMC has occurred on continental shelf sediments as a result of prolonged sub-aerial exposure of the continental shelf during Pleistocene sea-level fluctuations.

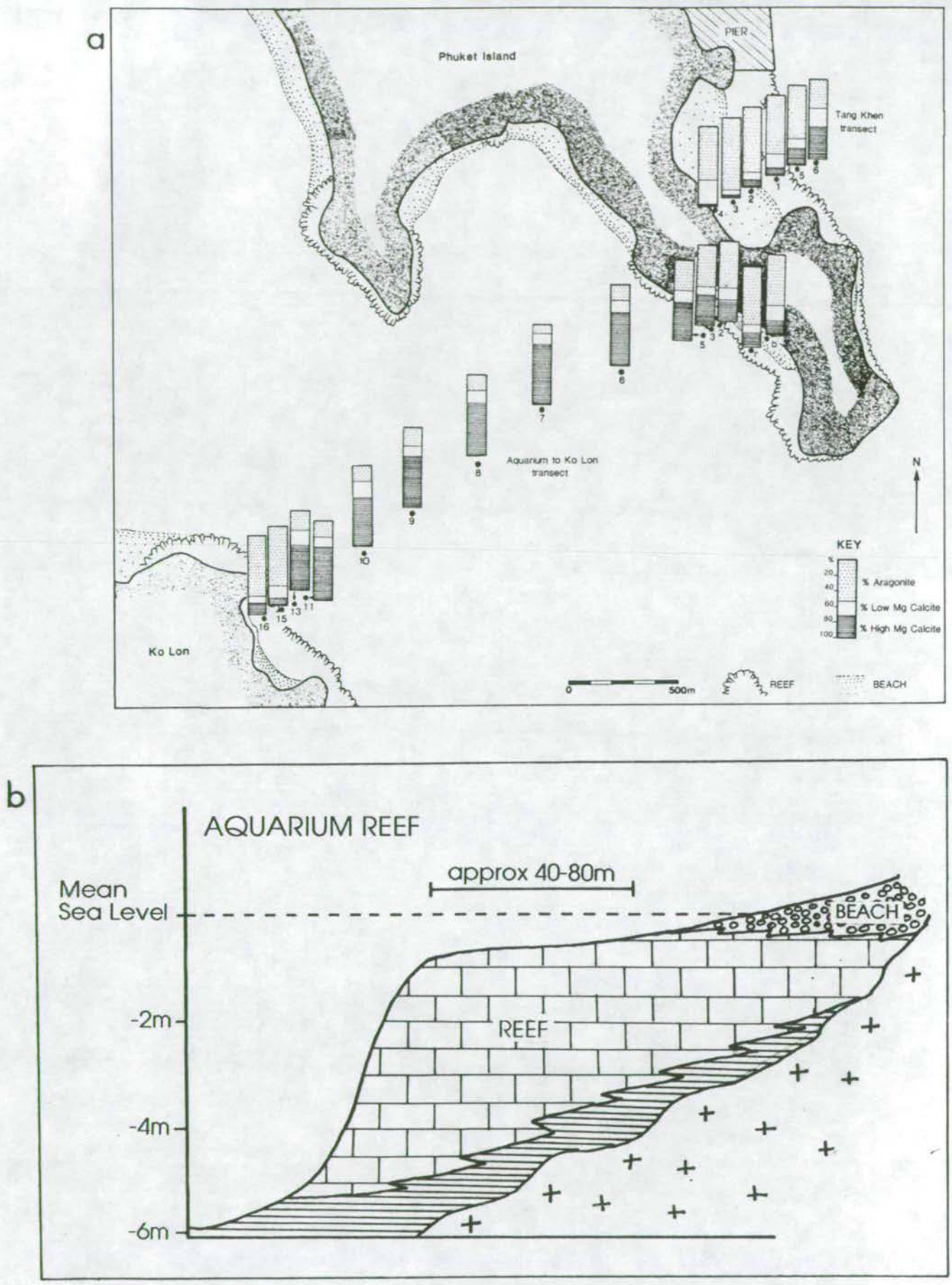

Figure 3.12 a. Variation in proportion of aragonite, LMC and HMC in the Tang Khen and Aquarium/Ko Lon areas of south east Ko Phuket.
b. Schematic diagram illustrating the scale of fringing reefs in the area.

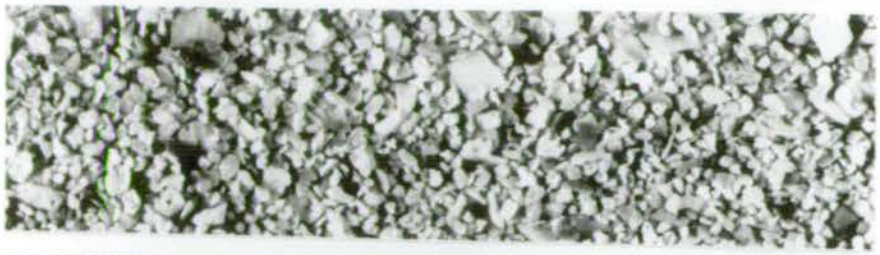

Aquarium
beach

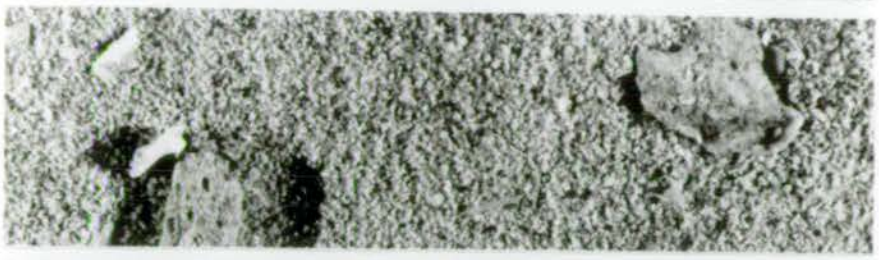

Aquarium
reef top

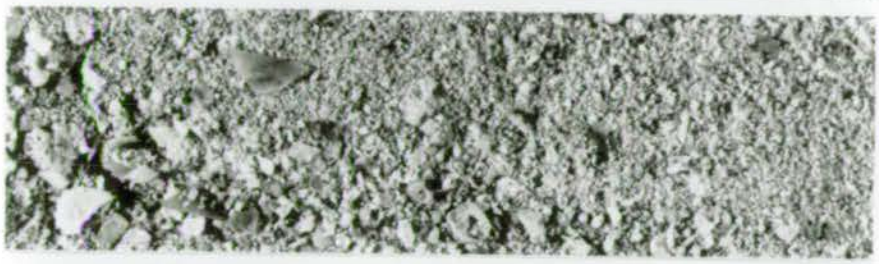

Aq-KL 1
reef front
(proximal)

Aq-KL 5
reef front
(distal)

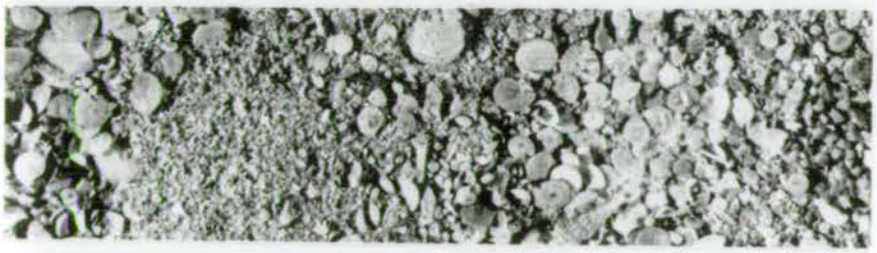

Aq-KL 8
shallow marine
(6 metres)

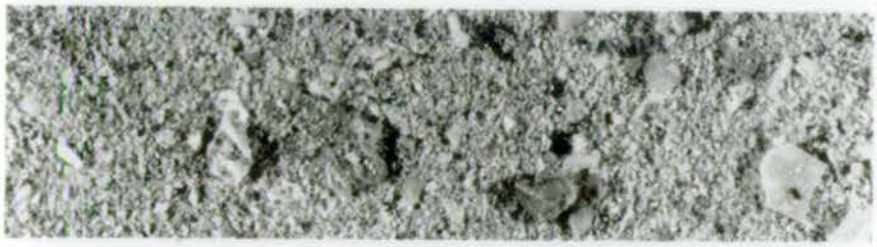

Aq-KL 15
reef front
(proximal)

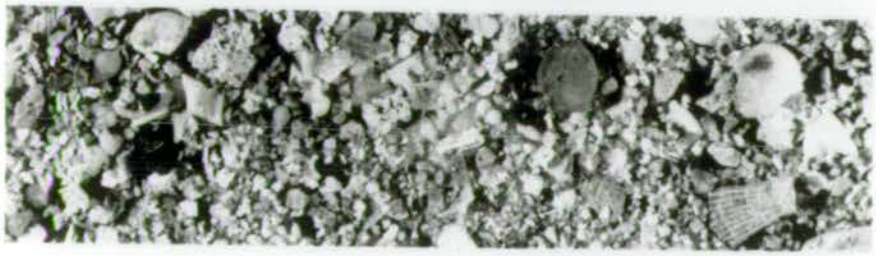

Aq-KL 16
reef top

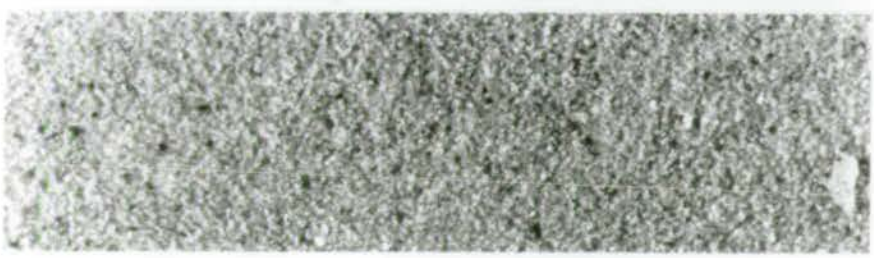

Aq-KL 17
beach

1 cm

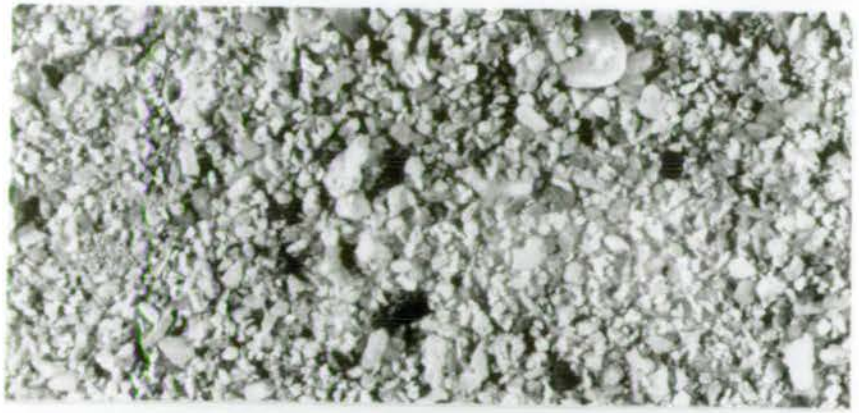

TK 4
beach strandline

TK 3
between
sand waves

TK 2
top of
sand wave

TK 5
reef front
(proximal)

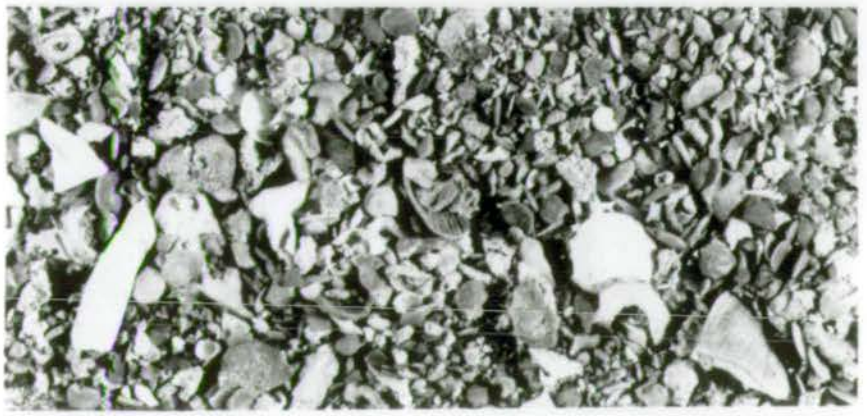

TK 6
reef front
1(distal)

1 cm

This he uses to explain the higher LMC and lower aragonite values in marine sediments compared to beach sands which although sub-aerially exposed are still not totally removed from marine influence hence diagenetic changes have not yet taken place. Both these studies therefore report opposite trends in carbonate mineralogy variation to Phangnga Bay where relative aragonite values stay constant, possibly decreasing slightly seaward and HMC increases seaward. This would suggest that despite the southern terrigenous sediments being of proposed relict origin, the carbonate mineralogy does not indicate any significant alteration of unstable calcitic forms to the stable LMC during sub-aerial exposure which suggests that the carbonate material is of recent origin. Pilkey (1964), studying carbonate mineralogy of sediments of the United States South Atlantic shelf reports a similar carbonate petrological assemblage as Phangnga Bay (ie, molluscs are the dominant contributor with bivalves more common than gastropods, echinoderms and bryozoan fragments are also reasonably common and there are a wide variety of 'minor contributors'). Although Pilkeys' study covers a much larger area than Phangnga Bay, extending out to the continental shelf slope, and trends of carbonate mineralogy are not evident in comparison to water depth or bottom temperature, he does conclude that selective solution and recrystallization of LMC and aragonite have not been important processes as there is no increasing trend of LMC with depth (ie, seawards). Any variations in carbonate mineralogy he puts down to faunal changes.

In the case of Phangnga Bay the evidence for the southern seaward non-carbonate sediments being relict is strong and so some of the carbonate material may also be relict. However, if this is the case then this relict carbonate material has been diluted by recent skeletal material which has not been sub-aerially exposed and is composed of a significant proportion of fauna which secrete a HMC skeleton.

3.4 CONCLUSIONS

Terrigenous and biogenic minerals are the 2 main components of the surface sediments of Phangnga Bay. The mineralogy of the terrigenous fraction reflects the intense chemical weathering of the catchment area rocks with most minerals altered to clays and only resistant minerals surviving. Only carbonate biogenic minerals have been identified here (although there is likely to be a small proportion

of biogenic silica) and the proportions of the carbonate minerals are influenced by the prevalence of various carbonate-secreting organisms in the sediments.

Quartz is the dominant terrigenous mineral with feldspar, mica, heavy minerals and lithic fragments forming < 5% of the terrigenous fraction. Comparing the mineralogy and texture of the coarse terrigenous fraction of sediments from mangrove channels in the north of the Bay with sediments from the southern area reveals that the latter are mineralogically and texturally more mature with less feldspar and mica, and with quartz grains showing greater roundness, sphericity and a lower proportion of composite grains. This suggests a longer transport history for these southern sediments which is consistent with these sands being transported the length of the Bay during low sea-level stands in alluvial environments and deposited in high energy coastal areas. Some drainage basin geology control on Bay mineralogy distributions is evident by the restriction of lepidolite in Bay sediments to the mouths of channels draining from lepidolite pegmatite areas. Although there is no knowledge of lepidolite pegmatite veins in the Ko Racha Yai area, their presence is suggested by lepidolite mica in surrounding sediments.

A heavy mineral assemblage in the south of the Bay is mature with unstable minerals removed through chemical alteration and mechanical abrasion. Resistant minerals are abundant. Hematite and goethite coatings on quartz grains are thought to reflect areas of highly oxidised surface sediments in high energy areas in the south and mangrove channels in the north.

The clay minerals kaolinite, illite and montmorillonite are present in the Bay sediments. The high proportion of kaolinite and lack of chlorite reflects the intense chemical weathering of the catchment area rocks. Higher kaolinite proportions in the north are thought to be a result of the faster settling velocity of kaolinite in comparison with montmorillonite which is present in higher proportions in the south of the area.

The biogenic component of the sediments affects the carbonate mineralogy. Aragonite is present in greater proportions than HMC and LMC which is a reflection of the high proportion of bivalves in the sediments. LMC seems to stay at a constant level whilst HMC increases in proportion southwards which is thought to be a result of increasing proportions of echinoderm fragments, calcareous red algae and benthic foraminiferans which all secrete HMC skeletons. The fact that HMC is present in the

southern sediments and has not altered to the more stable form of LMC indicates that although the terrigenous material is relict the same cannot be said for all of the carbonate material. It is likely that any relict carbonate material present has been diluted by more recently deposited carbonate material.

CHAPTER 4

THE GEOCHEMISTRY OF THE SURFACE SEDIMENTS

CHAPTER 4 - GEOCHEMISTRY OF SURFACE SEDIMENTS

4.1 INTRODUCTION

The objective of this chapter is to describe the geochemistry of the surface sediments of Phangnga Bay by way of elemental distributions, the inter-relationships between elements, grain size and mineralogy and the main factors controlling element variance.

4.2 ANALYTICAL TECHNIQUES

All elemental analyses were carried out by X-ray fluorescence spectrometry the details of which are described in Appendix B. $CaCO_3$ was measured by the weight-loss method involving digestion with dilute HCl and organic carbon (C_{org}) was measured using a LECO Carbon Analyser - both of these methods are also detailed in Appendix B. Analyses of 29 elements were carried out. Three of these, Na, Cu[1] and Sc, were present in quantities less than the analytical precision of the instrument and method (ie, negative results were as common and as large as positive readings) and so discussion of these elements is not taken any further. Results for the major element oxides (Fe_2O_3, MnO, TiO_2, CaO, K_2O, Al_2O_5, SiO_2, and MgO) were recalculated to elemental percentages (ie, non-oxide) except for P_2O_5 which tends to be recorded in the literature in oxide form (eg Cook and Mayo, 1980). A correction for salt content was also made the method of which is detailed in Appendix B. Elements are recorded as either weight percent or ppm.

4.3 ELEMENT PARTITIONING

The processes of weathering and sedimentation tend to break down the complicated assemblages of elements in igneous and metamorphic rocks and regroup them into 3 generally simpler systems namely Si in quartz (sandstone), Al and Si in clays (shale) and Ca in carbonates. These 3 main mineralogical and

FOOTNOTE 1 : Garson et al (1975) recorded average Cu concentrations in drainage samples from the drainage basin of Phangnga Bay as < 10 ppm, therefore sediments of Phangnga Bay are expected to have values equal or lower than this. Such values are below the analytical precision of the XRF method.

geochemical groups are present in Phangnga Bay either as the end member or as a mix of the three. If Si, Al and Ca are the major elemental indices of these groups, how do all the other elements partition themselves between these components and to what degree do each of the 3 components control the concentrations of the other elements?

Much work has been done on the physiochemical processes that affect the chemical compositions of sediments and the element partitioning effects that result from such processes (general reviews are contained in Calvert, 1976; Chester and Aston, 1976 and Curtis, 1977).

In order to determine which elements in Phangnga Bay sediments are associated with which of the geochemical/mineralogical components, inter-element correlation coefficients and factor analysis were performed on the data set.

4.3.1 Correlation Coefficients

Co-varying groups of elements may be distinguished by the use of correlation coefficients (see Appendix C). Correlation coefficients for each element are plotted in a correlation matrix (Table 4.1). It can be seen that the majority of elements studied correlate with Al, one (Sr) correlates with Ca and 2 (Zr and Sn) show no correlation with either. Many of the correlations between elements other than Al or Ca are second order correlations in which the two elements are not considered to be directly related but are related through a third element (ie, Al or Ca) with which the two elements are significantly correlated.

4.3.2 Factor Analysis

In order to try and sort out whether correlations are first or second order, principal component analysis (a type of factor analysis) was used (Appendix C).

Factor analysis is a statistical data reduction technique used to objectively examine relationships among numerous geochemical variables and to determine groupings of samples based on their geochemistry. Various types of factor analysis have been successfully applied to geochemical data sets (Spencer et al, 1968; Reinson, 1975; Loring, 1978; Gardner et al 1990; Shimmield and Mowbray, 1991 and others). Eigenvalues represent the proportion of total variance explained by that factor (or

ALL PHANGNGA BAY SEDIMENTS

	Fe	Mn	Ti	Ca	K2	P205	Al	Si	Mg	Nb	Zr	Y	Sr	Rb	Th	Pb	Zn	Ni	Cr	Ce	Nd	La	V	Ba	Sn	CaCO3	Corg	Mean	S.d.	Skew	Gravel	Sand	Silt
Mn	0.755*																																
Ti	0.918*	0.588																															
Ca	-0.681*	-0.415	-0.694*																														
K2	0.744*	0.578	0.796*	-0.622*																													
P205	0.707*	0.565	0.725*	-0.326	0.472																												
Al	0.894*	0.677*	0.93*	-0.617*	0.898*	0.627*																											
Si	0.322	0.145	0.317	-0.888*	0.273	0.021	0.203																										
Mg	0.377	0.304	0.327	0.022	0.107	0.601	0.241	-0.236																									
Nb	0.836*	0.672*	0.873*	-0.661*	0.912*	0.537	0.965*	0.288	0.148																								
Zr	0.605	0.234	0.728*	-0.579	0.445	0.518	0.551	0.371	0.265	0.552																							
Y	0.822*	0.697*	0.841*	-0.599	0.882*	0.581	0.949*	0.215	0.23	0.971*	0.528																						
Sr	-0.618*	-0.519	-0.576	0.874*	-0.482	-0.366	-0.498	-0.81*	-0.103	-0.555	-0.422	-0.535																					
Rb	0.65*	0.601	0.675*	-0.544	0.941*	0.364	0.842*	0.223	0.019	0.911*	0.35	0.875*	-0.437																				
Th	0.801*	0.655*	0.827*	-0.537	0.865*	0.544	0.959*	0.138	0.191	0.97*	0.476	0.978*	-0.449	0.868*																			
Pb	0.775*	0.672*	0.782*	-0.544	0.916*	0.482	0.943*	0.161	0.123	0.967*	0.414	0.964*	-0.438	0.934*	0.975*																		
Zn	0.9*	0.672*	0.907*	-0.645*	0.798*	0.625*	0.931*	0.269	0.244	0.918*	0.595	0.887*	-0.557	0.779*	0.892*	0.864*																	
Ni	0.901*	0.638*	0.91*	-0.589	0.701	0.732*	0.865*	0.218	0.381	0.811*	0.634*	0.8*	-0.519	0.614*	0.791*	0.74*	0.936*																
Cr	0.849*	0.589	0.842*	-0.557	0.593	0.714*	0.765*	0.226	0.399	0.713*	0.618*	0.712*	-0.521	0.508	0.689*	0.632*	0.886*	0.969*															
Ce	0.813*	0.627*	0.825*	-0.474	0.727*	0.635*	0.881*	0.087	0.267	0.855*	0.511	0.869*	-0.427	0.716*	0.886*	0.857*	0.928*	0.895*	0.858*														
Nd	0.787*	0.601	0.809*	-0.531	0.742*	0.581	0.866*	0.163	0.237	0.854*	0.512	0.862*	-0.487	0.733*	0.877*	0.834*	0.914*	0.863*	0.828*	0.966*													
La	0.823*	0.633*	0.831*	-0.559	0.719*	0.626*	0.869*	0.199	0.252	0.857*	0.533	0.863*	-0.537	0.716*	0.865*	0.82*	0.935*	0.905*	0.871*	0.95*	0.934*												
V	0.871*	0.631*	0.878*	-0.58	0.702*	0.652*	0.857*	0.216	0.279	0.82*	0.586	0.811*	-0.517	0.639*	0.807*	0.759*	0.944*	0.963*	0.958*	0.92*	0.889*	0.928*											
Ba	0.754*	0.518	0.815*	-0.61*	0.747*	0.579	0.809*	0.289	0.17	0.799*	0.542	0.776*	-0.536	0.702*	0.776*	0.743*	0.89*	0.872*	0.855*	0.886*	0.897*	0.892*	0.904*										
Sn	0.295	0.365	0.279	-0.186	0.534	0.141	0.462	-0.002	0.078	0.55	0.046	0.553	-0.148	0.623*	0.56	0.597	0.393	0.262	0.161	0.376	0.381	0.386	0.288	0.279									
CaCO3	-0.657*	-0.384	-0.676*	0.992*	-0.617*	-0.313	-0.607	-0.886*	0.051	-0.653*	-0.563	-0.588	0.871*	-0.54	-0.531	-0.543	-0.632*	-0.566	-0.526	-0.458	-0.515	-0.543	-0.555	-0.591	-0.205								
Corg	0.504	0.316	0.627	-0.077	0.437	0.542	0.62	-0.36	0.209	0.492	0.108	0.544	0.008	0.315	0.584	0.522	0.553	0.562	0.566	0.608	0.602	0.563	0.632	0.569	0.173	-0.066							
Mean	0.793*	0.376	0.884*	-0.718*	0.698*	0.56	0.812*	0.417	0.268	0.778*	0.836*	0.738*	-0.505	0.574	0.726*	0.679*	0.799*	0.792*	0.72*	0.698*	0.708*	0.706*	0.734*	0.712*	0.198	-0.707	0.436						
S.d.	0.286	0.381	0.181	0.004	0.011	0.33	0.172	-0.113	0.281	0.147	0.061	0.214	-0.208	0.087	0.196	0.146	0.292	0.287	0.334	0.378	0.336	0.413	0.338	0.281	0.089	0.016	0.202	-0.028					
Skew	-0.337	-0.027	-0.439	0.215	-0.258	-0.227	-0.36	-0.047	-0.214	-0.297	-0.403	-0.257	-0.022	-0.148	-0.291	-0.254	-0.325	-0.362	-0.3	-0.279	-0.239	-0.244	-0.294	-0.254	-0.023	0.189	-0.503	-0.523	0.022				
Gravel	-0.237	0.171	-0.324	0.465	-0.284	-0.065	-0.277	-0.415	-0.073	-0.287	-0.489	-0.221	0.19	-0.212	-0.246	-0.233	-0.254	-0.231	-0.181	-0.174	-0.213	-0.199	-0.167	-0.24	-0.086	0.473	0.047	-0.627*	0.311	0.491			
Sand	-0.756*	-0.62*	-0.844*	0.433	-0.636*	-0.704*	-0.791*	-0.076	-0.323	-0.731*	-0.581	-0.748*	0.433	-0.538	-0.717*	-0.667*	-0.786*	-0.816*	-0.77*	-0.749*	-0.718*	-0.731*	-0.792*	-0.699*	-0.204	0.413	-0.677*	-0.684*	-0.296	0.264	-0.102	.	
Silt	0.831*	0.499	0.93*	-0.603	0.709*	0.698*	0.849*	0.251	0.349	0.798*	0.775*	0.787*	-0.486	0.584	0.764*	0.711*	0.835*	0.859*	0.796*	0.763*	0.752*	0.758*	0.803*	0.75*	0.211	-0.587	0.624*	0.913*	0.14	-0.466	-0.335	-0.9*	
Clay	0.853*	0.545	0.922*	-0.605	0.747*	0.639*	0.893*	0.238	0.271	0.838*	0.659*	0.823*	-0.487	0.635*	0.824*	0.775*	0.881*	0.875*	0.803*	0.824*	0.806*	0.811*	0.851*	0.784*	0.29	-0.594	0.657*	0.867*	0.165	-0.42	-0.309	-0.863*	0.925*
Silt/Clay	0.845*	0.514	0.94*	-0.611*	0.725*	0.695*	0.869*	0.251	0.338	0.816*	0.761*	0.804*	-0.492	0.601	0.785*	0.733*	0.855*	0.872*	0.807*	0.785*	0.772*	0.778*	0.822*	0.766*	0.23	-0.595	0.647*	0.919*	0.147	-0.462	-0.334	-0.901*	0.947*

For geochemical and grain size data: N=157 r=0.609 (95%)

For organic carbon data: N=37 r=0.711 (95%)

Table 4.1 Correlation matrix of elements and grain size parameters for all sediments of the Bay.

principal component) and the factor loadings for each element reflect the effect of the underlying factors controlling the structure of the data. The identity of the factors may be deduced, using geochemical principles, from a consideration of the factor pattern and the distribution of factor loadings.

Results from principal components analysis (PCA) are listed in Table 4.2 and plotted graphically in Figure 4.1. From Table 4.2 it can be seen that 6 factors explain 94.3% of the total variance in the sediment geochemistry and the first 3 factors account for 86.2% of the variance. Principal component 1 (PC1) is statistically dominant accounting for 67.3% of the variance and, from Figure 4.1, it is clearly the biogenic carbonate factor as Ca and Sr show the only positive loadings (Ca and Sr also correlate strongly - this association is discussed in more detail later).

Eigenvalue	17.498	3.119	1.797	1.038	0.637	0.441
Proportion	0.673	0.12	0.069	0.04	0.025	0.017
Cumulative	0.673	0.793	0.862	0.902	0.926	0.943
Variable	PC1	PC2	PC3	PC4	PC5	PC6
Fe	-0.22	0.006	0.154	-0.147	-0.178	0.206
Mn	-0.204	0.013	-0.02	-0.323	-0.271	0.108
Ti	-0.223	-0.009	0.179	-0.016	0.141	0.2
Ca	0.145	-0.43	-0.096	-0.01	0.054	-0.19
K	-0.214	0.054	-0.234	-0.096	0.195	0.103
P205	-0.164	-0.217	0.329	-0.24	0.112	0.031
Al	-0.233	-0.038	-0.036	-0.01	0.048	0.186
Si	-0.006	0.553	0.11	0.031	-0.096	0.103
Mg	-0.025	-0.376	0.257	-0.538	-0.001	0.122
Nb	-0.23	0.052	-0.165	-0.016	0.132	0.017
Zr	-0.114	0.231	0.331	-0.13	0.706	-0.338
Y	-0.23	-0.01	-0.128	-0.016	0.13	0.023
Sr	0.126	-0.41	-0.145	0.17	0.172	-0.183
Rb	-0.197	0.075	-0.351	-0.102	0.175	-0.06
Th	-0.227	-0.053	-0.145	0.021	0.104	0.063
Pb	-0.227	-0.007	-0.202	-0.007	0.074	0.059
Zn	-0.234	0.017	0.024	0.055	-0.062	-0.026
Ni	-0.224	-0.028	0.192	0.065	-0.19	-0.132
Cr	-0.209	-0.055	0.271	0.119	-0.217	-0.201
Ce	-0.226	-0.096	0.017	0.133	-0.053	-0.204
Nd	-0.222	-0.086	-0.043	0.135	-0.024	-0.162
La	-0.222	-0.044	0.014	0.081	-0.192	-0.219
V	-0.227	-0.038	0.116	0.184	-0.142	-0.127
Ba	-0.22	-0.031	-0.026	0.193	-0.062	-0.276
Sn	-0.135	-0.016	-0.448	-0.315	-0.097	-0.06
Corg	-0.136	-0.241	0.076	0.474	0.201	0.606

Table 4.2 Results of Principal Components Analysis on geochemical data for all sediments of the Bay. (For each of the principal components a factor loading is given for each element).

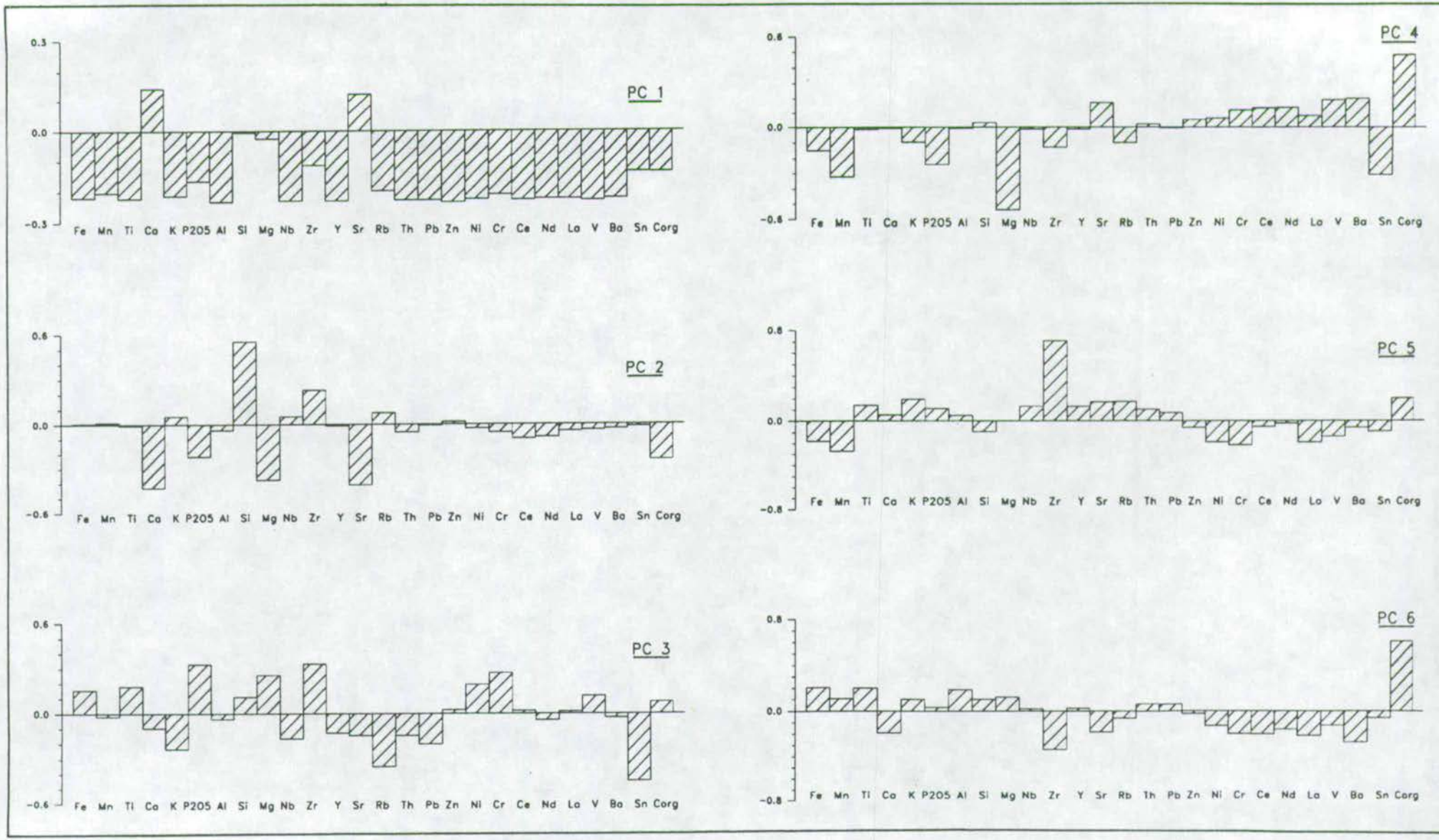

Figure 4.1 Graphical illustration of results of principal components analysis (PCA) on geochemical data (listed in Table 4.2) with loadings of each element for each principal component.

PC2 (accounting for 12% of the total variance) is a terrigenous quartz factor as both Si and Zr (found in quartz and zircon, minerals commonly associated with the coarse terrigenous fraction of sediments) have high positive loadings. Plotting these 2 main factors together (Fig 4.2a) shows the grouping of elements (circled on the graph) which define the 3 major mineralogical components of Phangnga Bay sediments. The majority of elements are associated with the aluminosilicate component (they are clustered around Al), none are closely associated with quartz and only Sr is closely associated with Ca. Hence, for the elements which are associated with aluminosilicates, their correlation with Al is first order whilst correlations between these elements are second order. Several elements lie outwith these 3 main groups (Fig 4.2a). Zr plots between the Si and Al group and Mg plots between the Ca and Al group. Sn, P_2O_5 and C_{org} plot near the Al group but outside the main cluster.

PC3 accounts of 6.9% of the elemental variance and appears to be an organo-phosphate factor with several associated metals. Fig 4.2b plots PC 1 against PC 3. The 3 main groups are still clearly defined but the Al-group becomes more dispersed and an additional grouping containing Rb and Sn can be picked out. The reasons for these described variations will be discussed for each element in the following sections.

4.3.3 Correcting for element partitioning

Since quartz is an essentially inert component within the system, with few elements substituting for Si (as is illustrated in the lack of element correlation with Si and its remote position in Figure 4.2a), the Phangnga Bay sediments can be viewed as a two-component geochemical system namely aluminosilicate-carbonate. It is evident from other studies (Hirst, 1962a,b; Moore, 1963; White, 1970; Reinson, 1975; Cook and Mayo, 1980; Norman and de Deckker, 1990 and others) that many elemental distributions simply reflect the aluminosilicate-carbonate distributions due to the fact that most elements are associated with one or the other of these 2 components.

Because of this partitioning of the majority of elements, any subsequent variations in an element's distribution due to other underlying factors are masked. Because of the physical grain size sorting effects on aluminosilicates (clays) and carbonates and quartz (sand) there is also an important element partitioning effect brought about

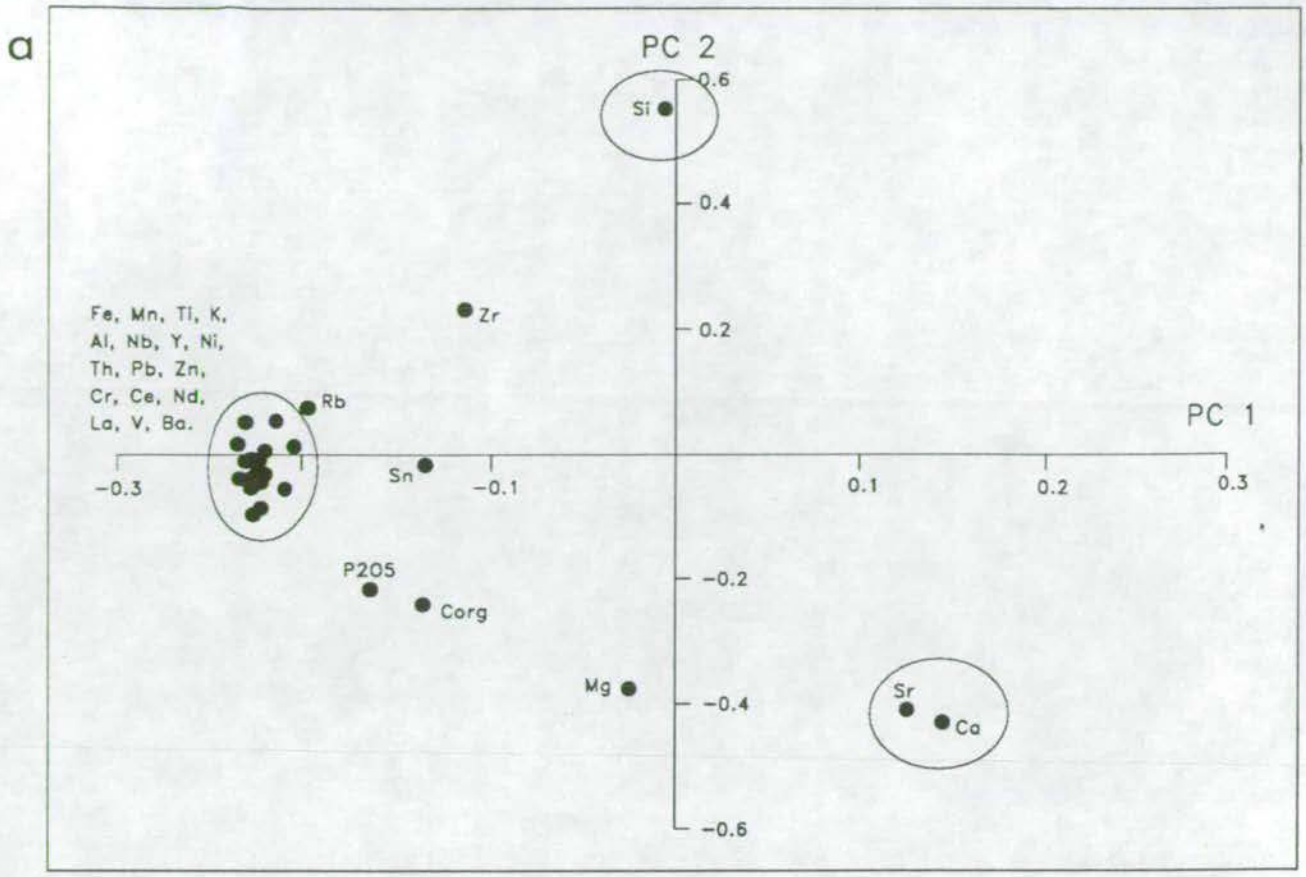

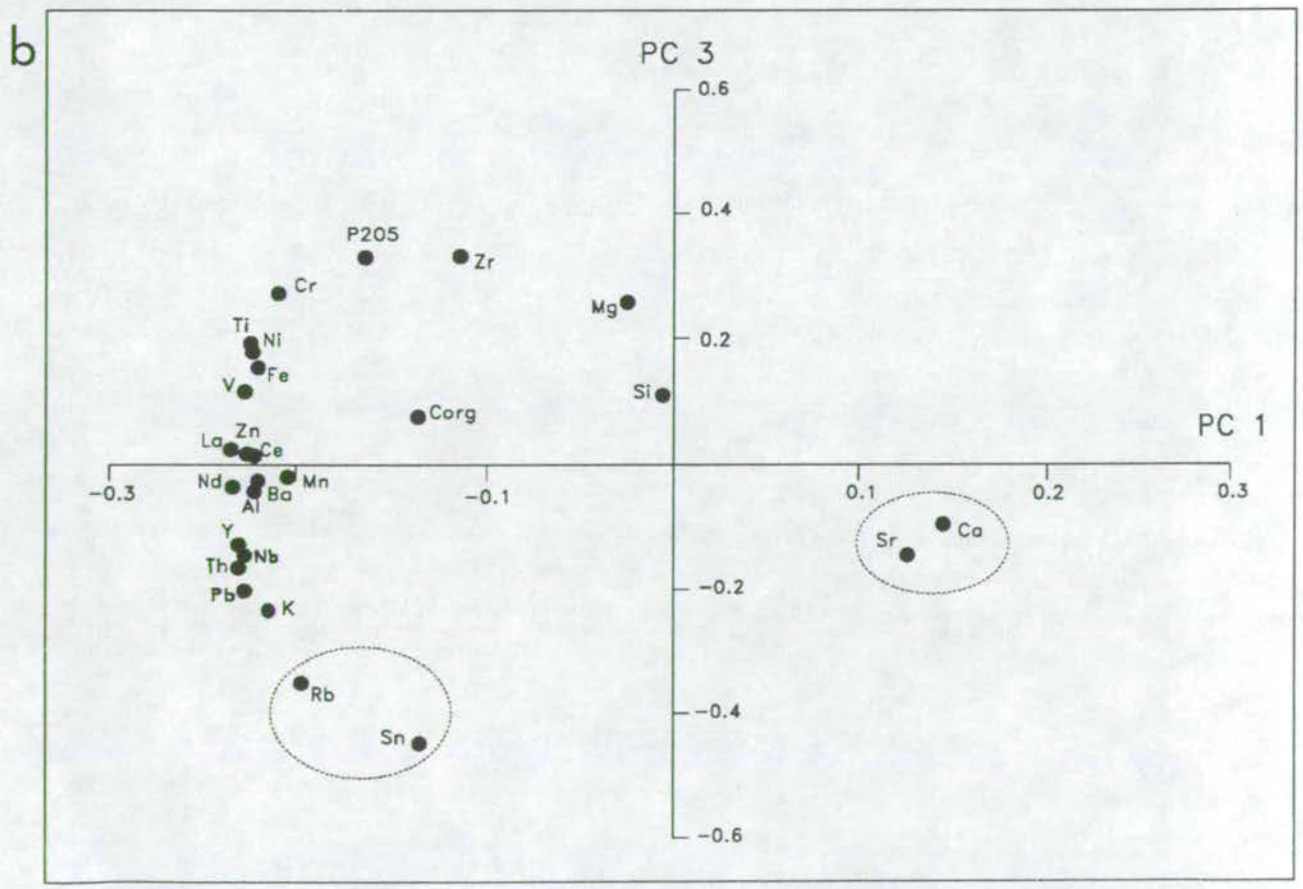

Figure 4.2 a. factor loadings of PC1 v. PC2 showing groupings of elements.
b. factor loadings of PC1 v. PC3 also showing groupings of elements.

by a textural control on the mineralogy of sediments which in the case of Phangnga Bay is very strong due to the large textural variability.

In order to 'unmask' the distributions of elements (both major and trace) their concentrations are recalculated as a ratio to either Al or Ca depending on which of these two elements they are associated with. Ratioing to Al also removes the textural control. It can be seen from Table 4.1 that Al correlates with mean grain size (in ϕ units hence increasing ϕ represents decreasing grain size) and this is corroborated by its correlation with the silt and clay fractions of the sediment. Figure 4.3 illustrates the distribution of Al concentrations throughout Phangnga Bay. The distribution mirrors that of mean grain size (Fig. 2.1) as would be expected from the strong positive correlation with mean grain size. Ca on the other hand correlates negatively with mean grain size thus positively but (not significantly at a 95% confidence level) with sand and gravel. Hence, although there is a relationship between Ca and grain size it is not as strong as that between Al and grain size. However, the correlations serve to illustrate that element partitioning controlled by the two major mineralogical components is also intimately linked with grain size variations.

4.4 MAJOR ELEMENT COMPOSITION

The major element compositions (non-oxide, salt corrected) of all surface sediment samples analysed are listed in Appendix D. An average value of these elements for all Phangnga Bay sediments is listed alongside World Average Shale, Sandstone and Limestone values as calculated by Turekian and Wedepohl (1961) (Table 4.3). The average Phangnga Bay sediment is something of a geochemical mix between these world average sandstones, shales and limestones which reflects the 3 component mineralogical nature of the Phangnga Bay sediments mentioned above.

4.4.1 Calcium

The matrix of correlation coefficients (Table 4.1) shows that Ca correlates strongly with $CaCO_3$. Although Ca may substitute in the lattice of montmorillonite clays, the error in measurement of $CaCO_3$ does not allow an accurate assessment of excess-Ca over $CaCO_3$-Ca which may indicate the amount contained in clays. However,

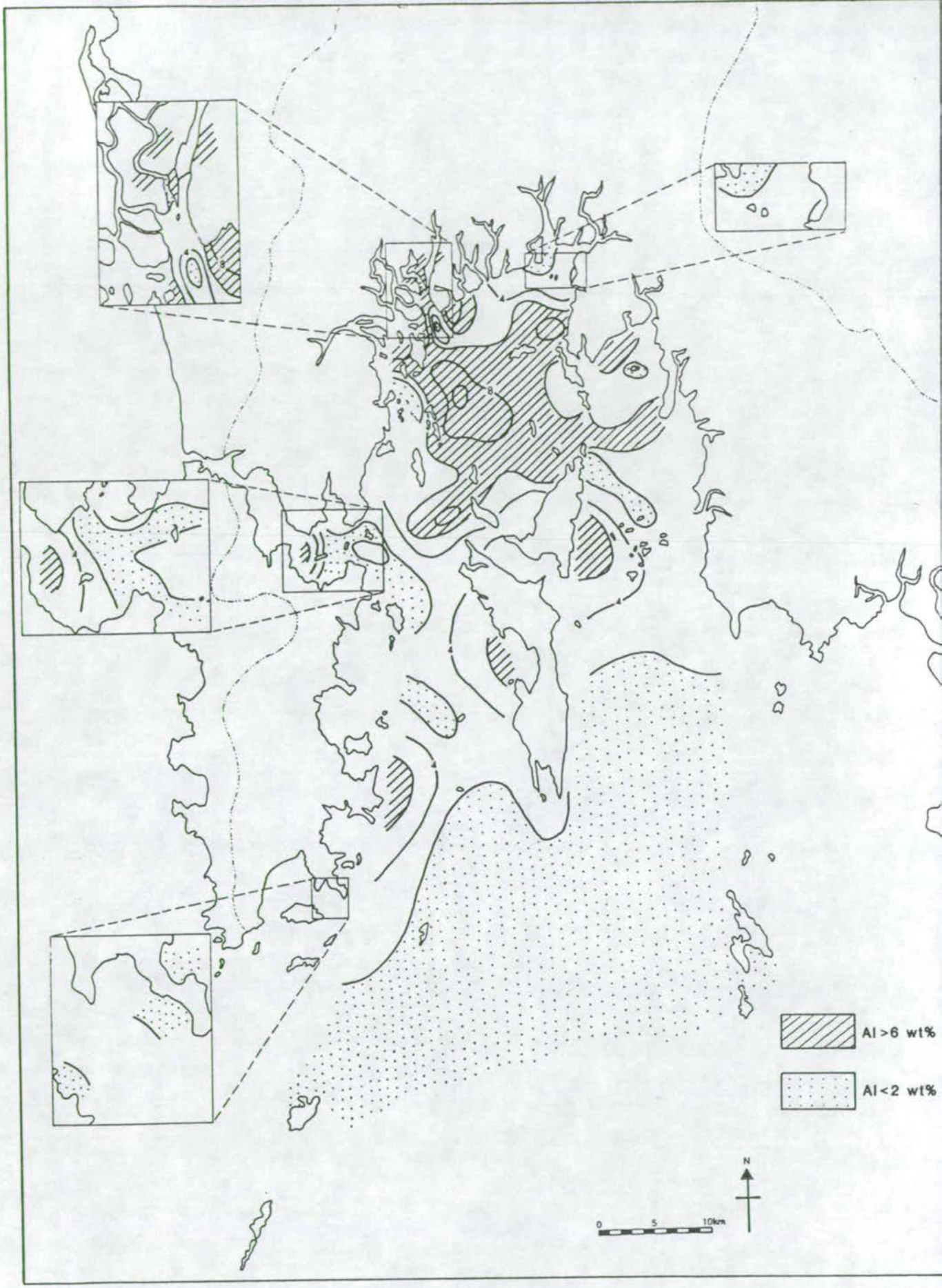

Figure 4.3 Areal distribution of Al concentrations in surface sediments.

	WORLD AVERAGE SHALE	WORLD AVERAGE SANDSTONE	WORLD AVERAGE LIMESTONE	ALL PHANGNGA BAY
				(n=156)
Fe (wt%)	4.72	0.98	0.38	1.61
Mn (ppm)	850	X0	1100	185
Ti (ppm)	4600	1500	400	1777
Ca (wt%)	2.21	3.91	30.23	10.86
K2 (wt%)	2.66	1.07	0.27	0.68
Al (wt%)	8	2.5	0.42	3.74
Si (wt%)	7.3	36.8	2.4	24.9
Mg (wt%)	1.5	0.7	4.7	1.0
Nb (ppm)	11	0.0X	0.3	11.8
Zr (ppm)	160	220	19	157
Y (ppm)	26	40	30	18.3
Sr (ppm)	30	20	610	892.6
Rb (ppm)	140	60	3	78.0
Th (ppm)	12	1.7	1.7	15.5
Pb (ppm)	20	7	9	22
Zn (ppm)	95	16	20	27
Ni (ppm)	68	2	20	12
Cr (ppm)	90	35	11	38
Ce (ppm)	59	92	11.5	55.3
Nd (ppm)	24	37	4.7	21.9
La (ppm)	92	30	X	24
V (ppm)	130	20	20	36
Ba (ppm)	580	X0	10	81
Sn (ppm)	6	0.X	0.X	12.0
P2O5 (ppm)	1600	390	920	746
Corg (wt %)*	0.94	0.36	0.47	1.24

After Turekian and Wedepohl (1961) (except * - after Ronov and Migdisov (1971))

Table 4.3 World average composition of shales, carbonates and sandstones compared to average Phangnga Bay sediments (X indicates the order of magnitude).

since the $CaCO_3$-Ca is very high in proportion to any Ca contained in clays it will be assumed here that all variation in Ca is reflected in the variation in $CaCO_3$ content hence a map of $CaCO_3$ content rather than Ca is plotted.

The contour map for weight % $CaCO_3$ concentrations in surface sediments (Fig 4.4) illustrates a trend of increasing $CaCO_3$ values southwards towards the more open marine setting. In the sheltered northern area of the Bay, $CaCO_3$ generally constitutes <10% of the sediment, however, there are local increases which are due either to areas of prolific calcareous macrofauna such as mussel and oyster beds, or to sedimentological effects which concentrate carbonate debris as lag deposits at mangrove mouths or beaches. The general trend of increasing $CaCO_3$ towards the open marine environment reflects the waning influence of terrigenous sediment supply southwards and thus, the improving environmental conditions required by the majority of the $CaCO_3$ secreting organisms ie, less turbid water, constant temperature and salinity, coarser and hence generally oxic sediments. Such a trend is recorded in similar environments eg, Broad Sound (Cook and Mayo, 1980), Mallacoota Inlet (Reinson, 1977), South Alligator River Estuary (Woodroffe et al 1979) and also on a larger scale in the Arabian Sea (Kolla et al, 1981).

4.4.2 **Silica**

The average SiO_2 content of Phangnga Bay sediments is more of the order of World average sandstones than carbonates or shales (Table 4.3). Because SiO_2 is the major component of the aluminosilicate and quartz (ie terrigenous) components, a pure Si distribution map will simply be the reverse of the $CaCO_3$ map (confirmed by the high negative correlation between $CaCO_3$ and Si - Table 4.1). However, by plotting Si/Al an indication of the amount of free Si in the form of quartz in the system can be obtained.

A Si/Al ratio distribution map for Phangnga Bay (Fig 4.5) shows an increasing trend southwards which indicates a large proportion of free quartz relative to clay minerals in the coarser sediments of this southern area. This abundance of quartz cannot be easily explained by present day depositional processes operating in Phangnga Bay - there are no large rivers depositing great quantities of sand into this southern area and although localised strong currents have been noted around Ko Racha Yai, there appears to be no present day hydrological regime operating which could account for this sediment type. The sedimentological evidence from grain size

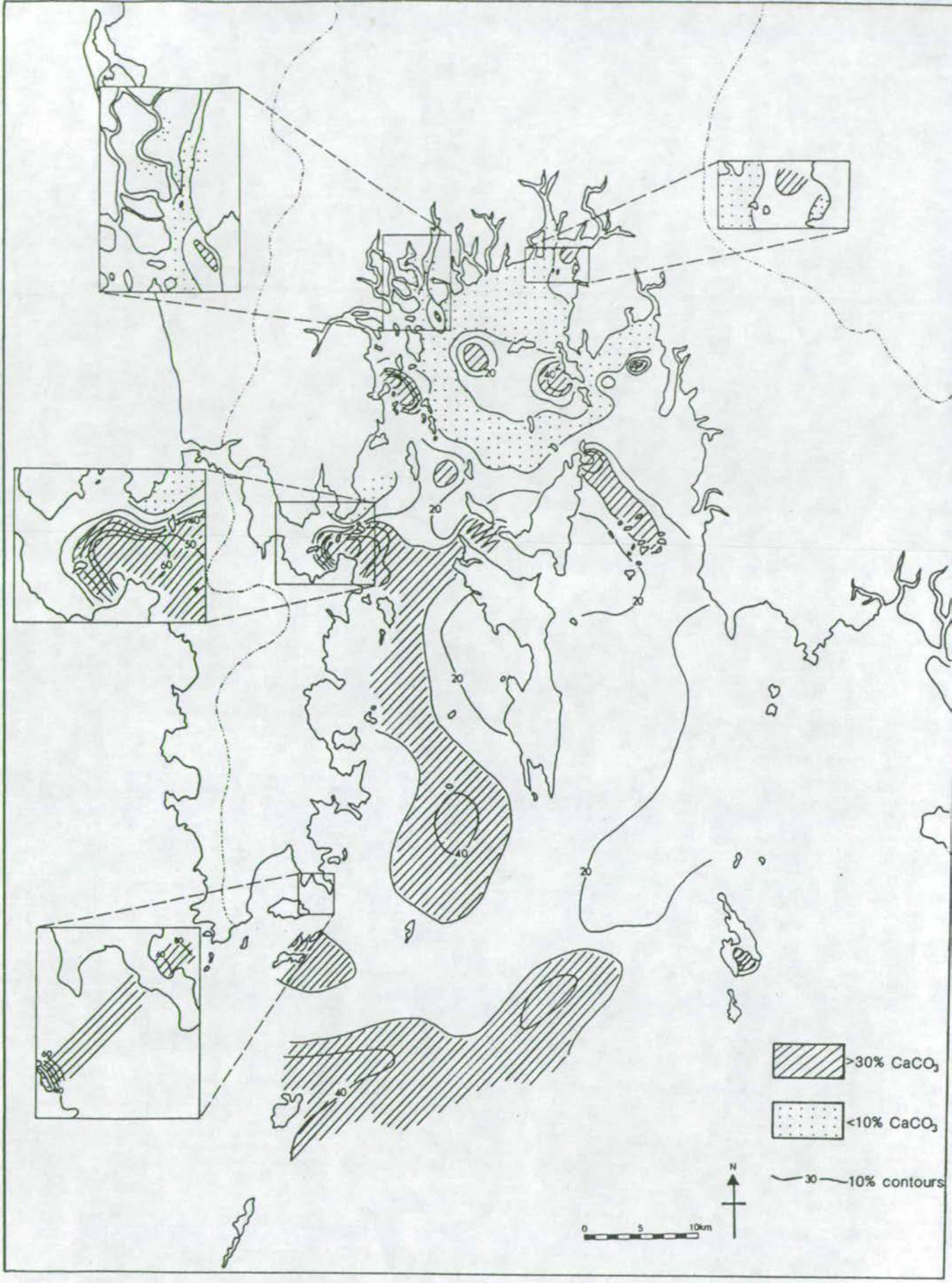

Figure 4.4 Areal distribution of $CaCO_3$ concentrations in surface sediments.

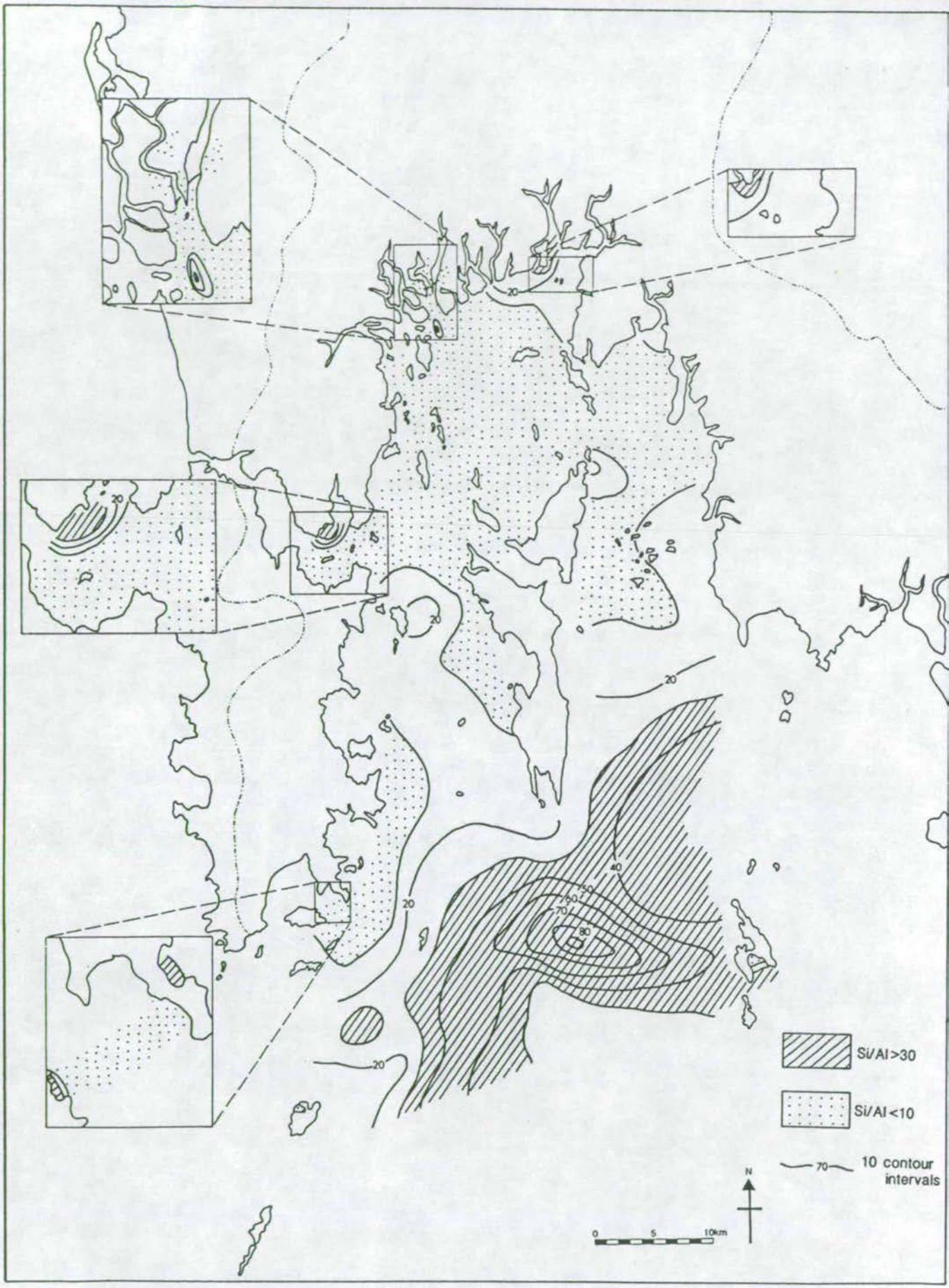

Figure 4.5 Areal distribution of Si/Al ratios in surface sediments.

analysis (Chapter 2) and the textural evidence from quartz grains (Chapter 3) indicates that the sediments are relict ie, deposited in a different set of conditions from those prevalent today. It is thought that they were deposited at low sea-level stands during Pleistocene glacial periods and may have been reworked in coastal environments during subsequent transgressions.

4.4.3 Magnesium

The average Mg content of Phangnga Bay sediments lies between the World average sandstone and shale values (Table 4.3). However, this generalisation hides wide variations in the Mg content throughout the Bay. Table 4.1 shows that Mg does not correlate strongly with any of the major elements nor with grain size. Figure 4.2a shows that Mg lies midway between Al-group elements and Ca. This is explained by the fact that Mg is found both in the lattice structure of clays as well as in the calcite structure.

Figure 4.6 plots $CaCO_3$ against Mg and shows the lack of correlation between the two. Lines have been drawn on the graph indicating the gradient of a 4% mole $MgCO_3$ (LMC), 13% and 19% mole $MgCO_3$ (HMC) line. There is no obvious trend of samples following any of these lines which suggests a mix of Mg-calcite types (confirmed by studies of the carbonate mineralogy - Chapter 3). Points plotting above the 19% mole $MgCO_3$ line show an excess of Mg which cannot be explained by Mg in carbonate and hence must be in clays. In truth, most of the sediments will contain a mix of Mg-clays and Mg-carbonates and so it cannot be said that all points below the 19% mole $MgCO_3$ line contain Mg solely in Mg-carbonates. However, it can be safely assumed that all points above the line contain most of their Mg in clays (at no site does 19% mole $MgCO_3$ constitute 100% of the carbonate so this line is an extreme limit of Mg in calcite). These sites above the 19% line have been plotted in Figure 4.7. They are all concentrated in the northern part of the Bay coinciding with areas of high clay and low carbonate concentrations.

Figure 4.8 illustrates that Mg/Al values increase southwards in the Bay. Although this may be reflecting increasing montmorillonite clay proportions southwards (as shown in Chapter 3) it may also be reflecting the increasing proportion of HMC southwards. In order to assess the amount of Mg contained in clays and carbonates separately, carbonate material was removed from 5 samples (8, 33, 94, 109 and 123G) by acidulation (using dilute Acetic acid to minimise attack of clays). These were then

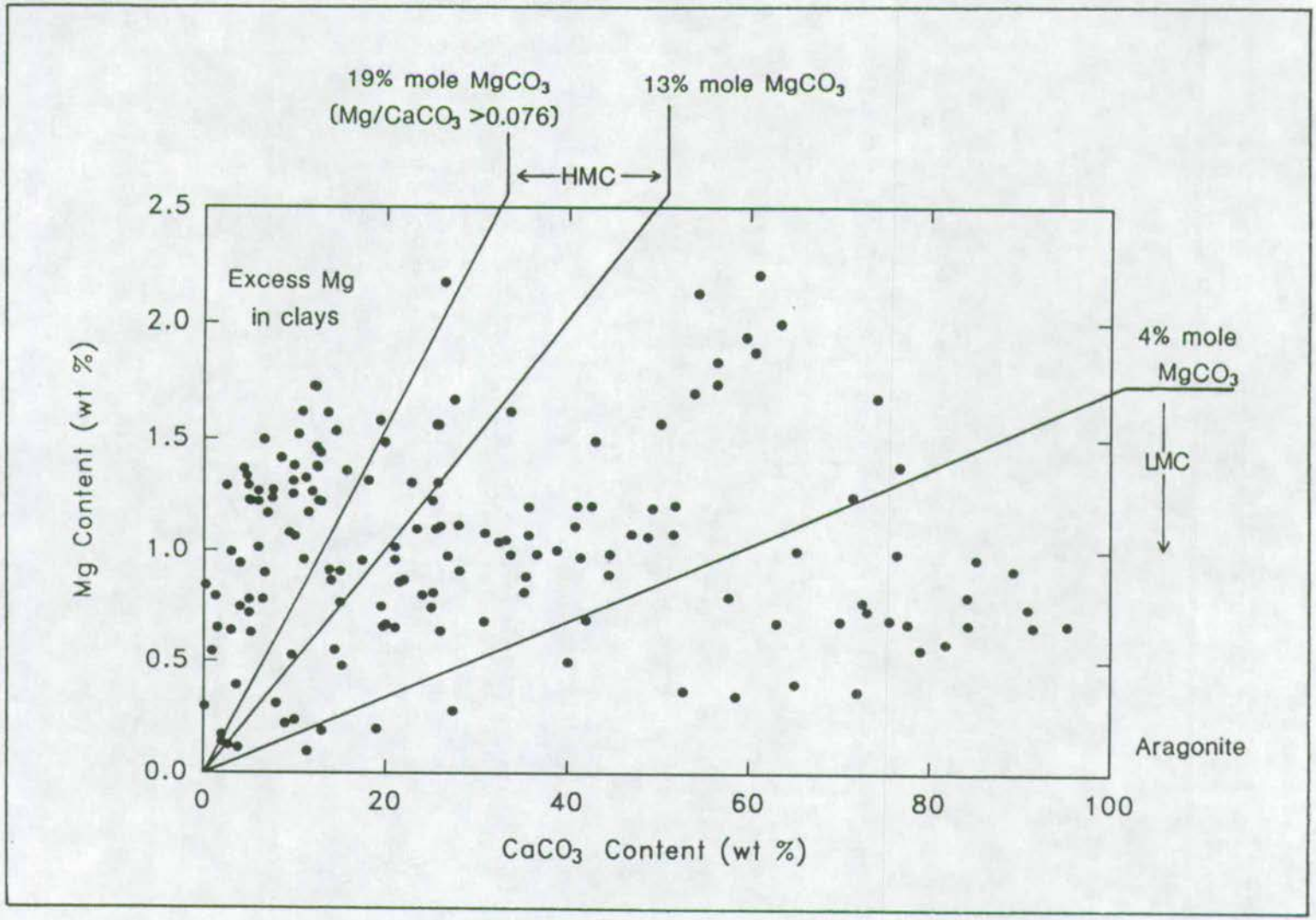

Figure 4.6 Graph of $CaCO_3$ v. Mg for surface sediments (see text for explanation).

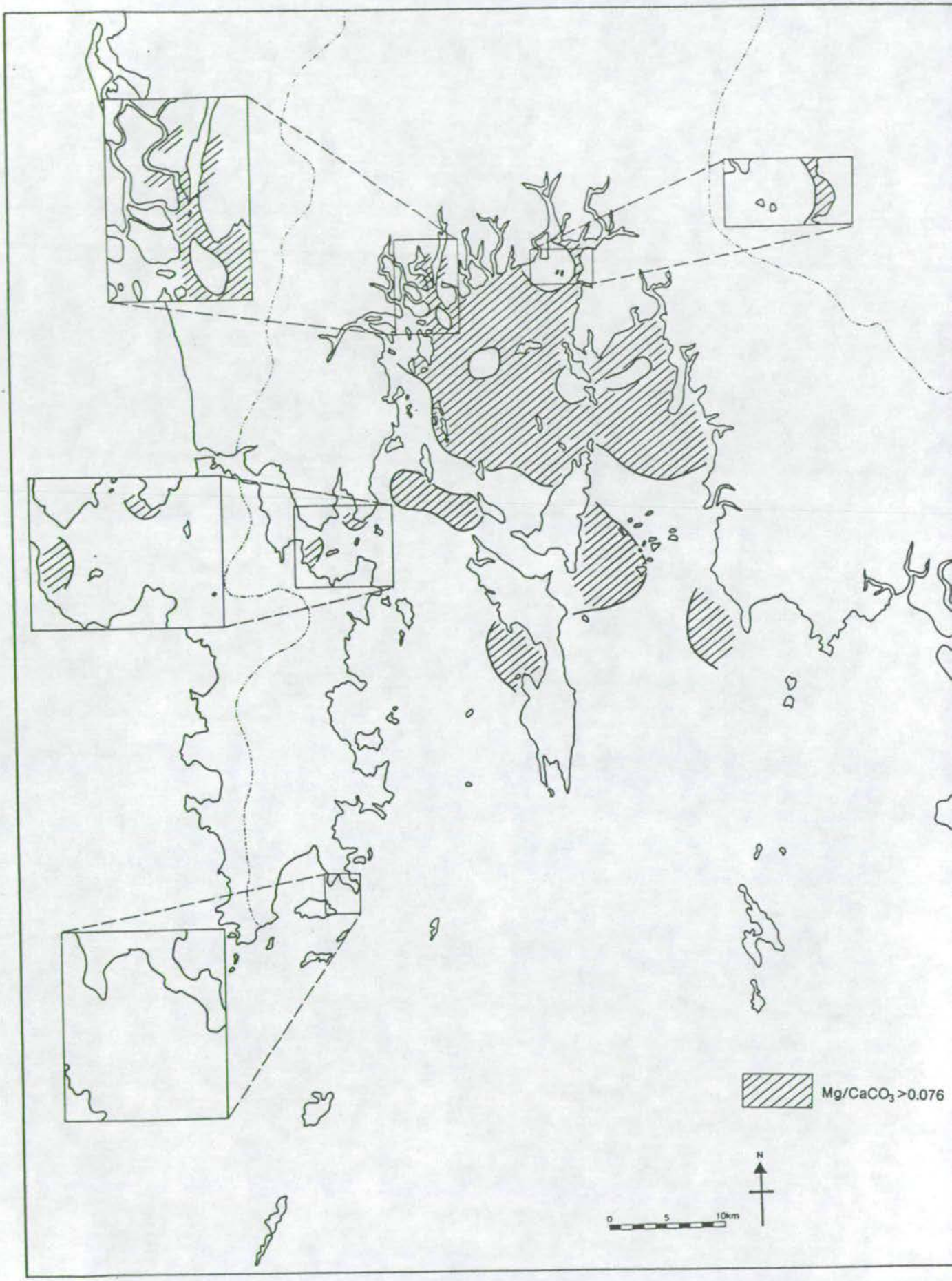

Figure 4.7 Areal distribution of samples which have a $Mg/CaCO_3$ ratio of > 0.076.

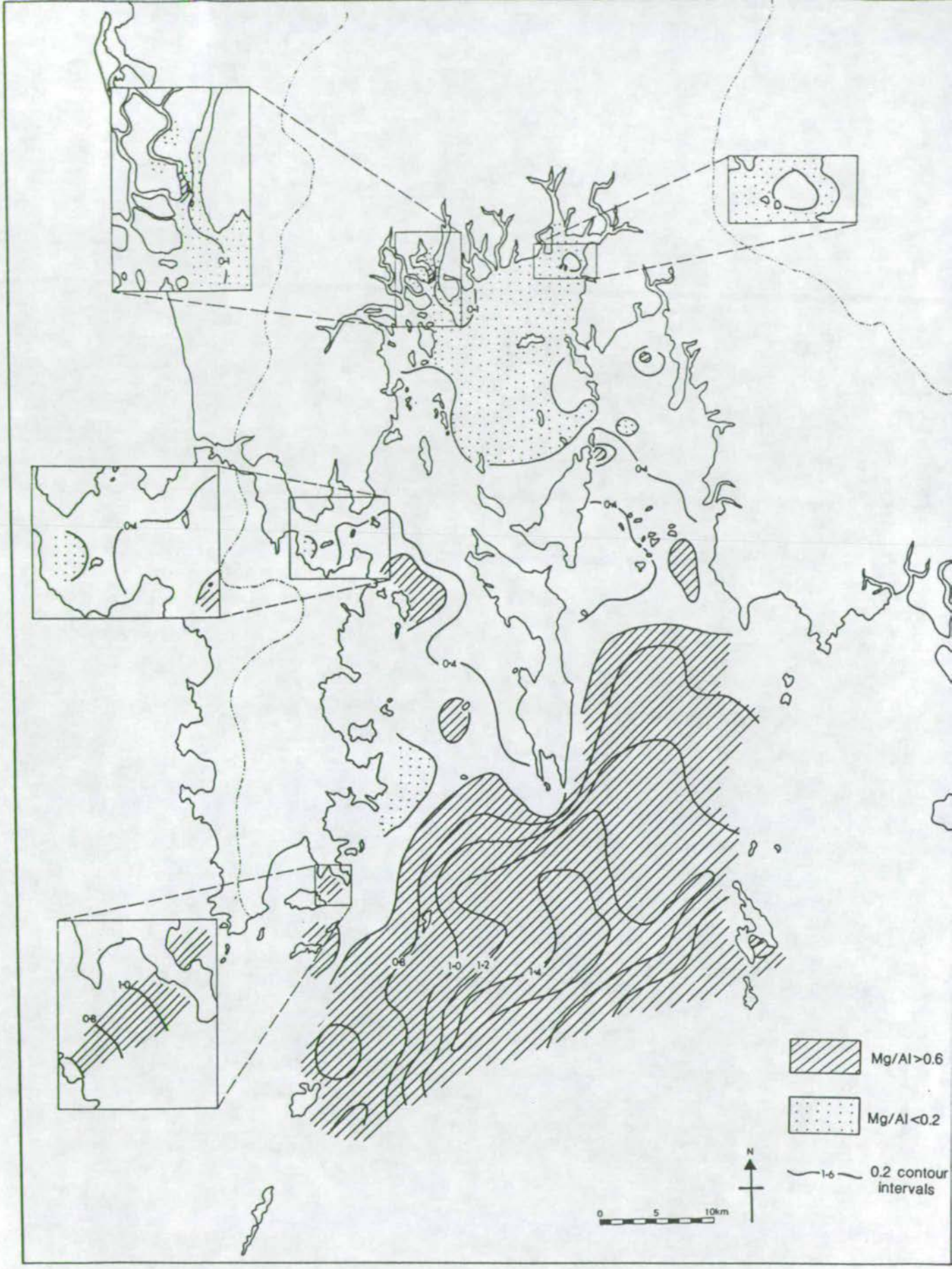

Figure 4.8 Areal distribution of Mg/Al ratios in surface sediments.

filtered, washed and dried before fusing for XRF major element analysis. On obtaining the Mg content of the carbonate-free samples (non-oxide and salt-free) an adjustment was made to correct the weight percent of the carbonate-free sample to that of the whole sample. A subtraction of the Mg_{CLAY} thus obtained, from the Mg_{TOTAL} leaves the $Mg_{CARBONATE}$. Table 4.4 lists the Mg_{CLAY}/Al and Mg_{CARB}/Ca ratios for the 5 samples (the figures are ratioed in order to normalise to equal clay and carbonate contents). It is clear that the Mg content of clays increases southwards as is expected from the increase in montmorillonitic clays reported in Chapter 3. Similarly the Mg content of carbonates increases southwards as is predicted by the increase in high magnesium calcite (Chapter 3). Therefore, the overall southward increase in Mg/Al ratios recorded in Figure 4.8 is a function of both increasing Mg in clays (due to an increasing proportion of montmorillonite) and increasing Mg in carbonates (due to biogenic control on carbonate type).

Figure 4.9 plots Mg against Al and illustrates the lack of correlation between these two parameters. However, when the data points are classified according to the $CaCO_3$ content (> or < 15% $CaCO_3$) two correlations do emerge. The high carbonate samples show a trend of relatively high Mg/Al ratios whilst the low carbonate samples show a trend of low Mg/Al ratios thus graphically illustrating the trend shown in Figure 4.7.

	Mg_{CLAY}/Al	$Mg_{CARB.}/Ca$
North ↓		
94G	0.12	0.0041
33G	0.134	0.0316
8G	0.39	0.0318
109G	0.568	0.0302
123G	0.513	0.0487
South		

Table 4.4
Ratios of Mg/Al (in clays) and Mg/Ca (in carbonates) for 5 samples from a north-south transect down the Bay.

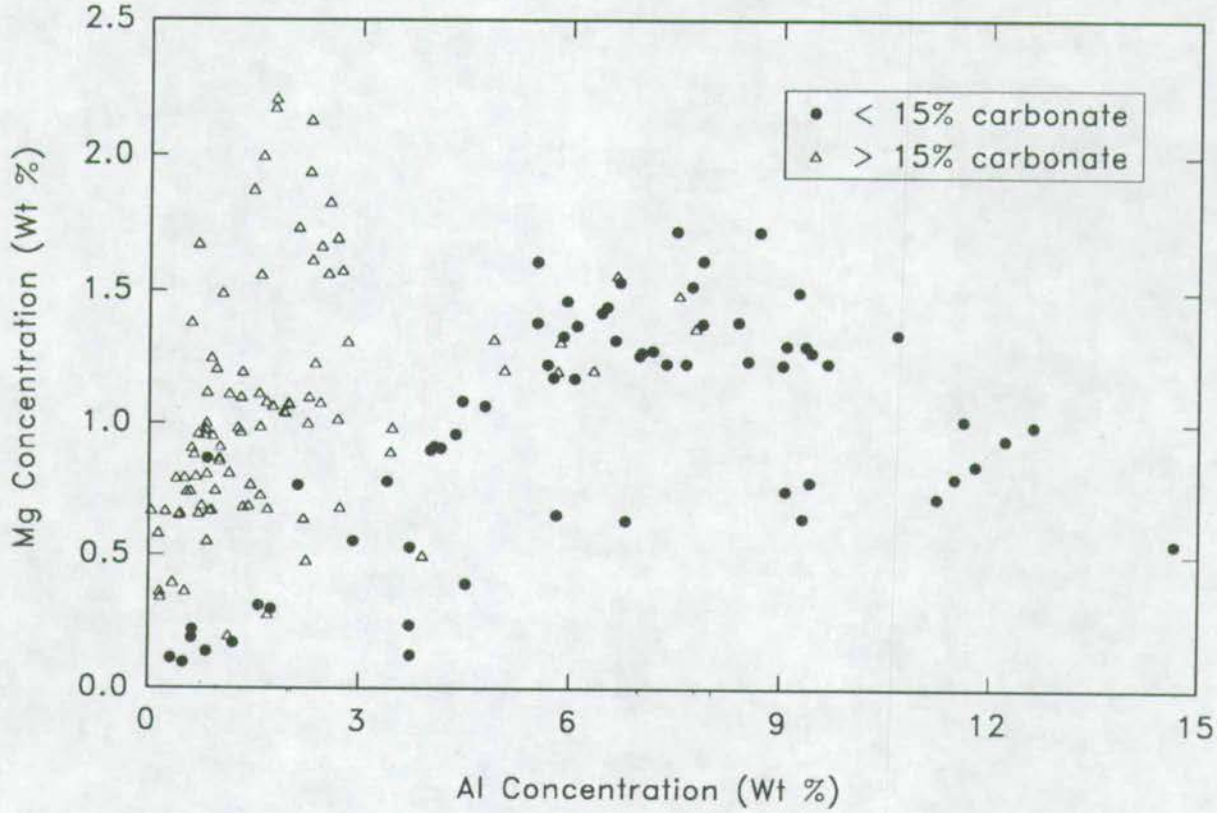

Figure 4.9 Graph of Mg v. Al for high carbonate (> 15%) and low carbonate (< 15%) sediments.

4.4.4 Iron

The average Fe content of Phangnga Bay sediments is intermediate between World average shales and sandstones (Table 4.3). Fe shows a strong positive correlation with both Al and grain size and a strong negative correlation with $CaCO_3$ (Table 4.1) thus indicating an Fe-clay relationship.

Particular attention has been focused on the mechanisms responsible for Fe removal from solution in rivers into particulate form available for deposition in estuaries (Boyle et al, 1977; Sholkovitz et al, 1978; Mayer, 1982 and others). It is generally agreed that Fe exists in rivers primarily as organic or inorganic colloids (possibly as the hydrous oxide of Fe, stabilized by organic colloids (Moore et al, 1979)) which flocculate on contact with sea-water thus forming larger particles and therefore effectively becoming part of the clay fraction thus the close association with Al. Investigations by Holliday and Liss (1976) showed that dissolved Fe was almost totally removed on mixing of river water with sea-water in the Beaulieu Estuary by the time the salinity had reached 15 ppt.

The Fe/Al distribution is plotted in Figure 4.10. It can be seen that the highest ratios are found in the southern and eastern parts of the Bay. Figure 4.11 graphically illustrates the Fe/Al relationship with lines of Fe/Al ratios corresponding to those picked out in the distribution map. The high Fe/Al ratios could be representing a change in clay type from low Fe clays (ie kaolinite) in the north to high Fe clays (montmorillonite and illite) in the south and indeed an increase in montmorillonite is recorded both in the mineralogy (Chapter 3) and in increasing Mg_{CLAY} contents. Hirst (1962a) suggested that the greenish colour of the sediments of the Gulf of Paria may be due to substitution of Fe^{3+} in Al^{3+} sites of illite and montmorillonite as ferric silicate has a green colour (Keller, 1953). The presence of Fe^{3+}-bearing illite and montmorillonite may also explain the greenish colour of sediments in the southern half of Phangnga Bay

It is also possible that glauconite which concentrates Fe in its structure, may be present in these sediments as an authigenic mineral. The relatively sediment starved area to the south of the Bay and the presence of the necessary "parent" minerals such as illite and carbonate grains means that the formation of glauconite in this area is possible. However, no glauconite was identified in sediments either by visual examination of the silt/sand fraction (where glauconite, if present, would be obvious

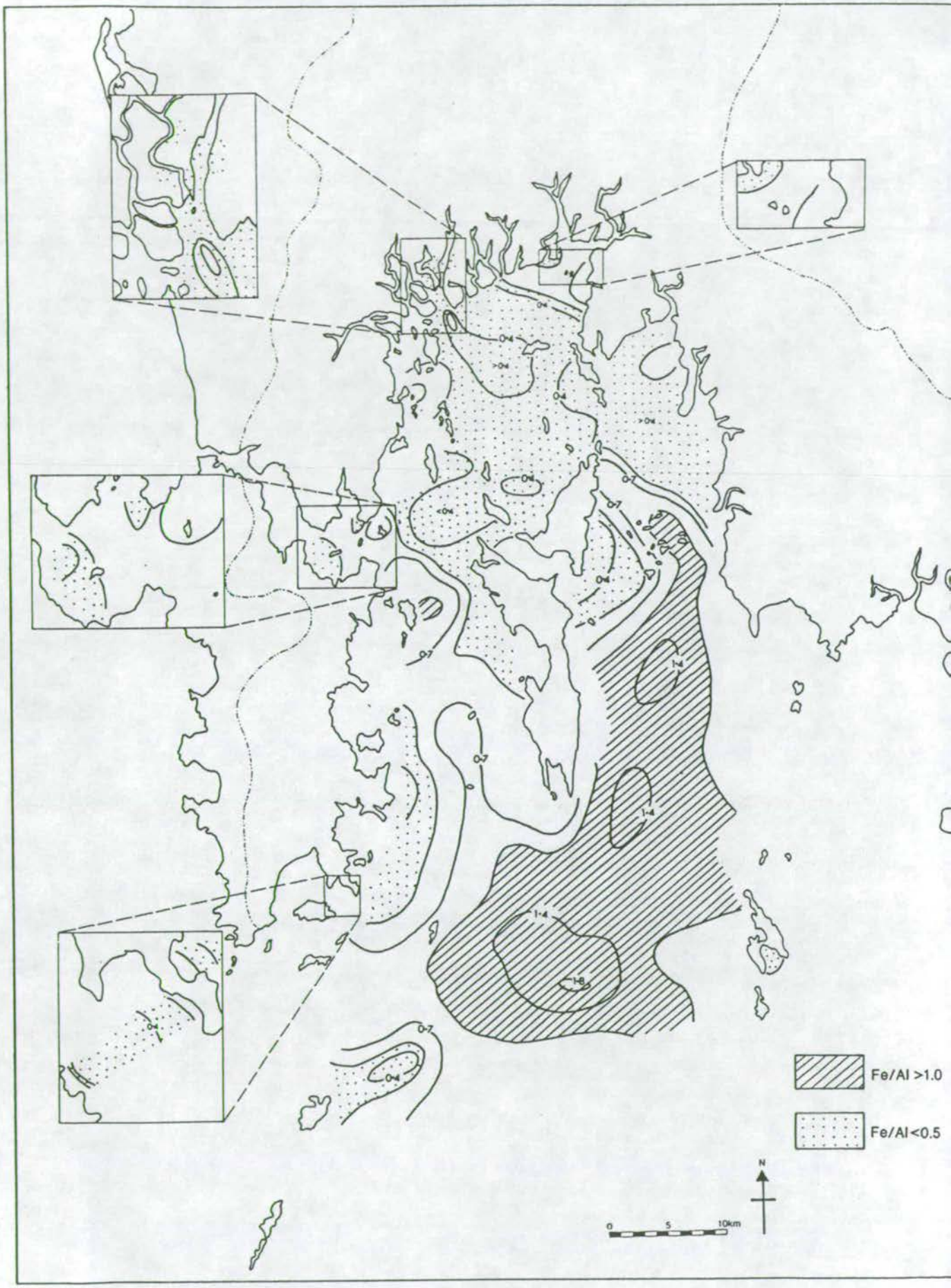

Figure 4.10 Areal distribution of Fe/Al ratios in surface sediments.

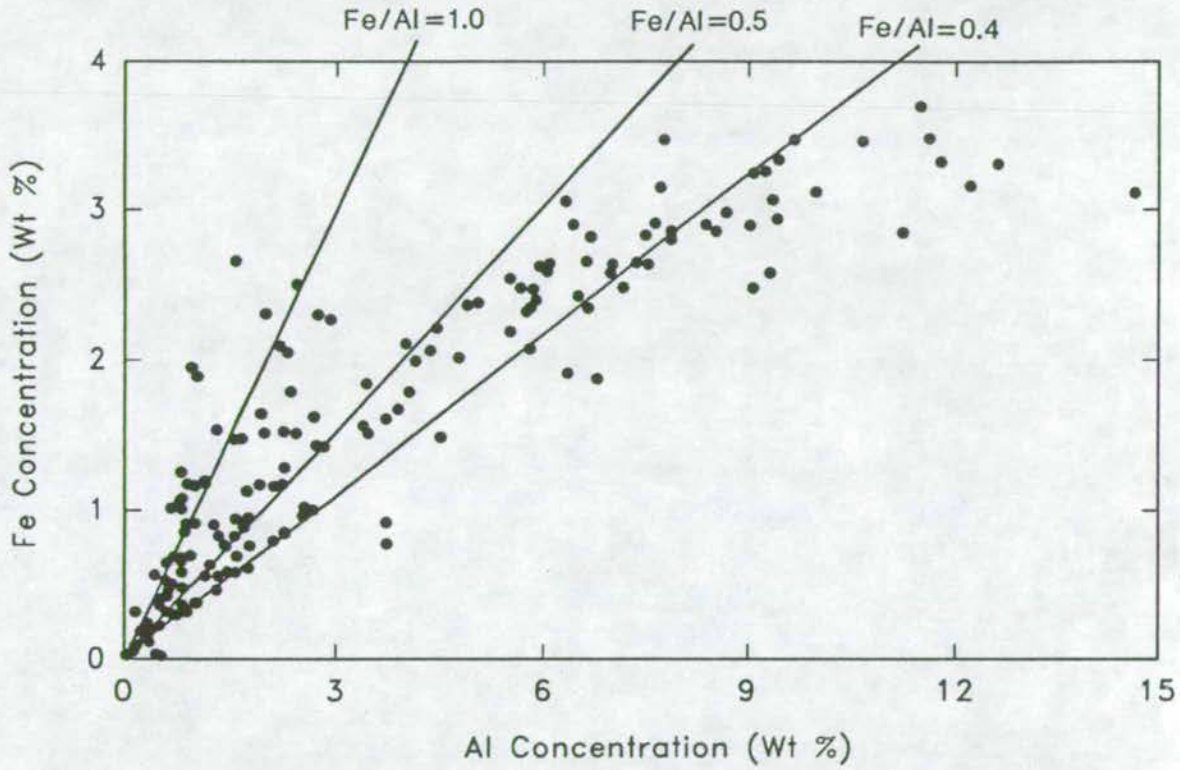

Figure 4.11 Graph of Fe v. Al for surface sediments.

as bright green grains) nor in XRD analyses - although admittedly, glauconite is difficult to identify in XRD traces due to its similarity to illite (Odin and Matter, 1981).

A more suitable explanation for the high Fe/Al concentrations in the south is the presence of Fe-bearing heavy minerals such as hematite, ilmenite and magnetite which are the main components of the heavy mineral fraction (Chapter 3) and which are concentrated in the fine sediment fraction. Ti, which is used as a heavy mineral indicator element (see next section) is also concentrated in this southern area in a SW-NE trend, as is Zr (concentrated in another heavy mineral, zircon). Slightly higher Fe/Al values are also found in the northern mangrove channel mouths and again this follows the pattern of Ti and Zr. The area of low Fe/Al ratios east of Ko Racha Yai coincides with the area of low Ti/Al ratios and suggests some unusual processes affecting sedimentation in this area - this will be discussed later.

4.4.5 Titanium

Hirst (1962a) illustrated that high Ti/Al ratios occur in the sands compared to the clays of the Gulf of Paria due to the contribution from Ti-bearing detrital minerals such as ilmenite. Spears and Kanaris-Sotiriou (1976) and Schmitz (1987) illustrated the preferential concentration of Ti in coarser sediment fractions due to its incorporation into heavy minerals such as ilmenite, rutile, titanomagnetite and augite. Schmitz (1987) noted that the Ti/Al ratio is a tool as useful as particle size measurements to estimate the energy of a depositional environment as the higher the energies of the suspension medium the greater the fraction of Ti-bearing minerals relative to the Al-rich clay fraction.

Ti is also an important chemical constituent of biotite mica and since this mineral is abundant in the acid igneous rocks of the drainage basin some contribution to the total Ti concentration in the Bay sediments might also be expected from this mineral. However, no biotite has been identified in any of the Bay sediments and this is not surprising considering that biotite is chemically altered relatively rapidly in humid tropical climates. The breakdown of biotite will release Ti ions but Goldschmidt (1954) states that practically no Ti can enter ocean water as a solute due to its prohibitive ionic potential. Therefore Ti is likely to be a primary component of clay minerals formed at the site of weathering rather than through halmyrolysis.

By plotting Ti/Al ratios the proportion of Ti in heavy minerals in the sediment can be estimated above that contained in clays. From delineating areas of high Ti/Al values (ie, heavy mineral concentrations) an indication of the energy of the environments of deposition can be established.

Figure 4.12 illustrates the Ti/Al ratios of Phangnga Bay sediments and shows a similar pattern to Fe/Al with an area of high Ti/Al ratios in a SW-NE trend across the southern area of the Bay with small areas of high Ti/Al concentrations in the north around the mangroves and in the channel between the north of Ko Phuket and the mainland. The area in the south coincides with the area of high quartz sand (Fig 4.5 and Fig 2.7) which is thought to represent relict sediments. High heavy mineral concentrations would be consistent with this model as reworking of these sediments in high energy alluvial and coastal environments would result in high heavy mineral concentrations. High concentrations in the north of the Bay result from recent sediment deposition as heavies settle out before travelling any distance into the low energy areas in front of the mangroves.

The low Ti/Al contents to the north east of Ko Racha Yai in the south coincide with similar low contents of other heavy mineral indicator elements (Fe, Zr and Sn). From the bathymetry map (Fig 1.4) it can be seen that there is a slight high in this area to the north east of Ko Racha Yai. If these sediments are indeed relict as is suggested by previous evidence, and were deposited in fluvial or shallow coastal environments then an area of higher elevation (either as an island in a coastal area or as a spur in a fluvial terrain) would not have received the same sediment cover as surrounding lower areas. Heavy minerals will be concentrated in lower areas due to the higher energy required to transport them. Therefore, this area of low heavy mineral concentrations may represent some vestige of the low sea-level stand topography.

4.4.6 Potassium

Table 4.1 illustrates potassium's positive correlation with Al and mean grain size and negative correlation with $CaCO_3$ thus indicating a strong association with the clay fraction of the whole sediment. This is similarly illustrated in Figs 4.2a and b. K is therefore plotted in Figure 4.13 as a ratio to Al.

Areas of high K/Al occur in the north of Phangnga Bay in mangrove channels and in front of the mangroves and also in the south west of the Bay to the south east of

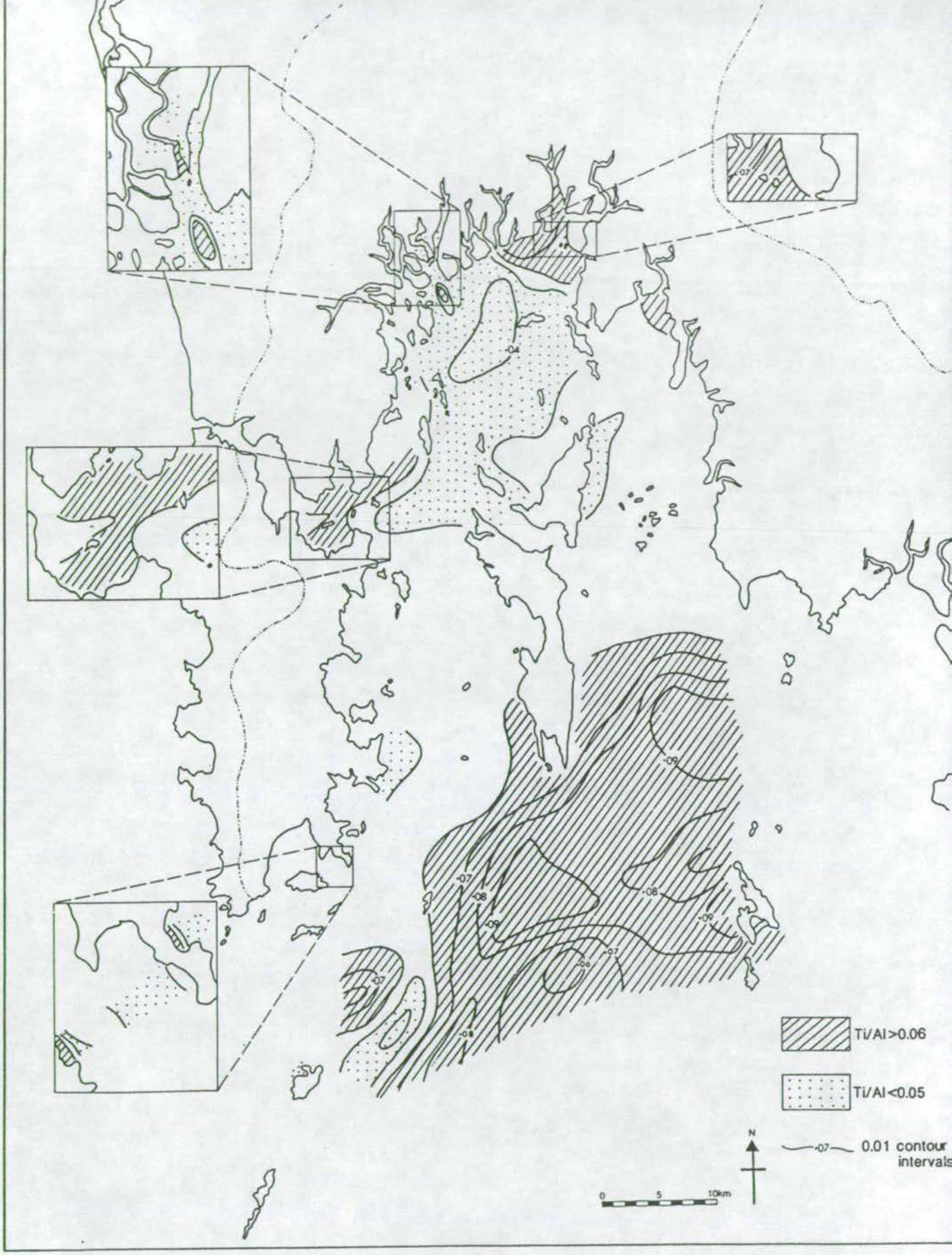

Figure 4.12 Areal distribution of Ti/Al ratios in surface sediments.

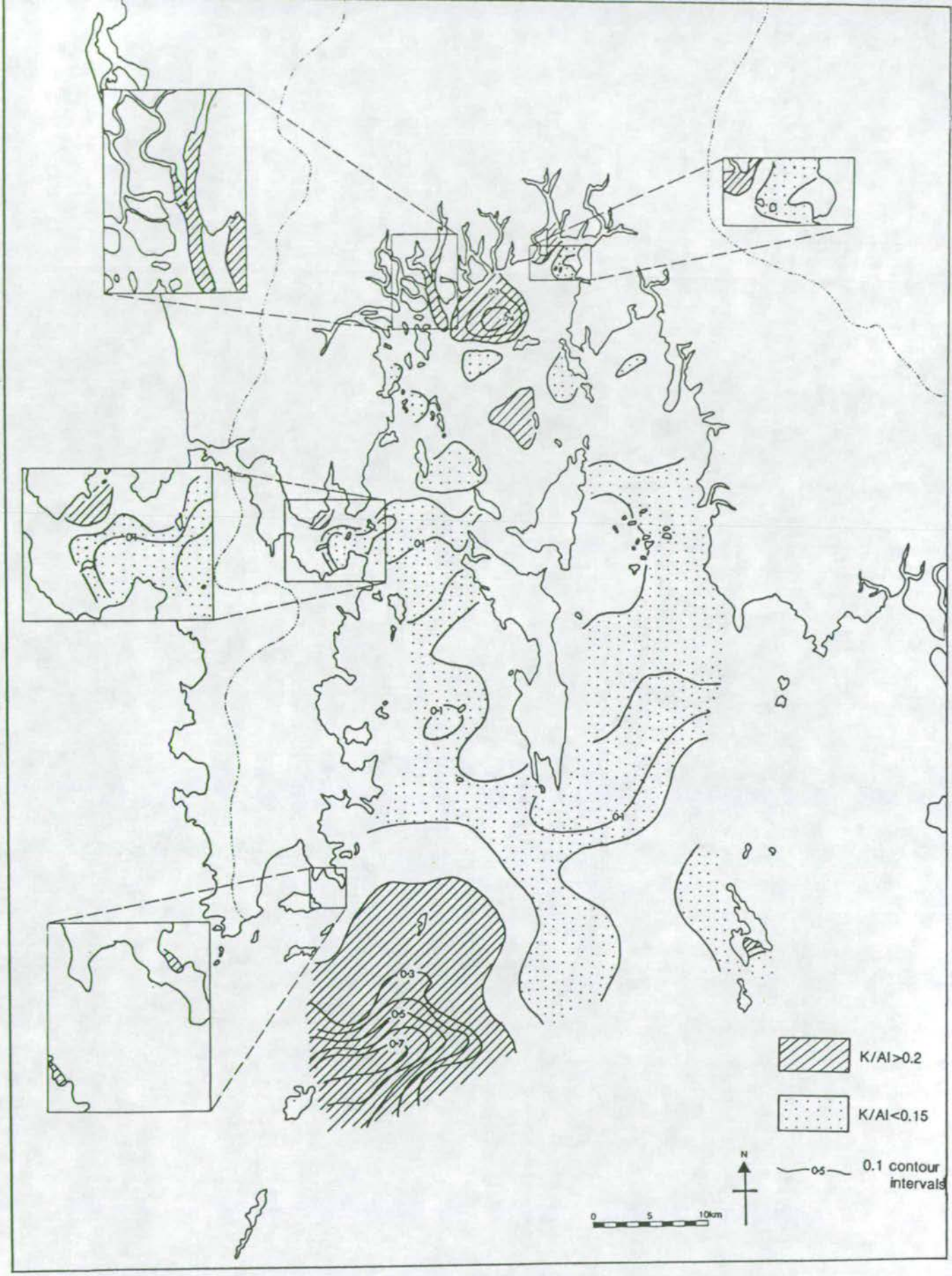

Figure 4.13 Areal distribution of K/Al ratios in surface sediments.

Ko Phuket. Conventionally an enrichment in K relative to Al indicates an enrichment of K-bearing feldspar (Calvert, 1976). This may explain the high K/Al ratios in the N of the Bay where K-feldspar has been identified in the sediments (Chapter 3) however, no K-feldspar has been identified in the sediments to the south-east of Ko Phuket. Lepidolite mica however, has been identified in sediments from both of these areas. K is a major elemental component of lepidolite mica and the high anomalies in the sediments are explained by the presence of this mineral. Rb is a common substituting element in lepidolite and similar anomalies in the element (see section 4.5.1.1) confirm this interpretation.

4.4.7 Phosphorus

The average P_2O_5 concentration of Phangnga Bay sediments (746 ppm) is between World average sandstones and limestones (Table 4.3). Table 4.1 shows that P_2O_5 correlates significantly with Al and positively but not significantly with mean grain size - there is also a weak negative correlation with $CaCO_3$ and a positive correlation with Fe that is stronger than that to Al. Table 4.3 shows that in world average sediments, P_2O_5 is concentrated in shales compared to sandstones and has an intermediate concentration in limestones. Hirst (1962a) and Reinson (1977) showed that P_2O_5 is concentrated in clays in sediments of the Gulf of Paria and Mallacoota Inlet respectively. Hence, in Phangnga Bay, P_2O_5 is likely to be concentrated in clays and this seems to be backed-up by the P_2O_5/Al correlation. The phosphate may occur in the clay fraction within finely-divided apatite (Hirst, 1962a). It may also occur as ferriphosphate in dispersed iron-oxides on mineral grain surfaces in the coarser grain size fraction which may explain the lack of a significant correlation with mean grain size.

Figure 4.14 plots P_2O_5 as a ratio to Al and illustrates a concentration of non-aluminosilicate P_2O_5 in dispersed sites around the north of the Bay and in a larger area trending SW-NE in the south of the Bay. Garson et al (1975) lists monazite ($(Ce,La,Th)PO_4$) as one of the main heavy minerals of granitic association in stream sediment samples from the hinterland of Phangnga Bay. Also, a Government Report on heavy mineral concentrations of sediments off Phuket (Chapter 3) listed monazite as present in these sediments. Monazite is moderately resistant to weathering and is frequently concentrated as a detrital mineral in stream and beach sands. The distribution of high P_2O_5/Al concentrations in the south of the Bay coincide with high Ti/Al concentrations which are interpreted as increased heavy

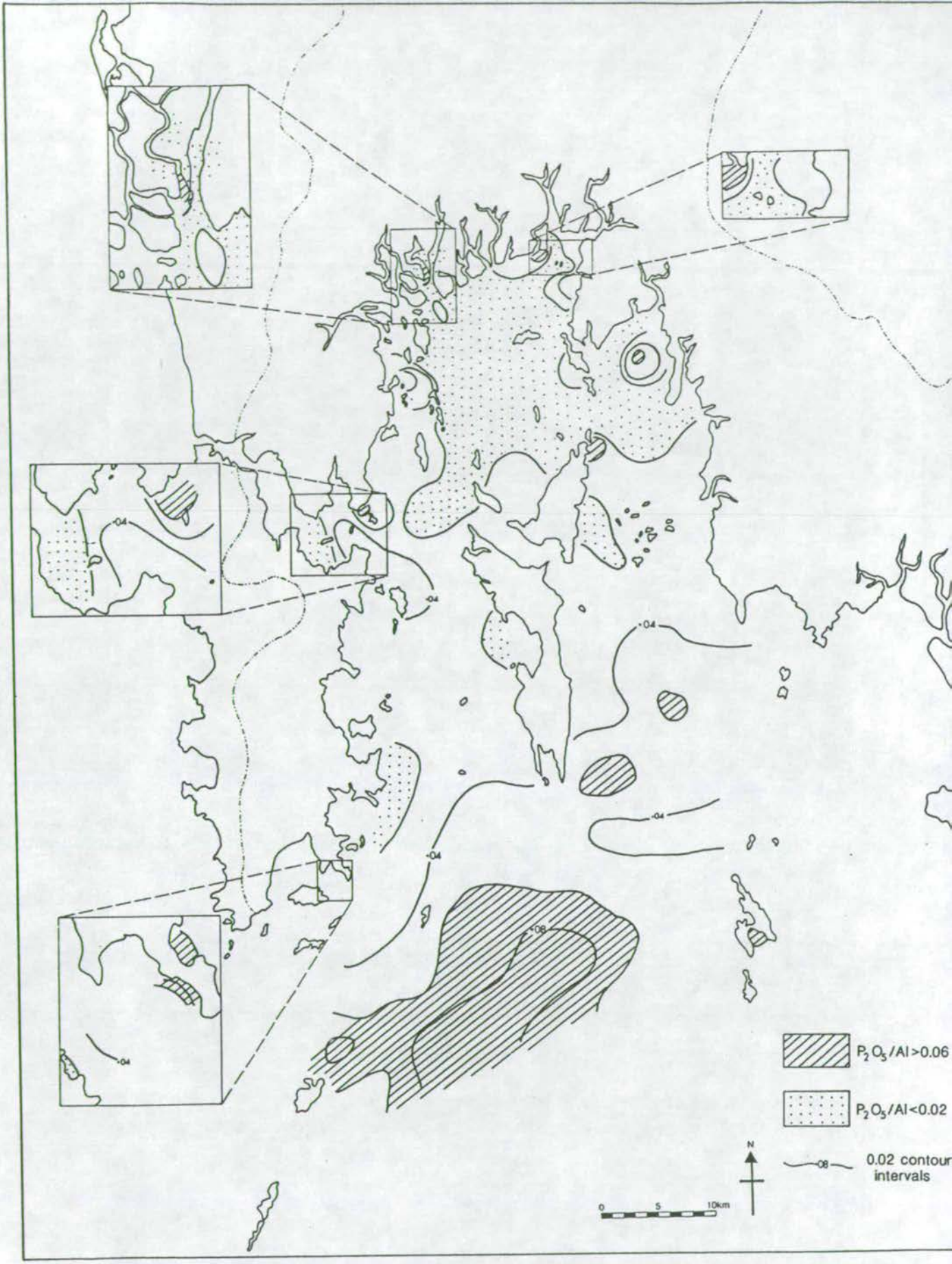

Figure 4.14 Areal distribution of P_2O_5/Al ratios in surface sediments.

mineral concentrations in these sediments. Therefore, although no monazite could be identified by XRD, a corresponding high monazite content would be plausible in this area to account for high P_2O_5 concentrations.

4.4.8 Manganese

The Mn content of Phangnga Bay sediments is relatively low compared to World average shales and carbonates (Table 4.3). Table 4.1 indicates that there is no significant correlation between Mn and grain size, however, Mn does correlate significantly with Al. Like P_2O_5, Mn exhibits a stronger correlation with Fe than with Al which may indicate a dual control on Mn distributions firstly by Fe-complexing (Fe and Mn oxides are readily precipitated together from solution) and then by grain size distribution. Gibbs (1973) found that the main transport mechanism for Mn differed from metals such as Ni, Cu, Cr and Co in rivers as Mn is mainly contained in precipitated metallic coatings as opposed to within crystalline solids or involved in ion exchange reactions. Before precipitation it occurs in the dissolved form as a colloid possibly as a hydrous oxide like Fe (Moore et al, 1979).

Fig 4.15 illustrates Mn/Al concentrations showing a similar pattern to P_2O_5 and Fe. Minerals containing Mn in the drainage basin rocks include rhodochrosite ($MnCO_3$) and Mn-rich almandine garnets in the granites and pegmatites on Ko Phuket (Garson et al, 1975). Garnets were recognised in the panned samples of sediments in the southern area of the Bay and form part of the heavy mineral fraction. Therefore, like P_2O_5 and Fe, high Mn/Al values may represent Mn contained in resistate terrigenous minerals concentrated in the low sea-level stand sediments. Gardner et al (1990) postulated that Mn may be present in the sediments of the Ebro continental shelf either in the form of rhodochrosite which forms diagenetically from Mn^{2+} and HCO_3^- released from Mn-oxides and organic matter in reduced sediments or as one of several Mn-oxyhydroxides. Such a location for Mn is a possibility in Phangnga Bay sediments. They also recorded the correlation of Mn with most other aluminosilicate-related elements as is the case with the Phangnga Bay sediments.

4.4.9 Organic Carbon and Iodine

These two elements are discussed together because of the close association of iodine with organic carbon (C_{org}).

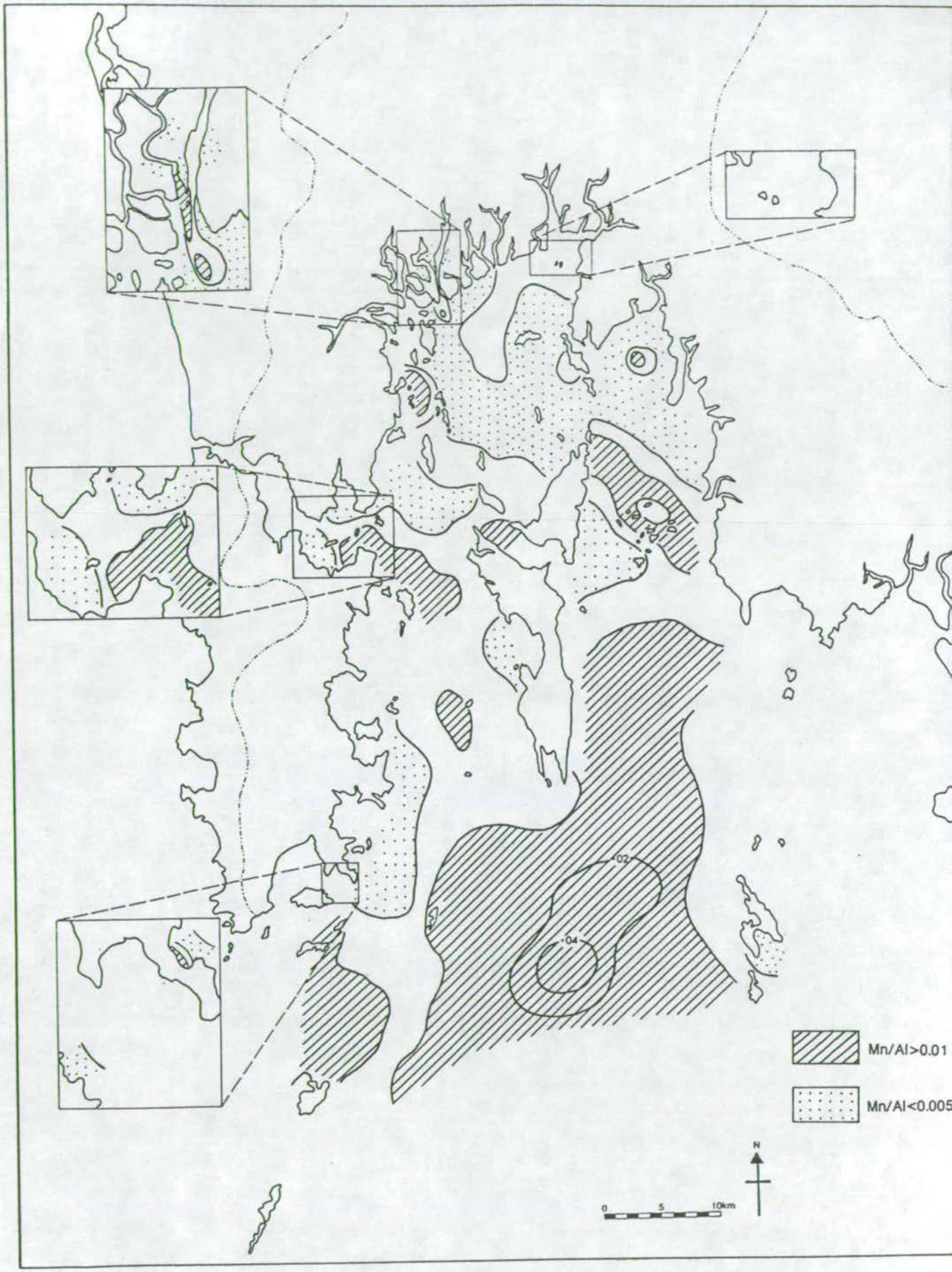

Figure 4.15 Areal distribution of Mn/Al ratios in surface sediments.

The average C_{org} values of Phangnga Bay are much higher than World average values for sandstones, shales and limestones. This is what is expected in a near-shore setting where terrestrial plant biomass production is high (27 dry tonnes/hectare/year - Christensen, 1978) and sediment accumulation rates are high (see Chapter 9).

The C_{org} concentrations recorded in Phangnga Bay sediments are similar to those of other tropical estuaries whose margins are dominated by mangrove swamps (Cook and Mayo, 1980; Risk and Rhodes, 1985) ie approximately 3% around the mangrove edge sediments decreasing to <1% oceanwards (see Fig 4.16a).

The origin of the organic material can be investigated by studying I/C_{org} ratios. Unlike most minor elements, iodine is exclusively contained in sediment organic matter. The I/C_{org} ratio is therefore frequently used to assess the iodine content of sediments. The I/C_{org} ratio is controlled by both the origin of the organic material (OM) and by the oxidation state of the sediment containing this OM. If the OM is derived from a marine source then high I/C_{org} ratios of approximately 250×10^{-4} are usually found (Shimmield and Pedersen, 1990) as marine organisms are known to concentrate iodine from sea water (Shaw, 1962). Terrestrial OM on the other hand, has no relationship with iodine and therefore I/C_{org} ratios in marine sediments rich in terrestrial OM are an order a magnitude lower. The oxidation state of the sediment also affects I/C_{org} ratios as iodine is released from OM on its degradation in anoxic sediments. Therefore, oxic sediment containing marine OM may have I/C_{org} ratios of $250\text{-}350 \times 10^{-4}$ whilst anoxic sediments with similar OM may have I/C_{org} ratios of only 30×10^{-4}.

The iodine content of 34 surface samples for which the C_{org} is known are given in Appendix D. The $I/C_{org} \times 10^{-4}$ ratios for these sediments are illustrated on figure 4.16b. The ratios are all low despite a variation in the oxidation states of the sediments, which indicates that the OM is dominantly from a terrestrial source. However, the increase in I/C_{org} ratios from $\sim 20 \times 10^{-4}$ to $\sim 45 \times 10^{-4}$ from north to south which could initially suggest an increase in the amount of marine-derived OM, may be a result of the anoxic nature of the fine-grained sediments in the north (thus loss of iodine through OM reduction) compared to the coarser, oxic sediments in the south (which retain iodine).

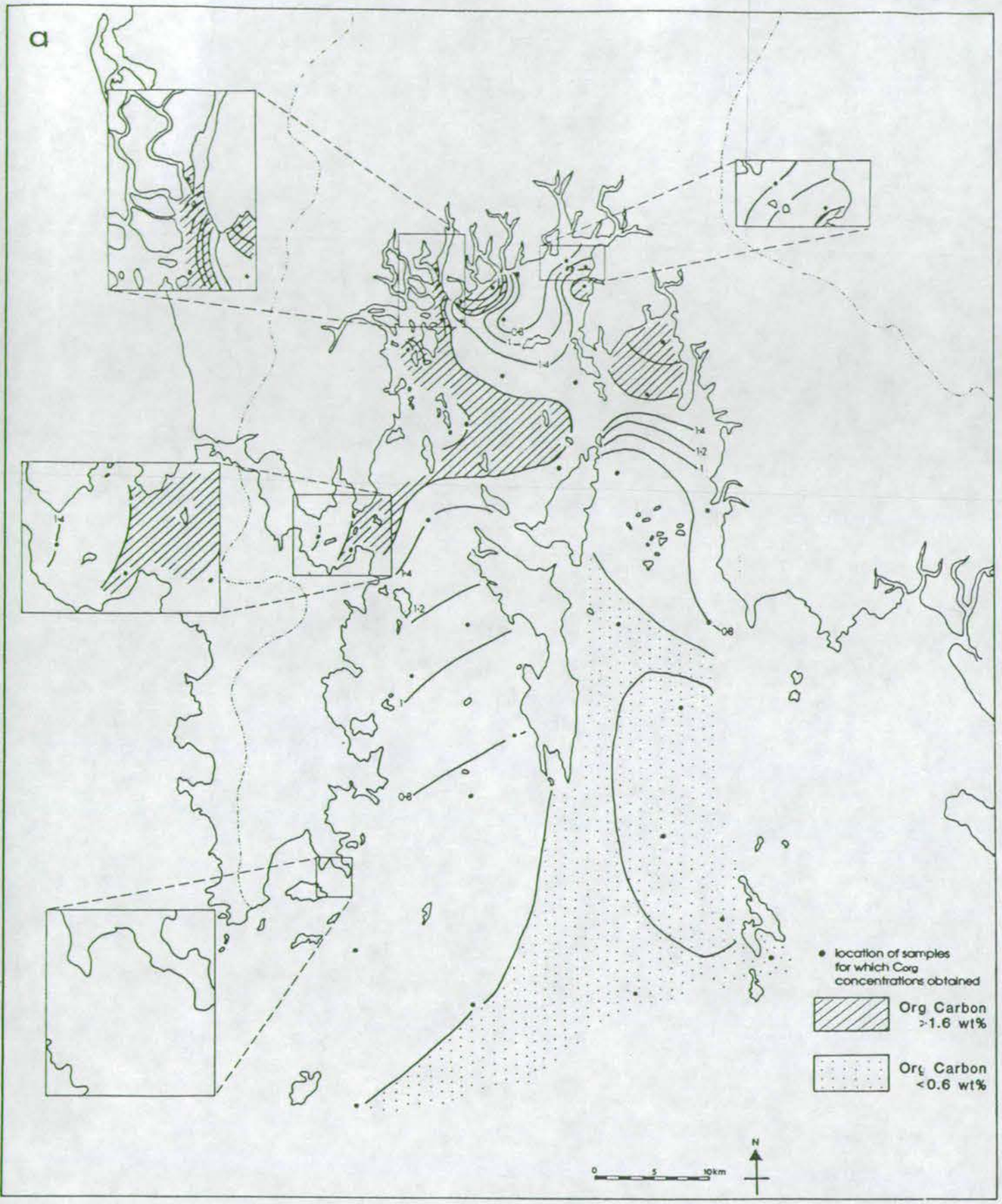

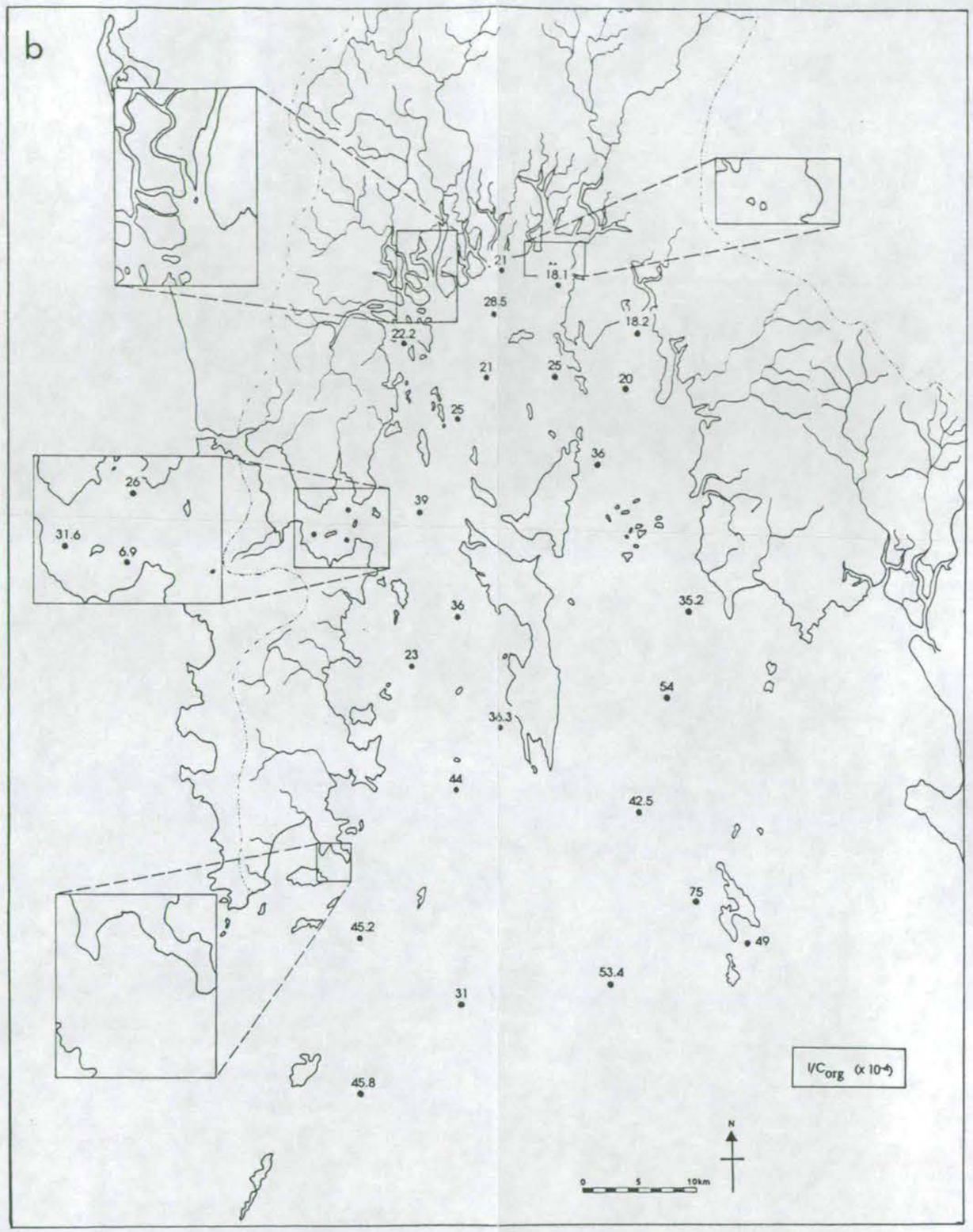

Figure 4.16 a. Areal distribution of organic carbon (Corg) in selected surface sediments.
b. Areal distribution of 1/Corg ($\times 10^{-4}$) in selected surface sediments.

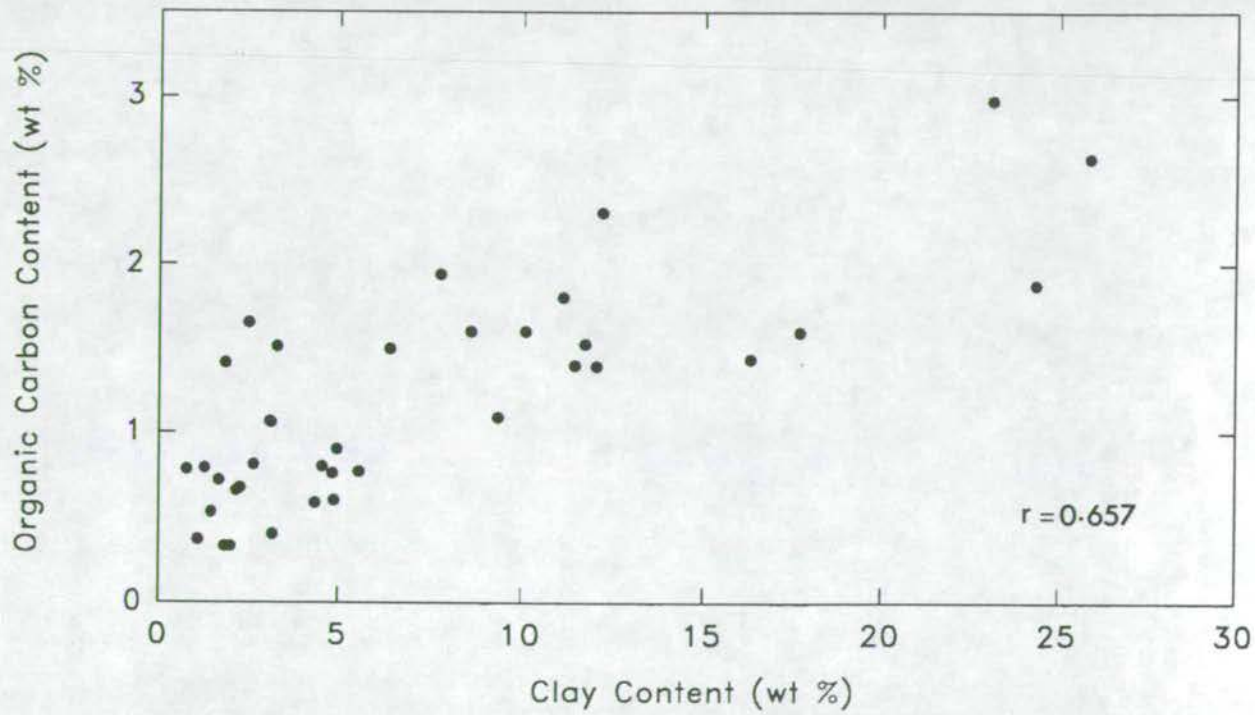

Figure 4.17 Graph of clay v. organic carbon content in selected surface sediments.

The oxidation state of iron directly controls the sediment colour (oxidised iron is orange, reduced is black). Since the oxidation state of iron is influenced by the amount of organics, the sediment colours are probably closely related to the amount of C_{org} in the sediments - dark grey to black in the mangrove swamps (C_{org} > 3 wt%), dark olive green-grey in the northern off-shore sediments (below a 1-2mm orange-brown surface oxidised layer) and pale brown-grey in the southern sediments (< 1 wt% C_{org}). The concentration of C_{org} is correlated to grain size (Table 4.1) with the strongest positive correlation being to clay content (see Fig 4.17) and a negative correlation to sand content (r = -0.677). This is as would be expected as sandy sediments tend to be more oxic than fine grained sediment thus organic matter degrades more rapidly. Additionally, it is unlikely that organic matter settles out in the higher energy southern area. C_{org} also correlates positively and significantly with Ti, Al and V and positively with most trace elements. This reflects the inter-relationship between clays and organic matter as well as the metal-complexing properties of both clays and organic matter.

4.5 TRACE ELEMENT COMPOSITION

Of the 16 trace elements studied, 13 show strong positive correlations with Al (Table 4.1). Because of this association, these elements will be discussed as a group and the remaining 3 elements will be discussed separately.

4.5.1 Aluminosilicate-associate elements

This group includes Rb, Ba, Th, Ce, Nd, La, Y, Nb, Cr, V, Pb, Zn and Ni. The distribution of these elements have been shown in previous studies (Cook and Mayo, 1980; Hirst, 1962 a & b; Moore, 1963) to be governed by the amount of aluminosilicates present. All the above elements show strong correlations with Al in Phangnga Bay sediments thus suggesting the above relationship to aluminosilicates is valid.

The elemental composition of clay minerals changes through the processes of transportation and deposition as a response to varying geochemical conditions, most importantly pH and salinity which vary significantly in the estuarine environment. These compositional changes result mostly from the substitution and ion exchange capacities of montmorillonite and illite clays which allow various ions in solution to either substitute for Al^{3+} or to be adsorbed on to clay particles. The

process of flocculation is particularly important in this respect as the negatively charged clay platelets attract a closely-held layer of cations supplied from the free ions in sea water. Organic matter on the particles, such as mucal films caused by bacterial activity and organics adsorbed from suspension, have positive charges and significantly enhance flocculation. Organic binding makes the flocculates very much harder to break up (Dyer, 1986). The latter is also significant with organic matter particles which are generally abundant alongside clays and with dispersed Fe and Mn oxides and oxyhydroxides (which are precipitated from solution) and are efficient adsorbers and desorbers of metal ions (Goldberg, 1954; Jenne, 1968). However, Loring (1978) calculated for the sediments of the St Lawrence estuary, that 61-93% of Zn, Cu and Pb concentrations are locked up in fine-grained sulphide, oxide and silicate minerals and the rest is weakly held in fine-grained organic material, oxide grain coatings and ion exchange positions. Therefore the presence of detrital minerals has to be considered when discussing these element concentrations. Additionally, the geochemical behaviour of the transition elements is known to be complex (Francois, 1988) due to the chalcophilic and biophilic nature of most of these elements.

Subdividing the 13 elements into groups displaying similar chemical properties (ionic radius and electronegativity being most important in the processes of cation exchange and adsorption) was at first considered necessary in order to try and explain the distributions of element/Al ratios. However, it is clear on studying element/Al correlation coefficients, principal component analysis results and plotting the element/Al graphs that there are 3 groups of elements each showing a distinctive correlation pattern with Al but with the ionic radii and electronegativities varying within each group (see Table 4.5).

4.5.1.1 Group 1 - Rb

Average Phangnga Bay Rb concentrations are similar to World average sandstones. Rb is plotted against Al in Figure 4.18 and shows a reasonably good correlation (r=0.795). However, high Rb samples above the Rb/Al=40 line indicate that there is a significant Rb anomaly in some sediments. The Rb/Al areal distribution is illustrated in Figure 4.19 and there are clearly 2 areas of high Rb anomalies, one in the north and one in the south. The northern distribution of these anomalies coincides with the presence of identifiable lepidolite mica in the sediments as described in Chapter 3. Lepidolite - K_2 (Li, Al)$_{5-6}$ (Si_{6-7} Al_{2-1} 0_{20}) (OH, F)$_4$ - is described by Deer et al (1966) as "one of the few minerals with appreciable Rb content" with Rb substituting for K ions

MAJOR ELEMENTS			TRACE ELEMENTS						
	IR	EN		IR	EN			IR	EN
Al^{3+}	0.535	1.5	Rb^{+}	1.52	0.8	Gp 1	Sr^{2+}	1.18	1.8
Ca^{2+}	1.00	1.0	Nb^{5+}	0.64	1.6	Gp 2	Zr^{4+}	0.72	1.4
			Y^{3+}	0.9	1.2				
Si^{4+}	0.4	1.8	Th^{4+}	0.94	1.3		Sn^{2+}	1.22	1.8
			Pb^{2+}	1.19	1.8		$^{4+}$	0.69	1.9
Mg^{2+}	0.72	1.2	$^{4+}$	0.774					
Fe^{2+}	0.61	1.8	V^{3+}	0.64	1.6	Gp 3			
$^{3+}$	0.55	1.9	Cr^{2+}	0.73	1.6				
			Zn^{2+}	0.74	1.7				
Ti^{4+}	0.605	1.5	Ni^{2+}	0.69	1.8				
			La^{3+}	1.03	1.3				
K^{+}	1.38	0.8	Ce^{3+}	1.01	1.1				
			Nd^{3+}	0.983	1.1				
Mn^{2+}	0.67	1.5	Ba^{2+}	1.35	0.9				

IR = ionic radius for 6-fold configuration (Shannon and Prewitt, 1969)

EN = electronegativity by Paulings method (source, Henderson 1982)

Table 4.5 Ionic ratios and electronegativities and charges of the major and trace elements studied here in their common geochemical form. (13 trace elements are separated into groups according to their apparently similar habit in these sediments.)

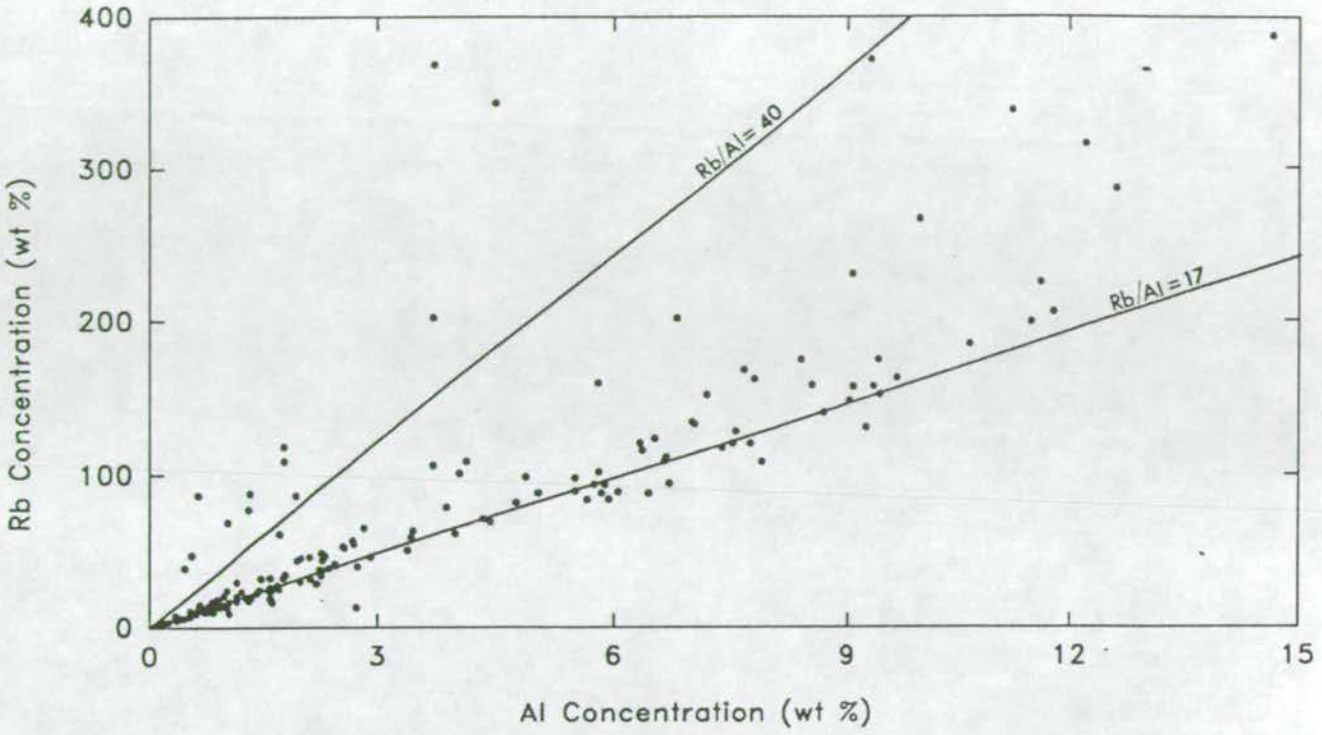

Figure 4.18 Graph of Rb v. Al for surface sediments.

Lepidolite Mica - Electron Microprobe Analyses (concentrations in wt %)							
Rb_2O	0.594	0.610	0.802	0.777	0.487	0.580	0.520
Na_2O	0.377	0.405	0.599	0.575	0.569	0.211	0.407
F	-	1.363	0.188	1.117	1.053	1.077	1.514
SiO_2	44.717	46.056	46.128	45.933	45.104	39.045	43.206
Al_2O_3	31.234	32.532	35.288	35.331	32.859	20.684	30.221
K_2O	10.001	10.339	9.957	10.043	9.906	7.588	9.477
TiO_2	0.192	0.176	0.069	0.077	0.173	2.312	0.173
Fe_2O_3	3.748	3.893	1.025	0.939	3.132	18.212	3.629
MnO	0.211	0.222	0.978	0.966	0.313	0.451	0.197
Total	91.074	95.596	95.034	95.759	93.595	90.160	89.345

Table 4.6 Results of electron probe analyses on 6 lepidolite grains (from sample site 35b).

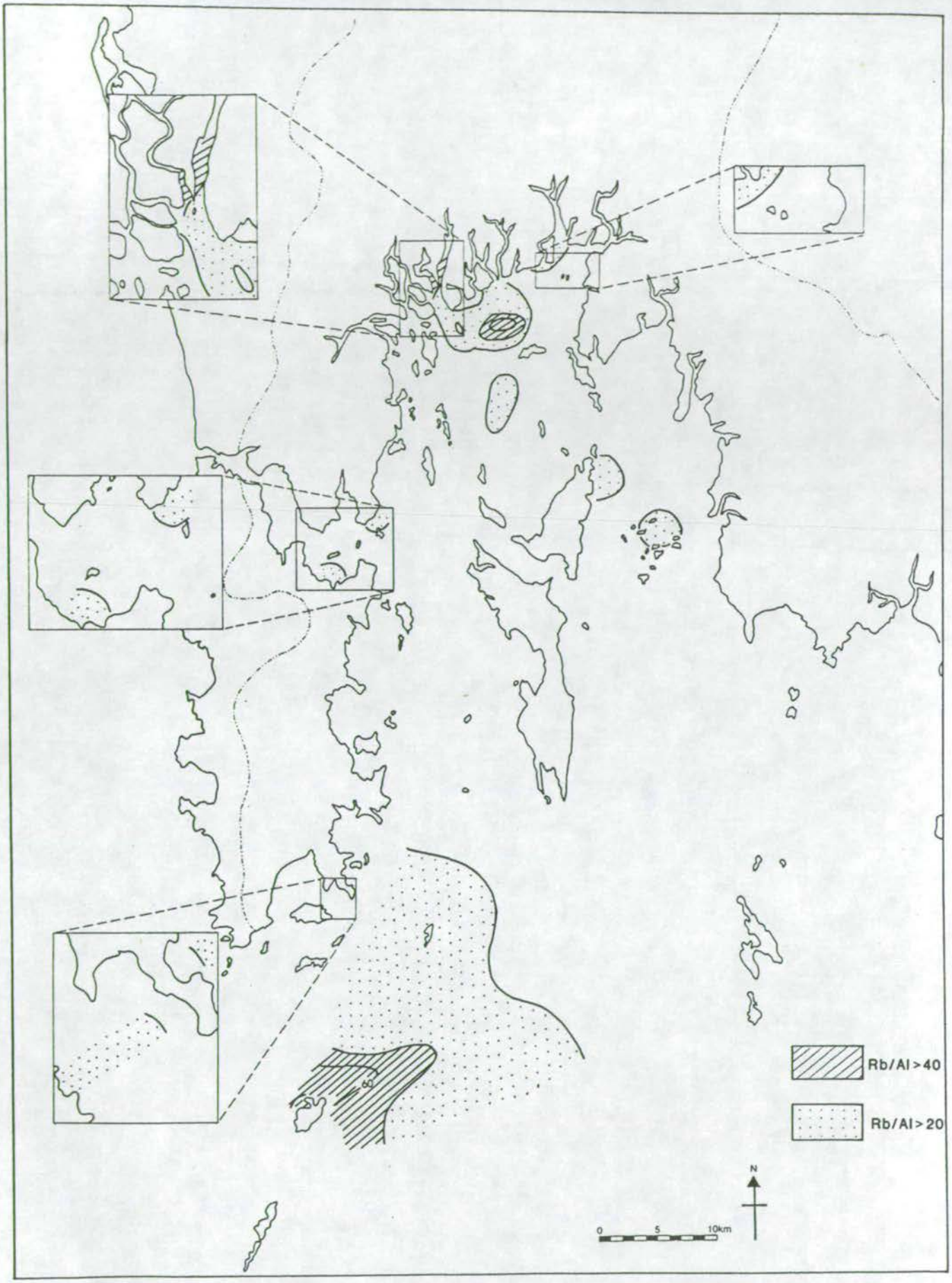

Figure 4.19 Areal distribution of Rb/Al ratios in surface sediments.

as is expected from the comparable ionic radii of Rb and K (Table 4.5). The significant strong positive correlation of Rb with K (r=0.901) is consistent with the theory that the Rb is contained within lepidolite mica. Indeed, Francois (1988) concluded that Rb concentrations in the sediments of Saanich Inlet are essentially controlled by mineral variations as opposed to the more complex chalcophilic or biophilic associations of transition metals.

In order to test whether the Rb is contained in lepidolite mica, a few lepidolite grains were mounted in resin, polished and analysed for their chemical composition using an electron microprobe (see Appendix B). A Rb peak was visible on traces for all grains analysed and although there are problems in quantifying this peak due to its proximity to the Si peak (and hence the difficulty in measuring a background level) seven analyses were obtained and these are listed in Table 4.6. (Totals do not add up to 100% due to the presence of H_2O and Li which are not measured with the microprobe). Rb_2O concentrations vary between 0.5% and 1%. Although lepidolites can have concentrations up to approximately 4% these are rare (Deer et al, 1962). There is a continuous chemical series between muscovite and lepidolite with < 3.3% Li_2O termed as lithian muscovite and > 3.3% Li_2O termed as lepidolite. It is extremely difficult to pin-point which precise terminology should be used by the analysis of XRD peak positions and without knowing the Li concentration this is made even harder. However, comparing the analyses of the Phangnga Bay samples with those published by Deer et al (1962), particularly the Si/Al ratios, suggests that lithian muscovite is a more accurate term for these minerals. The Phangnga Bay samples have an average SiO_2/Al_2O_3 ratio of 1.4 which is intermediate between lepidolites which average 2 and muscovites which average 1.2 (Deer et al, 1962). However, since the term lepidolite has been used previously in this work the terminology of Garson et al (1975) will be adopted whereby "lepidolite" refers to lithian muscovites or true lepidolites ie, any muscovite-type mica with appreciable Li content.

Having confirmed that the Rb is contained in lepidolite, the distribution of high Rb anomalies in the Bay sediments therefore reflects the amount of lepidolite in the sediments. The origin of the northern Rb anomaly is likely to be lepidolite sourced from the lepidolite pegmatite veins along the Phangnga fault zone (Fig 3.3). Although small flecks of mica are visible in the sediments around Ko Racha Yai where the other Rb anomaly is situated, they are too small to be picked out and analysed by XRD. However, it is highly likely, due to the Rb anomaly in this area, that this mica is also lepidolite. The geology of Ko Racha Yai is known to be entirely

biotite granite - the same granite type as is found on Ko Phuket and in NW Phangnga Province (L. Jiemton, Mineral Resources Centre, Phuket - pers. comm.). Additionally, the Klong Marui fault system is thought to run down the western side of Phangnga Bay and through the Ko Racha Yai area (Garson et al, 1975). Since the lepidolite-pegmatites to the NW of Phangnga Bay (Fig 3.3) are known to have formed in close association with the Klong Marui fault system it is entirely possible that similar pegmatites have formed in the southern extension of the fault system and they are either exposed on Ko Racha Yai itself of subaqueously around the island thus sourcing the Rb anomalies in this area. Interestingly there are no low Rb/Al values in the area to the north east of Ko Racha Yai where low Ti/Al, Fe/Al and Zr/Al ratios are thought to represent low heavy mineral concentrations on this slight bathymetric high possibly indicating a vestige of the low sea-level stand topography. Mica is not subject to the same sediment distribution controls as heavy minerals which are concentrated in topographically low areas, hence it could be more easily deposited on this topographic high.

4.5.1.2 Group 2 - Nb, Y, Th and Pb

The ionic radii and electronegativities of these elements are illustrated in Table 4.5. All of these elements show a strong correlation with Al (r = 0.943-0.965 - see Figure 4.20 a-d) and to K (r = 0.865-0.916). This is additionally illustrated in the Figure 4.2b where these 4 elements cluster together close to K compared to the other Al-associate elements. Although Th and Y ions are very similar in size (ionic radii of 0.94 and 0.9 respectively), Pb and Nb are quite different with ionic radii of 1.19 and 0.64 respectively. The high charges of these 4 elements suggest that substitution for K^+ in clays would not occur readily. However, the high positive correlations with K and Al suggest that adsorption onto clays is significant. Additionally, although Pb is known as a chalcophile element, it is found chiefly in acidic igneous rocks in K-bearing feldspars and micas (Krauskopf, 1956) thus possibly explaining the high Pb-K correlation.

4.5.1.3 Group 3 - V, Cr, Zn, Ni, La, Ce, Nd and Ba

All of these elements show a comparatively poor correlation to Al (r = 0.765-0.931) and K (r = 0.593-0.793) relative to group 2. The graphs in Figures 4.21 a-d and 4.22 a-d illustrate this difference. Scatter about the general trend of increasing element to Al is greater than for those elements in group 2. V, Cr, Zn and Ni have similar ionic radii and electronegativities as do La, Ce, Nd (light rare earth elements - LREE) whereas Ba has a comparatively large ionic radius (Table 4.5).

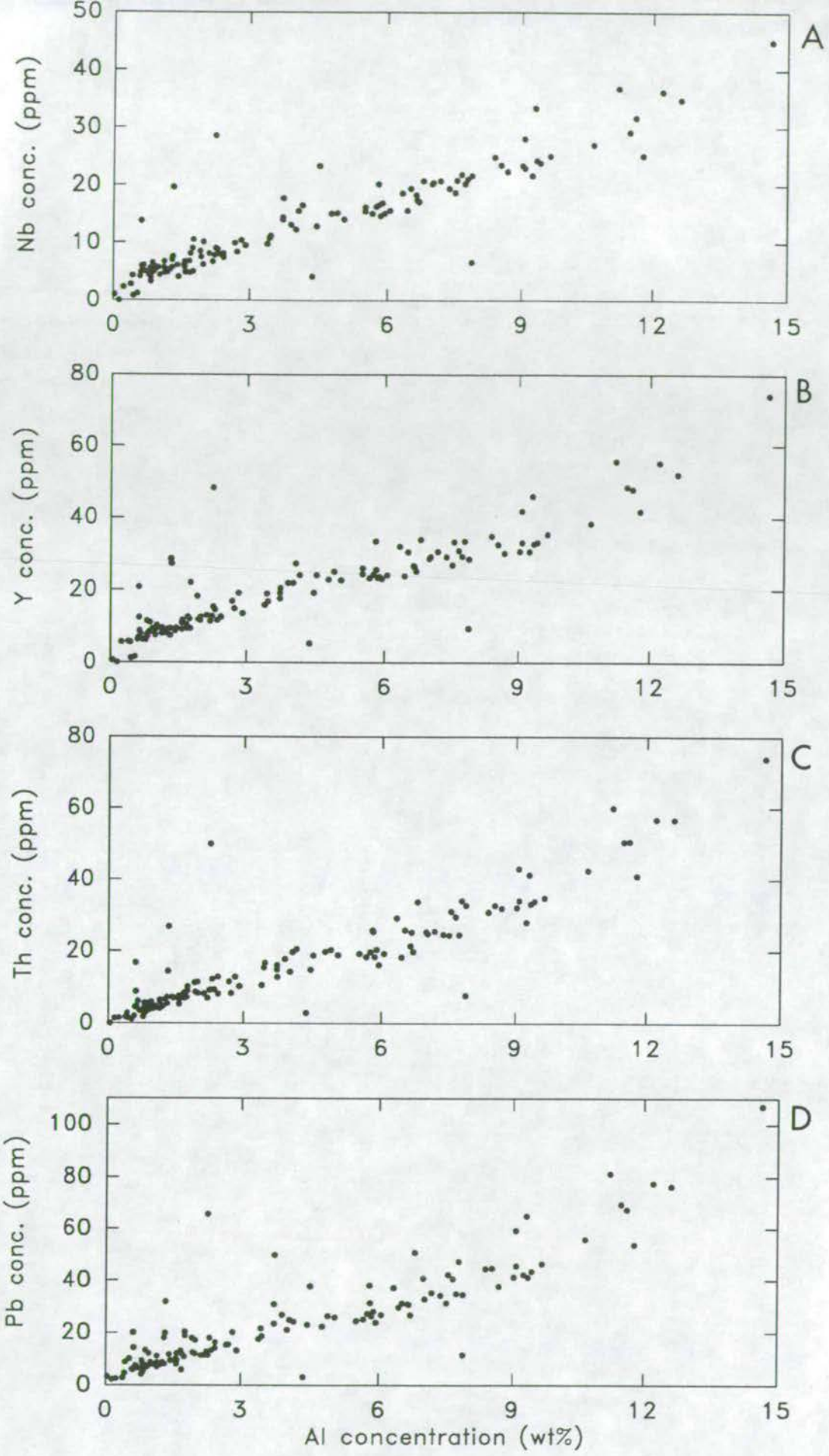

Figure 4.20 Graphs of "Group 2" elements:
a. Al v. Nb, b. Al v. Y, c. Al v. Th, d Al v. Pb

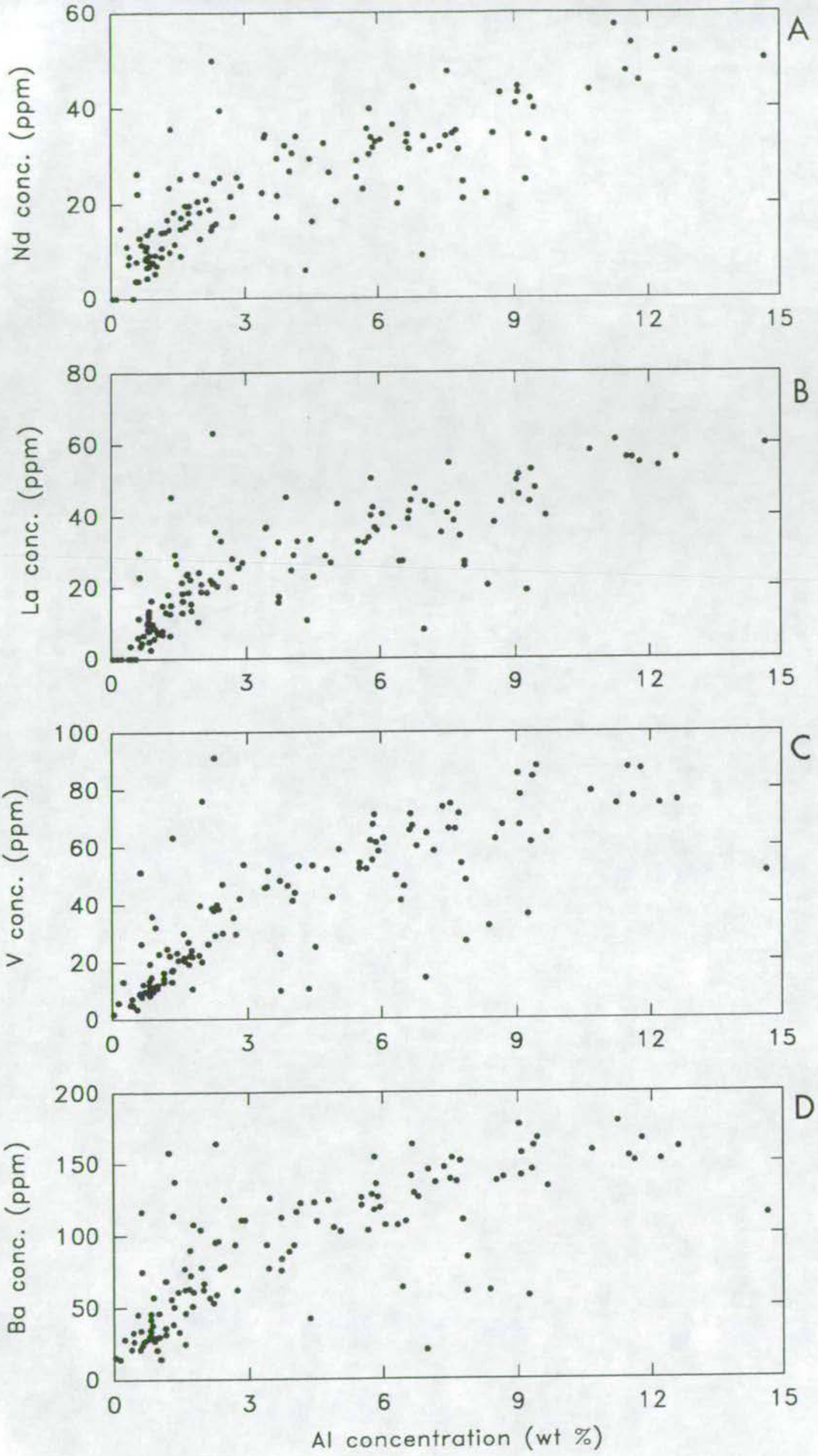

Figure 4.21 Graphs of "Group 3" elements:
a. Al v. Na, b. Al v. La, c. Al v. V, d. Al v. Ba

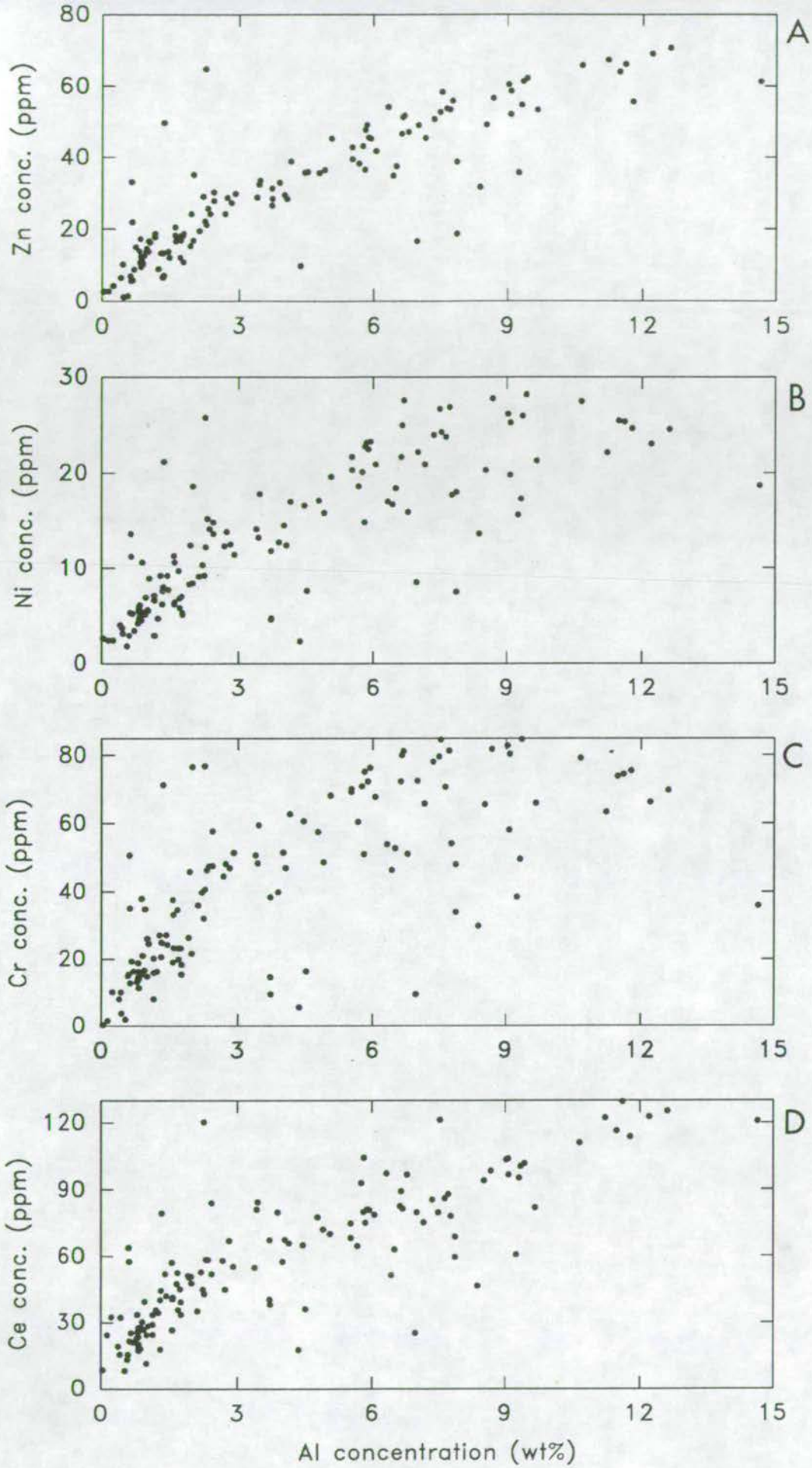

Figure 4.22 Graphs of "Group 3" elements (cont'd):
a. Al v. Zn, b. Al v. Ni, c. Al v. Cr, d. Al v. Ce

In Figure 4.2b Cr, Ni and V plot near Ti and Fe. As discussed earlier Ti and Fe are thought to be contained in heavy minerals as well as in aluminosilicates. Since Cr, Ni and V are commonly found in mafic minerals (Francois, 1988) it is possible that some of the variation in these element concentrations may be due to variations in the distribution of heavy minerals containing these elements. Equally, the close association with Fe and the proximity to P_2O_5 in Figure 4.2b may indicate an association of these transition metals with Fe-oxides which are effective scavengers of transition metals and P_2O_5. Certainly the fact that these elements plot away from Si and Zr (both representing resistate detrital minerals) indicates that there is an association with the aluminosilicates as well as with resistate minerals. La, Ce and Nd are chemically very similar and so their close grouping in Figure 4.2b is not surprising. They plot closely to Al suggesting a stronger association with clays than Cr, Ni and V however the scatter on the Al plots indicates some other control on concentrations possibly due to these LREEs being contained in heavy resistate minerals such as monazite.

Ba has a similar ionic radius to K and is therefore expected to preferentially substitute for K as is generally found in feldspars. Indeed Ba is often used as an indication of feldspar content in shallow marine sediments (Calvert, 1976). However, there is very little feldspar in Phangnga Bay sediments due to its rapid breakdown in the humid climate and so Ba is thought to be dominantly contained in aluminosilicate minerals.

The correlations to Al and K suggest that group 2 elements are preferentially adsorbed onto clays compared to group 3 elements. But the chemical properties (ie, ionic radii, electronegativity and charge) do not seem to adequately explain the grouping of these elements.

4.5.2 Non-aluminosilicate-associate elements

Sr, Zr and Sn fall into this category and each will be discussed in turn.

4.5.2.1 Strontium

Average Sr values for Phangnga Bay (893 ppm) are much higher than world average shales, sandstones or limestones (Table 4.3). However, such an average hides a wide variation in Sr concentrations in Phangnga Bay sediments from 15 ppm to 5092 ppm. Due to the similar ionic radii of Sr and Ca (Ca^{2+} = 1.0, Sr^{2+} = 1.18) Sr can substitute for Ca ions in the $CaCO_3$ lattice (as is suggested by the significant

positive Sr to Ca correlation - all other Sr correlations coefficients are negative). Because of the slightly larger size of Sr^{2+} compared to Ca^{2+}, it can be more easily accommodated in the aragonite lattice as opposed to the calcite lattice. This is reflected in Sr concentration variations between carbonate-secreting organisms with molluscs averaging 2500 ppm Sr in their structures whilst corals average 8000 ppm (Scoffin, 1987).

Sr may also be associated with clays as it can replace K in the clay lattice (Hirst, 1962b). Figure 4.23 plots Sr against Ca - samples with > 5 wt% Al (ie high clay) and < 5 wt% Al (ie, low clay) have been distinguished. In the inset of Figure 4.23 a regression line has been drawn through the Al > 5 wt% samples. This line intercepts the Y-axis at approximately 50 ppm Sr which represents the approximate Sr content of the clay fraction.

Below 8 wt% Ca, samples follow a tight trend but above this level there is a much greater scatter of points. The areal distribution of Sr/Ca ratios of samples with > 8 wt% Ca are illustrated on Figure 4.24. Areas of high Sr/Ca (> 80 $\times 10^{-2}$) correspond with coral reef build-ups with decreasing ratios away from these reefs. Coral reefs have developed around islands within the southern part of the Bay and as far up as the archipelago between Ko Yao Noi and Krabi Province (eastern Phangnga Bay) (see Chapter 1). Debris from these reefs is likely to be responsible for the high Sr/Ca ratios. The Sr to Ca plot (Fig 4.23) shows the Sr/Ca = 60 $\times 10^{-2}$ line which approximates to the average 2000ppm Sr composition found in molluscs. Most of the samples fall around this line indicating the dominance of molluscan fauna (described in Chapter 7) within the carbonate-rich sediments.

4.5.2.2 Zirconium

Average Zirconium values in Phangnga Bay are similar to World average shales. Zr differs from most of the other trace elements in that it shows no significant correlation with either Al or Ca. Zr is found most closely associated with the resistate mineral zircon and the lack of correlation with Al indicates that Zr does not readily form ions in solution and therefore does not substitute in clay mineral lattices and is not available for absorption by clays and organic matter. The correlation of Zr with the silt/clay fraction indicates the fine-grained nature of zircon grains and this has been similarly described in studies by Hirst (1962a) and Spencer et al (1968). (The correlation of Zr with mean grain size may also explain the positive correlation with Al and negative correlation with Ca ie, these are secondary correlations.) On Figure

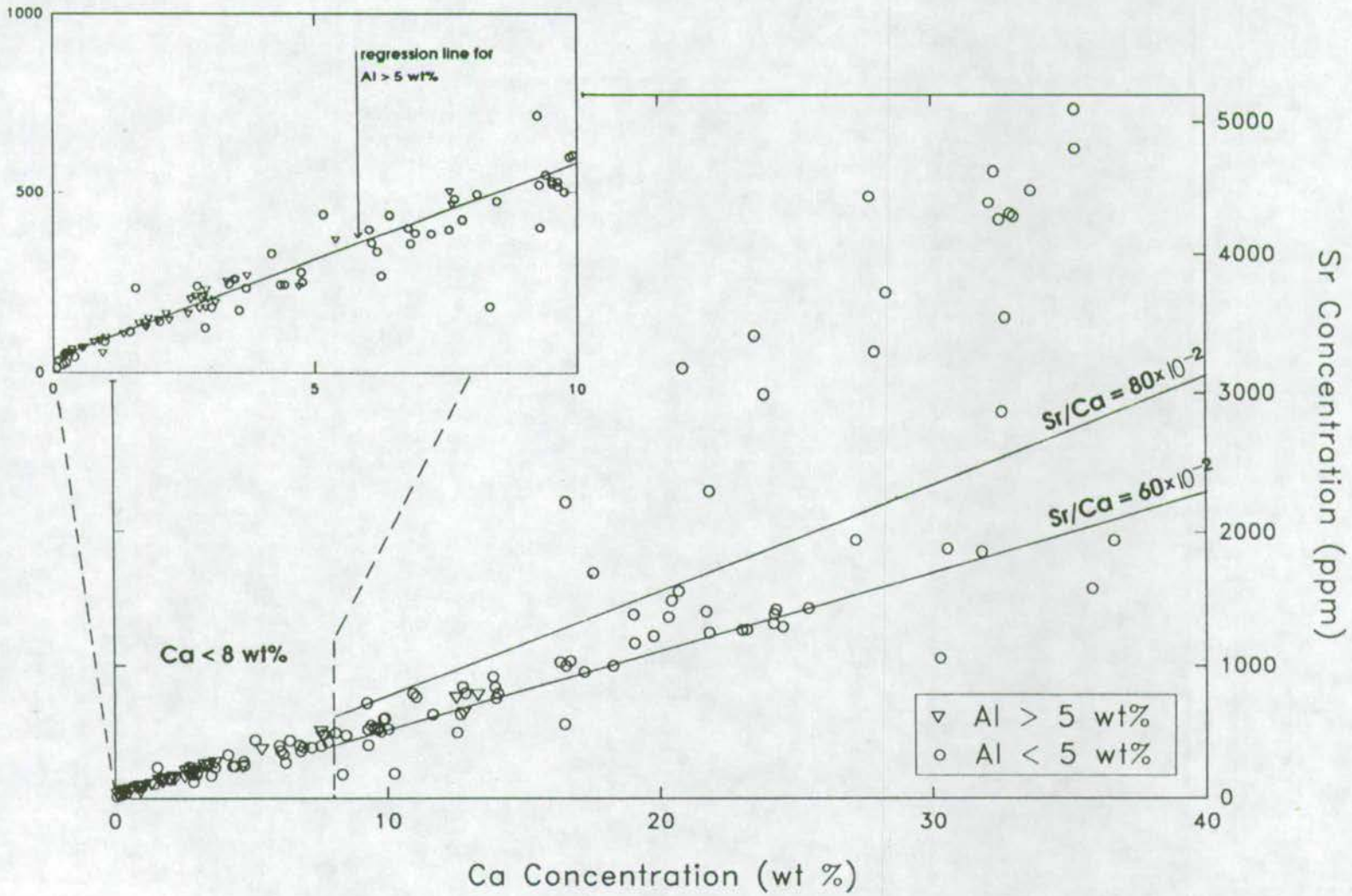

Figure 4.23 Graph of Sr v. Ca for surface sediments (inset shows detail of points from samples with < 8wt% Ca).

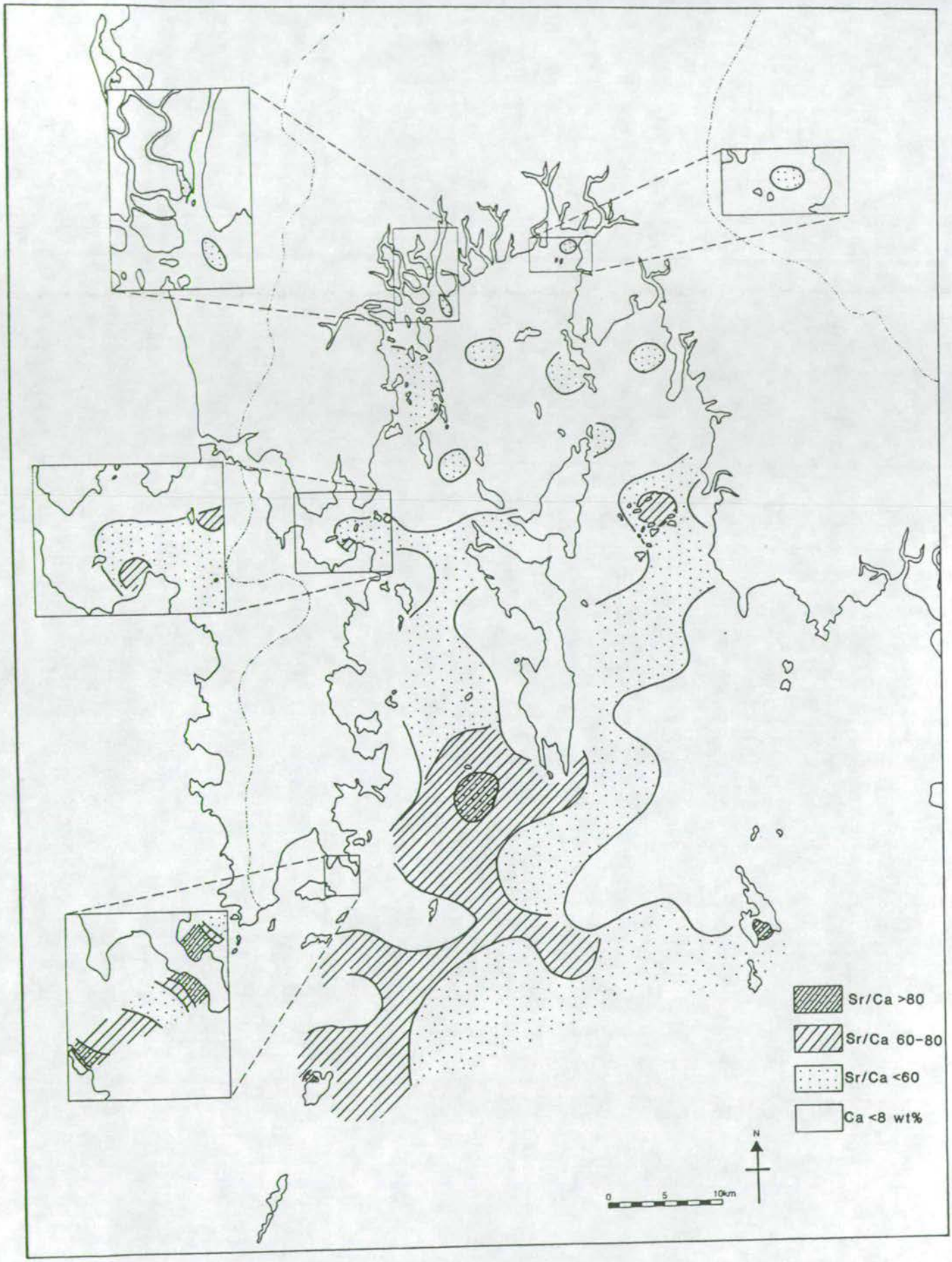

Figure 4.24 Areal distribution of Sr/Ca ratios for surface sediments (only ratios for Ca > 8wt% samples plotted).

4.2a & b Zr plots between the aluminosilicate group and Si reflecting its fine grain size (therefore found in the silt/clay fraction and partially associated with clays) but concentration by sorting with the quartz sand fraction.

Because of this grain size control, Zr is plotted as a ratio to Al (Fig 4.25). This diagram illustrates that high concentrations of Zr are found in mangrove channel mouths, beaches and in a SW-NE trending band across the south of the Bay in a similar pattern to Ti and Fe which as discussed earlier are heavy mineral indicators. The concentrations in beach and channel mouth sediments is explained by the high energy sorting capacities of these environments concentrating heavy minerals. The large area of high Zr values across the south is likely to be a reflection of the relict nature of these sediments as discussed in Chapters 2 and 3. If fluvial material was dumped along the southern edge of Phangnga Bay during low sea-level stands and this material was reworked in coastal environments in subsequent transgressions then concentration of heavy minerals would be expected in this area. The area of low Zr in the north of the Bay represents recent sedimentation - Zr settles out from fluvial transportation before making any progress into the comparatively calm northern waters of the Bay.

Zircons are often enriched in Y (due to the isostructural relationship of xenotime (YPO_4) and zircon - Deer et al, 1966) however, although the Zr/Y correlation coefficient is positive (Figure 4.1) it is not significant and the Y concentration is more strongly controlled by aluminosilicate content than zircon concentration.

4.5.2.3 Tin

Average Phangnga Bay sediment Sn concentrations are 2 orders of magnitude greater than World average sandstones and limestones and double the World average shale (Table 4.3). Like Zr, Sn shows no significant correlation with either Al or Ca (Table 4.1), however, unlike Zr, it also shows no significant correlation with mean grain size. In fact the only parameter that Sn does correlate significantly with is Rb. Hirst (1962a) thought that a high proportion of the total Sn content of sediments from the Gulf of Paria was contributed from the adsorption and co-precipitation of soluble Sn. However, Byrd and Andreae (1986), after studying the geochemistry of Sn in dissolved and particulate form in a series of polluted and pristine estuaries, concluded that rivers supply very little tin to the surface ocean in forms available for geochemical reactions. They note that although Sn may be mobilized during sediment diagenesis in most estuaries, this process is neither widespread or

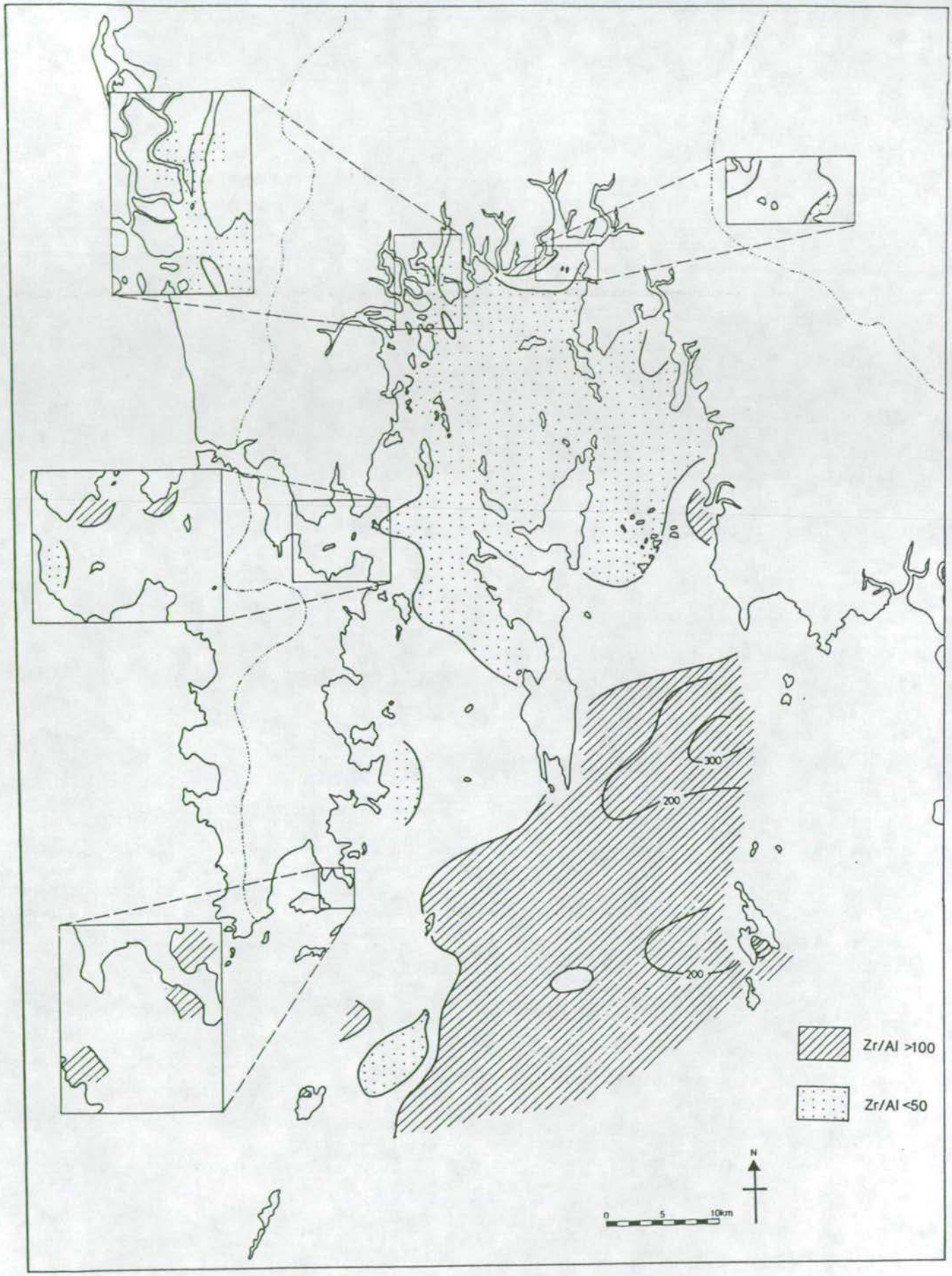

Figure 4.25 Areal distribution of Zr/Al ratios for surface sediments.

important. Most of the Sn weathered from the continents reaches the oceans locked in particulates which are deposited on the continental margins. Although Sn is found in organotin compounds (such as marine anti-fouling paints) which are extremely toxic to marine species (particularly molluscs and fish) and have been shown to be significant pollutants in some estuaries (Seidel et al, 1980), such an input is not yet considered significant in Phangnga Bay compared to the detrital input.

For this reason Sn is a particularly interesting mineral to study as the lack of control by the processes of adsorption or cation exchange by clays or carbonates and hence *to some extent* by hydrodynamic sorting processes, allows an indication of the extent of drainage basin geochemical control on the geochemistry of the sediments. The abundance of Sn in the form of cassiterite (SnO_2) in the surrounding hinterland is discussed in Chapter 1. The presence of cassiterite as a common detrital mineral in sediments derived from Sn-bearing acid rocks as illustrated by the alluvial Sn deposits of Peninsula Thailand, Malaysia and Indonesia attests to this minerals stability and resistance to weathering. Thus Sn ions are not likely to be formed and be made available for adsorption or cation exchange by clays or carbonates, hence the "independent" nature of the element. Figures 4.26a and b graphically illustrate the lack of association between Sn and either $CaCO_3$ or grain size. Figure 4.27 plots Sn on a $CaCO_3$-free basis (thus removing the biogenic dilution factor) for Phangnga Bay sediments, as well as concentrations of Sn measured in stream sediment samples from the drainage basin (data from Garson et al, 1975).

Two areas of anomalous Sn values are evident from this map. One in the north west of the Bay which is likely to be sourced from the tin-bearing granites north west of this area as indicated by the high Sn values in stream sediment samples. The other is in the south west of the Bay. Some of this Sn may be sourced from tin-bearing granites on Ko Phuket (note the < 20 ppm Sn concentration off the coast from Phuket Bay where dredging has recently taken place (Fig 3.4)). However, the correlation of Sn with Rb and the similar locations of anomalies of these two elements may also indicate an unknown source of Sn and lepidolite from on or around Ko Racha Yai. Since cassiterite, like zircon, is a heavy mineral some of the anomaly may also be accounted for by reworking of relict placer deposits during sea-level transgressions.

The lack of cassiterite/lepidolite-bearing rocks in the eastern hinterland and the corresponding lack of any high Sn or Rb anomalies in sediments from the eastern side of Phangnga Bay illustrate the control that the drainage basin geochemistry

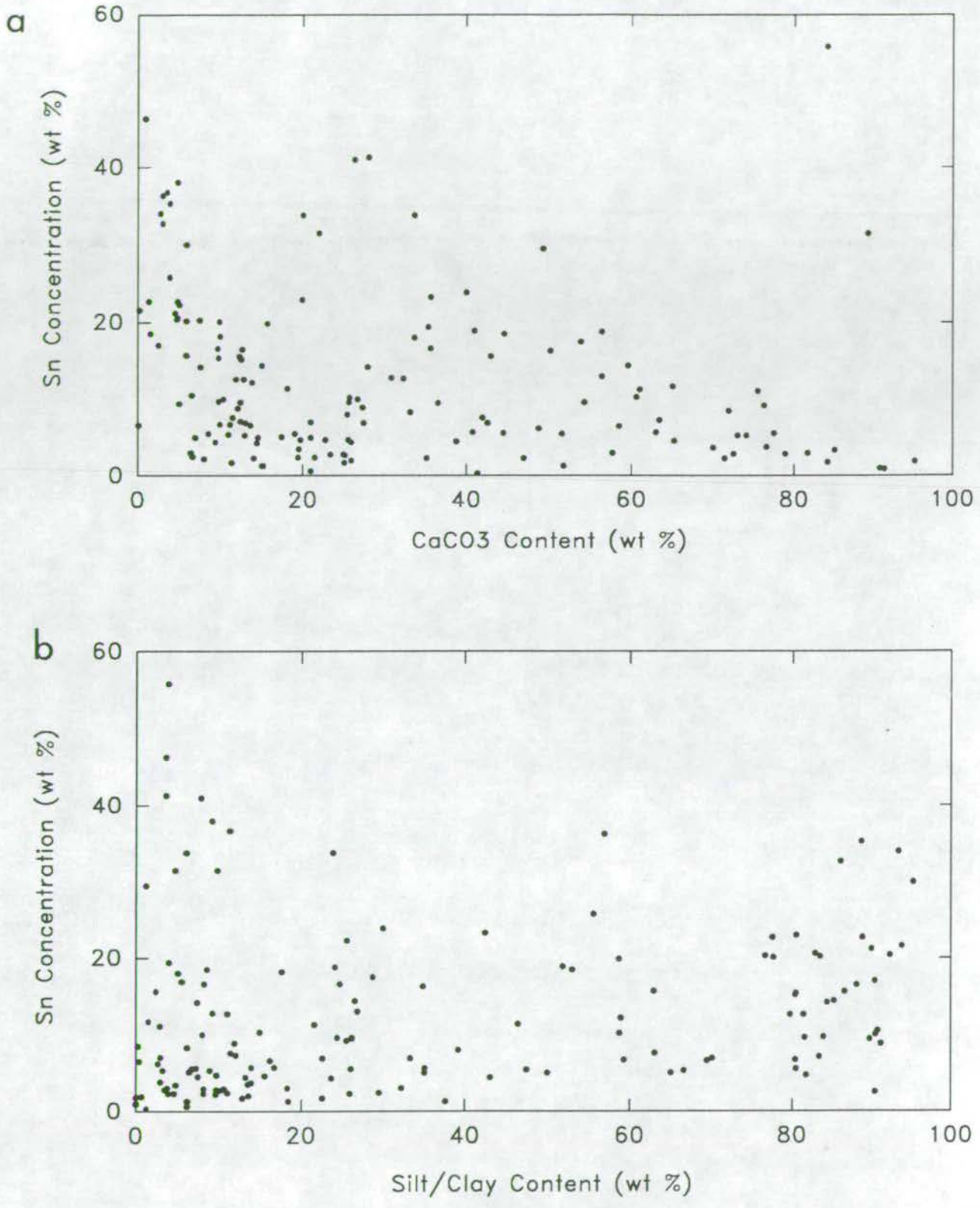

Figure 4.26 a. Graph of Sn v. $CaCO_3$ for surface sediments.
b. Graph of Sn v. % silt/clay for surface sediments.

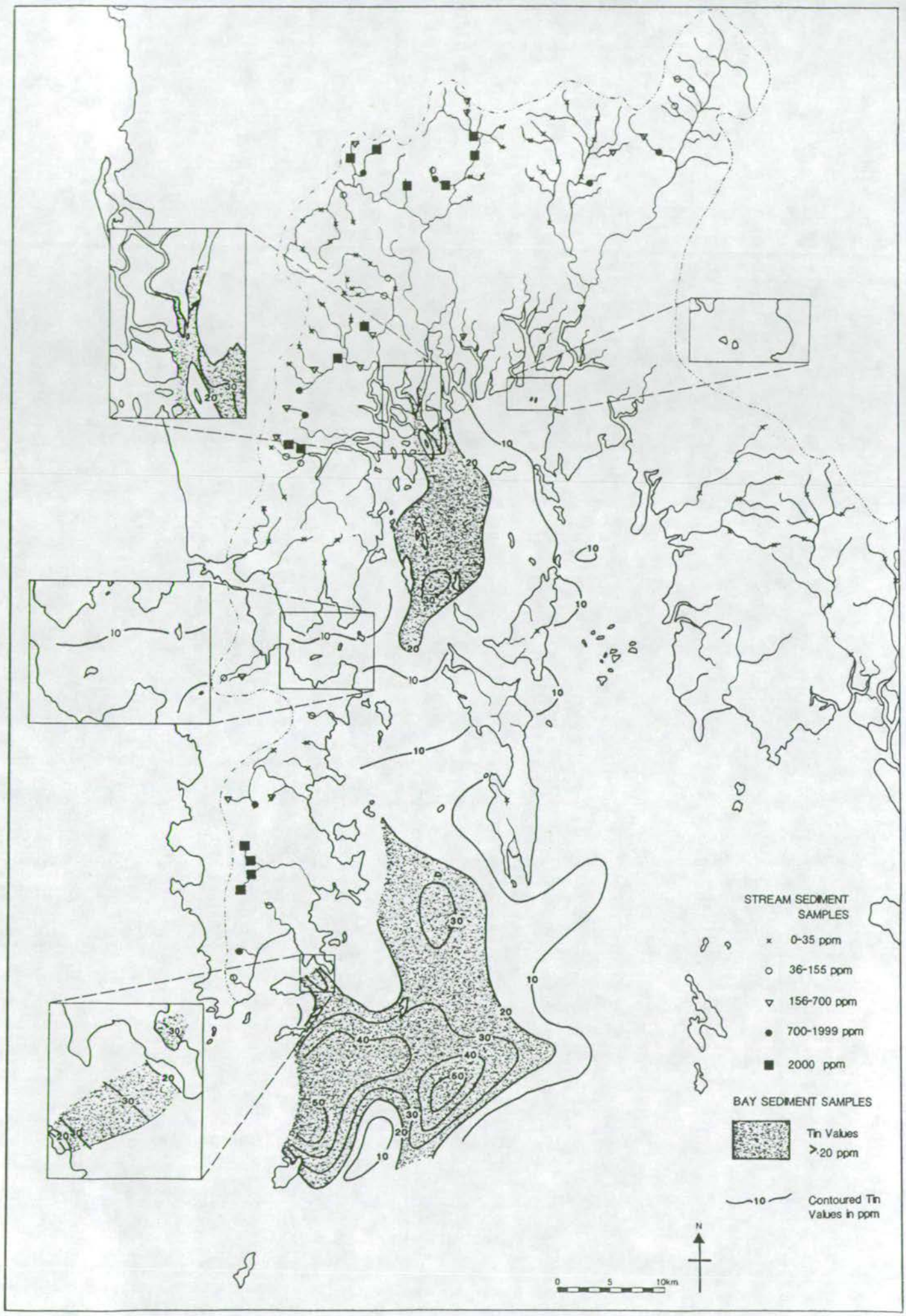

Figure 4.27 Areal distribution of Sn concentrations (for the $CaCO_3$-free fraction of the sediment).

can have on the Bay sediment geochemistry. However, this control obviously depends heavily on the chemical behaviour of the elements considered - only those that are independent of clay/organic matter adsorption processes and hence only those elements that do not readily form ions in solution will be dominantly controlled by the distribution of drainage basin geochemistry as opposed to the strong sedimentary depositional controls on clay distribution.

4.6 DISCUSSION AND CONCLUSIONS

The main controls on the geochemical nature of sediments may be considered as:

a. *source effects* (including variations in the composition of the parent material, conditions under which weathering and erosion occur and the nature of the chemical and physical agents of erosion).

b. *transport and deposition processes* (including the chemical composition and mechanical conditions of the transport agent (ie, wind, ice, water), the amount of mixing from different sources afforded by the transport mechanism, the amount of biogenic mineral precipitation in the transport and deposition environments).

c. *post-depositional processes* (including diagenetic reactions controlled by the redox conditions, the amount of sulphate and organic matter in the sediment, circulation of fluids in the sediment and the rate of sediment accumulation).

Both the source effects and transport and deposition processes affecting the surface sediment geochemistry in Phangnga Bay have been alluded to previously in this chapter and will be summarised in this section. Post-depositional processes have not been studied in this work, however, some consideration of the processes which may be operating in the sediments will be discussed here.

The source effects on sediment geochemistry have had a strong control on the type of material entering the Bay and made available for deposition. Firstly, the composition of the intrusive igneous source rocks in the drainage basin are unusual in their enrichment in Sn and associated elements (these include W and Li which have not been analysed for in this study). Not only have these rocks sourced

anomalous Sn and Rb values in the sediments of the Bay compared to World average sediments but the limited distribution of these rocks in the catchment area on the western side of the Bay (on Ko Phuket, in western Phangnga Province and along the Klong Marui fault which is thought to run north-south just to the east of Ko Phuket) has led to anomalously high Sn and Rb values only in the north and western side of the Bay. However, although there is this catchment geochemistry control on certain element distributions, this is only possible due to the geochemistry of these particular elements. Sn is concentrated in cassiterite in this area and since cassiterite is extremely resistant to chemical attack, the Sn is locked in particulate form and is unavailable for adsorption or cation exchange by clays or organic matter. The fact that Sn is contained in the heavy mineral fraction makes it less susceptible to the wide sedimentological distribution effects operating on the clay fraction and it is thus concentrated in areas comparatively near to source on the western side of the Bay. Although the associated mineral lepidolite mica is less resistant to weathering breakdown than cassiterite, Rb is still locked in its lattice and near-source lepidolite concentrations in bay sediments lead to anomalously high Rb/Al values.

The climatic conditions under which the source rocks in the catchment area have been eroded have also strongly affected the mineralogy and geochemistry of the resulting material deposited in the Bay. Intensive chemical weathering results from the warm humid conditions. A study of soil formation in a similar climate in Brazil (Kronberg et al, 1979) showed that intense chemical weathering leads to a product soil essentially in the system SiO_2-Al_2O_3-Fe_2O_3-H_2O. The first stages of weathering lead to the formation of smectitic clays and eventually after leaching of metal ions into solution only the minerals quartz, kaolinite, gibbsite, goethite and hematite are left. Since smectitic clays are present in Phangnga Bay sediments the weathering and leaching in the catchment basin cannot be so intense as to remove all metals from the soil as solutes - some formation and transport of smecttitic clays must occur. However, the main terrigenous minerals in the Bay sediments are kaolinite and quartz (hematite and goethite are also evident in some oxidised sediments) indicating that intense chemical weathering plays an important part in the composition of the Bay sediments. The production of large quantities of terrigenous organic matter in the catchment area (again as a result of the climatic conditions) leads to high organic matter concentrations particularly in the near-shore sediments and this is also an important factor in the geochemical composition of the sediment due to the metal ion adsorption properties of particulate organic matter.

The transport and deposition processes include the factors which control the fixing of metal solutes into particulate form available for deposition. They also include the processes which mix and sort the incoming terrigenous material into clay-dominated and quartz sand-dominated assemblages and distribute this material around the Bay. The abundance of biogenic carbonate is also effectively controlled by these processes due to their control on the varying physiochemical environments throughout the Bay, some of which are more conducive to carbonate-secreting organisms than others.

Most of the river-borne dissolved constituents entering the oceans are removed by a variety of processes which help maintain the relatively constant chemical composition of sea-water. Much of this removal occurs at the fresh-water/sea-water interface due to the wide variation in physiochemical conditions. The processes of flocculation, coagulation and precipitation of dissolved inorganic and organic matter during the mixing of river and sea water are the most important mechanisms for the removal of Fe, Mn, Al, P, C_{org} and trace metals. The close association of Fe, K, P_2O_5, Mn, C_{org}, Ti, Rb, Nb, Y, Th, Pb, V, Cr, Zn, Ni, La, Ce, Nd and Ba with Al (the "clay indicator" element) in all the sediments of the Bay shows that these elements, on release from their mineralogical matrix in the drainage basin rocks, either immediately become part of a neo-formed clay mineral (smectitic in composition) or are leached from the product soil as solutes and are carried by rivers into the Bay. On the change in physiochemical conditions (ie, pH and salinity) at the fresh-water/sea-water interface they flocculate (if in colloidal form) or substitute into clay lattices or are adsorbed onto clays/organic matter thus becoming part of the clay fraction.

The processes of deposition controlled by the hydrodynamic conditions in the Bay affect the sorting of the clay fraction from the coarser quartz-dominated fraction. The environments of deposition are discussed in the next chapter but suffice to say here that in some areas this sorting is complete with dominantly quartz sand sediments and dominantly clay sediments and in others the fractions are mixed in varying proportions. Different clays within the clay fraction are themselves sorted by their varying particle size (small kaolinite settles first, larger illite and montmorillonite particles settle further from source) thus affecting the overall sediment geochemistry.

The distribution of high anomalous Sn concentrations in the northern recent sediments gives a hint as to the prevailing currents operating in the Bay. The fact that the Sn anomalies are restricted to the western side (close to the source area in the drainage basin) indicates there are no major west to east circulatory currents sweeping around the northern area of the Bay. Looking at the bathymetry of the Bay and considering the distribution of Sn and the generally different patterns of element concentrations on either side of the Ko Yao islands, suggests that Phangnga Bay can be divided longitudinally into 2 sub-basins which are only connected by a narrow passage to the north of Ko Yao Noi. Such a division was recognised by Hummel and Phawandon (1967) who described the western side of the Bay as the Ancient Phangnga River basin and the eastern side as the Ancient Marui River basin.

A major part of the sediment variation in Phangnga Bay is due to a mix of recent and relict depositional processes. Most of the clay-dominated sediments which control the distribution of the majority of elements are of recent origin whilst in the south the sands are of relict origin deposited during low sea-level stands. Although quartz is the dominant terrigenous mineral in these sediments, heavy minerals are also significant in their concentrations.

The excess Fe, Ti, Mn, P_2O_5 and Zr values concentrated in the southern sediments are all thought to be due to this heavy mineral concentration. These heavy minerals were concentrated in alluvial/shallow coastal environments during low sea-level stands where clay minerals were winnowed away. Reworking of these sediments during subsequent transgressions was likely thus further concentrating the heavy minerals. The northern-most extent of these exposed sediments is controlled by the extent of deposition of recent fine sediments which if they are transported into this southern area, cannot settle due to higher energy conditions. The SW-NE trending line of demarcation from south Ko Phuket to Ko Yao Yai to Krabi reflects the higher energy hydrodynamic conditions in this southern part of the Bay especially during the strong SW monsoon. Ko Phuket protects the rest of Phangnga Bay from the storm waves generated in this monsoon. The lack of heavy mineral concentrations in a small area to the north east of Ko Racha Yai on a slight bathymetric high is perhaps representing some vestige of the low sea-level stand topography. Extreme heavy mineral concentrations would be expected in the relict alluvial channels of this topography however these would be of too low a resolution to be picked up on this sampling scale.

The third major mineralogical and geochemical component picked out by correlation and factor analysis is the biogenic carbonate fraction which controls Ca, Sr and to some extent Mg concentrations in the sediments. The major control on the $CaCO_3$ distribution is the physiochemical environment. Most carbonate-secreting organisms require relatively clear water, constant temperature and salinity and oxic sediments. Such conditions occur in the south of the area thus there are increasing Ca and Sr values southwards. The Sr and Mg concentrations are particularly affected by the type of carbonate-secreting organism. Echinoderms and benthic foraminifera in particular secrete skeletons of HMC, and aragonite-secreting organisms such as corals and molluscs include higher concentrations of Sr in their skeletons. Hence there is a strong biogenic control on the distributions of Ca, Sr and Mg in the sediments.

Although a diagenetic study is not part of this work it is relevant to postulate on changes that may take place below the surface oxidised layer found particularly in the finer sediments in the northern half of the Bay.

On deposition and burial of the sediment, oxidation of organic matter by the action of aerobic bacteria eventually removes all the dissolved oxygen in the pore water therefore reducing the oxidation potential (Eh) of the sediment. Thus below the thin orange oxidised layer is reduced sediment. Further organic matter oxidation is facilitated in this reduced sediment by obtaining oxygen from secondary sources such as sulphates (from sea-water and reduced by sulphate-reducing bacteria) and Fe-Mn oxides (from the sediment). The reduced Fe (Fe^{2+}) and sulphide may then combine to form pyrite. In most of the dark reduced sediments there is a strong hydrogen sulphide smell and the abundance of Fe suggests that it is likely that pyrite is forming. Other elements are known to form sulphides in reduced sediments (eg, Cu and Zn - Kitano et al 1980) and so it is possible that such sulphides are also present in the Phangnga Bay sediments. Reducing Fe^{3+} and Mn^{4+} to their soluble Fe^{2+} and Mn^{2+} states also allows their upward diffusion back into the oxidised zone where they re-precipitate as insoluble Fe^{3+} and Mn^{4+}. This is more usually the case for Mn rather than Fe as Mn-sulphide is highly soluble unlike Fe-sulphide.

The early diagenesis of clays deposited in shallow marine areas was considered by Drever (1971) in sediments of the Banderas Bay which drains the Rio Ameca Basin in Mexico. He concluded that Mg is taken up by clay minerals in anaerobic sediments

from pore waters replacing Fe which is removed from the clays to form sulphides. There was no evidence for the uptake of K^+ or Na^+ by the land derived clays except during initial ion exchange and glauconite formation. However, Nelson (1960) noted some uptake of K^+ as well as Mn^{2+} on degraded illite in estuarine sediments. In general, there is a lack of evidence showing significant changes in the structure of clay minerals do occur on shallow burial. Rather the effects of organic matter oxidation and sulphate reduction are more important in the early diagenesis of these sediments.

CHAPTER 5

THE SEDIMENTOLOGY AND GEOCHEMISTRY OF RECENT DEPOSITIONAL ENVIRONMENTS

CHAPTER 5 - SEDIMENTOLOGY AND GEOCHEMISTRY OF RECENT DEPOSITIONAL ENVIRONMENTS

5.1 INTRODUCTION

A depositional environment can be described as "a complex of physical, chemical and biological conditions under which a sediment accumulates" (Krumbein and Sloss, 1963). These conditions affect the grain size, mineralogy and geochemistry of the sediment and therefore their definition is an important aspect in examining the underlying controls on sediment variations. These variations have been described in the previous 3 chapters and some of the controls have been alluded to, however, this chapter aims to define these more precisely. Depositional environments will be classified according to their present day geomorphology and water depth and the sediment characteristics of these environments will be described. The next chapter classifies the sediments by the opposite approach of finding populations of sediments with similar characteristics using grain size and geochemical variables alone.

By defining the sedimentary and geochemical processes operating in the Bay at present, a model can be developed which can be used to predict the effect of anthropological influences such as the addition of heavy metal pollutants on the Bay sediments. Since such shallow sheltered marine environments act as a sink for any effluents or pollutants the potential effect of such additions needs to be predicted to enable a resource management programme to be effective.

The identification of depositional environments is a major objective in the study of ancient sedimentary sequences and only by the description of modern environments can these ancient analogues be defined. Since grain size and geochemical data in ancient sequences is easily obtained the results of this study can have applications in helping to identify ancient analogues.

5.2 DEFINITION OF THE DEPOSITIONAL ENVIRONMENTS

In general terms, Phangnga Bay can be described as a combination of estuarine, shallow, sheltered marine and more open marine depositional environments. The

estuarine environment is restricted to the northern limit of the Bay around the mangroves but its extent varies seasonally. In the rainy season the diluting effect of fresh water flow can extend up to 10km further south into the Bay than in the dry season when lowered salinities (25-30 ppt) are restricted to mangrove areas (Limpsaichol, 1989). However, within this broad description there are a number of depositional environments which can be distinguished by the geomorphology and water depth of the deposits which result from them. Eight such environments have been distinguished:-

1. The **mangrove swamp** environment develops in the upper part of the intertidal zone and extends into the supratidal area (the latter area was not examined at in this study). The largest development of mangrove swamps is around the northern coast of Phangnga Bay. There are smaller pockets in sheltered bays further south but these have not been sampled. The mangroves form very dense vegetation growing on soft grey-brown oxidised peaty mud which becomes anoxic below 1-2cm (Limpsaichol, 1978). The most important mangrove species colonising around Phangnga Bay are *Rhizophora apiculata* and *Rhizophora mucronata* (Christensen, 1978).

2. The **mangrove channels** are also located within the intertidal zone, dissecting the mangrove swamps and extending into the open intertidal zone. Some channels extend landward into entirely freshwater alluvial channels although most start as smaller channels within the mangroves and are only influenced by tidal processes. The channels are restricted in areal extent although they can reach up to 150m wide at the channel mouths. The channels are flanked by muddy banks stabilised by mangrove vegetation. Although no channels were viewed at low tide, it is known from other studies (Cook and Mayo, 1978, Risk and Rhodes, 1985) that they generally have a v-shape cross-sectional form.

3. The **open intertidal** environment extends from the mangrove swamp front to the lowest low water level although this boundary is gradational into the shallow marine environment (see below). The larger mangrove channels extend through the open intertidal zone and grade into the shallow marine environment with no exposure at low tide.

4. The **shallow marine** environment extends from the open intertidal environment and mangrove channel environment southwards and is entirely sub-tidal. The

southern-most limit bounds with the open marine environment and this boundary follows the 20m isobath. This is a somewhat arbitrary boundary and may not be very representative of an actual change in depositional conditions.

5. The **open marine** environment extends seaward from the shallow marine environment at depths greater than 20m, continuing outside of the field study area across the continental shelf.

6. The **beach** environment contains sand and gravel sediment deposited in the more exposed littoral areas which exist predominantly in bays in the southern part of the study area.

7. The **reef top** environment consists of fringing reefs commonly with intertidal reef flats 100-200m wide.

8. The **reef front** environment is generally a narrow zone (10-50m wide) from 1-10m water depth seaward of the reef where a mixture of reef-derived calcareous debris and terrigenous sediment accumulates on a gentle slope.

Most of these terms are self-evident and have been used for similar environments by other workers (Thom et al, 1975; Cook and Mayo, 1978; Risk and Rhodes, 1985; Bird, 1986). Both tidal range and biota (particularly mangroves and coral reefs) have an important influence on sedimentary processes operating within the Bay. The position within the tidal range affects sedimentological processes through variations in water depth and current strength - hence the term open intertidal is used. Similarly, mangroves act as a sediment trapper and binder and coral reefs act as a sediment supplier and may also act as a sediment trapper. Therefore these biotic terms are brought into the classification. This classification does not include textural or lithological terms for the reason that such terms may not adequately describe any variation in sediment types that may be present within one depositional environment.

A schematic diagram of these depositional environments is illustrated in Figure 5.1 and their areal distributions are illustrated in Figure 5.2. This latter diagram was compiled from bathymetric data, field observations and published map information. Sampling coverage of the 8 environments varies due to both their varying areal extent and restrictions on access for sampling (especially in mangrove swamps and

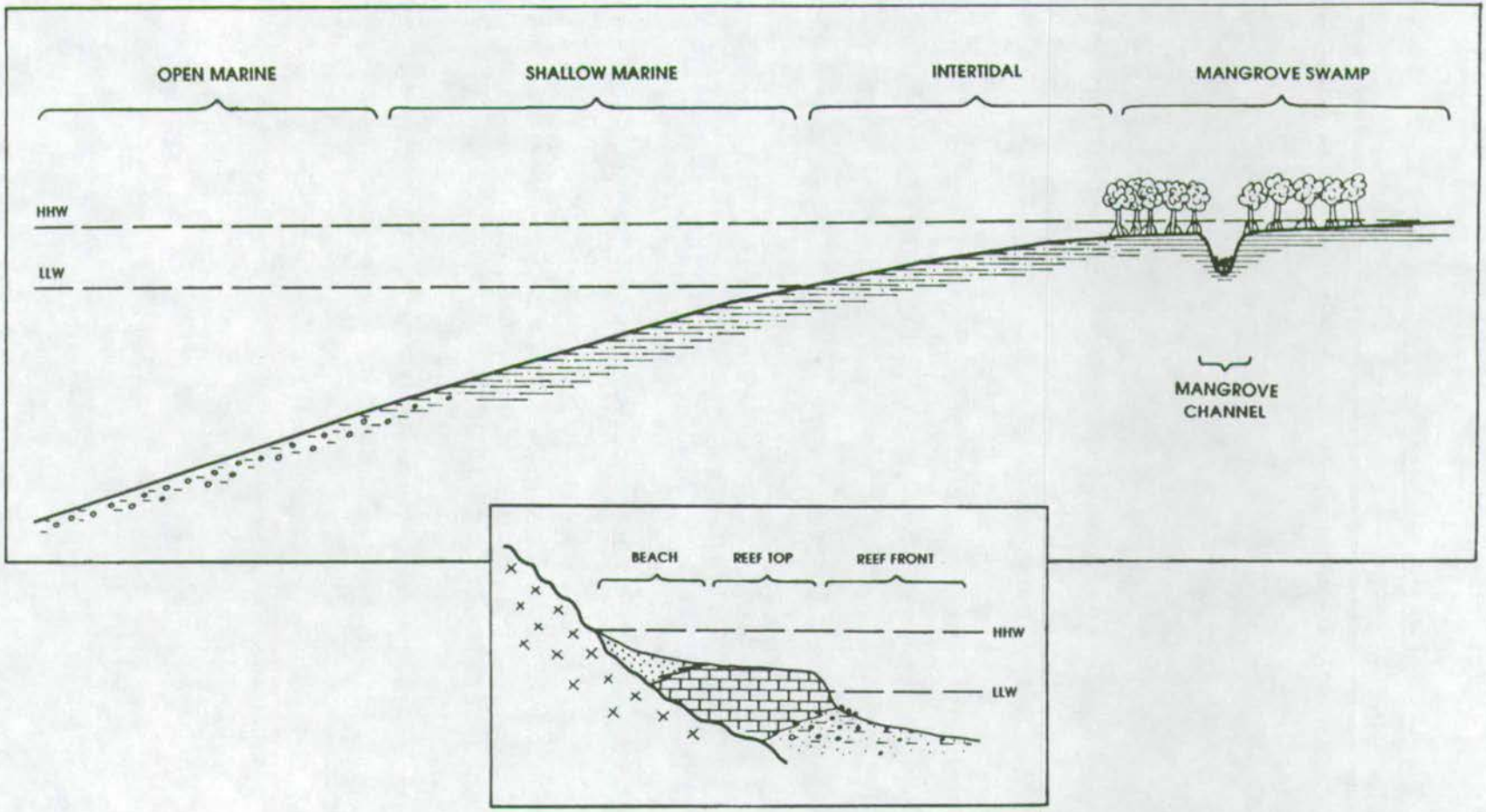

Figure 5.1 Schematic representation of the depositional environments of Phangnga Bay (horizontal scale is exaggerated)

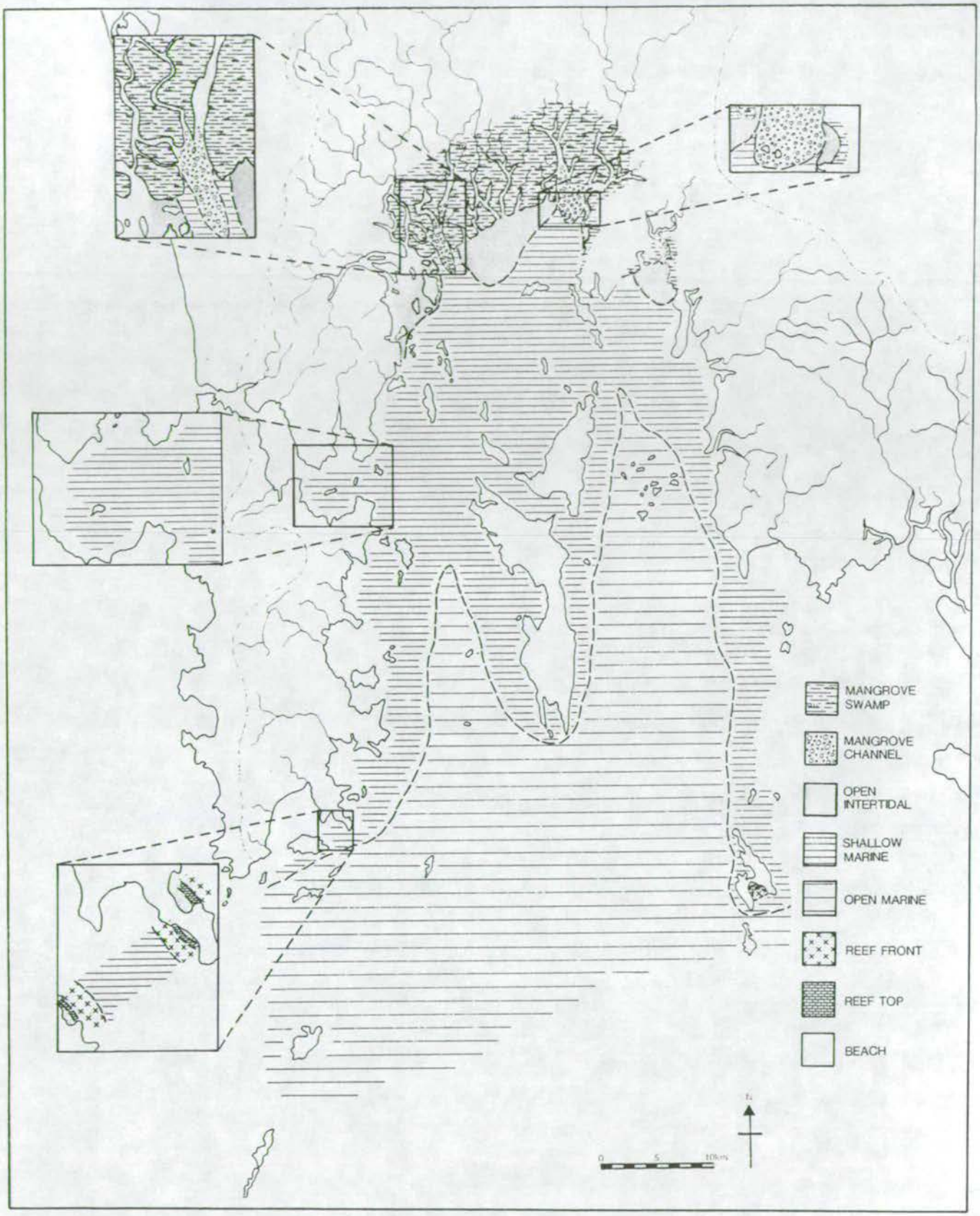

Figure 5.2 Areal distribution of the 8 depositional environments distinguished on the basis of water depth and geomorphology.

channels). Only mangrove channels which are extensions of alluvial systems have been sampled so no sediment information is available on the purely tidal mangrove channels in Phangnga Bay.

The beach, reef top and reef front environments have been sampled from the southern areas of the bay (ie, south east Phuket, Ko Lon and Ko Phi Phi - see figure 1.1b for their location). Small beaches have formed in the northern half of Phangnga Bay (sample sites 44a and 70a are samples from these) but reefs have not developed. The northern-most reefs are developed around the small group of islands east of Ko Yao Noi. Apart from the mangrove development in the north of the Bay, very little of the coastal area around Phangnga Bay has been sampled due to time constraints. However, areas of mangrove development are thought to show similar sedimentary patterns as the large development to the north, that is, mangrove swamps dissected by mangrove channels fronted by an open intertidal environment grading into the shallow marine environment. Rocky headlands tend to abut directly into the shallow marine environment.

5.3 GRAIN SIZE VARIATIONS BETWEEN ENVIRONMENTS

5.3.1 Summary statistics of grain size parameters

Table 5.1 lists the mean and standard deviation (1 σ) of each grain size parameter for each environment. T-tests have been carried out in order to compare means between environments. Since the reef top and beach environments are so obviously distinctive in their grain size and mineralogy from the mangrove, intertidal and shallow marine environments, a division of environments into two groups has been made for the purposes of comparing means with t-tests[1]. The means of the mangrove swamp, mangrove channel, open intertidal, shallow marine and open marine environments are compared in one group and the means of the open marine, reef front, reef top and beach environments compared in another group (Table 5.2).

[1] footnote. This division into two groups for t-tests was considered necessary to reduce the number of environmental comparisons from 28 to 16 thus making the results clearer and easier to handle. Since the reef top and beach sediments are obviously very different in mineralogy and geochemistry from the mangrove swamp, mangrove channel, intertidal and shallow marine sediments and would be very distinct in the geological record, comparing means were not considered useful. Reef front and open marine sediments do have some similarities and so are compared alongside the reef top and beach sediments.

	MANGROVE SWAMP		MANGROVE CHANNEL		INTER TIDAL		SHALLOW MARINE		OPEN MARINE		REEF FRONT		REEF TOP		BEACH		ALL PHANGNGA BAY	
	MEAN	STDEV	MEAN	STDEV	MEAN	STDEV	MEAN	STDEV	MEAN	STDEV	MEAN	STDEV	MEAN	STDEV	MEAN	STDEV	MEAN	STDEV
	(n=5)		(n=12)		(n=16)		(n=65)		(n=38)		(n=13)		(n=6)		(n=8)		(n=163)	
Mean (phi)	6.43	0.24	2.87	0.83	5.04	1.40	4.11	2.08	2.35	1.20	2.25	1.39	1.71	0.96	1.36	1.38	3.342	2.019
S.D. (phi)	1.93	0.18	2.35	0.47	2.01	0.46	2.27	0.56	1.74	0.31	1.96	0.48	1.39	0.51	0.87	0.39	1.992	0.5892
Skew	-0.18	0.42	0.86	0.38	0.64	0.91	0.27	0.84	0.84	0.43	0.56	0.54	0.02	0.99	-0.45	2.52	0.4489	0.9263
Gravel(wt%)	0.0	0.0	11.9	10.6	1.3	4.2	8.7	15.7	6.5	12.0	6.1	6.9	7.8	9.8	12.3	28.1	7.34	13.78
Sand (wt%)	11.8	6.6	73.7	11.4	39.6	30.1	39.4	24.8	82.1	15.2	75.2	22.9	87.0	10.8	87.3	28.3	58	36.95
Silt (wt%)	68.0	5.8	11.0	6.6	46.7	24.8	42.5	25.0	9.3	10.9	16.1	22.0	4.8	6.4	0.3	0.4	28.06	26.69
Clay (wt%)	20.1	2.0	3.4	2.2	12.5	7.6	9.5	5.8	2.2	2.2	2.6	2.7	0.5	0.4	0.1	0.1	6.604	6.565

Table 5.1

Mean and standard deviation of each grain size parameter for each depositional environment and for Phangnga Bay sediments as a whole.

1.	MS-MC	MS-IT	MS-SM	MS-OM	MC-IT	MC-SM	MC-OM	IT-SM	IT-OM	SM-OM
Mean (phi)	>	>	>	>	<	<	=	>	>	>
Sorting (phi)	<	=	<	>	>	=	>	<	>	>
Skewness	<	<	<	<	=	>	=	=	=	<

2.	OM-RF	OM-RT	OM-B	RF-RT	RF-B	RT-B
Mean (phi)	=	=	=	=	=	=
Sorting (phi)	=	=	>	>	>	>
Skewness	=	>	=	=	=	=

MS = mangrove swamp IT = intertidal OM = open marine RT = reef top
MC = mangrove channel SM = shallow marine RF = reef front B = beach

Independent two sample t-test (unpooled, ie test does not assume that the populations have equal variance.)

MS<MC - t-test indicates that the mean of the parameter for the mangrove swamp environment is less than the mean for the same parameter in the mangrove channel environment at a 95% confidence level.

MS=MC - t-test indicates that the means of the parameter are the same at a 95% confidence level for both environments.

MS>MC - t-test indicates that the mean of the parameter for the mangrove swamp environment is greater than the mean for the same parameter in the mangrove channel environment at a 95% confidence level.

Table 5.2

Results of an independent 2 sample t-test for two groups of depositional environments.
1. mangrove swamp, mangrove channel, open intertidal, shallow marine and open marine.
2. open marine, reef front, reef top and beach.

5.3.1.1 Mean grain size

As described in Chapter 2 there is a general trend of increasing mean grain size from the north to the south of Phangnga Bay. Since there is also a north-south trend of the main depositional environment distributions (from mangrove swamp to open intertidal to shallow marine to open marine) it would be expected that each of these environments will be characterized by increasingly coarser sediments.

The mean and standard deviation (1 σ) of all the grain size parameters are listed in Table 5.1. As expected, the average of mean grain sizes increases from 6.43 ϕ in the mangrove swamp to 5.04 ϕ in the intertidal, 4.11 ϕ in the shallow marine and 2.35 ϕ in the open marine environments. These increases are all significant at a 95% confidence level (Table 5.2). The mangrove channel sediments are significantly coarser than the mangrove swamp, open intertidal and shallow marine sediments but have a similar mean grain size to the open marine sediments.

There appears to be a trend of increasing grain size from the reef front (2.25 ϕ) to the reef top (1.71 ϕ) to beach (1.36 ϕ) environments however, from t-tests it is clear that none of the means of these environments are significantly different from each other or from the open marine sediments.

5.3.1.2 Sorting

The general trend of increased sorting from north to south is discussed in Chapter 2 but such a trend is not reflected in the average sorting values for each environment (Table 5.1). Open marine sediments (1.74 ϕ) are better sorted than mangrove swamp sediments (1.93 ϕ) and intertidal sediments (2.01 ϕ) which are better sorted than shallow marine sediments (2.27 ϕ). Mangrove channel sediments are on average very poorly sorted (2.35 ϕ). Most of the differences between sorting means are significant (Table 5.2) however, the mangrove swamp and intertidal sediments have similar sorting means as do the mangrove channel and shallow marine sediments.

Reef front, reef top and beach sediments however are, on average, better sorted with increased sorting corresponding to increased mean grain size from reef front to reef top to beach environments. The sorting of open marine sediments is similar to reef front and reef top sediments however, there is a significant increase in sorting between the open marine sediments and beach sediments and between the reef front, reef top and beach sediments.

5.3.1.3 Skewness

The most strongly positively-skewed sediments are found in mangrove channel and open marine environments (Fig 5.1), with decreasing skewness from open intertidal to shallow marine environments and a weak negative-skewness in mangrove swamp sediments. From Table 5.2, the mangrove swamp sediments have a significantly lower skewness value than the mangrove channel, intertidal, shallow marine and open marine sediments which do not have significantly different skewness means. Skewness apparently decreases from +0.56 in reef front to near zero in reef top to -0.43 in beach sediments but the differences between the skewness means are on the whole, not significant.

5.3.1.4 Size fractions

Average percent sediment size fractions show similar trends to average mean grain size with no gravel in mangrove swamp sediments to approximately 12% in mangrove channels and beach sediments. Average percent sand values are highest in open marine, reef top and beach environments and lowest in the mangrove swamp sediments. Percent silt and clay are therefore predictably highest in mangrove swamp, open intertidal and shallow marine environments and lowest in reef top and beach sediments.

5.3.1.5 Typical grain size distribution frequency graphs for each environment

A grain size frequency graph has been plotted for a sample from each depositional environment (Fig 5.3). These illustrate the general characteristics of sediments from each environment as described above and in the next section.

5.3.2 **Scatter plots of grain size parameters**

5.3.2.1 Using all samples

Figures 5.4 a,b and c plot mean versus sorting for each environment. Although each group plots within a reasonably confined area, there is considerable overlap between groups. The shallow marine environment shows the most scatter on the plot (Fig 5.4b) - this is statistically illustrated by this environment having the highest standard deviation of mean and sorting (Table 5.1). Mangrove swamps have the most well constricted distribution (lowest standard deviation in Table 5.1). Figure 5.4a shows that open intertidal sediments plot between mangrove swamp and mangrove channel sediments suggesting a mixture of sediments from the latter two environments occurs in the intertidal environment.

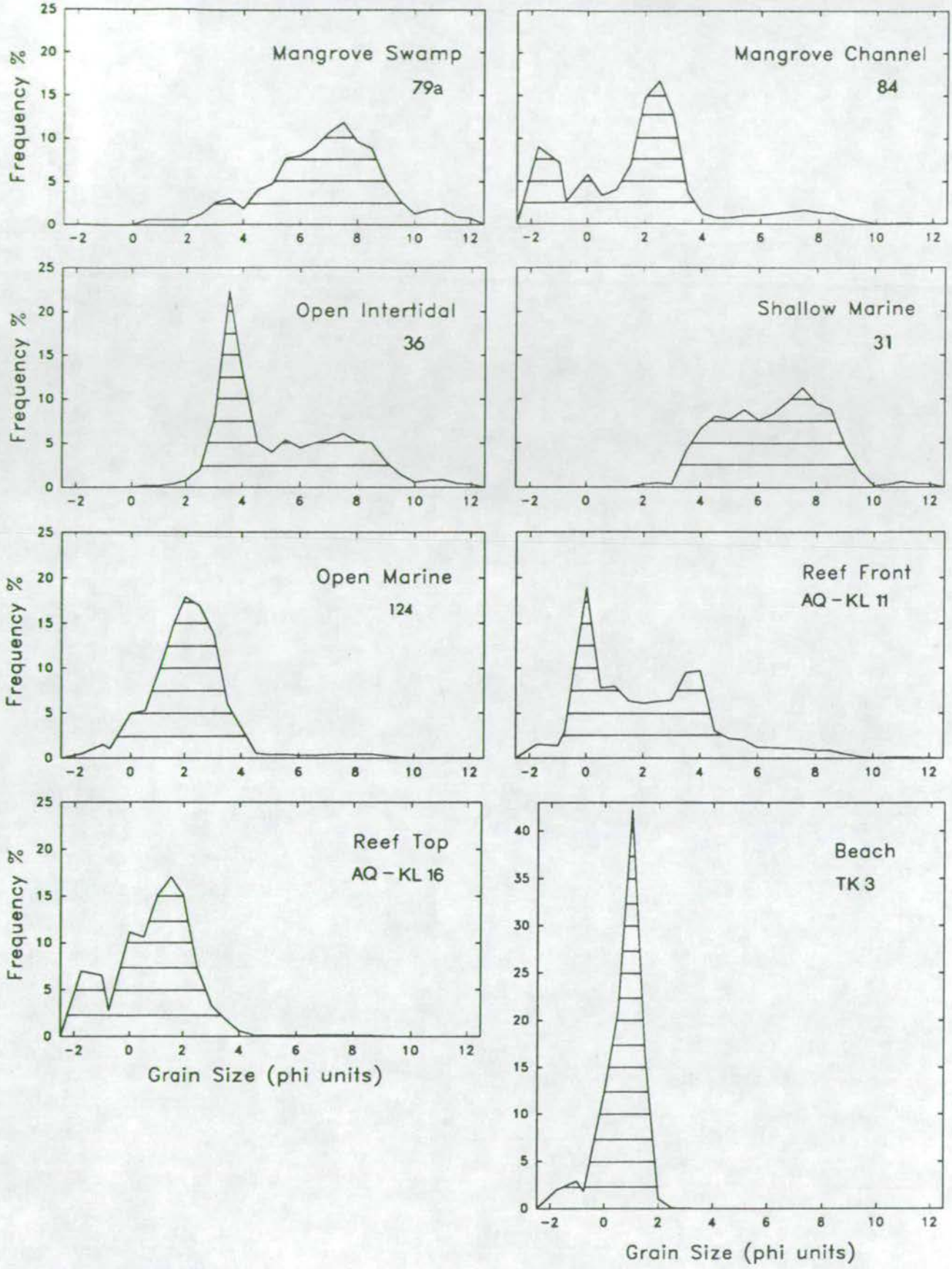

Figure 5.3 Typical grain size frequency histograms for a sediment from each depositional environment.

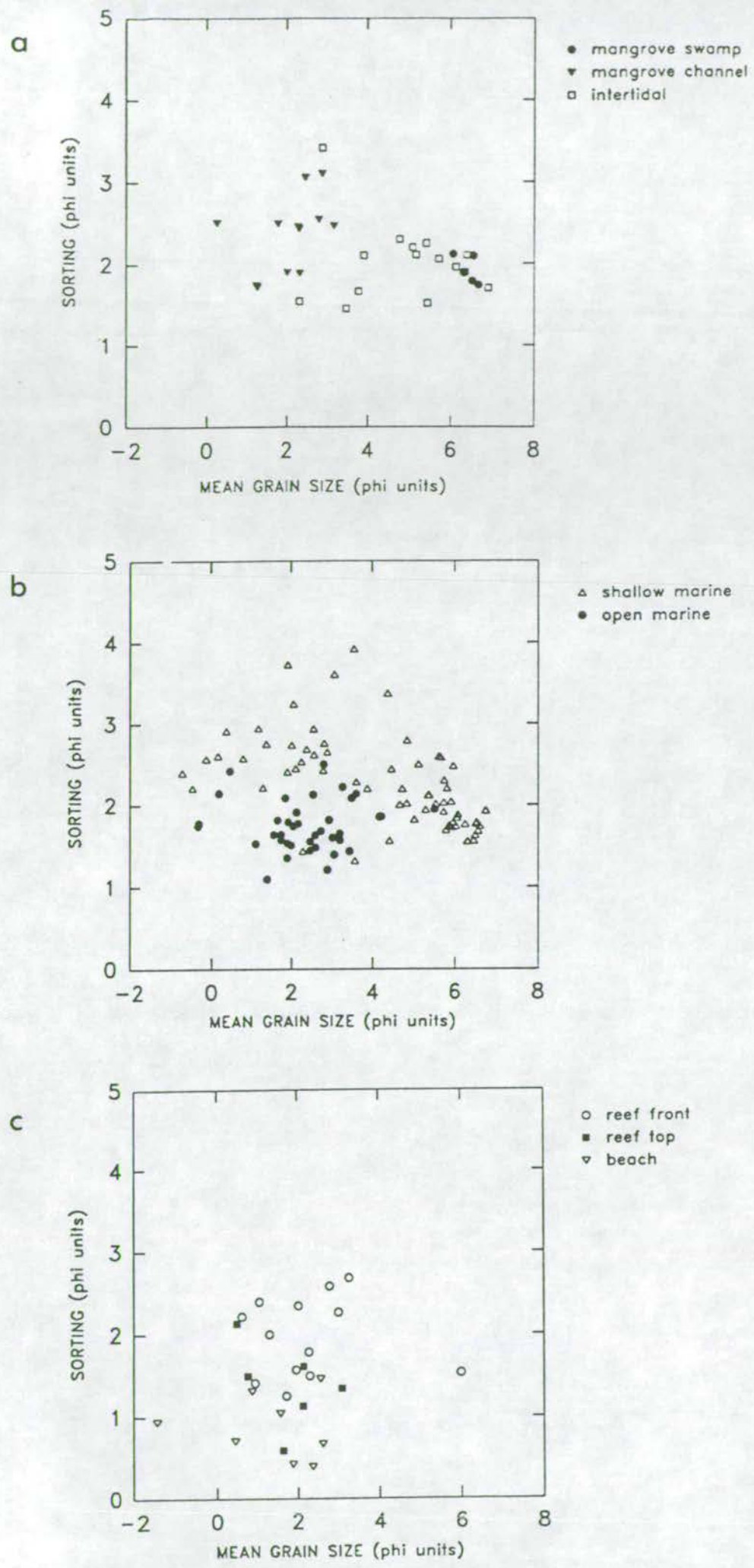

Figure 5.4

Mean grain size v. sorting for a. the mangrove swamp, mangrove channel and open intertidal environments; b. the shallow marine and open marine environments; c. the beach, reef front and reef top environments.

Plotting mean grain size against skewness (Fig 5.5 a-c) shows that all environments except for beach sediments, consist of sediments which show decreasing skewness values with decreasing mean grain size. In other words fine-grained sediments tend to have negative skewness and coarse-grained sediments have positive skewness. As with mean against sorting, sediments within one environment tend to plot within a restricted area although there is considerable overlap between groups. The shallow marine environment sediments show a wider scatter within this plot than the other environments. Beach sediments do not follow the general trend described above, rather they are composed of coarse-grained sediments which show a comparatively strong negative skewness.

Plotting sorting against skewness (Fig 5.6 a-c) does not show any particular trend although once again beach sediments plot outwith the main cluster of points.

5.3.2.2 Using sample suite means

Tanner (1991) suggests that a way of improving the bivariate grain size plots is to define sample suites (in this case the 8 depositional environments) and plot only suite means for each parameter. This greatly reduces the scatter, minimises overlap and pin-points the centre of gravity of the measurements for any one suite. Anomalous values no longer appear thus removing the overlap problem. This approach has been undertaken and the results illustrated in figure 5.7 a-c.

These plots neatly summarise the descriptions of the sediments of each environment as described above. Mean grain size versus sorting shows the greatest variation in the scatter of the points and thus shows the best environmental discrimination. In the mean grain size versus skewness plot the scatter is reduced. The sorting versus skewness plot only distinguishes the beach sediments from any of the other environments. However, the loss of information is considerable, and such plots should be used with caution if they are the sole descriptive tool for sediments from different environments.

5.3.3 **Textural classification and variations**

The sediments for each environment are described texturally in Figures 5.9 -5.16 on triangular plots of Gravel-Sand-Silt/Clay (using the classification terms of Folk, 1954 - Fig 2.7c) for the whole and carbonate-free sediment and Sand-Silt-Clay (using the classification of Shepard, 1954 - Fig 5.8) for the whole sediment only.

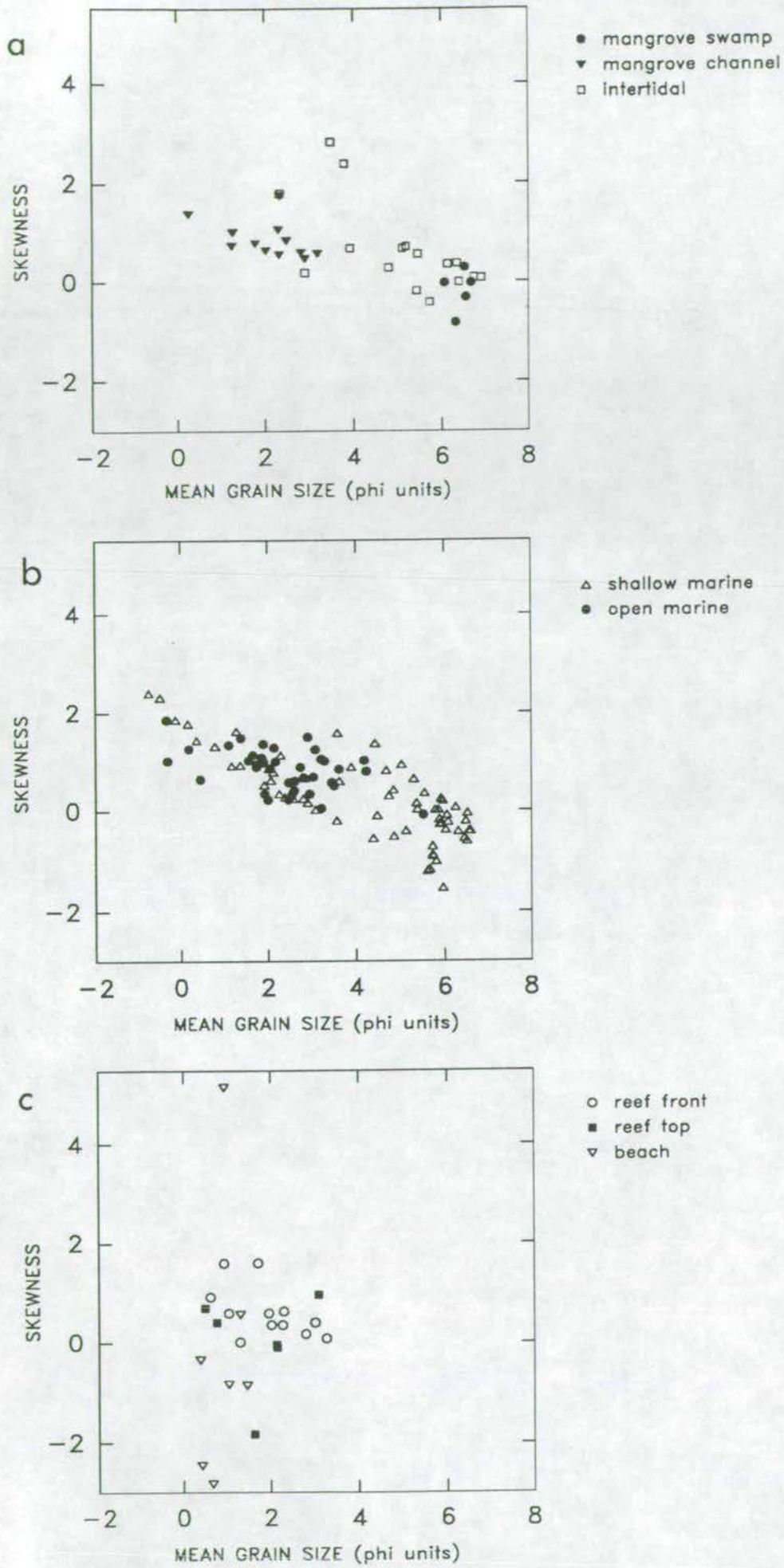

Figure 5.5

Mean grain size v. skewness for a. the mangrove swamp, mangrove channel and open intertidal environments; b. the shallow marine and open marine environments; c. the beach, reef front and reef top environments.

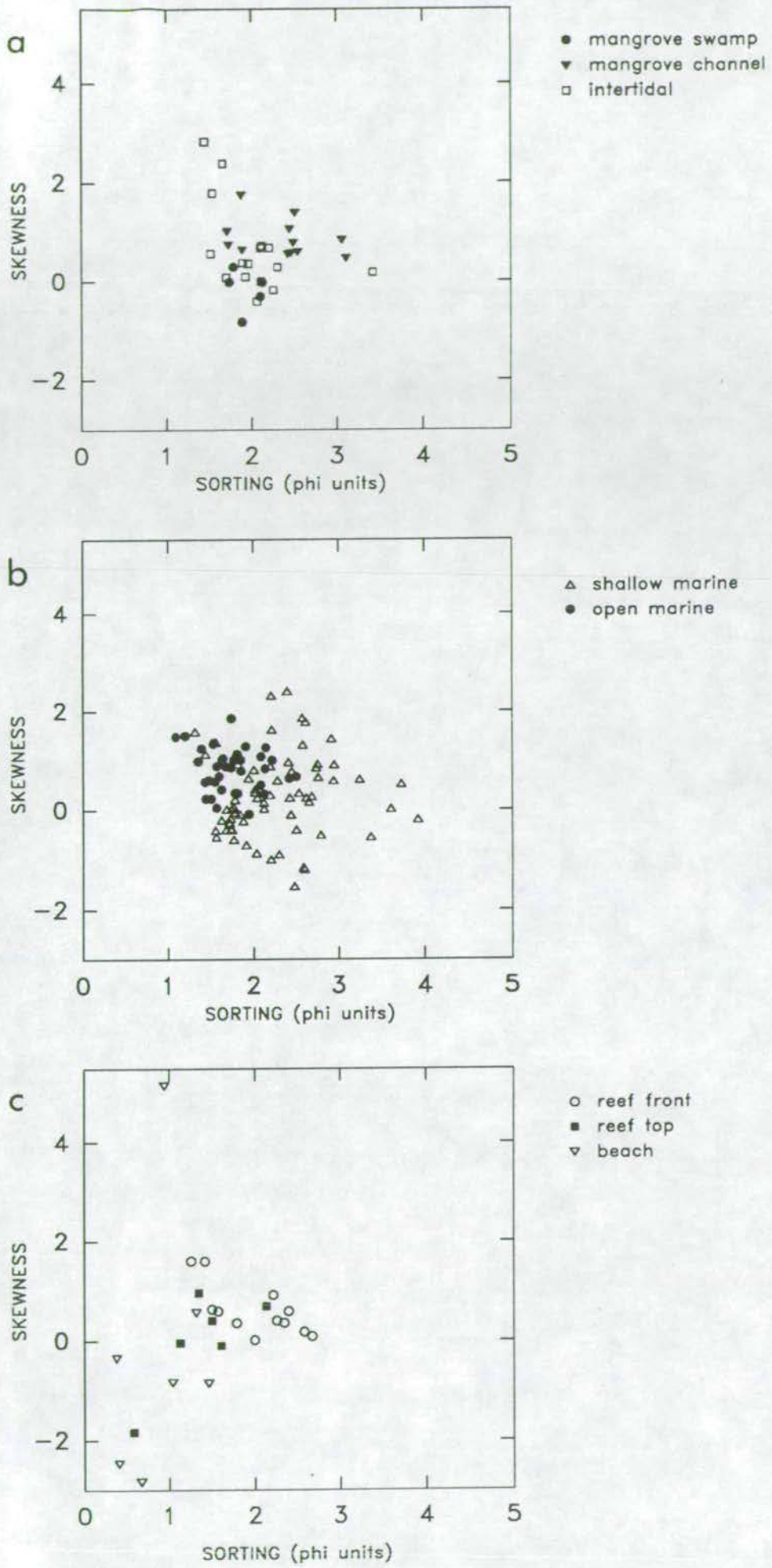

Figure 5.6
Sorting v. skewness for a. the mangrove swamp, mangrove channel and open intertidal environments; b. the shallow marine and open marine environments; c. the beach, reef front and reef top environments.

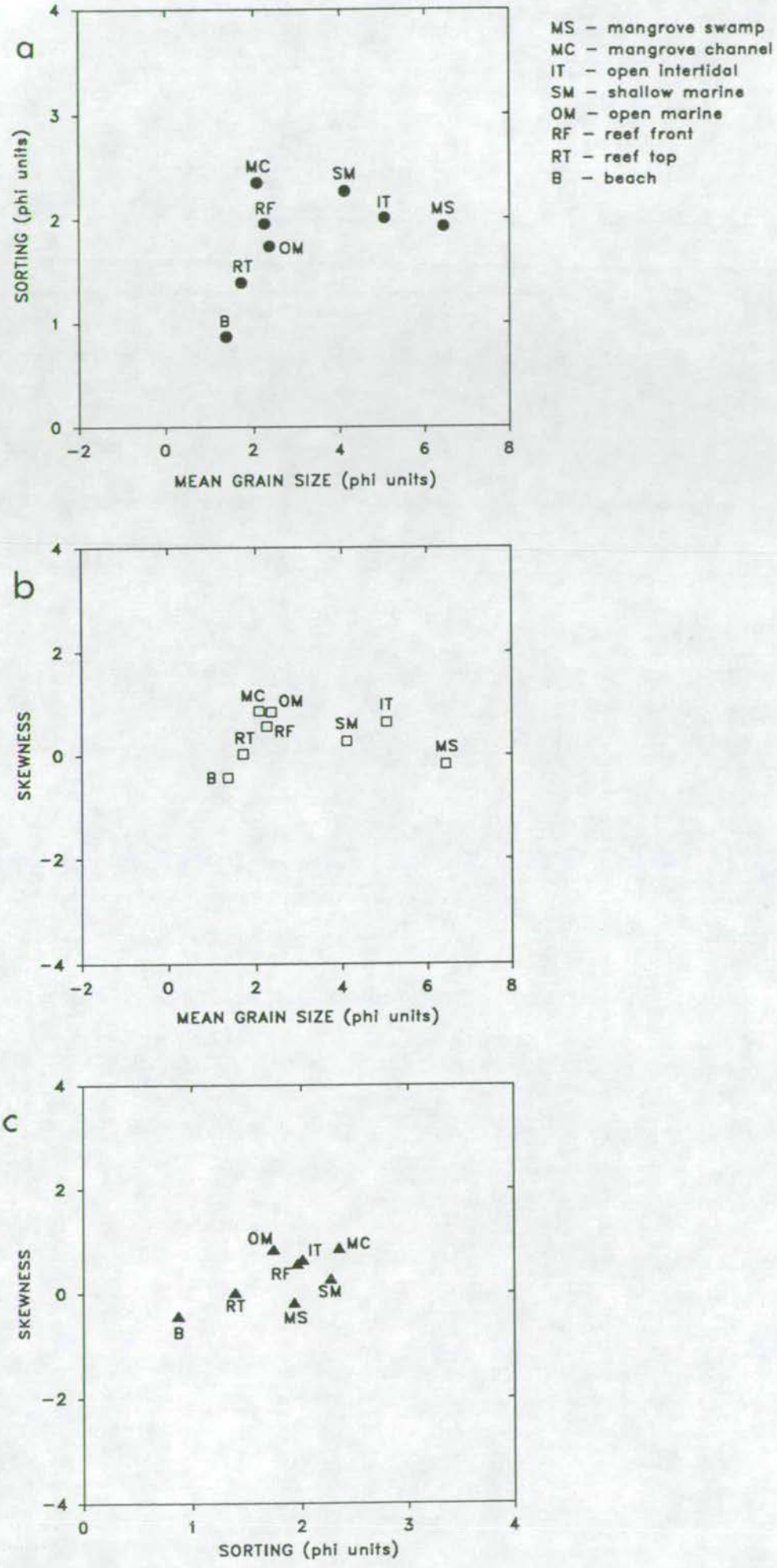

Figure 5.7

Graph of average values of a. mean grain size v. sorting; b. mean grain size v. skewness and c. sorting v. skewness for all 8 environments.

The mangrove swamp sediments (Fig 5.9 a-c) are sandy muds and muds (Folk) with no carbonate debris affecting the grain size distribution. In Shepard's terminology they are dominantly clayey silts. The mangrove channel sediments are in very close proximity to these sediments described above but texturally very different (Fig 5.10 a-c). They are dominantly gravelly muddy sands (Folk) of which only a small proportion of the gravel component can be accounted for by carbonate material. These are described as sands and silty sands in Shepard's classification. Open intertidal sediments range from sands to muds (Fig 5.11 a-c) with only one sample having a gravel component which is purely carbonate (this sample, 44b was taken from near a shell lag beach deposit, 44a). The non-gravel fraction ranges from sand to silty sand to clayey silts.

Comparing the above 3 environments it is again illustrated that the open intertidal sediments are a textural mix of both mangrove swamp and mangrove channel sediments. Similar sediments are found in the intertidal environment of Missionary Bay (Australia) by Risk and Rhodes (1985) who found mean grain size averaged 7 ϕ, the sediments are poorly sorted and sand is common especially near tidal channels or swamp margins.

The textural distribution of the shallow marine sediments (Fig 5.12 a-c) ranges from sandy gravel to sand to mud (Folk). However, when carbonate is removed all but 2 of the sediments plot on the sand-silt/clay line. Therefore the coarse component of the shallow marine sediments is dominated by shell debris. The non-gravel fraction ranges from sand to clayey silts. The open marine sediments (Fig 5.13 a-c), although also containing a gravel component and dominated by sands do not alter significantly on removal of carbonate. Therefore the coarse fraction is dominantly of terrigenous origin. A small fraction of the sand material is removed with carbonate removal. The majority of these sediments plot within the sand field of Shepard's classification so compared to the shallow marine sediments there is more coarse terrigenous sediment.

The reef front and reef top sediments (Fig 5.14 a-c and 5.15 a-c) are classified as gravelly sands and sands but on removal of carbonate the terrigenous fraction is composed of much finer sediments (sandy muds and muds). The finer whole sediment is composed dominantly of sands. Beach sediments (Fig 16 a-c) are clustered tightly in the sand field apart from one sample which contains carbonate gravel.

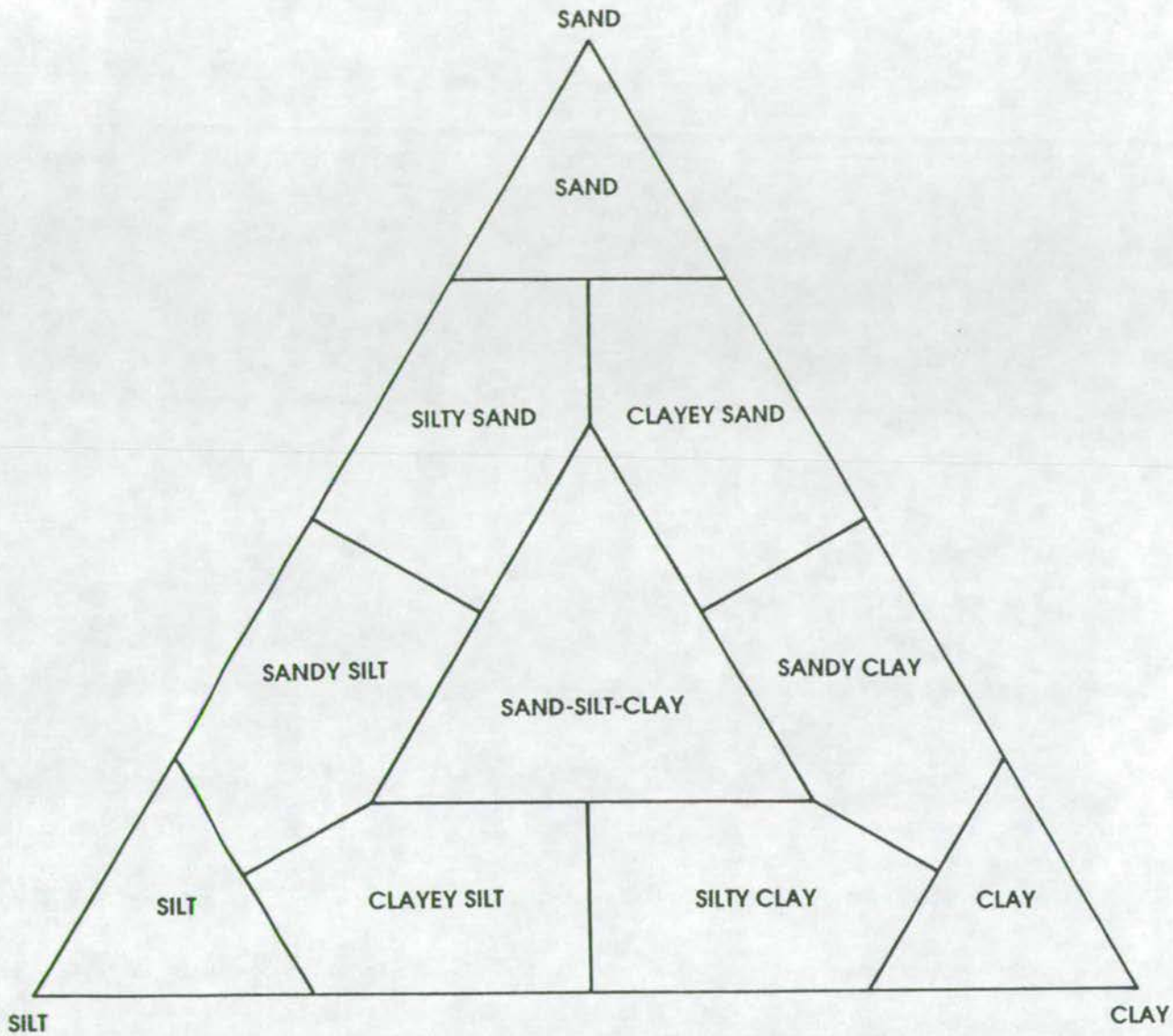

Figure 5.8 Classification of sediments according to sand, silt and clay proportions (Shepard, 1954).

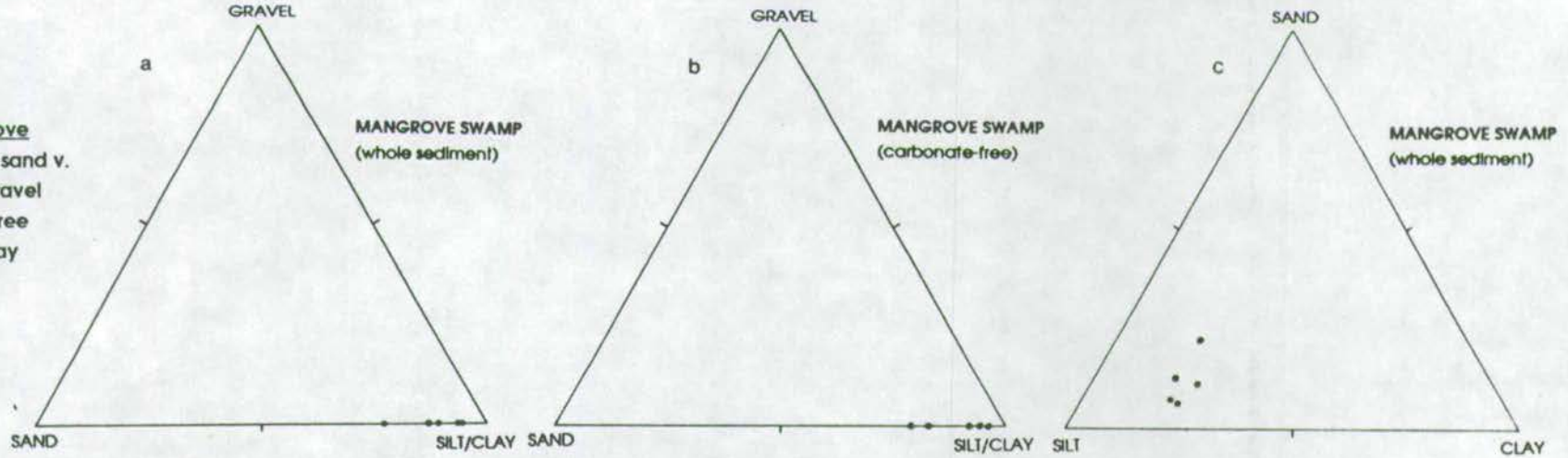

Figure 5.9
Textural grain size plots of mangrove swamp sediments for a. gravel v. sand v. silt/clay of whole sediments; b. gravel v. sand v. silt/clay of carbonate-free sediments and c. sand v. silt v. clay for whole sediments.

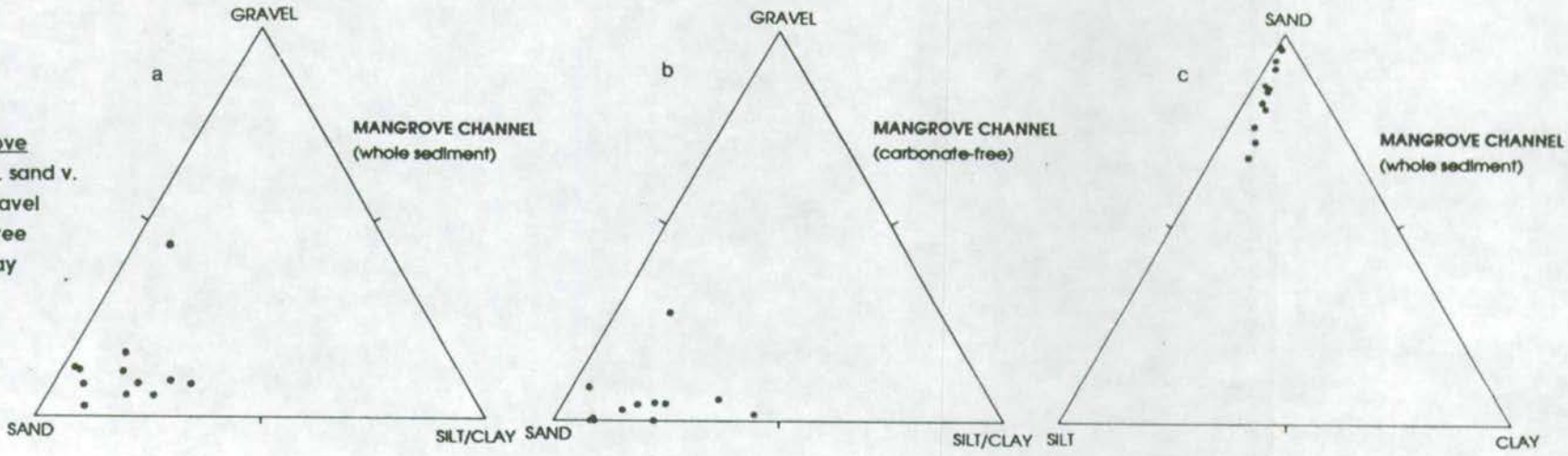

Figure 5.10
Textural grain size plots of mangrove channel sediments for a. gravel v. sand v. silt/clay of whole sediments; b. gravel v. sand v. silt/clay of carbonate-free sediments and c. sand v. silt v. clay for whole sediments.

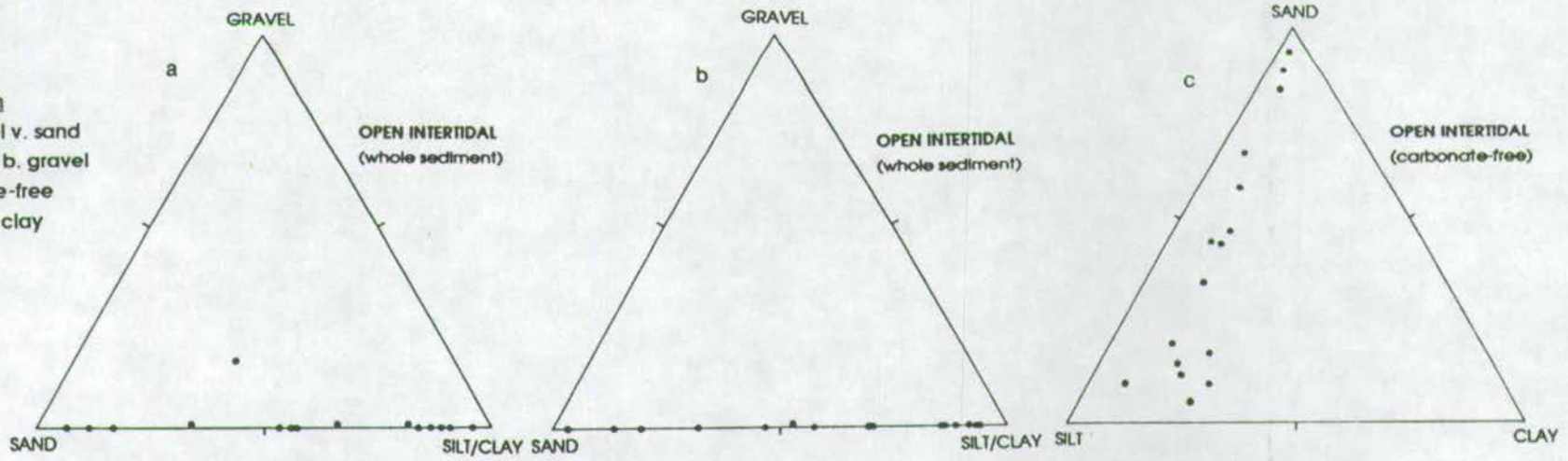

Figure 5.11
Textural grain size plots of open intertidal sediments for a gravel v. sand v. silt/clay of whole sediments; b. gravel v. sand v. silt/clay of carbonate-free sediments and c. sand v. silt v. clay for whole sediments.

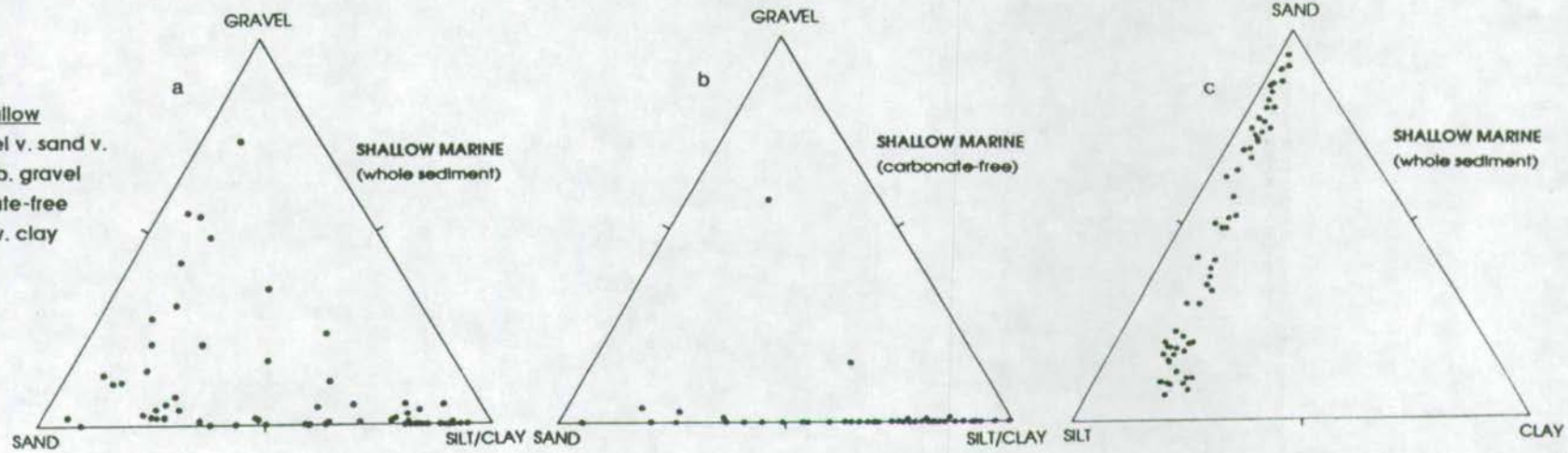

Figure 5.12
Textural grain size plots of shallow marine sediments for a. gravel v. sand v. silt/clay of whole sediments; b. gravel v. sand v. silt/clay of carbonate-free sediments and c. sand v. silt v. clay for whole sediments.

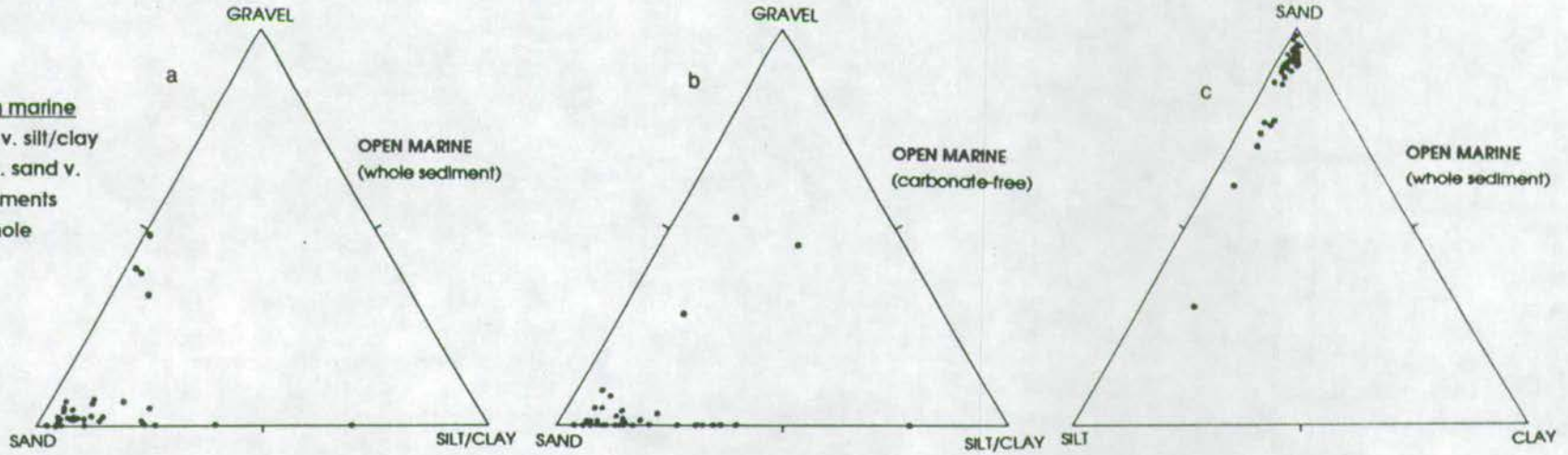

Figure 5.13
Textural grain size plots of open marine sediments for a. gravel v. sand v. silt/clay of whole sediments; b. gravel v. sand v. silt/clay of carbonate-free sediments and c. sand v. silt v. clay for whole sediments.

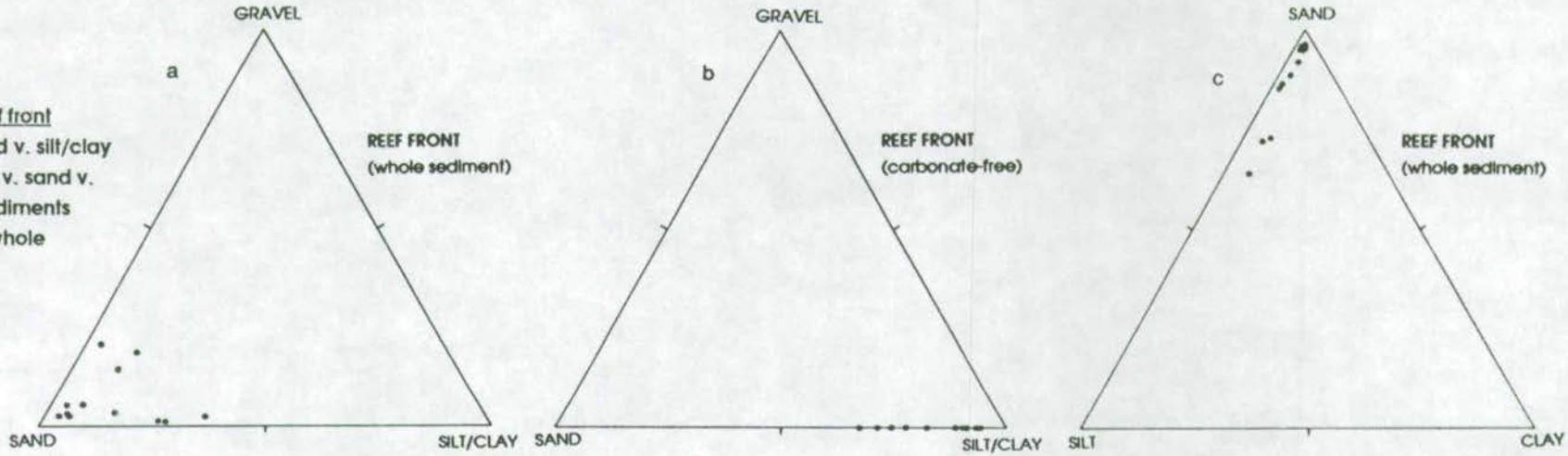

Figure 5.14
Textural grain size plots of reef front sediments for a. gravel v. sand v. silt/clay of whole sediments; b. gravel v. sand v. silt/clay of carbonate-free sediments and c. sand v. silt v. clay for whole sediments.

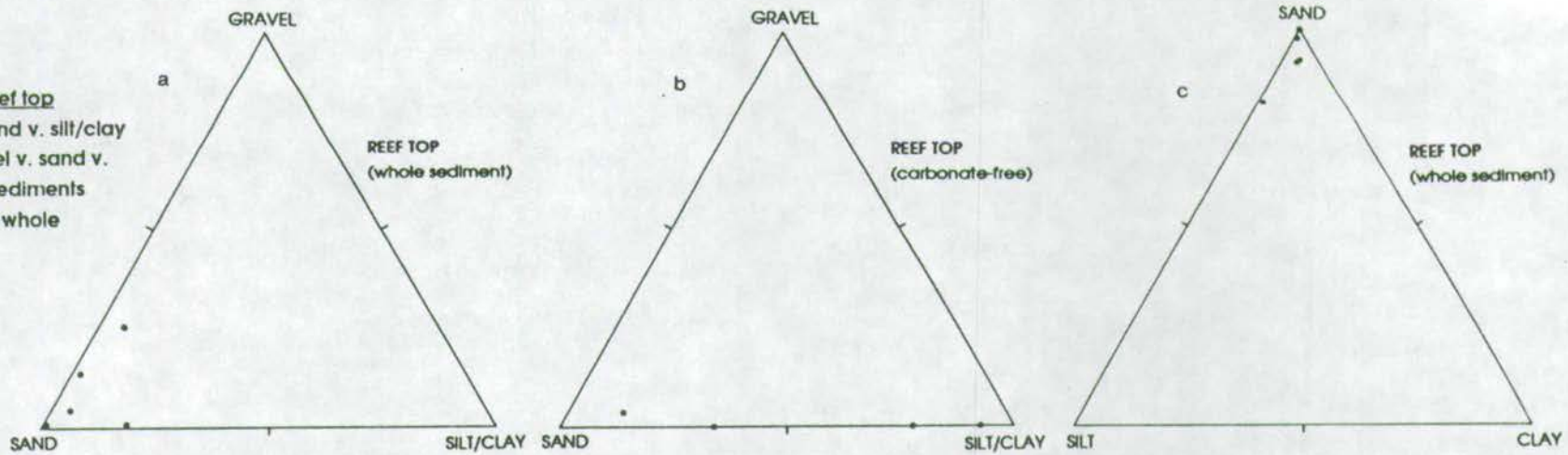

Figure 5.15
Textural grain size plots of reef top sediments for a. gravel v. sand v. silt/clay of whole sediments; b. gravel v. sand v. silt/clay of carbonate-free sediments and c. sand v. silt v. clay for whole sediments.

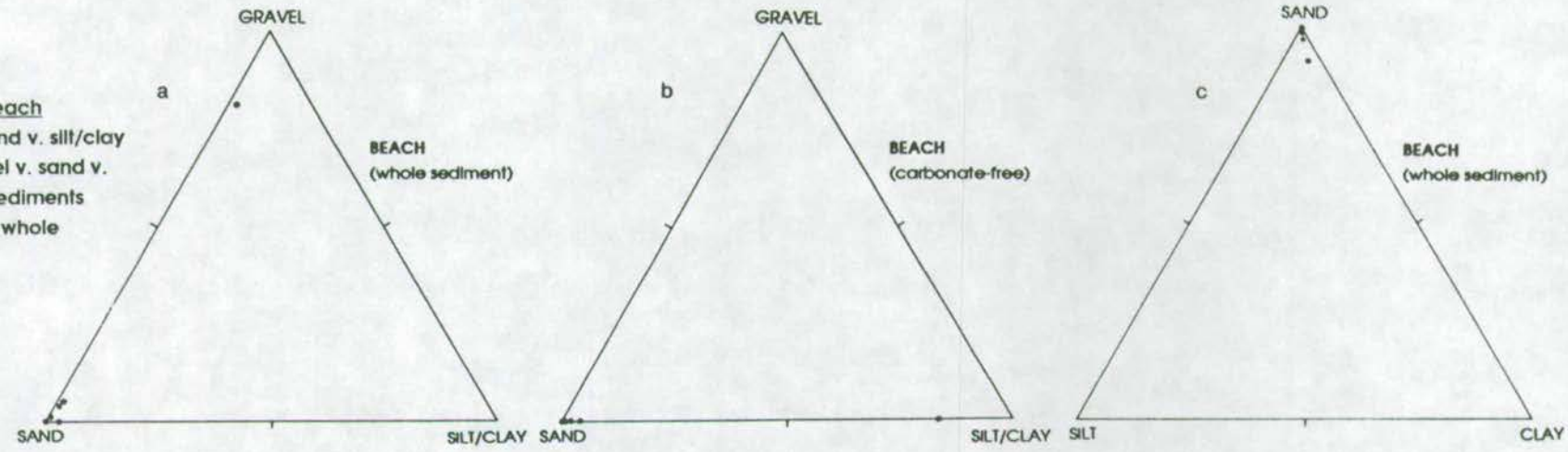

Figure 5.16
Textural grain size plots of beach sediments for a. gravel v. sand v. silt/clay of whole sediments; b. gravel v. sand v. silt/clay of carbonate-free sediments and c. sand v. silt v. clay for whole sediments.

On removal of carbonate the textural classification remains the same apart from one sample which is composed of a finer fraction.

5.3.4 Discussion

There are clearly important differences in the sediment grain size characteristics between the depositional environments. These differences can be explained by consideration of hydrodynamic energy levels and the sediment component supply in the different environments.

The increasing grain size and generally increasing sorting of sediments in different depositional environments from north to south is due to both the increasing hydrodynamic energy southwards and also the relict origin of coarse terrigenous sediment which is not yet covered by recent sediment as in the north (see Chapter 2). However, the shallow marine environment is poorly sorted compared to sediments in the mangrove swamp and open intertidal environments to the north and open marine environments to the south. This is due to the carbonate content of the shallow marine sediments which adds a gravel component to the mainly muddy sand terrigenous component hence decreasing the apparent sorting values. Although carbonate debris also adds to the sediment distribution of the open marine environment, there is a high proportion of quartz gravel and low mud content (due to higher energies preventing settling out) which gives an increased sorting value for this area. It has to be noted however, that the sediments of the shallow marine environment show greater variation in grain size parameters than any of the other depositional environments. This is due to the likely gradation in depositional conditions from the intertidal to the open marine environments rather than a sharp change in environments (unlike the mangrove swamp-mangrove channel boundary and the mangrove swamp-open intertidal boundary). The shallow marine environment is in effect a transitional zone between areas of tidally controlled deposition and off-shore environments and so some degree of overlap in sediment properties is to be expected.

The sediments of the mangrove swamp environment are of the finest grain size and show less variation in grain size parameters than any of the other environments. The lack of coarse material is due to the low energy conditions across the mangrove vegetated areas created by the prop roots and pneumatophores of mangrove trees acting as a baffle to any waves and tidal currents (Bird, 1986). The main

mangrove development has formed across the north of the Bay in the most sheltered area where wave action is at its weakest and only tidal currents are significant. The mechanisms controlling the deposition of fine material in this area are discussed in Chapter 2. This fine material, as well as having strong cohesive properties preventing resuspension, is bound by the mangrove roots and also by the feeding activities of the organisms living in and on the sediment surface (crabs, mud skippers etc) through their production of faecal pellets (van Straaten and Kuenan, 1958; Christensen, 1978).

Terrigenous coarse material is transported into the Bay through mangrove channels. Much of the medium to coarse sand and gravel fraction settles out in these channels and is not transported far into the Bay. The presence of fine material accounts for the poor sorting and may be deposited in this comparatively high energy environment in a number of ways. Firstly the steep banks of the channels are prone to slumping (Cook and Mayo, 1978) and the lumps of cohesive mud are relatively resistant to resuspension and transport. Secondly, if a typical salinity stratification develops in these channels as in other estuarine environments, (particularly during high fresh water discharge) where fresh water lies at the top of the water column moving seawards and salt water lies at the bottom moving landwards, a turbidity maximum may develop in the salt wedge. This is due to the residual circulation where mixing in the upper estuary transfers suspended sediment into the surface layer where it is transported seawards. In the lower energy middle estuary the sediment settles into the lower layer where it travels in the salt wedge intrusion, back to the head of the estuary. Thus a trap for suspended sediments is created leading to their eventual accumulation on the channel floor. Such a phenomenon is a well known feature of comparatively low energy tidal inlets (Allen et al, 1982; Barua, 1990).

Mangrove channels which do not form a continuation of alluvial channels and are only affected by tidal currents are not likely to have a coarse sediment lag over their floor. Rather, they are simply incisions into the mangrove muds and although some coarser material may be supplied from the open intertidal environment during flood tide, the channels mainly supply resuspended fine material to the open intertidal environment from the mangrove mudflats during ebb tide. Although this is only speculative for Phangnga Bay, such a process has been observed in Broad Sound (Cook and Mayo, 1978).

Fine sands and muds carried in suspension in the channels from fluvial systems are transported into the open intertidal environment, the coarser material settles whilst the fine material may either settle out through flocculation or be carried in suspension into the mangrove swamp environment.

The positioning of the coarse mangrove channel material within the very fine grained mangrove swamp sediments is due to a combination of fluvial and tidal currents concentrating within the channels which have prograded forward with the mangrove system from the original river mouth thus preserving their incut channel form and allowing a conduit for terrigenous material to be transported seaward. The high tidal and fluvial current strengths concentrated in these channels are immediately dissipated when the channel water overflows into the mangrove swamp environment.

The above explanation of sediment patterns in these 3 environments also explains the apparent textural mix of mangrove swamp and mangrove channel sediments in the open intertidal sediments. Of the terrigenous sediment transported from the hinterland the coarsest material settles out in streams and mangrove channels and a mix of sands and muds are transported to and settle out in the open intertidal environment. The finest material carried in suspension is transported into and settles out in the low energy mangrove swamp environment. The sediment of the open intertidal environment, although varying from sand to clayey silt in texture, is generally much finer than sediments found in a similar low energy depositional environment in Broad Sound (Cook and Mayo, 1978) where large sand waves and ridges have developed. This is due to the more humid tropical climate in Phangnga Bay's hinterland in which intense chemical weathering produces an influx of sediment into the Bay dominated by silt and clay rather than sand sized material.

It is known that in temperate estuaries of NE America and northern Europe much of the sediment deposited is derived from off-shore rather than nearby land sources. As discussed in Chapter 3, this is not thought to be the case in Phangnga Bay due the prevalence of clays from intense chemical weathering of rocks in the drainage basin and the high rainfall allowing their transport into the Bay. The lack of fine material off-shore to source the fine sediment accumulation in the north also indicates that an off-shore source is not likely.

The reef front, reef top and beach environments are not areally extensive in Phangnga Bay (see figure 3.12b for the scale of an average beach and fringing reef in the south of the Bay) and tend to be concentrated in the southern area away from any large inputs of terrigenous material which would hinder coral growth. In effect these 3 coastal environments replace those of mangrove channel, swamp and intertidal environments. They form in higher energy, more oceanward areas. This higher energy is reflected in the coarse mean grain size. Reef front sediments are texturally the finest of the 3 environments and are comparable to the open marine sediments although they contain more carbonate material. Reef top sediments are well sorted and coarse grained as this environment is subject to high energy conditions with tidal currents as well as waves breaking over the reef. Beach sediments are the most well sorted as would be expected due to the high sorting capacity of wave wash. They also show negative skewness values which is typical of beach sands from many part of the World (Moiola and Weiser, 1968). Carbonate material dominates these sediments. It is sourced from the coral reef itself as well as its associated molluscan and foraminiferan carbonate-secreting fauna. Terrigenous material is only present as sand sized particles since finer material, if present in suspension, cannot settle out.

5.4 GEOCHEMICAL VARIATIONS BETWEEN ENVIRONMENTS

Since the concentrations of most of the elements studied are controlled by the abundance of clays, quartz sand and carbonate material in the sediment (see Chapter 4) and these in turn are reflected in grain size distributions, much of the geochemical variation between depositional environments will be explained by the grain size variations discussed above. Table 5.3 lists the mean and standard deviation of elements for each environment and it is clear that increasing Al, K, Fe and other aluminosilicate element concentrations simply follow the trend of decreasing mean grain size. Si and Ca tend to show the reverse trend.

[1] footnote. It must be stressed that N varies considerably between environments and so care has to be taken in interpreting the correlation coefficients. Coefficients significant at a level of 95% or greater are indicated. The limiting correlation coefficient varies according to N (see Appendix C) and increases with decreasing N. Since the sample size of the mangrove swamp, reef top and beach environments are < 10, the limiting correlation coefficients are all > 0.9. Despite the limitations of small sample size, comparison of significant correlations between environments is considered useful in indicating various controls on geochemical variations in sediments.

	MANGROVE SWAMP		MANGROVE CHANNEL		INTER TIDAL		SHALLOW MARINE		OPEN MARINE		REEF FRONT		REEF TOP		BEACH		PHANGNGA BAY AS A WHOLE	
	MEAN	STDEV	MEAN	STDEV	MEAN	STDEV	MEAN	STDEV	MEAN	STDEV	MEAN	STDEV	MEAN	STDEV	MEAN	STDEV	MEAN	STDEV
	(n=4)		(n=13)		(n=16)		(n=62)		(n=37)		(n=12)		(n=5)		(n=7)		(n=156)	
Al (wt%)	11.84	2.15	2.74	1.54	6.86	3.74	4.97	2.92	1.40	0.96	1.21	0.65	0.51	0.33	0.26	0.16	3.743	3.322
Ca (wt%)	0.14	0.12	5.43	3.95	1.54	4.02	8.93	9.21	10.79	4.67	28.73	5.50	28.17	7.80	25.41	11.99	10.86	10.59
Si (wt%)	25.50	1.61	34.61	4.85	31.18	6.85	24.87	8.44	29.25	5.75	6.12	4.69	9.52	10.13	14.06	15.65	24.883	10.389
Mg (wt%)	0.741	0.134	0.536	0.529	0.847	0.363	1.102	0.417	1.068	0.283	1.272	0.486	0.617	0.160	0.471	0.229	1.0279	0.4377
Fe (wt%)	3.266	0.325	1.237	0.574	2.341	0.891	2.048	0.885	1.207	0.640	0.500	0.230	0.217	0.175	0.155	0.112	1.605	0.998
K2 (wt%)	1.920	0.344	0.701	0.637	1.372	0.772	0.802	0.558	0.312	0.330	0.150	0.094	0.146	0.178	0.121	0.189	0.679	0.636
Ti (ppm)	3660	412	1260	370	2880	1110	2448	1263	860	470	570	380	260	200	340	390	1777	1310
Mn (ppm)	376	220	169	74	239	101	223	87	169	115	64	32	10	25	28	97	185	118
Rb (ppm)	242.4	97.8	94.7	104.1	165.3	117.3	91.9	57.5	31.4	28.7	26.5	20.4	15.1	14.6	9.8	16.9	78.01	80.88
Nb (ppm)	31.9	8.8	10.0	5.0	20.9	10.1	14.9	7.1	6.4	2.3	5.0	3.2	1.9	1.6	3.7	2.8	11.84	8.648
Y (ppm)	53.1	14.4	15.3	7.7	30.6	14.6	22.8	9.6	10.7	5.0	10.1	5.1	2.5	2.5	2.7	1.8	18.33	12.92
Th (ppm)	53.8	14.1	11.2	7.9	28.0	17.5	20.2	10.6	6.5	3.8	8.5	4.8	2.6	1.9	1.8	1.3	15.54	13.75
Pb (ppm)	73.9	23.0	19.7	15.5	40.0	23.1	26.6	14.3	11.0	5.4	11.7	5.4	7.2	6.3	4.8	2.8	22.15	18.46
V (ppm)	79.1	18.8	29.6	16.4	55.0	23.2	47.8	20.1	20.3	14.8	16.8	7.2	7.6	3.3	6.2	3.9	35.74	24.32
Cr (ppm)	65.6	19.7	25.0	16.1	53.4	22.0	52.5	22.7	27.1	16.1	19.6	15.8	5.6	3.3	4.9	3.4	38.43	25.24
Zn (ppm)	61.4	4.2	23.4	10.8	44.0	18.8	36.3	16.1	15.7	8.4	11.5	4.9	5.1	3.0	4.8	2.9	27.43	18.61
Ni (ppm)	23.7	3.4	7.4	4.1	17.4	7.1	16.4	7.0	8.2	4.4	5.3	2.3	3.2	1.2	2.4	0.5	12.067	7.769
La (ppm)	58.5	3.8	21.6	11.8	38.7	13.9	32.0	12.2	13.0	8.0	10.2	8.0	-0.7	3.8	-2.7	6.3	23.71	16.85
Ce (ppm)	117.8	3.4	45.4	21.5	80.2	33.4	70.1	22.6	33.5	15.8	36.7	9.8	24.6	6.5	19.8	9.1	55.33	30.03
Nd (ppm)	48.3	2.2	19.4	9.9	32.5	14.1	28.1	10.1	13.0	6.7	12.7	5.4	5.5	6.5	5.7	5.8	21.85	13.17
Ba (ppm)	149.6	24.5	83.7	32.9	114.8	41.1	104.0	41.9	51.6	30.4	35.6	19.3	29.8	18.6	27.8	11.7	81.09	47.29
Sr (ppm)	45.5	11.2	217.6	145.2	91.1	128.2	548.9	527.1	661.8	345.4	3041.0	1289.0	3794.0	1165.0	2971.0	1575.0	892.6	1181.6
Zr (ppm)	179.4	29.9	112.3	34.6	196.1	43.5	186.4	69.5	132.7	51.3	124.4	35.7	113.0	28.7	88.8	30.6	156.81	64.28
Sn (ppm)	28.3	12.0	12.6	13.9	17.5	13.7	11.0	7.1	11.0	10.9	14.4	15.1	4.5	7.1	4.4	4.6	11.998	10.821
P2O5 (ppm)	812	204	482	247	840	212	842	263	631	236	661	173	354	134	241	108	746	385
CaCO3 (wt%)	1.8	2.2	17.47	11.93	6.81	10.31	25.9	21.6	29.32	11.51	72.42	12.14	70.88	18.64	67.1	31	29.75	25.08
Org C (wt%)					1.48	0.86	1.39	0.40	0.717	0.516								

Table 5.3 Mean and standard deviation of geochemical variables for each depositional environment and for Phangnga Bay sediments as a whole.

In order to look more deeply into the geochemical variations between depositional environments, the average element/Al ratio (or element/Ca ratio in the case of Sr) for each environment has been calculated and is listed in Table 5.4. In order to test whether the element ratio means are significantly different between environments, t-tests were performed on the mangrove swamp, mangrove channel, open intertidal, shallow marine and open marine environments and on the open marine, reef front, reef top and beach environments (Tables 5.5 and 5.6).

Correlation matrices[1] have also been constructed for each environment (Tables 5.7 to 5.14).

Discussion of each element's variation between environments will follow the order of element discussion in Chapter 4 with major elements followed by trace elements.

5.4.1 Aluminium

Since Al is concentrated in aluminosilicate minerals (ie, clays) the mean aluminium values for each environment mirror those of mean grain size with highest values in the mangrove swamp and intertidal sediments and lowest in the reef top and beach sediments (Tables 5.1 - 5.3).

In all environments, Al correlates positively although not always significantly with the Al-associate elements discussed in Chapter 4. Slight variations in trace element correlations with Al will be discussed further in the section on trace elements.

5.4.2 Calcium

The Ca concentration is controlled by the calcium carbonate content of the sediment (Chapter 4). Highest values are found in the reef front, reef top and beach sediments which all have a similar carbonate content (Table 5.6) and decrease significantly through the open and shallow marine sediments to the intertidal and mangrove swamp sediments. This reflects the general trend of increasing carbonate content from north to south in the Bay with the highest concentrations due to contributions from coral reefs in the southern area. Ca contents are therefore highest in areas of highest $CaCO_3$ production, ie around coral reefs and in environments with comparatively low terrigenous sediment input

	MANGROVE SWAMP		MANGROVE CHANNEL		INTERTIDAL		SHALLOW MARINE		OPEN MARINE		REEF FRONT		REEF TOP		BEACH	
	Mean (n=4)	S.D.	Mean (n=13)	S.D.	Mean (n=16)	S.D.	Mean (n=64)	S.D.	Mean (n=37)	S.D.	Mean (n=12)	S.D.	Mean (n=5)	S.D.	Mean (n=7)	S.D.
Fe/Al	0.282	0.049	0.503	0.202	0.390	0.115	0.497	0.248	0.964	0.362	0.439	0.107	0.431	0.257	0.775	0.599
Mn/Al	0.0030	0.0012	0.0070	0.0034	0.0040	0.0017	0.0064	0.0059	0.0145	0.0115	0.0056	0.0019	0.0015	0.0039	0.0101	0.0426
Ti/Al	0.0320	0.0078	0.0544	0.0213	0.0497	0.0181	0.0538	0.0156	0.0678	0.0186	0.0447	0.0062	0.0537	0.0344	0.1378	0.1259
K2/Al	0.1626	0.0080	0.2461	0.1445	0.2076	0.0836	0.1517	0.0488	0.2188	0.1828	0.1208	0.0209	0.3260	0.3960	0.3680	0.3050
P205/Al	0.0070	0.0020	0.0208	0.0125	0.0209	0.0280	0.0275	0.0211	0.0534	0.0205	0.0689	0.0395	0.0954	0.0690	0.2010	0.2970
Si/Al	2.22	0.51	16.51	9.45	9.11	13.26	9.06	13.88	28.96	17.17	4.57	1.41	20.96	20.74	59.30	52.00
Mg/Al	0.065	0.020	0.243	0.305	0.146	0.065	0.339	0.254	0.932	0.329	1.237	0.610	1.811	1.443	4.050	6.400
Nb/Al	2.67	0.28	3.91	1.17	3.40	1.13	3.49	3.09	5.45	1.78	4.20	1.99	3.66	3.09	18.75	11.96
Zr/Al	15.83	5.51	52.59	29.69	43.61	33.70	50.95	57.53	120.90	66.80	122.60	51.30	360.00	359.00	743.00	1124.00
Y/Al	4.45	0.43	6.07	2.41	4.94	1.32	5.57	4.59	8.82	3.25	8.69	3.37	5.34	5.63	12.67	6.98
Rb/Al	20.00	4.34	31.94	25.79	24.13	15.37	19.50	16.03	21.69	14.13	21.77	15.15	30.90	31.90	24.80	29.10
Th/Al	4.51	0.37	4.10	1.19	4.00	0.61	4.62	3.84	4.95	1.72	7.23	2.84	5.73	2.57	7.52	5.23
Pb/Al	6.16	0.79	6.93	2.87	5.89	1.08	6.01	4.55	8.63	2.55	10.65	4.28	13.75	5.31	29.50	29.60
Zn/Al	5.29	0.76	9.35	3.40	7.20	1.82	8.84	7.45	12.42	4.19	10.38	4.09	12.02	6.95	29.48	25.04
Ni/Al	2.08	0.57	2.95	1.22	2.98	1.13	4.04	3.33	6.29	1.72	5.39	3.80	8.50	5.50	18.63	23.86
Cr/Al	5.86	2.38	10.04	5.30	9.18	3.69	13.42	12.64	20.55	6.29	19.94	23.09	12.64	6.66	21.60	16.27
Ce/Al	10.16	1.57	18.18	5.74	13.84	5.77	19.13	14.72	26.24	6.67	37.18	17.11	71.50	59.80	114.30	75.10
Nd/Al	4.16	0.58	7.68	2.59	5.38	2.09	7.62	7.02	10.29	3.76	11.98	5.54	13.19	10.95	24.21	21.37
La/Al	5.04	0.74	8.54	2.86	7.00	3.41	8.53	7.06	9.73	3.78	8.96	6.50	1.24	1.79	4.51	7.81
V/Al	7.01	2.47	12.19	5.60	9.04	2.81	12.17	10.74	14.96	6.65	16.31	9.98	19.30	12.96	31.39	18.90
Ba/Al	13.20	4.09	39.05	30.30	20.87	10.69	27.28	25.06	39.80	14.93	30.95	16.61	71.70	38.20	155.70	126.00
Sr/Ca	248.60	73.00	60.50	45.40	135.10	53.70	68.25	25.14	60.22	8.93	104.10	36.30	133.90	7.15	124.80	37.40

Table 5.4 Mean and standard deviation of geochemical variables as a ratio to Al for each depositional environment.

	MS-MC	MS-IT	MS-SM	MS-OM	MC-IT	MC-SM	MC-OM	IT-SM	IT-OM	SM-OM
Ca	<	=	<	<	>	<	<	<	<	=
Al	>	>	>	>	<	<	>	>	>	>
Si	<	<	=	<	=	>	>	>	=	<
Si/Al	<	<	<	<	>	>	<	=	<	<
Mg/Al	<	<	<	<	=	=	<	<	<	<
Fe/Al	<	<	<	<	>	=	<	<	<	<
Ti/Al	<	<	<	<	=	=	<	=	<	<
K/Al	<	<	=	<	=	>	=	>	=	<
P2O5/Al	<	<	<	<	=	=	<	=	<	<
Mn/Al	<	=	<	<	>	=	<	<	<	<
Rb/Al	<	=	=	=	=	=	=	=	=	=
Mb/Al	<	<	<	<	=	=	<	=	<	<
Y/Al	<	=	<	<	=	=	<	=	<	<
Th/Al	=	>	=	=	=	=	<	=	<	=
Pb/Al	=	=	=	<	=	=	<	=	<	<
V/Al	<	=	<	<	>	=	=	<	<	=
Cr/Al	<	<	<	<	=	=	<	<	<	<
Zn/Al	=	<	<	<	>	=	<	=	<	<
Ni/Al	<	<	<	<	=	<	<	<	<	<
La/Al	<	<	<	<	=	=	=	=	<	=
Ce/Al	<	<	<	<	>	=	<	<	<	<
Nd/Al	<	<	<	<	>	=	<	<	<	<
Ba/Al	<	<	<	<	>	=	=	<	<	<
Sr/Ca	>	=	<	>	<	=	=	>	>	>
Zr/Al	<	<	<	<	=	=	<	=	<	<
Sn	<	=	>	>	=	=	=	>	<	=

MS = mangrove swamp IT = intertidal OM = open marine
MC = mangrove channel SM = shallow marine

Independent two sample t-test (unpooled, ie test does not assume that the populations have equal variances).

MS<MC - t-test indicates that the mean of the element for the mangrove swamp environment is less than the mean for the same element in the mangrove channel environment at a 95% confidence level.

MS=MC - t-test indicates that the means of the element are the same at a 95 % confidence level for both environments

MS>MC - t-test indicates that the mean of the element for the mangrove swamp environment is greater than the mean for the same element in the mangrove channel environment at a 95% confidence level.

Table 5.5 Results of an independent 2 sample t-test on geochemical data means for mangrove swamp, mangrove channel, open intertidal, shallow marine and open marine depositional groups.

	OM-RF	OM-RT	OM-B	RF-RT	RF-B	RT-B
Ca	<	<	<	=	=	=
Al	=	>	>	>	>	=
Si	>	>	>	=	=	=
Si/Al	>	=	=	=	<	=
Mg/Al	=	=	=	=	=	=
Fe/Al	>	>	=	=	=	=
Ti/Al	>	=	=	=	<	=
K/Al	>	=	=	=	<	=
P2O5/Al	=	=	=	=	=	=
Mn/Al	>	>	=	>	=	=
Rb/Al	=	=	=	=	=	=
Mb/Al	>	=	<	=	<	<
Y/Al	=	=	=	=	=	<
Th/Al	<	=	=	=	=	=
Pb/Al	=	=	=	=	=	=
V/Al	=	=	<	=	<	=
Cr/Al	=	>	=	=	=	=
Zn/al	=	=	=	=	<	=
Ni/Al	=	=	=	=	=	=
La/Al	=	>	=	>	=	=
Ce/Al	<	=	<	=	<	=
Nd/Al	=	=	=	=	=	=
Ba/Al	=	=	<	<	<	=
Sr/Ca	<	<	<	<	=	=
Sn	=	=	>	>	>	=
Zr/Al	=	=	=	=	=	=

OM = open marine RT = reef top
RF = reef front B = Beach

Independent two sample t-test (unpooled, ie test does not assume that the populations have equal variances).

OM<RF - t-test indicates that the mean of the element for the mangrove swamp environment is less than the mean for the same element in the mangrove channel environment at a 95% confidence level.

OM=RF - t-test indicates that the means of the element are the same at a 95% confidence level for both environments.

OM>RF - t-test indicates that the mean of the element for the mangrove swamp environment is greater than the mean for the same element in the mangrove channel environment at a 95% confidence level.

Table 5.6 Results of an independent 2 sample t-test on geochemical data means for open marine, reef front, reef top and beach depositional groups.

MANGROVE SWAMP ENVIRONMENT

	Fe	Mn	Ti	Ca	K2	P205	Al	Si	Mg	Rb	Zr	Y	Sr	Rb	Th	Pb	Zn	Ni	Cr	Ce	Nd	La	V	Ba	Sn	CaCO3	Mean	S.d.	Skew	Sand	Silt	Clay
Mn	-0.018																															
Ti	0.61	-0.798																														
Ca	0.107	-0.379	0.275																													
K2	-0.077	0.998*	-0.828	-0.414																												
P205	0.729	0.131	0.268	0.639	0.066																											
Al	0.099	0.972	-0.687	-0.545	0.97	0.076																										
Si	-0.687	-0.19	-0.325	0.645	-0.172	-0.064	-0.408																									
Mg	0.355	-0.899	0.945	0.117	-0.907	-0.057	-0.777	-0.258																								
Rb	-0.131	0.993*	-0.861	-0.371	0.997*	0.06	0.949	-0.099	-0.936																							
Zr	-0.533	-0.621	0.117	0.7	-0.605	-0.103	-0.782	0.868	0.216	-0.545																						
Y	-0.129	0.994*	-0.858	-0.4	0.998*	0.04	0.956	-0.122	-0.927	1	-0.564																					
Sr	0.52	-0.858	0.994*	0.29	-0.883	0.194	-0.757	-0.25	0.968	-0.911	0.205	-0.908																				
Rb	-0.214	0.981	-0.899	-0.394	0.99*	-0.017	0.931	-0.054	-0.946	0.996*	-0.504	0.996*	-0.94																			
Th	-0.04	0.999*	-0.805	-0.425	0.999*	0.083	0.978	-0.209	-0.891	0.994*	-0.635	0.995*	-0.864	0.984																		
Pb	-0.041	1	-0.812	-0.373	0.999*	0.121	0.967	-0.168	-0.909	0.996*	-0.603	0.996*	-0.871	0.985	0.998*																	
Zn	0.791	0.278	0.303	-0.52	0.248	0.26	0.473	-0.978	0.169	0.177	-0.909	0.195	0.213	0.119	0.287	0.255																
Ni	0.407	-0.903	0.97	0.217	-0.918	0.048	-0.796	-0.223	0.993*	-0.944	0.247	-0.938	0.989*	-0.961	-0.901	-0.913	0.156															
Cr	0.286	-0.954	0.934	0.264	-0.963	-0.019	-0.868	-0.098	0.986	-0.98	0.369	-0.976	0.967	-0.987*	-0.952	-0.961	0.021	0.99*														
Ce	0.113	0.728	-0.441	-0.884	0.74	-0.263	0.86	-0.696	-0.423	0.697	-0.901	0.718	-0.498	0.691	0.756	0.718	0.665	-0.487	-0.569													
Nd	0.18	0.73	-0.405	-0.861	0.738	-0.202	0.866	-0.73	-0.407	0.691	-0.928	0.712	-0.468	0.68	0.756	0.719	0.709	-0.466	-0.555	0.998*												
La	0.072	0.362	-0.154	-0.984	0.387	-0.516	0.551	-0.771	-0.039	0.335	-0.792	0.364	-0.184	0.343	0.405	0.352	0.662	-0.131	-0.199	0.9	0.889											
V	0.327	-0.933	0.946	0.217	-0.943	-0.018	-0.834	-0.163	0.994*	-0.965	0.507	-0.959	0.974	-0.975	-0.93	-0.942	0.085	0.996*	0.998*	-0.517	-0.501	-0.144										
Ba	0.12	-0.982	0.859	0.237	-0.981	-0.16	-0.911	0.007	0.961	-0.99*	0.465	-0.985	0.909	-0.983	-0.975	-0.986	-0.108	0.955	0.985	-0.596	-0.596	-0.202	0.977									
Sn	-0.317	0.945	-0.945	-0.271	0.957	-0.01	0.858	0.116	-0.987*	0.975	-0.351	0.971*	-0.975	0.985	0.944	0.953	-0.044	-0.994*	-0.999*	0.564	0.548	0.2	-0.998	-0.979								
CaCO3	-0.568	-0.525	0.016	0.716	-0.51	-0.074	-0.705	0.935	0.102	-0.445	0.993*	-0.466	0.101	-0.404	-0.542	-0.506	-0.942	0.137	0.261	-0.876	-0.904	-0.816	0.197	0.358	-0.243							
Mean	0.659	0.449	0.095	-0.65	0.428	0.15	0.635	-0.961*	-0.012	0.36	-0.977*	0.38	0.007	0.312	0.463	0.428	0.975*	-0.038	-0.169	0.812	0.846	0.767	-0.104	-0.28	0.148	-0.993*						
S.d.	0.108	-0.562	0.429	0.978*	-0.593	0.547	-0.703	0.612	0.309	-0.555	0.759	-0.581	0.455	-0.574	-0.603	-0.557	-0.519	0.399	0.451	-0.95*	-0.93	-0.959*	0.405	0.433	-0.456	0.752	-0.619					
Skew	-0.721	0.667	-0.932	-0.535	0.714	-0.585	0.613	0.203	-0.775	0.738	-0.157	0.744	-0.909	0.796	0.692	0.681	-0.256	-0.838	-0.795	0.55	0.5	0.399	-0.8	-0.691	0.814	-0.084	0.197	-0.215				
Sand	-0.441	-0.66	0.2	0.756	-0.651	-0.018	-0.817	0.857	0.272	-0.394	0.994*	-0.614	0.282	-0.561	-0.678	-0.644	-0.866	0.312	0.427	-0.941	-0.962*	-0.831	0.366	0.508	-0.412	0.985*	-0.939	0.803	-0.187			
Silt	0.193	0.737	-0.404	-0.851	0.743	-0.183	0.872	-0.732	-0.412	0.697	-0.933	0.718	-0.468	0.684	0.762	0.726	0.715	-0.469	-0.56	0.996*	1	0.881	-0.506	-0.601	0.552	-0.909	0.796	-0.923	0.165	-0.953*		
Clay	0.994*	0.019	0.587	-0.007	-0.036	0.658	0.156	-0.765	0.349	-0.095	-0.614	-0.09	0.495	-0.175	0.003	-0.004	0.855	0.391	0.263	0.212	0.276	0.185	0.31	0.099	-0.294	-0.652	0.744	0.057	0.125	-0.492	0.204	
Silt/Clay	0.443	0.658	-0.197	-0.756	0.649	0.018	0.815	-0.858	-0.27	0.592	-0.995*	0.612	-0.279	0.558	0.676	0.642	0.868	-0.309	-0.424	0.941	0.962*	0.832	-0.364	-0.506	0.409	-0.983*	0.939	-0.803	0.185	-1	0.952*	0.495

For geochemical data: N=4 r=0.987 (95%)

For grain size data: N=5 r=0.950 (95%)

Table 5.7 Correlation matrix of elements and grain size parameters for Mangrove Swamp sediments.

MANGROVE CHANNEL ENVIRONMENT

	Fe	Mn	Ti	Ca	K2	P205	Al	Si	Mg	Nb	Zr	Y	Sr	Rb	Th	Pb	Zn	Ni	Cr	Ce	Nd	La	V	Ba	Sn	CaCO3	Mean	S.d.	Skew	Gravel	Sand	Silt	Clay
Mn	0.374																																
Ti	0.739	0.356																															
Ca	0.214	0.169	0.158																														
K2	-0.078	0.487	-0.029	-0.502																													
P205	0.529	0.668	0.490	0.515	-0.136																												
Al	0.489	0.605	0.665	-0.210	0.663	0.321																											
Si	-0.527	-0.631	-0.492	-0.817	0.176	-0.807	-0.274																										
Mg	0.173	0.544	0.069	0.355	-0.093	0.753	-0.036	-0.545																									
Nb	0.196	0.750	0.348	-0.315	0.861*	0.209	0.874*	-0.176	0.026																								
Zr	0.527	-0.205	0.570	0.167	-0.575	0.065	-0.114	-0.186	-0.057	-0.342																							
Y	0.276	0.863*	0.444	-0.163	0.651	0.511	0.825*	-0.381	0.302	0.924*	-0.251																						
Sr	0.327	0.093	0.168	0.823*	-0.560	0.308	-0.218	-0.691	0.038	-0.287	0.392	-0.169																					
Rb	-0.131	0.511	-0.109	-0.462	0.987*	-0.142	0.604	0.146	-0.084	0.857*	-0.599	0.657	-0.481																				
Th	0.361	0.693	0.624	-0.227	0.571	0.400	0.919*	-0.294	0.052	0.889*	-0.104	0.933*	-0.158	0.547																			
Pb	0.112	0.661	0.224	-0.402	0.914*	0.110	0.837*	-0.055	-0.044	0.982*	-0.432	0.871*	-0.376	0.916*	0.828*																		
Zn	0.563	0.670	0.575	-0.226	0.488	0.292	0.806	-0.300	-0.015	0.806	0.129	0.818	0.042	0.497	0.870*	0.750																	
Ni	0.771	0.511	0.752	-0.023	0.065	0.518	0.658	-0.450	0.060	0.486	0.416	0.621	0.235	0.054	0.721	0.405	0.835*																
Cr	0.833*	0.453	0.726	-0.011	-0.064	0.494	0.504	-0.419	0.106	0.334	0.550	0.479	0.281	-0.080	0.568	0.235	0.750	0.959*															
Ce	0.676	0.627	0.749	-0.022	0.267	0.555	0.820	-0.471	0.032	0.668	0.183	0.767	0.138	0.244	0.862*	0.597	0.855*	0.934*	0.834*														
Nd	0.529	0.701	0.608	-0.156	0.439	0.474	0.835*	-0.359	0.020	0.793	-0.029	0.861*	0.011	0.432	0.918*	0.732	0.891*	0.866*	0.752	0.940*													
La	0.631	0.615	0.769	0.107	0.195	0.541	0.769	-0.544	-0.016	0.627	0.228	0.725	0.262	0.186	0.827*	0.545	0.822	0.908*	0.793	0.971*	0.914*												
V	0.779	0.452	0.779	-0.038	-0.055	0.500	0.556	-0.402	0.083	0.367	0.538	0.521	0.226	-0.084	0.637	0.260	0.746	0.960*	0.981*	0.873*	0.776	0.835*											
Ba	0.036	0.070	0.206	-0.588	0.160	-0.023	0.256	0.348	-0.267	0.267	0.072	0.289	-0.397	0.121	0.378	0.268	0.272	0.404	0.405	0.445	0.463	0.374	0.495										
Sn	-0.091	0.848*	-0.071	0.032	0.680	0.402	0.430	-0.366	0.513	0.727	-0.576	0.760	-0.164	0.729	0.504	0.713	0.603	0.068	-0.025	0.262	0.420	0.253	-0.028	-0.072									
CaCO3	0.292	0.220	0.179	0.990*	-0.477	0.571	-0.166	-0.848*	0.377	-0.273	0.178	-0.114	0.835*	-0.432	-0.188	-0.354	-0.156	0.051	0.060	0.052	-0.094	0.169	0.023	-0.566	0.060								
Mean	0.508	-0.137	0.565	-0.127	-0.226	-0.177	0.256	-0.010	-0.566	0.034	0.676	-0.007	0.342	-0.269	0.259	-0.027	0.496	0.637	0.671	0.508	0.380	0.543	0.692	0.572	-0.530	-0.114							
S.d.	0.512	0.646	0.606	0.207	-0.029	0.664	0.517	-0.692	0.239	0.437	0.202	0.659	0.382	-0.020	0.685	0.313	0.666	0.808	0.769	0.833	0.757	0.815	0.823	0.609	0.243	0.255	0.428						
Skew	-0.512	-0.016	-0.507	-0.350	0.181	-0.190	-0.166	0.387	0.269	0.013	-0.525	0.039	-0.493	0.198	-0.072	0.054	-0.171	-0.357	-0.388	-0.395	-0.171	-0.440	-0.395	-0.244	0.298	-0.413	-0.456	-0.335					
Gravel	-0.183	0.476	-0.293	0.312	0.017	0.599	-0.219	-0.414	0.890*	0.002	-0.370	0.230	-0.049	0.058	-0.091	-0.018	-0.249	-0.225	-0.197	-0.180	-0.115	-0.226	-0.221	-0.280	0.615	0.329	-0.795	0.086	0.270				
Sand	-0.311	-0.810	-0.286	-0.337	0.009	-0.557*	-0.228	0.771	-0.766	-0.311	0.026	-0.609	-0.224	-0.016	-0.411	-0.199	-0.330	-0.459	-0.473	-0.488	-0.470	-0.450	-0.495	-0.306	-0.580	-0.381	0.153	-0.762	0.066	-0.682			
Silt	0.626	0.483	0.710	0.073	-0.037	0.380	0.540	-0.503	-0.075	0.389	0.414	0.495	0.363	-0.054	0.621	0.264	0.714	0.846*	0.842*	0.830	0.727	0.835*	0.895*	0.722	0.010	0.108	0.758	0.877*	-0.421	-0.315	-0.477		
Clay	0.600	0.434	0.745	0.012	-0.019	0.387	0.605	-0.468	-0.106	0.426	0.400	0.545	0.297	-0.035	0.691	0.320	0.754	0.906*	0.852*	0.884*	0.786	0.894*	0.909*	0.752	-0.003	0.051	0.757	0.874*	-0.377	-0.547	-0.435	0.949*	
Silt/Clay	0.623	0.473	0.723	0.058	-0.032	0.384	0.559	-0.497	-0.083	0.400	0.413	0.510	0.348	-0.050	0.643	0.280	0.728	0.866*	0.849*	0.848*	0.767	0.855*	0.904*	0.734	0.007	0.094	0.762	0.881*	-0.412	-0.325	-0.469	0.998*	0.983*

For geochemical data: N=13 r=0.823 (95%)

For grain size data: N=12 r=0.834 (95%)

Table 5.8 **Correlation matrix of elements and grain size parameters for Mangrove Channel sediments.**

OPEN INTERTIDAL ENVIRONMENT

	Fe	Mn	Ti	Ca	K2	P205	Al	Si	Mg	Nb	Zr	Y	Sr	Rb	Th	Pb	Zn	Ni	Cr	Ce	Nd	La	V	Ba	Sn	CaCO3	Corg	Mean	S.d.	Skew	Gravel	Sand	Silt	Clay
Mn	0.749																																	
Ti	0.969*	0.587																																
Ca	-0.143	0.065	-0.253																															
K2	0.664	0.761	0.591	-0.413																														
P205	0.419	-0.032	0.536	0.09	-0.112																													
Al	0.911*	0.806*	0.854*	-0.273	0.839*	0.252																												
Si	-0.775	-0.732	-0.668	-0.492	-0.4	-0.384	-0.669																											
Mg	0.825*	0.391	0.861*	0.087	0.229	0.645	0.558	-0.728																										
Nb	0.76	0.838*	0.669	-0.311	0.955*	-0.02	0.939*	-0.543	0.301																									
Zr	0.25	-0.055	0.323	-0.177	0.039	0.072	-0.029	-0.02	0.408	-0.071																								
Y	0.806*	0.829*	0.713	-0.252	0.882*	0.072	0.957*	-0.608	0.37	0.973*	-0.034																							
Sr	-0.076	0.078	-0.178	0.992*	-0.404	0.154	-0.244	-0.536	0.19	-0.307	-0.096	-0.239																						
Rb	0.481	0.752	0.364	-0.286	0.956*	-0.303	0.714	-0.341	0.016	0.904*	-0.097	0.81*	-0.299																					
Th	0.81*	0.818*	0.722	-0.238	0.848*	0.123	0.972*	-0.621	0.379	0.963*	-0.147	0.987*	-0.231	0.773																				
Pb	0.768	0.849*	0.662	-0.252	0.908*	0.013	0.948*	-0.585	0.315	0.987*	-0.124	0.99*	-0.246	0.859*	0.985*																			
Zn	0.914*	0.81*	0.86*	-0.198	0.819*	0.257	0.981*	-0.718	0.587	0.918*	-0.011	0.922*	-0.171	0.703	0.943*	0.914*																		
Ni	0.946*	0.618	0.959*	-0.165	0.566	0.497	0.875*	-0.716	0.805*	0.685	0.155	0.738	-0.11	0.563	0.771	0.694	0.905*																	
Cr	0.887*	0.514	0.92*	-0.063	0.418	0.524	0.765	-0.716	0.827*	0.55	0.252	0.628	-0.004	0.211	0.653	0.562	0.816*	0.972*																
Ce	0.86*	0.79	0.788	-0.035	0.656	0.245	0.921*	-0.759	0.534	0.83*	-0.059	0.898*	-0.022	0.55	0.922*	0.865*	0.932*	0.878*	0.836*															
Nd	0.861*	0.785	0.789	-0.012	0.626	0.246	0.903*	-0.772	0.559	0.805*	-0.021	0.875*	0.007	0.523	0.902*	0.842*	0.922*	0.875*	0.843*	0.989*														
La	0.859*	0.764	0.81*	-0.084	0.684	0.259	0.921*	-0.743	0.559	0.83*	-0.049	0.88*	-0.069	0.561	0.906*	0.85*	0.942*	0.898*	0.857*	0.981*	0.971*													
V	0.911*	0.649	0.91*	-0.127	0.615	0.368	0.877*	-0.727	0.718	0.732	0.15	0.78	-0.087	0.438	0.801*	0.733	0.921*	0.975*	0.962*	0.92*	0.912*	0.948*												
Ba	0.801*	0.691	0.785	-0.29	0.825*	0.162	0.896*	-0.569	0.462	0.874*	0.061	0.857*	-0.275	0.71	0.867*	0.844*	0.941*	0.851*	0.79	0.861*	0.848*	0.897*	0.906*											
Sn	0.51	0.778	0.392	-0.293	0.941*	-0.301	0.752	-0.355	0.006	0.926*	-0.164	0.836*	-0.319	0.976*	0.818*	0.884*	0.746	0.612	0.258	0.619	0.592	0.624	0.491	0.751										
CaCO3	-0.057	0.125	-0.168	0.988	-0.378	0.139	-0.21	-0.552	0.182	-0.272	-0.156	-0.208	0.991	-0.269	-0.191	-0.208	-0.132	-0.077	0.019	0.02	0.047	-0.03	-0.054	-0.233	-0.277									
Corg	0.814	0.069	0.928	0.269	0.066	0.975*	0.624	-0.783	0.976*	0.262	0.334	0.455	0.577	-0.205	0.497	0.305	0.643	0.89	0.956*	0.702	0.758	0.716	0.857	0.656	-0.234	0.41								
Mean	0.929*	0.56	0.963*	-0.399	0.606	0.442	0.836*	-0.533	0.755	0.682	0.4	0.728	-0.33	0.385	0.721	0.668	0.825*	0.894*	0.851*	0.758	0.76	0.76	0.847*	0.755	0.421	-0.328	0.927							
S.d.	0.133	0.219	0.041	0.806*	-0.173	0.107	0.014	-0.634	0.305	-0.07	-0.089	0.021	0.812*	-0.144	0.021	-0.006	0.074	0.163	0.263	0.259	0.25	0.268	0.242	0.013	-0.156	0.816*	0.422	-0.148						
Skew	-0.742	-0.364	-0.761	-0.178	-0.151	-0.686	-0.539	0.721	-0.872*	-0.276	-0.264	-0.419	-0.266	0.051	-0.42	-0.342	-0.528	-0.767	-0.811*	-0.611	-0.607	-0.613	-0.709	-0.416	0.069	-0.268	-0.938*	-0.642	-0.493					
Gravel	-0.164	0.064	-0.275	0.993*	-0.42	0.05	-0.276	-0.478	0.06	-0.312	-0.231	-0.255	0.979*	-0.286	-0.236	-0.252	-0.194	-0.164	-0.058	-0.024	-0.004	-0.065	-0.115	-0.277	-0.287	0.982*		-0.425	0.829*	-0.164				
Sand	-0.908*	-0.531	-0.917*	0.046	-0.422	-0.627	-0.755	0.722	-0.85*	-0.55	-0.376	-0.653	-0.036	-0.224	-0.65	-0.58	-0.75	-0.869*	-0.867*	-0.753	-0.772	-0.718	-0.805*	-0.636	-0.258	-0.031	-0.94*	-0.901*	-0.11	0.818*	0.09			
Silt	0.86*	0.463	0.878*	-0.184	0.425	0.585	0.716	-0.601	0.796	0.528	0.452	0.633	-0.074	0.224	0.616	0.559	0.687	0.802*	0.792	0.675	0.701	0.634	0.725	0.584	0.217	-0.088	0.891	0.89*	-0.017	-0.769	-0.217	-0.978*		
Clay	0.89*	0.559	0.926*	-0.193	0.516	0.557	0.813*	-0.643	0.744	0.631	0.143	0.665	-0.151	0.312	0.699	0.616	0.84	0.924*	0.891*	0.8*	0.782	0.818*	0.892*	0.772	0.391	-0.128	0.827	0.903*	0.036	-0.65	-0.199	-0.831*	0.738	
Silt/Clay	0.911*	0.51	0.935*	-0.179	0.469	0.608	0.776	-0.642	0.824*	0.58	0.399	0.673	-0.097	0.257	0.667	0.601	0.759	0.872*	0.856*	0.74	0.756	0.711	0.803*	0.66	0.271	-0.102	0.94*	0.939*	-0.004	-0.778	-0.224	-0.991*	0.986*	0.84*

For geochemical and grain size data: N=16 r=0.798 (95%)

For organic carbon: N=6 r=0.933 (95%)

Table 5.9 Correlation matrix of elements and grain size parameters for Open Intertidal sediments.

SHALLOW MARINE ENVIRONMENT

	Fe	Mn	Ti	Ca	K2	P205	Al	Si	Mg	Nb	Zr	Y	Sr	Rb	Th	Pb	Zn	Ni	Cr	Ce	Nd	La	V	Ba	Sn	CaCO3	Corg	Mean	S.d.	Skew	Gravel	Sand	Silt	Clay
Mn	0.727*																																	
Ti	0.915*	0.49																																
Ca	-0.728*	-0.246	-0.808*																															
K2	0.887*	0.527	0.923*	-0.78*																														
P205	0.295	0.231	0.316	-0.152	0.21																													
Al	0.932*	0.616	0.945*	-0.726*	0.967*	0.267																												
Si	0.407	-0.038	0.505	-0.899*	0.452	0.075	0.36																											
Mg	0.365	0.248	0.383	-0.072	0.309	0.06	0.367	-0.179																										
Nb	0.849*	0.517	0.877*	-0.78	0.945*	0.131	0.945*	0.46	0.237																									
Zr	0.521	0.05	0.721*	-0.768*	0.587	0.089	0.548	0.683*	0.202	0.635																								
Y	0.819*	0.534	0.834*	-0.71*	0.91*	0.116	0.922*	0.372	0.309	0.98*	0.619																							
Sr	-0.727*	-0.297	-0.8*	0.974*	-0.775*	-0.078	-0.727*	-0.865*	-0.071	-0.779*	-0.742*	-0.711*																						
Rb	0.784*	0.54	0.774*	-0.689*	0.915*	0.112	0.903*	0.363	0.186	0.969*	0.5	0.968*	-0.691*																					
Th	0.789*	0.538	0.784*	-0.641	0.886*	0.118	0.911*	0.292	0.284	0.966*	0.5	0.972*	-0.644	0.965*																				
Pb	0.828*	0.579	0.798*	-0.675*	0.917*	0.111	0.928*	0.33	0.236	0.971*	0.48	0.97*	-0.679*	0.98*	0.98*																			
Zn	0.841*	0.54	0.824*	-0.707*	0.802*	0.137	0.862*	0.404	0.252	0.869*	0.559	0.854*	-0.708*	0.817*	0.841*	0.834*																		
Ni	0.803*	0.482	0.834*	-0.691*	0.745*	0.173	0.806*	0.416	0.308	0.778*	0.6	0.743*	-0.678*	0.689*	0.711*	0.703*	0.944*																	
Cr	0.705*	0.406	0.728*	-0.635	0.613	0.095	0.677*	0.415	0.238	0.666	0.587	0.637	-0.624	0.572	0.593	0.583	0.905*	0.963*																
Ce	0.654	0.469	0.638	-0.472	0.617	0.083	0.708*	0.182	0.28	0.719*	0.423	0.732*	-0.468	0.688*	0.75*	0.71*	0.887*	0.842*	0.847*															
Nd	0.591	0.361	0.608	-0.512	0.622	-0.017	0.677*	0.249	0.212	0.732*	0.471	0.744*	-0.513	0.713*	0.756*	0.714*	0.861*	0.81*	0.816*	0.949*														
La	0.593	0.338	0.615	-0.492	0.596	0.076	0.672*	0.228	0.196	0.7*	0.428	0.702*	-0.477	0.678*	0.711*	0.677*	0.879*	0.853*	0.863*	0.921*	0.89*													
V	0.754*	0.441	0.771*	-0.68*	0.712*	0.076	0.764*	0.423	0.206	0.77*	0.576	0.739*	-0.674*	0.699*	0.716*	0.706*	0.952*	0.956*	0.969*	0.885*	0.857*	0.895*												
Ba	0.63	0.33	0.68*	-0.625	0.633	0.137	0.678*	0.404	0.129	0.713*	0.569	0.696*	-0.6	0.666	0.677*	0.643	0.893*	0.89*	0.914*	0.901*	0.898*	0.913*	0.943*											
Sn	0.518	0.409	0.483	-0.352	0.649	-0.058	0.669*	0.053	0.289	0.75*	0.246	0.792*	-0.361	0.808*	0.838*	0.813*	0.592	0.417	0.322	0.635	0.641	0.586	0.469	0.481										
CaCO3	-0.706*	-0.222	-0.795*	0.992*	-0.777*	-0.155	-0.714*	-0.899*	-0.038	-0.765*	-0.749*	-0.69*	0.966*	-0.678*	-0.627	-0.663	-0.676*	-0.664	-0.604	-0.445	-0.5	-0.462	-0.653	-0.605	-0.329									
Corg	0.467	0.315	0.612	-0.143	0.514	0.497	0.576	-0.226	0.198	0.467	0.214	0.42	-0.142	0.366	0.454	0.407	0.51	0.495	0.435	0.541	0.384	0.474	0.544	0.537	0.226	-0.199								
Mean	0.739*	0.206	0.886*	-0.878*	0.806*	0.199	0.778*	0.693*	0.318	0.8*	0.864*	0.761*	-0.852*	0.675*	0.685*	0.689*	0.736*	0.752*	0.679*	0.55	0.592	0.54	0.694*	0.65	0.389	-0.856*	0.356							
S.d.	-0.248	0.142	-0.415	0.6	-0.501	-0.06	-0.344	-0.593	0.071	-0.403	-0.452	-0.345	0.583	-0.368	-0.294	-0.337	-0.21	-0.219	-0.159	-0.034	-0.139	-0.068	-0.211	-0.171	-0.11	0.63	0.031	-0.547						
Skew	-0.674*	-0.295	-0.784*	0.589	-0.652	-0.251	-0.69*	-0.354	-0.57	-0.64	-0.62	-0.619	0.576	-0.519	-0.577	-0.558	-0.623	-0.657	-0.568	-0.485	-0.472	-0.472	-0.549	-0.502	-0.379	0.562	-0.446	-0.795*	0.079					
Gravel	-0.416	0.116	-0.58	0.741*	-0.55	-0.088	-0.495	-0.677*	-0.341	-0.556	-0.677*	-0.539	0.702*	-0.479	-0.493	-0.477	-0.469	-0.465	-0.411	-0.402	-0.473	-0.409	-0.429	-0.473	-0.352	0.748*	-0.047	-0.794*	0.482	0.634				
Sand	-0.666*	-0.449	-0.706*	0.44	-0.587	-0.226	-0.619	-0.209	-0.226	-0.557	-0.533	-0.52	0.443	-0.431	-0.453	-0.472	-0.581	-0.647	-0.591	-0.368	-0.327	-0.347	-0.563	-0.623	-0.166	0.403	-0.463	-0.649	0.248	0.591	0.079			
Silt	0.751*	0.285	0.876*	-0.75*	0.763*	0.229	0.754*	0.534	0.372	0.739*	0.805*	0.701*	-0.731*	0.595	0.615	0.623	0.705*	0.761*	0.689*	0.492	0.499	0.486	0.67*	0.583	0.31	-0.714*	0.427	0.937*	-0.463	-0.808*	-0.584	-0.852*		
Clay	0.768*	0.364	0.854*	-0.715*	0.754*	0.223	0.773*	0.482	0.315	0.745*	0.694*	0.702*	-0.701*	0.613	0.658	0.661	0.751*	0.775*	0.699*	0.574	0.567	0.528	0.712*	0.614	0.359	-0.691*	0.463	0.897*	-0.377	-0.769*	-0.535	-0.824*	0.923*	
Silt/Clay	0.763*	0.304	0.883*	-0.753*	0.771*	0.23	0.767*	0.531	0.365	0.749*	0.794*	0.71*	-0.735*	0.606	0.631	0.638	0.722*	0.773*	0.7*	0.513	0.518	0.5	0.687*	0.596	0.323	-0.718*	0.438	0.94*	-0.452	-0.81*	-0.581	-0.857*	0.997*	0.949*

For geochemical data: N=62 r=0.667 (95%)

For grain size data: N=65 r=0.663 (95%)

For organic carbon: N=19 r=0.778 (95%)

Table 5.10 Correlation matrix of elements and grain size parameters for Shallow Marine sediments.

OPEN MARINE ENVIRONMENT

	Fe	Mn	Ti	Ca	K2	P205	Al	Si	Mg	Nb	Zr	Y	Sr	Rb	Th	Pb	Zn	Ni	Cr	Ce	Nd	La	V	Ba	Sn	CaCO3	Corg	Mean	S.d.	Skew	Gravel	Sand	Silt	Clay
Mn	0.547																																	
Ti	0.702	0.191																																
Ca	-0.275	0.375	-0.401																															
K2	0.036	-0.043	0.281	0.33																														
P205	0.422	0.487	0.449	0.467	0.616																													
Al	0.692	0.256	0.933*	-0.174	0.525	0.593																												
Si	-0.009	-0.491	0.051	-0.924*	-0.521	-0.689	-0.201																											
Mg	0.811*	0.591	0.598	0.157	0.298	0.687	0.702	-0.458																										
Nb	0.641	0.225	0.922*	-0.212	0.474	0.553	0.922*	-0.124	0.566																									
Zr	0.334	-0.117	0.635	-0.583	-0.148	-0.014	0.399	0.439	0.142	0.425																								
Y	0.414	0.261	0.676	0.143	0.618	0.73*	0.714*	-0.412	0.583	0.776*	0.252																							
Sr	-0.273	0.249	-0.336	0.936*	0.372	0.418	-0.109	-0.871*	0.107	-0.168	-0.541	0.164																						
Rb	0.181	0.051	0.431	0.284	0.971*	0.677	0.664	-0.52	0.403	0.605	-0.059	0.689	0.335																					
Th	0.451	0.177	0.755*	0.12	0.73*	0.727*	0.858*	-0.439	0.597	0.88*	0.205	0.89*	0.172	0.816*																				
Pb	0.458	0.311	0.594	0.276	0.825*	0.771*	0.796*	-0.569	0.637	0.754*	0.028	0.777*	0.295	0.906*	0.893*																			
Zn	0.85*	0.384	0.874*	-0.338	0.185	0.407	0.859*	0.017	0.642	0.827*	0.489	0.524	-0.276	0.357	0.623	0.583																		
Ni	0.808*	0.553	0.821*	-0.002	0.303	0.622	0.872*	-0.323	0.778*	0.856*	0.255	0.647	0.029	0.469	0.752*	0.725*	0.882*																	
Cr	0.796*	0.569	0.786*	-0.052	0.255	0.564	0.819*	-0.243	0.684	0.838*	0.274	0.606	-0.03	0.431	0.696	0.705	0.893*	0.967*																
Ce	0.621	0.283	0.755*	0.064	0.593	0.671	0.869*	-0.39	0.712*	0.819*	0.242	0.746*	0.108	0.707	0.876*	0.868*	0.752*	0.835*	0.802*															
Nd	0.452	0.094	0.575	0.027	0.638	0.506	0.729*	-0.297	0.557	0.641	0.181	0.504	0.085	0.698	0.73*	0.769*	0.569	0.605	0.58	0.823*														
La	0.681	0.354	0.693	0.08	0.321	0.536	0.777*	-0.369	0.776*	0.707	0.249	0.6	0.114	0.471	0.729*	0.708	0.737*	0.851*	0.809*	0.82*	0.682													
V	0.7	0.602	0.667	0.062	0.244	0.517	0.719*	-0.316	0.591	0.778*	0.159	0.551	0.082	0.404	0.648	0.668	0.827*	0.927*	0.962*	0.745*	0.505	0.757*												
Ba	0.306	0.095	0.546	0.178	0.807*	0.581	0.763*	-0.449	0.47	0.679	0.022	0.559	0.226	0.864*	0.795*	0.888*	0.532	0.626	0.59	0.801*	0.865*	0.651	0.572											
Sn	-0.098	-0.072	-0.103	0.234	0.054	0.075	-0.095	-0.2	-0.016	0.059	-0.286	0.138	0.254	0.013	0.165	0.033	-0.125	0.013	-0.049	-0.069	-0.138	0.09	0.037	-0.04										
CaCO3	-0.208	0.48	-0.359	0.978*	0.283	0.459	-0.14	-0.913*	0.188	-0.178	-0.56	0.14	0.905*	0.263	0.121	0.293	-0.266	0.066	0.038	0.092	0.05	0.134	0.157	0.191	0.138									
Corg	-0.159	-0.097	-0.327	0.099	0.013	-0.226	-0.133	-0.065	-0.091	-0.124	-0.695	-0.142	0.034	-0.032	-0.017	-0.069	-0.147	-0.066	-0.165	-0.088	0.015	0.004	-0.042	0.103	0.183	0.082								
Mean	0.449	-0.187	0.693	-0.688	-0.121	-0.028	0.539	0.474	0.311	0.427	0.807*	0.13	-0.619	-0.036	0.198	0.034	0.562	0.323	0.273	0.297	0.331	0.313	0.112	0.155	-0.36	-0.679	-0.399							
S.d.	0.636	0.477	0.491	0.135	0.04	0.351	0.513	-0.321	0.568	0.563	0.122	0.437	0.117	0.185	0.498	0.474	0.625	0.763*	0.768*	0.638	0.365	0.752*	0.774*	0.34	0.17	0.2	-0.137	0.031						
Skew	-0.359	-0.165	-0.405	0.317	0.132	-0.06	-0.28	-0.19	-0.26	-0.273	-0.462	-0.172	0.359	0.086	-0.074	0.015	-0.403	-0.226	-0.229	-0.188	0.051	-0.048	-0.184	0.132	0.133	0.315	0.278	-0.49	-0.177					
Gravel	-0.045	0.509	-0.122	0.598	0.206	0.374	-0.048	-0.566	0.092	0.086	-0.38	0.421	0.53	0.238	0.227	0.32	-0.053	0.203	0.258	0.111	-0.14	0.128	0.254	0.037	0.231	0.643	-0.185	-0.748*	0.309	0.296				
Sand	-0.487	-0.474	-0.752*	-0.1	-0.337	-0.626	-0.749*	0.368	-0.549	-0.791*	-0.291	-0.797*	-0.102	-0.492	-0.752*	-0.67	-0.675	-0.803*	-0.791*	-0.673	-0.361	-0.673	-0.749*	-0.482	-0.039	-0.159	0.239	-0.052	-0.584	0.097	-0.568			
Silt	0.566	0.106	0.948*	-0.38	0.213	0.399	0.881*	0.055	0.526	0.819*	0.651	0.553	-0.323	0.36	0.659	0.485	0.795*	0.728*	0.668	0.659	0.51	0.638	0.544	0.508	-0.151	-0.354	-0.205	0.754*	0.376	-0.395	-0.262	-0.644		
Clay	0.691	0.16	0.953*	-0.378	0.197	0.389	0.909*	0.032	0.633	0.832*	0.6	0.549	-0.315	0.352	0.676	0.554	0.853*	0.792*	0.74*	0.712*	0.589	0.735*	0.605	0.544	-0.133	-0.339	-0.126	0.751*	0.488	-0.346	-0.271	-0.614	0.961*	
Silt/Clay	0.59	0.116	0.954*	-0.382	0.212	0.4	0.89*	0.052	0.547	0.825*	0.646	0.556	-0.324	0.361	0.665	0.495	0.809*	0.742*	0.684	0.671	0.526	0.658	0.557	0.516	-0.149	-0.353	-0.192	0.758*	0.397	-0.389	-0.265	-0.643	0.999*	0.975*

For geochemical data: N=37 r=0.711 (95%)

For grain size data: N=38 r=0.705 (95%)

For organic carbon: N=12 r=0.834 (95%)

Table 5.11 Correlation matrix of elements and grain size parameters for Open Marine sediments.

REEF FRONT ENVIRONMENT

	Fe	Mn	Ti	Ca	K2	P205	Al	Si	Mg	Nb	Zr	Y	Sr	Rb	Th	Pb	Zn	Ni	Cr	Ce	Nd	La	V	Ba	Sn	CaCO3	Mean	S.d.	Skew	Gravel	Sand	Silt	Clay
Mn	0.761																																
Ti	0.952*	0.772																															
Ca	-0.848*	-0.622	-0.868*																														
K2	0.896*	0.728	0.979*	-0.826																													
P205	0.503	0.145	0.293	-0.175	0.229																												
Al	0.954*	0.776	0.994*	-0.848*	0.969*	0.28																											
Si	0.928*	0.799	0.982*	-0.895*	0.951*	0.28	0.962*																										
Mg	0.718	0.626	0.572	-0.654	0.665	0.643	0.54	0.655																									
Nb	0.697	0.866*	0.742	-0.602	0.751	0.205	0.761	0.702	0.336																								
Zr	0.455	0.334	0.673	-0.466	0.775	-0.147	0.648	0.635	-0.094	0.516																							
Y	0.811	0.935*	0.789	-0.543	0.76	0.372	0.802	0.779	0.608	0.935*	0.358																						
Sr	-0.792	-0.925*	-0.746	0.578	-0.696	-0.469	-0.731	-0.787	-0.781	-0.83	-0.253	-0.943*																					
Rb	0.549	0.788	0.623	-0.245	0.656	0.09	0.649	0.572	0.158	0.973*	0.516	0.871*	-0.724																				
Th	0.717	0.854*	0.783	-0.446	0.794	0.236	0.79	0.758	0.37	0.965*	0.583	0.933*	-0.836*	0.952*																			
Pb	0.627	0.812	0.631	-0.312	0.628	0.149	0.675	0.558	0.233	0.932*	0.358	0.886*	-0.724	0.943*	0.896*																		
Zn	0.593	0.707	0.63	-0.283	0.641	0.172	0.674	0.562	0.204	0.862*	0.437	0.849*	-0.644	0.895*	0.883*	0.89*																	
Ni	0.397	0.269	0.158	-0.027	0.123	0.715	0.181	0.11	0.456	0.342	-0.228	0.464	-0.455	0.262	0.26	0.378	0.319																
Cr	0.334	0.164	0.048	-0.06	-0.058	0.731	0.069	0.039	0.591	0.063	-0.5	0.303	-0.351	-0.036	0.025	0.148	0.147	0.875*															
Ce	0.178	0.04	0.212	0.03	0.282	0.215	0.245	0.121	-0.122	0.274	0.302	0.294	-0.073	0.385	0.398	0.37	0.663	0.155	0.086														
Nd	0.457	0.319	0.54	-0.452	0.516	0.024	0.557	0.513	0.197	0.238	0.387	0.338	-0.213	0.261	0.41	0.304	0.527	-0.264	-0.103	0.614													
La	0.709	0.752	0.686	-0.465	0.704	0.478	0.679	0.684	0.614	0.784	0.367	0.848*	-0.848*	0.699	0.754	0.651	0.683	0.501	0.317	0.285	0.201												
V	0.557	0.452	0.333	-0.151	0.248	0.681	0.388	0.262	0.507	0.497	-0.243	0.641	-0.56	0.437	0.442	0.615	0.592	0.838*	0.829	0.348	0.134	0.546											
Ba	0.732	0.532	0.709	-0.496	0.674	0.432	0.746	0.652	0.434	0.595	0.333	0.705	-0.549	0.56	0.679	0.6	0.808	0.306	0.299	0.688	0.731	0.555	0.618										
Sn	-0.232	0.079	-0.144	0.282	-0.113	-0.382	-0.147	-0.155	-0.325	0.13	0.085	-0.083	0.06	0.18	0.066	0.133	-0.172	-0.244	-0.448	-0.468	-0.289	-0.222	-0.325	-0.443									
CaCO3	-0.89*	-0.627	-0.875*	0.936*	-0.83	-0.399	-0.844*	-0.903*	-0.739	-0.47	-0.457	-0.597	0.681	-0.289	-0.489	-0.33	-0.275	-0.188	-0.181	0.074	-0.306	-0.624	-0.253	-0.447	0.292								
Mean	0.453	0.026	0.603	-0.46	0.654	0.137	0.578	0.555	-0.006	0.196	0.809	0.111	-0.047	0.155	0.309	0.04	0.2	-0.258	-0.365	0.331	0.524	0.159	-0.208	0.436	-0.094	-0.461							
S.d.	0.792	0.867*	0.883*	-0.765	0.884*	-0.081	0.896*	0.864*	0.38	0.798	0.639	0.803	-0.695	0.735	0.799	0.755	0.712	0.072	-0.079	0.17	0.481	0.617	0.259	0.592	0.019	-0.68	-0.024						
Skew	-0.341	-0.322	-0.554	0.586	-0.603	0.545	-0.548	-0.541	0.155	-0.297	-0.771	-0.187	0.074	-0.288	-0.332	-0.244	-0.239	0.45	0.566	-0.009	-0.358	-0.014	0.385	-0.157	-0.103	0.412	-0.573	-0.538					
Gravel	-0.173	0.171	-0.218	-0.002	-0.251	-0.503	-0.168	-0.215	-0.11	-0.026	-0.417	0.017	0.055	0.014	-0.136	0.191	0.022	-0.043	0.046	-0.211	-0.166	-0.18	0.097	-0.207	0.014	0.164	-0.61	0.211	-0.016				
Sand	-0.784	-0.776	-0.824*	0.73	-0.817	0.034	-0.863*	-0.761	-0.311	-0.744	-0.501	-0.756	0.596	-0.693	-0.72	-0.797	-0.717	-0.144	-0.01	-0.252	-0.486	-0.539	-0.404	-0.634	0.047	0.628	-0.797	-0.162	0.568	0.109			
Silt	0.886*	0.659	0.951*	-0.722	0.966*	0.296	0.957*	0.89*	0.387	0.75	0.755	0.736	-0.63	0.671	0.796	0.66	0.688	0.175	-0.013	0.376	0.576	0.651	0.338	0.754	-0.06	-0.73	0.911*	0.083	-0.519	-0.378	-0.961*		
Clay	0.843*	0.621	0.922*	-0.674	0.938*	0.234	0.936*	0.849*	0.304	0.728	0.765	0.698	-0.563	0.668	0.779	0.661	0.709	0.118	-0.056	0.425	0.637	0.598	0.318	0.767	-0.042	-0.663	0.916*	0.165	-0.559	-0.392	-0.951*	0.993*	
Silt/Clay	0.882*	0.654	0.949*	-0.717	0.963*	0.288	0.956*	0.885*	0.377	0.748	0.757	0.732	-0.622	0.672	0.794	0.661	0.692	0.168	-0.019	0.383	0.584	0.645	0.336	0.756	-0.058	-0.722	0.912*	0.092	-0.524	-0.38	-0.961*	1*	0.994*

For geochemical data: N=12 r=0.834 (95%)

For grain size data: N=13 r=0.823 (95%)

Table 5.12 Correlation matrix of elements and grain size parameters for Reef Front sediments.

REEF TOP ENVIRONMENT

	Fe	Mn	Ti	Ca	K2	P205	Al	Si	Mg	Nb	Zr	Y	Sr	Rb	Th	Pb	Zn	Ni	Cr	Ce	Nd	La	V	Ba	Sn	CaCO3	Mean	S.d.	Skew	Gravel	Sand	Silt	Clay
Mn	0.77																																
Ti	0.964*	0.727																															
Ca	-0.645	-0.116	-0.751																														
K2	-0.401	-0.673	-0.481	0.211																													
P205	0.429	0.813	0.461	0.154	-0.455																												
Al	0.7	0.706	0.587	-0.046	0.041	0.676																											
Si	0.594	0.062	0.708	-0.997*	-0.209	-0.203	-0.025																										
Mg	-0.378	0.038	-0.255	0.477	0.029	0.605	0.093	-0.481																									
Nb	0.897	0.576	0.954*	-0.776	-0.243	0.433	0.629	0.732	-0.134																								
Zr	-0.395	0.242	-0.315	0.637	-0.433	0.582	-0.12	-0.63	0.776	-0.391																							
Y	0.605	0.411	0.763	-0.647	-0.219	0.54	0.447	0.617	0.295	0.876	-0.071																						
Sr	-0.602	-0.057	-0.723	0.986*	0.101	0.126	-0.08	-0.982*	0.565	-0.796	0.629	-0.72																					
Rb	-0.253	-0.469	-0.353	0.248	0.966*	-0.229	0.285	-0.264	0.121	-0.112	-0.376	-0.105	0.129																				
Th	0.73	0.863	0.597	0.033	-0.214	0.728	0.946	-0.102	0.013	0.56	0.016	0.307	0.048	0.028																			
Pb	0.409	0.537	0.243	0.305	0.239	0.584	0.925	-0.371	0.177	0.292	-0.005	0.132	0.264	0.47	0.878																		
Zn	0.945	0.815	0.985*	-0.664	-0.604	0.562	0.581	0.621	-0.18	0.906	-0.163	0.737	-0.624	-0.464	0.633	0.246																	
Ni	0.16	0.529	0.187	0.344	-0.074	0.908	0.654	-0.389	0.803	0.268	0.582	0.475	0.256	0.144	0.601	0.663	0.258																
Cr	0.734	0.256	0.845	-0.956*	-0.177	0.089	0.277	0.938	-0.276	0.911	-0.548	0.826	-0.974*	-0.148	0.158	-0.085	0.763	-0.063															
Ce	-0.405	-0.144	-0.563	0.81	0.629	0.131	0.338	-0.833	0.375	-0.46	0.211	-0.429	0.74	0.726	0.262	0.66	-0.559	0.433	-0.685														
Nd	0.318	0.057	0.41	-0.373	0.379	0.355	0.523	0.341	0.4	0.657	-0.217	0.808	-0.514	0.495	0.247	0.37	0.328	0.533	0.594	0.073													
La	0.759	0.532	0.663	-0.307	0.198	0.448	0.938	0.241	-0.092	0.755	-0.427	0.536	-0.354	0.399	0.812	0.808	0.6	0.449	0.504	0.199	0.655												
V	0.889	0.802	0.741	-0.285	-0.297	0.412	0.791	0.226	-0.442	0.627	-0.332	0.256	-0.217	-0.124	0.881	0.645	0.743	0.172	0.365	-0.056	0.067	0.765											
Ba	0.653	0.044	0.61	-0.83	0.092	-0.38	0.196	0.817	-0.801	0.623	-0.93	0.283	-0.794	0.062	0.121	-0.035	0.487	-0.521	0.752	-0.484	0.21	0.478	0.509										
Sn	0.381	0.797	0.281	0.416	-0.26	0.874	0.792	-0.475	0.401	0.22	0.466	0.168	0.414	-0.019	0.88	0.832	0.375	0.817	-0.198	0.461	0.136	0.532	0.584	-0.364									
CaCO3	-0.913	-0.858	-0.98*	0.922	0.608	-0.413	-0.422	-0.928	0.276	-0.896	0.277	-0.766	0.881	0.568	-0.765	0.482	-0.999*	0.079	-0.896	0.957*	-0.293	-0.425	-0.635	-0.595	0.286								
Mean	-0.613	-0.422	-0.385	0.088	-0.17	-0.048	-0.698	-0.036	0.579	-0.335	0.56	0.109	0.04	-0.295	-0.72	-0.7	-0.335	0.033	-0.124	-0.275	-0.008	-0.732	-0.857	-0.548	-0.403	0.037							
S.d.	0.653	0.949*	0.593	-0.027	-0.797	0.673	0.497	-0.016	-0.089	0.368	0.304	0.168	0.075	-0.641	0.736	0.368	0.704	0.333	0.09	-0.206	-0.256	0.293	0.742	-0.014	0.706	-0.599	-0.409						
Skew	0.68	0.804	0.783	-0.454	-0.894	0.641	0.275	0.432	0.049	0.633	0.265	0.612	-0.392	-0.793	0.425	-0.022	0.869	0.292	0.518	-0.65	0.057	0.184	0.468	0.106	0.367	-0.868	0.043	0.771					
Gravel	0.799	0.849	0.637	-0.079	-0.292	0.537	0.844	0.016	-0.282	0.52	-0.152	0.17	-0.019	-0.09	0.951*	0.757	0.664	0.33	0.192	0.115	0.04	0.748	0.974*	0.309	0.743	-0.554	-0.843	0.801	0.433				
Sand	-0.794	-0.974*	-0.79	0.204	0.609	-0.875	-0.754	-0.147	-0.159	-0.696	-0.229	-0.596	0.178	0.393	-0.85	-0.548	-0.863	-0.632	-0.385	0.166	-0.269	-0.61	-0.747	-0.059	-0.78	0.941*	0.387	-0.868	-0.784	-0.795			
Silt	0.041	0.232	0.282	-0.22	-0.508	0.541	-0.102	0.228	0.657	0.312	0.567	0.68	-0.269	-0.477	-0.116	-0.298	0.352	0.472	0.329	-0.448	0.362	-0.173	-0.302	-0.353	0.079	-0.478	0.636	0.194	0.614	-0.219	-0.417		
Clay	0.498	0.876	0.542	0.057	-0.622	0.979*	0.603	-0.102	0.504	0.466	0.579	0.544	0.058	-0.414	0.702	0.468	0.655	0.808	0.15	-0.041	0.244	0.376	0.453	-0.321	0.824	-0.568	-0.057	0.78	0.77	0.568	-0.904	0.594	
Silt/Clay	0.071	0.278	0.305	-0.208	-0.528	0.582	-0.06	0.213	0.663	0.329	0.582	0.688	-0.255	-0.485	-0.067	-0.257	0.38	0.505	0.326	-0.434	0.364	-0.143	-0.262	-0.36	0.128	-0.483	0.608	0.234	0.658	-0.176	-0.457	0.999*	0.634

For geochemical data: N=5 r=0.950 (95%)

For grain size data: N=6 r=0.933 (95%)

Table 5.13 Correlation matrix of elements and grain size parameters for Reef Top sediments.

BEACH ENVIRONMENT

	Fe	Mn	Ti	Ca	K2	P205	Al	Si	Mg	Na	Zr	Y	Sr	Rb	Th	Pb	Zn	Ni	Cr	Ce	Nd	La	V	Ba	Sn	CaCO3	Mean	S.d.	Skew	Gravel	Sand	Silt	Clay
Mn	0.193																																
Ti	0.605	-0.265																															
Ca	-0.425	0.397	-0.962*																														
K2	-0.447	-0.221	-0.17	0.102																													
P205	-0.514	0.43	-0.932*	0.916*	0.036																												
Al	-0.116	-0.086	0.119	-0.169	0.839	-0.086																											
Si	0.448	-0.385	0.967*	-1	-0.125	-0.921*	0.147																										
Mg	-0.646	0.366	-0.909*	0.916*	0.386	0.866	0.082	-0.925*																									
Na	0.793	-0.198	0.959*	-0.87	-0.241	-0.908*	0.057	0.882	-0.908*																								
Zr	-0.4	-0.856	-0.091	-0.031	0.15	0.024	0.017	0.016	-0.015	-0.163																							
Y	0.446	0.725	0.405	-0.306	-0.193	-0.153	0.198	0.313	-0.234	0.385	-0.778																						
Sr	-0.616	-0.385	-0.775	0.687	0.226	0.616	-0.13	-0.697	0.621	-0.75	0.659	-0.869																					
Rb	-0.452	-0.185	-0.221	0.153	0.998*	0.089	0.839	-0.176	0.424	-0.282	0.131	-0.192	0.252																				
Th	0.538	-0.144	0.623	-0.681	-0.191	-0.468	0.297	0.68	-0.761	0.628	-0.042	0.398	-0.527	-0.196																			
Pb	-0.261	-0.332	-0.427	0.38	0.759	0.215	0.545	-0.394	0.41	-0.345	0.31	-0.564	0.594	0.782	-0.182																		
Zn	0.958*	-0.039	0.718	-0.547	-0.428	-0.667	-0.163	0.568	-0.739	0.879	-0.205	0.289	-0.565	-0.45	0.481	-0.269																	
Ni	0.205	0.048	-0.379	0.409	-0.664	0.46	-0.581	-0.395	0.055	-0.229	0.256	-0.272	0.419	-0.627	0.083	-0.101	0.138																
Cr	0.725	0.705	0.124	0.035	-0.365	0.095	0.042	-0.018	-0.15	0.289	-0.656	0.715	-0.521	-0.332	0.448	-0.243	0.508	0.317															
Ce	0.672	0.646	0.084	0.012	-0.569	0.08	-0.211	0.008	-0.268	0.243	-0.658	0.605	-0.467	-0.532	0.493	-0.339	0.451	0.458	0.911*														
Nd	0.496	0.718	0.203	-0.118	-0.433	0.106	0.039	0.128	-0.197	0.24	-0.617	0.874	-0.644	-0.411	0.524	-0.546	0.291	0.201	0.874	0.821													
La	0.335	-0.211	0.055	-0.038	-0.214	0.139	0.138	0.027	-0.214	0.142	0.441	-0.058	0.154	-0.199	0.544	0.082	0.306	0.622	0.382	0.278	0.321												
V	0.617	0.812	0.097	0.073	-0.286	0.151	0.101	-0.059	-0.031	0.223	-0.72	0.818	-0.571	-0.258	0.326	-0.309	0.401	0.174	0.968*	0.823	0.904	0.272											
Ba	0.084	0.007	0.354	-0.31	0.759	-0.439	0.75	0.3	-0.042	0.323	-0.294	0.275	-0.395	0.737	0.018	0.377	0.103	-0.875	-0.035	-0.269	-0.126	-0.376	0.059										
Sn	0.349	-0.225	-0.073	0.044	-0.388	0.156	-0.129	-0.039	-0.262	0.063	0.354	-0.228	0.266	-0.359	0.552	0.133	0.287	0.812	0.358	0.455	0.225	0.854	0.157	-0.584									
CaCO3	-0.426	0.411	-0.968*	0.99*	0.165	0.928*	-0.066	-0.992*	0.913*	-0.877	-0.056	-0.271	0.67	0.223	-0.599	0.442	-0.572	0.386	0.079	0.055	-0.074	-0.005	0.11	-0.264	0.084								
Mean	-0.547	-0.928*	0.199	-0.4	0.315	-0.306	0.271	0.361	-0.314	0.076	0.827	-0.6	0.356	0.288	-0.298	0.333	-0.174	-0.095	-0.666	-0.591	-0.563	0.262	-0.756	-0.01	0.264	-0.374							
S.d.	0.372	0.091	-0.245	0.347	-0.605	0.387	-0.444	-0.332	0.024	-0.074	0.221	-0.139	0.295	-0.577	0.11	-0.112	0.319	0.932*	0.453	0.451	0.297	0.755	0.342	-0.717	0.779	0.317	-0.129						
Skew	0.193	0.917*	-0.441	0.618	-0.09	0.57	-0.03	-0.606	0.551	-0.31	-0.688	0.504	-0.126	-0.048	-0.506	-0.058	-0.022	0.169	0.686	0.54	0.554	-0.057	0.778	0.023	-0.12	0.624	-0.801	0.303					
Gravel	0.164	0.998*	-0.279	0.406	-0.233	0.462	-0.087	-0.394	0.379	-0.223	-0.825	0.727	-0.369	-0.197	-0.138	-0.354	-0.068	0.07	0.699	0.637	0.736	-0.177	0.811	-0.028	-0.208	0.419	-0.846	0.131	0.908*				
Sand	-0.166	-0.997*	0.28	-0.406	0.239	-0.467	0.086	0.395	-0.377	0.223	0.819	-0.729	0.367	0.202	0.129	0.357	0.067	-0.08	-0.706	-0.643	-0.744	0.161	-0.816	0.037	0.194	-0.42	0.841	-0.143	-0.908*	-1*			
Silt	0.218	0.217	-0.09	0.08	-0.322	0.378	0.111	-0.081	-0.064	-0.051	0.081	0.298	-0.025	-0.29	0.57	-0.163	0.07	0.601	0.591	0.546	0.683	0.842	0.538	-0.484	0.738	0.138	0.049	0.674	0.272	0.279	-0.296		
Clay	0.222	0.197	-0.082	0.075	-0.31	0.37	0.123	-0.077	-0.066	-0.043	0.105	0.286	-0.017	-0.279	0.565	-0.152	0.081	0.598	0.582	0.525	0.67	0.859	0.53	-0.454	0.739	0.132	0.059	0.682	0.262	0.26	-0.277	0.999*	
Silt/Clay	0.219	0.214	-0.089	0.079	-0.32	0.376	0.113	-0.081	-0.065	-0.05	0.085	0.296	-0.024	-0.289	0.569	-0.161	0.072	0.601	0.59	0.563	0.681	0.845	0.536	-0.462	0.738	0.137	0.05	0.675	0.27	0.276	-0.293	1*	0.999*

For geochemical data: N=7 r=0.908 (95%)

For grain size data: N=5 r=0.891 (95%)

Table 5.14 Correlation matrix of elements and grain size parameters for Beach sediments.

and constant ambient conditions of water temperature, salinity and depth (ie, shallow and open marine environments) which are the most favourable conditions for growth of molluscs and other bottom-dwelling carbonate-secreting fauna.

Ca shows significant positive correlations with P_2O_5 and Mg in the beach environments and Sr in the reef top, open marine, shallow marine, open intertidal and mangrove channel environments (a positive but less significant correlation with Sr exists in the beach and reef front environments). Ca also correlates positively and significantly with gravel in the shallow marine and intertidal environments.

Strong negative correlations exist between Ca and Ti and Si in the reef front, reef top and beach environments and weaker negative correlations exist between Ca and all 'terrigenous' elements in all environments except mangrove swamp where the very low Ca concentrations show a weak correlation with Si and percent sand.

The only unusual association shown in the Ca correlation analysis is that with P_2O_5 and Mg in the beach environment. The association with Mg is expected due to the substitution of Mg ions in the calcite lattice and a positive although less significant correlation with Mg is evident in the reef top sediments which are the main source for the beach sediments. However, the Ca-P_2O_5 association is puzzling especially since there is no similar association in the reef top sediments. It is possible that remains of phosphate-secreting organisms are concentrated in the beach environment as trace amounts of apatite. This will be discussed further when looking at P_2O_5 variations.

5.4.3 Silica

As discussed in Chapter 4, Si concentrations reflect the amount of quartz which forms one of the three major geochemical and mineralogical components of Phangnga Bay sediments. It is of entirely terrigenous origin (biogenic Si concentrations are thought to be negligible in shallow coastal sediments which are dominated by a terrigenous input) although in Phangnga Bay there is thought to be a mix of recent and Pleistocene aged quartz sand and silt deposits.

The highest mean Si concentrations are found in the mangrove channel and intertidal sediments with significantly decreasing values from the open marine to mangrove swamp to shallow marine sediments. The shallow marine environment

shows the greatest variability in Si content (high standard deviation) which reflects the similar high variability in sediment grain size parameters. The mangrove swamp sediments show the least variability.

In all environments, Si correlates negatively and mostly significantly with Ca reflecting the geochemically antithetic relationship between the terrigenous sand and marine carbonate components. In the mangrove swamp, shallow marine and open marine environments, Si correlates positively with Zr (in zircon) reflecting the association of Zr with the coarser terrigenous fraction of recent and relict sediments. In all environments Si shows no significant correlation with any aluminosilicate elements reflecting the geochemically antithetic relationship between quartz sand and clays. Si correlates positively with sand in all environments except the shallow marine and reef front sediments where carbonate forms the sand size fraction and quartz dominates the silt fraction.

5.4.4 Magnesium

Mg is found in the highest concentrations in the reef front , shallow marine and open marine environments and decreases through the intertidal, mangrove swamp, reef top, mangrove channel and beach environments. However, Mg/Al ratios increase significantly southwards through the mangrove swamp, intertidal, shallow marine and open marine environments (Table 5.4 and 5.5). Mangrove channel values are similar to the intertidal and shallow marine environments. There is no significant variation in the mean Mg/Al values between the open marine, reef front, reef top and beach environments (Table 5.6).

As discussed in Chapter 4, Mg is contained in both smectitic clays and in carbonates and the proportion of Mg in these 2 components increases southwards. Therefore, high average Mg/Al concentrations are found in the southern depositional environments of open marine and reef front where a mix of clays and carbonates each with high Mg content are found. Highest values are found in the reef top and beach sediments where clays are absent and carbonate abundant.

Comparing correlation coefficients for Mg between environments, some idea of the varying habit of Mg can be deduced. In the mangrove swamp, intertidal, shallow marine, open marine and reef front environments, Mg tends to correlate positively with Fe, Ni, Ti, C_{org}, P_2O_5, Al, Al-associate elements and the silt/clay fraction. These

associations indicate that the main control on Mg content in these environments is fixation of Mg and other metals by clays (either by adsorption or substitution) and in organo-metal complexes. Despite Mg in carbonate increasing southwards into the shallow marine and open marine environments (Chapter 3), a carbonate/Mg association is not picked up until reaching the high carbonate/low clays environments of reef top and beach. The reason for this dominating Mg_{CLAY} trend is due to the greater Mg contents of clays compared to carbonates which is illustrated in Mg_{CLAY}/Al ratios two orders of magnitude greater than Mg_{CARB}/Ca ratios (Table 4.4).

5.4.5 Iron

The average Fe content of sediments (Table 5.3) is highest in the mangrove swamp environment and decreases in proportion to the amount of mud in the sediments of each environment. This strong Fe-clay association is picked out in the Fe-correlations in the environments. Fe correlates strongly and positively with the silt/clay fraction (particularly clay in the mangrove swamp environment), other typical aluminosilicate elements as well as P_2O_5 and C_{org} (in the open intertidal and shallow marine environments).

The mean Fe/Al values however show a significant increase from the mangrove swamp to open intertidal to shallow marine to open marine environments. Mangrove channels have an equivalent mean Fe/Al value to shallow marine sediments. Reef front, reef top and beach sediments have similar Fe/Al values which are less than in the open marine sediments. The increasing Fe/Al content southwards (which reflects excess-Fe over that which is contained in clays) is thought to be due to the increasing heavy mineral content of the sediments due to their relict origin (Chapter 4). The higher Fe/Al values in the mangrove channel sediments compared to the mangrove swamp and intertidal sediments are due to the concentration of heavy minerals in the higher energy environment.

This explanation for high Fe/Al ratios is backed up by the strong Fe-Ti correlations in all environments. Considering their similar ionic radii (Fe^{2+} - 0.78Å; Fe^{3+} - 0.64Å; Ti^{3+} - 0.67Å) and thus the likelihood of these elements substituting for each other this association is not surprising. However, there are other elements with similar ionic radii to Fe (eg, Cr, Zn and Ni) but which do not show such a consistently strong correlation with Fe in all environments. This Fe-Ti association may be due to these elements

being major components of the heavy mineral fraction (particularly in ilmenite, rutile and magnetite) as well as possibly being associated in the clay fraction.

Only total Fe (Fe_2O_3) has been measured in these sediments and so the relative proportions of the divalent and trivalent states are not known. Although the trivalent state is generally assumed to be dominant in surficial sediments (Cook and Mayo, 1978) it is likely, considering the reduced nature of the sub-surface sediments particularly in the mangrove swamp and intertidal environments (Limpsaichol, 1978 and observation during collection) that the more reduced form is also present and pyrite is present in low quantities due to the action of sulphate-reducing bacteria.

5.4.6 Titanium

Absolute Ti concentrations in the surface sediments show a decrease in concentration from the mangrove swamp to open intertidal to shallow marine to open marine environments. Mangrove channel sediments have a similar Ti concentration to the shallow marine sediments. Lowest Ti values are found in the reef front, reef top and beach environments. It is clear therefore that there is an association of Ti with the fine size fraction of the sediment and this is illustrated in the correlation of Ti with Fe, Al, Al-associate elements and the silt/clay fraction in the mangrove channel, intertidal, shallow marine and open marine environments. There is a corresponding negative correlation with Si, Ca and percent sand. Although Ti correlates with percent clay in the mangrove swamp sediments there is no corresponding correlation with K or Al which indicates that Ti is not adsorbed onto or substituted into clays.

The habit of Ti in these sediments is thought to be in fine grained Ti-bearing heavy minerals such as rutile. The positive correlation of Ti with Zr in all environments agrees with this association with heavy minerals.

Comparing Ti/Al ratios between environments shows that there is an increase in values southwards from the mangrove swamp to the open marine environments with the highest values in beach sediments. Ti/Al values reflect the proportion of heavy minerals in the sediments. High values in the shallow and open marine environments reflect the concentration of heavy minerals in the relict low sea-level stand sediments whilst similar values in the mangrove channel sediments indicate that there is a concentration of heavy minerals in these channels compared to the

surrounding mangrove swamp and open intertidal sediments. The highest Ti/Al values in beach sediments reflect the high energy reworking conditions of this environment where clays are winnowed out and heavies are concentrated.

5.4.7 Potassium

As with Al, absolute K concentrations in each environment are closely related to the mean grain size of the sediments - an increase in the silt/clay fraction results in increased K due to the presence of K in the clay lattices.

In all but the reef top and beach environments, K shows significant positive correlations with Nb, Y, Th, Pb and Rb and positive although not significant correlations with Al, Al-associate elements, C_{org}, P_2O_5 and the silt/clay fraction. These correlations therefore illustrate K's close association with clays as it forms an important component of the clay lattice. There are thus negative correlations with percent sand, Si, Ca and Sr in these environments.

In the reef top and beach environments however, K correlates positively and significantly with only Rb and positively with percent sand - most of the correlations with Al-associate elements are negative. As discussed in Chapter 4, Rb and K are found closely associated in the mica lepidolite and these correlations with Rb and sand in the high energy environments of reef top and beach indicate that lepidolite controls the Al concentration in these environments where clays are absent. The elements usually associated with clays are, in these environments, probably found in heavy minerals which are concentrated in the finer size fraction unlike lepidolite, therefore there are negative correlations with K.

5.4.8 Phosphorus

The highest P_2O_5 concentration is found in the shallow marine environment (842 ppm) with similar values in the intertidal and mangrove swamp environments and decreasing values through the reef front, open marine, mangrove channel and reef top sediments. This to some extent reflects the clay content of the sediments in each environment and the positive correlations in most environments with elements associated with clays also reflect this. However, P_2O_5 shows relatively few significant correlations with any elements or grain size parameters. In the intertidal environment there is a significant positive correlation with C_{org}. This correlation is less positive in

the shallow marine environment and negative in the open marine sediments. Therefore, P_2O_5 is likely to be present in an organic complex in the intertidal sediments but such an association decreased to the south where there is less organic matter available for complexing. There are however, significant correlations with Y, Th, Pb and less significant but positive correlations with other Al-associate elements and the silt/clay fraction in the open marine sediments. These relationships are probably the result of metal and phosphate fixation by clays either by ionic exchange with Al in the clay lattice or by surface adsorption. However, it is also possible that these elements are related in the resistate detrital minerals monazite and apatite (Chapter 4).

Mean P_2O_5/Al values increase significantly from the mangrove swamp to intertidal to shallow marine to open marine sediments (Table 5.5). Mangrove channel sediments have a similar P_2O_5/Al ratio as intertidal and shallow marine sediments. Open marine, reef front, reef top and beach sediments do not have significantly different mean P_2O_5/Al values.

In the beach sediments P_2O_5 correlates positively (but not significantly) with Ca, Mg and the gravel fraction and also positively with most of the Al-associate elements. Although absolute P_2O_5 concentrations are low in these sediments the P_2O_5/Al ratio is very high indicating that P_2O_5 is not associated with clays in this environment (which are absent anyway) but in some other mineralogical fraction. The association with Al-associate elements suggests P_2O_5 is present in the heavy mineral (monazite and/or apatite) fraction but the correlation with Ca and Mg indicates there may also be some P_2O_5 contained in or associated with the carbonate fraction, possibly in the form of marine phosphate.

5.4.9 Manganese

As mentioned in Chapter 4, average Mn values for Phangnga Bay sediments are low compared to World average sedimentary rocks. The highest absolute mean value is found in the mangrove swamp sediments (376 ppm - this is similar to the World average sandstone concentration). Mean Mn values decrease through the depositional environments following the trend of decreasing silt/clay content. No statistical data is available for the beach environment as Mn values in these sediments are below the level of machine precision (there is a mix of low positive and negative values).

In the mangrove swamp, mangrove channel, intertidal and reef front sediments, Mn correlates significantly with Al, and the group 2 Al-associate elements (Th, Y, Nb, Pb). There are less significant correlations with Fe, K, Rb and percent silt/clay. Correlations with Ca, Sr, sand and Zr are negative. In the shallow and open marine environments correlations with the above elements are positive but not significant indicating that the Mn-element associations are not as strong.

Cook and Mayo (1980) recorded a decrease in Mn/Fe values from the open marine sediments through to the mangrove swamp sediments and explained this by the varying behaviour of Fe and Mn in different redox conditions. In the acid conditions prevailing in the mangrove swamp and channel environments Mn is relatively soluble compared to Fe and so is preferentially leached from the sediments thus reducing the Mn/Fe ratio. Although there is not a continuous decrease in Mn/Fe ratios from the open marine through to the mangrove swamp environments there are lower ratios in the mangrove swamp and intertidal sediments compared to the coarser-grained mangrove channel and open marine sediments. This indicates that there may be some leaching of Mn in the mangrove swamp and intertidal sediments. However, it is likely that Mn concentrations are not totally controlled by ion exchange and adsorption processes with clays and organic matter but that the presence of Mn in detrital minerals also affects its concentration.

5.4.10 Organic Carbon

C_{org} means have only been calculated for the open intertidal, shallow marine and open marine environments since only a small number of samples were analysed for organic carbon. There is clearly a decrease in C_{org} content from the intertidal to the shallow marine to the open marine sediments which reflects the increasing distance from the main source organic matter in the north.

The C_{org} correlations also show a change through these 3 environments. In the intertidal sediments C_{org} correlates significantly and positively with P_2O_5, Mg, Cr and percent silt/clay and less significantly with Fe, Ti, Ni and other Al-associate elements. In the shallow marine sediments there are correlations with similar elements but the correlations are weaker and in no cases significant. In both these environments there are negative correlations with percent sand and Si. In the open marine sediments however, C_{org} shows no significant correlation with any element or grain

size parameter. Therefore, although there is a clear relationship between C_{org} and clays (and the associated clay elements) in the intertidal environment, the association is weaker in the shallow marine sediments and is not evident at all in the open marine sediments.

In the intertidal environment C_{org} is derived from terrigenous organic matter in the form of degraded vegetation debris sourced from the mangrove swamps in the north. As transition metals are known to be effectively scavenged by particulate organic matter, this C_{org} will form organo-metallic complexes with the abundant supply of metal ions similarly sourced from the terrigenous environment and these settle out in the calm, near-source areas in the north of the Bay. There is therefore a close association of C_{org} with metals in the intertidal environment (and most probably also in the mangrove swamp environment).

In the open marine environment however, some degradation of the organic material in the generally oxic sediments may have caused the release of the adsorbed metals which may then either be adsorbed by clays or may remain in solution in the sediment pore waters. Additionally, if some of the C_{org} is sourced from marine organic material then this material is less likely to complex with metal ions due to their diminished supply in this oceanward area.

It is known that Ba is incorporated into the calcareous tests of marine organisms such as protozoans (Finlay et al, 1983), benthic foraminiferans (Lea and Boyle, 1989) and corals (Lea et al, 1989), however, there is no significant correlation between Ba and Ca in any of the environments and indeed in the reef top and beach environments Ba/Ca correlations are negative. Therefore, in these sediments, Ba appears to be associated entirely with the terrigenous fraction as opposed to the biogenic component. This is perhaps not surprising as the involvement of Ba in biogeochemical processes is thought to be only significant in open oceanward environments away from terrigenous input.

5.4.11 Aluminosilicate-associate trace elements

5.4.11.1 Group 1 - Rb

Absolute Rb values vary between depositional environments according to the mean grain size variation. However, mean Rb/Al values show no significant difference between any of the environments (apart from a significantly lower mean between

the mangrove swamp and mangrove channel sediments). Rb is the only element which shows such a constant and significant mean ratio to Al through all of the depositional environments.

Anomalously high Rb/Al values are due to concentrations of lepidolite mica as discussed in Chapter 4. In every environment there is a significant positive correlation with K which supports the suggestion that Rb is contained in the lepidolite lattice by its substitution in the K sites. In the mangrove swamp, mangrove channel, open intertidal and shallow marine environment there are positive (although not significant) correlations with Sn. However, such a correlation is not evident in the open marine, reef front, reef top and beach sediments. Although Rb and Sn are closely related in terms of the distribution pattern of Rb/Al and Sn ($CaCO_3$-free) anomalies (Figs 4.19 and 4.27) these distributions are controlled by catchment basin geology rather than solely sedimentological depositional controls. The significantly similar mean Rb/Al values between each environment are also a result of this catchment geology control rather than depositional environment control.

5.4.11.2 Group 2 - Nb, Y, Th, Pb

As these elements are all closely associated with Al their mean absolute concentrations follow the trend of Al concentrations and hence mean grain size between the depositional environments.

Their mean ratios to Al also show similar trends between environments (generally increasing values north to south from the mangrove swamp to open intertidal to shallow marine to open marine sediments with mangrove channel sediments similar to shallow and open marine sediments) however, the 4 elements do not show identical patterns in concentrations between these 5 environments. On the whole there are no significant differences between the mean element/Al ratios of the open marine, reef front, reef top and beach environments.

In the mangrove swamp and channel, open intertidal, shallow marine and open marine environments these 4 elements behave similarly and show significant positive correlations between themselves and with the Al, K, Fe, other Al-associate elements and percent silt/clay. In the reef front, reef top and beach environments, although the above described correlations are evident, the correlation coefficients for each of the 4 elements are different.

Nb and Y show a similar pattern of means comparisons between environments in the t-tests (Tables 5.5 and 5.6). Mangrove channel, intertidal and shallow marine sediments all show similar Nb/Al and Y/Al ratio means with a lower mean in the mangrove swamp and higher mean in the open marine environment. Th and Pb however, both show more equivalence between ratio means between these 5 environments.

5.4.11.3 Group 3 - V, Cr, Zn, Ni, La, Ce, Nd, Ba

As with the group 2 elements, these 8 elements are all closely associated with the clay fraction and show similar trends in absolute values as mean grain size and Al content.

Mean element/Al ratios between depositional environments also show similar trends with increasing ratios from the mangrove swamp to open intertidal to shallow marine to open marine environments and similar means between the mangrove channel, intertidal and shallow marine sediments. Mean element/Al ratios are also very similar between the open marine, reef front, reef top and beach sediments.

The correlation coefficients for the 8 elements in the intertidal, shallow marine and open marine sediments show strong associations with Fe, Mn, Ti, Al, K, other Al-associate elements and percent silt/clay (as well as between the 8 elements themselves). There are low positive correlations with Ca, Si and percent sand. Similar correlations are evident in the mangrove swamp, mangrove channel, reef front, reef top and beach sediments although there are greater variations in the correlation coefficients between the 8 elements. Much of the variation may be due to the small sample size of these environments compared to the intertidal, shallow marine and open marine environments rather than to any significant changes between environments.

5.4.12 **Non-aluminosilicate-associate trace elements**

5.4.12.1 Strontium

From Table 5.3 it is clear that the highest absolute Sr values are found in the reef front, reef top and beach sediments and the lowest are in the mangrove swamp sediments. This reflects the $CaCO_3$ content of these environments as Sr substitutes for Ca in the calcite lattice. It also reflects the biogenic control on Sr substitution as

higher Sr values are found in aragonitic structures which include corals (see Chapter 4).

The mean Sr/Ca ratios for each depositional environment are plotted on Table 5.4. Mangrove swamp sediments have the highest Sr/Ca ratio. As discussed in Chapter 4, this reflects the Sr contained in clays as opposed to carbonate. In the mangrove swamp sediments Sr correlates significantly and positively with other Al-associate elements as well as the percent clay fraction thus supporting the Sr/clay association. The mangrove swamp values are similar to the open intertidal sediments suggesting that Sr is also contained in clays in this environment. The shallow and open marine sediments have a lower mean Sr/Ca ratio than the mangrove swamp and intertidal sediments and the open marine sediments also have a lower value than the reef front, reef top and beach sediments. This reflects the lack of Sr in clays in the open marine environment and the comparatively low Sr content in carbonates since most of the carbonate material is molluscan which has a lower Sr/Ca content than corals. The mangrove channel sediments have a similarly low content as the shallow and open marine sediments. In the shallow and open marine, reef front, reef top and beach sediments Sr correlates positively and sometimes significantly with Ca, (hence $CaCO_3$), percent gravel and percent sand.

5.4.12.2 Zirconium

Since the absolute Zr concentration in the sediments has a strong grain size control (Chapter 4) the concentrations for each depositional environment (Table 5.3) follow the general trend of mean grain size with decreasing Zr concentrations from the open intertidal to mangrove swamp environments to the open marine and reef/beach environments.

However, when this grain size control is effectively removed by plotting Zr/Al the trend reverses and the highest significant mean values are found in the open marine, reef front, reef top and beach sediments. The mangrove channel, open intertidal and shallow marine sediments have similar mean Zr/Al values but the mangrove swamp sediments have a significantly lower value than all the other environments.

In the mangrove swamp environment Zr correlates positively with Ca, Si and percent sand and negatively with percent silt/clay and Al-associate elements. A similar correlation pattern is evident in the reef top and beach environments but in all other

environments Zr correlates positively with Al, Ti, the silt/clay fraction and most Al-associate elements and negatively with Si, Ca and percent sand and gravel. It was suggested in Chapter 4 that Zr is contained dominantly in the heavy mineral zircon as opposed to within clays and the correlation patterns tend to support this. In the very fine sediments of the mangrove swamp environment, zircon, although fine grained, would form part of the comparatively coarser fraction and thus shows correlations with Si, Ca and percent sand and negative correlations with clay and clay elements. In the coarser, mixed grain size sediments of the mangrove channel, intertidal, shallow marine, open marine and reef front environments the zircon forms part of the comparatively fine fraction and thus correlates with percent silt/clay and clay elements rather than sand and carbonate.

Although high Zr/Al values reflecting high zircon content would be expected in the higher energy reef top and beach environments, the high values in the open marine sediments reflect the relict sediment control on sediment mineralogy and geochemistry rather than recent depositional controls as heavy minerals are concentrated in the low sea-level stand coarse sediments not yet covered by recent, lower energy sediments.

5.4.12.3 Tin

Although absolute Sn concentrations show a decrease from the mangrove swamp to open intertidal to shallow marine to open marine environments like many of the Al-associate elements due to north-south increase in grain size, it was shown in Chapter 4 that Sn does not correlate with silt/clay content and is therefore independent of grain size controls. The catchment geology is the main factor controlling Sn distributions and although there are some significant differences between means for depositional environments these are more to do with the location of the 2 main high Sn anomalies (one in the north covering the mangrove channel and open intertidal environments and one in the south in the open marine environment) than any sedimentary depositional control.

The correlations for Sn in each environment also suggest this. Although there are a few significant correlations with clay type elements and percent silt/clay in the mangrove swamp and channel, intertidal and shallow marine sediments there are no significant correlations in the other environments.

5.4.13 **Discussion**

It was shown in Chapter 4 that absolute concentrations of elements are controlled by the 3 major mineral components (quartz, clays and carbonates) which themselves reflect the grain size composition of the sediment. Therefore, it is not surprising that absolute concentrations of elements in sediments from different environments vary according to the grain size variations between environments.

Variations in Si and Al between environments reflects percent sand and clay respectively and are therefore controlled by the environmental processes discussed in section 5.3.4. Ca reflects percent carbonate in the sediment and the variations between environments are due to the variation in conditions favourable for the growth of Ca-secreting organisms such as corals and molluscs. Hence, Ca concentrations are low in the sediment laden waters of the mangrove swamp, channel, and intertidal environments where there are also salinity fluctuations, and high in the open marine sediments and environments associated with coral reefs.

The majority of the other elements show a reasonably consistent increase in their ratio to Al in the sediments from the mangrove swamp to open intertidal to shallow marine to mangrove channel to open marine environments which is thought to be due to an increase in heavy minerals containing these elements. The mangrove channel sediments are geochemically (and sedimentologically) very similar to the open marine sediments which is thought to be due to the increase in heavy mineral content through high energy deposition and reworking in the relict sediments of the open marine environment, and through early settling out from transport in the mangrove channel sediments. These elements show virtually no variation in their ratios to Al between the open marine, reef top, reef front and beach environments.

Rb, K, Sn and Sr are all exceptions to the above generalisation. Sr/Ca increases north to south through the environments with the highest values in the reef top and beach environments. This reflects the variation in carbonate mineralogy with the highest Sr concentrations found in corals. There is no evidence of an association of Sr with clays in any of the clay-rich environments.

Rb, K and Sn have all been shown to be strongly controlled by the drainage basin geochemistry rather than by the sedimentological controls affecting the majority of the other elements studied.

5.5 CONCLUSIONS

By comparing the grain size and geochemical variations between sediments from the 8 depositional environments distinguished on the basis of geomorphology and water depth, it is clear that grain size variations are of more use in distinguishing between the environments than are geochemical variations. Although absolute geochemical values simply reflect the grain size characteristics of the sediment, ratioing the elements can effectively remove this grain size mask. There does appear to be a general increase in element/Al ratios from the mangrove swamp to open intertidal to shallow marine to open marine environments with mangrove channel sediments showing similar characteristics to shallow marine sediments. This is thought to be due to an increased heavy mineral concentration in the mangrove channel sediments (from recent deposition) and in the open marine sediments (from relict deposition). Open marine, reef front, reef top and beach sediments are geochemically very similar.

Cook and Mayo (1980) also came to the conclusion that grain size characteristics were of more use in distinguishing between sediments of different depositional environments although they suggested that elemental ratios such as Mn/Fe, Cu/Pb and Cu/Zn may offer potential in environmental discrimination. This is due to the environmentally sensitive nature of the ions and the preferential concentration or leaching arising from changes in the pH, salinity etc. Mn/Fe ratios did not give convincing evidence of environmental discrimination in Phangnga Bay and unfortunately Cu values were too low to allow their comparison with Pb and Zn.

CHAPTER 6

A NUMERICAL APPROACH TO SAMPLE CLASSIFICATION

CHAPTER 6 - A NUMERICAL APPROACH TO SAMPLE CLASSIFICATION

6.1 INTRODUCTION

The approach taken in the previous chapter was to determine the sediment grain size and geochemistry characteristics of distinct depositional environments distinguished on the basis of the known present day observational parameters of water depth and geomorphology. Although this approach is of use in describing and accounting for the sedimentary processes operating at present it does not really help in identifying such environments in the geological record where water depth and geomorphology are not immediately obvious. It is clear from the grain size parameter scatter plots (Figs 5.4-5.6) that the sediment characteristics of the 8 environments overlap to the extent that these environments could not be distinguished on the basis of grain size parameters alone. This chapter approaches the problem of sediment sample classification by using numerical techniques ie, by taking the sediment grain size and geochemical parameters and with the use of scatter plots, histograms and statistical analysis, identifying clusters (or populations) of samples based on these measurable variables.

The first part of this chapter will attempt to classify the sediment samples into separate sedimentological groups on the basis of grain size parameters and to interpret the geological meaning of these groups in relation to the sediment processes operating in the Bay. The second part of this chapter will attempt to classify the sediments on the basis of grain size and geochemical variables together and compare this numerical classification with that of the observational classification described in the previous chapter.

6.2 CLASSIFICATION USING GRAIN SIZE PARAMETERS

6.2.1 **Bivariate Scatter Plots**

6.2.1.1 Identifying populations

Bivariate scatter diagrams of grains size parameters are commonly used in sedimentological studies in an attempt to characterise depositional environments. Some success in this method has been achieved in distinguishing between river,

beach and dune deposits (Stewart, 1958; Friedman, 1961 & 1962; Moiola and Weiser, 1968) although this is only with sand sized material. However, although general fields can be distinguished on these plots, there is always some overlap between the previously determined depositional environments and this is also the case with the sediments in the Phangnga Bay depositional environments (Figs 5.4 - 5.6). Despite the fact that separate depositional environments are not indicated by precise and distinct groupings of samples, clusters of samples may indicate broader sedimentological groupings which may point to sediment processes operating in the Bay. Therefore an attempt is made here to delineate clusters on scatter plots and use these to describe broad sedimentological groupings of samples.

A scatter plot of mean grain size versus sorting (Fig 6.1) with sample point concentration contours indicates that there are 2 main clusters of sample points around 6 phi and 2 - 3 phi mean grain size. These are also evident in the frequency distribution of mean grain size (Fig 6.4a) where two modes at 2 - 2.5 phi and 5.5 - 6 phi suggest 2 distinct populations of sediment. The cluster around 2 - 3 phi mean grain size (Fig 6.1) is split into two by varying sorting values. However, 2 distinct populations are not evident in the frequency distribution plot of sorting (Fig 6.4b) although there is a shoulder of values between 1.75 and 2.25 phi after the mode of 1.5 - 1.75 phi suggesting that there may be two closely placed populations.

A sinusoidal trend of samples in the mean grain size versus sorting plot was reported by Folk and Ward (1957) with 2 basic end-member populations of gravel and sand. This trend was shown to continue into the clay population by Thomas et al (1972) as a result of mixing of various proportions of the end-members. This sinusoidal curve is due to the 2 end-member populations (one coarser than the other) being better sorted than the mix of the 2 populations represented by poorly sorted samples inbetween. Similarly a mix of some much finer or much coarser population will cause a trend of more poorly sorted samples on either side (see Fig 6.5). A similar although less well defined sinusoidal trend was also shown by some samples from Broad Sound (Cook and Mayo, 1978). There is no similar clearly defined trend in the Phangnga Bay samples (Fig 6.1) however, the 2 main clusters although not tight, are separate and suggest that there are 2 "end-member" populations distinguished mainly on the basis of mean grain size. The poorly-sorted nature of both of these populations indicates that the sediments are mostly a mix of coarser and finer end-members with different proportions of each end-member controlling the resulting mean grain size. This mix may be either a result of the actual mixing of separate fine

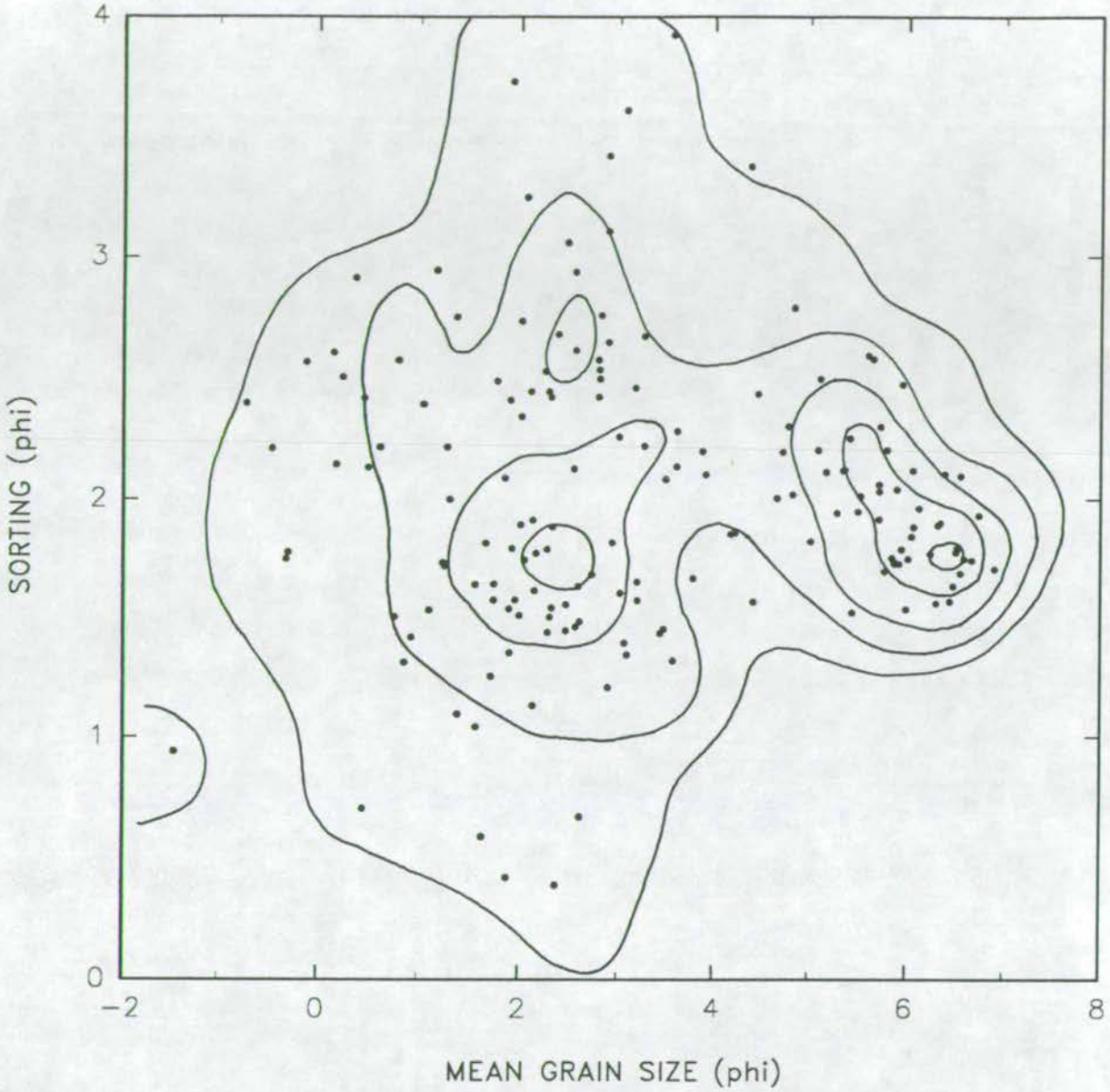

Figure 6.1 Scatter plot of mean grain size v. sorting for all surface samples of the Bay. (Sample concentration contours were constructed by placing a grid of 1/2 phi by 1/2 phi squares on the plot, counting the number of samples within each square and drawing contours by interpolating between these values plotted at the centre of each square.)

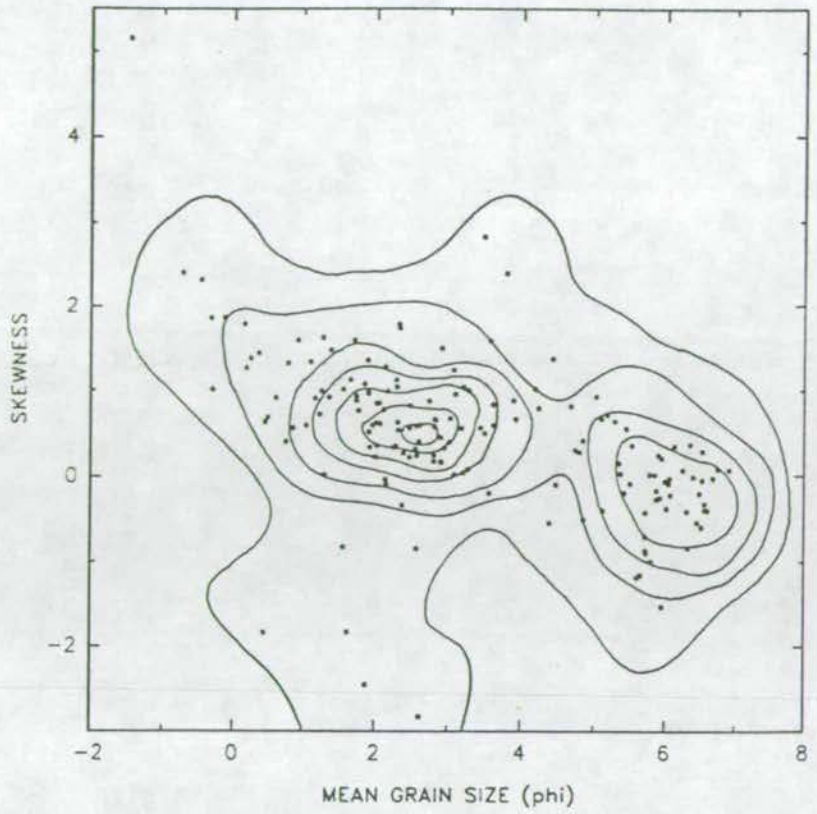

Figure 6.2 Scatter plot of mean grain size v. skewness.

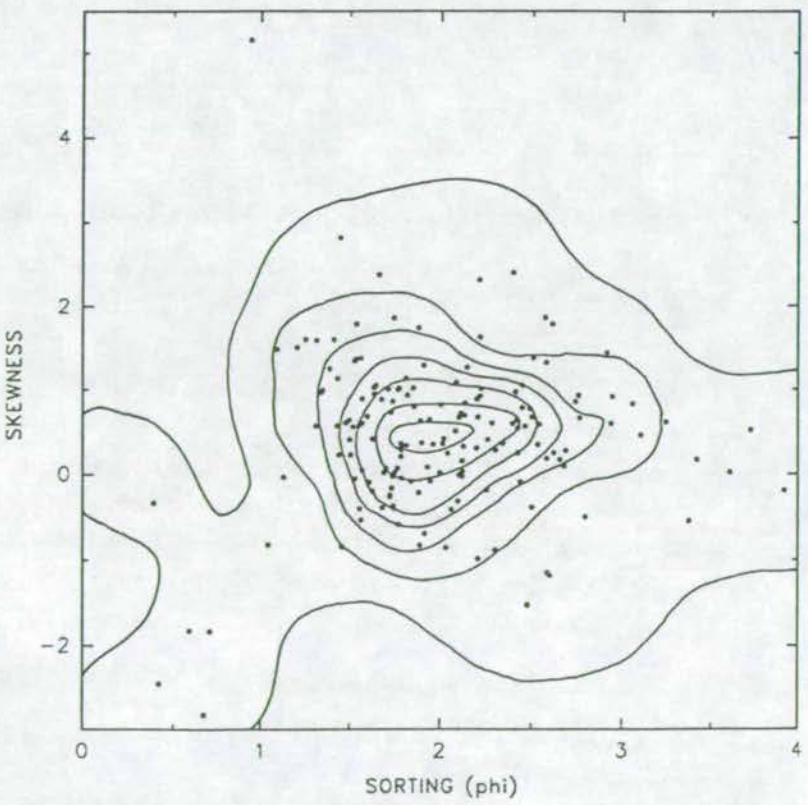

Figure 6.3 Scatter plot of sorting v. skewness.

and coarse fractions within the Bay itself during transport and deposition or, the result of sorting of a mixed input of sediment as a result of varying hydrodynamic regimes. Whether there is a mixing of 2 populations of a sorting of one population will be discussed later (see section 6.2.1.4).

A plot of mean grain size versus skewness (Fig 6.2) again illustrates the two main populations, the coarser grained of which has a skewness of >0 whilst the finer grained one has a skewness of +1 to -1. There is a general trend as recognised earlier (Chapter 2) of decreasing skewness with decreasing grain size. Figure 6.3 illustrates the scatter plot of sorting versus skewness. The 2 populations described above are not evident here, rather there is just one quite widely scattered group.

6.2.1.2 The effect of varying sample size on clustering

Four samples plot outside the main clusters on all the 3 scatter plots (Figs 6.1-6.3). These samples have a mean grain size of approximately 2 phi, are well sorted (0.5 phi) and are strongly negatively skewed (-2). Despite their distinctiveness they do not constitute a cluster and are liable to be ignored. Thus, a drawback of the use of these scatter plots when trying to distinguish depositional environments and processes is the variation in sample size of each depositional environment.

Drawing contours on the plot is a simple numerical method of helping the eye pick out clusters. But simply by looking for these clusters we are, in effect looking for the most well sampled environments (which in this case are the shallow marine and open marine environments - compare the 2 clusters on figure 6.1 with figure 5.4). Environments from which comparatively few samples have been taken (eg, the beach environment here), do not constitute a cluster if they plot outwith the main body of sediments (as in this case). They are hence seen as rather peripheral points whereas, if each environment had the same number of samples a cluster in these peripheral areas should emerge. However, it is impractical to take the same number of samples from each environment and in the geological sense quite unrepresentative of what is actually there. Although it is important to bear in mind the peripheral samples, the clusters, in effect, represent the dominant sediment types and hence the dominant depositional processes operating in the Bay.

6.2.1.3 Sedimentary Units

Since the mean grain size versus sorting plot shows less co-variation than the other 2 plots, this plot will be studied further. Now clusters have been picked out with the

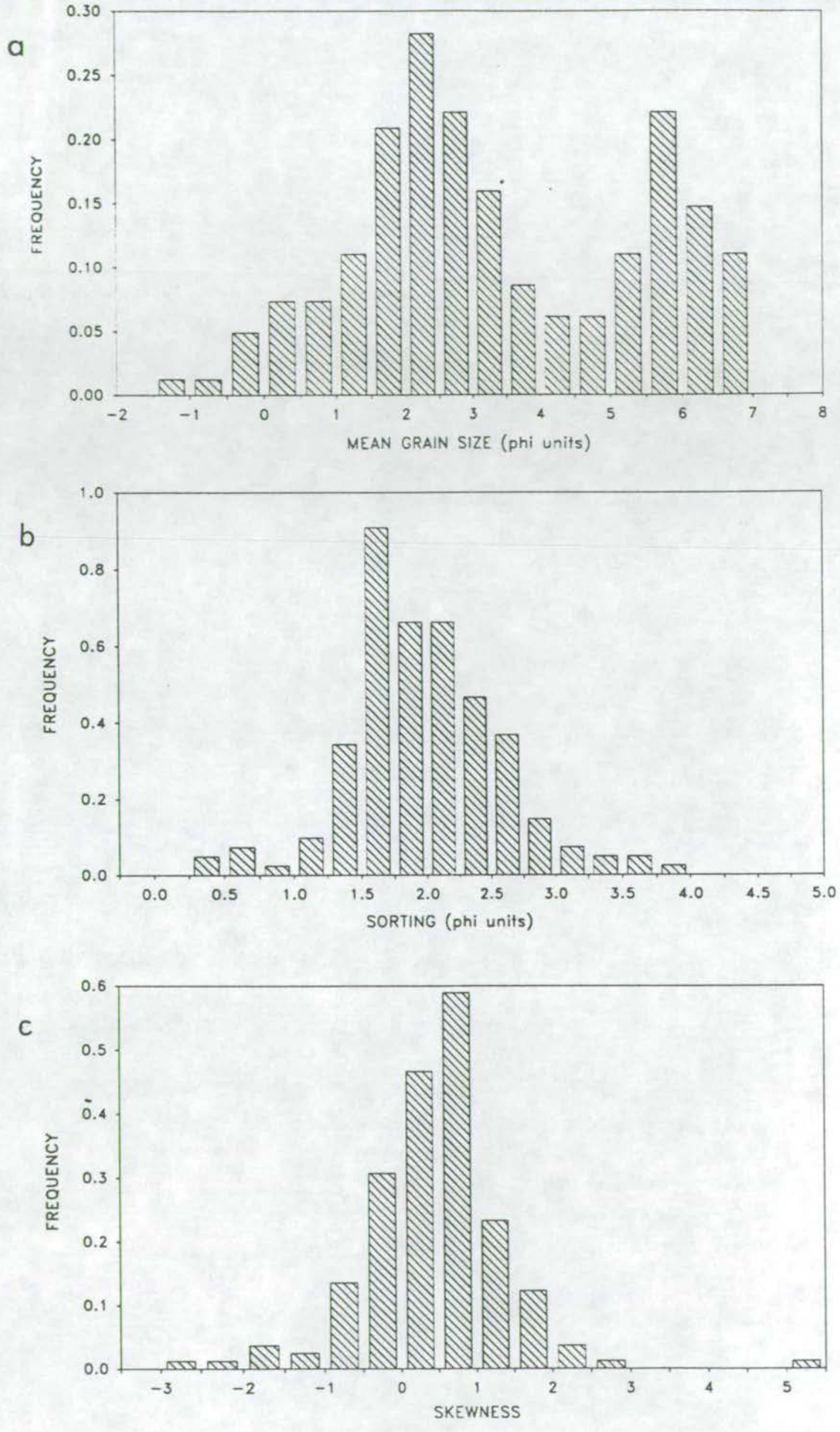

Figure 6.4 Frequency histograms of a. mean grain size; b. sorting and c. skewness values for all surface sediments.

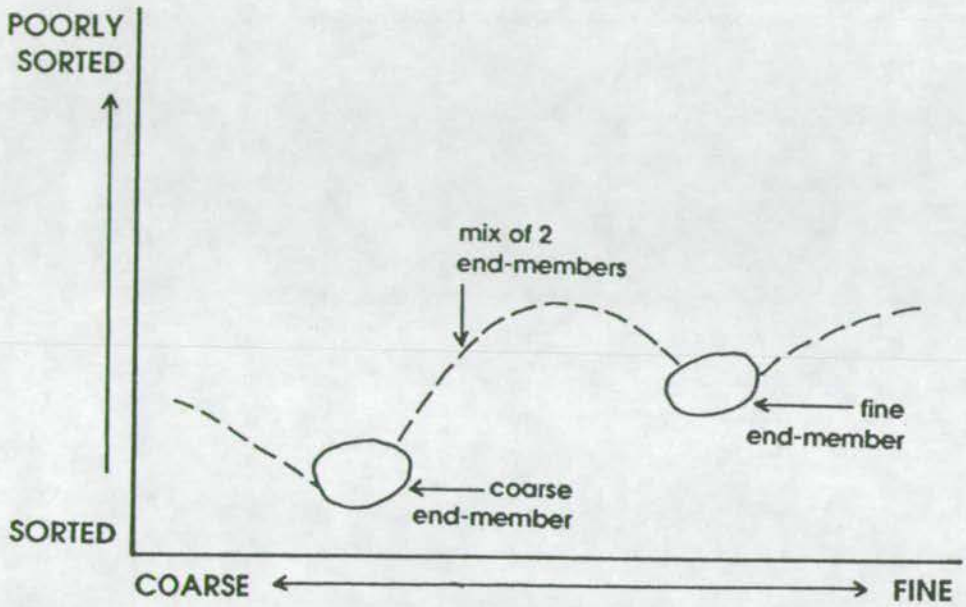

Figure 6.5 Schematic graph illustrating the sinusoidal trend developed on bivariate scatter plots of mean grain size v. sorting through the mixing of 2 grain size populations.

help of contours, lines partitioning the samples into fields representing sedimentary units can be drawn (Fig 6.6). Since grains size parameters are generally hydraulically controlled and therefore represent to some extent the depositional conditions of sedimentation, some generalisations can be made by the positioning of the 4 fields delineated on this plot.

Unit A is described as the **sorted sand unit**. These sediments have a comparatively coarse mean grain size (fine to coarse sands) and are moderately well to well sorted. They are the best sorted sediments compared to the rest of the samples. The typical frequency histograms of this group (Fig 6.7) indicate that there is one dominant mode. The low sorting values reflect high energy sorting and the one dominant mode suggests uniform depositional conditions. Griffiths (1967) illustrated that in all subaqueous depositional environments the best sorted sediments had mean grain sizes in the fine sand category - the sediments of this unit are approximately in this category. Figure 6.11 illustrates the areal distribution of the samples of each of the 4 units. Clearly the samples of the sorted sand unit are in shallow coastal beach and reef areas. They are therefore subject to high energy removal of silt and clay fractions and the sediment in the unit is approximately in equilibrium with the prevailing high energy conditions.

Unit B is termed the **poorly-sorted sand unit**. It consists of poorly-sorted fine-coarse sands and by its position on the plot indicates moderate energy conditions. Frequency distribution plots of 2 typical samples (Fig 6.8) indicate unimodal distributions although spread about the mean is obviously greater than the sorted sand unit and there is a silt/clay component. The samples of this unit are found almost exclusively in the southern part of the Bay (Fig 6.11) although samples are also found in mangrove channels and channel mouths in the north. Moderate energy conditions are likely in these northern areas due to the concentration of tidal currents in channels. In the south, present day hydrodynamic energy levels may be sufficient to account for the grain size characteristics of the sediment. But since it is certain that there is no present day source for these sediments, their relict origin must account for their grain size characteristics. At low sea-level stands, moderate energy alluvial or shallow open coastal conditions would have been predominant in this area thus depositing these sandy sediments. The energy conditions present today may be preserving the characteristics of this sediment and preventing a veneer of recent fine material from settling out.

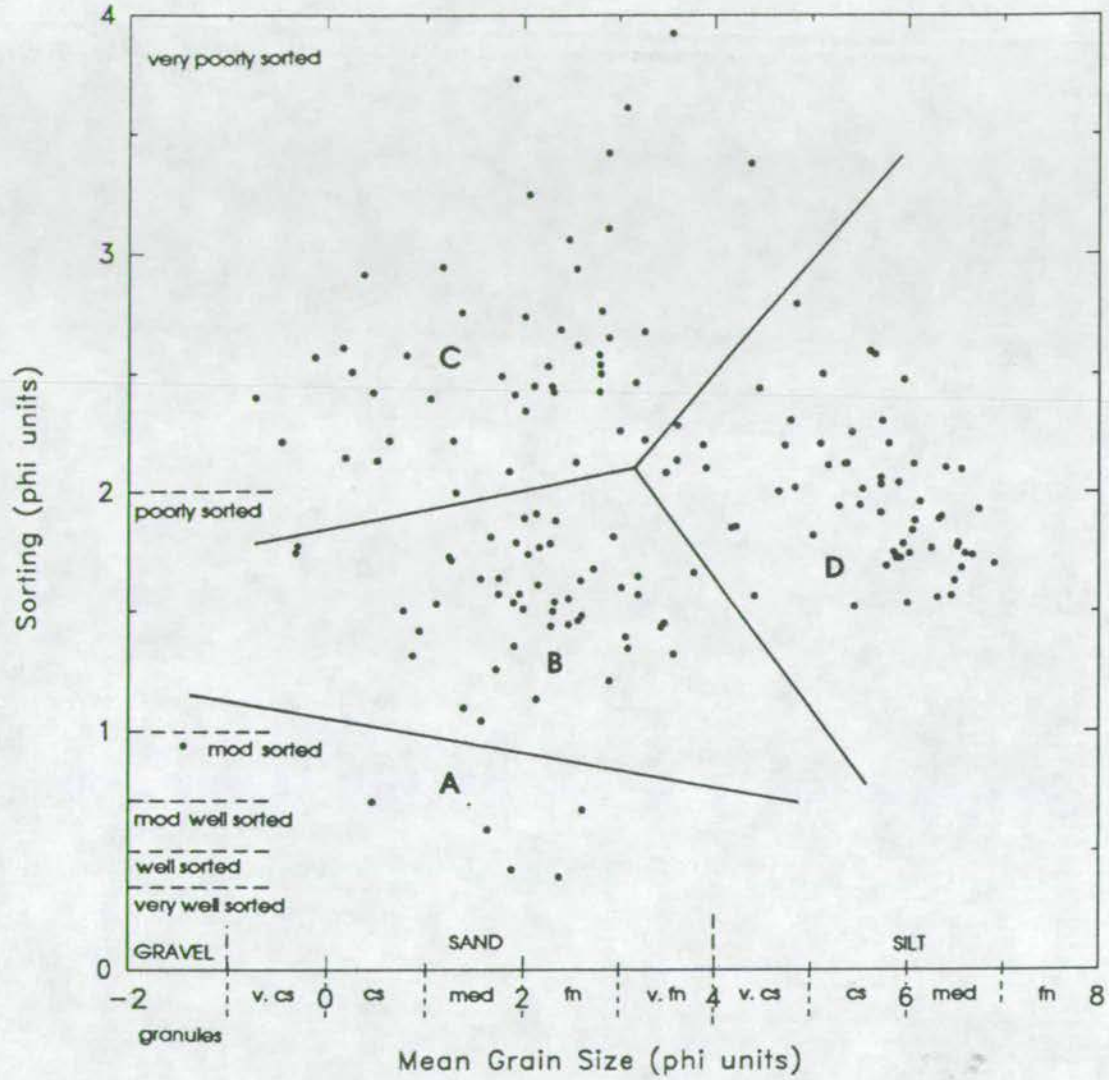

A = sorted sand unit

B = poorly-sorted sand unit

C = very poorly-sorted sand unit

D = poorly-sorted silt unit

Figure 6.6 Mean grain size v. sorting scatter plot with four fields delineated representing 4 sedimentary units

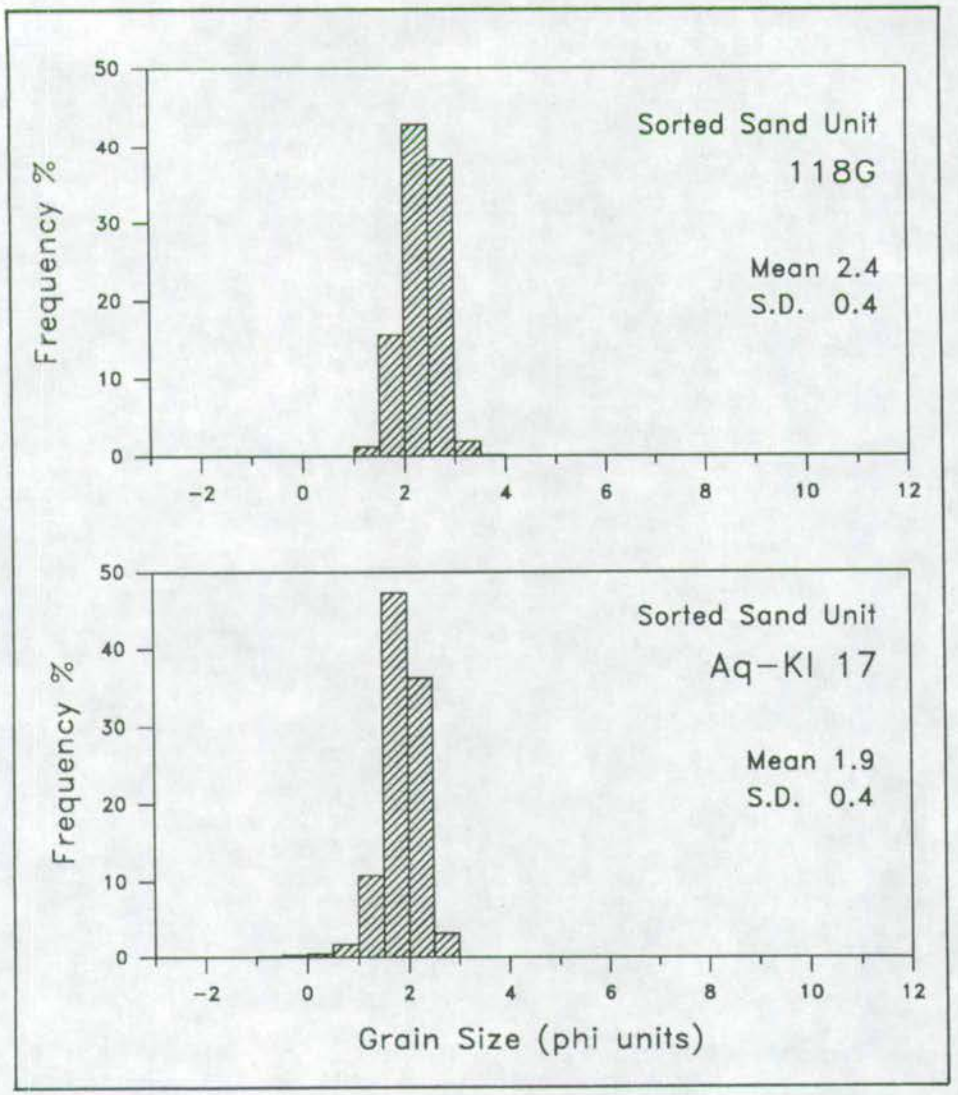

Figure 6.7 Typical grain size frequency histograms of the Sorted Sand Unit.

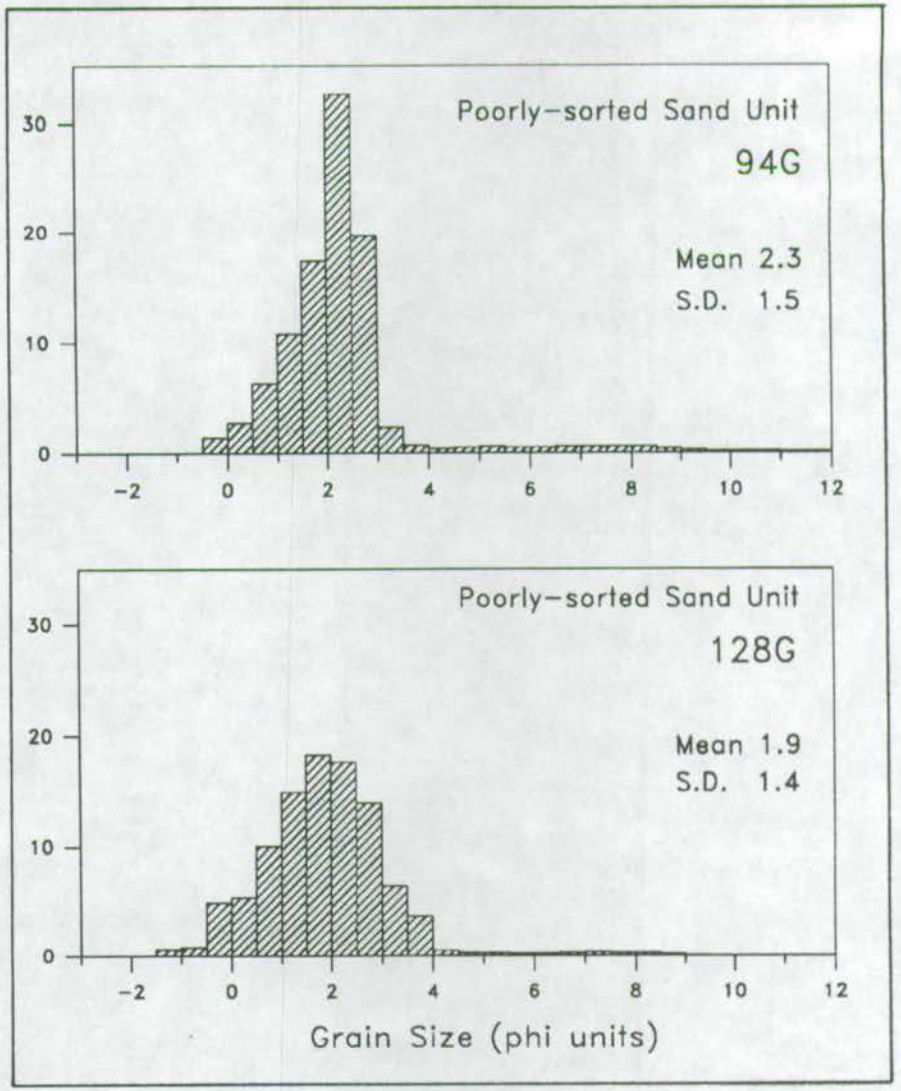

Figure 6.8 Typical grain size frequency histograms of the Poorly-sorted Sand Unit.

Unit C, the **unsorted sand unit**, consists of sediments of a similar mean grain size as the poorly-sorted sand unit however, the sediments are very poorly-sorted. The grain size suggests moderate energy conditions but the poor sorting suggests a mixed source of sediment. The polymodal nature of the distributions shown in the frequency histograms of 2 typical samples (Fig 6.9) also suggest a mixture of sediments populations. The distribution of these samples (Fig 6.11) in the sheltered northern part of the Bay would suggest low rather than moderate energy conditions. The coincident distribution of these samples with areas of high carbonate (Fig 4.4) accounts for the 'mixed source' interpretation. The *in situ* carbonate material adds a coarser fraction to the sediment (the modal peak at 0 phi on Fig 6.9 (Aq-KI 8)is due to benthic foraminifera infauna material) thus indicating higher energy conditions than are actually present in these areas (the known strong current areas excluded). The effect of *in situ* carbonate material on the grain size characteristics indicates that care has to be taken in making interpretations of hydrodynamic conditions from these bivariate scatter plots if whole sediment measurements are used.

Unit D, the **poorly-sorted silt unit**, is composed of relatively fine mean grain sized sediments (medium-coarse silts) which are poorly-sorted. Low energy conditions are suggested by the characteristics of this unit, and deposition from suspension is probably the dominant sedimentary process. Figure 6.10 show the frequency distribution histograms of 2 typical samples from this unit. The sediments of this unit are found in the northern sheltered part of the Bay (Fig 6.11) and the interpretation that they are deposited in low energy conditions dominantly from suspension is consistent with this distribution.

6.2.1.4 The origin of 'end-member' populations

The idea that the two main populations picked out in Figure 6.1 are approximate 'end-member' populations is reasonably accurate in the light of the postulated origin of these 2 populations - the coarser one is from relict sedimentation, the finer from recent sedimentation. The idea that the end-members are original distinct populations of sediment is perhaps inaccurate. Mixing in the sedimentological sense may be defined as '2 sediment populations having unique size frequency distributions that are mixed in various proportions to provide a suite of sediment samples with attributes falling between these 2 end-member 'source' distributions' (Syvitski, 1991). However, end-member distributions may also represent the result of singular depositional processes. This is thought to be the case for the 2 end-members identified here.

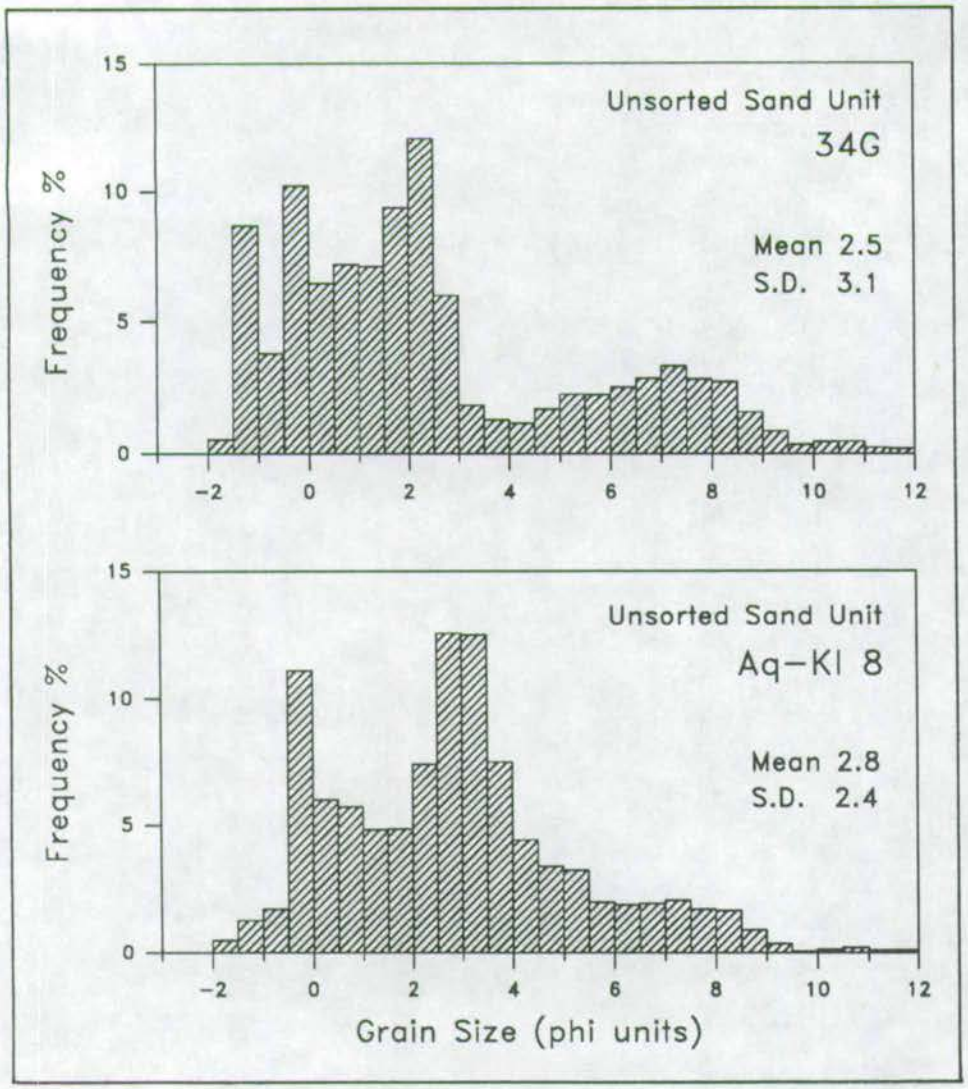

Figure 6.9 Typical grain size frequency histograms of the Unsorted Sand Unit.

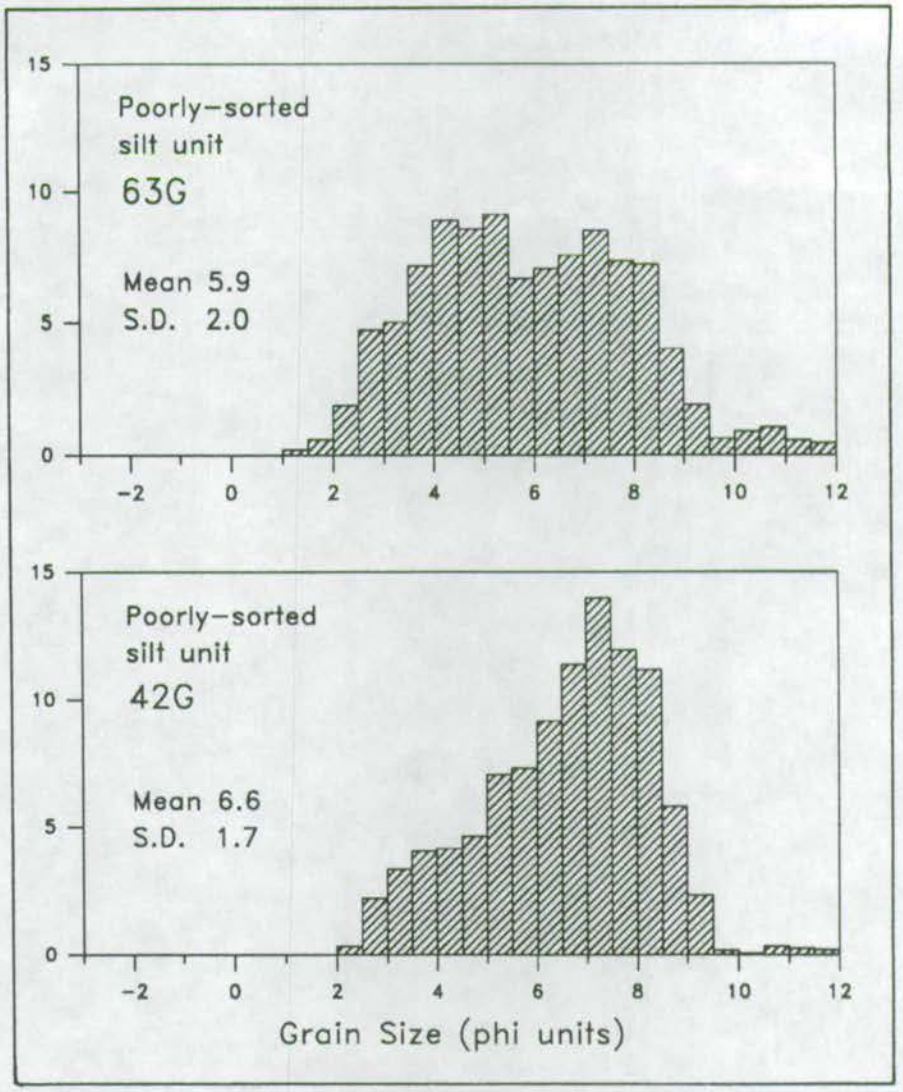

Figure 6.10 Typical grain size frequency histograms of the Poorly-sorted Silt Unit.

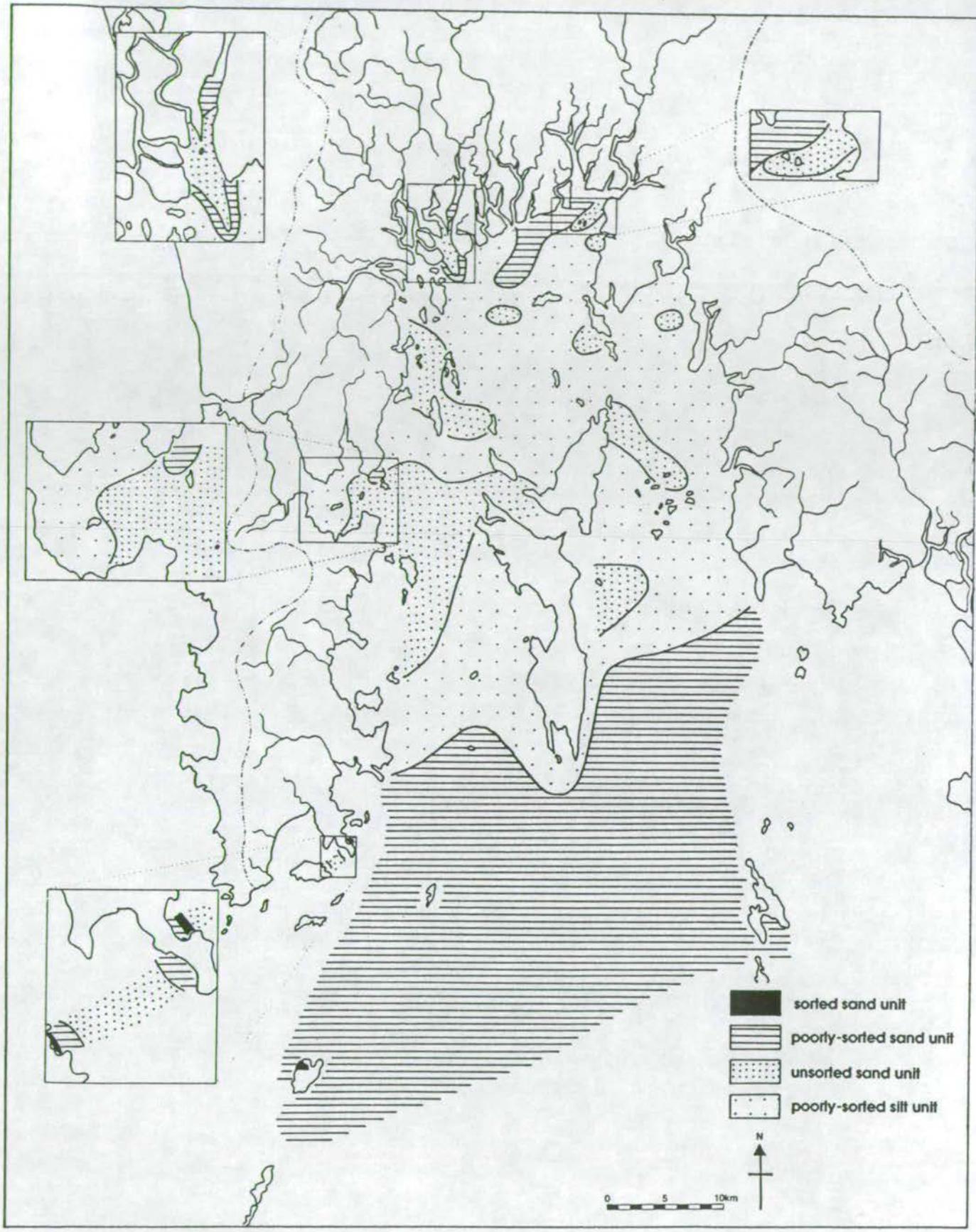

Figure 6.11 Areal distribution of the 4 sedimentary units delineated by the mean grain size v. sorting grain size plot.

If the coarser relict population is considered first, during low sea-level stands sediment sourced from the drainage basin travelled through the drainage system essentially as a mix of the original weathered material, ie coarse bedload and saltation material and finer suspended material. On reaching the river mouth the whole mix of material entered the unsheltered high energy coastal environment somewhere to the south of Phangnga Bay where fines will have been carried off-shore and only coarse material will have settled. With sea-level rise, reworking of alluvial material in this coastal environment will have resulted in only coarse material remaining. Hence the relict sediments are a result of the sorting of an originally mixed sediment load with fines removed and coarse material remaining.

The present high sea-level stand conditions mean that where this mix of material now enters the marine environment, conditions are sheltered and calm. This allows coarse material to settle out early on in mangrove channels and channel mouths and fines travel further off-shore and settle out or, be transported into the mangrove swamps where some material settles at slack tide. Thus the original mixed sediment load is sorted on reaching the marine environment.

This idea of mixing versus sorting as originators of end-member populations is discussed by Syvitski (1991) in his review of the use of factor analysis in grain size data analysis (see the next section of this chapter). He concludes that identifying end-members as a result of sediment sorting of a single population may be difficult in closed systems such as sedimentary basins where there may be a continuum between proximal and distal prodelta sediments and a reverse continuum related to the seaward transport of coarse delta front sediments transported by turbidity currents. This is not a problem in Phangnga Bay and the idea of sorting resulting in 2 end-members seems particularly relevant when considering contiguous diachronous sediment bodies sourced from the same area but deposited under different sedimentological conditions.

6.2.1.5 Discussion

The grouping of the sediment samples into these 4 basic units and the simple deductions on hydrodynamic conditions of deposition made for each group seem consistent with the areal distribution of these groups in the Bay. However, if such deductions were to be made on ancient equivalents some knowledge of the carbonate content would be required, or better still, a carbonate-free analysis of the grain size distribution made.

6.2.2 Factor Analysis

A further attempt at classifying the sediment samples into distinct depositional units is made by using principal components analysis (a type of factor analysis). In this method, the use of somewhat arbitrary statistical grain size parameters is avoided and the input data is actual weight percentages in each grain size interval which is considered to totally describe each sediment sample. In this way the results are obtained in an almost completely objective manner without any *a priori* knowledge of the significance of any particular grain-size parameters. Principal components analysis (PCA) is discussed in Chapter 4 and in Appendix C.

Factor analysis has been used in several studies in an attempt to understand sediment processes using the size frequency distribution of sediment samples (Klovan, 1966; Allen et al 1971; Dal Cin, 1976; Chambers and Upchurch, 1979) and in all of these studies the method has provided useful geological information. Syvitski (1991) reviews the use of factor analysis as applied to problems involving the use of grain size data.

6.2.2.1 Results

The results of the PCA are listed in Table 6.1 and the coefficients for each of the first 3 principal components are illustrated graphically in figure 6.12. 77% of the variance in the data is explained by the first 3 principal components. The first principal component is a 'coarse' sediment factor with positive loadings for grain size intervals coarser than 2.5 phi. PC2 is a 'medium' grain size factor with high positive loadings between 2.5 and 4 phi whilst PC3 is a 'fine' factor with high positive loadings between 9.5 and 12 phi. Principal components 4, 5 and 6 are not so clearly definable and are not considered further here as the majority of the variance is explained by the first 3 factors.

By plotting the principal component scores for each sample (calculated from the standardized variables ie, subtract the mean and divide by the standard deviation of each variable, then multiply by the coefficients listed in Table 6.1) samples may cluster into easily identifiable groups in a way similar to the clustering of the elements into groups using the coefficients of the principal components (Chapter 4). Figure 6.13 a & b illustrate the distribution of samples on a PC1 versus PC2 plot and PC1 versus PC3 plot. On figure 6.13a there are no obvious distinct clusters of samples

	PC1	PC2	PC3	PC4	PC5	PC6
Eigenvalue	14.86	3.678	3.136	2.011	1.497	0.855
Proportion	0.531	0.131	0.112	0.072	0.053	0.031
Cumulative	0.531	0.662	0.774	0.846	0.899	0.93
Phi Intervals	PC1	PC2	PC3	PC4	PC5	PC6
-1.75	0.087	-0.291	-0.111	0.319	-0.35	0.184
-1	0.118	-0.349	-0.105	0.279	-0.257	0.077
-0.5	0.146	-0.356	-0.074	0.212	-0.035	0.005
0	0.159	-0.302	-0.023	0.085	0.231	-0.061
0.5	0.169	-0.263	0.035	-0.072	0.396	-0.193
1	0.163	-0.206	0.075	-0.195	0.407	-0.173
1.5	0.182	-0.111	0.143	-0.352	0.178	0.071
2	0.156	0.024	0.167	-0.395	-0.152	0.297
2.5	0.151	0.181	0.185	-0.282	-0.312	0.124
3	0.1	0.35	0.149	0.08	-0.175	-0.314
3.5	0.007	0.369	0.006	0.37	0.203	-0.217
4	-0.07	0.273	-0.094	0.299	0.344	0.222
4.5	-0.188	0.059	-0.163	-0.001	0.219	0.474
5	-0.218	0.004	-0.155	-0.062	0.134	0.349
5.5	-0.241	-0.03	-0.124	-0.08	0.062	0.156
6	-0.247	-0.057	-0.102	-0.096	-0.008	-0.019
6.5	-0.243	-0.063	-0.13	-0.109	-0.032	-0.089
7.	-0.244	-0.069	-0.125	-0.109	-0.045	-0.133
7.5	-0.242	-0.071	-0.127	-0.11	-0.054	-0.166
8	-0.243	-0.072	-0.117	-0.105	-0.055	-0.177
8.5	-0.244	-0.072	-0.104	-0.098	-0.052	-0.177
9	-0.247	-0.078	-0.055	-0.08	-0.05	-0.178
9.5	-0.235	-0.096	0.121	-0.013	-0.052	-0.197
10	-0.166	-0.099	0.401	0.101	-0.013	-0.032
10.5	-0.164	-0.089	0.405	0.119	0.028	0.074
11	-0.188	-0.085	0.363	0.101	0.038	0.088
11.5	-0.197	-0.084	0.34	0.091	0.038	0.083
12	-0.198	-0.081	0.334	0.088	0.041	0.092

Table 6.1 Results of Principal Components Analysis on grain size data for all sediments of the Bay.

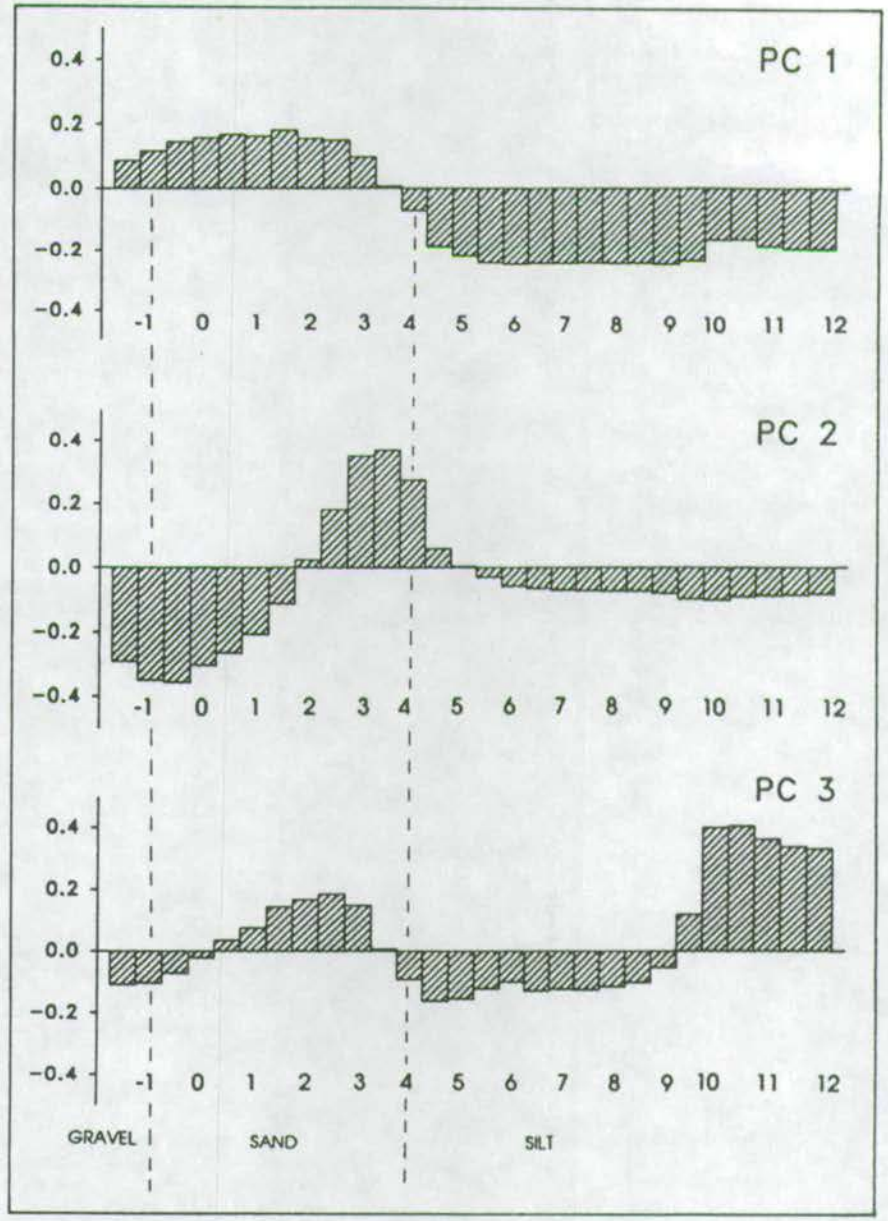

Figure 6.12 Graphical representation of results of principal components analysis given in Table 6.1.

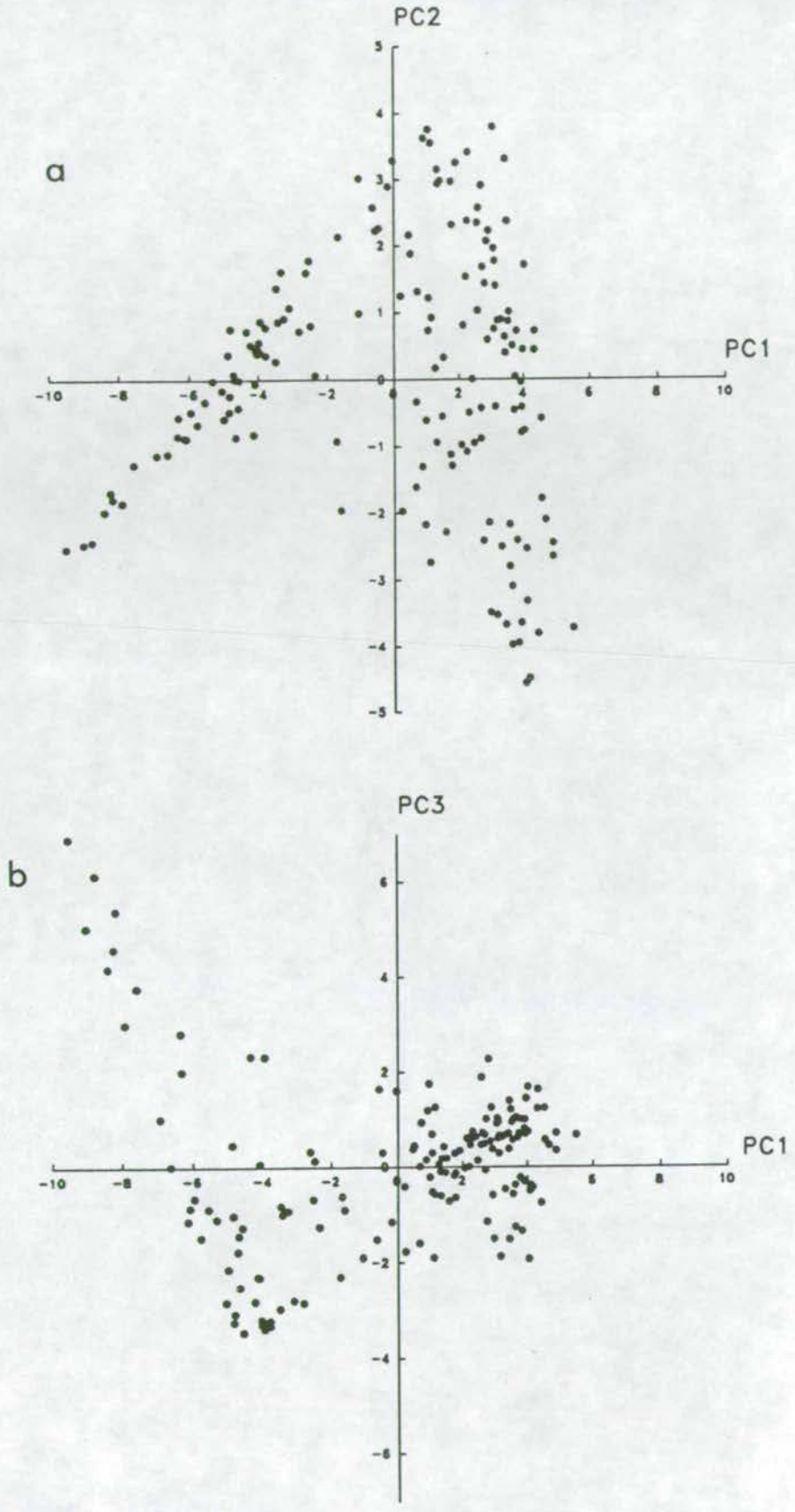

Figure 6.13 Principal component scores of grain size data (using weight % in each grain size interval) for each sample plotting a. PC1 v. PC2 and b. PC1 v. PC3.

which could be termed a population. However there is a clear shape to the scatter of points something like an upside-down V. This suggests 3 'end-members' at each apex with a continuum of sediment types from the bottom left apex to the top apex to the bottom right apex.

6.2.2.2 Interpretation

Considering the interpretation of PC1 and PC2, the bottom left apex is very fine grained sediment samples (negative PC1 and PC2), the top apex is 'medium' sediment samples (high PC2, low PC1) and the bottom right apex is coarse sediment (high PC1, low PC2). This interpretation is also illustrated in figure 6.13b (PC1 v. PC3) which is approximately the inverse pattern of 6.13a with high PC3 values indicating fine-grained samples. The distribution patterns of these sediment types in the Bay is illustrated in figure 6.14 - samples are classified by calculating the component scores for each sample and assigning the sample to that sediment type for which it has the highest score. From these distribution patterns the generalised interpretations of these apexes are given in figure 6.15. The fine sediments are of recent origin, the coarse sediments are dominantly of relict origin (although there are some recent channel sands and recent, shell-rich sediments in this coarse sediment grouping) and there is a continuum of samples inbetween of moderate grain size. However, there is no mixing of both fine and coarse sediments indicated by the gap between these 2 end-members. Since the finest sediments can only accumulate in sheltered low energy areas in the far north of the Bay, and the relict coarse material is only exposed in the higher energy southern part of the Bay it is not surprising that there is no mixing.

6.2.2.3 Discussion

This method has picked out the extremes of depositional energy conditions and their antithetic relationship and it also illustrates the continuum of depositional regimes between these two extremes.

Although this in itself is useful information obtained from an objective analysis of the data, the original idea of separating the samples into unique and distinct populations has not been achieved. Plotting the PC1 versus PC2 diagram using the sample divisions obtained with the use of bivariate plots (Fig 6.16) it is clear that although the 4 sedimentary units do plot in quite well defined areas, it would not be possible to delineate these without the *a priori* knowledge of these units. We also still have the problem of the carbonate material in the sediment and its affect on the

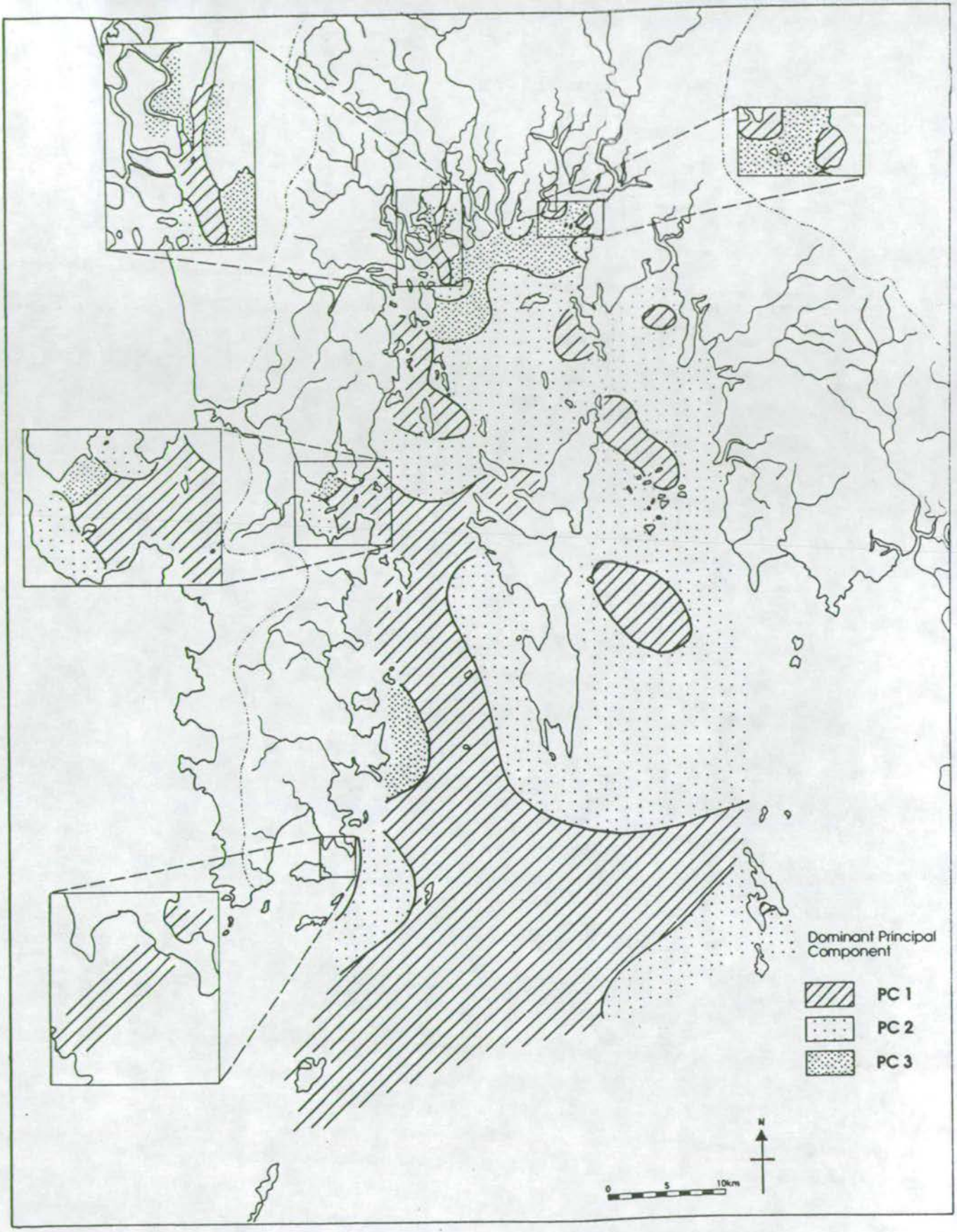

Figure 6.14 Areal distribution of sediments classified by the dominant principal component. (Samples are classified by calculating the principal component scores for each sample and assigning the sample to that sediment type for which it has the highest score).

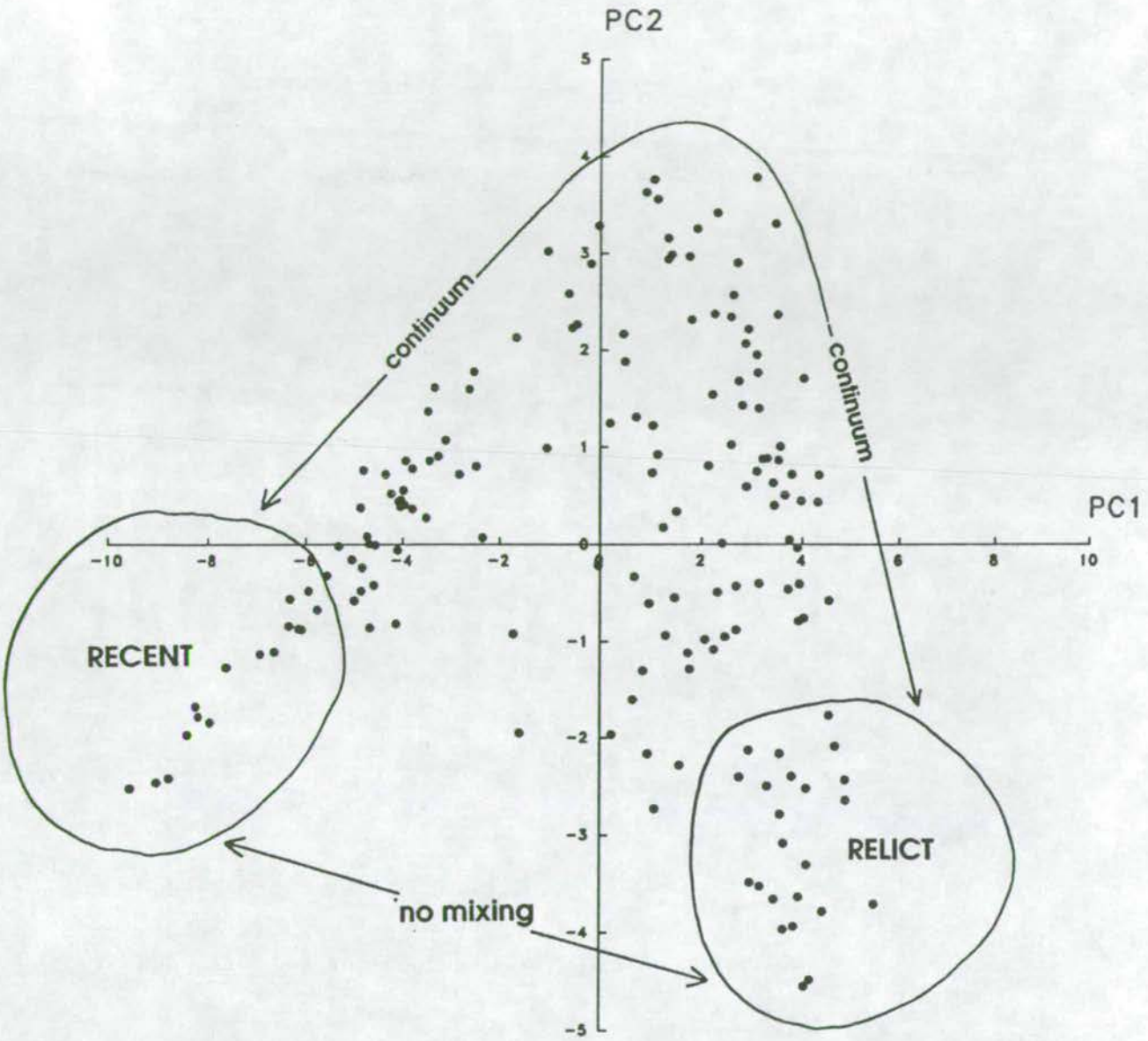

Figure 6.15 Interpretation of the distribution of sample points when plotting PC1 scores v. PC2 scores.

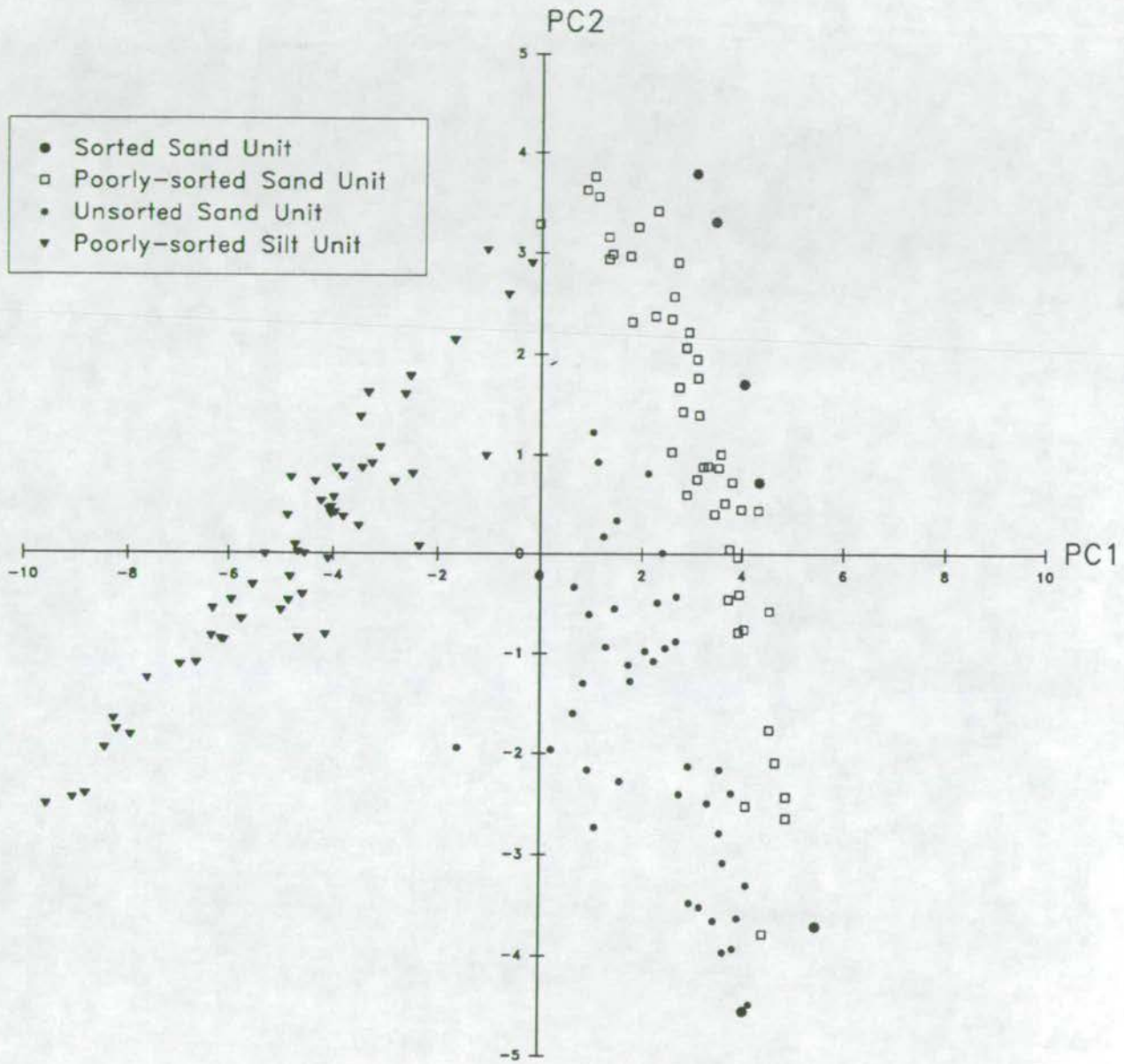

Figure 6.16 PC1 scores v. PC2 scores with samples classified according to the units delineated by the mean grain size v. sorting scatter plot.

grain size distribution which cannot be accounted for unless a comparison of principal component plots using the whole sediment versus the carbonate-free sediment is carried out (with the inherent problem of obtaining an accurate particle size distribution on sediment which has been chemically treated to remove the carbonate). Alternatively, some method of incorporating the percent carbonate content, and indeed other geochemical compositional data into the analysis of sediment populations could be used and this is what is attempted with the use of cluster analysis.

6.3 CLASSIFICATION USING GRAIN SIZE AND GEOCHEMICAL VARIABLES

6.3.1 **Cluster Analysis**

Cluster analysis is a method of classification which involves putting similar objects into an unknown number of distinct categories, with the objects in each category being more similar to each other than to the objects in all the other categories. Although in the ideal data set, clusters would be obvious enough to be picked out using 2-D plots, the data available here is obviously not of this type and so a more complicated mathematical clustering technique is required.

There are a great profusion of clustering techniques which are adequately explained in relevant texts (eg, Everitt, 1974) as are the principles of the technique which will be summarised here.

The basic procedure with all methods is similar. They begin with the computation of a similarity or distance matrix between the samples [1]. The choice of the similarity or distance measure used depends on the type of data, whether binary or continuous, whether there are missing values, whether weighting is required and the type of clustering strategy that is to be used. In this work the distance measure of Squared Euclidean Distance is used as it is the most commonly used distance measure and evidence suggests it is the most accurate for this type of data (Everitt, 1974). Since

[1] **similarity measures** calculate the closeness of samples and values range from 1 for most similar to 0 for most dissimilar - **distance measures** calculate the dissimilarity between samples with 0 meaning the least distance ie, most similar and increasingly positive numbers indicating decreasing similarity.

Euclidean distance is badly affected by scale changes between variables, the variables are standardised (transformed to have a mean of 0 and a standard deviation of 1).

Clustering strategies are divided into various groups depending on what sort of output they produce. In this case a dendrogram was required and so the agglomerative, hierarchical, group average method was used with unweighted data.

Since the concentrations of the majority of the trace elements are controlled by the amount of Al or Ca in the sediment, these elements are dependant on Al or Ca and their inclusion in the analysis adds weight to the effect of Al or Ca concentrations on the results. Since the choice of trace elements measured is purely arbitrary, their weighting effect is also arbitrary and therefore an unknown factor is introduced into the analysis which hinders interpretation of the results. Additionally, in order to emphasize environmental distributions and avoid effects due to provenance, Sn, Rb and Zr were also eliminated from the analysis. Since it is known that the proportion of the main components of the sediments are represented by the concentrations of Si, Al and Ca, these 3 elements along with the 3 grain size parameters (mean grain size, sorting and skewness) were used for the cluster analysis. Therefore the sediments are grouped into clusters on the basis of their grain size characteristics and their main component geochemistry.

6.3.1.1 Results

A dendrogram representing the results from cluster analysis is given in Figure 6.17. In order to compare the results with the 2 previous sample classifications (obtained from both knowledge of the geomorphology and water depth of the deposits and from a bivariate scatter plot of mean grain size against skewness) the classification of each sample is indicated below the plot (numbers refer to the geomorphological classification, letters refer to the bivariate plot classification). 'Natural breaks' between groups on the dendrogram are indicated by shading and each group is numbered. Groups 1 and 5 could each possibly be divided into 2 further groups (labelled a & b).

Although the 8 depositional environments do not at first appear to be well picked out by the clustering, on closer inspection, it can be seen that most of the open

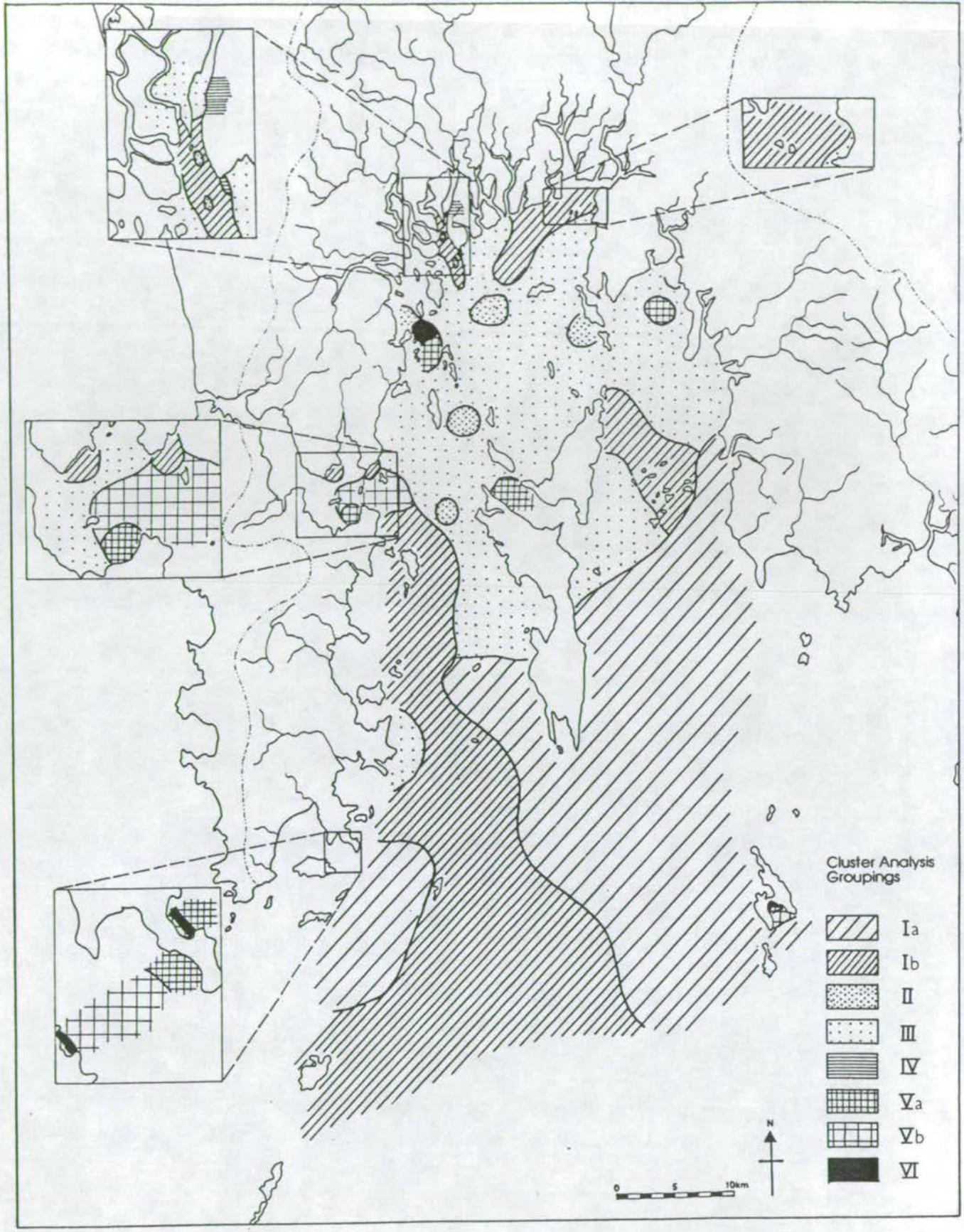

Figure 6.18 Areal distribution of the 6 cluster groups (including sub-groups) as delineated from the dendrogram.

Phuket. This latter area, although not near coral reefs like the 3 areas further south, is extremely rich in $CaCO_3$ (Fig 4.4) which perhaps explains the inclusion of these sediments in this group. The differences between cluster groups Va and Vb are not immediately obvious although there may be more terrigenous material in the Va sediments. Cluster group VI sediments are all from beach environments. The 2 beach samples, 44a and Aq-kl 17, plot quite separately from the other groups due to their unusual characteristics - very coarse shelly material (44a) and very well sorted, fine sand (Aq-kl 17).

Therefore by consideration of the distribution of the groups identified by cluster analysis, the general characteristics of each group can be described and are listed below:

Cluster group Ia, Ib — mainly coarse, relict sediments
- Ia — low $CaCO_3$ content
- Ib — high $CaCO_3$ content

II — recent, high $CaCO_3$ content (> 30%) sediments (concentrations of shell material in North of the Bay)

III/IV — Recent fine-grain sediments

Va, Vb — near reef, high carbonate sediments
- Va — ? high terrigenous content
- Vb — ? low terrigenous content

VI — beach sediments

6.3.1.3 Discussion

An important aspect of cluster analysis is verification of the results by seeing whether the groupings are geologically meaningful. Since the distributions fit in with the known distributions of the variables (especially mean grain size and $CaCO_3$ content) and can be explained as such, then the cluster groups do appear to geologically meaningful. This classification is thus more specific and meaningful than that obtained from bivariate plot of grain size parameters.

6.4 CONCLUSIONS

In this chapter, an attempt has been made at classification of sediment samples into populations using both the grain size and geochemical characteristics of the

DEPOSITIONAL ENVIRONMENT

1 — Mangrove Swamp
2 — Mangrove Channel
3 — Open Intertidal
4 — Shallow Marine
5 — Open marine
6 — Reef Front
7 — Reef Top
8 — Beach

SEDIMENTARY UNIT

a — sorted sand unit
b — poorly-sorted sand unit
c — unsorted sand unit
d — poorly-sorted sand unit

Dissimilarity Coefficient

0.173
0.155
0.137
0.118
0.100
0.082
0.064
0.046
0.028
0.010
0.0

I
Ia
Ib
II
III
IV
V
Va
Vb
VI

Depositional Environment 5 5 4 5 5 2 5 — 5 2 — 2 5 5 4 3 4 2 2 4 5 3 2 3 2 3 4 5 4 2 4 — 4 5 5 7 4 5 4 3 4 — 4 2 2 4 4 5 4 4 3 4 4 4 3 2 3 4 4 3 1 3 4 1 3 1 3 3 4 3 3 1 4 8 4 4 5 6 7 6 6 7 6 6 4 4 6 4 — 4 6 — 6 7 8 8

Sedimentary Unit d — d b b c c b c c c — c b b d c c b b c c d d b a c c b b c c b — b a a c a a

fk = Tang Khen transect
aq = Aquarium to Ko Lon transect

Figure 6.17 Dendrogram produced by cluster analysis (the agglomerative, hierarchical, group average method used with unweighted data) of Si, Al, Ca, mean grain size, sorting and skewness of surface sediments. 6 groups have been shaded (with 2 sub-groups in I and V). Classifications of depositional environments (from water depth and geomorphology) and sedimentary units (from a bivariate scatter plot of mean grain size v. sorting) are listed along the bottom of the dendrogram for comparison. Sample site numbers are listed along the bottom row.

sediments via both simple and complex techniques of classification. Comparison of these classifications with that obtained by knowledge of the water depth and geomorphology of the deposits allows a measure of the usefulness of these methods to be established.

Bivariate scatter plots of grain size parameters are used over and over again in sedimentary studies, possibly because of their simplicity, in order to try and classify samples and induce conditions of deposition. As was shown in Chapter 5, considerable overlap between sediments of the 8 depositional environments does not allow these environments to be distinguished in this way although the average for each environment may be more indicative of the differences between environments. However, this approach requires *a priori* knowledge of the environments which is effectively starting with the result and working round in a circle.

The numerical approach involves starting off with the descriptive data for each sample and trying to find similarities between samples which may result in groups of samples being established. Such an approach may be of use when studying sedimentary rocks if limited information is available on other discriminatory factors such as structures, fauna, geometry etc.

Identifying clusters in scatter plots of grain size parameters allows some deductions on the conditions of deposition to be made. However, the identification of these clusters, although aided by contour plots, is rather arbitrary and as discussed in section 6.2.1.2 is strongly affected by the number of samples taken from each type of environment. Four sedimentary units were delineated and when plotted on a distribution map the groupings appear to be geologically viable. However, only a broad classification was obtained, using rather arbitrary grain size parameters which, by simplifying the data, may lose an important part of the information.

The use of simplifying grain size parameters is avoided in the method of principal components analysis which takes account of the weight percent in each size fraction. However, although this method provided useful information on the main depositional energy regimes present in the Bay and effectively pin-pointed 2 'end-members' of low energy and high energy with a continuum inbetween, the samples were again not separated into distinct groupings and only a 3-grade classification was obtained. A problem with both the above methods is that no account could

be taken of the carbonate material in the sediment which affects the grain size distribution without necessarily being transported and deposited along with the terrigenous material. Also the overlap of sediment types between environments means that drawing a line between 'clusters' is a rather arbitrary affair.

Cluster analysis allows a mix of variables to be used in the analysis thus the $CaCO_3$ content can be accounted for. Although the grain size parameters were also used (thus losing some information compared to the principal components analysis) the moments method of calculating these parameters does take account of each weight percent in each size fraction and so is the best method available for calculating these parameters. The selection of clusters is not totally objective as the level of dissimilarity chosen as a cut-off is very much up to the interpreter, however, groupings are far more obvious. The distribution of the groupings on an areal map of the Bay indicates that they are geologically viable and their interpretation indicates that they are more specific than the classifications obtained from bivariate plots and principal components analysis.

The conclusion from this comparison of techniques is that depositional environments are not uniquely identified from numerical analysis of grain size data alone although useful information is obtained from consideration of hydrodynamic conditions of deposition. However, when both grain size and basic major component geochemical data are used with a more complicated (but workable) classification technique, environmental discrimination is much improved.

It is rarely the case that environmental classification in ancient deposits is based on just one descriptive tool such as grain size. Factors such as depositional structures, surrounding lithologies, geometry of the deposit and faunal assemblages are all studied and put together to indicate a depositional environment. However, since grain size and geochemical data are usually easily obtainable from sedimentary rocks, such a classification technique could give important information on the depositional conditions of sedimentation of the deposit

CHAPTER 7

THE DISTRIBUTION OF BIOGENIC COMPONENTS IN THE SURFACE SEDIMENTS

CHAPTER 7 - THE DISTRIBUTION OF THE BIOGENIC COMPONENTS IN THE SURFACE SEDIMENTS

7.1 INTRODUCTION

This chapter aims to describe the distribution of the biogenic components of the surface sediments of Phangnga Bay and discuss the implications of such distributions in terms of helping to determine ancient estuarine and bay sequences particularly the seaward and landward directions. Some mention of these biogenic components was made in Chapter 3 where the mineralogy of the biogenic carbonate fraction was discussed in relation to the distribution of some of the biogenic components identified in the sediments. Identifications of the bivalves and gastropods found in the Bay are listed in the second part of this chapter and their distribution in relation to the water depth and percent mud of the sediment in which they are found is discussed.

7.2 THE MAIN BIOGENIC COMPONENT DISTRIBUTIONS

7.2.1 **Method**

Estimates of the abundance of various biogenic components in the sediment have been made on two types of sample:

1. 1-5mm fraction of the grab sample - once whole sediment samples of the grab sediment were obtained, the rest of the grab contents were sieved through 5mm and 1mm sieves and the 1-5mm fraction collected.

2. > 5mm fraction of the dredge sample - the contents of the dredge bag were emptied and washed on a 5mm sieve table and a representative sample of the material collected.

Sieved grab samples were obtained from the sample stations illustrated in figure 7.1[1] and the coverage of dredge samples was restricted to the sites listed in figure 7.2[1] (areas not covered by dredge sampling are delineated by dashed lines which are

[1] Figures 7.1 and 7.2 are also included as enclosures in the form of overlays.

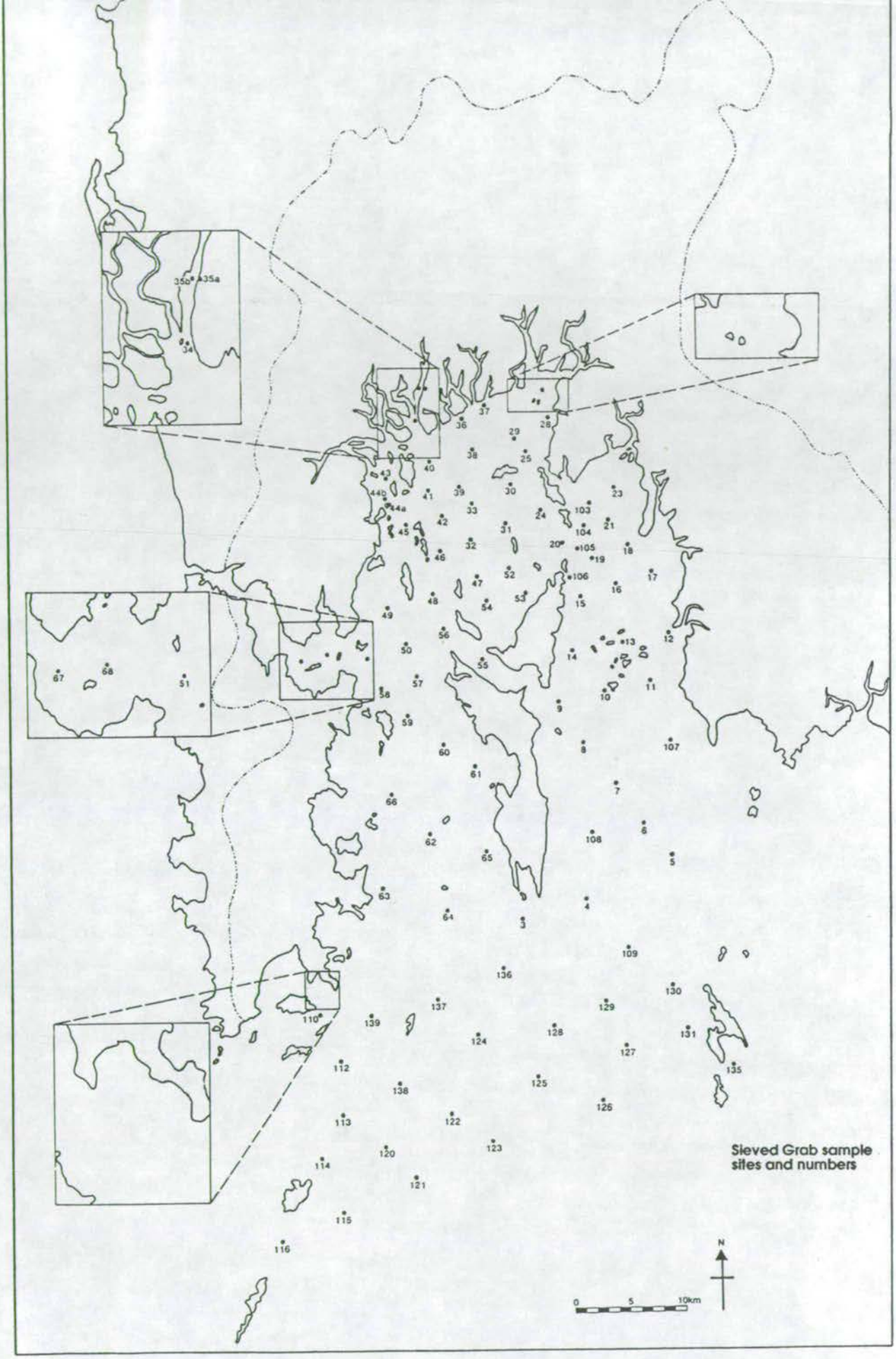

Figure 7.1 Distribution of sites from which sieved grab samples (1-5mm) were collected.

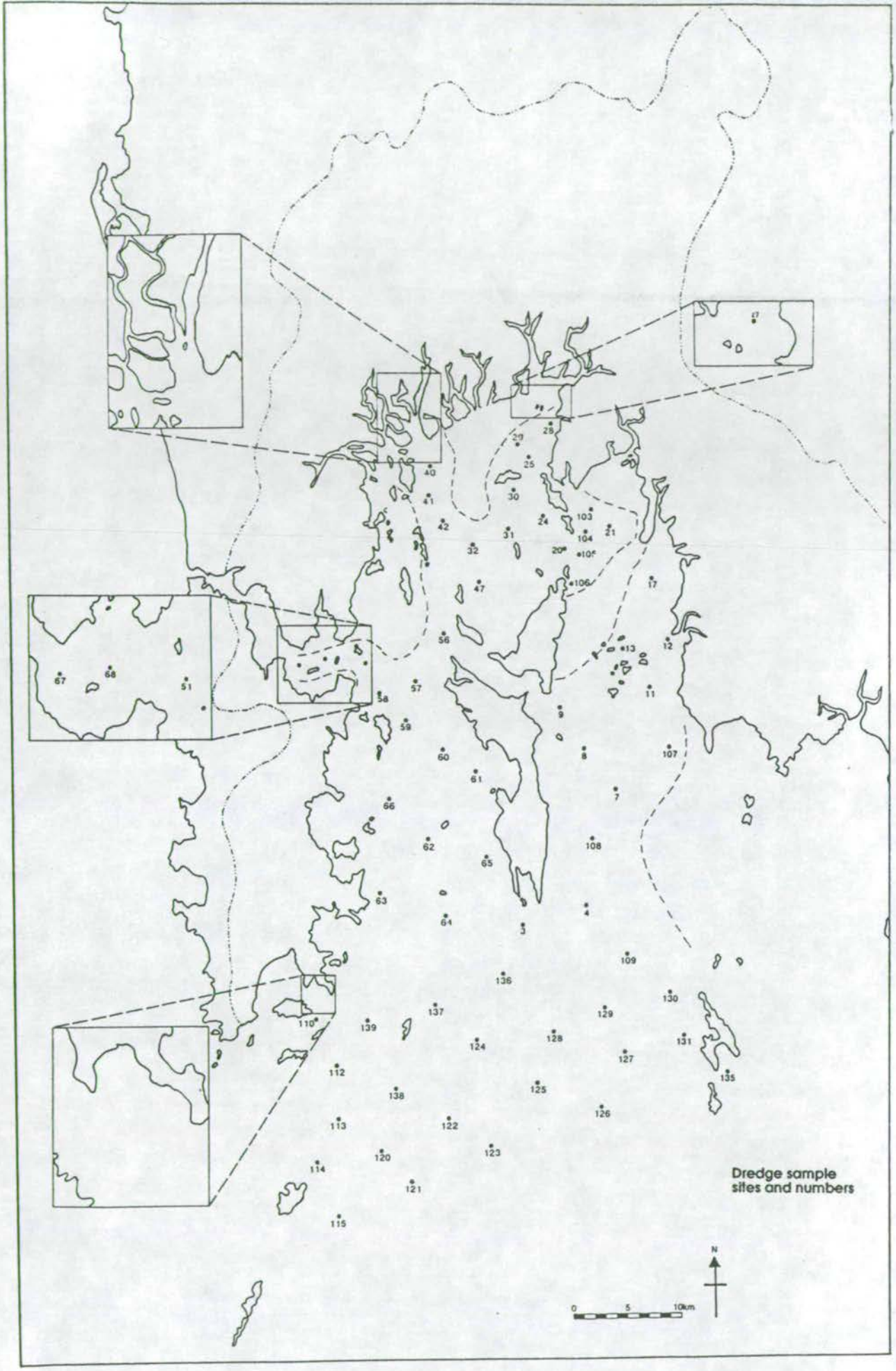

Figure 7.2 Distribution of sites from which dredge samples (>5mm) were collected.

also present on the following distribution maps). Both the above types of sample were stored and transported back to Britain in plastic bags and then washed and dried at 60°C before analysis. The proportion of each component, including terrigenous material, was visually estimated (with the use of a binocular microscope) in percent for each sample. The percent of each of the biogenic components was then recalculated as part of the biogenic fraction (ie, non-terrigenous) only. The results have been plotted on areal distribution maps of the Bay (Figs 7.3 - 7.17) and contours drawn to indicate areas of none, trace or relatively abundant amounts (in weight % intervals) of each component.

It has to be remembered that the figures on the maps refer to the percent of the biogenic fraction from certain size fractions rather than of the whole sediment. It is not possible to calculate absolute abundances (as a percent of the whole sediment), as in the measured grain size analysis of most sub-samples of the whole grab sample, the percent > 1mm is very small and in some cases non-existent despite the fact that some of this coarser material was collected when the entire contents of the grab were washed through a sieve. The dredge material was collected over a distance of approximately 150m and therefore it would be inaccurate to try and recalculate absolute abundances of each component found in the dredge using the grain size analysis of a sub-sample from a grab. Since large shells were removed from the grab sub-sample before grain size analysis such a recalculation becomes even more meaningless. The distribution maps reflect the variation in relative amounts of each component and if compared with the percent $CaCO_3$ map (which reflects the percent biogenic component) some idea of the absolute amount of each component can be obtained.

7.2.2 **The biogenic components**

Bivalves, gastropods (including pteropods), scaphopods, echinoid fragments (plates and spines), barnacles, foraminifera, crab fragments (Plate 17J), ophiuroid (brittle star) plates, coral fragments and plant material have been identified as the major components of the biogenic fraction. There is a wide variation in the condition of the biogenic material from comminuted shell debris to live specimens. However, despite the range of organisms, very few were found live even in the dredge samples. A few live, burrowing echinoids (identified as *Metalia sternalis* - by Somchai Bussarawit, PMBC) and ophiuroids were collected in the dredge samples along with

small mantis shrimps, crabs, flat fish and an octopus. The most abundant live organisms found in the sediments were polychaete worms surrounded by tubes constructed from the surrounding sediment (see Plate 5, Chapter 3 for an example of these tubes). Few molluscs were found live. A description of the condition of these shells found will follow in section 7.3.

In a study of the species abundance and distribution of macrobenthic fauna in Phangnga Bay (Sawangarreruks and Boonruang, 1988) in 1986 it was found that of the benthic organisms, 32% were crustaceans, 27% echinoids, 24% molluscs, 9% polychaetes and 7% fish and other chordates. It is not clear whether these are live or dead abundances but the figures give an indication of the types of benthic organisms which are common in the Bay.

7.2.2.1 Bivalves

Bivalves form the highest proportion of the biogenic fraction both as whole shells and as fragments. In the 1-5mm grab samples (Fig 7.3) they form > 50% of the biogenic component in the central and southern areas and in parts of the northern area of the Bay. Only in small mud-rich areas in the north and a current swept area in the south do they constitute < 25% of the biogenic fraction. In the dredge samples (Fig 7.4) they constitute > 50% of the sediment in all but 2 samples. Their dominance in the dredge samples reflects their larger size compared to the other components studied hence trends are not so evident in this map. In the 1-5mm fraction however, there is a general trend of increasing bivalve proportions southwards. This trend reflects quite closely that of $CaCO_3$ which suggests that much of the variation in carbonate content is caused by fluctuations in the absolute amount of bivalves.

7.2.2.2 Gastropods

In the 1-5mm grab fraction gastropods are distributed in varying proportions in the north and central areas of the Bay (Fig 7.5) but are present in only trace amounts in the coarser sediments in the south. Larger gastropods are more common in this southern area as is shown by their distribution in the > 5mm dredge samples (Fig 7.6). Small gastropods (<5mm) form a greater proportion (> 10%) of the biogenic fraction in patchy areas in the north and central parts of the Bay. However, there are no clear north-south trends.

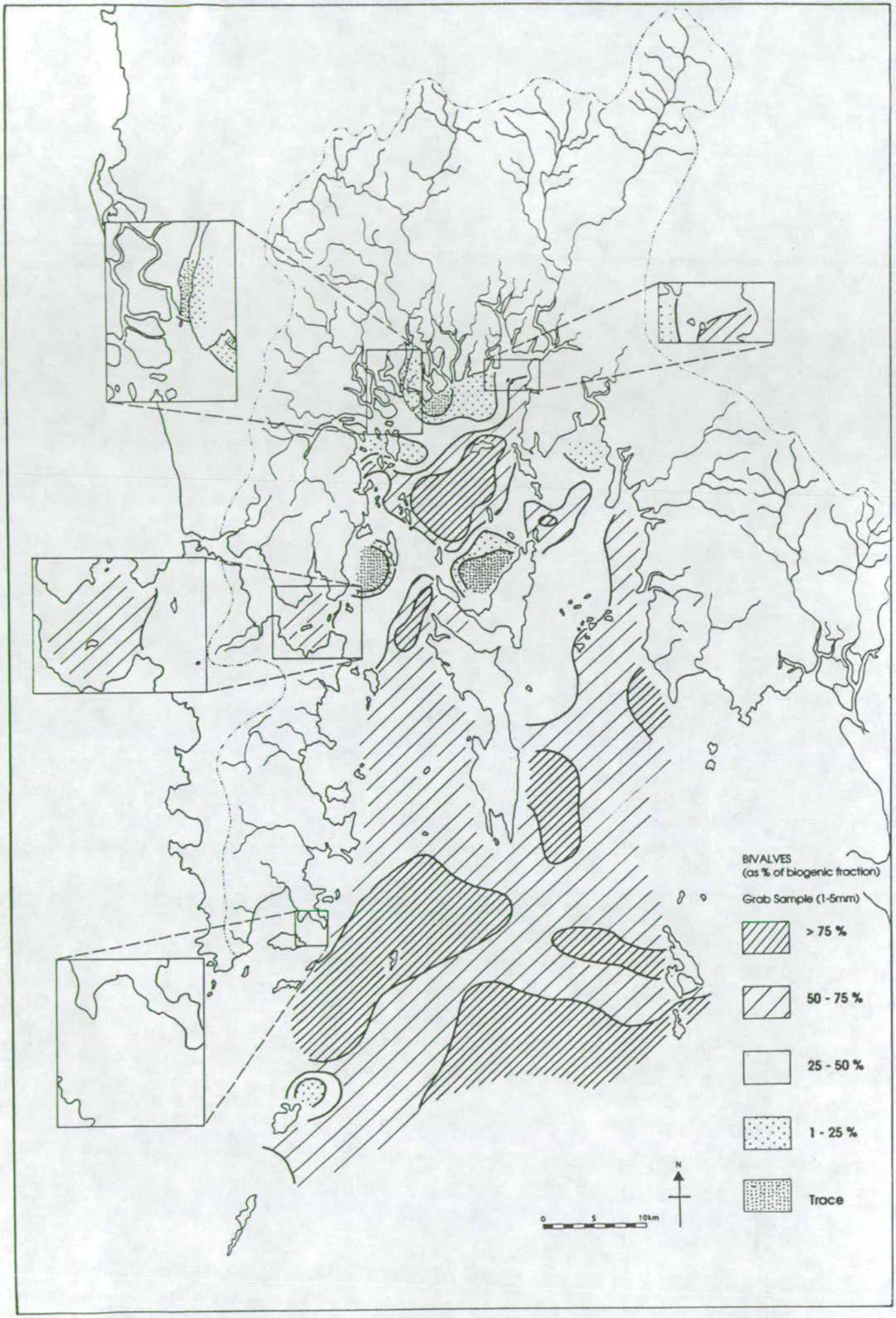

Figure 7.3 Distribution of bivalves in grab samples (1-5mm) as a percent of the biogenic fraction.

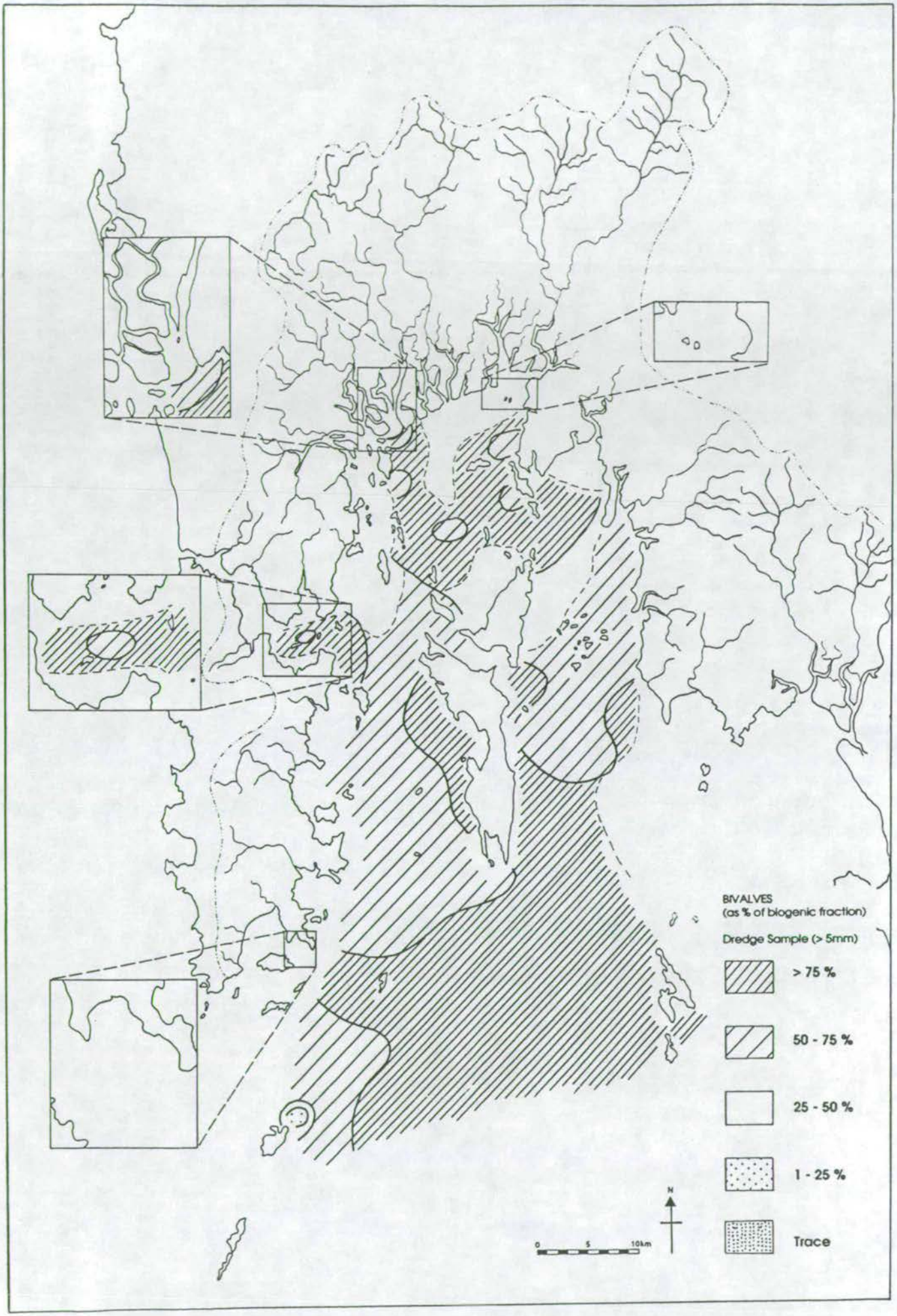

Figure 7.4 Distribution of bivalves in dredge samples (> 5mm) as a percent of the biogenic fraction.

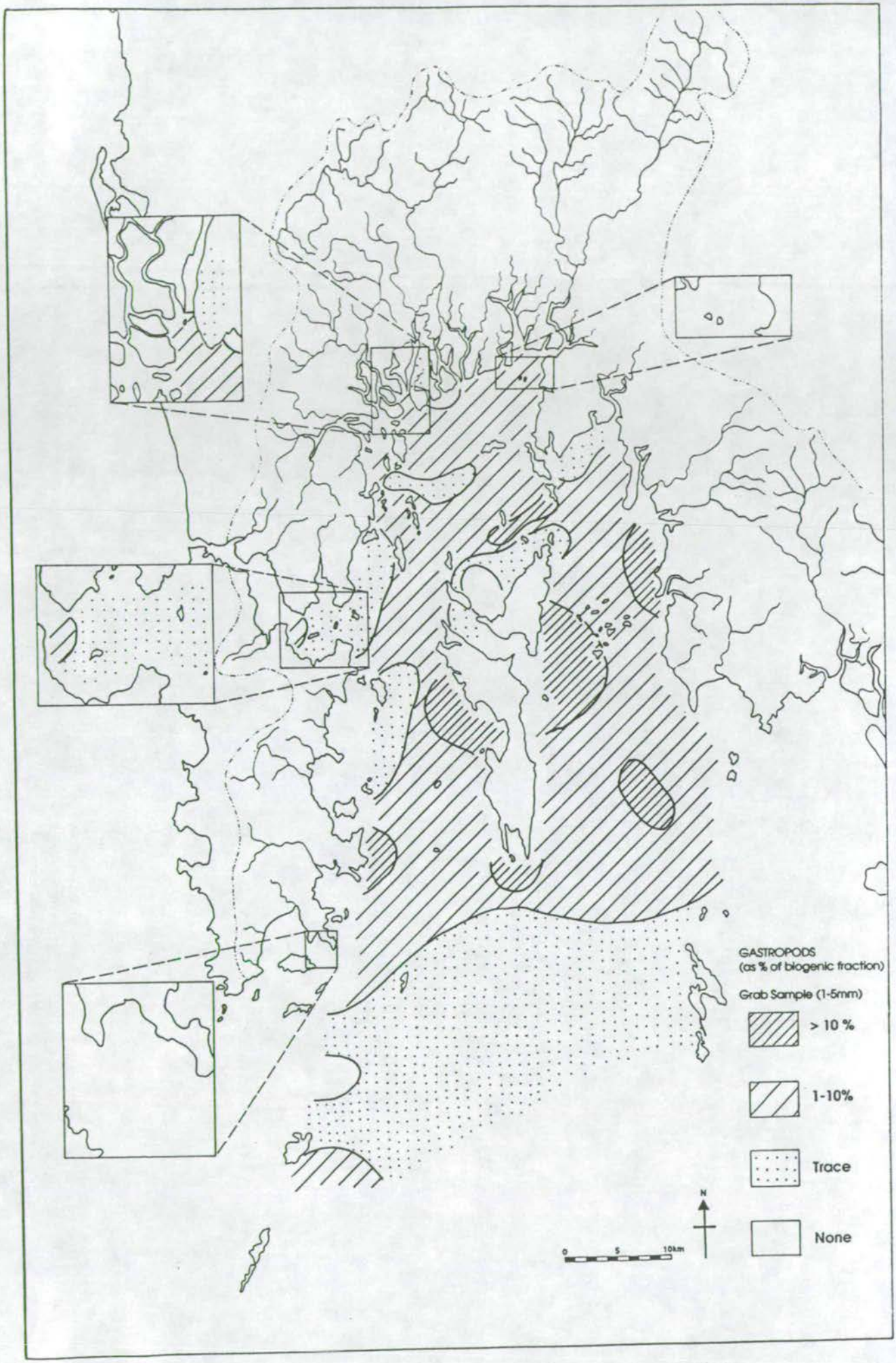

Figure 7.5 Distribution of gastropods in grab samples (1-5mm) as a percent of the biogenic fraction.

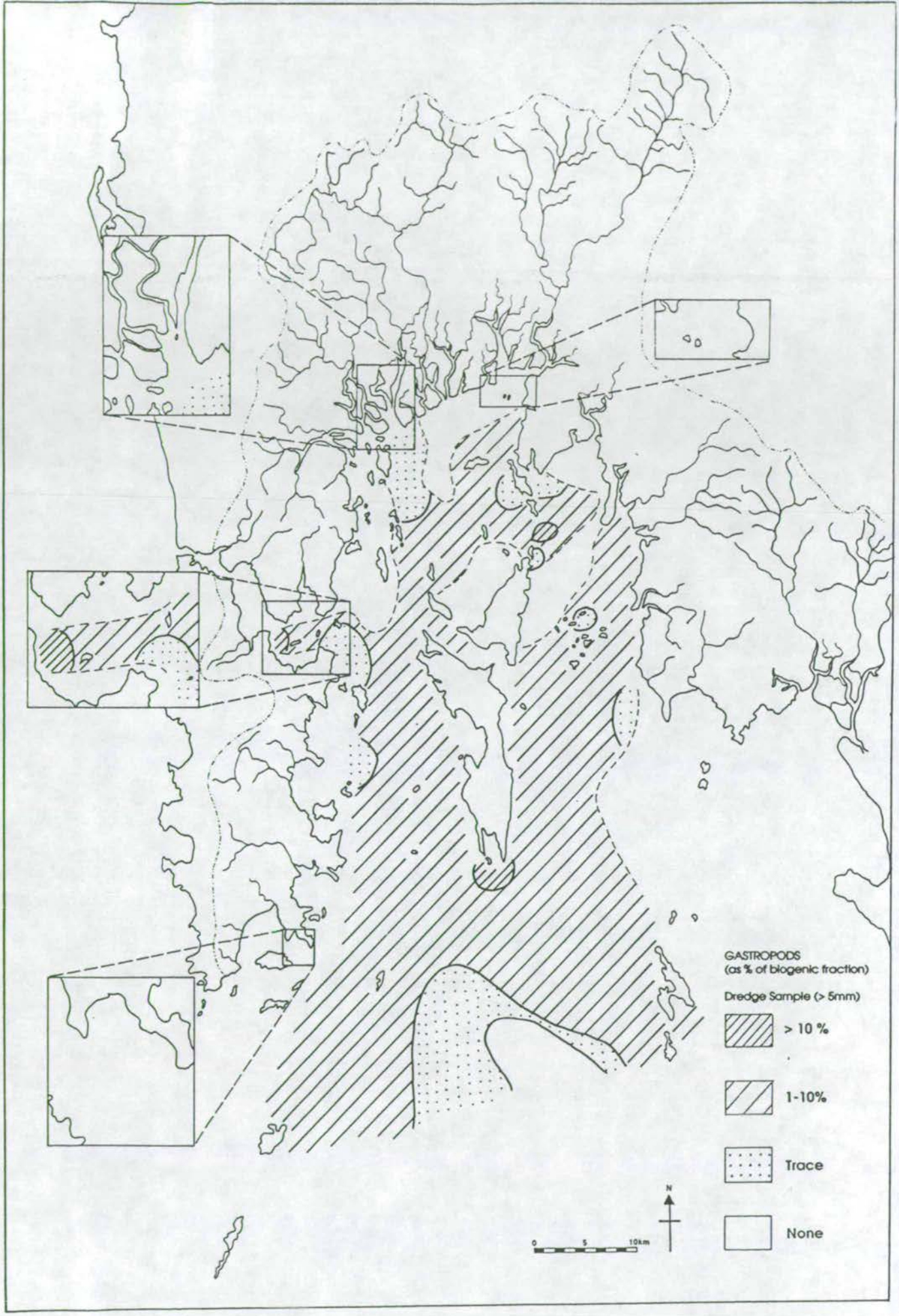

Figure 7.6 Distribution of gastropods in dredge samples (> 5mm) as a percent of the biogenic fraction.

7.2.2.3 Scaphopods

This class of mollusc is represented by the genera *Dentalium sp.* (see Plate 15A), and because of their distinctive "tusk" shape, they are easily identifiable in the biogenic fraction either as whole specimens or as fragments. Like gastropods, their distribution in either the grab or the dredge samples (Figs 7.7 and 7.8) does not show any clear north-south trend although they are only present in trace amounts if at all in the south of the Bay compared to patchy areas of > 1% and > 10% in the north and centre of the Bay. In the mangrove and intertidal areas in the far north, there is no evidence of this mollusc.

7.2.2.4 Echinoids

Live specimens of burrowing echinoids collected in the dredge and grab samples have been identified as *Metalia sternalis* and it is possible that most of the plate fragments and spines are from this species. Proportions of echinoid fragments in the biogenic fraction of the grab sample (Fig 7.9) are highest in the south and east side of the Bay with highest proportions (> 10%) in the NE area. No fragments were found near the mangroves (in the mangrove swamp, channel or intertidal environments). The larger fragments from the dredge samples (Fig 7.10) show a wide distribution of sites where the fragments make up between 1 and 10% of the biogenic fraction. The generally larger proportion of echinoid fragments in the dredge samples reflects the large size of some of the fragments compared to most of the other components. Echinoids are purely marine organisms and this seems to be reflected in their absence from the mangrove/estuarine areas where salinities are periodically lowered.

7.2.2.5 Pteropods, ophiuroid plates, coral and bryozoan fragments

These 4 biogenic components have been plotted together because of their low individual relative abundances and because they are all known to be solely marine organisms. Their distribution in the grab and dredge fractions (Figs 7.11 and 7.12 respectively) reflects this marine association clearly as their proportion of the biogenic component above trace values is limited to the central and southern parts of the Bay. Their proportion is much lower in the dredge sediment as a result of the small size of both pteropods and plates. Much of the material of this group in the dredge fraction is coral fragments.

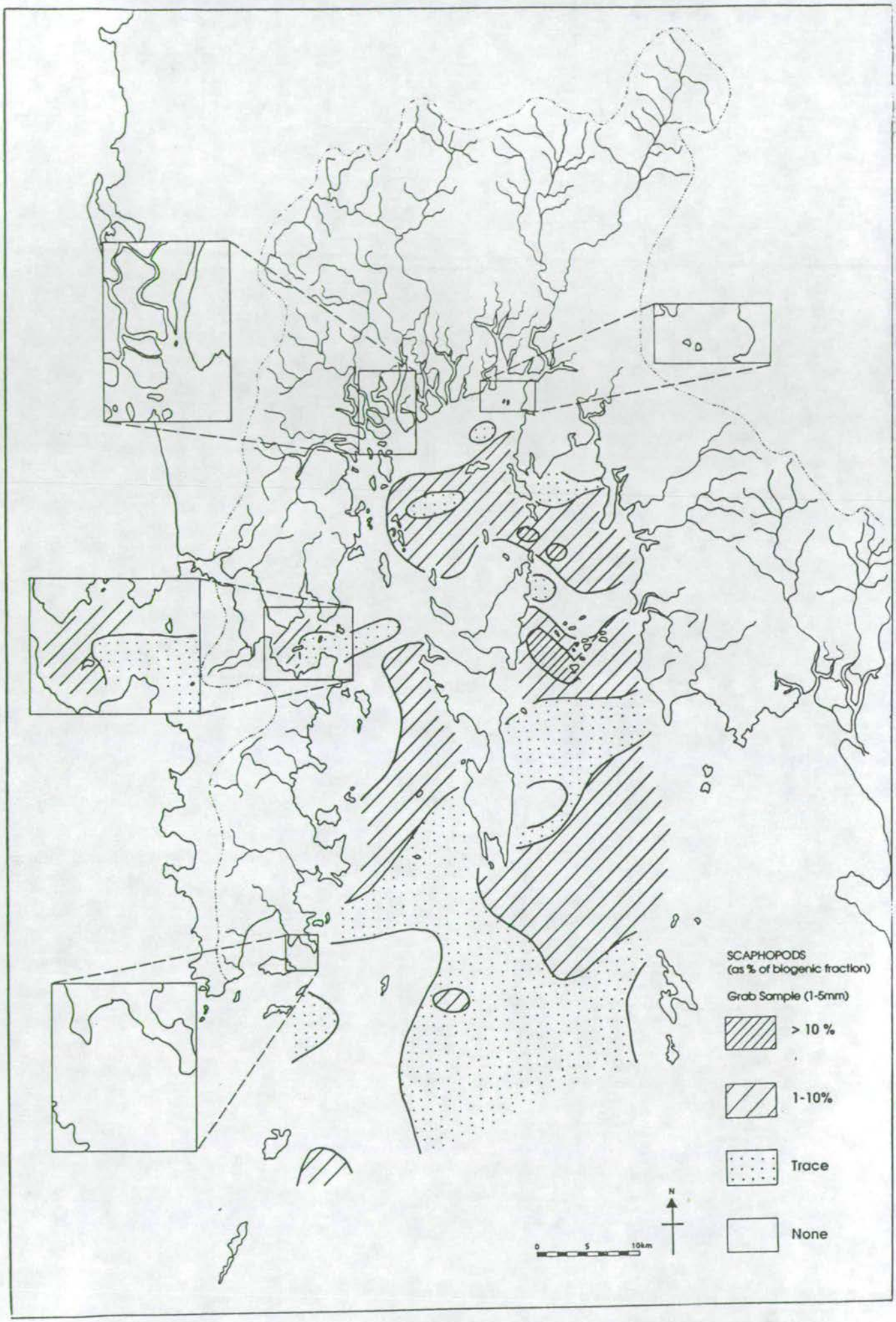

Figure 7.7 Distribution of scaphopods in grab samples (1-5mm) as a percent of the biogenic fraction.

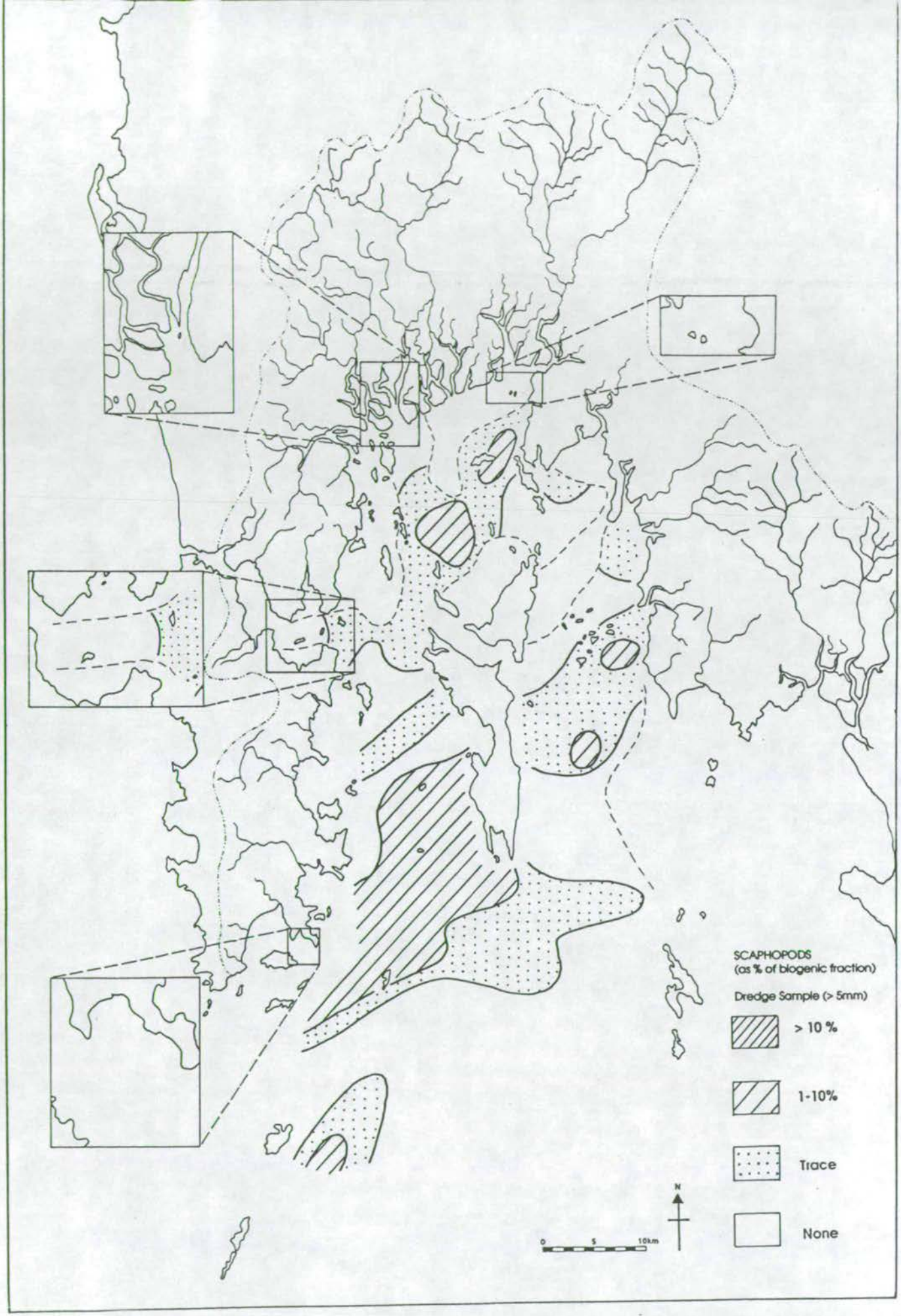

Figure 7.8 Distribution of scaphopods in dredge samples (> 5mm) as a percent of the biogenic fraction.

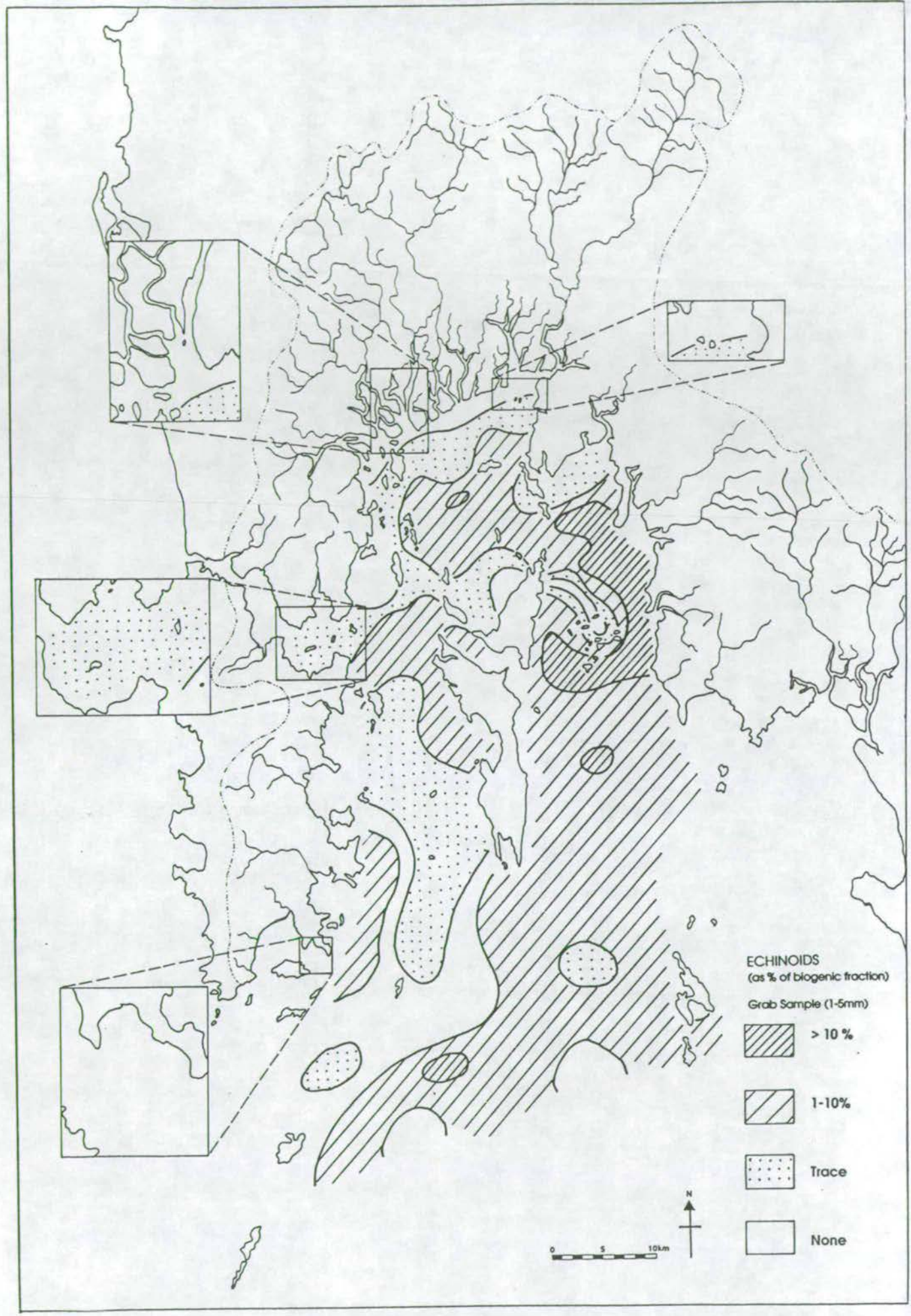

Figure 7.9 Distribution of echinoids in grab samples (1-5mm) as a percent of the biogenic fraction.

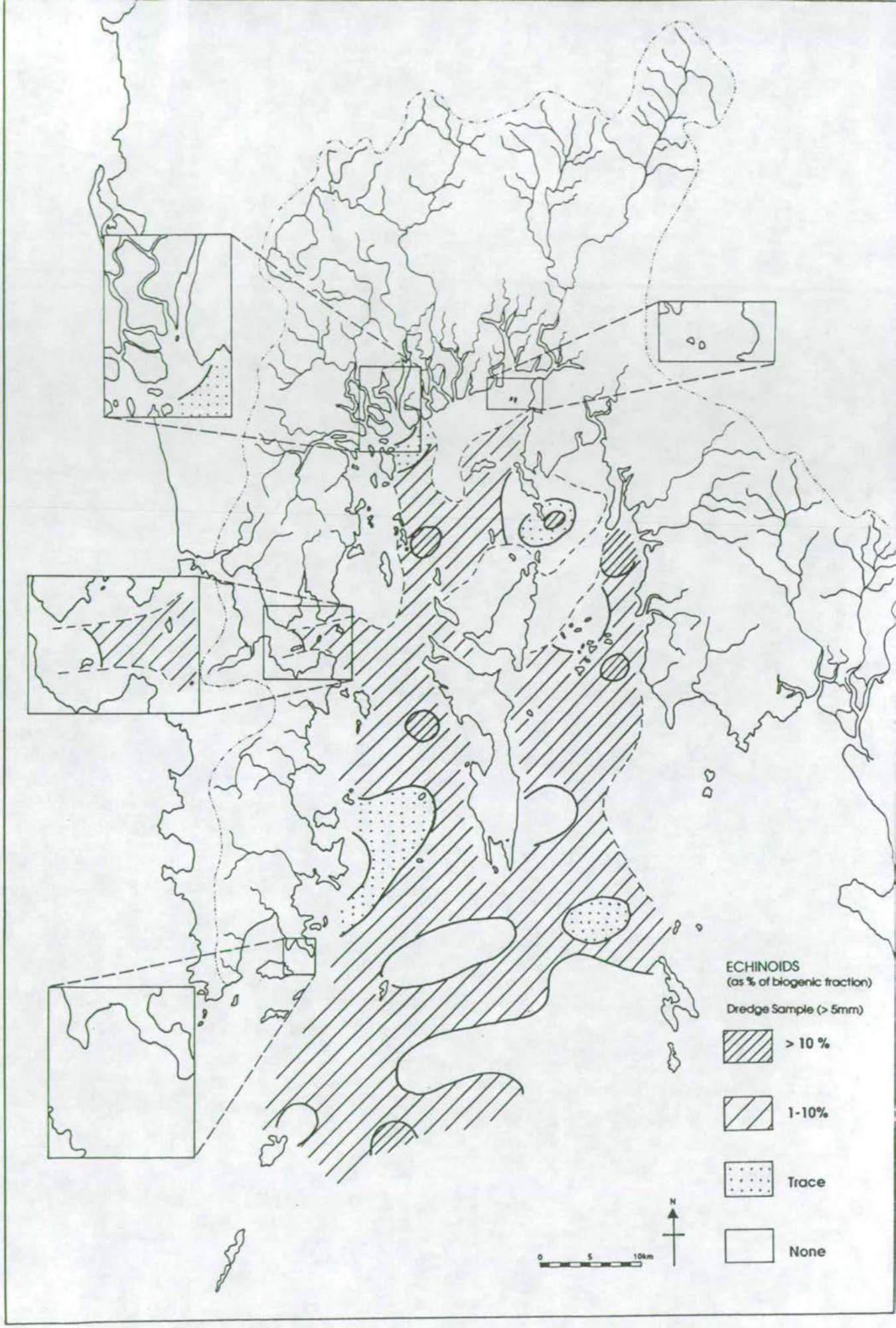

Figure 7.10 Distribution of echinoids in dredge samples (> 5mm) as a percent of the biogenic fraction.

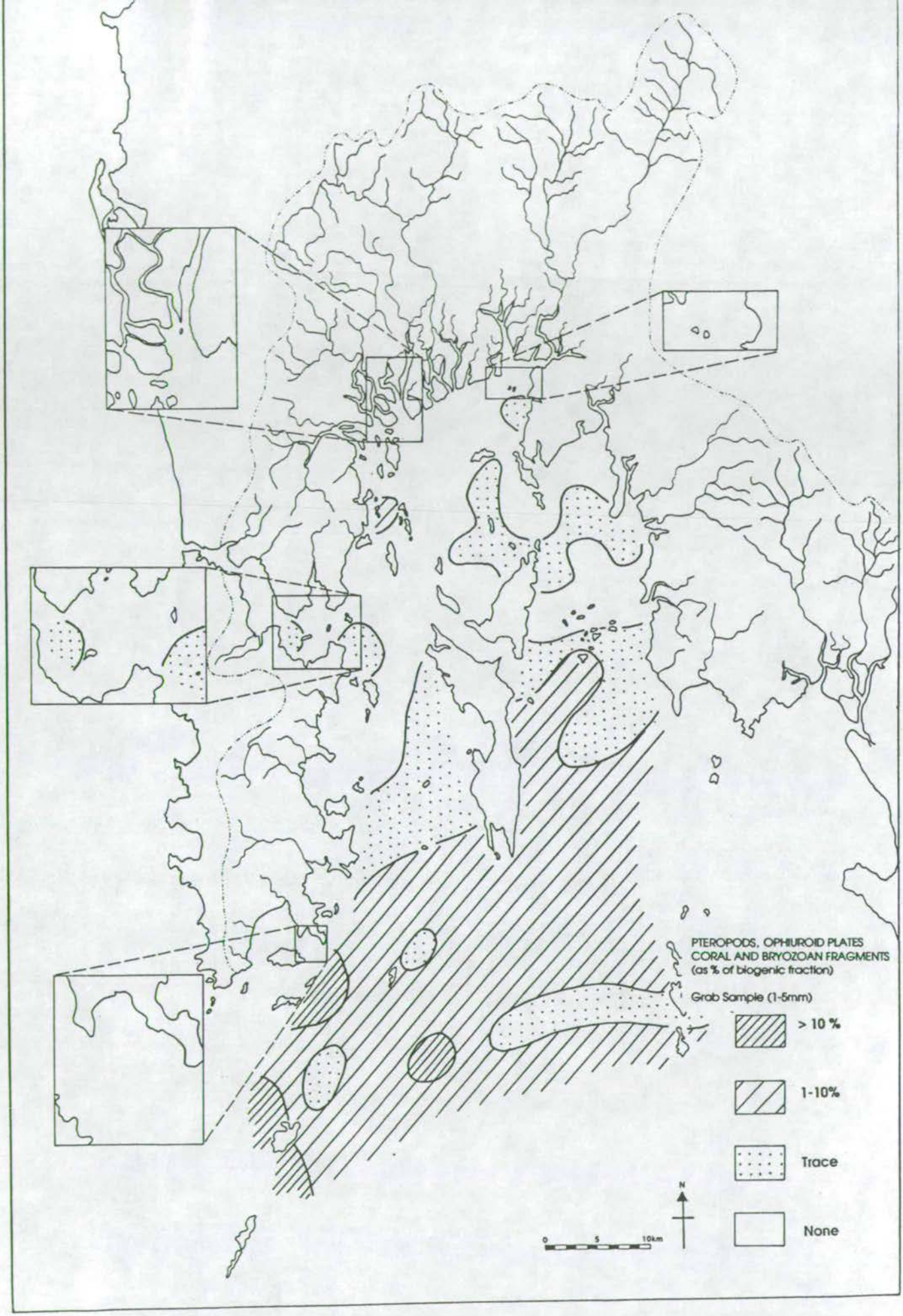

Figure 7.11 Distribution of pteropod, ophiurid plates, coral and bryozoan fragments in grab samples (1-5mm) as a percent of the biogenic fraction.

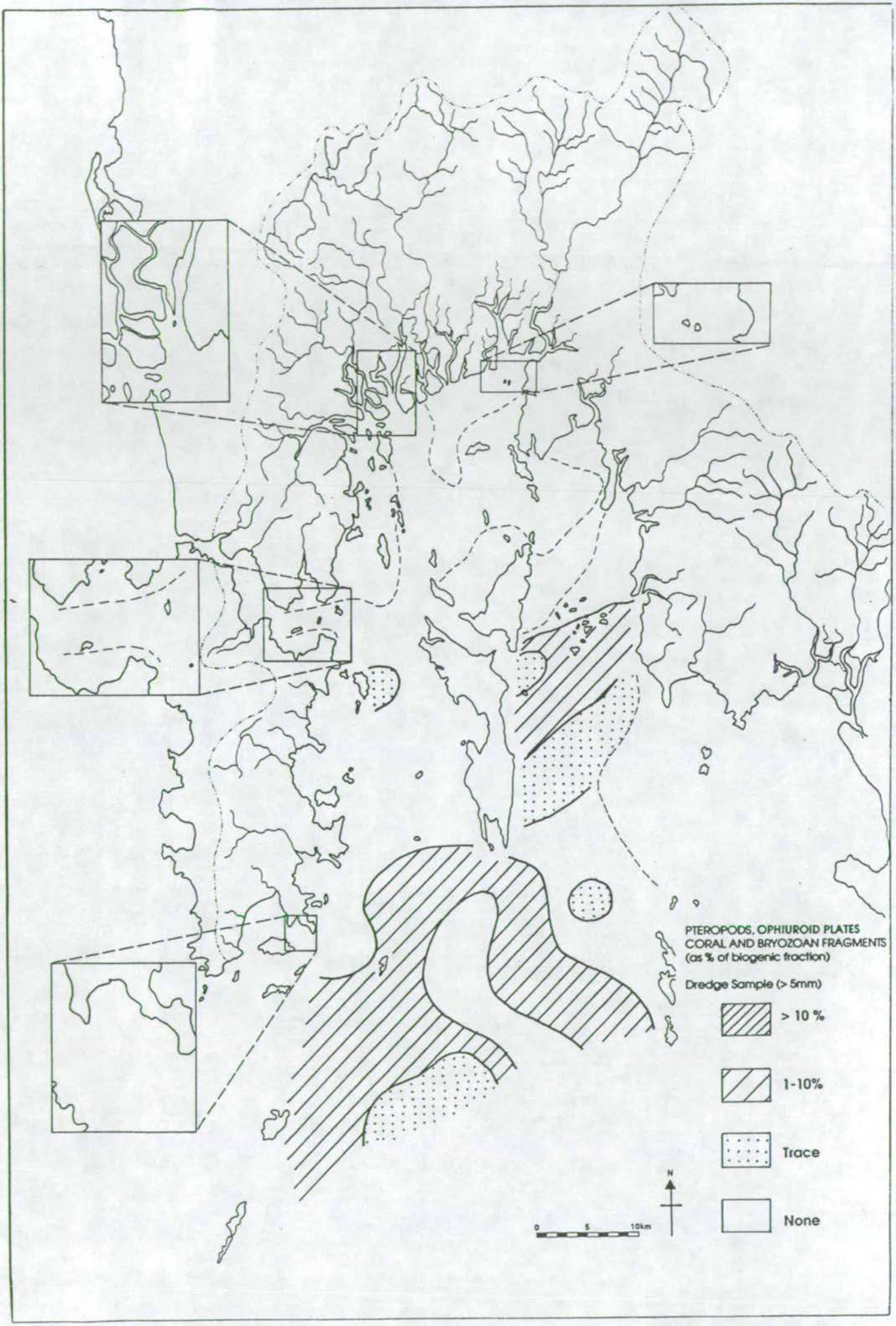

Figure 7.12 Distribution of pteropod, ophiurid plates, coral and bryozoan fragments in dredge samples (> 5mm) as a percent of the biogenic fraction.

7.2.2.6 Barnacles

The highest proportion of barnacles (fragments and whole) are found in the north and central parts of the Bay in both the grab and dredge samples (Figs 7.13 and 7.14 respectively). In most of the southern area, barnacles are absent. The distribution within the northern area is very patchy in both types of sample.

Whole barnacles collected in the sieves are 1 to 2cm in height and some were found attached to bivalves and gastropod shells. Since most barnacles attach to a solid substrate by a cement-like secretion (Scoffin, 1987), their patchy distribution in the Bay may be due to the lack of such substrates in some areas. Barnacles can produce significant quantities of carbonate as is evident in some areas in the north of Phangnga Bay where barnacle fragments make up to 80% of the biogenic fraction.

Although barnacles are solely marine organisms, their absence from the southern, deeper, more oceanward area of the Bay indicates their preference for sediment-laden water. Since barnacles are filter feeders, they obtain food from suspended material thus these more turbid waters in the north may be preferable to the clear southern waters. Although they are substrate dependant there is little evidence of them around the coastal rocks of Ko Racha Yai or Ko Phi Phi where the waters are clear and fine suspended sediment is absent.

7.2.2.7 Foraminifera

Because of their small size, no foraminifera were found in dredge samples and so only a grab sample map has been drawn (Fig 7.15). They are absent from the sediments of most of the north and central parts of the Bay but form a small proportion (< 10%) of the biogenic fraction in the southern part of the Bay. As illustrated in Plate 13 (Chapter 3), they form a major part of the biogenic fraction in the shallow marine sediments of the Aquarium-Ko Lon transect area but such quantities seem to be restricted to this area (biogenic percentages are omitted from this area on the maps as the research vessel did not visit this area and so seived grab and dredge samples were not obtained).

7.2.2.8 Plant material

Plant material is found in the sediments mainly in the form of fine, disseminated black fibrous material. However, a few twigs and recognisable leaf fragments were found in sites near mangroves. As can be seen from both the grab and dredge sample

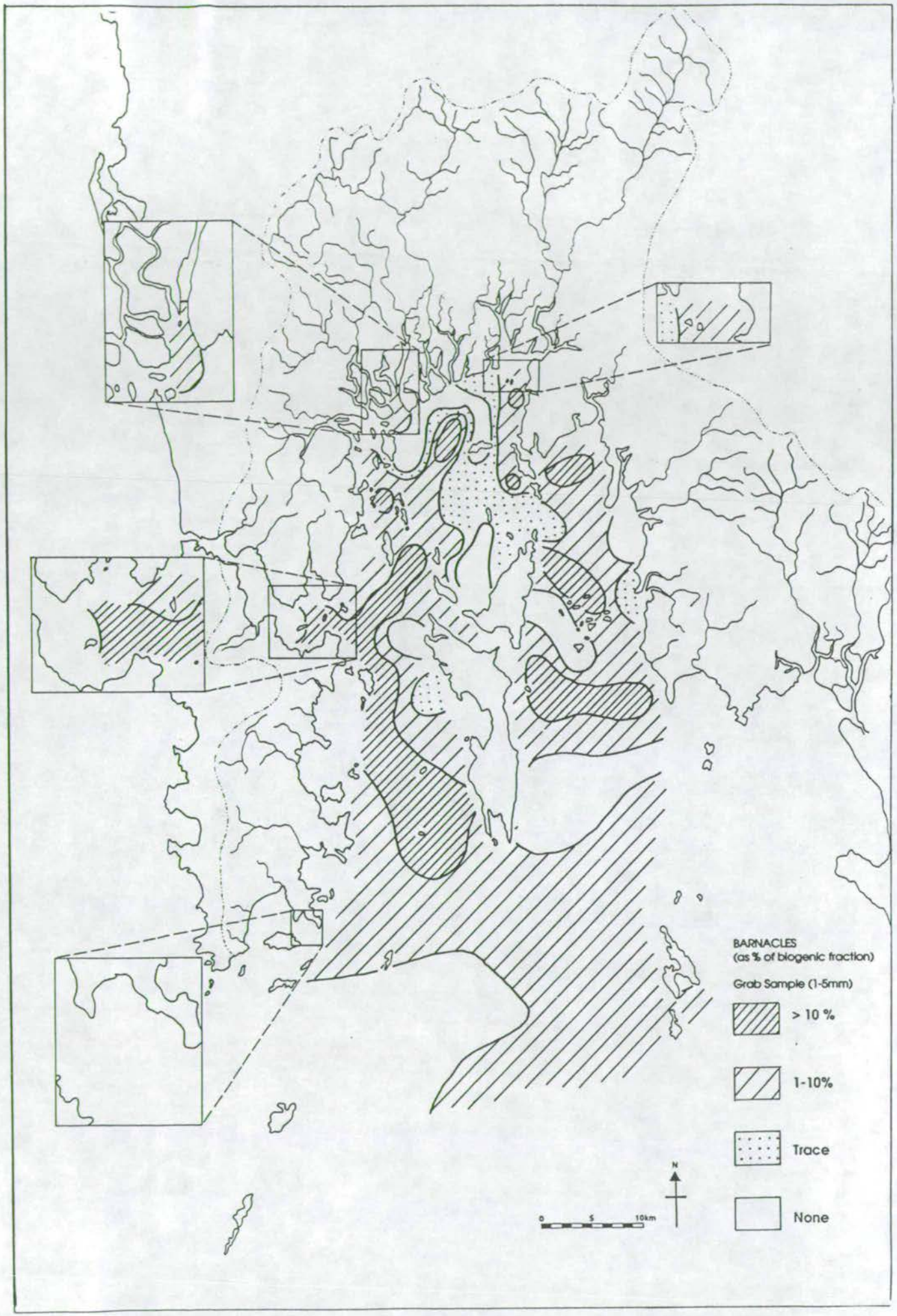

Figure 7.13 Distribution of barnacles in grab samples (1-5mm) as a percent of the biogenic fraction.

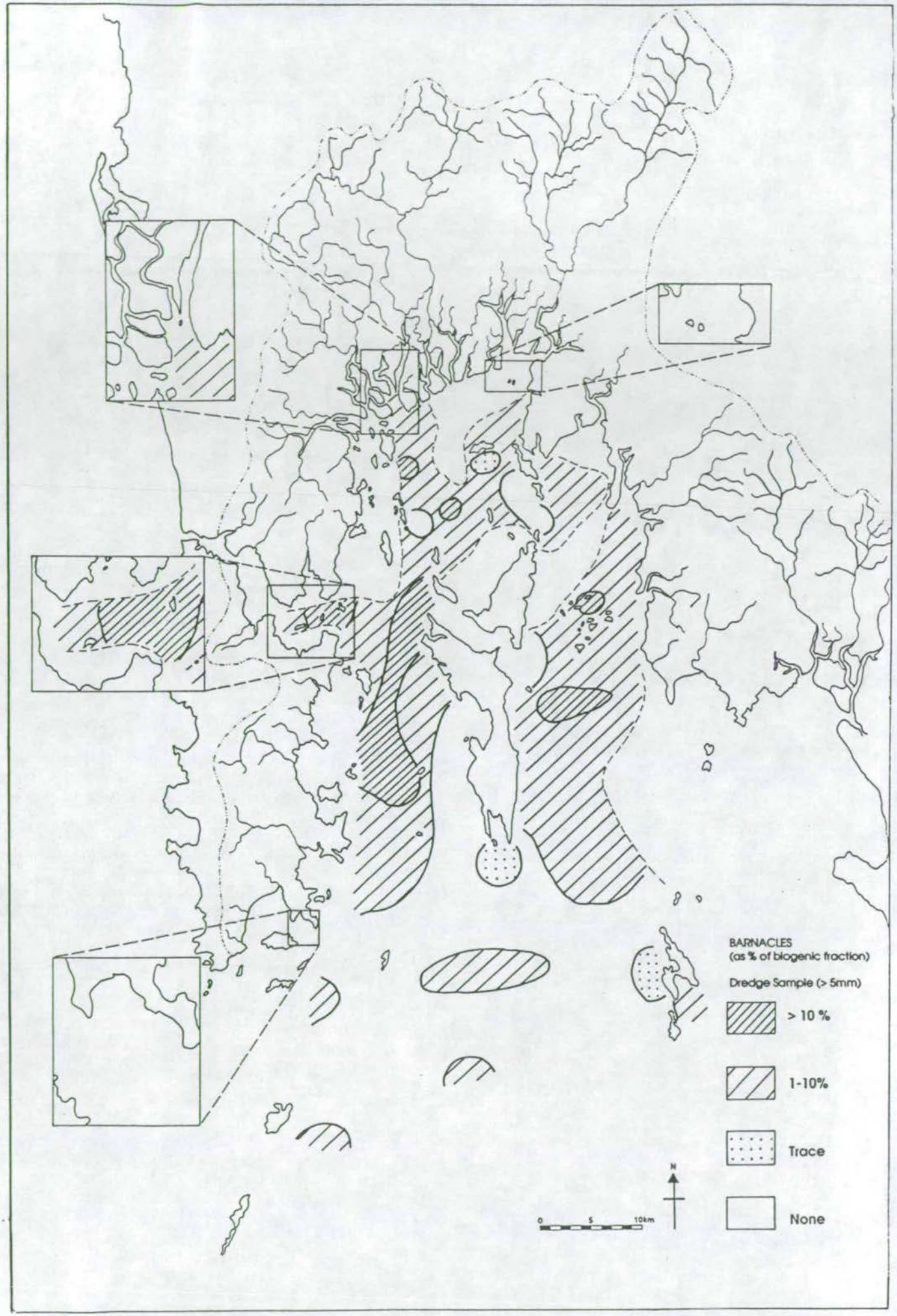

Figure 7.14 Distribution of barnacles in dredge samples (> 5mm) as a percent of the biogenic fraction.

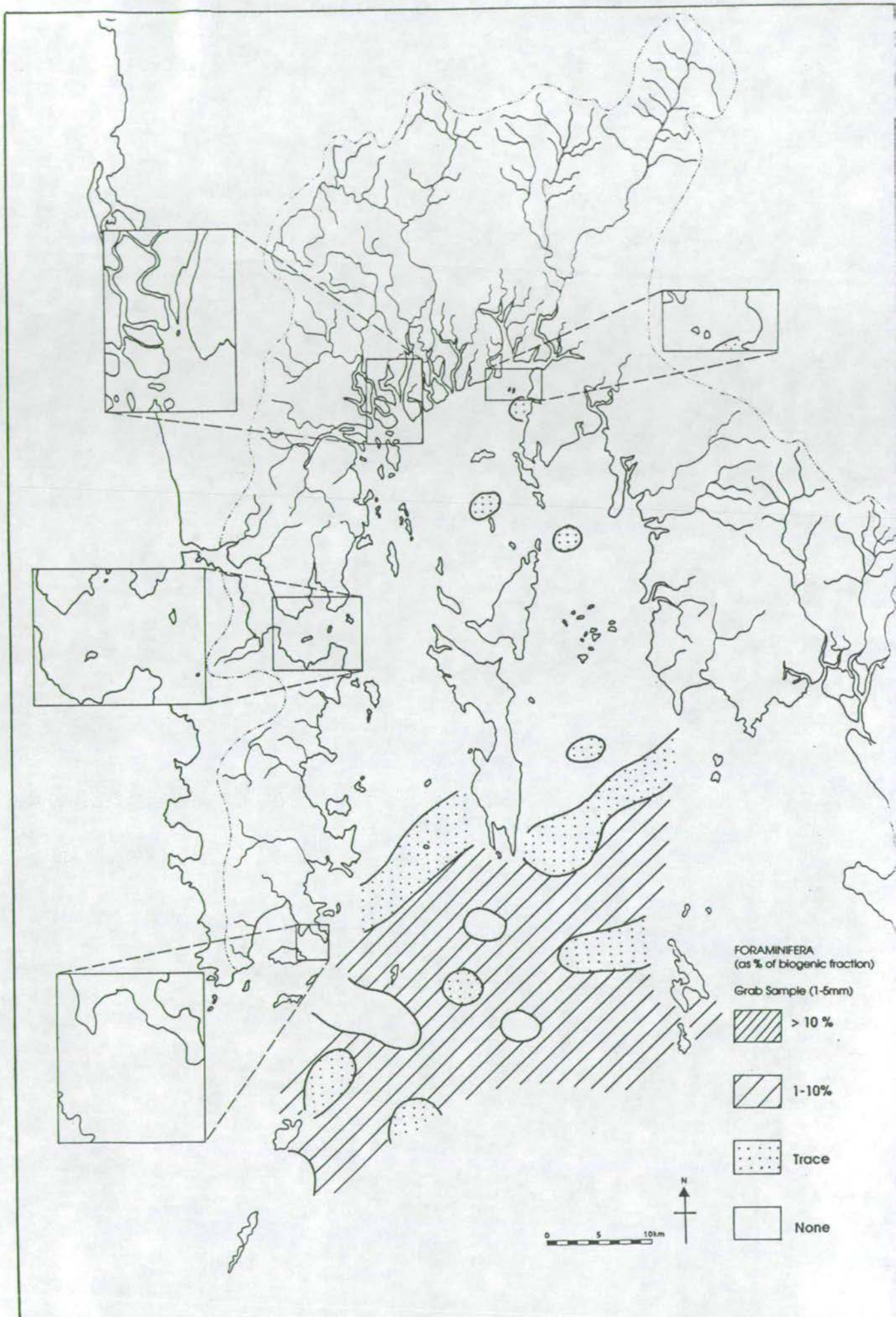

Figure 7.15 Distribution of foraminifera in grab samples (1-5mm) as a percent of the biogenic fraction.

maps (Figs 7.16 and 7.17 respectively), plant material is found in the highest proportions in the north of the Bay. The highest proportions are found in the grab fraction (up to 100% of the biogenic fraction in a mangrove channel sediment) in the far north of the Bay in the mangrove channel and swamp sediments and in the intertidal area. Since the source of this material is plants in the drainage basin, particularly the mangrove swamps, it is not surprising that the highest proportions are found in the north of the Bay where streams from the largest part of the drainage basin drain into the Bay through the large mangrove swamp development. Although plant material may be transported into the southern area, it is unlikely to be deposited due to the higher energy conditions in the south preventing the settling of this low density material.

7.2.3 **Discussion**

The distribution of any type of organism in nature is the result of a complex of environmental factors. In the case of shallow marine, bottom dwelling macrofauna, factors which have been found to be significant in various studies include water and sediment salinity (Sanders et al, 1965), sediment grain size characteristics (Sanders, 1958), which affect sediment penetrability and water content and the amount of algae and sea grass cover (Kalejta and Hockey, 1991) and oxygen levels (Wade, 1972).

Sanders et al (1965) found that infauna in the Pocasset estuary in Massachusetts experienced less physiological stress from salinity fluctuations due to the comparatively constant salinities within the sediments. Epifauna however, were subject to extreme stress due to the rapid salinity fluctuations of the overlying water. He suggested that the rate of change of salinity was of greater importance in affecting the ability of species to cope with salinity changes rather than the actual amount of salinity change. Sanders (1958) found that the sediment grain size affected the distributions of filter-feeders and deposit-feeders. Filter-feeders dominated in the sandy sediments where they obtained food from suspended material whilst deposit-feeders which live on organic matter on or in the sediment, dominated in muddy sediments. Kalejta and Hockey (1991) found that vegetation cover in the form of algal mats or sea grass affected the ability of some organisms to burrow into the sediment although the vegetation provided a food source for other organisms. Sanders (1968) suggested that the most diverse communities are found in shallow tropical marine sediments and deep sea sediments due to the relative

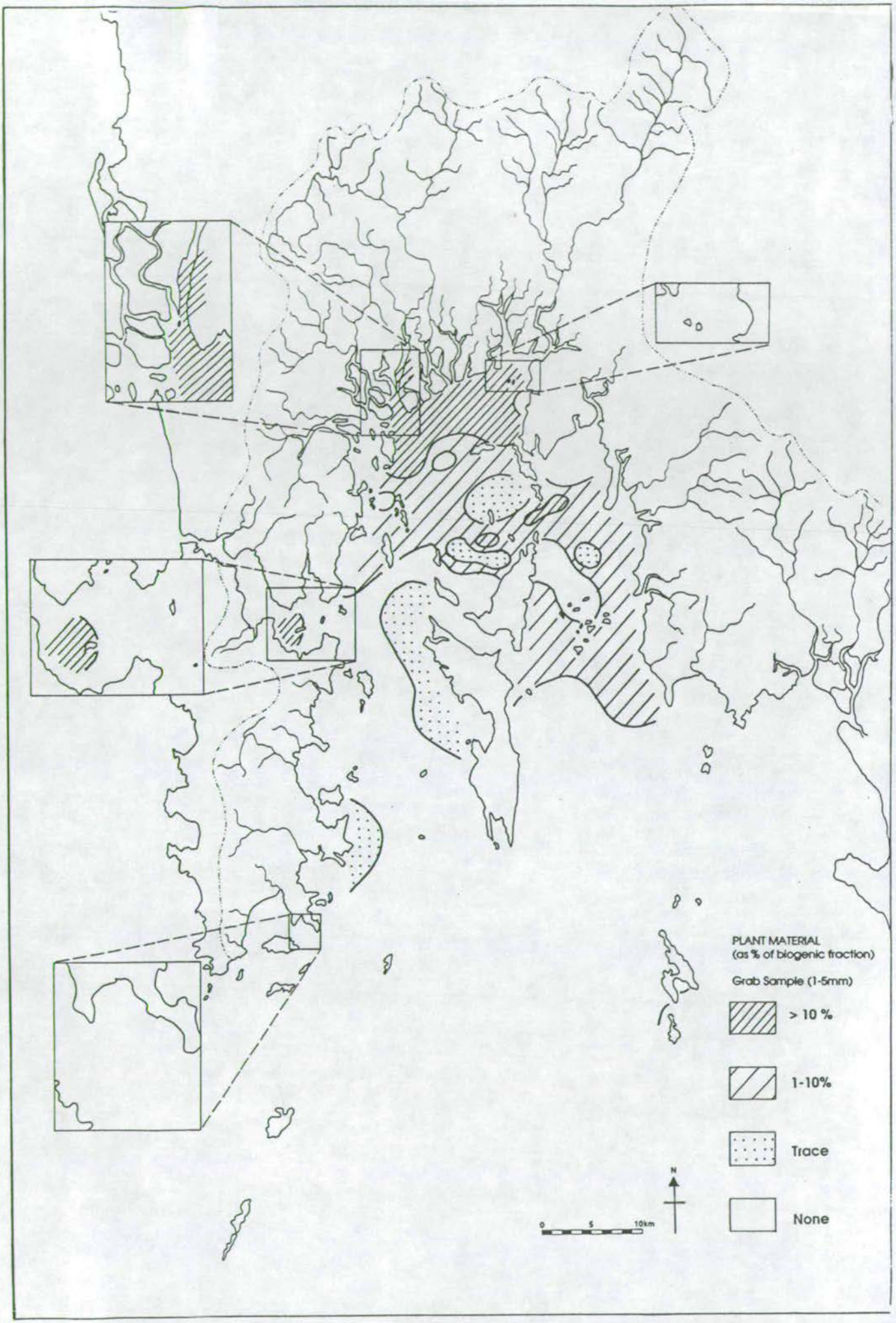

Figure 7.16 Distribution of plant material in grab samples (1-5mm) as a percent of the biogenic fraction.

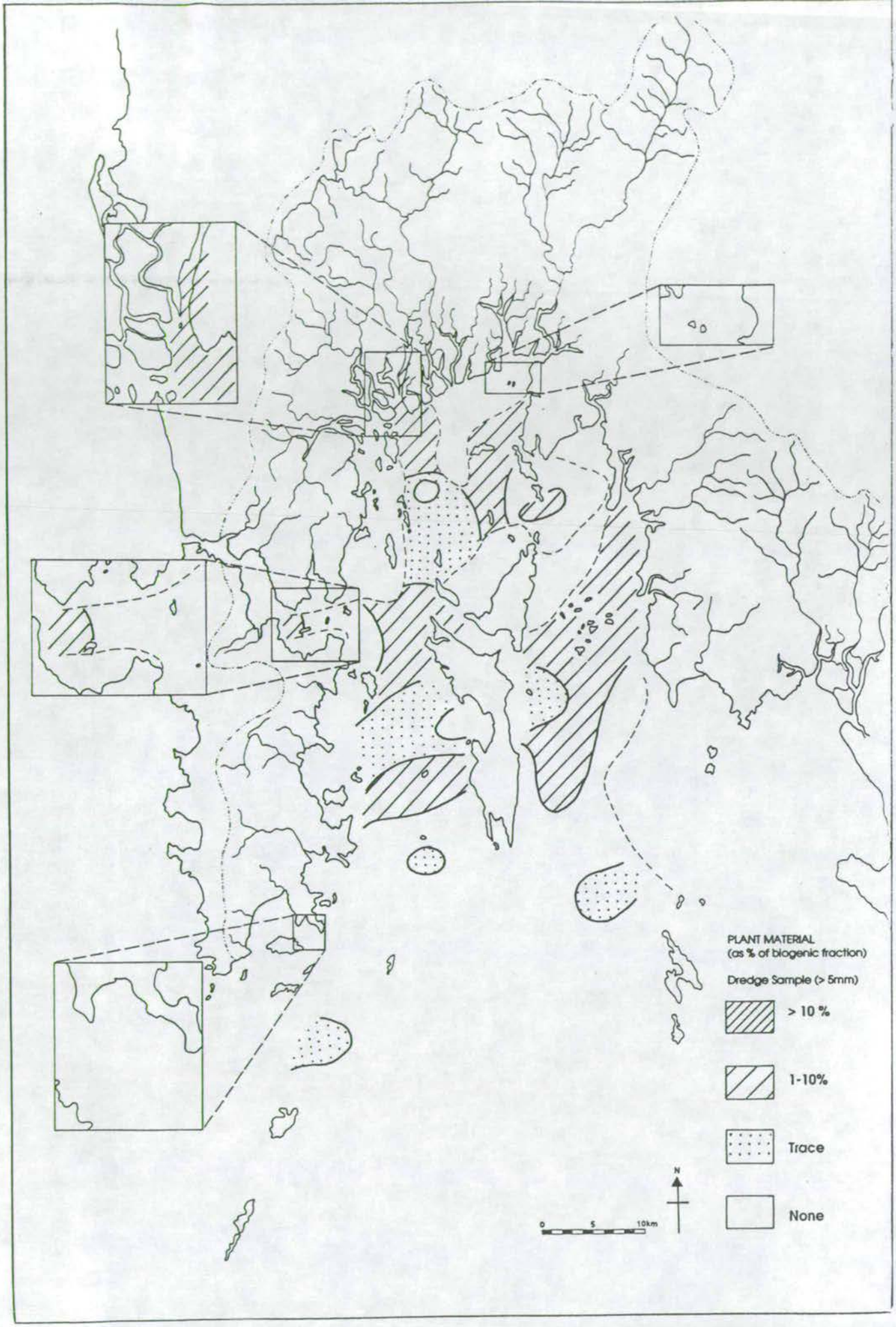

Figure 7.17 Distribution of plant material in dredge samples (> 5mm) as a percent of the biogenic fraction.

constancy of environmental conditions. Wade (1972) found this to be the case in Kingston Harbour in Jamaica where he suggested that the high benthic diversity is a result of an environment which is stable and undisturbed. However, he noted that not all tropical soft-bottomed communities are of high diversity due to local fluctuations in salinity and oxygen levels.

Cook and Mayo (1978) found that most groups (coral, coralline algae, gastropods and bryozoans) show logical trends of increasing relative abundance towards more congenial marine conditions. Some of the biogenic components of Phangnga Bay also show this increase in abundance towards the more open marine environment - these components include bivalves, pteropods, ophiuroids, corals and foraminifera. These "congenial" conditions include, constant salinity and temperature and comparatively clear, sediment-free waters. However, gastropods (particularly small < 5mm species), scaphopods and barnacles show higher relative proportions in the north of the Bay which may reflect their preference for calmer waters and/or finer-grained sediments. The greater turbidity of the waters in the north and central parts of the Bay (illustrated in a satellite image - Plate 18, Chapter 9) means that there is an increased food supply for these organisms most of which are filter-feeders. Echinoid fragments tend to show a more widespread distribution throughout the Bay (although they are not present in the mangrove swamp, mangrove channel or open intertidal areas) from the coarse sediments in the south to the fine sediments in the north. The restriction of plant material to the sediments in the north of the Bay reflects proximity to source although this distribution may also be exaggerated by the higher energy conditions in the south preventing settling of this low density material.

Parker (1956) applied several features of the distribution of macro-organisms found in the Mississippi delta area to ancient environments and assemblages preserved in nearby Miocene and younger sediments around the Gulf of Mexico. He found that river deltas and salt marshes could be detected by the presence of numerous wood and plant fibres. This is also the case for equivalent environments (ie mangrove swamps) in Phangnga Bay. Near-shore areas in the vicinity of large rivers where salinities are reduced and sedimentation rates are rapid could be detected by the presence of comparatively few molluscan remains. A similar feature is present in Phangnga Bay in the intertidal areas where there are no or low amounts of molluscs or echinoids. Parker (1956) also found that shallow continental shelf areas could be characterised by large numbers of molluscs and echinoids which are seldom found

in waters where chlorinity falls below 17 ppt - large numbers of molluscs and echinoids are also evident in the shallow and open marine environments of Phangnga Bay.

Alongi (1989) noted that despite the lack of data on benthic communities inhabiting tropical continental shelves compared to temperate regions, there do appear to be a few common characteristics that distinguish these communities from the continental shelves of temperate latitudes. These are:

a. faunal composition is dominated by large epibenthos eg, echinoids.
b. infaunal assemblages are composed mainly of pioneering, small surface deposit and/or suspension feeders, reflecting benthic adaptation to respond quickly to erratic, low nutrient inputs and physical disturbances (eg, tropical storms).
c. abundant crustaceans due to abundant epibenthos and surface fauna.

Alongi (1989) found it apparent that infaunal regimes on the Great Barrier Reef shelf are influenced or regulated by several conditions which include low or patchy inputs of detritus, continual warm temperatures and disturbances by trawling and climatic events.

In Phangnga Bay there is a similar benthic community as that described above (32% crustaceans and 27% echinoids seems to confirm points a and c above). Although land-derived detritus inputs are thought to be high, considering the whole of the study area, the inputs are patchy as Alongi (1989) described for the Great Barrier Reef shelf. Also, temperatures are continually warm in this region. Although it is not known whether prawn trawling is a major activity in the Bay, tropical storms and tin-dredging activities are known disturbance mechanisms which affect the sediment and thus the associated fauna. As discussed later, it is thought that storm disturbance will be greatest in the shallow areas in the north of the Bay thus affecting macrofaunal distributions in these areas. Although tin-dredging of the bottom sediment within Phangnga Bay itself is not areally extensive (restricted to an area south east of Ko Phuket and within the northern mangroves) the effect on the sediment fauna is devastating and as is recorded in work by Prasertwong (1983), the benthic community can take up to 15 years to recover. He studied the faunal assemblages of 6 dredging plots in Phuket Bay (see Fig 3.4) which has been operated on in different years from 1965 to 1982. In the most recently disturbed

plots, opportunist groups such as amphipods and polychaetes were abundant - these groups tend to reproduce rapidly and are relatively tolerant of sediment changes. Seven years after dredging the biomass of the community increased although the impact of dredging was still pronounced. The density, biomass and diversity in the benthic community from the oldest plot were similar to that of an undisturbed area.

The increase in $CaCO_3$ (and hence non-terrigenous, biogenic material) southwards may also be a consequence of decreasing rates of terrigenous sedimentation as well as increasing absolute amounts of biogenic carbonate secretion. Where sedimentation rates are low (eg, in the south, where it is thought that relict sediments have not been covered by Holocene deposits) carbonate content may be high due to the lack of dilution from terrigenous material. Conversely, where sedimentation rates are high (eg, in the north of the Bay) the carbonate content is low due to dilution from terrigenous material. This idea is discussed further in the next section.

7.3 BIVALVE AND GASTROPOD DISTRIBUTIONS

7.3.1 **Introduction**

A more detailed study of macrofauna distributions has been made by studying the species distribution of bivalves and gastropods in order to try and identify assemblages of species which may typify a particular area of the Bay. Bernasconi et al (1991) identified molluscan assemblages which indicate bathymetric regimes in the Nile delta. They used these to identify such regimes down cores from the same area during the last 7000 years.

7.3.2 **Method**

For each sieved grab (1-5mm) and dredge (> 5mm) sample individual valves of bivalves and whole gastropods were picked out. No attempt was made at a quantitative survey due to time restrictions, however, any obvious abundance of a particular species was noted. The specimens were then identified by comparison with specimens in collections at the British Museum (Natural History) and a check-list drawn up (see Appendix E). In all, 62 different bivalves and 67 gastropods were

picked out in the samples. Of these, 22 bivalves and 29 gastropods were identified down to genus level only and 40 bivalves and 38 gastropods were identified down to species level.

Tables 7.1 and 7.2 indicate the sites where each species was found (the information from grab and dredge samples has been combined in these tables). These sites are separated into 4 groups distinguished on the basis of water depth (exposed, 0-5m, 5-20m and >20m). From figure 1.4 (bathymetric map of the Bay) it can be seen that in general, water depth increases with distance from land and so the 4 groupings of sites also represent the relative distance of the sites from land with the "exposed" group closest to land and the "> 20m" group furthest away in the more open marine setting (an exception to this is site 34 which is sited in a mangrove channel which is therefore close to land but in relatively deeper water than surrounding sites). The depositional environment (as defined in Chapter 5) of each station is also indicated on the tables and it is clear that the "exposed" sites are mainly sediments of the open intertidal environment, the "0-5m" and "5-20m" sites are in the shallow marine environments and the "> 20m" sites are mainly open marine sediments. Within each group the sites are ordered according to the mud content (< 63μm fraction) of the sediment.

It has to be noted that species listed were collected as dead specimens whose distribution is influenced both by the distribution of the living forms and the prevailing processes of erosion, transport and deposition. Since an aim of the overall project is to examine sedimentation in the Bay and to relate this information to past geological environments, it is the geological aspects of the faunal occurrences which are of greatest significance ie, what is actually left to be preserved in the sediment. The listed sample sites where each species were found do not necessarily indicate that these species lived in these areas. Current transport processes may redistribute dead and disarticulated shells producing accumulations where perhaps no living species occur. The only place where this was obviously the case is the shelly beach gravel at site 44a. The shell material here is rounded, pitted and abraded suggesting reworking through transportation (as there are no live *in situ* specimens) and beach reworking. The mollusc shell material in all areas of the Bay is composed of a mix of broken shell fragments, whole valves and articulated valves. The presence of shell fragments does not necessarily indicate disintegration through transport as attack by scavengers or reworking by burrowing organisms may damage the shells but not transport them far from life position. Although relatively

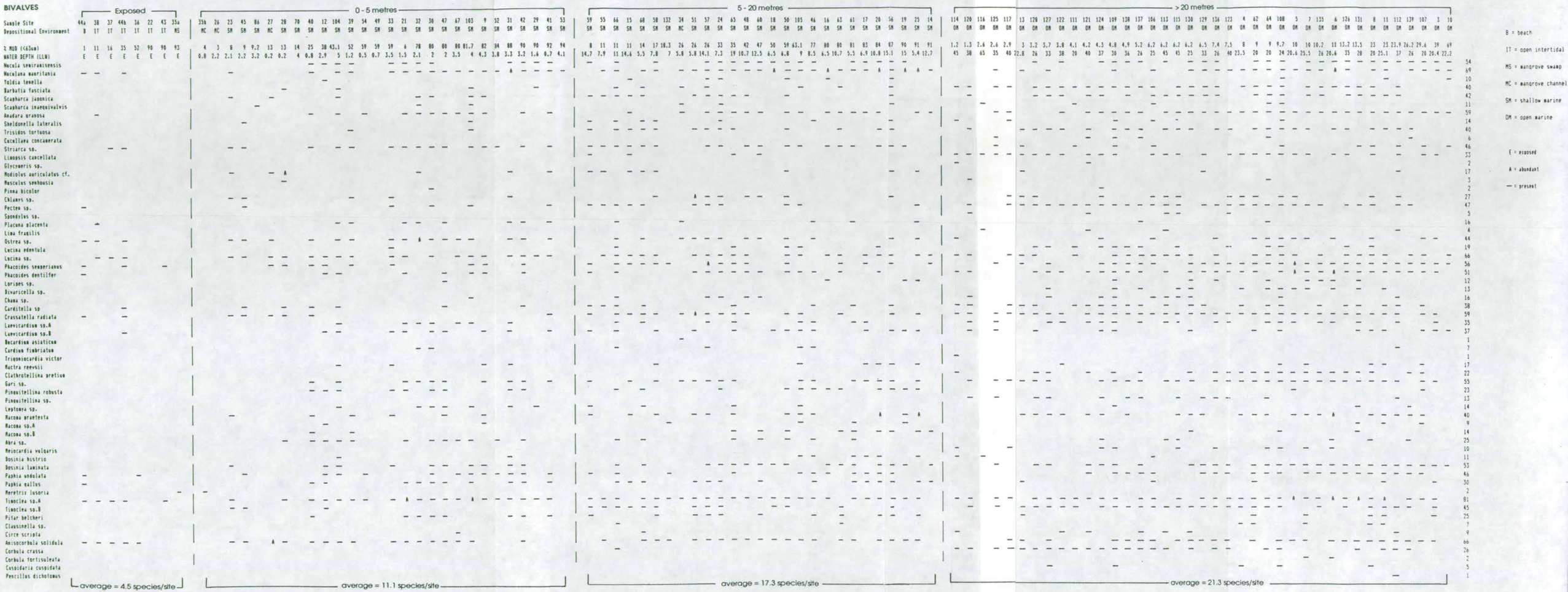

Table 7.1 Distribution of bivalve species in the Bay. Sample sites are grouped according to water depth and then arranged within each group according to mud content of the sediments. Average numbers of species/site are given at the bottom of the table and the number of sites in which a species occur are listed in a column on the right of the table.

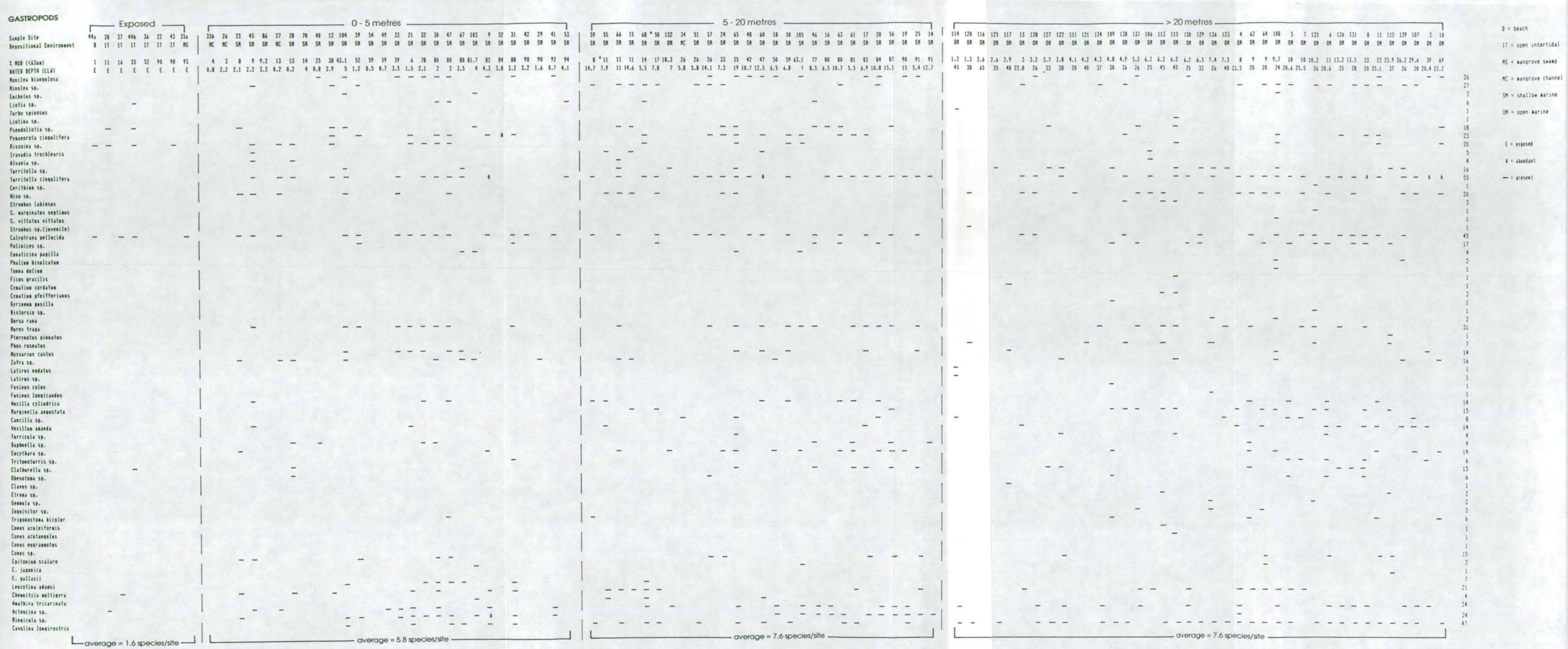

Table 7.2 Distribution of gastropod species in the Bay. Sample sites are grouped according to water depth and then arranged within each group according to mud content of the sediments. Average numbers of species/site are given at the bottom of the table and the number of sites in which a species occur are listed in a column on the right of the table.

large pieces of shell material can be moved in weaker currents than would move terrigenous sand material of the same size due to the low density and platey form of the carbonate, it is not thought that current transport processes have played a large part in redistributing shelly material in the Bay. In areas where currents are strong (eg, Ko Racha Yai and the northern tip of Ko Yao Noi) there is no suitable substrate for the benthic fauna as all mud and sand material has been removed.

Infaunal species have a higher preservation potential than epifaunal species as they are, in effect, buried on death and are not subject to the dispersal processes of a surface-living species. Unfortunately there is little information on the distribution of infaunal species relative to epifaunal species of the organisms identified here as the sieved material was collected from a 10-15cm depth of sediment which was sieved as a whole. Also on identification there was little information available on the particular habit of that species (particularly whether infaunal of epifaunal) and as species of one genus vary in their habit (particulary in the molluscan phylum) generalisations on habitats of genera from textbooks cannot be inferred for different species of that genus.

7.3.3 **Mode of Preservation**

The majority of bivalve shells in the samples are disarticulated. However, some specimens of *Modiolus auriculatus cf.* (pl 16G), *Musculus senhousia*, *Timoclea sp.A* (pl 15J), *Nuculana mauritania* (15C) and *Anisocorbula solidula* (16A) are articulated and closed. *Timoclea sp.A* and *Nuculana mauritania* are the most commonly articulated bivalves. As mentioned above, very few of the shells in any of the samples show any sign of abrasion. Those that do are found in shelly gravel sediments (Stations 23, 28, 44a, 45, 106, 114 and 116) which are found either near shorelines or in areas of strong currents (the latter 3 stations) where shell material will be subjected to a high degree of reworking. Elsewhere in the Bay the dominant occurrence of fine grained sediments (muds, silt and sand muds) prevent abrasive forces from affecting the shells. Both bivalves and gastropods show some evidence of bioerosion in the form of borings through the shell (Plate 17B) and also encrustation by oysters, barnacles and serpulid worm tubes (Plate 10 - Chapter 3). However, the majority of the shell specimens appear mineralogically unaltered and unaffected by discolouration, encrustation and bioerosion.

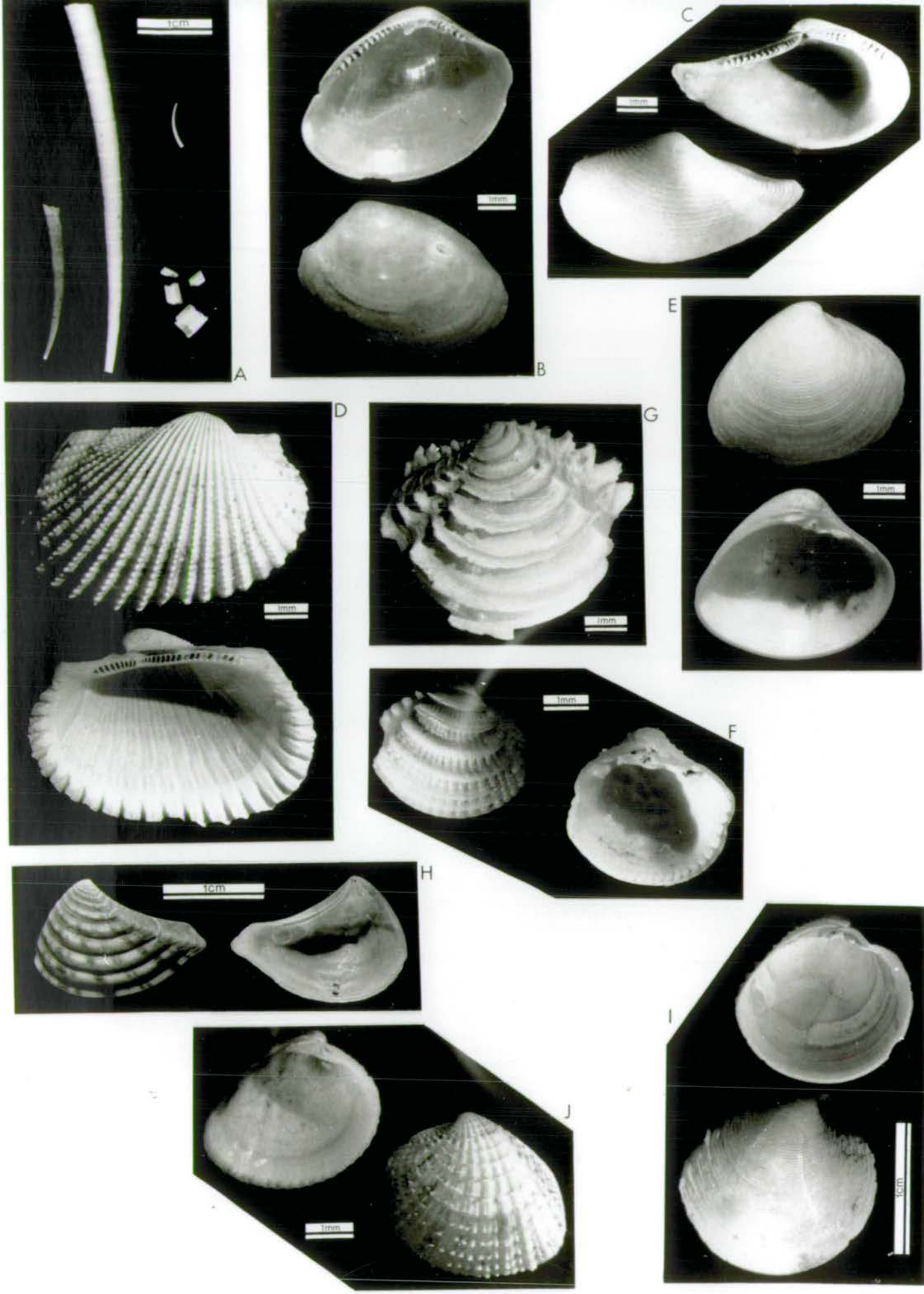

Plate 15 **A.** *Dentalium sp.* **B.** *Nucula semiramisensis* **C.** *Nuculana mauritania* **D.** *Anadara granosa* **E.** *Lucina sp.* **F.** *Phacoides semperianus* **G.** *Phacoides dentilfer* **H.** *Crassatella radiata* **I.** *Dosinia laminata* **J.** *Timoclea sp.A*

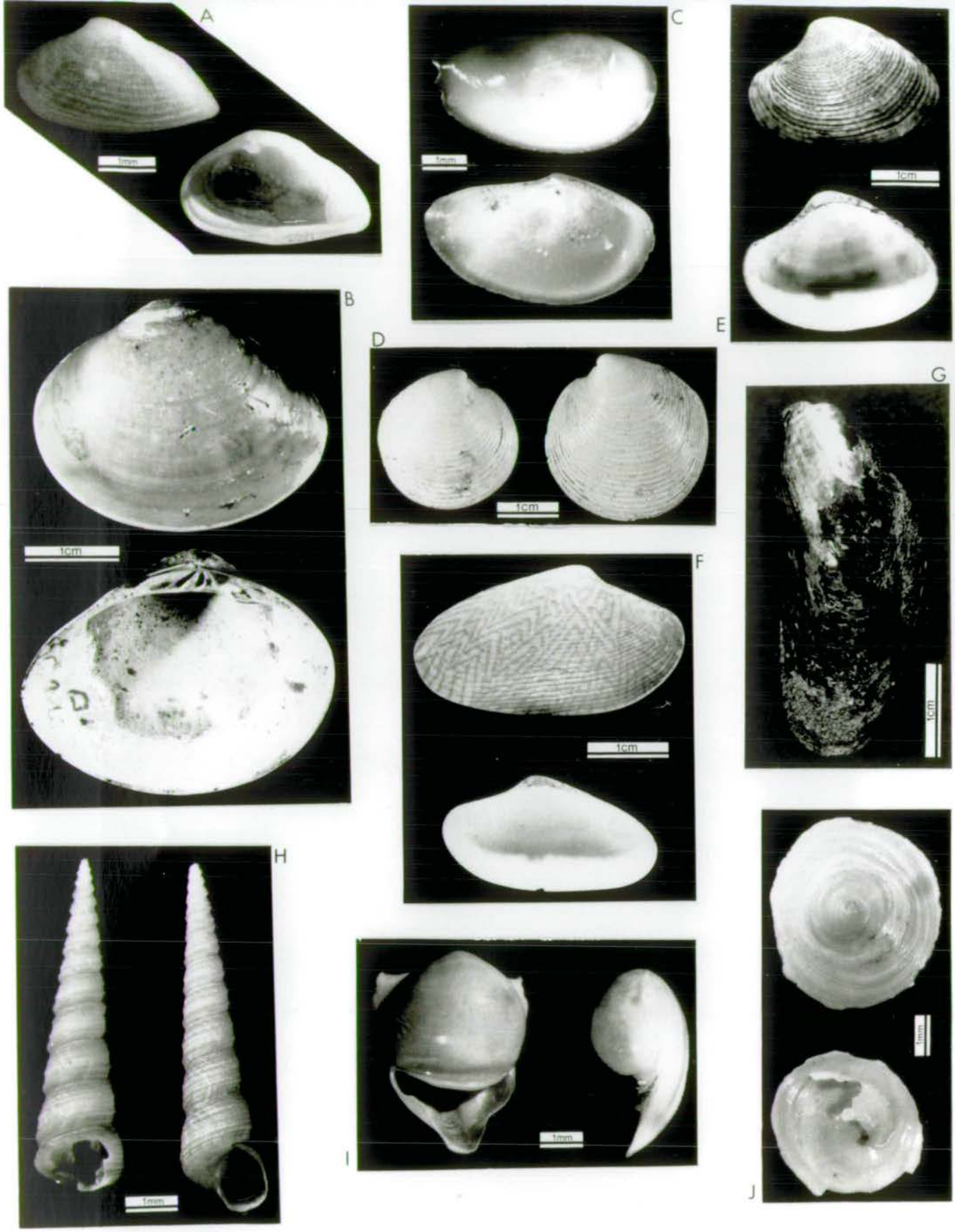

Plate 16

A. *Anisocorbula solidula* **B.** *Meretrix lusoria* **C.** *Yoldia tenella*
D. *Dosinia histrio* **E.** *Paphia gailus* **F.** *Paphia undulata*
G. *Modiolus auriculatus* **H.** *Turritella cingulifera* **I.** *Cavolina longirostris*
J. *Calyptraea pellucida*

7.3.4 Bivalve distributions

7.3.4.1 Comparisons between the 4 site groups

To summarise the variation in the number of bivalve species found in each of the 4 depth groups, the average number of species found at each site in a group is given at the bottom of Table 7.1. This clearly illustrates an increase in the number of bivalve species with increasing water depth from 4.5 species/site in the "exposed" group to 11.1 in the "0-5m" group to 17.3 in the "5-20m" group to 21.3 in the "> 20m". Considering the ordering of sites according to mud content within each group, only the "0-5m" group shows any variation with fewer species in the low mud sites. This is again summarised using species/site averages with 5.3 species/site in < 25% mud sites and 13.3 species/site for > 25% mud sites.

Therefore bivalve species distributions appear to be more strongly controlled by water depth (which is also indicative of distance from land) rather than by sediment characteristics. However, there does seem to be some sediment-type control in the shallow water areas.

7.3.4.2 Individual species variations

The number of sites in which individual bivalve species are found is listed on the right-hand side of Table 7.1. The most common species (present in > 50 sites) are: *Nucula semiramisensis* (pl 15B), *Nuculana mauritania* (pl 15C), *Anadara granosa* (pl 15D), *Lucina sp.* (pl 15E), *Phacoides semperianus* (pl 15F), *Phacoides dentilfer* (pl 15G), *Crassatella radiata* (pl 15H), *Gari sp.*, *Dosinia laminata* (pl 15I), *Timoclea sp. A* (pl 15J) and *Anisocorbula solidula* (pl 16A). These species are included on Table 7.3 which includes other relatively common bivalves found in the Bay and the water depth groups in which they are most commonly found.

Only *Meretrix lusoria* (pl 16B) is exclusively found in the "exposed" and "0-5m" groups. Looking at Table 7.1, it is restricted to sites 35a and 35b which are mangrove swamp and channel sediments within the main mangrove development where brackish waters prevail. *Yoldia tenella* (pl 16C) and *Dosinia histrio* (pl 16D) are restricted to the "5-20m" group of sites and 7 species are found exclusively in the "> 20m" deeper, more oceanward sites.

Paphia gallus (pl 16E) and *Paphia undulata* (pl 16F) are both harvested by the local fisherman in Phangnga Bay. *Paphia gallus* is not found in any of the "exposed"

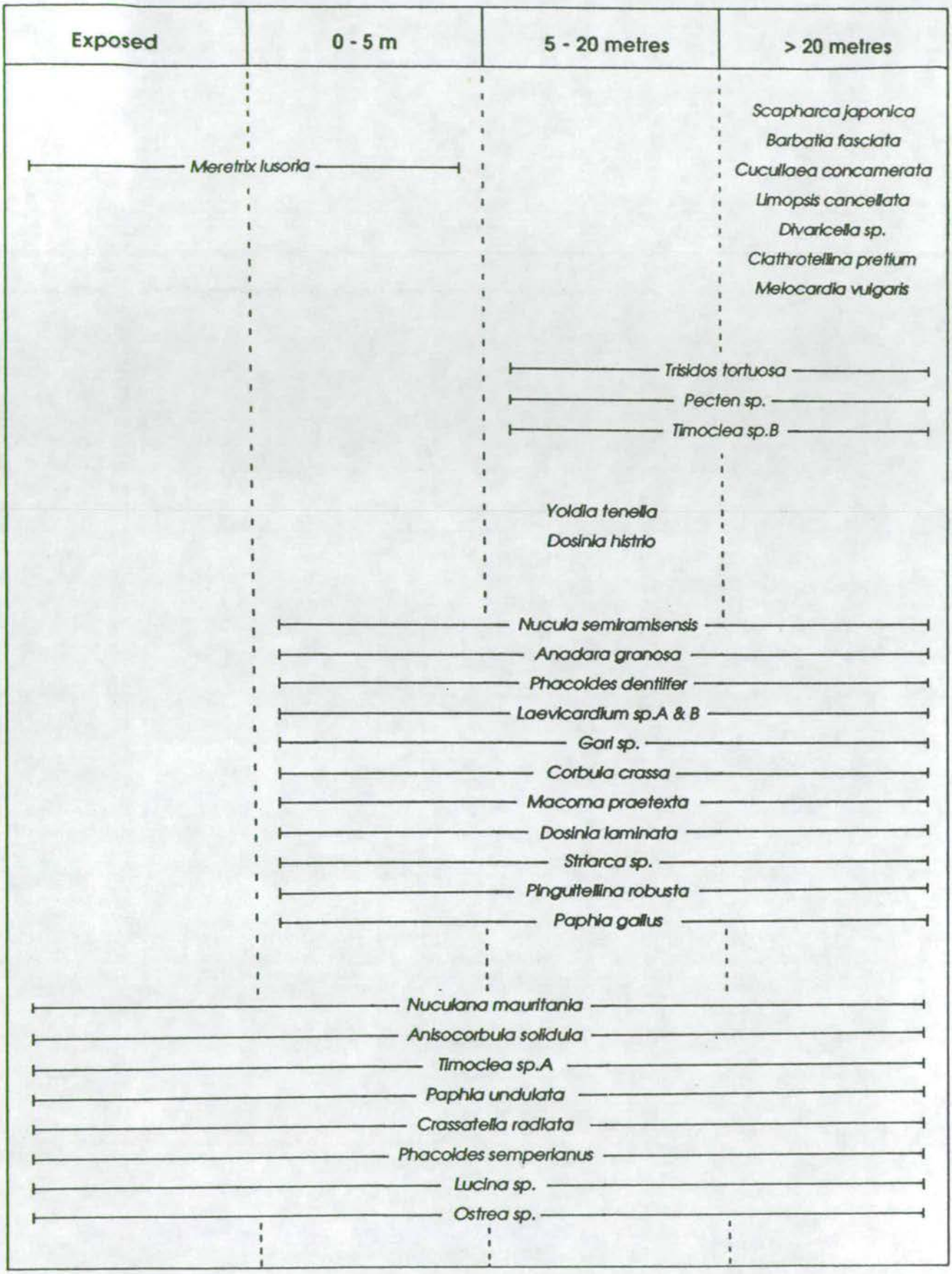

Table 7.3 Distribution of the most common bivalves in the 4 depth zones of the Bay.

group sites whereas *Paphia undulata* is distributed throughout most of the Bay. Considering their use as a food source their distribution may be related to over-harvesting in some areas (eg, in the exposed, intertidal areas for *Paphia gallus*). *Modiolus auriculatus* (also a harvested species) was found in abundance at site 28 where living individuals were found byssally attached in clumps.

7.3.5 Gastropod distributions

7.3.5.1 Comparisons between the 4 site groups

Gastropod distributions show a different pattern from the bivalves in that less genera are present in most of the sites (see group average of number of species in each site at the bottom of Table 7.2). However, like bivalves, there are fewer species in the "exposed" group sites than the others and slightly fewer in the "0-5m" group than the "5-20m" and "> 20m" sites. There does not appear to be any difference in species numbers between high and low percent mud sites within each group. Therefore, there is similar water depth control on species distributions as for bivalves, but no evidence of a strong sediment-type control.

7.3.5.2 Individual species variations

Turritella cingulifera (pl 16H) is the most common gastropod, found in 55 sites in the Bay, followed by the pteropod, *Cavolina longirostris* (pl 16I) and *Calyptraea pellucida* (pl 16J).

The other species that are present in more than 20 sites are illustrated in Plate 17 and include: *Monilea biangulosa* (pl 17A), *Minolea sp.* (pl 17B), *Pymaeorota cingulifera* (pl 17C), *Rissoina sp., Niso sp.* (pl 17D), *Murex trapa* (pl 17F), *Chemnitzia multigyra* (pl 17G), *Acteocina sp.* and *Ringicula sp.* (pl 17I). These species plus some of the other more common species are included in Table 7.4 which illustrates the sediment groups in which each species is dominantly found. No species are restricted to one group, however, 6 species are restricted to the "5-20m" and "> 20m" group and 3 are restricted to the "0-5m" and "5-20m" group. It was noted on studying the samples that larger gastropods (> 1cm) are more prevalent in the southern areas particularly in the "> 20m" group - this is also evident in comparing the gastropod proportions in the grab (1-5mm) and dredge (> 5mm) samples (Figs 7.5 and 7.6).

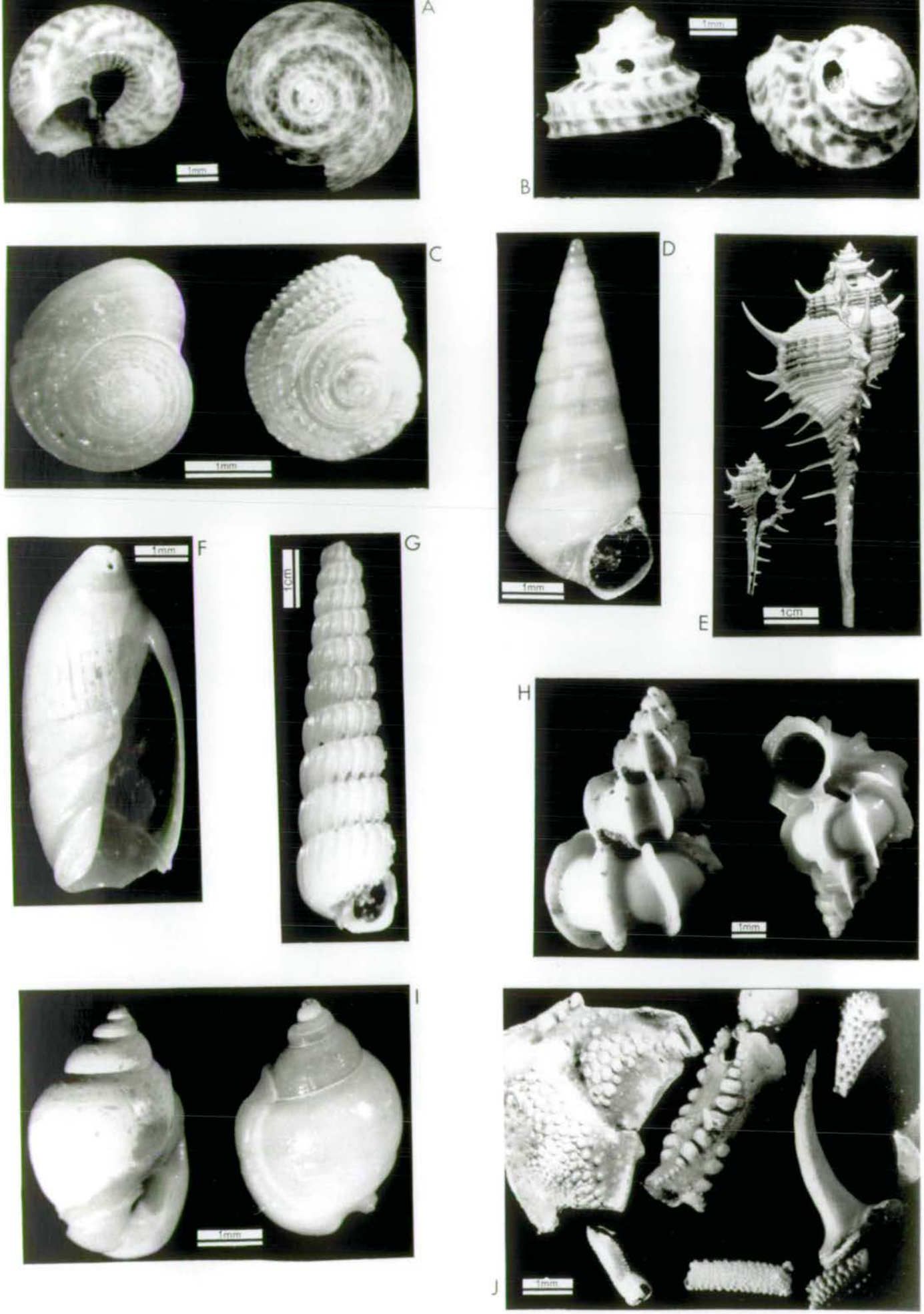

Plate 17 **A.** *Monilea biangulosa* **B.** *Minolea sp.* **C.** *Pymaeorota cingulifera*
D. *Niso sp.* **E.** *Murex trapa* **F.** *Ancilla cylindrica* **G.** *Chemnitzia multigyra*
H. *Epitonium scalare* **I.** *Ringicula sp.* **J.** Crab fragments

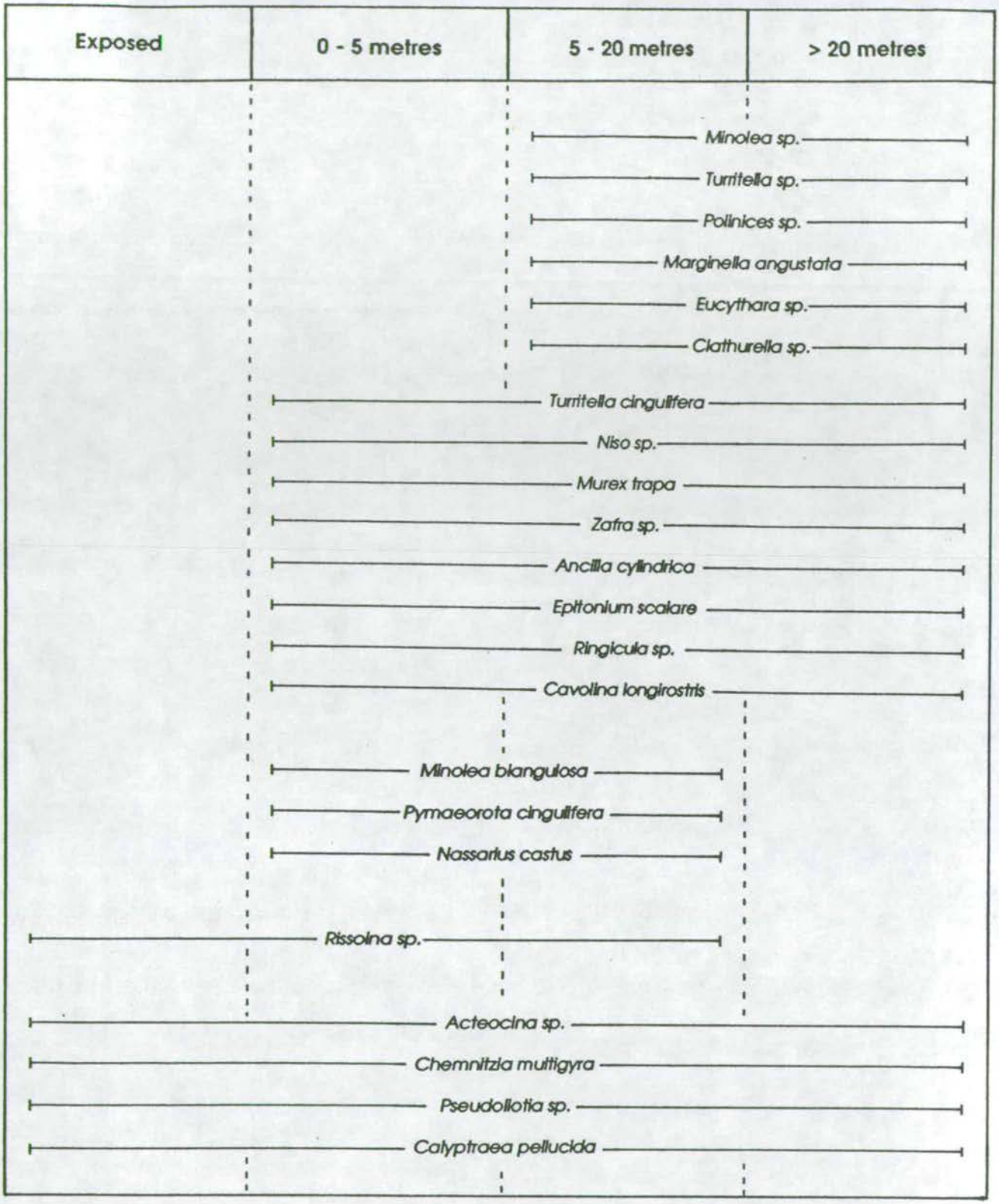

Table 7.4 Distribution of the most common gastropods in the 4 depth zones of the Bay.

7.3.6 Discussion

Without a detailed quantitative survey of bivalves and gastropods abundances it is difficult to make precise judgements on the factors controlling these macrofauna distributions because of the difficulty in using multivariate statistical techniques without absolute abundance data. Studies by Cassie and Michael (1968), Hughes and Thomas (1971), Shin (1982) and Absalão (1991) used such abundance data combined with sample station data (such as sediment type, water depth, temperature, salinity etc) to pin-point the important controls on faunal distribution. Shin (1982) concluded that organic carbon content and % silt/clay were the dominant controlling factors on infaunal macrofauna assemblages in North Bay, western Ireland. Similarly, Cassie and Michael (1968) concluded that the grain size characteristics (particularly % mud) are the dominant factors in controlling faunal distributions on Karore Bank, New Zealand. Hughes and Thomas (1971) however, suggested that distance from shore controls benthic fauna in Bideford River estuary, Canada with the extent of sea ice in winter and influx of fresh water during the spring thaw being important. Absalão (1991) studied the mollusc associations of Lagos dos Patas, South Brazil and by cluster analysis and multiple discriminant analysis concluded that a bathymetry controlled gradient of stability/disturbance is the dominant environmental parameter affecting distributions. As disturbance of the sediment surface from storms becomes less frequent with increasing water depth, the species abundance increases. The second most important factor is sedimentological with percent sand and percent mud being the measured parameters. More fauna were found in high percent mud sediments.

Since the water depth seems to have more affect on distributions in Phangnga Bay (with an increasing number of bivalves and gastropods found from the "exposed" group through to the "> 20m" group) it is suggested here that a disturbance factor may be an important control on bivalve and gastropod distributions. Since tropical storms periodically affect this region it is likely that the shallow water, finer sediments in the north of the Bay are more affected by disturbance than the deeper and coarser sediments to the south. Resuspension of sediments during storms could exclude the majority of benthic organisms which are adapted to stable environments (Levington, 1972). Although Absalão (1991) found that the sites with a combination of high mud and low disturbance (ie greater depth) were the sites with highest species richness this does not seem to be the case in Phangnga Bay (apart from bivalves in the "0-5m" group).

Despite very low mud contents in the south, species abundance is high. Again it has to be remembered here that the specimens collected and identified were dominantly dead specimens (mainly in the form of disarticulated shells) whereas in all of the above-mentioned surveys, only specimens found alive were included. Since we are considering the geological aspects of faunal abundance and distribution, the description of what is actually contained in the sediment is of importance rather than what is currently alive which may be of more use to an ecologist. Clearly more carbonate material exhibiting greater species abundance is accumulating in the deeper water sediments compared to the shallow sediments. This may be a result of different sedimentation rates rather than preferred habitats for species. Sedimentation rates in the south have been very low since the last sea-level rise as low sea-level stand Pleistocene sediments are still thought to be exposed at the sediment/water interface in this area. Therefore, carbonate material from carbonate-secreting macrofauna accumulates on and within the surface sediments without being diluted by terrigenous material. The recent origin of this carbonate material was suggested in Chapter 3 (section 3.3.3) as alteration from aragonite and HMC to LMC does not seem to have occurred as would be expected if the carbonate material was also relict and had been subject to sub-aerial processes. Therefore, this carbonate material probably represents approximately 6000 years of carbonate accumulation. Hence it is not surprising that more species were collected in the same size of sample material as was collected in the northern sediments which have a high terrigenous dilution component. These northern sediments have accumulated faster thus burying much of any carbonate material that has been deposited through time.

Working out which factor is the most important in controlling faunal distributions is difficult without more information on absolute abundances of living material and also on ages of the different fractions of the carbonate material present in the southern sediments. Although there is a clear distinction between "exposed" sites and the other 3 groups in the lack of fauna in the former group, whether there are any real sediment-type and water depth factors involved in controlling faunal distributions in the other groups is difficult to say due to the fact that a greater temporal range of carbonate material may have been sampled in the southern-most sediments.

7.4 CONCLUSIONS

Bivalves, pteropods, ophiuroids, corals and foraminifera show an increase in relative abundance towards the more open marine conditions in the south of Phangnga Bay. This increase is thought to reflect more stable, congenial conditions in this area such as constant temperature and salinity and clear, sediment-free waters. Gastropods, scaphopods and particularly barnacles show higher relative abundances in the north of the Bay which may reflect their preference for calmer waters and/or finer-grained sediments. Plant material is restricted to the north of the Bay which reflects the near-by land-derived source of this material.

The dominance of bivalves and echinoids in the biogenic component is thought to be a characteristic of tropical benthic communities, along with abundant crustaceans and the possibility of disturbance from climatic events or human activities. These characteristics are all evident in Phangnga Bay.

The dominance of bivalves in the biogenic component is reflected in their higher species/site values throughout the Bay than for gastropods. However, both gastropods and bivalves show increased species/site values from shallow water sites in the north to deep water sites in the south which may again reflect the greater possibility of disturbance of sediments by storms in the north. Assemblages of bivalves and gastropods have been picked out which identify particular bathymetric areas of the Bay.

Although both water depth and sediment type are likely to play some part in controlling benthic faunal distributions in the Bay, it is also thought that high carbonate content and high species/site values in the south may be a result of sampling approximately 6000 years of carbonate deposition since the last low sea-level stand as very little recent terrigenous material is thought to have been deposited in this area. In the north however, high terrigenous input has diluted and buried the remains of carbonate-secreting organisms.

CHAPTER 8 - SUB-SURFACE SEDIMENT GEOCHEMISTRY AND SEDIMENTOLOGY

8.1 INTRODUCTION

By studying the sub-surface character of Phangnga Bay sediments a record of geochemical and sedimentological changes through time can be obtained. With the addition of radiocarbon dates an absolute timescale can be accorded to some of these changes. Sedimentological variations may represent the progradation of the mangrove delta system through time and geochemical variations may reflect these sedimentological changes as well as indicate man-induced effects on sedimentation. In the latter case the effect of tin mining and dredging may be recorded in the sediment column.

8.2 METHODS

8.2.1 Core collection

Cores were taken from 43 sample sites (marked 'C' on Fig 1.5) using either a gravity corer operated from the research vessel or with a length of 4cm diameter plastic piping manually pushed in and retrieved from the sediment in shallow areas. The details of core collection are given in Chapter 1.

13 of the cores have been studied in detail, the location of these is illustrated on Figure 8.1. These cores were selected so as to represent the transition from mangrove swamp and channel, to mangrove front (open intertidal) to off-shore environments. Table 8.1 lists the details of each core site and the type of coring method used.

Core Number	Collection Date	Water Depth (at lowest low water)	Coring Method M=manual G=gravity corer
78	6/1/90	Exposed	M
26	18/1/89	2.2m	M
88	6/1/90	Exposed	M
36	19/1/89	Exposed	M
38	19/1/89	Exposed	M
30	18/1/89	2m	G
53	19/1/89	4.1m	M
60	20/1/89	12.5m	G
21	18/1/89	1.5m	G
16	17/1/89	6.5m	G
9	17/1/89	4.3m	G
44b	19/1/89	Exposed	M
67	5/1/90	3m	M

Table 8.1
Details of the core sites and the sampling method for the cores studied.

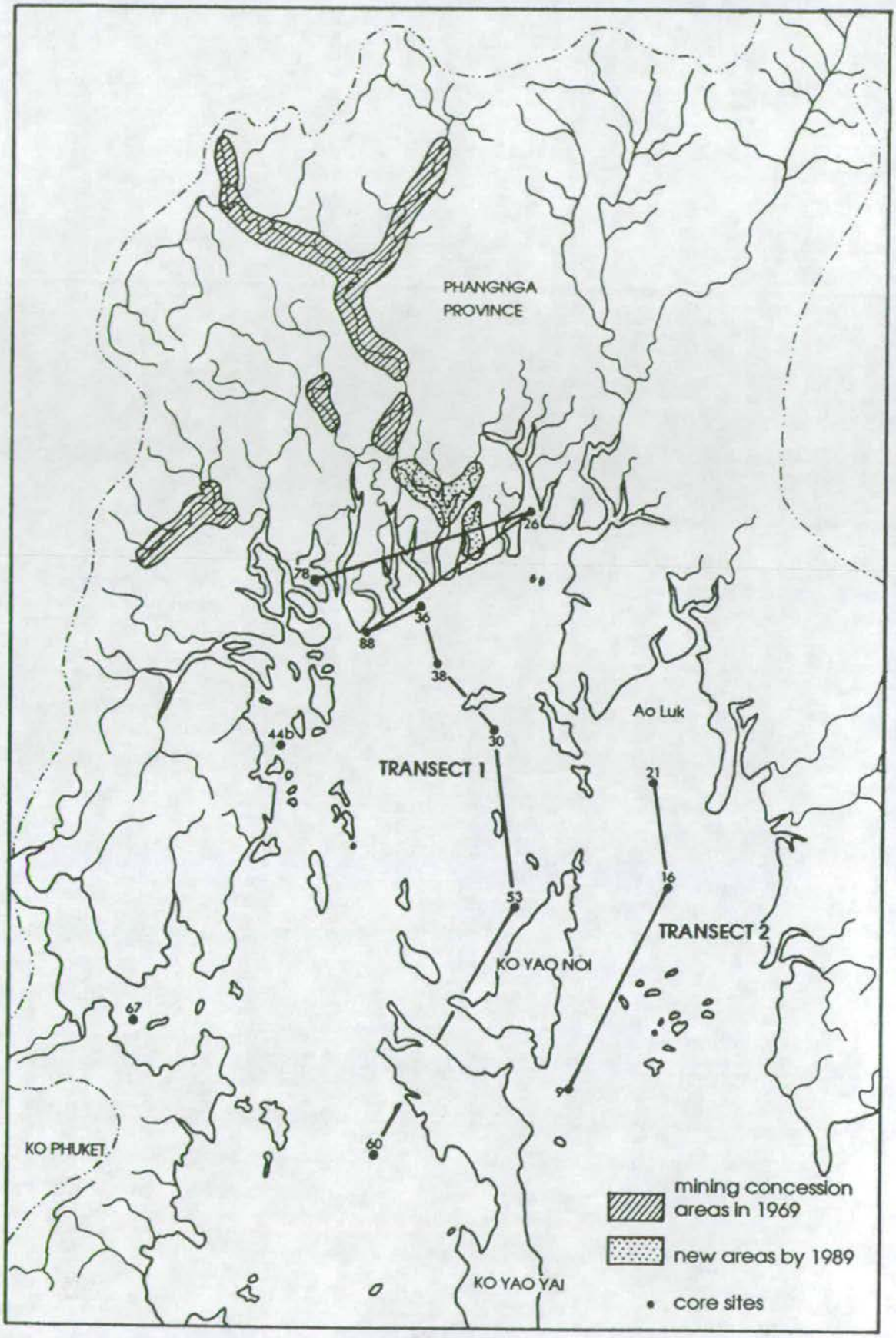

Figure 8.1 Location of cores studied and concession areas for tin-mining and dredging in the north of the Bay.

CHAPTER 8

SUB-SURFACE SEDIMENT SEDIMENTOLOGY AND GEOCHEMISTRY

8.2.2 Dry Bulk Density calculation

The dry bulk density calculation is as follows:

$$\text{Dry Bulk Density} = \frac{\text{Mass of Dry Sediment}}{\frac{\text{Mass of Dry Sed.}}{2.45} + \frac{\text{Mass of water}}{1.02}}$$

The average density of the sediment is taken as 2.45g/cm^3 and the density of sea-water is taken as 1.02g/cm^3. A slight correction is made to account for the salt content of the sediment. The dry bulk density therefore describes the density of the sediment in relation to the volume of the sediment and the water as a whole. As the sediment is compacted with depth, water is expelled and the dry bulk density increases. The dry bulk density varies however, with the grain size composition of the sediment. Fine grained sediments have a greater volume of pore spaces therefore higher water contents (hence lower dry bulk density) than coarse grained sediments.

8.2.3 Geochemical analysis

XRF analyses were carried out on samples taken from approximately 5cm intervals downcore (10cm intervals for cores over 70cm in length). These samples have been analysed for major elements in order to measure the variation in major mineralogical components (aluminosilicates, quartz and carbonate). Sn, Rb and Zr concentrations were also measured to assess the variation in sub-surface sediments of minerals which are mined/dredged. Appendix B describes the XRF method and Appendix D lists the geochemical results for the core material studied. Results have not been corrected for salt as it is thought that the salt content of porewaters will vary considerably downcore especially in the northern brackish water sites. Therefore, any salt correction may create more error than is present in the first place. Since the correction to the elements studied is so small anyway, the error in uncorrected results is considered negligible.

8.2.4 Graph Plots

Figures 8.2 - 8.14 illustrate the sedimentological logs, dry bulk density, Al, Ca, Si/Al, Rb/Al, Zr ($CaCO_3$-free basis) and Sn ($CaCO_3$-free basis) variation downcore for the 13 cores studied. Since the horizontal scales for each parameter vary between cores, dashed vertical lines representing a constant composition for eachparameter have been drawn on all graphs and the part of the core showing a composition greater than that marked is shaded to enable easy comparison between graphs. Vertical scales are the same for each core and the horizons from which radiocarbon dated samples were taken are marked with the corrected radiocarbon date (see Chapter 9 for more details on radiocarbon dates).

8.3 SEDIMENTOLOGICAL VARIATIONS

Sedimentological changes downcore are measured by a combination of core logging during sample collection, dry bulk density (DBD) variations over and above the general downcore increase from compaction, and geochemical variations in the Al (clays), Si/Al (excess Si in the form of quartz) and Ca (biogenic carbonate). Each core will be described in turn and then the trend of the sub-surface sediments across the transition of environments discussed.

8.3.1 Transect 1

8.3.1.1 Core descriptions

Core numbers 78, 26, 88, 36, 38, 30, 53 and 60 (Figures 8.2 - 8.9) form a transect across depositional environments from within the mangrove swamp to the open marine environment.

Core 78 - (Fig 8.2) a 1m core taken from mangrove swamp muds approximately 4m from the edge of a mangrove channel. The entire length of core is composed of dark brown to black mud with peaty fragments dispersed throughout the sediment. The Al content is comparatively high (8-10%) and Ca, Si/Al and DBD values consistently low downcore.

Core 26 - (Fig 8.3) a 45cm core taken from a large mangrove channel to the NE of the Bay. Al values are low (< 3%) whereas Si/Al values are high (12-36) and fluctuate

Figure 8.2

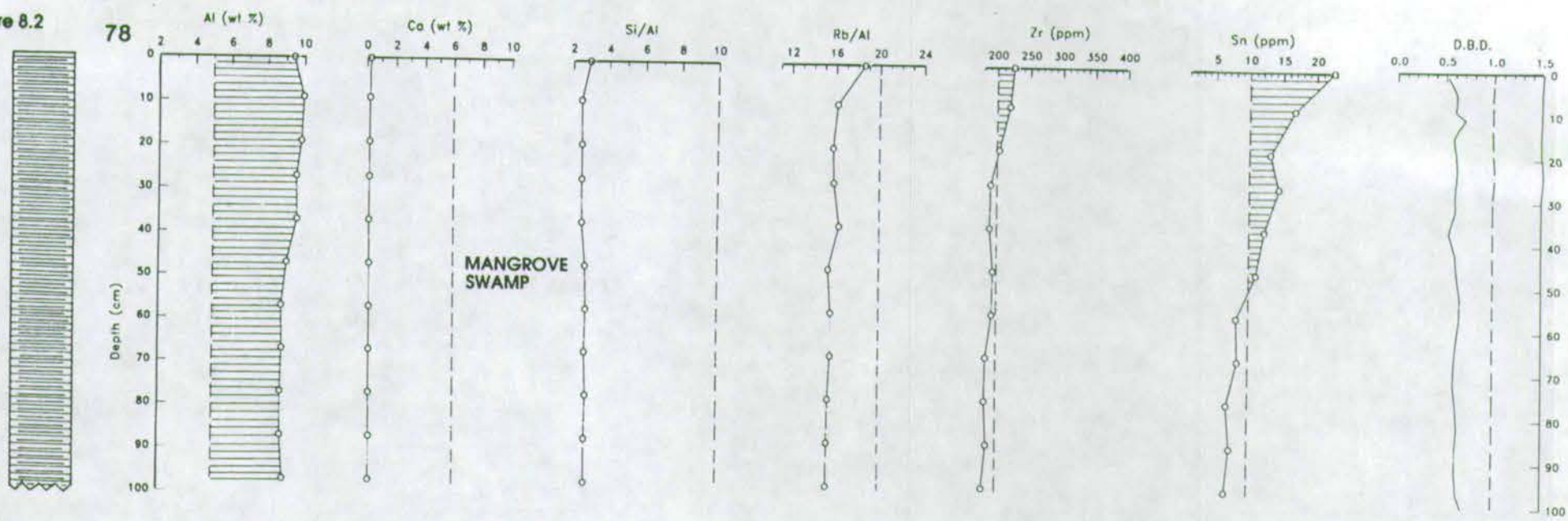

Figure 8.3

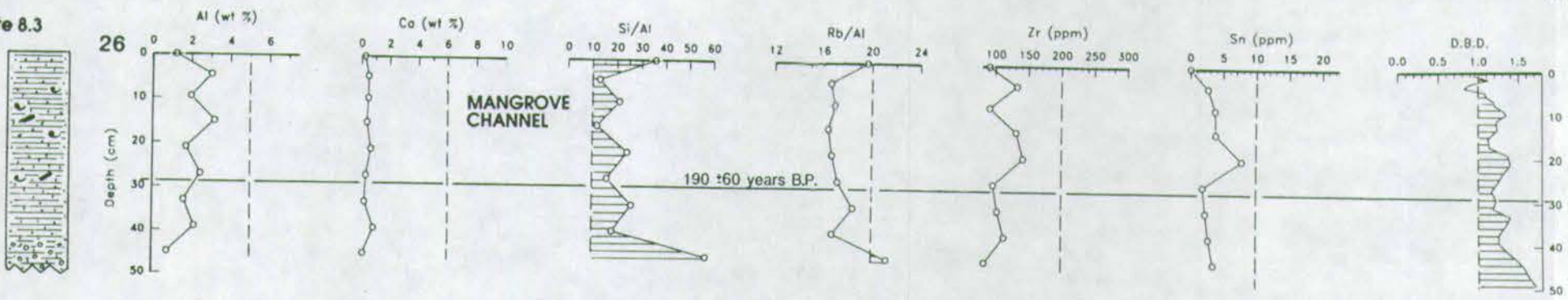

Figure 8.4

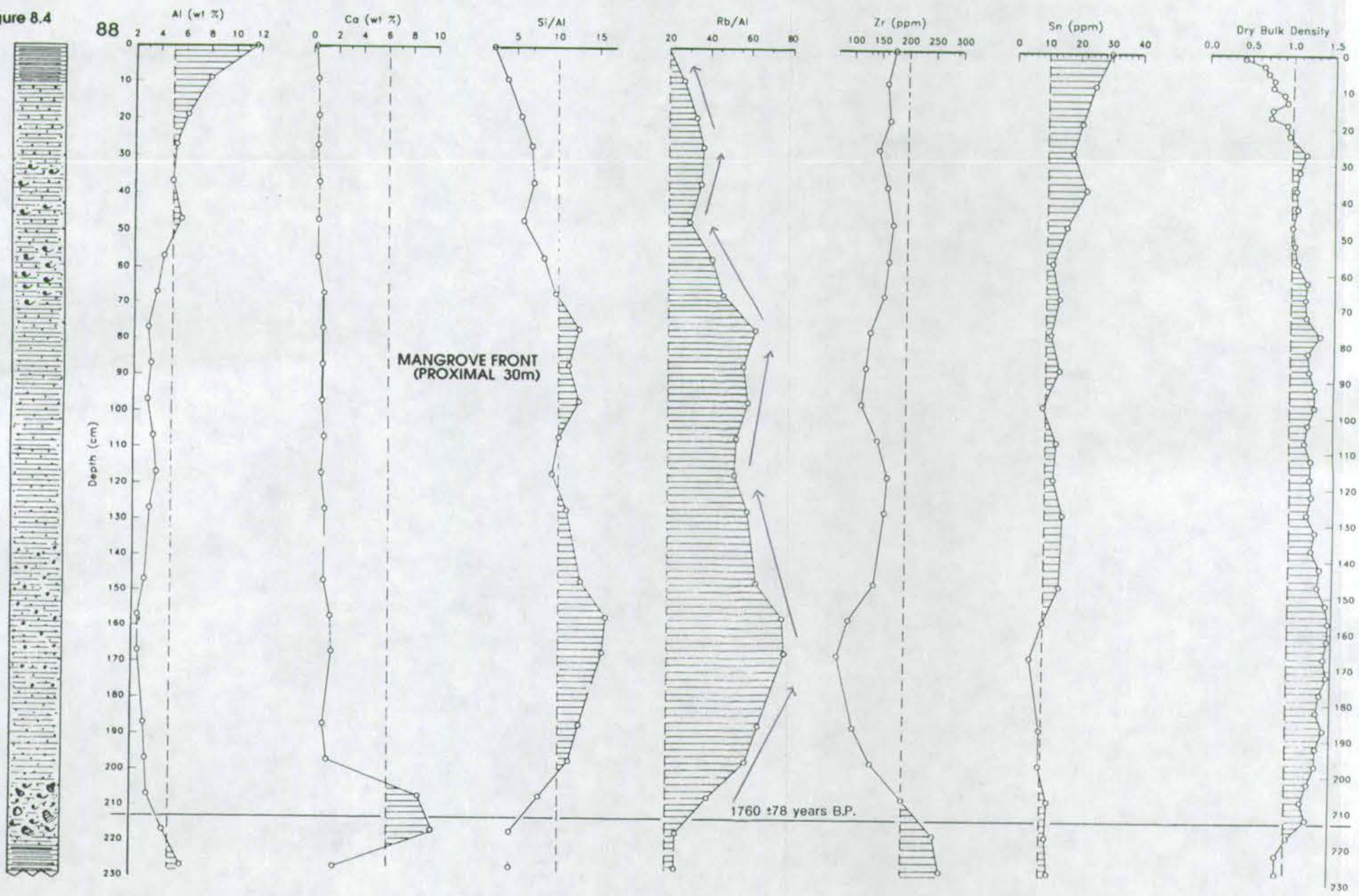

Figure 8.5

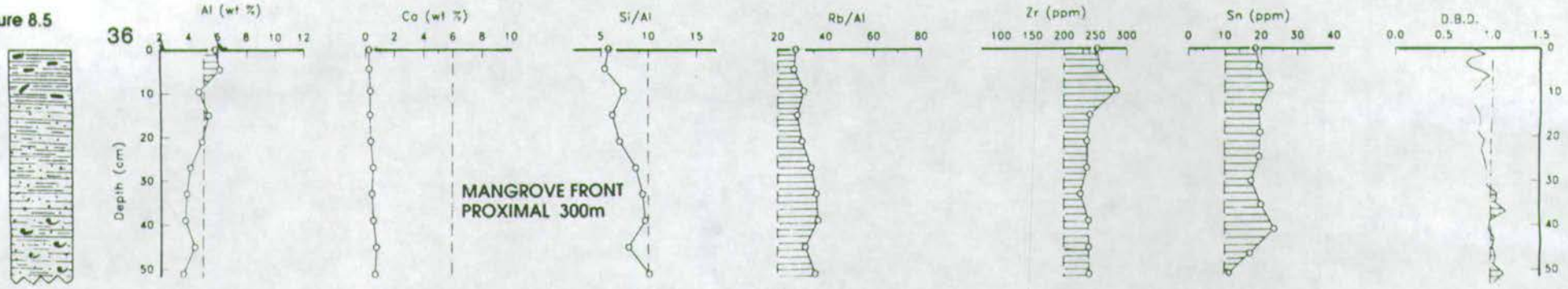

Figure 8.6

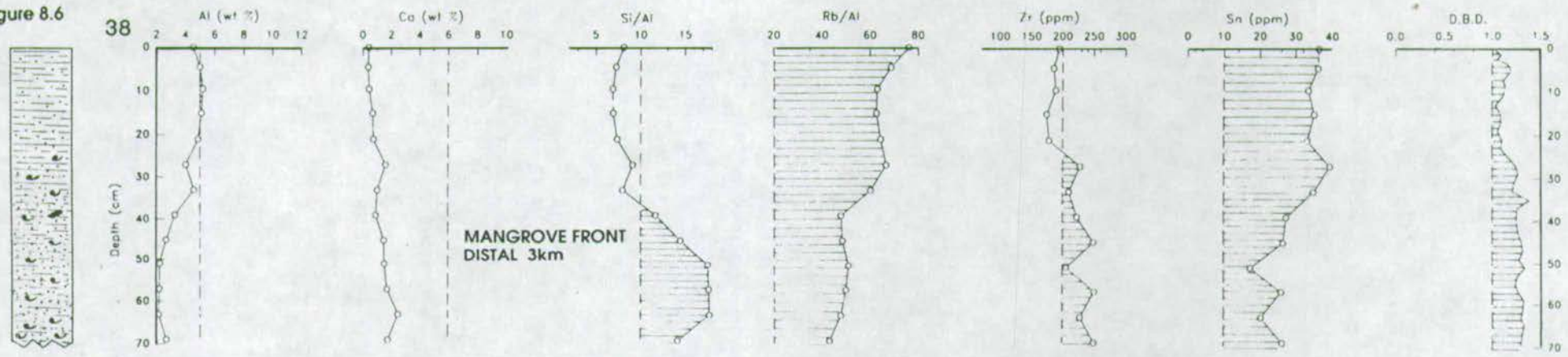

Figure 8.7

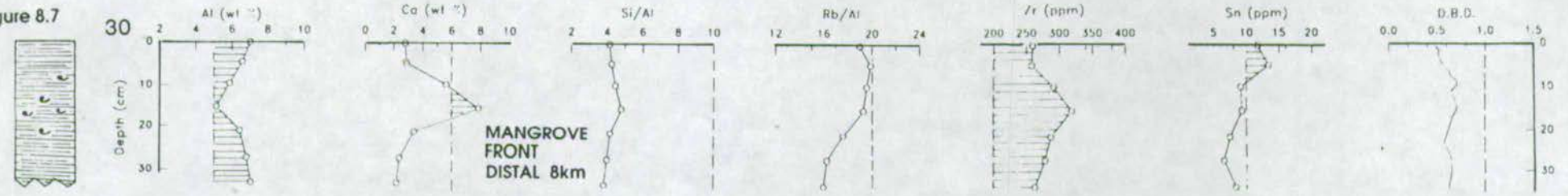

Figure 8.8

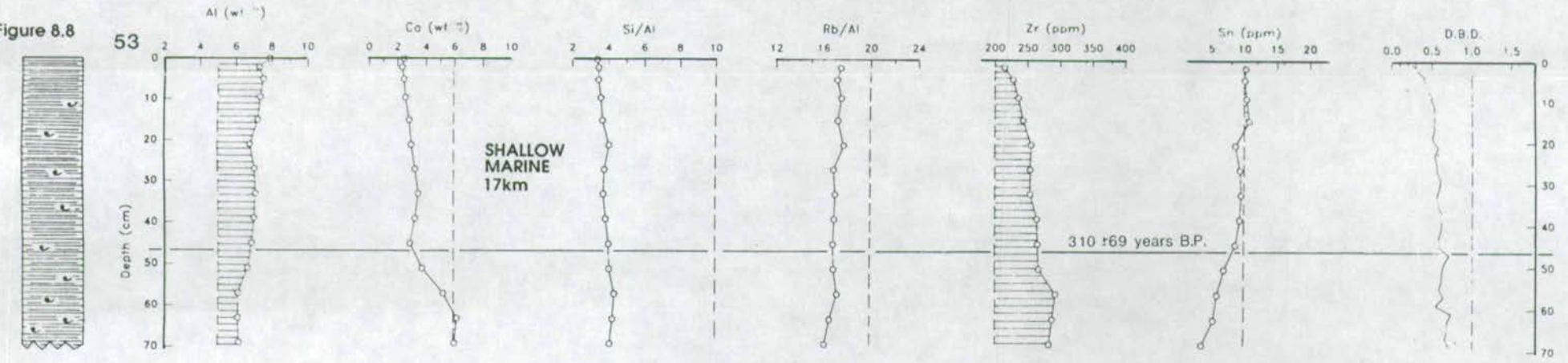

Figure 8.9

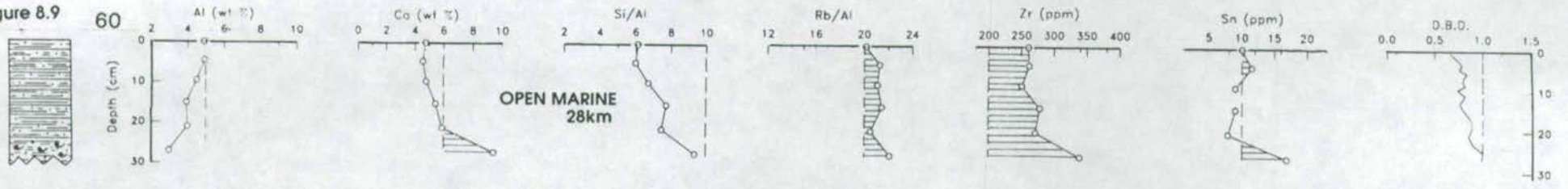

repeatedly downcore. This pattern is followed by the DBD pattern (since the DBD was calculated for every sample downcore the DBD resolution is higher than the geochemical analyses and so is a useful check on the validity of the fluctuations shown by the geochemical data). Ca values are consistently low although a few shell fragments were found along with woody fragments. The lithology is entirely muddy sand with coarser material at the base of the core. The Si/Al fluctuations possibly reflect sequences of graded bedded muddy sands developed through continual reworking of the sediments with tidal and fluvial currents.

Core 88 - (Fig 8.4) a 2.3m core taken from 30m in front of the mangrove edge. Although this core is muddy for the top 20cm, below this layer, muddy sands predominate. At approximately 2m there is a shelly horizon 15-20cm thick composed of small (1-2mm) gastropods and bivalve fragments in a muddy sand matrix. Below this layer muds start to predominate again. The combination of increasing Al, decreasing Si/Al and decreasing DBD upwards indicates a fining upwards sequence within which are 3 smaller sequences (marked with arrows on the Si/Al plot) consisting of coarsening then fining upward cycles. The implications of this are discussed later.

Core 36 - (Fig 8.5) a 50cm core taken approximately 300m from the mangrove edge. This core shows a very similar pattern to the top 50cm of core 88. Al values increase upwards (although values at the top are lower that core 88) with a 10cm thick muddy top to the core with organic matter fragments. Si/Al and DBD decrease upwards and Ca remains constant and low.

Core 38 - (Fig 8.6) a 70cm core taken approximately 3km from the mangrove edge. This core again shows an increase in Al, decrease in Si/Al and DBD and low constant Ca content. The Si/Al fluctuation is however more pronounced than the above 2 cores and there is not a muddy top to the core.

Core 30 - (Fig 8.7) a 35cm core taken approximately 8km from the mangrove edge. This core is dominated by fine muds reflected in the high Al content (5-8%), low Si/Al and DBD. Ca content fluctuates from 2-8% with a 10cm thick band of shell fragments at 15cm reflected in the high Ca values.

Core 53 - (Fig 8.8) a 70cm core taken approximately 17km from the mangrove front. Like core 30 this core is dominated by fine muds again reflected in the high Al

content (6-8%), low Si/Al and generally low Ca although this increases at the base of the core to 6%.

Core 60 - (Fig 8.9) a 27cm core taken from the western side of Phangnga Bay in the open marine environment. Al increases upwards but are comparatively low (< 5%). Si/Al and DBD values are also low but show a decrease upwards. Shell fragments in the base of the core are reflected in high Ca values (> 6%) compared to lower values above.

8.3.1.2 Discussion

The sub-surface sediment features of this transect generally reflect the surface sediment features. Fine organic muds predominate in the mangrove swamps, muddy sands in the mangrove channels, fine muddy sands with occasional shell debris in front of the mangroves followed by muds further off-shore. Finally relict muddy sands predominate towards the south of the Bay with less influence from recent sedimentation.

Shelly horizons are occasionally found within the sediment sequence (cores 88, 30 and 60) which may reflect localised lag deposits formed by storm reworking. In the cores proximal to the mangrove front (cores 88, 36 and 38) mud content increases towards the surface possibly reflecting the progradation of intertidal mangrove muds over older sediments.

The overall fining upwards trend in core 88 represents the progradation of mangrove muds over coarser grained shallow marine sediment. This is the opposite of the generalised view of progradational deltaic sequences as typified by the Gilbert model of fine grained bottomsets, sandy foresets and coarse grained topsets (Reading, 1978). The coarsening upward cycle is interpreted as representing a passage from marine facies upwards into terrestrial facies whilst the reverse, a fining upward cycle is interpreted as a transgressive, retrogradational sequence. In Phangnga Bay the opposite is the case - a fining upward sequence represents fine grained intertidal/mangrove muds overlying coarse grained relict off-shore sediments, ie, a fining up sequence represents the progradation of a modern day, sheltered, mangrove delta system.

Within the general fining upwards trend are 3 smaller scale sequences of coarsening and fining cycles. There are various possible explanations for these sequences:

1. a change in sediment type and supply ie, alternating influxes of coarse grained and fine grained sediment possibly in response to:

a) climatic variation eg, increased rainfall leads to increased run off therefore more coarse grained material.

b) base level shift by sea-level fluctuation or tectonic uplift/submergence - a change in sediment supply may be caused by down cutting of channels (supplies more coarse sediment to the mangrove front) or accretion (coarse material trapped inland so only fines are deposited at the mangrove front).

c) anthropogenic effects such as deforestation, agriculture, mining and urbanisation all cause increased run off thus a change in the sediment supply.

2. deep reworking of mixed sediments by storm action causing coarse grains to settle first followed by fines.

Although 2. cannot be ruled out (there are monsoonal storms in the area which may periodically be reworking events) and may explain the shelly horizon at the base of the core, the lack of a clearly defined erosive surface and basal lag at the base of each sequence tends to discount this theory. The log shows a sequence of coarsening followed by fining which is a more gradual change than would be expected from storm reworking.

Fluctuations in sediment type and supply would therefore be a more likely explanation. Whether climatic control or base level shift is the controlling factor is not known - both are possible on this time scale but detailed information on climatic variation, tectonic activity and sea-level variations for this area over the last 6,000 years is not available. The effect of mans' activities on sedimentation is discussed later when looking at Sn variations downcore but it is likely that these effects, if at all important, have only been prevalent in the last few hundred years and cannot explain the 1700 years of sedimentation represented by these sequences (see the radiocarbon date on core 88 at 212cm - Figure 8.2)

It is thought that the Thai/Malaysian Peninsula area is presently tectonically stable (Garson et al, 1975). However, work by Geyh et al (1979) on Pleistocene and Holocene sea-level changes in the Strait of Malacca just south of Phangnga Bay, suggest a sea-level maximum (+2.5m to +5.8m) between 6000 and 4000 years ago

with a subsequent lowering since then. Similarly, the dating of corals from reef flats around Ko Phuket (Scoffin 1991, pers comm) indicates that sea-level was a minimum of one metre above present level between about 5000 and 6000 years ago Whether the subsequent sea-level fall took place slowly and gradually or through an oscillatory process is not known. This latter point is quite important because if sea-level lowered by oscillatory fluctuations then this may explain the 'pulses' of varying sedimentation visible in core 88. If sea-level fell sharply over a short period then channels would down cut, coarse sediment transport would increase and be deposited at the channel mouths/mangrove front. If sea-level then stayed stable for a while then the system would re-equilibrate and eventually only fine sediments would be deposited at the mangrove front again. This process may also have implications for the growth of the mechanism of mangrove growth - it may grow in rapid spurts covering a wide area as a response to these sedimentation pulses rather than in a continuous, gradual manner. These ideas will be discussed further in Chapter 9.

8.3.2 **Transect 2**

Cores 21, 16 and 9 also form a transect from mangrove front (distal) to open marine environments.

8.3.2.1 Core descriptions

Core 21 - (Fig 8.10) a 35cm core from approximately 6km south of the mangrove development in Ao Luk (Fig 8.1) composed dominantly of muds which increase upwards (increasing Al, decreasing Si/Al and DBD up core). The lower part of the core contains shell debris as well as whole gastropods and bivalves which is reflected in the high Ca content.

Core 16 - (Fig 8.11) a 40cm core taken from approximately 6km south of core 21. This core is very similar to the above core with high Al content. Shell debris is distributed sparsely throughout the length of the core.

Core 9 - (Fig 8.12) a 40cm core taken from approximately 10km south of core 16, 2km to the east of Ko Yao Noi. Similar to the above 2 cores although there is less visible shell debris and the sediments become slightly sandy near the base.

Figure 8.10

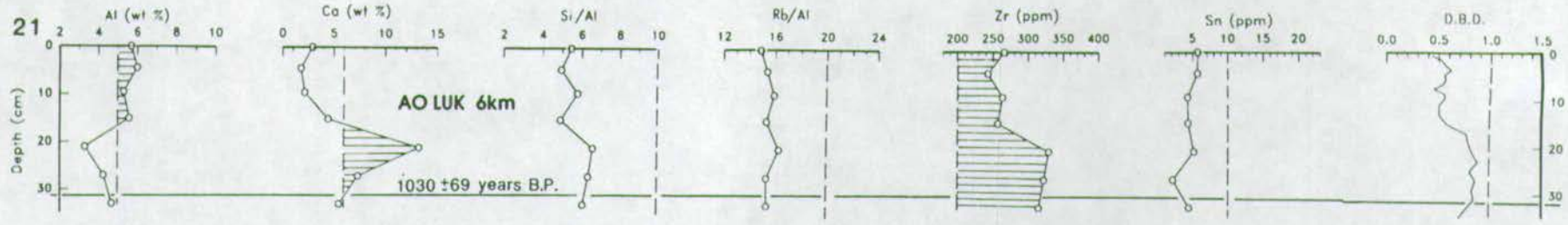

Figure 8.11

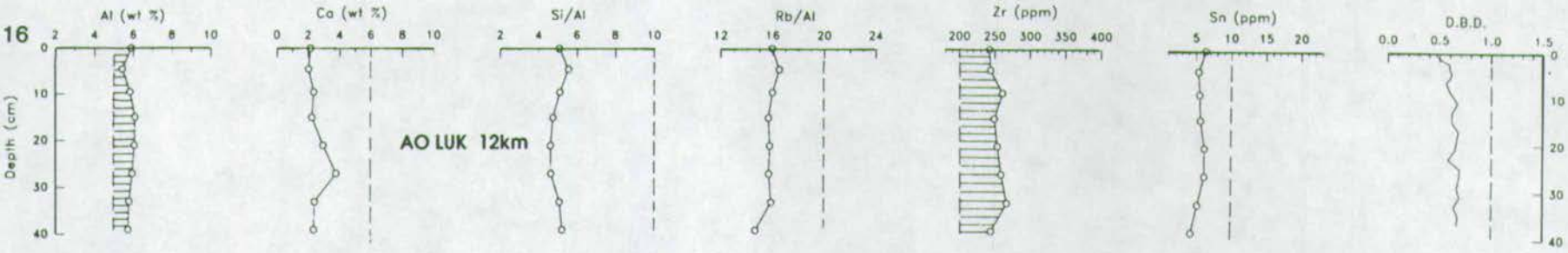

Figure 8.12

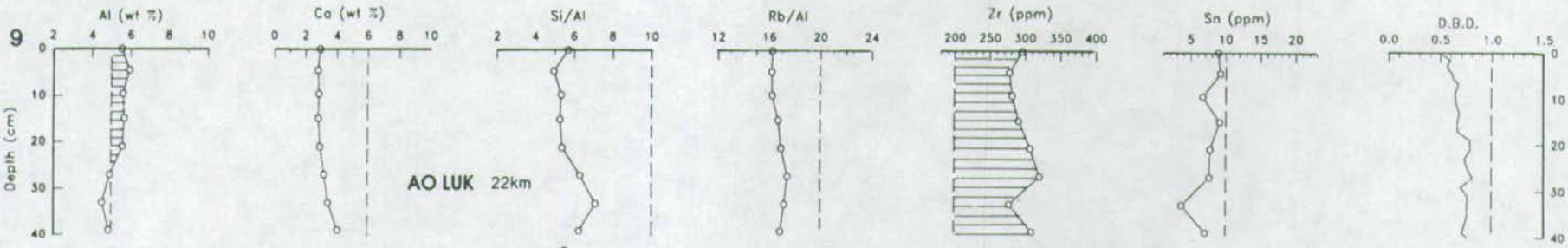

Figure 8.13

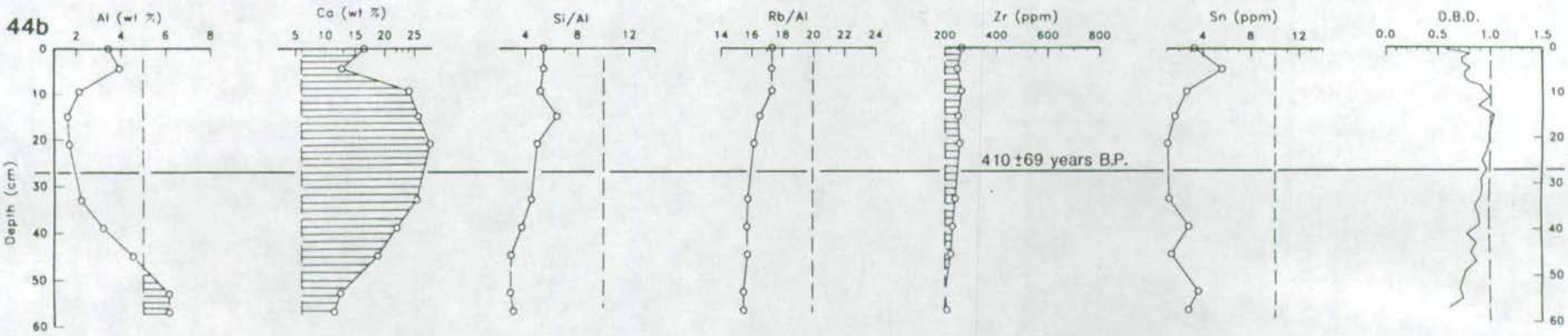

Figure 8.14

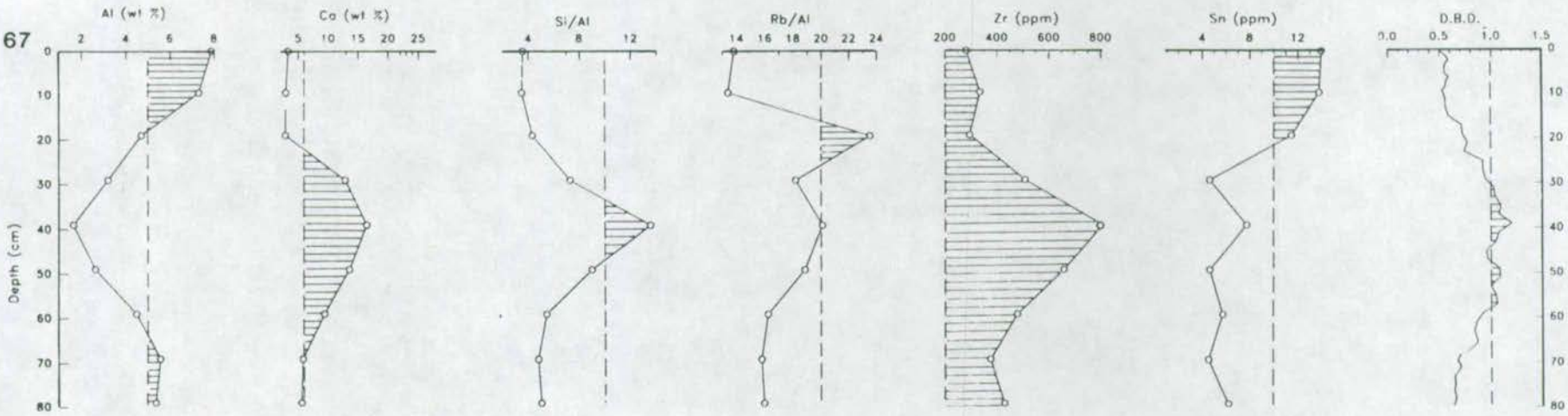

8.3.2.2 Discussion

The low quartz sand content of these cores reflects the comparatively small drainage basin of Ao Luk. The small streams draining through the mangrove swamp formed around the north of Ao Luk will bring a comparatively small amount of terrigenous material into this bay and this is reflected in the slower sediment accumulation rates calculated from the radiocarbon date on a shell from core 21 (Chapter 9). These cores serve as a comparison for the main transect of cores especially in geochemical terms as no tin mining or dredging has taken place in the catchment area and so sedimentation is essentially undisturbed.

8.3.3 **Cores 44b and 67**

Core 44b - (Fig 8.13) a 55cm core taken from approximately 150m north of a shell beach (sediment sample 44a) in the north west of Phangnga Bay. The sediment downcore is dominated by shelly debris (reflected in Ca concentrations > 10%) in a muddy matrix . The top 10cm and below 50cm are muds with less shell debris. The shell material is likely to be sourced from the nearby beach sediments as most of the fragments are worn and abraded shells rather than whole articulated samples. The nearness to mangrove swamps to the west may account for the dominantly fine grained matrix.

Core 67 - (Fig 8.14) an 80cm core taken from the channel between the north of Ko Phuket and the mainland. The sediments of this core change in character from muds for the top 20cm, to shell mud, to shelly sands at around 40cm and then back to muds at 70cm. The hydrodynamic processes operating in this stretch of water are not known and so the influence of the narrow opening to the Andaman Sea on water flow and sedimentation in this area is not known. However, the increase in Sn values in the top 20cm coinciding with a decrease in shell debris and an increase in mud suggest that some sediment transport through the opening is possible. Much dredging activity has and still is taking place off the west coast of Ko Phuket and the mainland (see satellite photo - Chapter 9). The fine material including cassiterite stirred up from such activity may have been transported through the narrow strait to the north of Ko Phuket on incoming tides and into the bay to settle around the area of core 67.

8.4 GEOCHEMICAL VARIATIONS - Rb, Sn and Zr

8.4.1 Introduction

These 3 elements have been chosen to study man-induced effects on sedimentation because of their resistance to diagenetic changes. Sn in cassiterite, Zr in zircon and Rb in lepidolite mica are resistant to any major changes in concentration downcore caused by shallow sediment diagenetic reactions. Most of the other trace elements studied in surface sediments are susceptible to redox reactions through burial as they are associated with clay minerals and organic matter which are not stable under such varying conditions. Therefore variations downcore are likely to reflect these diagenetic changes and may mask any anthropogenic influences. An investigation of diagenetic changes downcore is beyond the scope of this study.

As discussed in Chapter 4, Rb and Sn in the form of lepidolite mica and cassiterite are useful geochemical indicator elements for examining the effect of drainage basin geochemistry on sediment geochemistry. They show anomalously high values in the NW of the Bay due to recent drainage from Sn-bearing granites and lepidolite pegmatites and in the south of the Bay from either relict coastal placer deposits or local sub-aqueous outcrops of Sn-bearing rocks. Zircon is not concentrated in any particular rock type in the hinterland of Phangnga Bay and because of its extreme resistance to weathering it is likely to be a constituent of the sedimentary (non-carbonate) and metamorphic lithologies as well as a primary mineral in the igneous rocks. For this reason zircon acts as a background indicator mineral against which cassiterite variations can be compared as these two heavy minerals should theoretically behave similarly in sedimentary environments.

8.4.2 Results and discussion

Because of the mining and dredging activities around the north western hinterland of Phangnga Bay (the mining concession areas since 1969 are illustrated on Figure 8.1), some increase in the concentrations of Sn and Rb might be expected upcore in sub-surface sediments of the Bay. Higher concentrations of metals found towards the top of cores are commonly interpreted to reflect increasing anthropological stress on the system (Nadeau and Hall, 1988). Graphs of the downcore concentrations of these elements are plotted in Figures 8.2 - 8.14 along with Zr

concentrations, and show that in some cores Sn and Rb values do increase against constant or slightly decreasing Zr values.

Cores which show Sn values > 10 ppm (78, 88, 36, 38, 30, 60 and 67) are distributed in the NW of the Bay (coincident with areas of anomalously high Sn concentrations in surface sediments) and in nearly all of these cores (78, 88, 38, 30 and 67) Sn increases in concentration upwards. The fact that the increases in Sn are not reflected by the Zr trend indicates that Sn anomalies are not the result of natural weathering and transport processes. In effect, hydraulic pumping and dredging are increasing the rate of 'weathering' of specific areas of Sn-bearing rocks and although much of the cassiterite is extracted, some (especially very fine grains) will be washed downstream along with tailing minerals which consist largely of lepidolite and quartz (Garson et al, 1975). These minerals are eventually deposited in the Bay sediments.

Cores 9, 16 and 21 from the Ao Luk transect all show Sn concentrations lower than 10 ppm with no increasing trend up core.

The main increase in Sn values in cores 78, 88 and 38 starts at depths around 50cm. The accumulation rates in the northern area of the Bay vary between 1.1 and 1.5 mm/year (Chapter 9) which gives sediments at a depth of around 50cm an age of approximately 330-450 years. The earliest record of tin mining in the Phangnga area dates from 1583 (Gerini, 1905) when small tin mines were in operation. Tin production has undoubtably increased since then especially with the introduction of hydraulic gravel pumping and dredging (the latter was first introduced in Phangnga Bay in 1906 (Jones, 1925)). Thus the first increase in Sn values roughly coincides with the first reports of tin-mining in the area and the further increasing concentrations follow the trend of increasing tin mining activity.

High Rb/Al values (>20) are present in those cores which show high Sn concentrations as is expected knowing the association of Sn in cassiterite and Rb in lepidolite in surface sediments (Chapter 4). However, the Rb/Al trend tends to follow more closely the Si/Al trend suggesting that mica and quartz are subject to different depositional processes than cassiterite. Whilst Sn shows an increase up core, Rb/Al and Si/Al tend to decrease (core 38 is an exception to this - both Rb/Al and Sn show increasing trends upcore compared to decreasing Si/Al). The release of quartz, mica and other associated payground minerals from dredging and mining

operations would be equalled by a release in clay minerals (dominantly kaolinite) formed from feldspar alteration in the highly weathered rocks (it is the degradation of feldspar minerals in the rock matrix which makes possible the use of hydraulic jet methods in mining). Therefore clays would also be washed downstream and probably in greater quantities than coarser materials due to their transport by suspension. Therefore the increase in clays upcore may be a result of mining operations rather than part of the natural progradation of the mangrove delta system as suggested earlier.

8.5 CONCLUSIONS

Although it was not possible to study all of the collected core material in detail, a study of a selection of cores has given some insight into sediment processes which have operated through time in the northern part of the Bay.

A transect of cores from the main mangrove development in the north of the bay through the intertidal, shallow marine and open marine environments revealed that sub-surface sediment features (such as grain size which is indicated by DBD, Si/Al variations and logs downcore) generally reflect the surface sediment features with fine organic muds in the mangrove swamp, muddy sands in the mangrove channel, fine muddy sands with shell debris in front of the mangroves with muds further off-shore. Relict muddy sand is found towards the south. An increase in mud content upcore in mangrove front areas may reflect the progradation of the whole mangrove system over coarser grained off-shore sediments. Thus the progradation of a sheltered shallow marine depositional system is represented by a fining upward sequence of sediments.

A transect of cores from the north-eastern side of the Bay shows a lower quartz sand content and slower sediment accumulation rates (Chapter 9) than the transect in the north west of the Bay which is a result of the lower sediment input in the north east area from the smaller drainage basin. The lack of Sn-bearing granites in this eastern area is reflected in the comparative lack of Sn downcore in these sediments. This serves as a comparison to the main transect where most cores show higher Sn values and a trend of increasing Sn upcore. Zr acts as a background indicator element and shows no corresponding increase upcore. This strongly suggests that the increasing Sn values are a result of Man's tin-mining and dredging activities in the

catchment area which have increased significantly over the last 100 years. The trends of Rb/Al and Si/Al in these cores suggests that the mica and quartz grains bearing these elements are subject to different processes than cassiterite.

It would be expected that because of the increased load of material released in mining areas and the subsequent transport of this material downstream and into the Bay, sedimentation rates in this north-western part of the Bay will have increased through time. However, without a geochronology of the whole core length rather than one point in the core, such measure of rate of change of sedimentation rate is not possible. Although apparent sediment accumulation rates are faster in this area than elsewhere this could be a function of a naturally larger sediment load entering the Bay from the larger catchment area.

It is clear that tin mining operations have had some impact on the geochemistry of sediments in the northern part of Phangnga Bay by increasing Sn and Rb concentrations through deposition of mining outwash. However, the effect on major mineralogical components (hence grain size) and sedimentation rates is not clear as the natural processes of mangrove delta progradation could also explain the grain size variations visible in sub-surface sediments.

CHAPTER 9

QUATERNARY DEPOSITIONAL HISTORY OF THE BAY AND ANALOGUES IN THE GEOLOGICAL RECORD

CHAPTER 9 - QUATERNARY DEPOSITIONAL HISTORY OF THE BAY AND ANALOGUES IN THE GEOLOGICAL RECORD

9.1 INTRODUCTION

By the calculation of accumulation and progradation rates from radiocarbon dates, from further consideration of sub-surface sediment characteristics from core material and from comparisons with studies of similar areas, a picture of the Quaternary depositional history of Phangnga Bay will be established in this chapter. Although it is easier to postulate on the more recent Holocene depositional history since the last major sea-level rise, some consideration will be given to low sea-level stand sedimentation patterns. The second part of this chapter will consider the comparison of sedimentation in Phangnga Bay with possible analogues in the rock record.

9.2 QUATERNARY DEPOSITIONAL HISTORY

9.2.1 **Deposition during pre-Holocene low sea-level stands**

Throughout the preceding chapters reference has been made to the "relict" coarse sediments found in the southern, ocean-ward part of the Bay. Considering the present-day conditions of sedimentation in the Bay (discussed in Chapter 2 and 5) and the widespread presence of identified relict sediments elsewhere on continental shelves (referenced in section 2.4.1.2) it is thought certain that the terrigenous fraction of these coarse sediments represent sedimentation during glacial periods either in shallow coastal or alluvial/floodplain depositional environments.

Batchelor (1979) used seismic profiles and onland Quaternary sediment exposures to develop a Cenozoic stratigraphy of sediments deposited on the Sundaland shelf of which the Phangnga area is a part (Fig 9.1). Although the work was aimed at improving the methods of tin exploration in the region, the ideas developed are of use in considering the pre-Holocene depositional history of the Phangnga Bay region.

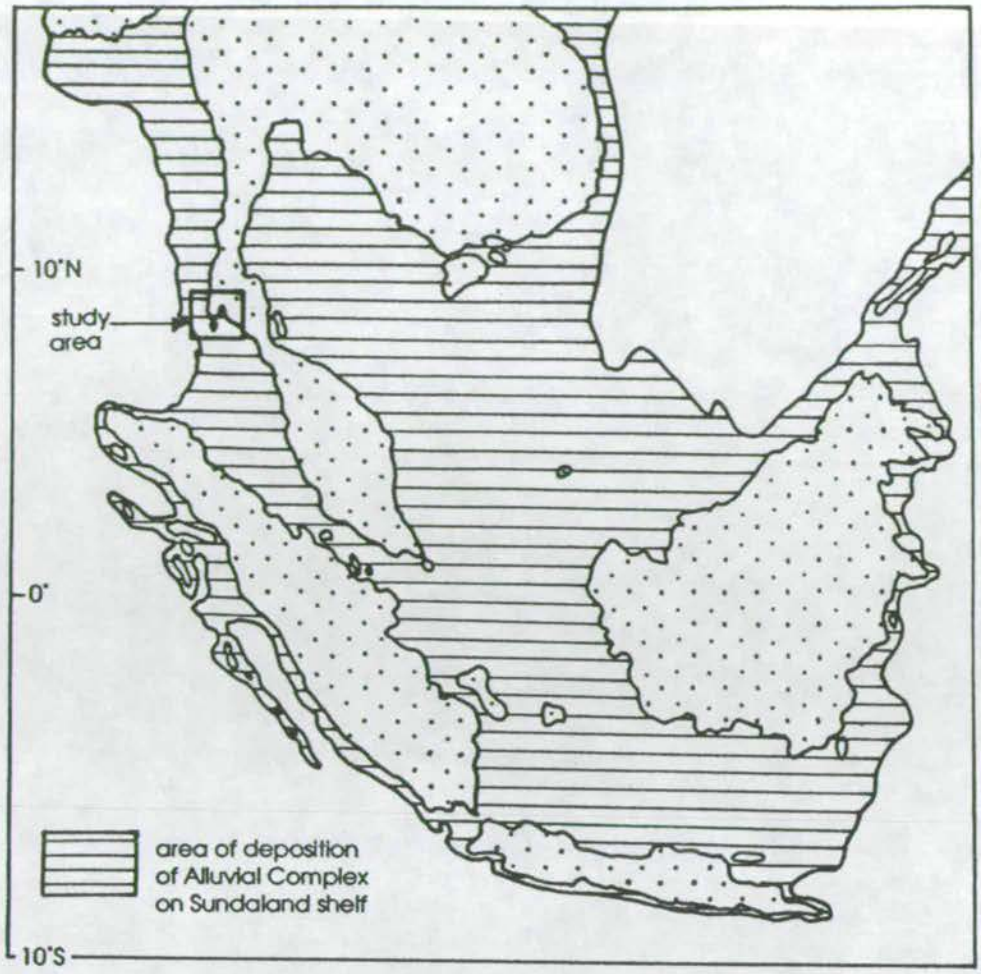

Figure 9.1 Extent of Sundaland shelf area and extent of deposition of the Late Pleistocene Alluvial Complex (from Batchelor, 1979).

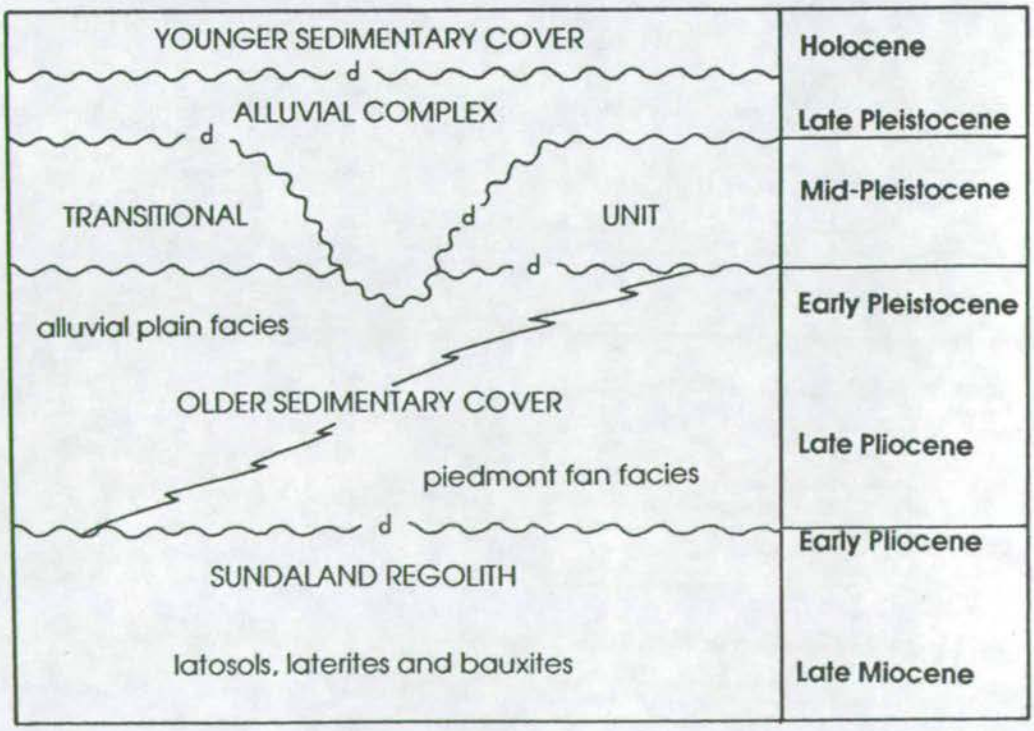

d = disconformity

Figure 9.2 Regional Late Cenozoic stratigraphic relationships of the Sundaland area (from Batchelor, 1979).

Batchelor's stratigraphy is summarised in figure 9.2 and is described below. During the late Miocene to early Pliocene, sea-level hovered below the continental shelf break (Vail et al 1977) thus continental red bed sedimentation and deep laterisation took place on the exposed Sundaland continent. These deposits are termed the Sundaland Regolith. Sea-level started to rise from the late Pliocene to early Pleistocene and rainfall increased thus increasing denudation with the resultant formation of alluvial plains and piedmont fan facies of the Older Sedimentary Cover. After varying continental sedimentation in the mid-Pleistocene (the Transitional Unit) sea-level rose over the continental shelf break resulting in large scale shifts in coastline position from the mid-Pleistocene to Holocene. Before sea-level reached its present level at the beginning of the Holocene, alluvial sediments of the Alluvial Complex consisting mainly of meander channel and floodplain deposits developed over exposed areas of the shelf.

It is these Alluvial Complex sediments that are thought to be presently exposed in the southern area of Phangnga Bay and were derived from sedimentation associated with the two ancient rivers which flowed down either side of the Ko Yao islands (Hummel and Phawandon, 1967). Geyh et al (1979) dated submerged brackish peats in the Malacca Straits (just south of the Phangnga region) and concluded that sea-level in this region was 40-60m below the present level 36 - 10ka ie, for much of the Late Pleistocene. Eustatic sea-level curves developed for the Late Pleistocene (eg, Chappell, 1974) show sea-level hovering at approximately -30 to -60m (Fig 9.3). The water depths in the south of the study area are in the 30-60m

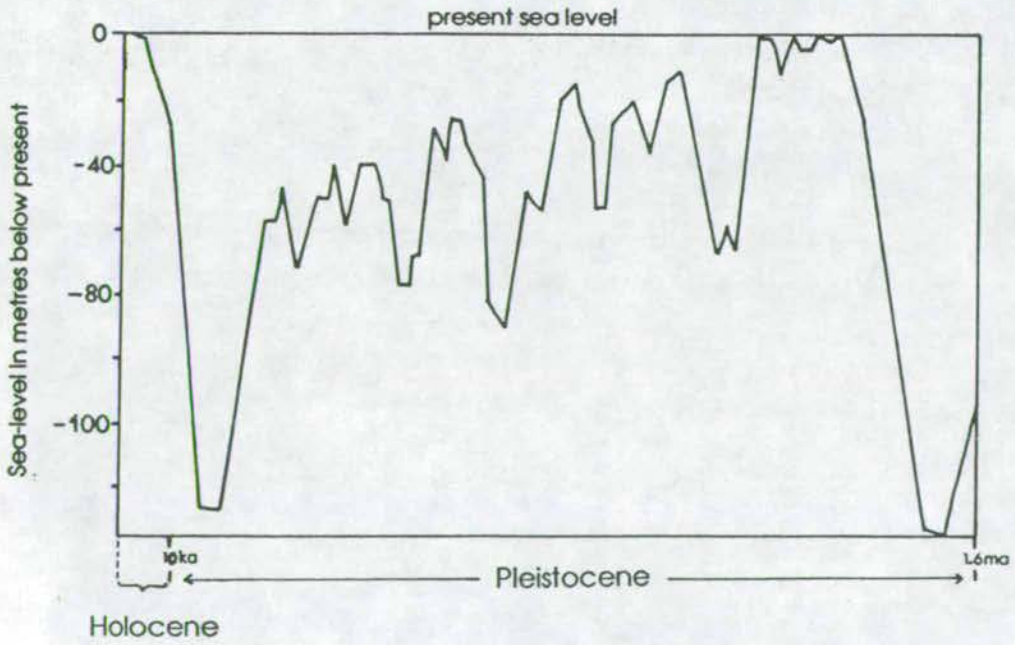

Figure 9.3 Quaternary sea-level curve from coral terraces in New Guinea (from Chappell, 1974).

range (Fig 1.4) and it is suggested that these sediments represent shallow coastal reworking of the Alluvial Complex sediments. The large area of high Sn anomalies in this region (Fig 4.27) may represent a coastal placer deposit. Batchelor (1979) discusses the various types of Sn placer found in the SE Asia area. He notes that they have had a lengthy development from the mid-Miocene when primary mineralisation was first exposed and that some placers in the Alluvial Complex have been reworked and further concentrated by waves and tides. Some of these can be laterally extensive and not restricted to narrow strandline morphologies. It would be interesting to see if the high Sn anomalies extend further south and east of the study area following a 30-60m bathymetric level as would be expected if these sediments are a result of coastal reworking during the Late Pleistocene. Some vestige of the low sea-level stand topography may also be evident by the lack of heavy minerals (shown by low Fe/Al, Zr/Al, Ti/Al and Sn values) to the NE of Ko Racha Yai where there is a slight bathymetric high. Concentration of heavy minerals would not occur on knolls but only in the surrounding lower areas. Interestingly, Rb/Al does not show any lower values in this area. This may be because mica (containing the Rb) is not subject to the same depositional processes as heavy minerals and is more likely to be carried over and deposited in higher areas.

Batchelor (1979) also notes that in the Malacca straits area (between Malaysia and Sumatra) anomalous Sn-rich areas are found restricted to off-shore granites and their mineralised contact zones. As was discussed in Chapter 4 (section 4.5.2.3) it is thought that such a mineralised zone may outcrop subaqueously in the Ko Racha Yai area and may account for the Sn and Rb anomalies to the north and east of this island.

There are, therefore, two possible origins of the high Sn and Rb anomalies in the south-western part of the study area:

a. a relict coastal placer deposit

b. recent sediment sourced from a tin-rich mineralisation zone.

It is thought likely that a combination of these two origins explains the anomaly. Highest Sn values are centred near Ko Racha Yai possibly recently sourced from an exposed Sn-rich zone but significantly high Sn values spread over quite a large area away from the island which may represent relict placers reworked in high energy coastal environments during low sea-level stands.

9.2.2 Holocene Deposition

A picture of Holocene sedimentation in Phangnga Bay may be built up with the use of accumulation and progradation rates and consideration of the characteristics of surface and sub-surface sediments along with comparisons from other studies.

9.2.2.1 Sediment Accumulation rates

In order to calculate accumulation rates of Holocene sediments in the north of the Bay, 7 samples of shell and wood from cores were radiocarbon dated by accelerator mass spectrometry at the AMS Unit, Oxford, Britain. Samples were taken from a range of depths in 6 different cores. The position of these cores is illustrated in figure 9.4a.

The radiocarbon dates are listed in Table 9.1. A correction of -450 ±35 years for all shell sample dates has been applied to account for the apparent age of marine carbonate (from the age of Australian coastal water carbonate (Gillespie and Pollach, 1979) as there is no available age for Thai coastal waters) and +40 years to correct ages to the date of collection (as all dates are published as radiocarbon years B.P. 1950). Sediment accumulation rates have been calculated by dividing the depth by the age and are also listed in Table 9.1 and alongside the core sites on figure 9.4a.

An attempt was made to select skeletal carbonate samples of the same genera for radiocarbon dating, however, this was not possible for these cores and so a variety of genera were used. It is thought that the *Paphia* samples provide more reliable dates than both *Ostrea* and Barnacle fragments. *Paphia* is an infaunal bivalve which is known to burrow to 4-6cm in the sediment (Limpsaichol, pers comm) and is therefore more likely to be preserved in place than *Ostrea* or Barnacles which are epifaunal and thus more prone to dispersal through sediment transportation processes. The *Ostrea* sample from core 44 at a depth of 44-46cm gives an anomalous date and accumulation rate compared to the sample above it in the same core and other samples at similar depths (Table 9.1). It is thought that the *Ostrea* fragment may represent a reworked deposit possibly from a storm event. Dates from the other non-*Paphia* fragments appear consistent.

The dates from cores 87 and 88 are remarkably similar. These cores were taken 50m apart, from in front of a large development of mangroves and the similarity of the

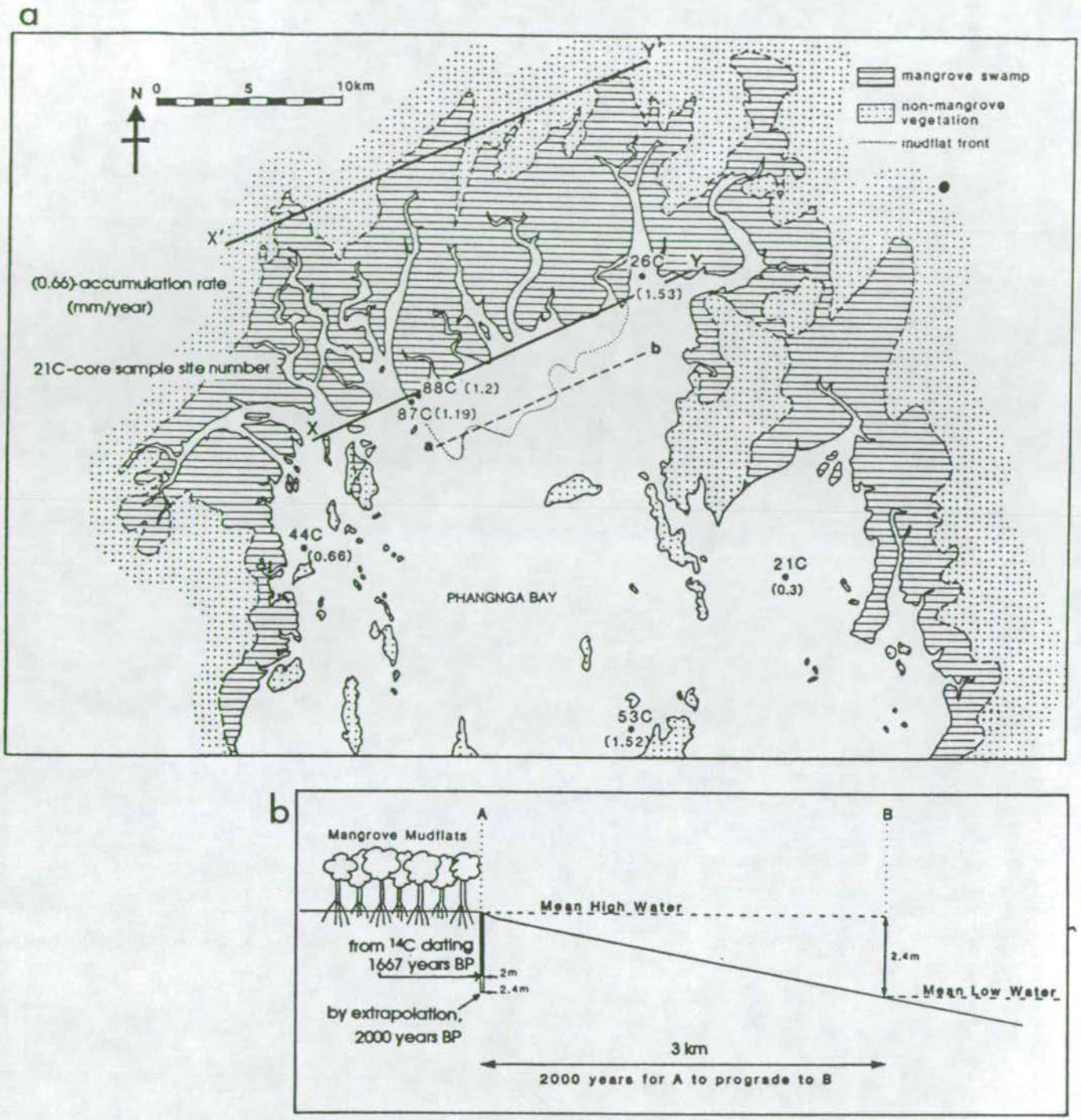

Figure 9.4 a. Location of cores for which radiocarbon dates and hence accumulation rates have been obtained.
b. Method of calculation of progradation rates of mangroves (see text for explanation).

Laboratory Reference	Core No.	Depth down core (cm)	Uncorrected Sample Type	Corrected ^{14}C Age (years)*	Age (years)#	Apparent Accumulation Rate (mm/year)
OxA-2699	21	30-32	*Paphia undulata* (infaunal bivalve)	1440 ±60	1030 ±69	0.3 ±0.02
OxA-2700	26	28-30	wood fragment (?mangrove)	150 ±60	190 ±60	1.53 ±0.5
OxA-2701	44	44-46	*Ostrea sp.* (oyster)	3220 ±70	2810 ±78	0.15 ±0.006
OxA-2702	44	26-28	*Paphia gallus* (infaunal bivalve)	820 ±60	410 ±69	0.66 ±0.1
OxA-2703	53	46-48	*Paphia undulata* (infaunal bivalve)	720 ±60	310 ±69	1.52 ±0.3
OxA-2704	87	185-190	Barnacle fragment	1980 ±70	1570 ±78	1.19 ±0.06
OxA-2705	88	210-215	*Ostrea sp.* (oyster)	2170 ±70	1760 ±78	1.2 ±0.06

* the age in radiocarbon years B.P. (Before Present - AD 1950) provided by the Oxford AMS laboratory.

the age in radiocarbon years before year of collection (1990) and with a marine reservoir correction.

Table 9.1 Details of radiocarbon dates of samples from cores in the north of the Bay.

	Ao Luk 21C	Mangrove Channel Sand 26C	Open Intertidal Mud 53C
AAR	0.3	1.53	1.52
CAR	0.25	1.37	1.17
UAR	0.48	2.3	3.3
Flux	19.4	179	78.6

AAR - apparent accumulation rate (mm/year)
CAR - compacted
UAR - uncompacted
Flux in $mg/cm^2/year$

Table 9.2 The 3 types of accumulation rate and flux calculated for cores 21C, 26C and 53C.

accumulation rates is good evidence for the consistency of the dates. The dated sample from core 26 is a woody fragment possibly of mangrove origin taken from a mangrove channel deposit. In this case the core was taken from near the mouth of the channel in line with cores 87 and 88 at the front of the mangroves (Fig 9.4a) and shows a similar accumulation rate. This indicates that despite more material being available for deposition in channels (due to the concentration of river-borne sediment in these areas) the scouring effect of tidal currents and river flow prevents sediment from accumulating any faster than the adjacent mangrove mudflats.

The date from core 53 also gives a similar accumulation rate to cores 26, 87 and 88, however this core was taken from approximately 16km south of the mangroves and north of Ko Yao Noi (Fig 9.4a). Plate 18 shows an image of Phangnga Bay taken by Satellite on 4th February 1988. This image shows the pattern of sediment-laden water quite clearly as lighter areas within Phangnga Bay and west of Phuket Island (patches of cloud are also evident as lighter areas over southern Phangnga Bay and Ko Yao Yai and also west of Phuket - they can be picked out from the gradational patterns of water turbidity by their more sharply defined shape and occasionally from the shadows below them). It can be seen from this image that sediment-laden water outflowing from the mangroves (either from fluvial input or resuspension of fine intertidal and mangrove muds) flows south and is trapped in the area of core 53 in the lee of the island which protects the area from the tidal inwashing of sediment-free marine water from the south and allows sediment to accumulate. Cores 21 and 44 are also from areas south of the main mangrove development (Fig 9.4a) but do not appear to be affected by the main plume of sediment coming south from these mangroves (Plate 18). The mangrove catchment areas directly affecting the regions of cores 21 and 44 are smaller than the mangrove development north of cores 26, 87 and 88 and so would be expected to be discharging a smaller volume of sediment into these areas. The slower sediment accumulation rates seem to confirm this theory.

The accumulation rates listed in Table 9.1 are calculated by dividing the depth of the dated sample by its age. This is the apparent accumulation rate (AAR) and takes no account of the varying density of sediment throughout the core. Soft sediment cores consist of an upper part which has a high water content and therefore relatively low dry bulk density (DBD) above compacted and dewatered sediment of relatively high DBD. By "decompacting" the core to the DBD of the surface sediment and dividing the resultant thickness of the core by the time taken

Plate 18 T.M. satellite image of Phangnga Bay on 4th February, 1988.
(image obtained from the Edinburgh University, Department of Geography, Gemstone system)

for it to deposit, an uncompacted accumulation rate (UAR) is obtained. This approximates to the net sediment accumulation experienced by sessile benthos. Alternatively, by 'compacting' the core to the DBD of the lower part, a compacted accumulation rate (CAR) is obtained which approximates to that which would be determined for an equivalent sediment in the rock record. A sediment flux (expressed in $mg/cm^2/year$) can be determined by multiplying the AAR by the mean DBD of the whole core down to the dated horizon.

The 3 types of accumulation rate and the flux have been calculated for 3 cores (see Appendix D for data tables). These cores show a relatively constant composition throughout their depth and therefore DBD does not vary significantly as a result of differing grain size. The accumulation rate and flux results are summarised in Table 9.2.

For core 21, the UAR and CAR are not very different from the AAR. However, all these values as well as the flux are low compared to Cores 26 and 53 which is consistent with the theory of comparative lack of sediment input and deposition in the Ao Luk area. Core 26 is composed of mangrove channel sands which despite showing a very similar AAR to the muds of Core 53, show a higher CAR, lower UAR and much higher flux. The greater flux is due to the higher ρ_{bulk} density of quartz sands compared to clays. This similarity of AARs between both these cores and cores 87 and 88 reflects the comparable vertical accretion of the mangrove channels with the surrounding mangrove swamps and intertidal muds subjected to a similar sediment supply. However, the lower CAR of the muds of core 53 compared to the sands of core 26 show the greater susceptibility of muds to compaction. It is likely that the muds surrounding the channel sands will show the same increased compaction as illustrated by core 53. Hence on burial and preservation of these sediments the muds will compact around the relatively resistant channel sands as illustrated in figure 9.5.

Such a phenomenon is well known in the geological record. An example is the compaction of coal and muds around channel sands in the Upper Cretaceous Ferron Sandstone member of the Mancos shale in central Utah (Ryer and Langer, 1980). In this example it was calculated that a coal bed had compacted 11 times more than the surrounding channel sand.

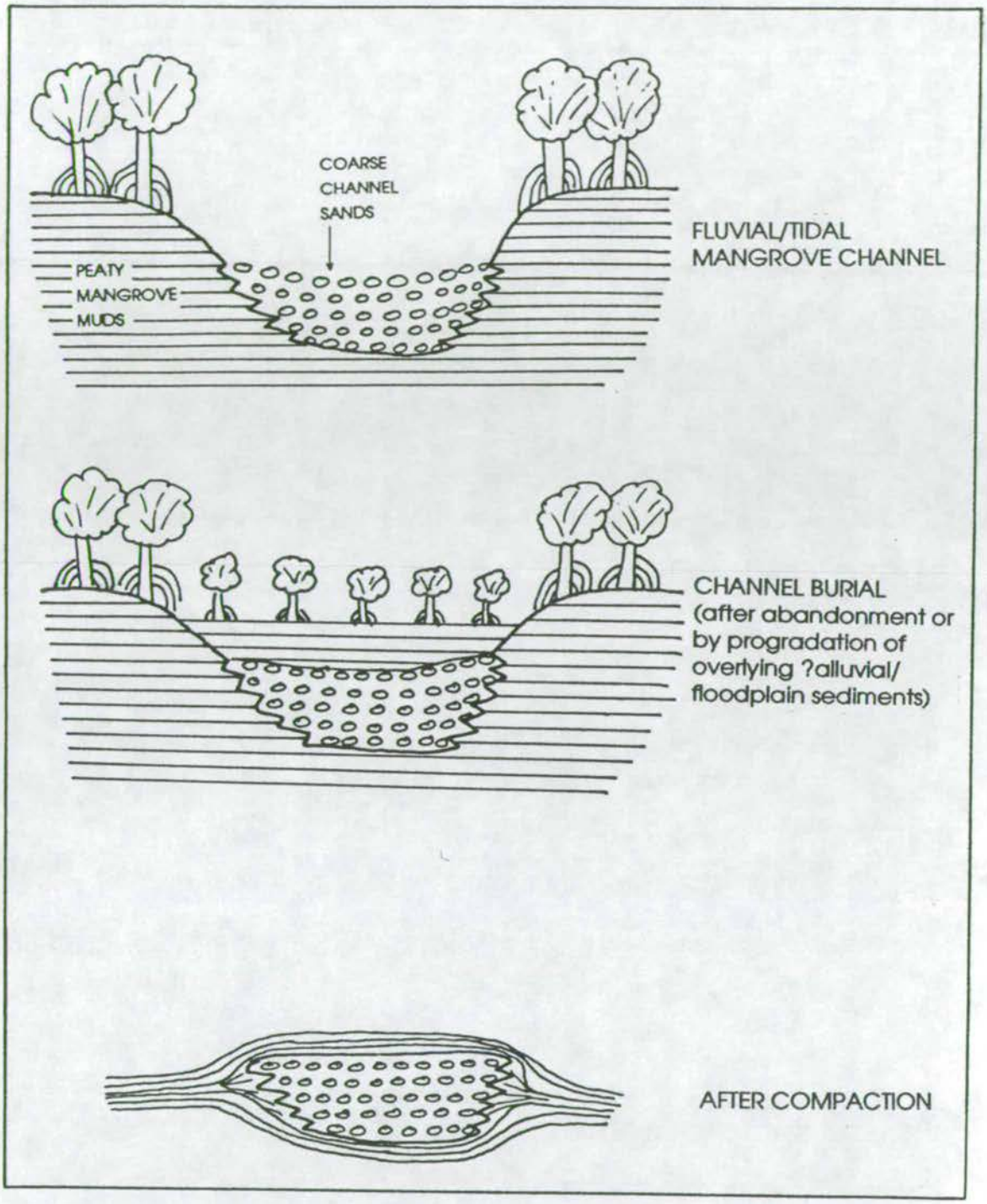

Figure 9.5 Schematic illustration of the process of greater compaction of mangrove muds around coarser channel sands.

9.2.2.2 Mangrove system progradation rates

Radiocarbon dates not only provide an indication of the vertical accumulation of sediment but also help in estimating the horizontal accumulation or progradation rate of the entire mangrove system. In the calculation of the progradation rate 2 methods have been used:

1. Figure 9.4a illustrates how **past mangrove growth** has been used to estimate mangrove swamp progradation rates. Line XY has been drawn across the present-day front of the mangrove development. Line X'Y' has been drawn across the approximate northern-most extent of mangrove development. The distance between these lines is approximately 10km and reflects the extent of mangrove growth since sea-level stabilised 6000 years ago (Thom et al, 1969 and Lowe and Walker, 1984) after the Holocene transgression. A simple calculation gives a progradation rate of 1.67m/year. The main problem with this method is that the extent of alluvial plain sediment progradation over the northern area of the mangrove swamp environment in the last 6000 years is not known. As the mangrove front progrades seaward a succession of environments from mangrove swamp to wholly terrestrial vegetation and sedimentation would develop and this whole system would be expected to prograde over the originally more seaward deposits. So if line X'Y' is to represent the coastline 6000 years ago when sea-level reached its maximum after transgressing and mangroves started to develop, then it should probably be further north and the rate of 1.67m/year is the **minimum** progradation rate.

b. The second method involves **predicting the future progradation rate** of the mangrove system using radiocarbon dates. The method for this is illustrated in figure 9.4a and 9.4b. If we assume that the present day level of the mangrove swamp represents mean high water and that the line of the southern-most extent of mudflats (line a'b' on figure 9.4a from published maps) represents mean low water then the height between these 2 levels is the mean tidal range which for northern Phangnga Bay is 2.4m (Siripong et al, 1987). These levels are illustrated on figure 9.4b and the horizontal distance between them of 3km is taken from figure 9.4a (ie, the distance between line XY and ab). The radiocarbon date of shells from cores 87 and 88 taken from directly in front of the mangroves, gives an accumulation rate of 1.2mm/year therefore the calculated age at 2.4m depth is 2000 years. The prediction is that it will take 2000 years for 2.4m of sediment to accumulate at point B (Fig 9.4b) thus bringing that point up to the mean high water level which

will represent the mangrove edge. This means it will take 2000 years for the mangrove edge to move south 3km which gives a progradation rate of 1.5m/year.

If we move the mudflat edge 0.5km either way (which allows for some error in the assumed positioning of this edge as well as in the positioning of the mean high and low water levels) then rates of 1.25 and 1.75m/year are obtained.

A major assumption in both models is that progradation rates have been continuous over the last 6000 years. A change of slope in the depositional basin would alter the rate of progradation (ie a steeper slope would require more vertical accretion to reach sea-level thus inhibiting horizontal accretion), however it is thought that the area over which these mangroves have developed is of a constant very low angle slope. This is evidenced from the development of tower karst limestone islands in this part of the Bay which are known to form from the extreme tropical weathering of limestone platforms and tend to develop very flat alluvial plains between the resulting outcrops as is seen in southern China (Scoffin, 1987 and K.Dobbie, pers comm). Phangnga Bay's tower karst is thought to have developed from the erosion of the Rat Buri limestone (Garson et al, 1975) during the low sea-level stands of the glacial periods when the northern part of the Bay would have been high and dry and a similar flat alluvial plain will have developed. Rates of progradation may also have varied due to climatic alterations affecting the volume of sediment discharge into the Bay. Over the last 6000 years the monsoons are thought to have weakened in intensity after their peak in strength 12-6ka (COHMAP members, 1988). This weakening to present day levels may also represent decreased precipitation hence decreased run off. Precise precipitation levels for the past 6000 years are not known and so it is assumed that run off has remained relatively constant over this time interval, however, it remains a possibility that run off has decreased and so absolute progradation rates may have gradually decreased.

Despite the various assumptions the figures produced above are well within an order of magnitude of each other and the figures of 1.67m/year and 1.5m/year from both methods are highly comparable.

Comparing these results to rates from other mangrove areas shows that Phangnga Bay has similar progradation rates to Broad Sound in Eastern Australia where accumulation rates for mangroves were calculated at 0.6 to 2.4mm/year and progradation rates of 1.2 to 1.7m/year (Cook and Mayo, 1978). Accumulation rates

for Missionary Bay also in Eastern Australia (Risk and Rhodes, 1985) are much faster (10mm/year) however progradation rates are slower (1m/year) indicating that the mangrove deposits are accumulating comparatively faster vertically than horizontally. This may be in response to tectonic subsidence which will increase the relative sea-level thus increasing the accommodation space for vertical accretion. Alternatively it may reflect a steeper gradient in the depositional basin which will slow horizontal progradation. Although these rates are geologically rapid, Coleman et al (1970) report progradation rates of 6m/year in the Klang delta (which is south of Phangnga Bay on the west of the Malaysian peninsula) and rates of 125m/year have been recorded in Sumatra and up to 200m/year in Java (MacNae, 1968).

Kukal (1971) gives a chart of the comparison of sedimentation rates between various depositional systems. For bays and lagoons the rate varies between 100 - 3000 cm/1000 years (0.1 - 3 mm/year) and for deltas the rate is given as > 50cm/1000 years (> 0.5mm/year). Such figures are comparable with the rates measured in Phangnga Bay.

9.2.2.3 Evolution of the predicted stratigraphic sequence

Figure 9.6 is a series of simplified, somewhat schematic stratigraphic cross-sections through the Late Pleistocene to Holocene as predicted by surface sedimentation, cores and studies from similar areas. The cross-sections run from the sheltered north of the Bay ("tower karst") to the open southern area ("Ko Racha"). Vertical "scale" is greatly exaggerated and the horizontal scale is not accurate as the central area is fore-shortened. However, the diagrams serve to illustrate what is thought to be the evolution of the stratigraphic sequence in the Bay.

Late Pleistocene sedimentation (Fig 9.6a) was sub-aerial throughout most of the Bay but coastal reworking of earlier alluvial sediments may have occurred in the south partly accounting for the high Sn concentrations in this area (section 9.2.1). It is possible that the alluvial plain was heavily vegetated and at a low angle of slope with meandering river channels (Batchelor, 1979). Park et al (1991) noted that the erosional pre-Holocene surface of Gunhung Bay in Korea formed during low sea-levels shows up in shallow seismic stratigraphy as a strong mid-reflector and v-shape patterns in this reflector indicate the existence of channels. It is possible that coral reefs developed around Ko Racha Yai although this is purely conjectural.

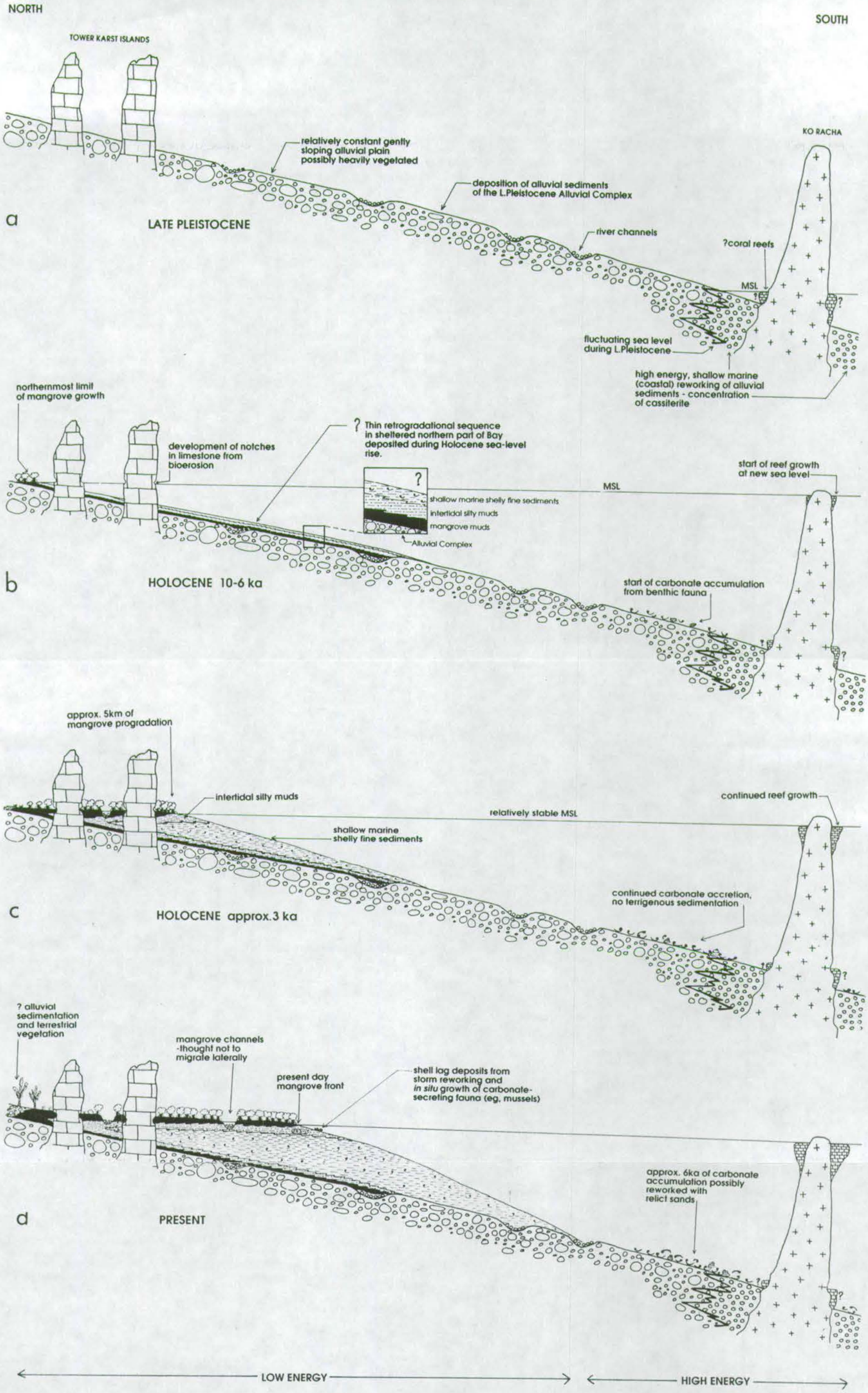

Figure 9.6 Schematic and simplified stratigraphic cross-sections of deposition in Phangnga Bay in a. Late Pleistocene; b. Early Holocene; c. Mid-Late Holocene and d. Present.

The **Early Holocene** (approximately 10-6ka - Fig 9.6b) is characterised by a rapid and large sea-level rise (Fig 9.3) as a result of the melting of the Pleistocene ice-sheets. Hence the coastline is thought to have moved rapidly north to a region near the present northern-most limit of the mangroves. The alluvial valleys on either side of the central Ko Yao islands were flooded. Any fine material in the surface sediments of the south of the Bay will have been winnowed out through coastal reworking as the coastline moved north. In the diagram a thin transgressive sequence of mangrove muds, intertidal silts and shallow marine shelly sediments has been included. As sea-level rose into the sheltered part of the Bay it is possible that fine sediments sourced from the north started to accumulate allowing the growth of mangroves which can establish and reach maturity in 10-30 years (Tomlinson, 1986). As sea-level continued rising the mangrove sea/land boundary moved north and mangrove muds were overlain by intertidal and then shallow marine sediments. Although such a transgressive sequence is conjectural for Phangnga Bay, such a sequence has been recorded in Missionary Bay, Australia (Risk and Rhodes, 1985). Conversely, Cook and Mayo (1978) found no evidence of a transgressive sequence in Broad Sound, Australia and concluded that the Holocene sea-level rise was so rapid that there was no associated sedimentation. However, the Broad Sound area is arid and terrigenous input is low at the present time and probably throughout the Holocene. Phangnga Bay however, has a wetter more humid climate and with an adequate source of fine terrigenous material from deep weathering of the hinterland rocks it is quite possible that some transgressive sedimentation occurred.

The notches at the base of the tower karst islands will have started to form from biological erosion possibly from boring sponges or other intertidal borers such as gastropods, chitons and echinoids which are known to play a role in intertidal notch formation (Scoffin, 1987). In the south, the colonisation of the sediments by benthic fauna will have begun and their carbonate remains start to accumulate without dilution from terrigenous material. The fringing reefs evident around the islands in the south will have established.

Once sea-level reached its maximum approximately 6000 years ago, continued sedimentation in the north in intertidal areas allowed the colonization by mangroves into the shallower areas and the mangrove system and whole sediment sequence started to prograde to form a regressive fining-upward sequence. This is illustrated in figure 9.6c for the **Mid-Holocene** (approximately 3ka). As the mangrove muds prograded so did the mangrove channels which were initially the mouths of the

fore-shortened alluvial channels. Although there is some slumping of mud from the sides of these channels, the root system of the mangrove is an effective sediment binder and the major mangrove channels are thought to be 'bound' in a fairly constant position and simply prograde along with the mangrove swamp front (Thom, 1982). Assuming that progradation rates have stayed constant throughout the last 6000 years, approximately 5km of mangroves will have developed by 3ka. Intertidal silts and shallow marine sediments will also have prograded forward as one system.

Figure 9.6d illustrates schematically the **present-day** stratigraphic sequence. In the north, with continued sediment accumulation in the mangroves the sediment surface will be raised above the limit of tidal inundations and mangrove vegetation will be replaced by more wholly terrestrial vegetation with associated alluvial/soil progradation over the mangrove deposits. Garson et al (1975) describe the estuarine deposits of the north of Phangnga Bay gradually passing into alluvial deposits which form extensive flat areas flanking the courses of larger streams and rivers. The alluvial deposits include a wide range of unconsolidated river-deposited sediments ranging from boulder accumulations and gravels to fine silts and muds. The 2m cores from the front of the mangroves show a gradual fining-upward sequence which is thought to represent the progradation of the mangrove system over intertidal silts. Thus as according to Walthers law, the vertical sequence reflects the lateral sequence. Such a feature of fining up sediment is also seen in Missionary Bay and Broad Sound.

Restricted areas of comminuted shelly debris within a muddy matrix of sediment are found in the north of the Bay and these may be the result of storm reworking of some of the shallow sediments in the north. Also, *in situ* production of carbonate material from mussel and oyster beds accounts for some of these carbonate accumulations. Carbonate accumulation also continues in the south - there may be some reworking from currents (particularly around Ko Racha Yai) and deep wave action (particularly during the south west monsoon). Reefs continue to grow although vertical reef growth has been superseded by horizontal reef flat consolidation and progradation.

It has been assumed that relative sea-level stayed constant after the Holocene transgression. However, there is evidence of previously higher sea-levels in this region (Hummel and Phawandon, 1967). Small patches of marine sediments are found at various localities above present sea-level on Phuket Island and also near

the west coast in Phangnga Province where clays and silts rest on an erosion surface in mudstones of the Phuket Group (Chapter 1) approximately 10m above present sea-level. This erosion surface is commonly covered with abundant recent marine mollusc shells and locally shows mollusc borings. However, there is no evidence of raised reef or beach deposits. From the study of onshore sediments from the south-western Malaysia peninsula, Geyh et al (1979) concluded that sea-level rose to +5.8m between 8-4ka and then fell to the present level. Since the Thai/Malaysian peninsula area is tectonically stable it is likely that such high levels are also applicable to the Phangnga region. However, such levels are not high enough to account for the marine deposits at 10m above present level in the region and so it is more likely that these deposits are a result of Pleistocene high sea-level stands. However, the fact that sea-level has fallen since its peak after the Holocene transgression suggests that progradation of the Holocene sediments may have been accelerated as the vertical accommodation space for accretion will have decreased and sediment will have been deposited at the front of the system rather than on top thus increasing progradation. Also, a fall in sea-level causes incision of streams due to the corresponding fall in base level. Such incision results in increased sedimentation at the coast.

As a summary to the above section, the terminology of sequence stratigraphy will be applied to the Late Quaternary sediments of Phangnga Bay. The Late Pleistocene sedimentation represents a lowstand systems tract which is bounded above by a sequence boundary (an erosional unconformity). This is possibly overlain by a transgressive systems tract (if there are Early Holocene sediments) which is then overlain by a highstand systems tract of progradational sediments (Fig 9.7)

9.2.2.4 The development of mangroves

Mangrove swamps are tropical analogues of temperate salt marshes and develop only where coastal physiography and energy conditions are favourable. They are most extensive where there is a low shore gradient in a sheltered area (eg, Phangnga Bay). On coasts which are exposed, mangroves are localised in the lee of other coastal landforms (Woodroffe, 1983). Although mangroves are often associated with fine-grained sediments they are able to grow on a wide range of substrate types including sandy, reefal or rocky substrates.

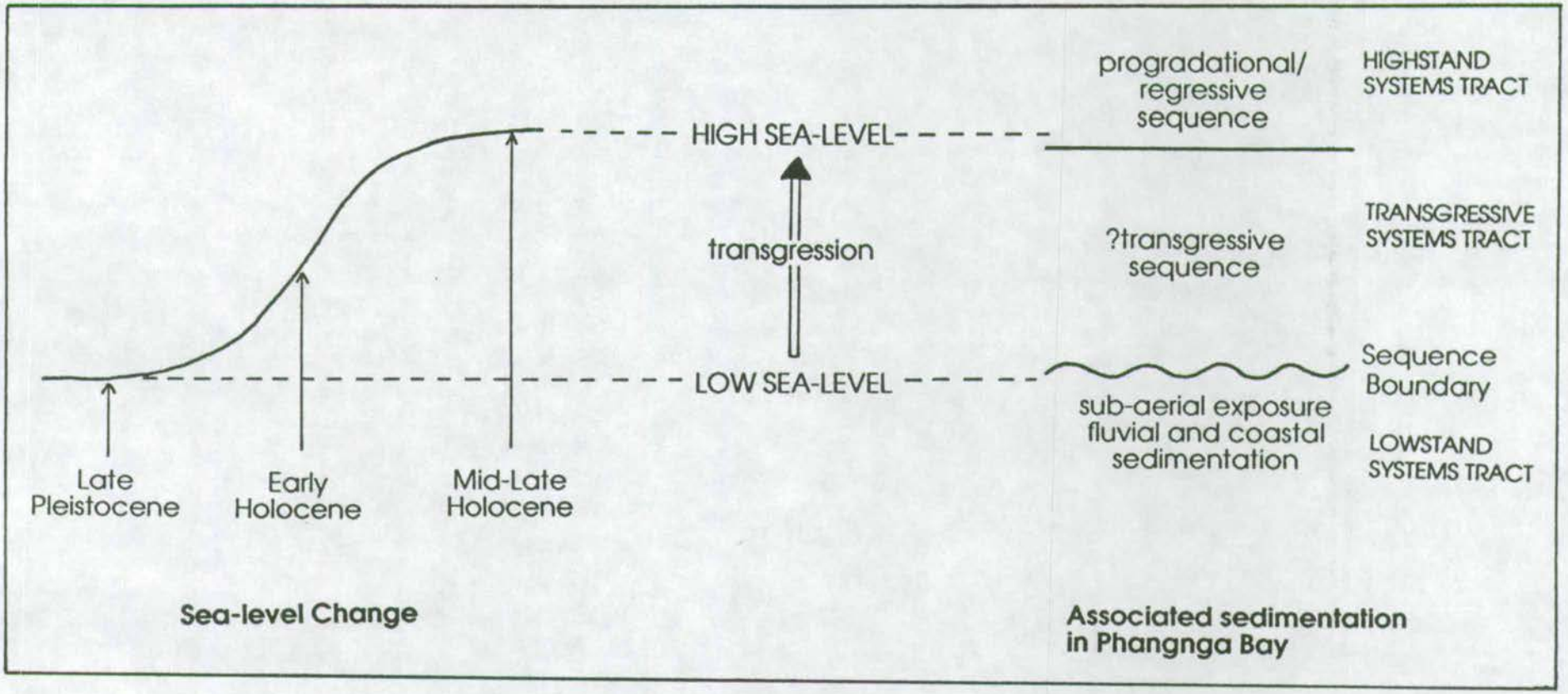

Figure 9.7 Application of the terms of sequence stratigraphy to the Quaternary sedimentation in Phangnga Bay.

In the varied literature on mangrove systems and the processes affecting their formation and development, there are two main schools of thought on the inter-relationships between the mangroves themselves and the sediment they grow on.

The first and generally older school follows the classic successional view of mangrove dynamics where purely biotic processes induce soil accumulation and as this accumulation gradually changes the environmental conditions for the biota, (eg, decreased tidal inundation, increased fresh water flushing) a different type of plant succeeds the previous type and so there is a succession of plant types from purely mangroves seaward to purely terrestrial plants landward (Watson, 1928; Rosevear, 1947; Kuenzler, 1974). Associated with the concept of species replacement through time is the belief that the seaward species has the ability to prograde into shallow water. The viviparous nature of seedlings (ie, the seeds have reached an advanced stage of development on release from the parent plant) of most species of mangroves appears to support this and several early workers regarded mangroves as "makers of land" (Curtis, 1888; Philips, 1903; Davis, 1938) ie, without the mangroves no sediment would accumulate.

The second, more recent school of thought suggests that mangroves are simply opportunist organisms only colonising suitable available substrates. Several studies on harbour and estuarine environments in eastern Australia have shown that vegetation on mangrove shorelines is dynamic but the movements of the mangrove margins are found to occur subsequent to sedimentation on seaward flats (Bird, 1971; Bird and Barson, 1977; Thom et al, 1975, Butler et al, 1977). In these geomorphologically active areas where allochthonous sediment inputs can be large, the general view appears to be that mangroves can modify the rate at which sediment processes can take place but generally do not change the pattern of landform evolution.

The discussion revolves around the question of whether the fine sediment would still be there and prograde so actively without the binding action of the mangrove roots and pneumatophores. A study of mangrove and intertidal morphology in Westernport Bay, Australia (Bird, 1986) addressed the question of whether mangroves promote sedimentation and therefore the evolution of depositional landforms or whether they simply occupy sites that have become ecologically suitable thereafter stabilising and protecting the intertidal morphology that would have formed independently. The conclusion is that mangroves trap sediment thus

forming a terrace - this sediment would otherwise have remained mobile in the intertidal zone. This terrace does not form in open intertidal areas and if die-back of mangroves occurs, the terrace is rapidly eroded. Measurements showed sustained accretion in the mangrove fringe in contrast with variability in surface levels on adjacent mudflats.

A general consensus seems to be being reached that a shallow water substrate must be available for the mangroves to establish (they can only colonise a stable shore out to approximately mid-tide level (Bird, 1986)) and sedimentation in front of the mangrove fringe must continue in order for the mangroves themselves to prograde. But once the mangroves have established, they promote further sedimentation as well as helping preserve the sediments assuming conditions such as sea-level remain stable. With vertical accretion and horizontal progradation the process of succession of plant species becomes apparent. However, this is a generalisation and probably only strictly applicable to areas of prograding mudflats (common along the west coast of the Thai/Malaysia peninsula). In other areas, the variety in magnitude and frequency of geomorphic processes through time (eg, cyclones, wave action, river run-off) may interrupt patterns of landform development and create a close mixture of actively accreting and eroding landforms such as is evident in the Cambridge Gulf-Ord River region, Northern Australia (Thom et al, 1975).

At first glance the large development of mangroves in the north of Phangnga Bay may be regarded as a typical prograding mudflat type with deposition of shallow intertidal sediments over which the mangroves can prograde with a succession of vegetation types landward of the mangrove fringe. Certainly this has probably been the case for most of the Holocene but the present day mangrove fringe does not have the characteristics of a prograding mangrove system. Bird (1986) describes the characteristics of an advancing mangrove fringe as a gradual seaward sloping profile of the mangrove canopy with mangrove seedlings surviving along the seaward margin to advance the vegetation (Fig 9.8a). By contrast, in Phangnga Bay the seaward margin of the mangroves is abrupt with only mature trees on the seaward edge and trunks and stems of mangrove trees visible from the sea (Fig 9.8b and Plate 19). Bird (1986) describes this as the aspect of a stable vegetation fringe - he concludes that in these areas accretion rates are generally too slow to permit extensive advance of the mangrove fringe. Could this be the case for the Phangnga Bay mangroves? Unfortunately there is little information

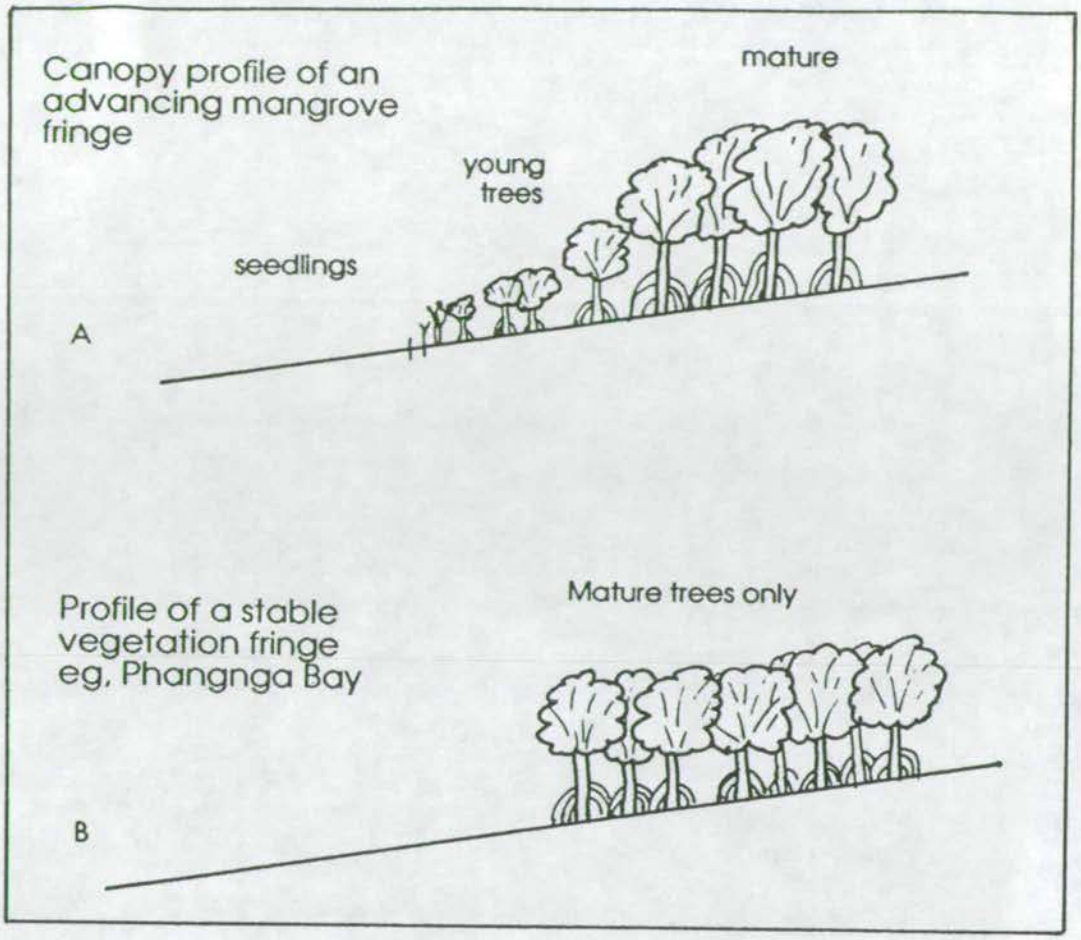

Figure 9.8 Comparison of characteristics of an advancing mangrove fringe (a. - from Bird, 1986) with that seen in Phangnga Bay (b. - and also Plate 19).

Plate 19 Front of main mangrove development in the north of Phangnga Bay illustrating the mature trees and lack of young plants at the mangrove front (author for scale!).

available on other mangrove developments around the Bay and whether such a feature of lack of young mangroves at the front is of regional extent. However, some theories which may explain this feature for the main mangrove development will be put forward here:

1. Man's influence - since there is a great deal of human activity in the area (the local population fish in the open intertidal areas and fix stakes in the open intertidal area to mark shell beds, they also rely on the water for transportation around the area in long-tailed boats) and this may have an adverse affect on the growth of mangroves at the mangrove fringe. Disturbance by the propellers of the boats may prevent the mangrove seeds from settling and germinating, and may damage young trees. Such an explanation is unlikely considering the large extent of the mangrove front (approx 20 km) and it is unlikely that the boats will travel right at the mangrove front (where young trees will start to grow) even at high tide it would be easier to determine direction of travel by travelling away from the edge of the mangroves.

2. relative sea-level rise - if relative sea-level has recently risen in this area, the water depth limit of germination of the mangrove seeds will have moved landward and the sediment surface will have to accrete in order for the mangroves to prograde seawards again

3. decrease in sedimentation rate - this is the mechanism proposed by Bird (1986) for the maintenance of a stable vegetation fringe of mangroves in Westernport Bay, Australia. Sediment reaching the mangrove areas has decreased due to Man's intervention (cutting of drainage and transport channels through the mangroves and intertidal flats) and also due to a decrease in fine sediment sourced from a nearby intertidal area which has been completely eroded. With a decrease in sedimentation rate in Phangnga Bay, the open intertidal mudflats in front of the mangrove fringe will not accrete to a height suitable for mangrove germination, hence progradation of the mangrove front stops.

The latter two ideas are in a way related in that they result in altering the water depth in front of the mangrove fringe which if too deep, prevents the germination of the mangrove seedlings hence prevents mangrove progradation. In the recent literature on mangroves, particularly their geomorphological characteristics, little attention has been paid to the actual form of progradation. It seems to be

generally assumed that the mangrove fringe, (especially of large developments such as the one in the north of Phangnga Bay) prograde relatively constantly and gradually. However, in other fields of sedimentology it is being suggested that sedimentation in such areas as deltas, occurs in pulses (C.Kay, pers comm) in response to a variation in climate conditions eg, increased rainfall (hence increased run-off) or relative sea-level fluctuations (affecting base-level therefore denudation rates hence sediment input and deposition rates). The pulses may occur on all time scales. It is suggested here that comparatively short term pulses of sedimentation have controlled the sedimentation rate and hence mangrove progradation in Phangnga Bay. Such an idea was suggested in Chapter 8 to explain the 3 fining-up cycles in core 88. It will be built upon here and may offer an explanation as to why the mangrove front seems to be at a standstill at present.

Sea-level indicators for the time interval between 4-5ka in the Malaysian peninsula region have been found at +2.5 and +5.8m (Geyh et al, 1979). Subsequent lowering of sea-level is indicated by peat samples at +2m (2ka) and mangroves at 0.8m (1ka). However, Geyh et al (1979) note that the data does not show whether the lowering of sea-level took place steadily or through an oscillatory process. A gradual fall would result in constant sediment input and progradation rates. However, as mentioned in Chapter 8, an oscillatory fall would result in the base-level altering in steps which may result in 'pulses' of sedimentation from stream erosion down to base-level on sea-level fall (Fig 9.9). Such an influx would probably increase sedimentation rates allowing fairly rapid progradation of mangroves over a rapidly accreting mudflat. With a following sea-level stillstand (possibly with a slight rise - see Fig 9.9) equilibrium would be reached and sedimentation would decrease thus progradation would cease.

Therefore each oscillation results in a pulse of sedimentation and progradation followed by a stillstand. The large mangrove system in Phangnga Bay may have prograded rapidly in spurts followed by a period of no progradation. Is this what is happening now? Could the system be in a stillstand at present hence the mangrove system is at equilibrium (as is suggested by Bird (1986) for the mangroves of Westernport Bay, Australia)?

Obviously much of this is theoretical and highly generalised but it does offer an explanation of the sediment cyclicity in core 88 and possibly the apparent lack of mangrove progradation at present in Phangnga Bay. Much more work is needed

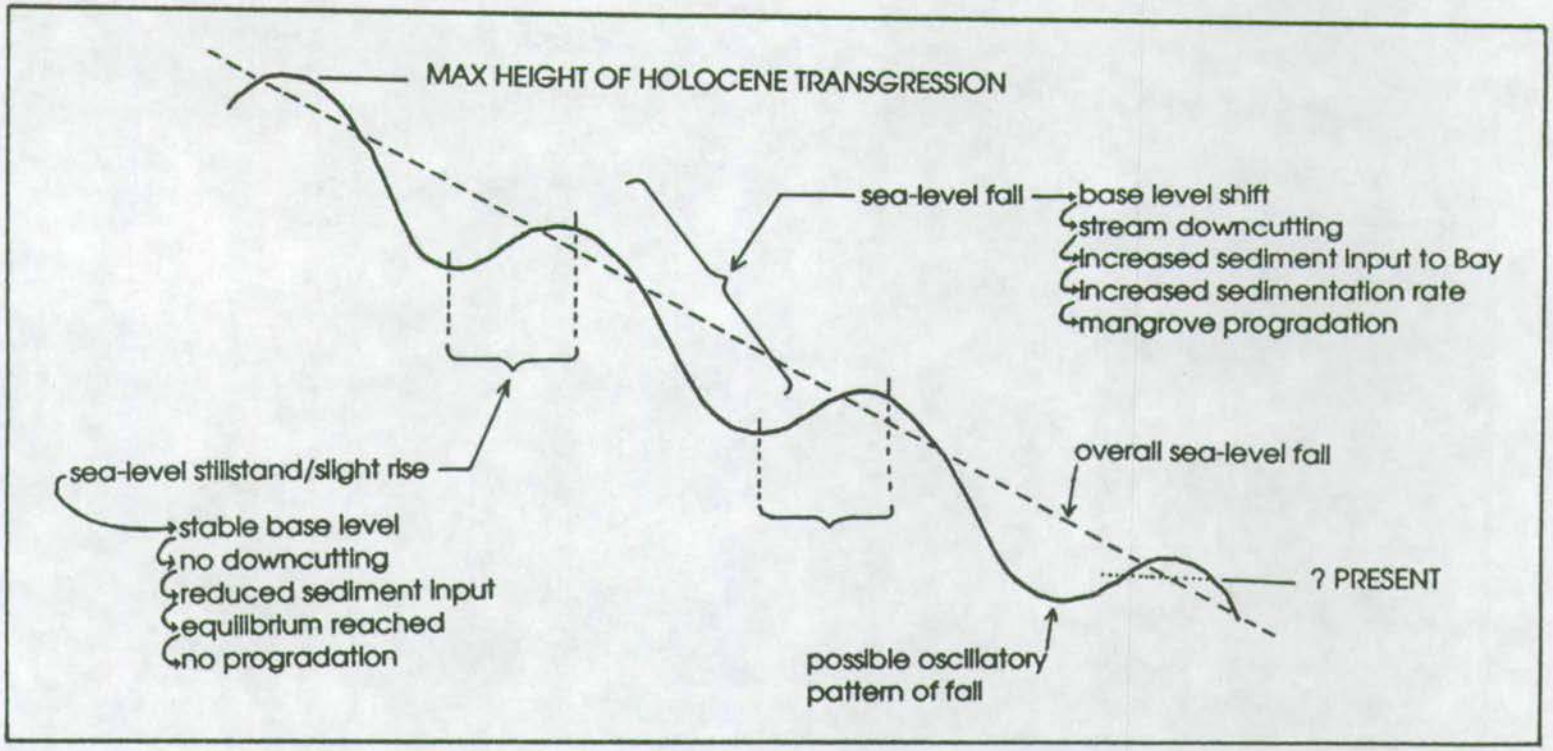

Figure 9.9 Effects of an oscillatory sea-level fall on sedimentation and mangrove progradation.

not only on sea-level fluctuations during the Holocene in this and other regions but also on detailed sub-surface sedimentation patterns in similar mangrove areas.

9.3 ANCIENT ANALOGUES

In looking for ancient analogues of sedimentary environments in Phangnga Bay it is necessary to summarise the sedimentary patterns in the area. Phangnga Bay is a shallow, sheltered bay where a large area of prograding muddy tidal flats have developed in the most landward, sheltered part of the area in semi-estuarine conditions. Such a sequence could be termed deltaic although the 'delta' is confined laterally by the sides of the Bay and channel shifting, evident in other modern deltas such as the Mississippi, does not occur. Mangrove vegetation has developed over these flats - in the geological record these would be represented by rootclays and coal horizons. In the south, in deeper but more open and high energy conditions quartz sand deposited in environments different from those present today are mixed with carbonate material which has accumulated since the last major sea-level rise. These quartz sediments are older than the muddy, intertidal sediments and are overlain by the fines deposited in the sheltered area.

9.3.1 **Ancient estuarine sequences**

In the geological record, there are examples of estuarine environments although they are not numerous (Reading, 1986). Those that have been described, such as the, Bathonian Great Estuarine Series in Skye (Hudson, 1963), the Tertiary Lower Bagshot Beds of southern England (Bosence, 1973) and Pleistocene sequences in Holland (de Raaf and Boersma, 1971) describe sequences dominated by sandy material. Criteria for recognising tidal processes in sedimentary successions include structures representing bi-polar flow, cross-beds and flaser bedding. However, sandy material has to be present to preserve and make recognisable such structures. As Alexander et al (1991) note, a paucity of sand-sized material in the mudflats of Nam Yang Bay (Korea) makes observations of sedimentary structures difficult - such a problem is evident for the fine material in the north of Phangnga Bay. Similarly, the numerous studies of sand-dominated intertidal sedimentation in present coastal environments over the years has perhaps biased the recognition of

estuarine environments in the geological record to coarse sediment dominated examples.

9.3.2 Ancient tidal flat sequences

There have been some studies which have recognised and described ancient tidal flat associations as opposed to more wide ranging 'estuarine' sequences (Kuijpers, 1971; MacKenzie, 1972; Sellwood, 1972). The examples have been recognised on the basis of an assemblage of structures and facies considered to indicate tidal processes and a fining-up sequence which reflects tidal flat progradation with thin coal and rootlet horizons capping the sequence. However, the sequences studied by the above-mentioned authors are again sand-dominated environments.

Mud-dominated intertidal sequences have been recognised in the Upper Devonian 'Catskill Delta' formation of central Pennsylvania by Walker and Harms (1971). Shales and siltstones with sparse marine fauna are thought to represent progradation of a muddy shoreline where wave action was slight, tidal range relatively low and there was a high supply of mud compared to sand. Although thin rootlet horizons have been identified there are no coals. De Vries Klein (1970) identified a siltstone/mudstone facies in the mid-Dalradian of Islay (Scotland) which he described as deposited in high tidal flat environment. This sequence overlies a massive-bedded, cross-stratified sandstone sequence which is interpreted as shallow marine or low tidal flat sedimentation. Thus the 2 sequences together represent a continuous progradational sequence rather than the progradational muds overlying an unconformity with alluvial sands below as is seen in Phangnga Bay.

9.3.3 Carboniferous analogues

The climate over much of the north Atlantic region during the Westphalian/Pennsylvanian was humid tropical and major coal-bearing strata are associated with this period in NW Europe and eastern USA. An enormous low-lying fluvio-deltaic plain covered much of the area and although the scale of such deposits are not comparable with Phangnga Bay, breaking the sequence down into smaller formations in restricted areas reveals that there may be some analogues to the Phangnga Bay situation. Two examples from the Lower-Mid Pennsylvanian of the USA will be cited here and no doubt there will be similar analogues from other areas of mid-Carboniferous sedimentation.

The mid-Pennsylvanian Allegheny formation of the north Appalachian plateau area (Ferm, 1970) is a sequence of deltaic deposits which are dominated by muddy sediments and overlain by rootlet horizons and coals. The muddy nature of the sediments is attributed both to a limited detrital supply and the development of the delta in shallow, narrow embayments (like northern Phangnga Bay) as opposed to many modern deltas which prograde out onto open continental shelves where fines are swept away (as in the south of Phangnga Bay). The delta has built out over marine limey clays and marls rather than sandstones but the actual deposition of the muds in a deltaic type of setting appears somewhat analogous to the recent deposition of sediments in Phangnga Bay.

Kvale and Archer (1990) describe the Brazil formation of the Lower Pennsylvanian of Indiana as being deposited in a mud-rich setting formed in a tropical environment near the ancient Pennsylvanian equator. The formation lacks obvious bi-polar current indicators, trace fossils are rare and generally absent and brackish water macrofossils are rare. They describe the best evidence of tidal influence as being rhythmically bedded mudstones and interbedded sandstones and siltstones, the rhythmicity being related to neap-spring tidal cycles. The siltstones are overlain by coals and whole trees are preserved which are thought to have grown in tidal areas suggesting they are Lower Pennsylvanian equivalents of mangroves. (Although extant mangrove communities can be traced as far back as the early Tertiary, establishing the presence of mangrove vegetation earlier than this relies heavily on non-morphological, geological information. Rooted horizons in sediments that contain marine or brackish water faunas or authigenic marine minerals provide one of the most reliable indications of fossil mangroves (Raymond and Phillips, 1983)). Although no large sand-dominated channel systems have been identified in the sub-surface of the Brazil formation, the authors suggest the Mahakam Delta on the east coast of Kalimantan as a modern example of the depositional environments of the Brazil formation. Because of lack of exposure it is not known what underlies the intertidal fine grained deposits of this formation.

9.3.4 A Paleogene analogue

A more recent analogue in the geological record is possibly the sediments of the Paleogene Wilcox group in south Texas (Breyer and McCabe, 1986). Paleocene and early Eocene sediments in the Rio Grande embayment of south Texas record a

progressive shallowing of water depths following an initial transgression. Paralic and fluviatile sediments of the Wilcox group overlie marine muds which were deposited on a broad continental shelf. Although the original continental shelf sediments are not described it is possible they are sandstones analogous to those in the south of Phangnga Bay which were drowned by a marine transgression. The Wilcox group is composed of mudstones deposited in intertidal areas between channel sandstones. Coal horizons are underlain by rootclays. The swamp and channel complex was thought to extend 10-30km inland from the main coastline which is on a similar scale to Phangnga Bay. The sequence is repeated throughout the group and is thought to represent repeated regressive and transgressive episodes with corresponding expansion and contraction of the peat swamps within the estuarine complex.

9.3.5 **Discussion**

Although some possible ancient analogues to the Phangnga Bay sedimentary pattern have been presented here, they are by no means common in the geological record, particularly in comparison to more coarse clastic sediment dominated coastlines. Indeed, Reading (1986) notes that "ancient tide-dominated or tide-influenced deltas have only been sparsely recognised in the geological record so far".

Could this simply be due to the bias towards studies of present-day sand-dominated intertidal and shallow marine environments which are more common in temperate latitudes (eg, eastern seaboard of USA and the North Sea coastlines)? This may have lead to a bias towards identifying such environments in the geological record since fine-grained equivalents (more common in tropical climates) are overlooked or mis-interpreted because of the lack of data on recent analogues.

This has perhaps lead to the generalised conventional ideas on shallow coastal sediment environments (especially those represented in the geological record and interpreted from electric logs and cores) that make the general assumption that coarse material represents onshore/shallow coastal environments whilst fine muds represent off-shore, quiet, deeper water depositional environments. Although in open coastline environments this is undoubtably true, in sheltered coastal bays and estuaries such as Phangnga Bay the reverse is the case. Although sedimentary structures to indicate shallow, intertidal conditions of deposition may be difficult to identify in fine-grained sediments, the study of the biogenic content of the

sediments of Phangnga Bay in this work shows that landward sediments can be clearly distinguished by a large proportion of wood and plant material in the sediment and greater proportions of marine carbonate fauna in the off-shore sediments. Even if the top part of the sequence is removed by erosion before burial (eg, the rootlet and coal horizons) the intertidal and off-shore sediments will still have this biogenic landward/seaward indicator.

On the other hand, is the lack of ancient analogues of the Phangnga Bay environment a result of a real lack of such environments in the geological record? Shallow sheltered environments are especially prevalent in times of high sea-level stands such as at the present due to the drowning of alluvial valleys created by down-cutting of rivers to base-level at low sea-level stands. Thom (1982) suggests that the present abundance of mangroves on the World's tropical and sub-tropical coasts may be partly due to Holocene sea-level changes. Perhaps the lack of such environments in the geological record is a reflection of this reliance on high sea-levels for their formation, since on sea-level fall, these deposits are unlikely to be preserved in entirety. They will be subject to sub-aerial erosional processes on sea-level fall whilst low sea-level deposits forming along more open coastlines (and hence being coarser-grained) will have a higher preservation potential by being blanketed by sub-aqueous deposition on sea-level rise.

9.3.6 **Economic aspects**

Environmental reconstruction of sediments preserved in the geological record is important in the search for hydrocarbons and many mineral deposits. It enables the search to be directed in the most prospective area once the palaeoenvironmental position is known particularly in respect to the shoreline.

As mentioned above, the mangrove swamps of Phangnga Bay may, if preserved, form a coal horizon. Equally, if the Phangnga Bay system is considered as a model of some ancient source-trap system, then petroleum source beds could be the open intertidal muds and silts containing mangrove plant debris (hence high C_{org}) as well as the preserved mangroves themselves. Risk and Rhodes (1985) suggest that the high lipid content of mangrove-derived organic matter (OM) makes such material an ideal petroleum-precursor. Because of the high rate of production of OM in the mangrove environment, the low energy of the environment preventing sediment mixing and relatively rapid sediment accumulation rates, anoxic conditions are

produced in the sediment and thus OM has a high preservation potential. Possible reservoir units would be the channel sands, beach sands and possibly even the underlying low sea-level stand deposits. Thus the model of Phangnga Bay sedimentation may have a predictive value in petroleum exploration.

A facet of this study which may have an immediate economic application is the location of heavy mineral deposits, particularly cassiterite. Although dredging is currently taking place off the south east coast of Phuket (in inshore areas - see figure 3.4), in the mangroves in the north and on the west coast of Phangnga province and Ko Phuket, there has been no dredging to the NE of Ko Racha Yai where the highest sediment Sn values have been found in this study. As discussed in Chapter 4 (sections 4.5.1.1 and 4.5.2.3) it is thought that there may be a nearby source for this Sn in the form of lepidolite pegmatite veins either on Ko Racha Yai or sub-aqueously exposed near the island. It is also a possibility that here has been Pleistocene coastal reworking of the sediments in this area thus concentrating heavy minerals and creating a placer deposit. It is not known whether it is possible to operate dredges in the water depths of this area nor whether such recovery would be economically viable considering the low Sn price which has been continually falling throughout the 1980's.

CHAPTER 10

SUMMARY OF CONCLUSIONS

CHAPTER 10 - SUMMARY OF CONCLUSIONS

This chapter aims to tie together the different facets of this study and summarise the ideas on Quaternary sedimentation of Phangnga Bay that have been put forward throughout this work.

The major conclusion of this work is that the surface sediments of Phangnga Bay represent a diachronous surface of deposition with recent fine grained sediments in the northern sheltered part of the Bay and relict coarse grained quartz and carbonate sediments in the open, southern area deposited during Pleistocene low sea-level stands. The evidence for this comes from considerations of the sediment depositional processes presently operating in the Bay. Terrigenous sediment currently being transported into the Bay from the surrounding catchment area is efficiently sorted on entry to the Bay with coarse material settling out in mangrove channels, silts and clays deposited in the shallow, low energy area in the north of the Bay and the finest material deposited in tidal mangrove swamps or transported southwards and out of the Bay. The presence of a large area of coarse sediments in the southern area cannot be explained by present day depositional processes and it is thus considered to be of relict origin. The mineralogical assemblage and texture of the quartz grains indicates that these sediments in the south are more mature than the quartz channel sands of the mangrove channels thus indicating a longer transport history and a greater degree of reworking. The geochemistry of these sediments suggests that heavy minerals are concentrated in this area. This all points to the sediments being deposited in high energy conditions which would have been prevalent during low sea-level stands when the coastline will have moved back and forth over this area thus reworking sediments sourced from the north and removing fines.

However, present-day, comparatively high energy conditions in the south compared to the sheltered north of the Bay have prevented a veneer of fine recent sediments from covering the relict sediments thus preserving them as surface sediment.

More localised depositional processes explain smaller scale variations in sediment grain size and geochemical patterns. The position of coarse grained mangrove channel sediment within very fine grained mangrove swamp sediments is a result of the concentration of tidal and fluvial currents within the channels and the dissipation

of tidal current energy over the mudflats (as well as the variation in tidal velocities and cohesiveness of muds in mangrove swamp areas). Strong localised currents result in coarse grained lag surfaces and concentrations of calcareous-secreting organisms result in localised $CaCO_3$ concentrations particularly in the north. These carbonate accumulations also affect the sediment grain size by adding a coarse fraction.

In general, $CaCO_3$ concentrations increase southwards reflecting the improved conditions for carbonate-secreting organisms. Variations in the proportions of different carbonate-secreting organisms in the sediment affect the carbonate mineralogy as well as the distribution of certain elements, particularly Mg and Sr. As an example, organisms which secrete HMC skeletons generally increase in proportion southwards thus explaining the increase in Mg_{CARB}/Ca ratios southwards. Similarly, high Sr values are found near coral reefs as a result of the incorporations of Sr in coral skeletons.

Bivalves, pteropods, ophiuroids, corals and foraminifera show an increase in relative abundance towards the more open marine conditions in the south of Phangnga Bay. This increase is thought to reflect more stable, congenial conditions in this area such as constant temperature and salinity and clear, sediment-free waters. Gastropods, scaphopods and particularly barnacles show higher relative abundances in the north of the Bay which may reflect their preference for calmer waters and/or finer-grained sediments. Plant material is restricted to the north of the Bay which reflects the near-by land-derived source of this material. The dominance of bivalves and echinoids in the biogenic component is thought to be a characteristic of tropical benthic communities, along with abundant crustaceans and the possibility of disturbance from climatic events or human activities. These characteristics are all evident in Phangnga Bay. Although both water depth and sediment type are likely to play some part in controlling benthic faunal distributions in the Bay, it is also thought that high carbonate content and high species/site values in the south may be a result of sampling approximately 6000 years of carbonate deposition since the last low sea-level stand as very little recent terrigenous material is thought to have been deposited in this area. In the north however, high terrigenous input has diluted and buried the remains of carbonate-secreting organisms.

Terrigenous mineralogy is controlled by both source effects (particularly the geology and climate of the drainage basin) and also by transport and depositional processes, particularly mixing and sorting. Quartz and clays are the dominant terrigenous minerals in the surface sediments. This along with the dominance of kaolinite and lack of chlorite in the clay mineralogy reflects the high degree of chemical weathering of the granites in the drainage basin (thus reducing the mineralogy of the rocks down to resistate minerals (dominantly quartz) and alteration products (clays)). The transport and depositional processes which affects the terrigenous sediments in the alluvial systems of the drainage basin and in the Bay waters, act to effectively sort the originally mixed sediment load into dominantly coarse grained and dominantly fine grained fractions. The coarse fraction settles out in the mangrove channels and channel mouths on entering the low energy conditions in the northern part of the Bay and the fines are then left to settle in the shallow marine environment or be transported and deposited in the mangrove swamps by tidal action. Since most of the major and trace elements are strongly associated with the clay fraction due to the adsorption and flocculating properties of clays and associated organic matter, much of the variation in the distribution of these elements is controlled by the distribution of clays. Exceptions to this are Si which is contained mainly in quartz, Ca contained in $CaCO_3$ and the elements Sn, Zr and Ti which are contained in cassiterite, zircon, ilmenite and rutile. The elements distributions are thus controlled by the processes governing quartz sand distribution, carbonate distribution and heavy mineral distributions.

Consideration of the characteristics of the surface sediments and the processes controlling their deposition has helped to formulate a picture of the Late Quaternary depositional history of sediments in the Bay. In the Late Pleistocene, sedimentation was sub-aerial throughout much of the Bay with the coastline hovering somewhere along the 40-60m bathymetric depth. Thus alluvial and shallow coastal sedimentation took place depositing the coarse relict sediments that are currently found in the south of the Bay. With sea-level rise in the Early Holocene these coarse sediments will have been reworked through shallow coastal processes thus producing the well-sorted, coarse grained, mineralogically and texturally mature sediments. It is possible that a transgressive sequence of sediments were deposited in the northern part of the Bay as sea-level rose. Once sea-level reached its maximum approximately 6000 years ago a progradational sequence of sedimentation started to develop resulting in the large development of mangroves present in the north of the Bay at present. Mangrove muds overlie intertidal silty

muds which overlie shallow silts containing shelly material. This sequence overlies low sea-level stand alluvial sediments in the north but has not yet covered these sediments in the south due to high energy conditions preventing settling of fines. Radiocarbon dates have provided apparent accumulation rates of sediment in the north of the Bay of up to 1.5mm/year at the main mangrove front and 0.3mm/year in the smaller Ao Luk area. Progradation rates calculated from these rates and also from the width of the main mangrove system in the north are approximately 1.5m/year which is rapid in geological terms and comparable to mangrove progradation rates in similar areas in Australia.

This model of deposition in Phangnga Bay is likely to be of use in the understanding of ancient depositional environments. A feature of the Phangnga Bay sediments is that they become coarser seawards and because the Holocene sedimentation has been progradational (in effect regressive) this is reflected in fining upward sequences in shallow sediment cores from the northern area. Therefore, Phangnga Bay sedimentation serves as a modern model for a regressive, fining-upward sequence. Such sequences are recognised in the Late Carboniferous successions (eg, the mid-Pennsylvanian Allegheny formation of the Appalachian plateau and the lower-Pennsylvanian Brazil formation of Indiana) and a rock analogue in the Palaogene is possibly the Wilcox group in south Texas. In general however, there seem to be few rock analogues to the Phangnga Bay model which may be a result of the lack of preservation of such environments in the geological record since they are more likely to develop at high sea-level stands and are thus subject to erosion on sea-level fall. However, it may also be a result of a lack of recognition of such environments in the geological record due to the apparent bias towards studies of modern sand-dominated coastal environments.

Looking at the economic aspects, the Phangnga Bay system may be considered as a model of some ancient petroleum source-trap system with mangrove organic matter providing a source and associated channel sands or the underlying alluvial sands providing a possible reservoir. In more applicable economic terms however, the study has pin-pointed areas of high Sn concentrations which may prove economically recoverable.

REFERENCE LIST

REFERENCE LIST

Absalao R.S. (1991) "Environmental descrimination among soft-bottom mollusc associations off lagoa dos Patos, south Brazil" Est. Coast. Shelf. Sci. 32 pp 71-85

Agraival Y.C., McCave I.N. and Riley J.B. (1991) "Laser diffraction size analysis" in "Principles, methods and Application of particle size analysis" J.P.M. Syvitski, Cambridge University Press, Cambridge, 362 pp

Alexander C.R., Nittrouer C.A., DeMaster D.J., Park Y-A and Park S-C (1991) "Macrotidal mudflats of the southwestern Korean coast: a model for interpretions of intertidal deposits" J. Sed. Pet. 41 pp 74-88

Allen G.P. (1971) "Relationship between grain size distribution and current patterns in the Gironde Estuary" J.Sed.Pet. 41 pp 74-88

Allen G.P., Castaing P. and Klingebiel A. (1971) "Preliminary investigation of the surficial sediments of the Cape Breton Canyon (SW France) and the surrounding continental shelf" Mar. Geol. 10 M27-M32

Allen G.P., Laurier D. and Thouvenin J. (1982) "Etude sedimentologique du Delta de la Mahakam" Compagnie Francaise des Petroles, Notes et Memoires 15

Alongi D.M. (1989) "Benthic processes across mixed terrigenous-carbonate sediment facies on the central Great Barrier Reef shelf" Cont. Shelf Res. 9 pp 629-663

Ashley G.M. (Ed) (1988) "The hydrodynamics and sedimentology of a back-barrier lagoon-salt marsh system, Great Sound, New Jersey" Mar. Geol. 82 pp 123-132

Barua D.K. (1990) "Suspended sediment movement in the estuary of the Ganges-Brahmaputra-Meghna river system" Marine Geology 91 pp 243-253

Batchelor B.C. (1979) "Geological characteristics of certain coastal and offshore placers as essential guides for tin exploration in Sundaland, Southeast Asia" Geol. Soc. Malaysia Bull. 11 pp 283-313

Bearman G. (Ed) (1979) "Seawater: its composition, properties and behaviour" Pergamon Press, Oxford, 165 pp.

Bernasconi M.P., Stanley D.J. and Geronimo I.D. (1991) "Molluscan faunas and paleobathymetry of Holocene sequences in the northeastern Nile delta, Egypt" Mar. Geol. 99 pp 29-43

Bird E.C.F. (1964) "Coastal Landforms - an introduction to coastal geomorphology with Australian examples" Australian National University, Canberra, 193 pp.

Bird E.C.F. (1971) "Mangroves as land-builders" Victoria Nat. 88 pp 189-197

Bird E.C.F. (1986) "Mangroves and intertidal morphology in Westernport Bay, Victoria, Australia" Marine Geology 69 pp 251-271

Bird E.C.F. and Barson M.M. (1977) "Measurement of physiographic changes on mangrove-fringed estuaries and coastlines" Mar. Res. Indonesia 18 pp 73-80

Biscaye P.E. (1965) "Mineralogy and sedimentation of recent deep-sea clay in the Atlantic Ocean and adjacent seas and oceans" Geol. Soc. Am. Bull. 72 pp 803-801

Bosence D.W.J. (1973) "Facies Relationships in a Tidally Influenced Environment." Geol. Mijnb. 52 pp 63-67

Boyle E.A, Edmond J.M and Sholkovitz E.R. (1977) "The mechanism of iron removal in estuaries" Geochim. Cosmochim. Acta. 41 pp 1313-1324

Breyer J.A. and McCabe P.J. (1986) "Coals associated with tidal sediments in the Wilcox group (Paleogene) South Texas" J. Sed. Pet 56 pp 510-519

Brown B.E. and Holley M.C. (1984) "Coral assemblages of intertidal reef flats at Ko Phuket, Thailand" PMBC Res. Bull. 30 pp 1-10

Butler A.J., Depers A.M., McKillup S.C. and Thomas D.P. (1977) "Distribution and sediments of mangrove forests in South Australia" Trans. Roy. Soc. S. Austr. 101 pp 35-44

Byrd J.T. and Andreae M.O. (1986) "Geochemistry of tin in rivers and estuaries" Geochim. Cosmochim. Acta. 50 pp 835-845

Calvert S.E. (1976) "The mineralogy and geochemistry of near-shore sediments" in "Chemical Oceanography - Vol 6" J.P.Riley and R.Chester (Eds), Academic Press, London, pp 187-280

Carr D.J., Khokiattiwong S., Scoffin T.P. and Tudhope A.W. (1991) "Grain size, calcium carbonate content and accumulation rates of recent sediments in Phangnga Bay, South Thailand" PMBC Res. Bull. 55 pp 77-96 (see appendix F)

Cassie R.M. and Michael A.D. (1968) "Fauna and sediments of an intertidal mud flat: a multivariate analysis" J. exp. mar. Biol. Ecol. 2 pp 1-23

Chambers R.L and Upchurch S.B. (1979) "Multivariate analysis of sedimentary environments using grain size frequency distributions" Math. Geol. 11 pp 27-43

Chapman V.J. (1977) "Wet Coastal Ecosystems - Ecosystems of the World 1" Elsevier, Amsterdam 428 pp

Chappell J. (1974) "Relationships between sea levels, ^{18}O variations and orbital perturbations during the past 250,000 years" Nature 252 pp 199-202

Chatananthawej B and Bussarawit S. (1987) "Quantitative survey of the macrobenthic fauna along the west coast of Thailand and the Andaman Sea" PMBC Res. Bull. 47 23 pp

Chester R. and Aston S.R. (1983) "The geochemistry of deep-sea sediments" in "Chemical Oceanography - Vol 6" J.P.Riley and R.Chester (Eds), Academic Press, London, pp 281-391

Christensen B. (1978) "Biomass and primary production of *Rhizophora apiculata Bl.* in a mangrove swamp in South Thailand" Aquatic Botany 4 pp 43-52

COHMAP Members (1988) "Climatic changes ofthe last 18.000 years: observations and model simulations" Science 241 pp 1043-1052

Coleman J.M., Sherwood M.G. and Smith W.G. (1970) "Sedimentation in a Malaysian high tide tropical delta" in "Deltaic Sedimentation, Modern and Ancient" SEPM Spec Publ 15 J.P. Morgan (Ed) pp 185-197

Cook P.J. & Mayo W. (1978) "Sedimentology and Holocene History of a Tropical Estuary (Broad Sound, Queensland)." BMR Geology and Geophysics Bulletin 170 206pp

Cook P.J. & Mayo W. (1980) "Geochemistry of a Tropical Estuary and its Catchment - Broad Sound, Queensland." BMR Geology and Geophysics Bulletin 182 211 pp

Curray J.R. (1965) "Late Quaternary history, continental shelves of the United States" in "The Quaternary of the United States" H.E. Wright and D.G. Frey (Eds) American Geological Institute, Washington. 356 pp

Curtis A.H. (1888) "How the mangroves form islands" Garden and Forest 1 pp 100-123

Curtis C.D. (1977) "Sedimentary geochemistry: environments and processes dominated by involvement of an aqueous phase" Philos. Trans. R. Soc. Ser. A 286 pp 353-372

Dal Cin R. (1976) "The use of factor analysis in determining beach erosion and accretion from grain size data" Mar. Geol. 20 pp 95-116

Davis J.H. (1938) "Mangroves, makers of land" Nature Mag. 31 pp 551-553

Deer W.A, Howie R.A. and Zussman J. (1962) "Rock-forming minerals, Volume 3 - Sheet Silicates" Longmans, London, 270 pp

Deer W.A., Howie R.A. and Zussman J. (1966) "An Introduction to the Rock Forming Minerals" Longman, England, 528 pp

De Luca Rebello A., Haekel W., Moreira I., Santelli R. and Schroeder F. (1986) "The fate of heavy metals in an estuarine tropical system" Mar. Chem. 18 pp 215-225

Demirpolat S. (1991) "Surface and near-surface sediments from the continental shelf off the Russian River, northern California" Mar. Geol. 99 pp 163-173

Diaz J.I., Nelson C.H., Barber J.H. and Giro S. (1990) "Late Pleistocene and Holocene sedimentary facies on the Ebro continental shelf" Mar. Geol. 95 pp 333-352

Ditlev H. (1978) "Zonation of corals (Scleractinia: coelenterata) on intertidal reef flats at Ko Phuket, Eastern Indian Ocean" Mar. Biol. 47 pp 29-39

Drever J.T. (1971) "Early diagenesis of clay minerals, Rio Ameca basin, Mexico" J. Sed. Pet. 41 pp 982-994

Duane D.B. (1964) "Significance of skewness in recent sediments, western Pimlico Sound, North Carolina" J. Sed. Pet. 34 pp 864-874

Dyer K.R. (1986) "Coastal and estuarine sediment dynamics" J. wiley and Sons, Chichester, 342 pp

Emery K.O. (1952) "Continental shelf sediments off Southern California" Bull.Geol.Soc.Am. 63 pp 1105-1108

Emery K.O. (1968) 'Relict sediments on continental shelves of the World' Am.Ass.Pet.Geol.Bull. 52 pp 445-464

Evans G. (1965) 'Intertidal flat sediments and their environments in the Wash' Quat. Jour. Geol. Soc. London 121pp 209-245

Everitt B. (1974) 'Cluster Analysis' Heinemann, London, 122 pp

Ferm J.C. (1970) 'Allegheny deltaic deposits' in 'Deltaic Sedimentation Modern and Ancient' SEPM Spec. Publ. 15 pp 246-255

Finlay B.J, Hetherington N.B and Davidson W. (1983) 'Active biological participation in lacustrine barium geochemistry' Geochim. Cosmochim. Acta. 47 pp 1325-1329

Fitton J.G and Dunlop H.M. (1985) 'The Cameroon line, West Africa and its bearing on the origin of oceanic and continental alkali basalt' Earth Plan. Sci. Lett. 72 pp 23-38

Folk R.L. (1954) 'The distinction between grain size and mineral composition in sedimentary-rock nomenclature' J. Geol. 62 pp 344-359

Folk R.L. (1974) 'Petrology of Sedimentary Rocks' Hemphill, Austin.

Folk R.L. and Ward W.C. (1957) 'Brazos River Bar: a study in the significance of grain size parameters' J. Sed. Pet. 27 pp 3-26

Francois R. (1988) 'A study on the regulations on the concentrations of some trace metals (Rb, Sr, Zn, Pb, Cu, V, Cr, Ni, Mn and Mo) in Saanich Inlet sediments, British Columbia, Canada' Mar. Geol. 83 pp 285-308

Friedman G.M. (1961) 'Distinction between dune, beach and river sands from their textural characteristics' J. Sed. Pet. 31 pp 514-529

Friedman G.M. (1962) 'On sorting, sorting coefficients and the log-normality of the grain size distribution of sandstones' J. Geol. 70 pp 737-753

Frith D.W., Tantanasiriwong R. and Bhatia O. (1976) ' Zonation of Macrofauna on a mangrove shore, Phuket Island' PMBC Res. Bull. 10 37 pp

Gardner J.V, Dean W.E. and Alonso B. (1990) 'Inorganic geochemistry of surface sediments of the Ebro Shelf and slope, northwestern Mediterranean' Mar. Geol. 95 pp 225-245

Garson M.S. & Mitchell A.H.G. (1970) 'Transform Faulting in the Thai Peninsula' Nature 228 pp 45-47

Garson M.S., Mitchell A.H.G., Young B. & Tait B.A.R. (1975) 'The Geology of the Tin Belt in Peninsula Thailand around Phuket, Phangnga and Takua Pa.' I.G.S. Overseas Memoir No.1 112 pp

Gerini G.E. (1905) 'Historical retrospect of Junkceylon Island' Journal of the Siam Society 2 141 pp

Geyh M.A., Kudrass H.R. and Streif H. (1979) 'Sea level changes during the Late Pleistocene and Holocene in the Straits of Malacca' Nature 278 pp 441-443

Gibbs R.J. (1973) "Mechanisms of trace metal transport in rivers" Science 180 pp 71-73

Gillespie R. and Pollach H.A. (1979) "The suitability of marine shells for the Radiocarbon dating of Australian prehistory" in "Conference Proceedings - Radiocarbon Dating" R. Berger and H.E. Seuss (Eds), Univ. of California Press, Berkeley, pp 404-421

Goldberg E.D. (1954) "Marine geochemistry 1: chemical scavengers of the sea" J. Geol. 62 pp 249-265

Goldschmidt V.M. (1954) "Geochemistry", Clarendon

Goldsmith J.R. and Graf D.L. (1958) "Relations between lattice constraints and composition of the Ca-Mg carbonates" Am. Miner. 43 pp 84-101

Goldsmith J.R., Graf D.L. and Heard H.C. (1961) " Lattice constants of the Calcium-Magnesium carbonates" Am. Miner. 46 pp 453-457

Grant A. and Middleton R. (1990) "An assessment of metal contamination of sediments in the Humber estuary, U.K." Est. Coast. Shelf. Sci. 31 pp 71-85

Griffiths J.C. (1967) "Scientific Method in Analysis of Sediments" McGraw-Hill, New York

Griffin G.M. and Ingram R.L. (1955) "Clay minerals of the Neuse River Estuary" J. Sed. Pet. 15 pp 194-200

Hardy R. and Tucker M. (1988) "X-Ray powder diffraction of sediments" in "Techniques in Sedimentology" M. Tucker (Ed.) Blackwell Scientific Publications, Oxford 394 pp

Hirst D.M. (1962a) "The geochemistry of modern marine sediments from the Gulf of Paria I - the relationship between the mineralogy and the distribution of major elements. Geochim. Cosmochim. Acta 26 pp 309-334

Hirst D.M. (1962b) "The geochemistry of modern marine sediments from the Gulf of Paria II - the location and distribution of trace elements." Geochim. Cosmochim. Acta 26 pp 1147-1187

Holliday L.M. and Liss P.S. (1976) "The behaviour of dissolved Fe, Mn and Zn in the Beaulieu Estuary" Est. Coast. Mar. Sci. 4 pp 349-353

Hudson J.D. (1963) "The Recognition of salinity-controlled Mollusc Assemblages in the Great Estuarine Series (Middle Jurassic) of the Inner Hebrides." Palaeontology 6 pp 318-326

Hughes R.N. and Thomas M.L.H. (1971) "The classification and ordination of shallow-water benthic samples from Prince Edward Island, Canada" J. exp. mar. Biol. Ecol. 7 pp 1-39

Hummel C.L. and Phanwandon P. (1967) "Geology and mineral deposits of the Phuket mining district, South Thailand" Report Investigation, Royal Thai Department of Mineral Resources, No 5. (in Thai)

Hylleberg J., Nateewathana A., Chatananthawej B. (1985) "Temporal changes in sediment characteristics on the west coast of Phuket Island" PMBC Res. Bull. 37 16 pp

Jenne E.A. (1968) "Controls on Mn, Fe, Co, Ni, Cu and Zn concentrations in soils and water: the significant role of hydrous Mn and Fe oxides" in "Trace Inorganics in Water" R.A.Baker (Ed.) Adv. Chem. Series 73, Am. Chem. Soc. pp 337-387

Jones W.R. (1925) "Tin fields of the World", London

Kalejta B and Hockey P.A.R. (1991) "Distribution, abundance and productivity of benthic invertebrates at the Berg River Estuary, South Africa" Est. Coast. Shelf Sci. 33 pp 175-191

Keller W.D. (1953) "Illite and montmorillonite in green sedimentary rocks" J. Sed. Pet. 23 pp 3-9

Keller W.D. (1956) "Clay minerals as influenced by environments of their formation" Am. Ass. Pet. Geol. Bull. 40 pp 2689-2710

Khokiattiwong S., Limpsaichol P., Petpiroon S., Sojisuporn P. and Kjerfve B. (1991) "Oceoanographic variations in Phangnga Bay, Thailand under monsoonal effects" PMBC Res. Bull 55 pp 43-76

Kitano Y., Sakata M. and Matsumoto E. (1980) "Partitioning of heavy metals into mineral and organic fractions in a sediment core from Tokyo Bay" Geochim. Cosmochim. Acta 44 pp 1279-1285

Klovan J.E. (1966) "The use of factor analysis in determining depositional environments from grain-size distributions" J. Sed. Pet. 36 pp 115-125

Kolla V., Ray P.K. and Kostecki J.A. (1981) "Surficial sediments of the Arabian Sea" Mar. Geol. 41 pp 183-204

Krauskopf K.B. (1956) "Factors controlling the concentrations of 13 rare metals in sea-water" Geochim. Cosmochim. Acta 9 pp 1-32

Kronberg B.I., Fyfe W.S., Leanoardos O.H. and Santos A.M. (1979) "The chemistry of some Brazilian soils: element mobility during intense weathering" Chem. Geol. 24 pp 211-229

Krumbein W.C and Sloss L.L. (1963) "Stratigraphy and Sedimentation" Freeman, San Francisco pg 234

Kuenzler E.J. (1974) "Mangrove swamp systems" in Coastal Ecological systems of the United States", The Conservation Foundation, Washington D.C. 1 pp 346-371

Kuijpers E.P. (1971) "Transition from fluviatile to tidal marine sediments in the Upper Devonian of Seven Heads Peninsula" Geol. Mijnb. 50 pp 443-450

Kukal Z. (1971) "Geology of Recent Sediments" Academic Press, London, 490 pp

Kulm L.D., Rousch R.C., Harlett J.C., Neudeck R.H., Chambers D.M. and Runge E.J. (1975) "Oregon continental shelf sedimentation: interrelationships of facies distribution and sedimentary processes" J. Geol. 83 pp 145-176

Kvale E.P. and Archer A.W. (1990) 'Tidal deposits with low-sulphur coals, Brazil Formation (Lower Pennsylvanian) Indiana' J. Sed. Pet. 60 pp 563-574

Lea D.W. and Boyle E.A. (1989) 'Barium content of benthic foraminifera controlled by bottom-water composition' Nature 338 pp 751-753

Lea D.W., Shen G.T. and Boyle E.A (1989) 'Coralline barium records temporal variability in equatorial Pacific upwelling' Nature 340 pp 373-376

Levington J. (1972) 'Stability and trophic structure in deposit feeding and suspension feeding communities' Am. Nat. 106 pp 472-486

Limpsaichol P. (1978) 'Reduction and oxidation properties of the mangrove sediment, Phuket Island, Southern Thailand.' PMBC Res. Bull. No 23 13 pp

Limpsaichol P. (1989) 'Coastal Environment of Phangnga Bay' Phuket Marine Biological Centre Final Technical Report 61 pp

Loring D.H. (1978) 'Geochemistry of Zinc, Copper and Lead in the sediments of the estuary and Gulf of St Lawrence' Can J. Earth Sci 15 pp 757-772

Lowe J.J. and Walker M.J.C. (1984) 'Reconstructing Quaternary Environments' Longman, London, 389 pp

MacKenzie D.B. (1972) 'Tidal sand flat deposits in Lower Cretaceous Dakota Group near Denver, Colorado' Mount. Geol. 9 pp 269-277

MacNae W. (1968) 'A general account of the fauna and flora of mangrove swamps and forests in the Indo-West-Pacific region' Adv. Mar. Biol. 6 pp 73-270

Maiklem W.R. (1967) 'Black and brown speckled foraminiferal sand from the southern part of the Great Barrier Reef' J. Sed. Pet. 37 pp 1023-1030

Mayar L.M. (1982) 'Retention of iron in estuaries' Geochim. Cosmochim. Acta 46 pp 1003-1009

McCave I.N., Bryant R.J., Cook H.F. and Coughanowr C.A. (1986) 'Evaluation of a Laser-Diffraction-Size analyser for use with natural sediments' J. Sed. Pet 56 pp 561-564

McManus D.A. (1975) 'Modern versus relict sediment on the continental shelf' Geol. Soc. Am. Bull. 86 pp 1154-1160

McManus J., Buller A.T. and Green C.D. (1980) 'Sediments of the Tay Estuary VI. Sediments of the lower and outer reaches' Proc. Royal. Soc. Edin. 78B pp s133-s153

McManus J. (1988) 'Grain Size Determination' in 'Techniques in Sedimentology' M.Tucker (Ed), Blackwell Scientific Publications, Oxford, 394 pp.

Milliman J.D. (1974) 'Marine Carbonates' Springer-Verlag, Berlin 375 pp

Mitchell A.H.G. (1977) 'Tectonic Settings for Emplacement of South-East Asian Tin Granites.' Geol. Soc. Malaysia Bull. 9 pp 123-140

Mohr E.C.J. and Van Baren P.A. (1954) 'Tropical Soils' Bandung 498 pp

Moiola R.J and Weiser D. (1968) 'Textural parameters: an evaluation' J. Sed. Pet. 38 pp 45-53

Moore J.R. (1963) 'Bottom sediment studies, Buzzards Bay, Massachusetts' J. Sed. Pet. 33 pp 511-558

Moore R.M., Burton J.D., Williams P.J. and Young M.L. (1979) 'The behaviour of dissolved organic material, Fe and Mn in estuarine mixing' Geochim. Cosmochim. Acta 43 pp 919-926

Nadeau J.E. and Hall M.J. (1988) 'Distribution patterns of metals in sediments of the Great Sound Complex, New Jersey' Mar. Geol. 82 pp 113-122

Nelson E. (1960) 'Clay mineralogy of the bottom sediments, Rappahannock River, Virginia' in 'Clays and Clay Minerals' A. Swineford (Ed.) Proc. 7th Nat. Conf., Washington, 1958, London, Pergamon Press pp 135-147

Nielsen C. (1976) 'An illustrated checklist of bivalves from PMBC beach with a reef-flat at Phuket, Thailand' PMBC Res. Bull. 9 25 pp

Norman M.D. and De Deckker P. (1990) 'Trace metals in lacustrine and marine sediments : a case study from the Gulf of Carpentaria, northern Australia' Chem. Geol. 82 pp 299-318

Norrish K. and Hutton J.T. (1969) 'An accurate X-ray spectrographic method for the analysis of a wide range of geological samples' Geochim. Cosmochim. Acta 33 pp 431-453

Odin G.A. and Matter A. (1981) 'De glauconiarum origine' Sedimentology 28 pp 47-61

Ogorelec B, Misic M. and Faganeli J. (1991) 'Marine geology of the Gulf of Trieste (northern Adriatic): sedimentological aspects' Marine Geology 99 pp 79-92

Park S.C., Kim Y.S. and Hong S.K. (1991) 'Shallow seismic stratigraphy and distribution patterns of Late Quaternary sediments in a macrotidal Bay: Gunhung Bay, west coast of Korea' Mar. Geol. 98 pp 135-144

Parker R.H. (1956) 'Macro-invertebrate assemblages as indicators of sedimentary environments in east Mississippi delta region' Bull. Am. Ass. Pet. Geol. 40 pp 295-376

Philips O.P. (1903) 'How the mangrove tree adds new land to Florida' Jour. Geogr. N.Y. 2 pp 10-21

Pilkey O.H. (1964) 'The size distribution and mineralogy of the carbonate fraction of United States South Atlantic shelf and upper slope sediments' Mar. Geol. 2 pp 121-136

Powers M.C. (1953) 'A new roundness scale for sedimentary particles' J. Sed. Pet. 23 pp 117-119

Prasertwong P. (1983) 'Recolonisation of marine benthic fauna after offshore tin-mining' Thesis Report, Marine Science Dept., Chulalongkorn University, Thailand.

Prior W.A and Glass H.D. (1961) "Cretaceous-Tertiary clay mineralogy of the Upper Mississippi embayment" J. Sed. Pet. 31 pp 38-51

Pritchard D.W. (1967) "What is an Estuary: Physical Viewpoint" in "Estuaries" Lauff G.H. (Ed.) American Association for the Advancement of Science No 83

Raaf de J.F.M. & Boersma J.R. (1971) "Tidal Deposits and their Sedimentary Structures." Geol. Mijnb. 50 pp 479-503

Rateev M.A., Gorbunova Z.N., Lisitzyn A.P. and Nosov G.L. (1969) "The Distribution of Clay Minerals in the Oceans" Sedimentology 13 pp 21-43

Raymond A. and Phillips T.L. (1983) "Evidence for an Upper Carboniferous mangrove community" in "Tasks for vegetation science - Chapter 2" Junk Publishers, The Hague pp 19-30

Reading H.G. (1986) "Sedimentary Environments and Facies" 2nd Edition, Blackwell Science Publications, Oxford 615 pp

Reineck H.E. (1967) "Layered sediments of tidal flats, beaches and shelf bottoms of the North Sea" in "Estuaries" G.H. Lauff (Ed.) Am. Ass. Adv. of Science, Washington D.C. pp 191-206

Reinson G.E. (1975) "Geochemistry of muds from a shallow restricted estuary, Australia" Marine Geology 19 pp 297-314

Reinson G.E. (1977) "Hydrology and Sediments of a Temperate Estuary - Mallacoota Inlet, Victoria." BMR Geology and Geophysics Bulletin 178 91 pp

Reynolds R.C.Jr and Hower J. (1970) "The nature of interlayering in mixed-layer illite-montmorillonites" Clays Clay Miner. 18 pp 25-36

Risk M.J. and Rhodes E.G. (1985) "From mangroves to petroleum precursors: an example from tropical North East Australia" A.A.P.G. Bull. 69 pp 1230-1240

Robbins J.A. & Eddington D.N. (1975) "Determination of Recent Sedimentation Rates in Lake Michigan using ^{210}Pb and ^{137}Cs." Geochim. Cosmochim. Acta 39 pp 285-304.

Ronov A.B. and Migdisov A.A. (1971) "Geochemical history of the crystalline basement and the sedimentary cover of the Russian and North American platforms" Sedimentology 16 pp 137-185

Rosevear D.R. (1947) "Mangrove Swamps" Farm and Forest 8 pp 23-30

Ryan B.F., Joiner B.L. and Ryan T.A. (1985) "Minitab Handbook" 2nd Edition, PWS Publishing, Boston, 379 pp

Ryer T.A. and Langer A.W. (1980) "Thickness change involved in the peat-to-coal transformation for a bituminous coal of Cretaceous age in central Utah" J. Sed. Pet. 50 pp 987-992

Sanders H.L (1958) "Benthic studies in Buzzards' Bay: I. Animal-sediment relationships" Limnol. and Ocean. 3 pp 245-258

Sanders H.L. (1968) "Marine benthic diversity: A comparative study" Am Nat 102 pp 243-282

Sanders H.L., Mangelsdorf P.C. and Hampson G.R. (1965) "Salinity and faunal distribution in the Pocasset River, Massachusetts" Limnol. and Ocean. 10 pp 216-229

Sawangarreruks S. and Boonruang P. (1988) "Species abundance and distribution of macrobenthic fauna in Phangnga Bay" PMBC Report (in Thai)

Schmitz B. (1987) "The TiO_2/Al_2O_3 ratio in the Cenozoic Bengal Abyssal Fan sediments and its use as a paleostream energy indicator" Mar. Geol. 76 pp 195-206

Scoffin T.P. (1987) "An introduction to carbonate sediments and rocks" Blackie, Glasgow, 274 pp

Seidel S.L., Hodge V.F. and Goldberg E.D. (1980) "Tin as an environmental pollutant" Thallassia Jugoslavica 16 pp 209-223

Sellwood B.W. (1972) "Tidal flat sedimentation in the Lower Jurassic of Bornholm, Denmark" Palaeogeogr. Palaeoclimat. Palaeoecol 11 pp 93-106

Shackleton N.J. (1987) "Oxygen isotopes, ice volume and sea level" Quat. Sci. Review 6 pp 183-190

Shaw T.I. (1962) "Physiology and Biochemistry of Algae" (Ed. R.A.Lewin), Academic Press, New York, 247 pp

Shepard F.P. (1932) "Sediment on continental shelves" Bull. Geol. Soc. Am. 43 pp 1017-1034

Shepard F.P. (1954) "Nomenclature based on Sand-Silt-Clay ratios" J. Sed. Pet. 24 pp 151-158

Shimmield G.B and Pedersen T.F. (1990) "The geochemistry of reactive trace metals and halogens in hemipelagic continental margin sediments" Aquatic Science 3 pp 255-279

Shimmield G.B. and Mowbray S.R. (1991) "The inorganic geochemical record of the northwest Arabian Sea: A history of productivity variation over the last 400 K.Y. from sites 722 and 724" Proceedings of the Ocean Drilling Program, Scientific Results, Vol 117 pp 409-420

Shin P.K.S. (1982) "Multiple discriminant analysis of macrobenthic infaunal assemblages" J. exp. mar. Biol. Ecol. 59 pp 39-50

Sholkovitz E.R., Boyle E.A. and Price N.B. (1978) "The removal of dissolved humic acids and iron during estuarine mixing" Earth Planet. Sci. Lett. 40 pp 130-136

Siesser W.G. (1971) "Mineralogy and diagenesis of some South African coastal and marine carbonates" Marine Geol. 10 pp 15-38

Siripong A. (1980) "Environmental Mapping of the Phangnga Area Utilizing Landsat MSS CCT Data" Marine Science Dept Report, Chulalongkorn University, Thailand

Siripong A. (and collaborators) (1987) 'Estuarine Ecosystems of the Phangnga Bay Vol. Chemical and Physical Oceanography' Research Report to the National Research Council of Thailand 162 pp

Spears D.A. and Kanaris-Sotiriou R. (1976) 'Titanium in some Carboniferous sediments from Great Britain' Geochim. Cosmochim. Acta 40 pp 345-351

Spencer D.W. (1963) 'The interpretation of grain size distribution curves of clastic sediments' J. Sed. Pet. 33 pp 180-190

Spencer D.W., Degens E.T. and Kulbicki G. (1968) 'Factors affecting element distributions in sediments' in 'Origin and Distribution of the Elements' L.H. Ahrens (Ed.) Pergamon Press, Oxford pp 981-988

Stewart H.B. (1958) 'Sedimentological reflections on depositional environments in the San Migue Lagoon, Baja California, Mexico' Bull. Am. Ass. Petrol. Geol. 42 pp 2567-2618

Straaten L.M.J.U. van (1950) 'Environment of formation and facies of Wadden Sea sediments' Tijdschr. Kon. Nederl. Aardr. Gen 67 pp 354-368

Straaten L.M.J.U. van and Kuenen Ph.H. (1958) 'Tidal action as a cause of clay accumulation' J. Sed. Pet. 28 pp 406-413

Swift D.J.P. (1969) 'Outer shelf sedimentation: processes and products' in 'The new concepts of continental margin sedimentation: Application to the geological record' D.J. Stanley (Ed.) Am. Geol Inst., Washington, pp DS-4-1 - DS-4-46

Swift D.J.P. (1970) 'Quaternary shelves and the return to grade' Mar. Geol. 8 pp 5-30

Swift D.J.P., Stanley D.J. and Curray J.R. (1971) 'Relict sediments on continental shelves: a reconsideration' J. Geol. 79 pp 322-346

Syvitski J.P.M (1991) 'Factor analysis of size frequency distributions: significance of factor solutions based on simulation experiments' Chapter 18 in 'Principles, Methods and Applications of Particle Size Analysis' Ed J.P.M. Syvitski, Cambridge University Press, Cambridge, 368 pp

Tanner W.F. (1991) 'Suite statistics: the hydrodynamic evolution of the sediment pool' Chapter 16 in 'Principles, Methods and Applications of Particle Size Analysis' Ed J.P.M. Syvitski, Cambridge University Press, Cambridge, 368 pp.

Tantanasiriwong R. (1978) 'An illustrated checklist of marine shelled gastropods from Phuket, adjacent mainland and offshore islands' PMBC Res. Bull. 21 63 pp

Terwindt J.H.J. (1971) 'Lithofacies of inshore estuarine and tidal inlet deposits' Geol. en Mijn. 50 pp 515-526

Terwindt J.H.J. (1988) 'Palaeo-tidal reconstructions of inshore tidal depositional environments' in 'Tide influenced sedimentary environments and facies' P.L. de Boer (Ed.) D. Reidel Publ. Co., Netherlands, pp 233-263

Thom B.G. (1982) 'Mangrove Ecology - A Geomorphological Perspective' in 'Mangrove Ecosystems in Australia' ed. B.F.Clough Australia National University Press, Canberra pp 3-17

Thom B.G., Hails J.R. and Martin A.R.H. (1969) 'Radiocarbon evidence against higher post-glacial sea levels in easter Australia' Mar. Geol. 7 pp 161-168

Thom B.G., Wright L.D. and Coleman J.M. (1975) 'Mangrove ecology and deltaic-estuarine geomorphology: Cambridge Gulf-Ord River, Western Australia' Jour. Ecol. 63 pp 203-232

Thomas R.L., Kemp A.L.W. and Lewis C.F.M. (1972) 'The distribution, composition and characterisitics of the surficial sediments of Lake Ontario' J. Sed. Pet. 66 pp 66-84

Tomlinson P.B. (1986) 'The Botany of Mangroves' Cambridge University Press, Cambridge 413 pp

Tucker M.E. (1973) 'The sedimentary environments of tropical African estuaries: Freetown Peninsula, Sierra Leone' Geol.en Mijn. 52 pp 203-215

Tucker M.E. (1988) 'Techniques in Sedimentology' Blackwell Scientific Publications, Oxford 394 pp

Turekian K.K. and Wedepohl K.H. (1961) 'Distribution of the elements in some major rock units of the Earths crust' Bull. Geol. Soc. Am. 72 pp 175-192

Vail P.R., Mitchum R.M. and Thompson S. (1977) 'Seismic stratigraphy and global changes of sea-level Part 4: global cycles of relative changes of sea-level' Mem. Am. Ass. Pet. Geol. 26 pp 49-97

Van Andel T.J. and Postma H. (1954) 'Recent sediments of the Gulf of Paria' Reports of the Orinoco Shelf Expedition Vol 1 North Holland, Amsterdam

Vries Klein de G. (1970) 'Tidal origin of a Precambrian quartzite - the lower fine-grained quartzite (mid-Dalradian) of Islay, Scotland' J. Sed. Pet. 40 pp 38-54

Wade B.A. (1972) 'A description of a highly diverse soft bottom community in Kingston Harbour, Jamaica' Mar. Biol. 13 pp 57-69

Walker R.G and Harms J.C. (1971) 'The ''Catskill Delta'': a prograding muddy shoreline in central Pennsylvania' Jour. Geol. 79 pp 381-399

Watson J.G. (1928) 'Mangrove forests of the Malay Peninsula' Malay Forest Rec. 6 pp 1-275

Wentworth C.K. (1922) 'A scale of grade and classification terms for clastic sediments' J. Geol. 30 pp 377-392

White S.M. (1970) 'Mineralogy and geochemistry of continental shelf sediments of the Washington-Oregon coast' J. Sed. Pet. 40 pp 38-

Whitehouse U.G., Jeffrey L.M. and Debrecht J. D. (1960) 'Differential settling tendencies of clay minerals in saline waters' Proc. 6th Conf. Clays Clay Miner. pp 1-79

Windom H., Smith R. and Rawlinson C. (1988) 'Trace metal transport in a tropical estuary' Mar. Chem. 24 pp 293-305

Wishart D. (1987) 'Clustan' computing programme version 3.2

Woodroffe C.D. (1983) 'Development of mangrove forests from a geological perspective' Ch.1 in Tasks for Vegetation Science, Vol 8 H.J.Teas (Ed.) pp 1-17

Woodroffe C.D., Chappell J., Thom B.G. and Wallensky E. (1989) 'Depositional model of a macrotidal estuary and floodplain, South Alligator River, Northern Australia' Sedimentology 36 pp 737-756

ACKNOWLEDGEMENTS

A piece of work such as this cannot be completed alone and I would therefore like to take this opportunity to thank all the people who contributed their time, expertise and knowledge to this study - they filled in a lot of gaps in my ability and knowledge.

Firstly, I thank the staff of the Phuket Marine Biological Centre who contributed far more than just their time and equipment to the fieldwork. Both Mr Prawin Limpsiachol, Dr Hansa Chansang and Mr Somkiat Khokiattiwong helped in both the logistics and the actual collection of samples - Somkiat also gave considerable help as an interpreter on the ship. The crew of the sample ship, the Pramong 14, were a great bunch - they worked hard, cooked superb food and were keen to communicate with us despite the language barrier. Unfortunately they lost their ship only two weeks after our last trip with them. I hope they now have a replacement vessel and are continuing their work in the Bay. There were many other people who contributed to a really enjoyable time in Thailand whose names I have forgotten and so cannot be mentioned here. However, I look forward to my return visit and maybe meeting a few of them again.

I am grateful for the great deal of help with sample collection that was also given by my supervisors Dr Terry Scoffin and Dr Sandy Tudhope and also by Dr Alison MacLennan.

The staff of the Geology Department at Edinburgh University gave freely of their time in helping me with analysis of samples and thesis production. Dodie James and Dr Godfrey Fitton helped with XRF, Geoff Angell with XRD, Stuart Kearns with the electron microprobe, Christine Armstrong, Shane Voss and Dr Cliff Ford with computing (but I could have done without the computer games - I could have finished a lot earlier!), Diane Baty and Yvonne Cooper with photography and Jane Foster with thin-sectioning. As usual, the department secretaries held the whole thing together with their efficiency and friendliness. Dr John Taylor and Dr David Reid helped in identification of specimens at the British Museum (Natural History). Dr Brian Price, Dr Sandy Tudhope, Dr Terry Scoffin and Dr Graham Shimmield all gave advice and some discussion to the results of the analytical work.

I have really enjoyed my time in Edinburgh and the time spent outside the Department made bearable the monotonous days of sample grinding, pressing etc etc in the Department. Thanks for this must go to the friends I made in the Diving Club, flatmates and also my contemporaries in the Department. I suppose I'd better mention a few of the latter bunch in case they ever read this: Andrew Patience, Steve Batty, Dave Whitmarsh, David Walker, Karen Dobbie, Andy Poole, George Ritchie, Tim Brand, Steve Mowbray, Ian Fitzsimons, Subrata Ghosh and Ned and Christine.

I gratefully acknowledge the receipt of a PhD grant from the Natural Environment Research Council of Great Britain.

Finally, to Andrew. This work would not have got very far without all your advice, interest and answers to all the questions that no-one else could be bothered with. For all the meals, Munros, coffees and companionship, thank you.

Debbie

APPENDICES

APPENDIX A

SAMPLE SITE DETAILS

Site	Date	Water Depth at LLW	LOCATION Northings	Eastings	SAMPLING BOAT Large	Small	SAMPLES Core	Grab	Dredge	DESCRIPTION
3	17/1/89	20.4	7°52'48''	98°35'07''	✓		✓	✓	✓	grey-green fine sand
4		23.5	53'25''	39'35''	✓			✓	✓	grey-green muddy sand
5		20.6	55'12''	44'25''	✓			✓		"
6		20.6	57'30''	42'57''	✓			✓		"
7		25.5	59'45''	41'12''	✓			✓	✓	"
8		17.5	8°01'35''	39'35''	✓		✓	✓	✓	"
9		4.3	03'52''	37'50''	✓		✓	✓	✓	dark grey-green mud
10		22.2	04'30''	40'25''	✓		✓	✓		grey-green mud
11		25.1	04'55''	42'50''	✓			✓	✓	grey-green sandy mud (shells)
12		2.9	07'50''	43'52''	✓		✓	✓	✓	"
13		22.8	07'15''	41'15''	✓			✓	✓	grey, shelly, muddy sand
14		12.7	06'37''	38'40''	✓		✓	✓		grey-green silty mud
15		14.6	09'50''	39'07''	✓			✓		grey-green shelly, sandy mud
16		6.5	10'15'	41'07''	✓		✓	✓		grey-green silty mud
17	18/1/89	6.9	10'45''	43'30''	✓		✓	✓	✓	"
18		8.5	12'45''	42'00''	✓		✓	✓		grey-green mud
19		15.0	11'37''	29'35''	✓			✓		grey-green silty mud
20		10.8	13'07''	38'07''	✓		✓	✓	✓	grey-green shelly silty mud
21		1.5	14'10''	40'40''	✓		✓	✓	✓	silty mud (shells)
22		Exp'd	17'00''	41'55''		✓	✓	✓		grey-green mud
23		2.1	16'00''	41'15''	✓		✓	✓		shell gravel (minor mud)
24		7.3	14'47''	37'20''	✓		✓	✓	✓	grey-green silty mud (OM + shells)
25		5.4	18'07''	36'10''	✓		✓	✓	✓	"
26		2.2	23'25''	37'05''		✓	✓	✓		grey mud
27		0.2	21'25''	37'20''		✓	✓	✓		muddy sand (OM + shells)
28		0.2	19'55''	37'55''		✓	✓	✓		shelly gravel (mussel beds)
29		1.6	19'00''	35'45''		✓		✓		grey mud (OM)
30		2.0	15'55''	35'35''	✓		✓	✓	✓	grey-green mud (shells)
31		3.3	14'15''	35'22''	✓		✓	✓	✓	grey-green mud (OM + shells)
32		2.1	13'25''	33'15''	✓			✓	✓	grey-green mud
33		2.5	15'10''	33'27	✓		✓	✓		grey-green mud (OM + shells)
34		5.8	20'10''	30'25''	✓		✓	✓	✓	grey-brown shelly sandy mud
35a	19/1/89	Exp'd	21'52''	30'55''		✓		✓		orange med-cs sand
35b		0.8	21'52''	30'40''	✓			✓		red-brown mud (OM)
36		Exp'd	19'55''	32'37''		✓	✓	✓		grey-brown silty mud (OM)
37		Exp'd	20'45''	33'40''		✓	✓	✓		grey-brown muddy sand (OM + shells)
38		Exp'd	18'20''	33'20''		✓	✓	✓		"
39		1.2	15'20''	32'37''		✓	✓	✓		greey grey-brown mud (fine OM + shell)
40		0.8	17'35''	31'00''	✓		✓	✓	✓	grey-brown sandy mud (OM + shells)
41		0.7	16'10''	30'52''	✓		✓	✓	✓	grey-brown silty mud (OM + shells)
42		2.5	14'50''	31'35''	✓		✓	✓	✓	grey mud
43		Exp'd	16'45''	28'30''		✓	✓	✓		grey-brown mud
44a		Exp'd	15'10''	28'40''		✓		✓		shelly gravel
44b		Exp'd	15'22''	28'22''		✓	✓	✓		grey gritty mud (OM + shells)
45		2.2	14'20''	29'35''		✓	✓	✓		muddy shell gravel
46		8.5	12'45''	31'12''	✓		✓	✓	✓	green-brown silty mud (OM + shells)
47		2.0	11'22''	33'20''	✓		✓	✓	✓	grey-green shelly mud
48		10.7	10'15''	30'55''	✓		✓	✓		green-grey silty mud (shells)
49		0.7	09'35''	28'30''		✓	✓	✓		grey mud
50		6.8	07'35''	29'10''	✓		✓	✓		green-grey shelly mud
51		5.8	06'50''	27'07''	✓		✓	✓	✓	"
52		3.8	12'00''	35'30''		✓		✓		grey mud

Site	Date	Water Depth at LLW	LOCATION Northings	Eastings	SAMPLING BOAT Large	Small	SAMPLES Core	Grab	Dredge	DESCRIPTION
53	19/1/89	4.1	8°10'40''	98°36'20''		✓	✓	✓		grey mud
54	↓	0.5	09'55''	33'52''		✓	✓	✓		"
55		7.9	06'40''	33'30''		✓	✓	✓		muddy shell grit
56	↓	15.1	08'20''	31'15''	✓		✓	✓	✓	green-grey mud
57	20/1/89	14.1	05'37''	29'52''	✓		✓	✓	✓	green-grey shelly mud
58	↓	7.8	04'52''	27'52''	✓			✓	✓	"
59		14.7	03'35''	29'15''	✓			✓	✓	green-grey shelly muddy sand
60		12.5	02'00''	31'20''	✓		✓	✓	✓	green-grey muddy fine sand
61		5.5	00'30''	33'07''	✓		✓	✓	✓	grey-green silty mud
62		18.6	7°56'00''	30'15''	✓			✓	✓	grey-green muddy shelly sand
63	↓	10.7	53'25''	27'40''	✓		✓	✓	✓	grey-green silty mud
64	5/1/90	20.0	52'10''	31'10''	✓			✓	✓	grey-green muddy sand
65	↓	19.0	55'55''	33'30''	✓		✓	✓	✓	"
66		11.0	59'03''	28'06''	✓		✓	✓	✓	"
67		3.5	8°06'30''	23'30''	✓		✓	✓	✓	grey-green mud
68		6.5	06'50''	24'55''	✓			✓	✓	muddy grit
69		4.5	05'45''	25'25''		✓		✓		coarse shelly sand
70		4.0	05'40''	24'05''		✓		✓		grey mud
71		4.5	07'40''	24'20''		✓	✓	✓		"
72		4.5	08'00''	25'25''		✓		✓		green-grey mud
73		4.0	07'45''	26'30''		✓		✓		green-grey muddy sand
74		7.5	07'25''	27'15''		✓		✓		"
75	↓	9.0	06'45''	26'00''		✓	✓	✓		"
76	6/1/90	5.5	23'00''	28'45''		✓		✓		dark brown/black mangrove mud
77	↓	Exp'd	22'40''	29'20''		✓	✓	✓		"
78		Exp'd	22'15''	29'45''		✓	✓	✓		"
79a		Exp'd	20'40''	30'06''		✓		✓		"
79b		6.0	20'38''	30'15''		✓		✓		sandy, shelly mud
80		Exp'd	18'25''	30'15''		✓	✓	✓		grey mud
81		Exp'd	18'30''	30'25''		✓		✓		"
82		2.0	18'40''	30'35''		✓		✓		"
83		2.0	18'45''	30'45''		✓		✓		shelly mud
84		1.5	18'55''	30'55''		✓		✓		"
85		10.5	19'00''	31'05''		✓		✓		"
86		5.0	19'10''	31'15''		✓		✓		grey mud
87		Exp'd	19'25''	31'10''		✓	✓			"
88		Exp'd	19'30''	31'20''		✓		✓		"
89		Exp'd	19'15''	31'35''		✓		✓		"
90		Exp'd	19'00''	31'50''		✓		✓		"
91		Exp'd	18'50''	32'05''		✓		✓		sandy mud
92		6.0	18'30''	32'20''		✓		✓		grey-green mud
93		0.5	18'10''	32'40''		✓		✓		"
94		Exp'd	21'25''	36'30''		✓		✓		fine sandy mud
95		5.5	21'20''	36'55''		✓		✓		shelly mud
96		6.5	21'15''	37'20''		✓		✓		sandy mud
97		6.0	21'10''	37'45''		✓		✓		sand mud (shells)
98		2.0	21'05''	38'05''		✓		✓		grey mud
99	↓	Exp'd	21'00''	38'15''		✓		✓		"
100	7/1/90	Exp'd	17'15''	42'00''		✓		✓		"
101	↓	Exp'd	16'40''	41'35''		✓		✓		"

Site	Date	Water Depth at LLW	LOCATION Northings	Eastings	SAMPLING BOAT Large	Small	SAMPLES Core	Grab	Dredge	DESCRIPTION
102	7/1/90	3.0	8°16'00''	98°41'00''		✓		✓		grey mud (mussel clumps)
103		4.5	14'40''	40'40''	✓			✓		olive green mud
104		5.5	13'00''	40'15''	✓			✓	✓	shelly sandy mud
105		9.0	12'00''	39'45''	✓			✓	✓	olive-green mud
106		25.0	10'40''	39'00''	✓			✓	✓	orange gravel
107		18.0	02'03''	44'12''	✓		✓	✓	✓	grey-green sandy mud
108		24.0	7°56'57''	39'54''	✓			✓	✓	"
109		30.0	50'15''	41'28''	✓			✓	✓	"
110	8/1/90	15.0	46'30''	23'54''	✓					rocky bottom - no recovery
111		19.0	45'30''	22'38''	✓			✓		coarse orange gravel
112		37.0	43'54''	24'45''	✓			✓	✓	orange-green med-cs sand
113		45.0	41'04''	24'36''	✓			✓	✓	orange coarse sand
114		45.0	38'05''	23'25''	✓			✓	✓	coarse sandy gravel
115		45.0	35'10''	24'40''	✓			✓	✓	green-orange sand
116		65.0	33'45''	21'30''	✓			✓	✓	"
117		40.0	36'40''	21'35''	✓			✓		"
118	9/1/90	Exp'd	36'20''	22'15''		✓		✓		white fine sand
119		5.0	36'20''	22'15''		✓		✓		white fine-med sand (shells)
120		38.0	38'30''	26'40''	✓			✓	✓	slightly muddy orangey sand
121		40.0	36'25''	29'20''	✓			✓	✓	"
122		38.0	40'50''	30'45''	✓			✓	✓	shelly sand
123		40.0	38'25''	33'30''	✓			✓	✓	slightly muddy green-orange sand
124		37.0	44'25''	33'10''	✓			✓	✓	"
125		35.0	42'10''	36'20''	✓			✓	✓	"
126		35.0	40'45''	40'0''	✓			✓	✓	grey-brown muddy sand
127		33.0	44'15''	41'30''	✓			✓	✓	"
128		26.0	45'55''	38'30''	✓			✓	✓	"
129		33.0	47'05''	40'30''	✓			✓	✓	"
130		25.0	47'30''	44'05''	✓			✓	✓	"
131		28.0	44'50''	44'05''	✓			✓	✓	"
132		7.5	44'00''	46'20''		✓		✓		white carbonate sand
133	10/1/90	4.5	44'00''	46'45''		✓		✓		"
134		Exp'd	44'08''	46'15''		✓		✓		fine white sand (shells)
135		26.0	43'30''	46'45''	✓			✓	✓	green-brown muddy sand
136		26.0	48'20''	35'10''	✓			✓	✓	"
137		26.0	47'05''	30'30''	✓			✓	✓	"
138		36.0	42'45''	28'00''	✓			✓	✓	"
139		26.0	46'15''	26'35''	✓			✓	✓	"

Site	Date	Water Depth at LLW	LOCATION Northings	Eastings	SAMPLING BOAT Large	Small	SAMPLES Core	Grab	Dredge	DESCRIPTION
Khen 1	3/1/90	Exp'd	7°48'30''	98°24'30''		✓		✓		Sed. from between corals at seaward edge of reef
" 2		Exp'd	"	"		✓		✓		From sand wave on beach behind reef
" 3		Exp'd	"	"		✓		✓		From between sand waves on beach
" 4		Exp'd	"	"		✓		✓		From strandline at top of beach
" 5		3.0	"	"		✓		✓		1-2m off reef front
" 6		4.0	"	"		✓		✓		50m off reef front
o Lon 1	31/12/90	2.5	7°48'13''	98 24'26''		✓		✓		cs carb sand (seagrass and coral)
" 2		3.5	48'13''	24'25''		✓		✓		fine carb sand
" 3		4.25	48'12''	24'24''		✓		✓		"
" 4		5.0	48'12''	24'23''		✓		✓		cs shelly sand
" 5		6.0	48'11''	24'21''		✓		✓		"
" 6		5.75	48'07''	24'04''		✓		✓		soft shelly mud (forams)
" 7		6.0	48'00''	23'54''		✓		✓		"
" 8		6.0	47'49''	23'46''		✓		✓		"
" 9		5.5	47'42''	23'38''		✓		✓		sandy shelly mud (forams)
" 10		4.75	47'36''	23'24''		✓		✓		"
" 11		4.75	47'26''	23'18''		✓		✓		muddy foram sand
12		4.5	47'25''	23'18''		✓		✓		"
13		4.5	47'25''	23'17''		✓		✓		"
14		4.0	47'24''	23'16''		✓		✓		"
15		3.0	47'23''	23'15''		✓		✓		cs shell/coral sand
16		Exp'd	47'22''	23'12''		✓		✓		cs coral sand
17		Exp'd	47'18''	23'10''		✓		✓		fine quartz sand

APPENDIX B

ANALYTICAL METHODS

APPENDIX B - ANALYTICAL METHODS

B.1 INTRODUCTION

Figure B.1 is a flow diagram which illustrates the treatment of surface grab samples after collection and the procedures followed in order to prepare the samples for the variety of analytical techniques used. Figure B.2 is a similar diagram illustrating the treatment of core samples. Each of the procedures is described in the following sections.

B.2 GRAIN SIZE ANALYSIS

To enable accurate grain size determination it was essential to preserve the sediments wet to prevent aggregation of clays through drying. No attempt was made to wash salt from the sediment as, with the high amount of fine grained sediment, it was thought there was a high risk of loosing fine sediment fractions with repeated washings. However, the samples were treated with H_2O_2 to oxidise organic matter on return to the lab in Thailand (a maximum of 5 days after collection after being stored on ice). This was considered necessary as the samples could not be analysed for grain size distributions until back in Britain and growth of bacteria feeding on organic matter was likely to occur during transit. This may have adversely affected the fine sediment fractions as well as making treatment of samples rather unpleasant. 30% by volume H_2O_2 was added to the grab samples in small amounts (10-30ml) in open-topped plastic containers, and stirred. Once reaction with H_2O_2 was complete (ie, bubbling had stopped) the containers were sealed until used for grain size analysis.

Figure B.3 is a flow diagram depicting the method used for grain size analysis. All weight measurements were made in grams to 2 decimal places. As according to the method described by McManus (1988 - pg66), the coarse fraction (>62μm) was dry sieved on a sieve shaker for 15 minutes and each size fraction weighed. The fine fraction was analysed using a Coulter LS-100 laser particle size analyser. This instrument measures the particle size of grains passing through a laser beam by measuring the dispersion of the beam. The method is based on the principle that particles of a given size diffract light through a given angle, the angle increasing with

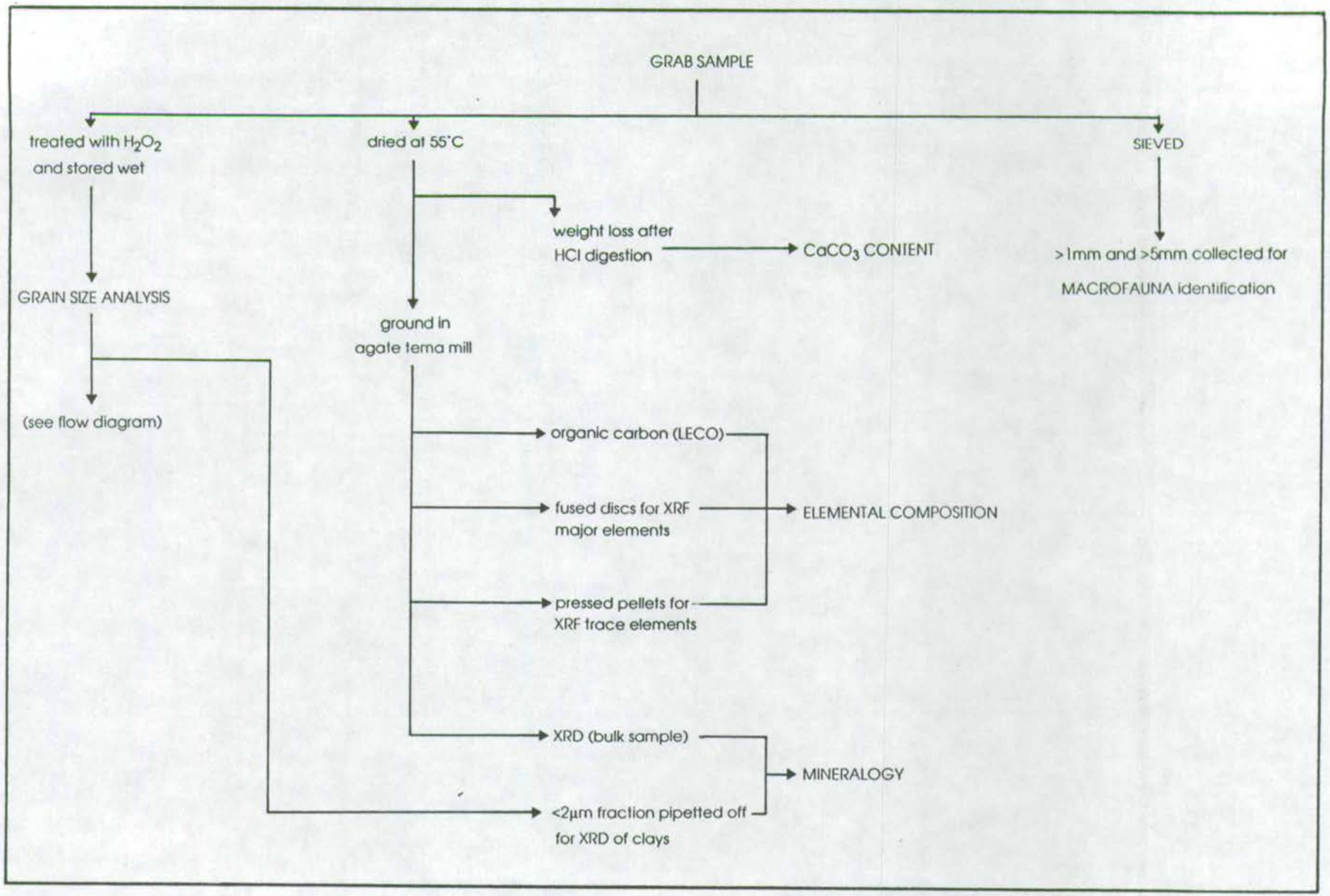

Figure B.1 **Flow diagram of sequence of treatments of grab sample sediments**

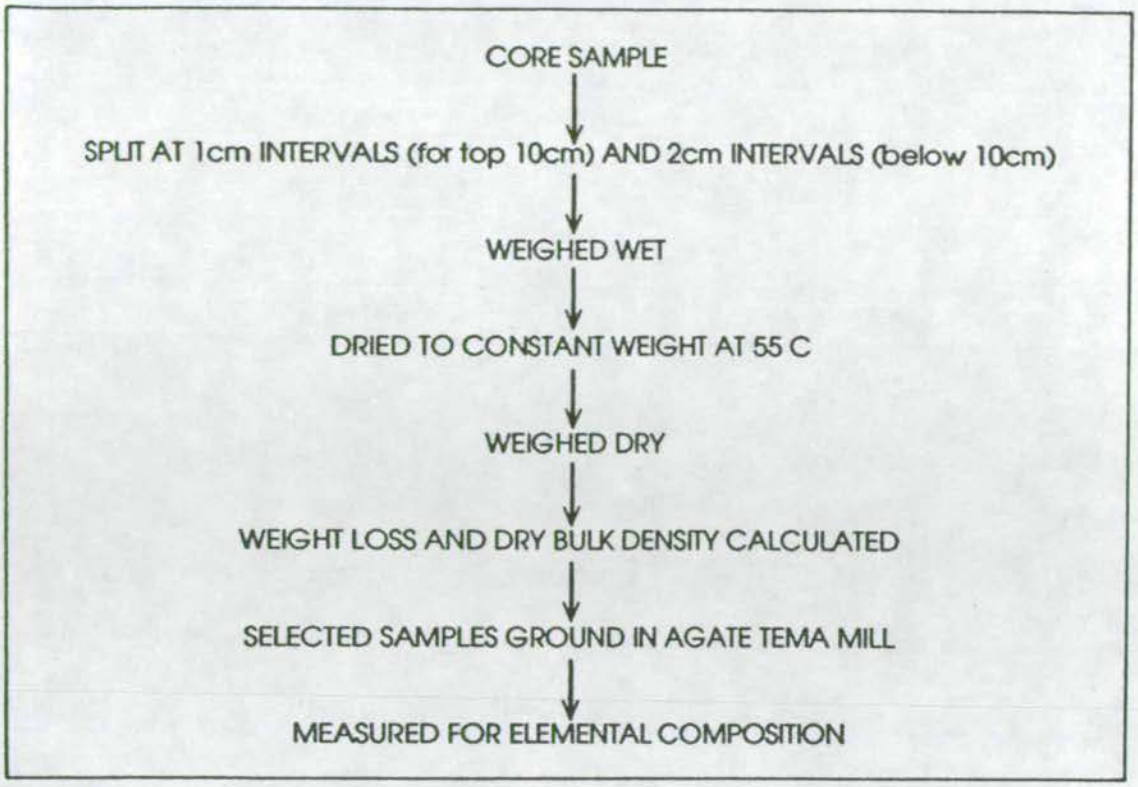

Figure B.2 Flow diagram of sequence of treatments of core sample sediments

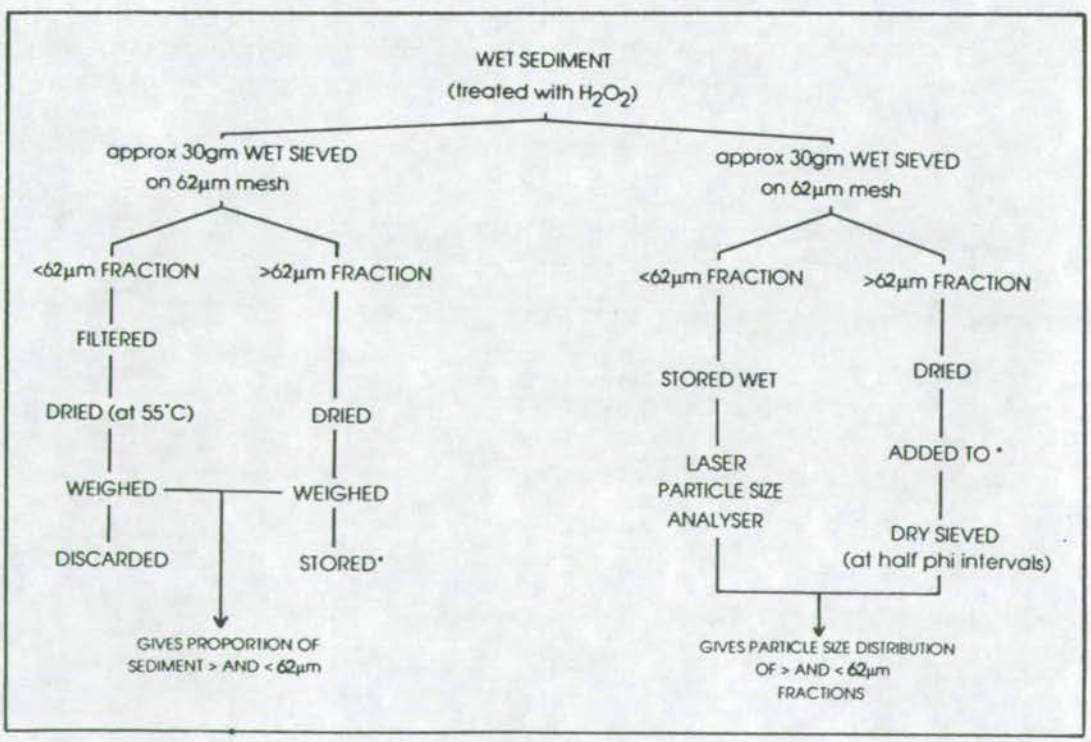

Figure B.3 Flow diagram of method of grain size analysis

decreasing grain size. A beam is passed through a suspension of the sample and diffracted light is focussed on a detector which senses the angular distribution of scattered light energy. A stream of constantly agitated particles can be passed through the beam and a diffraction pattern established which, with the use of computer software, can be used to calculate the size distribution. 30-40 samples a day can be analysed by this method. Actual measurement of the sample takes 1 minute and a computer printout obtained in 5 minutes. The time consuming process is cleaning out the sample holder and tubes and ensuring that the clean water in the system is free of bubbles which will also deflect the laser beam.

A drawback of this instrument is that spurious modes are recorded at constant positions for every sample which appears to be an artifact of the instrument (Fig. B.4). A similar artifact in a different make of laser particle size analyser was recorded by McCave et al (1986) which they put down to an inability of the instruments inversion scheme (the method of converting the light dispersion pattern to grain size data) to cope with noise produced by light scattered from clay (<2μm) in the sample. A revision of the principals and methods of laser diffraction size analysis is given in Agralval et al (1991). In this paper they report that there are difficulties for the geologist who is trying to find the total sediment distribution however this is common to other well-used devices and is by no means peculiar to the laser analyser. However, they do point out the problem of defining polymodal size distribution and suggest that dissection of polymodal size distributions and the tracing of populations through modal structure should be left to other devices. Whatever, the explanation for the spurious modes from the Coulter instrument, the occurrence of these modes prevents the results from this instrument being used in modal analysis of sediment populations.

An overlap of the 62μm boundary occurs (Fig. B.4) due to the fact that the laser particle size analyser is effectively measuring the diffraction of light by spherical grains of glass beads, however, not all grains are spherical and most will have a different Refractive Index than glass beads which affects the diffraction properties. Sieving separates grains of differing actual grain diameters. Therefore, the 2 methods are measuring different properties of the sediments. This problem occurs in any grain size analysis technique where the coarse and fine fractions are measured separately using different principles in each method. In all the samples run, the overlap totalled <4% of the total and so was ignored when combining results for the fine and coarse fractions

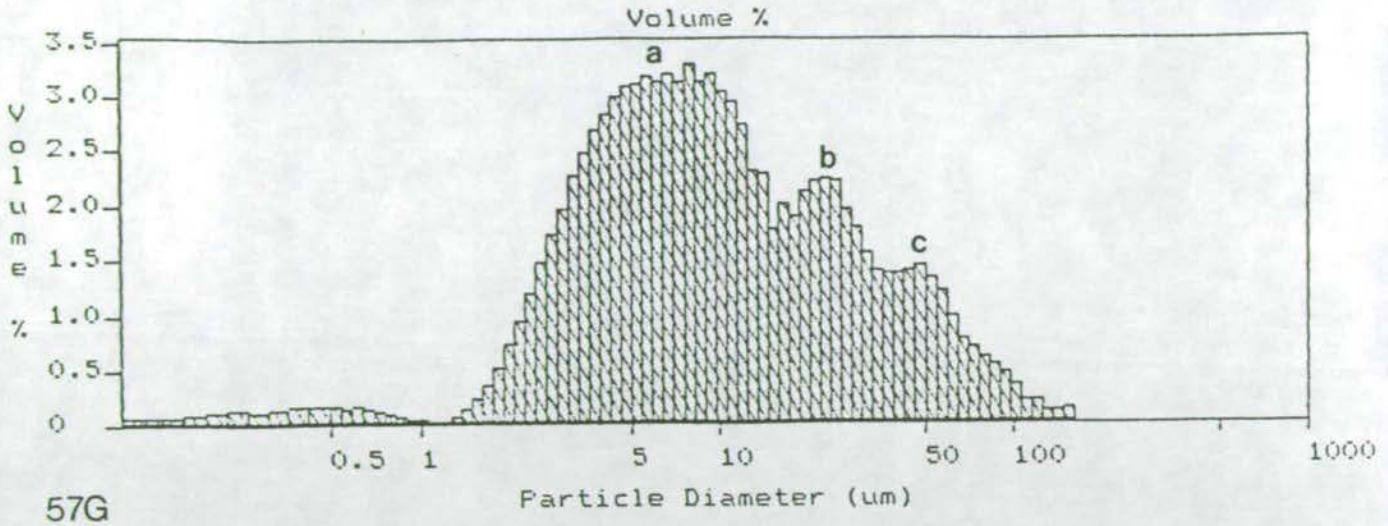

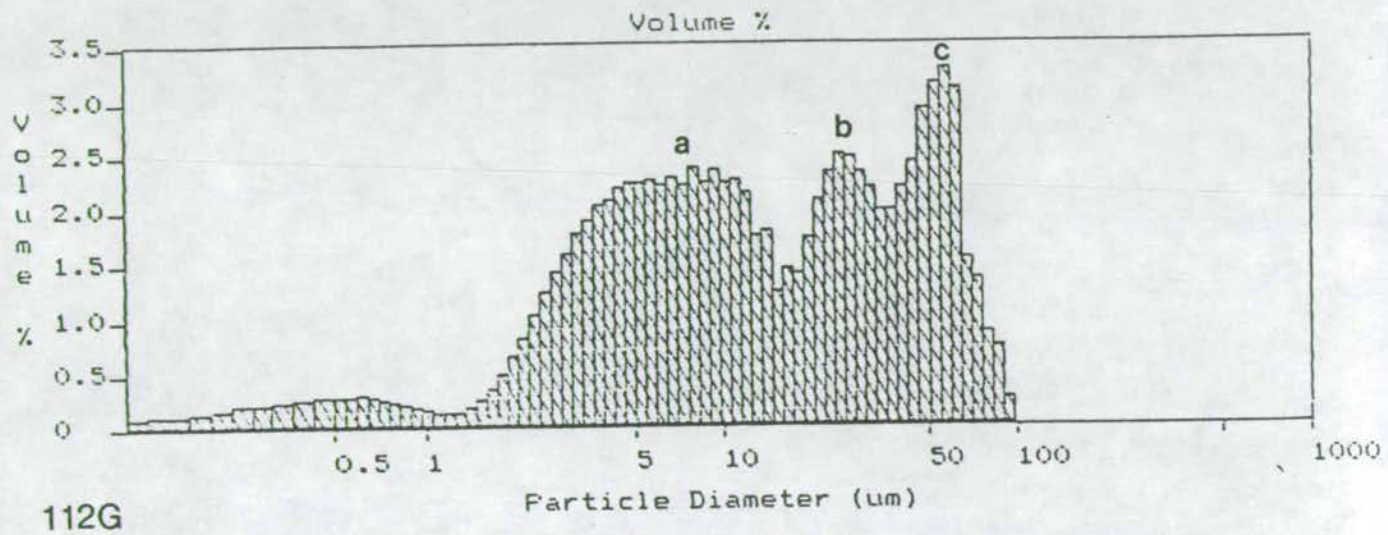

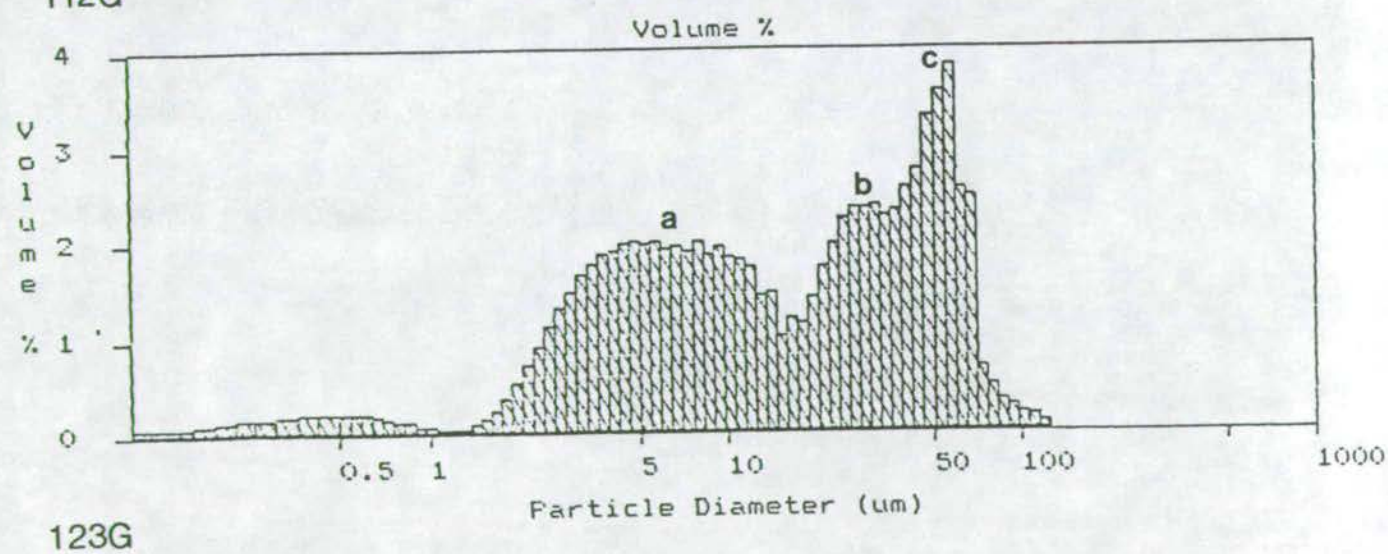

Figure B.4 Illustration of spurious modes recorded on laser particle size analyser (a result of an artifact of the instrument)

Although the laser particle size analyser is not perfect in its measurement of grain size, it is considerably faster than pipette analysis and does give highly reproducible results which are considered adequate for the purpose of comparing between samples in this study.

To check reproducibility, 10 replicate analyses of one sample were run through the whole analytical method and the mean grain size calculated by the method of moments (see text). The precision was calculated as 0.2 ϕ (1σ)

In order to measure the grain size distribution of the carbonate-free fraction of the sediment, $CaCO_3$ was removed from approximately 40 grams of wet untreated sample by addition of 10% HCl until all reaction had stopped. The sample was then sieved on a 62μm mesh and the percent gravel (> 2mm), percent sand (>62μm, < 2mm) and percent mud/silt (< 62μm) calculated.

B.3 X-RAY DIFFRACTION

B.3.1 **Bulk Samples**

These were dried and ground to a powder in an agate tema mill. A slurry was made by mixing approximately 0.5 grams of ground sample with acetone and pipetting this onto a glass slide. The slide was left to dry and then loaded into a Philips PW 1800 X-Ray Diffractometer. The machine was operated at 40kV and 50ma using Cu K α radiation and a monochromator. A 2°-60° 2θ trace was obtained for all the samples. Although software was available for automatically identifying minerals, all traces were examined manually and characteristic peaks of minerals identified using published tables.

B.3.2 **Clay Minerals**

These are only partially recognisable in X-Ray diffraction (XRD) traces of whole rock analyses and for this reason the clay fraction is separated for analysis. The <2μm fraction is collected by allowing a well stirred suspension of the whole sample to stand in a settling column for approximately 4 hours (exact timing was calculated from Stokes Law and varied according to temperature) then removing a 10ml

sample by pipette from 5cm depth. The original material was sediment which had been initially treated with Hydrogen Peroxide to remove organic material then stored wet. For this reason no deflocculent was added at any stage as clays were not thought to have aggregated in a any way through drying. An oriented mount was then prepared by allowing a 10ml suspension to dry out at 30°C onto a glass slide. Once the oriented mounts were prepared they were analysed by XRD from 2° to 25° 2θ as untreated samples. Then each slide was subjected to a series of treatments and analysed by XRD after each treatment which allows clarification of the clay minerals present. These treatments were:

1. glycolation at 60°C for 1 hour in a desiccator.
2. heated to 400°C for 30 minutes.
3. heated to 550°C for 30 minutes.

The clay minerals were identified by their characteristic basal spacing which, depending on the mineral, altered with the various treatments (details of the behaviour of each clay mineral with these treatments is given in the text - Chapter 3).

B.4 $CaCO_3$ CONTENT DETERMINATION

The $CaCO_3$ content of the sediments was obtained by treating approximately 5 grams of ground sediment (accurately weighed to 5 decimal places) with 1M HCl, heating to dryness on a hot plate and then repeating the procedure until reaction with HCl had ceased. The resulting dry weight of the residue was accurately measured and the percent weight loss calculated. Care was taken in ensuring all crucibles were clean and weighed accurately, and that no sample was lost (this was facilitated by adding HCl drop by drop to prevent the sample bubbling over and by keeping all the sample in one crucible throughout the whole procedure). Repeat analysis on one sample gave an analytical precision of 3% (1 σ, n=6) for approximately 20% $CaCO_3$.

B.5 ORGANIC CARBON DETERMINATION

In order to measure the organic carbon (C_{org}) content of sediments the carbonate carbon has to be removed first. Approximately 0.5 grams of sediment were accurately weighed (to 5 decimal places) and placed in LECO ceramic crucibles where they were treated with 3M HCl. Care was taken to ensure that the sediment was only just dampened as wetting would allow percolation of the acid through the porous walls of the crucible possible taking some Corg with it. The crucibles were placed on a hot plate until the acid evaporated and the procedure repeated, with thorough stirring of the samples after acid addition, until there was no reaction with HCl which indicated that all carbonate carbon was removed. Because strongly hydroscopic $CaCl_2$ forms from the reaction of HCl with $CaCO_3$, the samples were kept on a hot plate until transferred to the LECO combustion chamber. This prevented the samples from hydrating which would inhibit full combustion.

A LECO 521-200 induction furnace equipped with dust trap, sulphur trap and catalyst furnace was used for igniting the samples in a stream of CO_2-free oxygen. A LECO 572-100 carbon analyser used a gas burette to measure the change in volume which results when the O_2 and CO_2 mixture from the combustion furnace was flushed through CO_2-absorbing KOH. The C_{org} content was calculated from this change in volume measured in the burette and corrected for the ambient temperature and barometric pressure at the time of measurement and for the weight of the sediment sample.

HCl fumes formed by combusting $CaCl_2$ are oxidised in the MnO_2 trap (for SO_2 absorption) thus producing chlorine gas which can interfere with KOH absorption giving erroneous (high) results. Therefore, samples with >40% $CaCO_3$ were not analysed for C_{org}.

Analytical precision was 3.8% (1 σ, n=6) for approximately 2% C_{org} and 8.5% for approximately 0.5% C_{org}.

B.6 X-RAY FLUORESCENCE

B.6.1 Major Elements

Si, Al, Fe, Mg, Ca, K, Ti, Mn and P were analysed using X-ray fluorescence (XRF) spectrometry. Dried and ground bulk samples were made into glass discs by fusing the sample with lithium tetraborate flux (Johnson Matthey Spectroflux 105) using the technique described by Norrish and Hutton (1969) and Fitton and Dunlop (1985). Because the samples had relatively high organic carbon contents which would damage the platinum crucibles in which the samples were melted, all samples were pre-ignited in silica crucibles and the loss on ignition (LOI) calculated from weight loss measurements. The sample discs were analysed on a Philips PW 1480 X-ray spectrometer with a chromium tube and LiF(200) crystal. The analytical precision of the results is listed in Table B.1. Results were first of all corrected to take account of the LOI. Then a salt correcton was applied (described below) before recalculating the oxide percentages to non-oxide percentages (except P2O5) using the formulas listed in Table B.2.

B.6.1.1 Salt Correction

To ascertain the salt concentration of the interstitial water of selected surface and core sediments the chloride concentration of solutions taken from these sediments was measured using a High Pressure Liquid Chromatogram. Analysing the salt concentration of the pore waters is necessary in order to adjust XRF major element concentrations to take account of the cations found in salt (Na and Mg being the cations most affected by this adjustment). Although the correction is small its magnitude varies due to a change from brackish to marine conditions and this variation needs to be taken into account to ensure accurate elemental analyses and comparisons.

Method - Approximately 1gm of dried, chemically untreated sediment was dispersed in 500ml of Millepore filtered water, shaken thoroughly and left for 24 hours to allow chloride to completely dissolve. The solution was then filtered through a 0.45um millepore filter and approximately 30ml collected and stored in clean, dry polythene bottles. Care was taken to ensure no dilution or contamination took place at this stage. Each sample was injected into the ion-chromatogram and the areas of sample Cl peaks were compared (with the help of computer software) with standard Cl solutions. To calculate the ppt salt concentration of the dried sediment the following equation was used:-

Element Oxides	Mean Weight % (n=6)	1σ	Estimated Total Precision * (as % rel. st. dev. 1σ)
SiO_2	62.392	0.1	0.16
Al_2O_3	5.392	0.024	0.45
Fe_2O_3	3.598	0.012	0.33
MgO	3.236	0.012	0.37
CaO	22.144	0.058	0.26
Na_2O	0.881	0.036	4.09
K_2O	0.771	0.0065	0.84
TiO_2	0.281	0.004	1.40
MnO	0.031	0.0015	4.80
P_2O_5	0.128	0.004	1.60
Total	98.854	0.292	0.29
LOI#	18.6	0.04	0.21

* Total precision includes counting error, disc reproducibility and error in the regression line.

\# LOI (loss on ignition) calculated before fusing - above element percentages not recalculated to take account of LOI.

Table B.1. Precision of X-ray fluorescence major element analyses

OXIDE TO ELEMENT CONVERSIONS		
Si02 to Si	=	0.4674 x Si02
Al203 to Al	=	0.529 x Al205
Fe203 to Fe	=	0.6995 x Fe203
MgO to Mg	=	0.6032 x MgO
CaO to Ca	=	0.715 x CaO
Na20 to Na2	=	0.7419 x Na20
K20 to K2	=	0.8302 x K20
Ti02 to Ti	=	0.5994 x Ti02
MnO to Mn	=	0.7744 x MnO

Table B.2 Calculations used to convert major element oxides to elements

$$\% \text{ salt conc. of dried sed.} = \frac{\text{Cl conc.(ppm)/2}}{\text{Dried Sed wt. (mg)}} \div 0.5504 \times 100/1$$

The Cl conc is divided by 2 to make the concentration to ppm/litre. After dividing by the dry sediment weight the ppm/litre/mg is divided by 0.5504 to convert the Cl concentration to the total salt concentration (this figure is calculated from the data for total composition of sea salt given in Bearman (1989)- original source unknown). The water content of the sediment varies but is known from water loss measurements. Therefore to adjust the % salt concentration of dried sediment to percent of pore water the following equation is used:-

$$\% \text{ salt in water} = \% \text{ salt in dried sed.} \times \frac{\% \text{ sed. of total}}{\% \text{ water of total}}$$

Once the salt concentration in the water has been established (see results below) corrections are applied to the XRF major element analyses according to the following formulae:

1. for elements which form part of the salt content of water:

wt % Na = Total wt % Na - (0.306 x salt)

wt % K = Total wt % K - (0.011 x salt)

wt % Ca = Total wt % Ca - (0.012 x salt)

wt % Mg = Total wt % Mg - (0.037 x salt)

ppm Sr = Total ppm Sr - (4.13 x salt)

2. for the remaining elements:

Elemental % (salt free) = Element_{tot} x (100 / 100 - salt)

Results - The ppt salt concentrations as measured by HPLC analysis for 16 stations are listed in Table B.3. As expected, salinity varies considerably from nearshore areas out towards areas furthest from land. Work by Siripong et al (1987) shows net salinities of the whole water column per tidal cycle in the northern mangrove area in March (1980) to be 26.971 - this corresponds to 27 ppt at station 78 measured by HPLC. At the main channel mouth Siripong et al (1987) records 31.781 ppt (this compares to an HPLC measurement of 32.1 ppt at station 34) and 32.336 to 32.684 ppt for 7 measurements taken from the northern area of the Bay away from coastal areas

HPLC CHLORINE ANALYSIS - CALCULATIONS							
SAMPLE	Cl SOLN CONC ppm	DRY SED WT. mg	NaCl FACTOR	% SALT IN DRY SED	SED:WATER RATIO x:1	% SALT IN WATER	PPT
21G	33.03	1003.77	0.5504	2.99	0.754	2.3	22.5
22G	27.18	1017.23	0.5504	2.43	0.923	2.2	22.4
32G	37.45	1015.58	0.5504	3.35	1.000	3.3	33.5
33G	35.51	1013.09	0.5504	3.18	1.000	3.2	31.8
34G	13.08	998.84	0.5504	1.19	2.700	3.2	32.1
37G	10.35	1028.74	0.5504	0.91	2.030	1.9	18.6
38G	13.81	1037.72	0.5504	1.21	2.125	2.6	25.7
44G	25.43	1021.80	0.5504	2.26	1.500	3.4	33.9
47G	34	1011.24	0.5504	3.05	0.923	2.8	28.2
51G	16.23	1013.17	0.5504	1.46	2.030	3.0	29.5
60G	29.16	1012.70	0.5504	2.62	1.080	2.8	28.3
67G	25.57	1032.61	0.5504	2.25	0.785	1.8	17.7
71G	33.18	1068.71	0.5504	2.82	1.040	2.9	29.3
75G	20.07	1065.18	0.5504	1.71	1.857	3.2	31.8
78G	29.1	1349.70	0.5504	1.96	1.381	2.7	27.0
88G	28.02	1003.37	0.5504	2.54	1.380	3.5	35.0

Table B.3 **Results of HPLC chlorine analysis for salt content calculations**

	112G Ca = 12.7 wt% Al = 2.3 wt%			90G Ca = 0.22 wt% Al = 12.21 wt%		
Element	Mean ppm (n=6)	1σ	Estimated Total Precision * (as % rel. st. dev. 1σ)	Mean ppm (n=6)	1σ	Estimated Total Precision * (as % rel. st. dev. 1σ)
Nb	8.8	0.48	5.5	36.2	0.52	1.4
Zr	175.1	6.89	3.9	167.8	3.65	2.2
Y	14.4	0.463	3.2	55.0	0.534	0.97
Sr	792.3	5.17	0.6	46.3	0.51	1.1
Rb	48.1	0.71	1.5	314.7	3.4	1.1
Th	11.1	0.674	5.8	56.4	0.95	1.7
Pb	19.1	0.743	3.9	79.8	0.766	0.96
Zn	23.9	0.87	3.6	68.2	0.447	0.66
Ni	15.4	0.354	2.3	25.1	0.65	2.6
Cr	43.2	2.87	6.6	64.7	0.92	1.4
Nd	20.4	3.08	15.0	50.9	3.69	7.2
Ce	48.6	4.18	8.6	118.4	6.7	5.7
La	25.8	4.22	16.3	58.7	3.02	5.1
V	39.9	2.23	5.6	73.4	1.55	2.1
Ba	88.8	11.26	12.6	156.5	5.71	3.6

* Total precision includes counting error, disc reproducibility and error in the regression line.

Table B.4 **Precision of XRF trace element analyses**

(28.2 to 33.9 ppt by HPLC). This variation is probably caused by a combination of experimental error in the HPLC method and time variation between sample collection for both methods. Salt correction figures for different areas of the bay are taken from a combination of these water salinity measurements and HPLC measurements. A salt correction figure of 26.971 is used for the near shore and mangrove channel areas (delineated as the approximate boundary of low salinity in the NE-monsoon (Limpsaichol et al, 1988)) 32.51 ppt is used for the northern non-coastal areas of the Bay, and 32.94 ppt for the southern area. The boundary delineating the latter 2 areas is taken from Limpsaichol et al (1988) where salinity concentration distributions are illustrated for both NE and SW monsoon seasons. Since all samples were collected in January (1989 and 1990) all salinity figures used are for the NE monsoon season.

B.6.2 Trace Elements

Sc, Ba, V, La, Ce, Nd, Cr, Ni, Cu, Zn, Pb, Th, Rb, Sr, Y, Zr, Nb and Sn were analysed on the same spectrometer as for the major elements but using a Rhodium tube. Dried and ground samples were made into pressed powder discs using 6 grams of sample. The spectrometer was already calibrated for 17 of these 18 elements but for Sn a series of standards were made up from Analar $CaCO_3$ and SnO_2 and these were used to calibrate the machine before each batch of samples were run for Sn. Analytical precision for each element from 2 samples of varying composition are listed in Table B.4.

B.7 ELECTRON MICROPROBE ANALYSES

In order to measure the chemical composition of lepidolite mica grains a 'Cameca Camebax Microbeam' electron microprobe was used. The standard used was Rb Mn F_3. Although there are difficulties in quantitively measuring the Rb peak due to its close proximity to the Si peak, a Rb peak was identified and attempts at quantifying the Rb concentration from this peak are listed in the text of Chapter 4.

APPENDIX C

STATISTICAL ANALYSES

APPENDIX C - STATISTICAL ANALYSES

C.1 INTRODUCTION

All statistical calculations were computed using the Minitab programme. The following sections define some of the important points to note about the method of each test. For a more detailed description including formulas, refer to Ryan, Joiner and Ryan (1985) and the Minitab reference manual (release 7).

C.2 CORRELATION COEFFICIENTS

The Pearson product moment correlation coefficient was used. Only the lower triangle of the correlation matrix is computed. The programme uses 'pairwise deletion' of missing values, ie calculates the correlation coefficient using only the samples that have data for both variables.

Confidence Limits on Correlation Coefficients (calculated manually)
In order to know which correlation coefficients are significant at a level of 95% or greater the following hypothesis test is investigated:

ρ = population correlation coefficient of variables X and Y
r = sample correlation coefficient of variables x and y

(Capital symbols refer to population characteristics whilst lower case symbols refer to the sample characteristics).

n = sample size

$$W = 0.5 \log_e \frac{1 + \rho}{1 - \rho}$$

$$w = 0.5 \log_e \frac{1 + r}{1 - r}$$ (both w and W can be found from tables)

The variable w is approximately Normally distributed (only very good when $n > 50$) with mean = W and standard deviation = $1 / \sqrt{n - 3}$.

The standardised Normal variable, $z = |w - W| \sqrt{n - 3}$.

$H_o \rightarrow \rho = 0.5$ ie, 25% ($100 (0.5)^2$) of the variability of X or Y is "explained" by a fitted straight line on a graph of X versus Y.

We need to find the limiting correlation coefficent r, with a sample size of 157 (for the whole of Phangnga Bay) for a 95% confidence limit (standardised Normal variable = 1.96).

$\therefore |w - W| \sqrt{n - 3} = 1.96$

$\therefore |w - 0.5493| \sqrt{154} = 1.96$

$\therefore w = 0.7072$

hence $r = 0.609$

Therefore, when $\rho = 0.5$, the limiting correlation coefficient corresponding to a confidence level of 95% is 0.609. Hence, in the correlation matrix (Table 4.1), when the correlation coefficient is > 0.609 we reject the null hypothesis that $\rho = 0.5$ and can say that there is correlation between x and y. Similarly when $r < 0.609$ we accept the null hypothesis and say there is no significant correlation.

"n" changes for each environment (and in some cases between parameters within one environment) therefore the confidence limits change accordingly. These variations are noted on each table.

C.3 PRINCIPAL COMPONENTS ANALYSIS

This is a data reduction technique used to identify a small set of variables that account for a large proportion of the total variance in the original variables. The components are calculated from the correlation matrix. The output from the Minitab programme includes the eigenvalues (ie the variances of the principal components) and the proportion and cumulative proportion of the total variance explained by each principal component as well the the coefficients for each principal component. The principal component scores are calculated from the standardized variables, ie subtract the mean and divide by the standard deviation of each variable then multiply by the coefficients.

C.4 INDEPENDANT TWO SAMPLE T-TEST

For this test the programme used does not assume that the two populations have equal variances (ie, it does not use the pooled t method). On average the analysis will be slightly conservative (ie slightly less likely to reject a true null hypothesis) however it removes the possibility of large error gained if the equal variances assumption is wrong. The critical points for a 95% confidence level and for the number of degrees of freedom were read from t-tables.

C.5 CLUSTER ANALYSIS

The cluster analysis software 'CLUSTAN' (version 3.2) was used on the Edinburgh University Unix mainframe system to carry out the cluster analysis. For future reference, the following programme was used within Clustan:-

assign, file = ------, specification = ------ (input file)
read data, variables continuous 1-6, cases 154, infile = ------
read labels, cases
assign file = ---, specification = --- (output file)
cluster, method average, measure seuclid, transform standardise,
save tree outfile = ---
select graphics device, plotter
plink, layout title "---", labels, coefficients, dendrogram full

For further information on Clustan see Wishart (1987).

APPENDIX D

DATA TABLES

Major Element analyses of surface sediments (recalculated from oxides and salt-corrected)

SAMPLE	Fe	Mn	Ti	Ca	K2	P205	Al	Si	Mg
3G	1.28	0.013	0.154	9.86	0.213	0.099	2.27	30.44	1.10
4G	1.25	0.015	0.072	9.64	0.056	0.063	0.82	32.08	0.98
5G	0.69	0.006	0.071	7.83	0.111	0.034	0.71	34.32	0.66
6G	1.16	0.014	0.092	6.83	0.086	0.061	1.00	35.47	0.86
7G	2.66	0.024	0.096	10.03	0.159	0.079	1.58	29.15	1.56
8G	1.79	0.019	0.126	9.29	0.342	0.062	2.36	28.29	1.23
9G	2.19	0.024	0.322	2.92	0.937	0.120	5.52	31.35	1.38
10G	2.54	0.025	0.292	3.70	0.916	0.108	5.51	28.27	1.61
11G	2.50	0.026	0.125	9.53	0.266	0.088	2.44	27.98	1.67
12G	1.16	0.009	0.165	4.17	0.293	0.070	2.12	36.11	0.77
13G	2.31	0.042	0.113	11.06	0.290	0.076	1.99	28.91	1.07
14G	2.83	0.027	0.375	2.62	1.263	0.134	7.50	27.25	1.73
15G	1.64	0.021	0.097	10.94	0.263	0.064	1.94	27.30	1.04
16G	2.40	0.020	0.323	2.15	1.011	0.113	5.89	29.91	1.33
17G	2.63	0.023	0.335	2.87	0.921	0.117	5.94	30.24	1.46
18G	2.82	0.027	0.366	2.95	1.062	0.118	6.69	28.83	1.53
19G	3.15	0.025	0.389	1.62	1.362	0.117	7.72	27.73	1.52
20G	2.66	0.025	0.349	2.00	1.216	0.109	6.63	30.46	1.32
21G	2.48	0.025	0.319	2.90	0.930	0.102	5.67	30.86	1.22
22G	2.11	0.014	0.281	1.46	0.754	0.098	4.01	35.04	0.90
23G	0.49	0.015	0.042	31.84	0.111	0.053	0.83	4.68	0.55
24G	2.39	0.030	0.240	13.31	0.526	0.109	5.05	19.17	1.20
25G	3.25	0.029	0.431	1.33	1.571	0.115	9.25	26.74	1.50
26G	0.63	0.008	0.086	0.25	0.345	0.035	1.21	43.21	0.17
27G	1.43	0.010	0.146	10.25	0.406	0.056	2.72	32.49	0.68
28G	0.37	0.003	0.060	3.58	0.093	0.024	0.50	38.23	0.10
29G	2.65	0.026	0.379	1.00	1.294	0.118	7.36	29.20	1.23
30G	2.64	0.022	0.346	2.79	1.304	0.108	7.01	28.99	1.27
31G	2.91	0.024	0.341	2.20	1.598	0.106	7.64	29.68	1.23
32G	2.90	0.030	0.379	1.74	1.673	0.104	8.38	28.14	1.38
33G	3.47	0.040	0.299	4.70	1.383	0.111	7.77	25.37	1.36
34G	1.88	0.027	0.205	0.94	1.490	0.080	6.79	33.28	0.63
35AG	3.11	0.069	0.308	0.09	2.417	0.080	14.65	25.72	0.54

SAMPLE	Fe	Mn	Ti	Ca	K2	P205	Al	Si	Mg
35BG	0.78	0.020	0.080	0.07	2.301	0.018	3.73	39.96	0.12
36G	2.08	0.021	0.263	0.23	1.442	0.078	5.80	33.79	0.65
37G	1.13	0.013	0.134	0.19	0.341	0.046	1.75	42.21	0.30
38G	1.48	0.028	0.159	0.40	2.101	0.046	4.52	36.53	0.39
39G	3.05	0.039	0.234	12.79	0.618	0.100	6.32	17.97	1.20
40G	1.61	0.018	0.195	2.90	0.718	0.062	3.72	34.95	0.53
41G	3.24	0.026	0.408	0.91	1.588	0.115	9.08	26.48	1.30
42G	3.46	0.039	0.403	0.78	1.730	0.121	10.66	25.40	1.34
43G	3.07	0.021	0.439	0.35	1.627	0.120	9.35	26.64	1.29
44AG	0.19	0.024	0.010	35.89	0.035	0.035	0.24	0.75	0.67
44G	1.84	0.027	0.178	16.52	0.276	0.089	3.44	18.53	0.89
45G	0.94	0.033	0.072	30.29	0.023	0.075	1.59	5.91	0.73
46G	2.86	0.029	0.367	1.77	1.477	0.109	8.53	27.49	1.24
47G	2.58	0.026	0.334	3.10	1.320	0.120	6.98	29.46	1.26
48G	2.35	0.033	0.250	12.52	0.621	0.114	5.81	20.29	1.20
49G	2.02	0.021	0.293	3.68	0.770	0.105	4.78	32.12	1.07
50G	2.35	0.027	0.311	7.59	0.763	0.114	6.65	22.37	1.56
51G	1.51	0.021	0.118	23.01	0.349	0.073	2.44	12.53	1.08
52G	2.48	0.024	0.348	1.81	1.440	0.118	7.17	29.46	1.28
53G	2.86	0.023	0.402	2.43	1.265	0.137	7.87	26.53	1.62
54G	1.79	0.021	0.241	5.17	0.758	0.122	4.06	31.00	0.91
55G	0.76	0.015	0.061	30.56	0.028	0.098	1.45	5.45	0.77
56G	2.98	0.039	0.404	2.71	1.438	0.129	8.68	25.96	1.72
57G	1.51	0.020	0.176	12.68	0.296	0.097	3.46	23.72	0.98
58G	1.47	0.024	0.082	16.36	0.133	0.072	1.57	22.05	1.11
59G	1.18	0.019	0.063	13.95	0.106	0.048	1.14	26.62	0.82
60G	2.37	0.032	0.256	4.74	0.784	0.119	4.90	29.93	1.32
61G	2.43	0.026	0.343	3.47	1.136	0.126	6.51	29.35	1.44
62G	1.47	0.019	0.095	9.41	0.159	0.054	1.67	30.64	1.08
63G	2.64	0.022	0.365	5.40	1.005	0.118	7.54	25.76	1.49
64G	0.90	0.010	0.069	17.58	0.179	0.051	1.27	22.40	0.99
65G	1.62	0.018	0.164	6.04	0.510	0.072	2.68	32.95	1.02
66G	0.77	0.010	0.083	17.24	0.199	0.045	1.42	22.28	0.69

Major Element analyses of surface sediments (cont'd)

SAMPLE	Fe	Mn	Ti	Ca	K2	P205	Al	Si	Mg
67G	2.80	0.022	0.406	3.31	1.287	0.120	7.87	28.16	1.38
68G	0.92	0.014	0.101	24.49	0.138	0.098	1.69	13.25	0.68
69G	0.83	0.020	0.081	27.18	0.057	0.075	1.34	9.62	0.69
70G	2.00	0.012	0.268	2.75	0.687	0.083	4.15	32.27	0.91
71G	0.43	0.004	0.065	3.46	0.186	0.015	0.62	38.21	0.19
72G	2.07	0.011	0.279	2.84	0.700	0.090	4.36	33.53	0.96
73G	0.46	0.002	0.076	3.35	0.159	0.092	0.63	41.69	0.22
74G	1.51	0.020	0.109	20.70	0.168	0.083	1.98	16.31	1.08
75G	1.52	0.025	0.123	24.19	0.153	0.088	2.26	11.80	1.00
77G	3.32	0.030	0.387	-0.00	1.814	0.063	11.79	23.81	0.84
78G	2.94	0.018	0.368	0.24	1.623	0.072	9.41	27.62	0.78
79AG	3.69	0.034	0.401	0.25	1.826	0.110	11.49	24.90	0.79
79BG	0.95	0.029	0.099	8.34	0.712	0.094	1.77	29.07	2.17
80G	3.33	0.024	0.431	0.29	1.641	0.097	9.43	27.65	1.27
81G	2.90	0.026	0.410	0.58	1.578	0.101	9.02	27.93	1.22
82G	3.47	0.024	0.427	0.54	1.746	0.103	9.67	26.74	1.23
83G	0.56	0.012	0.119	6.27	0.241	0.026	1.14	37.37	0.20
84G	0.89	0.015	0.107	9.30	0.385	0.049	1.70	32.72	0.28
85G	1.67	0.027	0.156	12.55	0.505	0.079	3.90	24.51	0.50
86G	2.85	0.035	0.308	0.22	2.134	0.078	11.23	23.13	0.72
88G	3.48	0.042	0.408	0.23	1.884	0.096	11.62	26.17	1.01
89G	2.48	0.027	0.303	0.23	1.880	0.075	9.07	30.56	0.75
90G	3.16	0.031	0.369	0.22	2.255	0.078	12.21	25.29	0.94
91G	0.92	0.019	0.112	3.55	1.415	0.022	3.72	36.55	0.24
92G	3.30	0.037	0.378	0.34	2.181	0.093	12.62	24.93	0.99
93G	2.58	0.034	0.293	0.35	2.613	0.062	9.31	30.51	0.64
94G	0.37	0.003	0.076	0.18	0.229	0.102	0.83	45.23	0.14
95G	0.83	0.009	0.098	3.02	0.242	0.021	1.57	39.29	0.31
96G	1.17	0.011	0.145	4.77	0.321	0.038	2.24	34.65	0.48
97G	2.27	0.021	0.173	4.42	0.520	0.050	2.91	34.04	0.55
98G	2.09	0.015	0.115	6.93	0.230	0.060	2.20	32.76	0.64
99G	2.59	0.026	0.330	0.88	0.999	0.091	6.05	30.46	1.17
100G	1.56	0.012	0.207	0.98	0.570	0.066	3.39	36.99	0.78

SAMPLE	Fe	Mn	Ti	Ca	K2	P205	Al	Si	Mg
101G	2.90	0.022	0.362	1.75	1.152	0.108	6.43	28.41	1.42
102G	2.64	0.015	0.335	1.53	1.039	0.099	6.08	30.08	1.37
103G	2.47	0.023	0.311	7.63	0.875	0.097	5.85	24.12	1.31
104G	2.22	0.019	0.251	2.02	0.811	0.076	4.46	33.55	1.08
105G	2.33	0.026	0.320	2.57	1.028	0.091	5.75	31.24	1.17
106G	1.95	0.039	0.041	18.29	0.164	0.072	0.96	19.98	1.21
107G	2.30	0.027	0.148	6.09	0.361	0.077	2.73	31.79	1.58
108G	1.53	0.018	0.091	7.57	0.141	0.042	1.31	33.18	1.10
109G	1.08	0.014	0.071	4.34	0.141	0.027	0.83	38.14	0.87
111G	0.91	0.058	0.043	25.44	0.122	0.083	0.88	12.37	1.25
112G	2.05	0.021	0.127	12.86	0.514	0.088	2.31	23.80	1.62
113G	0.86	0.010	0.071	7.68	0.212	0.045	0.87	34.45	0.67
114G	0.56	0.017	0.076	20.33	1.016	0.116	1.33	17.37	1.20
115G	1.17	0.012	0.097	12.76	1.133	0.084	1.92	25.82	1.05
117G	0.61	0.011	0.040	19.04	1.296	0.079	1.76	18.89	1.07
118G	0.02	-0.001	0.003	32.91	0.541	0.029	0.54	3.47	0.74
119G	0.03	-0.002	0.003	33.04	0.458	0.024	0.45	3.41	0.66
120G	0.47	0.010	0.043	16.56	0.979	0.103	1.31	22.57	0.97
121G	0.48	0.011	0.054	13.99	0.159	0.055	0.64	27.08	0.88
122G	0.65	0.009	0.049	11.66	0.140	0.049	0.61	29.89	0.91
123G	0.66	0.013	0.052	14.06	0.165	0.065	0.82	26.29	1.00
124G	1.01	0.008	0.063	8.11	0.140	0.049	0.67	34.04	0.80
125G	1.89	0.048	0.059	16.73	0.107	0.100	1.03	21.46	1.49
126G	1.20	0.019	0.081	9.76	0.204	0.056	1.14	30.95	1.11
127G	0.53	0.009	0.052	8.48	0.100	0.033	0.59	34.06	0.74
128G	0.57	0.010	0.041	7.23	0.048	0.027	0.43	35.67	0.65
129G	1.17	0.022	0.071	6.20	0.162	0.046	0.91	35.63	0.95
130G	1.06	0.008	0.054	6.79	0.108	0.036	0.79	35.37	0.96
131G	0.70	0.008	0.091	6.43	0.137	0.051	0.94	35.82	0.75
132G	0.20	0.001	0.034	23.82	0.044	0.044	0.39	15.47	0.79
133G	0.06	0.000	0.007	35.28	0.021	0.029	0.14	1.02	0.58
134G	0.03	-0.001	0.002	35.28	0.017	0.031	0.04	1.23	0.67
135G	0.59	0.003	0.065	9.25	0.101	0.048	0.83	32.49	0.81

Major Element analyses of surface sediments (cont'd)

SAMPLE	Fe	Mn	Ti	Ca	K2	P205	Al	Si	Mg
136G	1.01	0.013	0.074	9.64	0.120	0.042	0.82	31.57	1.12
137G	0.68	0.012	0.055	13.88	0.170	0.046	0.80	26.75	0.98
138G	0.91	0.009	0.054	9.92	0.308	0.050	1.00	31.30	0.87
139G	1.42	0.012	0.145	9.53	0.667	0.064	2.82	27.66	1.31
AQ-KL1	0.23	0.004	0.020	33.67	0.060	0.048	0.51	1.69	0.80
AQ-KL2	0.31	0.003	0.029	32.51	0.067	0.065	0.70	3.15	0.96
AQ-KL3	0.32	0.003	0.024	32.71	0.073	0.083	0.60	2.27	1.38
AQ-KL4	0.51	0.005	0.027	32.59	0.061	0.100	0.69	2.15	1.68
AQ-KL5	0.69	0.010	0.076	21.82	0.153	0.062	1.60	9.03	2.00
AQ-KL6	0.76	0.012	0.084	24.16	0.224	0.065	1.78	10.02	2.21
AQ-KL7	0.85	0.011	0.106	23.19	0.260	0.068	2.28	10.66	2.13
AQ-KL8	1.02	0.013	0.123	19.77	0.417	0.071	2.56	15.00	1.83
AQ-KL9	1.00	0.012	0.136	19.08	0.408	0.075	2.67	15.73	1.70
AQ-KL10	0.85	0.012	0.113	21.81	0.271	0.073	2.27	12.54	1.94
AQ-KL11	0.59	0.010	0.082	24.25	0.219	0.065	1.47	11.05	1.88
AQ-KL12	0.80	0.010	0.112	21.70	0.293	0.075	2.11	13.38	1.74
AQ-KL13	0.96	0.010	0.133	20.45	0.329	0.084	2.54	14.49	1.57
AQ-KL14	0.59	0.005	0.075	28.31	0.223	0.067	1.58	6.80	0.99
AQ-KL15	0.32	0.003	0.037	32.32	0.099	0.050	0.89	3.26	0.67
AQ-KL16	0.41	0.001	0.046	16.58	0.118	0.025	0.52	24.53	0.37
AQ-KL17	0.25	-0.001	0.115	1.57	0.126	0.003	0.33	45.23	0.11
TK1	0.38	0.005	0.040	32.13	0.090	0.055	1.03	3.18	0.68
TK2	0.09	-0.002	0.030	20.88	0.036	0.022	0.17	19.90	0.34
TK3	0.18	-0.002	0.037	23.49	0.061	0.029	0.35	16.27	0.40
TK4	0.32	0.002	0.039	27.87	0.030	0.019	0.16	11.58	0.36
TK5	0.30	0.004	0.031	27.70	0.111	0.039	0.75	2.62	0.69
TK6	0.38	0.010	0.040	36.68	0.113	0.056	1.01	3.50	0.91

Organic Carbon and Iodine contents of selected surface sediments

SAMPLE NUMBER	Organic Carbon (wt %)	Iodine (ppm)	SAMPLE NUMBER	Organic Carbon (wt %)	Iodine (ppm)
6G	0.003	16.2	67G	1.438	45.4
8G	0.585	-	69G	1.650	11.4
12G	0.800	-	72G	1.600	41.6
15G	0.657	23.7	79AG	2.980	-
21G	1.600	32.0	81G	2.312	-
22G	1.940	35.3	86G	1.413	-
24G	1.497	37.4	88G	1.880	-
28G	1.510	27.3	93G	1.400	-
33G	1.525	32.0	95G	0.811	-
37G	0.600	12.6	98G	1.065	-
38G	0.400	11.4	107G	0.770	27.1
43G	2.640	58.6	109G	0.369	15.7
46G	1.803	45.1	112G	0.902	40.8
50G	1.395	54.4	115G	0.791	36.2
53G	1.597	-	122G	0.782	24.2
60G	1.090	39.2	126G	0.530	28.3
64G	0.673	29.6	128G	2.146	-
65G	0.760	27.6	131G	0.330	24.7
66G	1.059	24.4	135G	0.718	35.1

Calcium Carbonate content of surface sediments (calculated from weight loss by acidulation)

SAMPLE NUMBER	wt %	SAMPLE NUMBER	wt %	SAMPLE NUMBER	wt %	SAMPLE NUMBER	wt %	SAMPLE NUMBER	wt %
3G	25.50	35AG	0.90	65G	21.00	97G	14.40	130G	21.00
4G	26.80	35BG	2.70	66G	42.00	98G	26.00	131G	19.50
5G	19.70	36G	1.50	67G	12.50	99G	7.00	132G	57.70
5G	21.50	37G	0.10	68G	63.00	100G	6.50	133G	81.70
7G	25.60	38G	3.60	69G	70.00	101G	8.50	134G	84.20
8G	25.12	39G	41.00	70G	15.00	102G	4.40	135G	25.20
9G	12.40	40G	9.70	71G	13.00	103G	22.80	136G	28.00
10G	13.60	41G	4.90	72G	11.00	104G	9.40	137G	33.70
11G	27.50	42G	4.70	73G	9.00	105G	11.50	138G	22.00
12G	15.00	43G	2.50	74G	47.00	106G	51.80	139G	25.70
13G	35.69	44AG	95.20	75G	65.20	107G	19.40	AQ-KL1	84.10
14G	12.10	44BG	44.50	76G	7.00	108G	23.40	AQ-KL2	85.10
15G	32.40	45G	73.00	77G	0.20	109G	14.00	AQ-KL3	76.60
16G	11.20	46G	7.50	78G	5.00	111G	71.40	AQ-KL4	74.10
17G	12.40	47G	9.80	79AG	1.30	112G	33.70	AQ-KL5	63.40
18G	14.50	48G	35.70	79BG	26.40	113G	20.00	AQ-KL6	61.00
19G	10.40	49G	10.00	80G	6.00	114G	49.30	AQ-KL7	54.30
20G	9.80	50G	25.80	81G	6.00	115G	33.20	AQ-KL8	56.40
21G	12.90	51G	51.60	82G	5.00	116G	41.40	AQ-KL9	53.90
22G	6.70	52G	7.60	83G	19.00	117G	48.80	AQ-KL10	59.60
23G	78.90	53G	10.80	84G	27.40	118G	90.80	AQ-KL11	60.60
24G	42.60	54G	13.80	85G	40.00	119G	91.40	AQ-KL12	56.40
25G	6.60	55G	72.50	86G	5.00	120G	41.40	AQ-KL13	50.20
26G	2.00	56G	12.30	88G	6.00	121G	35.40	AQ-KL14	76.30
27G	30.80	57G	36.60	89G	4.00	122G	28.10	AQ-KL15	77.50
28G	11.40	58G	40.80	90G	4.00	123G	38.80	AQ-KL16	52.70
29G	5.20	59G	35.20	91G	10.00	124G	24.00	AQ-KL17	3.80
30G	11.90	60G	18.10	92G	3.00	125G	43.00	TK1	80.33
31G	12.60	61G	12.80	93G	3.00	126G	26.00	TK2	58.50
32G	9.90	62G	30.90	94G	2.00	127G	25.00	TK3	65.00
33G	15.70	63G	19.90	95G	8.00	128G	21.00	TK4	71.90
34G	5.20	64G	44.60	96G	15.20	129G	17.40	TK5	75.50
								TK6	89.20

Trace Element analyses of surface sediments
(Sr corrected for salt)

SAMPLE NUMBER	Nb ppm	Zr ppm	Y ppm	Sr ppm	Rb ppm	Th ppm	Pb ppm	Zn ppm	Ni ppm	Cr ppm	Ce ppm	Nd ppm	La ppm	V ppm	Ba ppm	Sn ppm
3G	9.0	233.4	15.3	597.2	37.7	9.2	11.5	21.1	12.2	40.7	43.0	15.3	21.3	29.3	59.0	8.0
4G	5.6	192.4	11.3	528.9	10.3	4.8	8.4	17.2	4.6	18.8	26.2	8.7	10.4	11.9	30.3	10.0
5G	5.0	213.7	6.2	421.2	10.2	3.5	6.5	14.9	3.4	16.3	21.1	11.4	6.5	9.8	27.1	4.7
6G	5.7	203.9	9.0	353.3	13.3	4.5	8.1	16.6	5.5	26.1	24.4	9.2	7.6	12.0	29.7	2.4
7G	6.7	143.2	11.6	520.1	19.4	5.3	12.1	16.5	10.6	33.2	40.6	9.0	18.3	21.2	24.8	4.7
8G	8.0	129.8	11.6	520.2	39.3	9.3	13.3	24.1	14.1	47.5	58.4	15.8	20.3	38.5	77.1	1.7
9G	16.2	274.0	26.0	225.6	89.6	19.3	24.6	39.5	20.3	70.1	68.2	29.0	32.8	54.4	120.8	9.6
10G	15.5	241.4	24.4	265.1	98.0	19.3	24.5	42.9	21.7	69.3	74.8	25.5	29.5	52.5	126.1	6.6
11G	7.4	126.0	12.4	522.9	40.9	8.1	16.3	27.8	13.6	47.6	52.0	25.4	24.2	30.1	78.6	6.9
12G	8.1	238.7	12.9	325.6	32.3	8.2	11.4	19.4	9.1	36.0	35.2	20.9	18.6	26.4	56.7	1.3
13G	10.1	99.6	12.5	759.6	45.9	8.3	17.2	35.1	18.6	76.6	47.9	12.6	20.9	76.1	66.7	16.6
14G	18.7	200.6	26.9	199.2	120.6	24.4	31.4	52.7	26.7	79.6	79.7	34.0	40.7	66.2	138.6	8.8
15G	7.5	74.9	11.8	784.1	44.4	8.6	12.5	24.1	12.4	45.9	50.5	20.5	24.2	39.7	77.8	12.7
16G	16.9	229.5	23.7	158.9	93.9	20.4	28.1	45.6	22.5	72.3	81.1	31.7	36.7	61.5	126.4	6.7
17G	15.1	239.7	23.1	208.7	84.3	16.2	23.9	45.3	23.3	76.3	80.8	32.9	35.9	58.4	119.0	7.1
18G	17.1	242.4	25.2	199.9	94.6	19.8	26.8	51.7	27.6	81.2	81.4	31.3	44.3	67.3	129.1	5.0
19G	20.2	230.7	29.3	133.5	120.5	24.5	34.9	53.4	26.9	81.3	88.0	35.1	43.0	71.4	151.3	10.0
20G	18.3	273.7	26.7	143.7	109.1	21.4	31.0	46.6	21.7	72.3	82.6	32.7	39.1	65.7	141.0	9.7
21G	15.1	246.1	23.3	175.2	84.1	18.4	25.2	38.3	18.6	60.5	64.6	23.0	32.5	52.3	103.2	5.3
22G	12.3	286.6	21.9	111.1	62.0	14.3	21.1	29.5	14.5	51.5	57.5	26.7	24.7	41.3	93.1	2.5
23G	3.3	72.2	7.6	1853.4	12.5	3.1	5.2	11.1	6.1	14.6	27.8	13.6	7.7	19.5	33.3	2.9
24G	14.1	175.6	22.7	773.7	88.3	18.9	25.9	45.3	19.6	68.2	70.1	20.4	43.4	59.1	102.6	6.9
25G	21.6	201.8	30.6	104.0	130.8	28.0	42.2	35.7	15.6	38.5	60.7	24.8	19.0	36.4	57.6	10.5
26G	4.9	89.7	8.0	26.1	23.8	4.7	7.7	8.8	4.7	16.2	35.7	14.1	13.0	24.7	157.7	-1.7
27G	4.9	108.5	5.9	183.6	13.3	3.3	4.7	5.8	2.6	4.7	26.2	6.4	11.8	9.6	33.3	-0.3
28G	—	—	—	—	—	—	—	—	—	—	—	—	—	—	—	1.7
29G	19.4	234.8	29.2	94.3	117.6	24.6	34.3	50.7	24.0	78.1	85.5	31.8	35.2	73.7	147.0	9.4
30G	20.4	241.2	29.2	172.8	133.0	24.8	32.9	49.0	22.2	72.5	79.8	33.9	43.9	64.7	145.3	12.6
31G	21.8	217.6	30.9	141.7	168.2	29.5	40.6	53.7	23.8	70.7	86.1	34.5	38.6	66.1	137.0	16.5
32G	24.8	246.9	34.9	124.2	174.8	30.8	44.5	31.7	13.6	29.9	46.6	21.9	20.4	32.4	61.4	20.1

Trace Element analyses of surface sediments (cont'd)

SAMPLE NUMBER	Nb ppm	Zr ppm	Y ppm	Sr ppm	Rb ppm	Th ppm	Pb ppm	Zn ppm	Ni ppm	Cr ppm	Ce ppm	Nd ppm	La ppm	V ppm	Ba ppm	Sn ppm
33G	21.0	179.5	33.5	234.6	162.2	34.0	47.3	55.9	17.7	54.1	78.1	31.2	34.3	54.1	110.3	19.9
34G	20.7	110.5	33.9	52.0	201.9	33.7	50.8	47.1	15.9	51.1	96.8	44.3	47.5	60.2	126.2	22.3
35AG	44.9	162.4	74.2	29.1	387.6	73.9	107.0	61.3	18.7	36.0	120.8	50.2	59.9	51.0	113.7	46.3
35BG	17.7	55.8	20.5	13.6	368.7	12.8	49.8	28.4	4.7	9.4	38.2	21.6	17.3	9.9	83.6	34.0
36G	20.2	251.1	33.4	40.5	159.4	25.8	38.1	36.6	14.8	51.0	79.9	30.3	40.1	55.4	117.4	18.5
37G	9.0	190.1	11.9	21.5	32.6	7.2	10.9	18.0	7.0	23.2	45.2	18.1	22.2	24.2	51.0	6.6
38G	23.3	192.6	24.1	42.6	343.5	18.8	37.8	35.9	7.6	16.3	36.1	16.2	22.9	25.2	109.6	36.7
39G	18.6	139.2	32.0	640.4	120.6	29.2	37.2	54.1	17.0	53.9	97.3	36.4	36.6	50.0	106.8	18.9
40G	14.4	192.9	19.1	121.2	106.3	16.1	23.5	31.3	11.8	38.4	67.3	29.4	32.6	48.2	112.2	16.6
41G	22.9	210.3	33.1	88.0	157.2	34.0	45.6	58.6	25.3	80.4	96.7	43.0	45.8	78.0	156.9	20.4
42G	27.0	172.2	38.3	81.5	185.9	42.5	55.8	65.8	27.5	79.2	111.0	43.7	58.2	79.1	158.6	21.2
43G	24.2	209.5	32.7	61.9	157.5	33.1	41.2	61.3	26.0	84.7	100.5	41.8	52.9	84.3	162.0	17.0
44AG	2.3	30.4	5.6	1583.2	3.6	1.5	2.5	4.2	2.4	10.1	32.4	14.9	-4.0	13.2	28.1	1.9
44BG	10.8	155.7	18.9	558.1	59.6	15.4	21.7	32.4	13.2	48.4	81.1	33.8	36.6	46.1	77.1	5.6
45G	4.9	63.2	11.5	1059.1	24.1	7.1	9.5	16.6	6.4	23.3	41.4	17.1	16.2	20.5	46.3	5.3
46G	23.4	216.5	32.6	121.9	158.1	32.7	44.7	49.1	20.3	65.6	94.1	34.5	38.1	62.6	137.5	20.3
47G	20.2	233.8	28.7	190.5	134.3	25.3	40.8	16.6	8.5	9.4	25.2	9.0	7.9	14.3	20.2	15.4
48G	16.6	164.6	25.6	750.9	102.0	25.4	31.4	47.7	22.8	75.2	104.3	39.8	50.5	67.8	154.1	23.3
49G	15.1	272.9	22.9	230.4	82.2	19.8	22.4	35.6	17.1	57.5	77.6	32.6	28.8	52.1	124.3	6.7
50G	17.4	196.2	26.3	500.6	111.6	25.2	30.8	51.2	25.0	80.0	89.3	34.3	41.2	71.3	163.1	10.2
51G	8.1	124.5	12.6	1267.9	41.9	12.8	14.1	30.2	14.8	57.7	84.0	39.5	33.0	47.1	124.9	5.5
52G	20.7	228.4	30.6	146.5	152.0	25.5	35.3	45.4	20.9	65.8	75.3	31.0	42.7	58.5	136.5	14.2
99G	15.6	236.7	24.1	84.3	89.1	19.3	26.9	41.8	20.9	67.8	78.7	33.3	40.5	63.0	107.0	—
54G	15.5	303.3	27.3	436.0	101.0	19.7	24.9	28.4	12.4	47.0	67.5	30.5	29.0	44.0	116.0	12.2
55G	4.1	63.2	9.4	1877.1	24.8	7.0	9.4	12.0	7.7	24.3	42.0	11.5	26.6	20.7	33.0	2.9
56G	22.3	207.5	30.2	207.0	140.4	31.9	37.7	56.6	27.8	81.8	98.5	43.0	43.8	67.6	140.0	15.6
57G	11.2	146.2	16.8	630.2	63.7	16.7	18.7	33.5	17.8	59.5	84.4	34.4	36.9	51.7	125.7	9.5
58G	6.2	88.7	10.8	1025.8	24.5	7.5	10.2	18.2	11.3	37.6	57.1	25.3	21.4	30.0	77.1	5.7
59G	4.8	53.0	7.9	833.8	17.5	5.9	11.1	18.6	6.6	15.9	33.5	10.7	7.8	16.4	31.4	2.3
60G	15.2	229.6	25.1	274.6	98.7	20.3	26.4	36.4	15.8	48.7	72.1	26.5	26.8	42.4	105.4	11.4
61G	19.4	287.8	30.5	253.6	123.6	25.8	31.3	37.5	18.4	52.7	63.0	23.0	27.2	46.3	109.4	12.6
62G	6.8	113.9	10.4	549.0	27.9	8.1	13.1	17.9	9.7	34.6	47.6	19.6	23.6	27.1	63.0	12.8

Trace Element analyses of surface sediments (cont'd)

SAMPLE NUMBER	Nb ppm	Zr ppm	Y ppm	Sr ppm	Rb ppm	Th ppm	Pb ppm	Zn ppm	Ni ppm	Cr ppm	Ce ppm	Nd ppm	La ppm	V ppm	Ba ppm	Sn ppm
63G	20.8	249.5	33.3	362.9	128.4	31.0	42.2	58.4	24.3	84.6	121.3	47.6	54.7	74.8	153.5	23.0
64G	5.4	96.4	9.1	1694.2	19.9	6.6	8.8	13.2	9.2	27.1	34.5	16.7	18.0	22.3	55.9	18.5
65G	9.9	192.0	16.9	393.8	55.2	11.5	15.4	24.1	12.3	44.6	58.0	21.5	28.0	35.5	93.5	5.0
66G	6.1	106.4	8.6	952.7	22.8	7.2	11.7	13.6	9.2	27.2	52.0	18.3	29.2	23.3	60.9	7.6
67G	21.6	258.7	28.6	249.9	108.7	32.7	34.6	38.7	18.0	48.1	68.8	24.5	27.0	48.3	84.5	15.2
68G	6.6	98.0	9.3	1293.3	25.6	7.7	11.5	18.6	7.5	34.0	59.6	20.9	25.8	27.0	60.7	5.7
69G	4.8	94.4	9.3	1940.8	19.7	6.9	5.9	12.0	6.8	23.2	52.5	15.2	23.9	19.3	89.8	3.7
70G	19.6	281.0	27.3	236.2	108.8	26.8	31.9	49.6	21.2	71.3	79.4	35.6	45.4	63.3	137.4	14.4
71G	16.5	289.0	24.1	255.8	87.0	20.6	24.3	38.8	17.0	62.8	65.9	34.0	32.9	53.4	122.2	6.9
72G	13.8	263.0	20.8	206.1	71.8	16.8	20.1	33.1	13.6	50.7	63.9	26.3	29.7	51.3	116.4	5.4
73G	4.2	84.7	5.2	242.3	14.2	2.9	3.1	9.7	2.3	5.5	17.6	5.9	10.7	10.5	42.1	-1.4
74G	6.0	96.5	12.3	1558.2	30.5	8.8	14.3	21.9	11.2	35.1	57.6	22.1	22.9	26.5	75.0	2.3
75G	6.2	123.9	11.5	1388.5	34.5	11.4	12.0	16.7	8.4	21.6	50.8	18.2	18.8	20.2	62.3	4.6
77G	28.5	158.7	48.2	51.3	206.6	49.9	65.6	64.8	25.8	76.8	120.3	49.9	63.2	91.1	164.0	21.6
78G	25.1	223.3	41.7	47.8	175.0	41.0	53.8	55.6	24.7	75.5	113.7	45.6	54.8	86.9	166.5	22.7
79AG	29.2	173.1	48.4	53.9	200.3	50.5	69.4	64.0	25.5	73.9	116.3	47.6	56.2	87.4	154.4	22.7
79BG	10.5	82.2	22.0	178.7	108.9	10.1	18.9	18.6	5.1	18.3	33.6	16.1	13.5	22.0	60.9	41.0
80G	23.8	213.8	33.1	54.2	152.4	33.8	43.4	62.2	28.2	85.4	101.8	39.8	47.7	88.0	167.4	20.2
81G	23.3	195.0	30.7	67.2	148.1	32.1	41.3	60.4	26.2	82.8	103.5	40.8	49.9	85.4	176.9	15.7
82G	25.0	193.0	35.3	65.9	163.1	34.8	46.4	53.3	21.3	66.0	81.9	33.1	40.0	64.7	133.5	20.6
83G	6.7	139.3	9.5	265.3	30.1	6.5	8.7	17.7	2.9	8.0	24.5	8.8	14.9	14.4	68.6	5.5
84G	8.1	91.0	12.5	399.4	61.8	8.4	11.9	16.7	5.8	19.9	35.8	19.5	18.6	22.3	72.4	8.9
85G	13.1	114.4	21.9	494.5	79.2	17.8	26.9	32.9	12.7	39.9	79.8	32.1	45.3	46.5	88.7	23.9
86G	36.8	151.3	55.6	41.9	338.5	60.0	81.3	67.3	22.2	63.4	122.2	57.4	61.1	74.7	179.1	38.0
88G	31.7	173.9	47.8	48.3	226.0	50.6	67.4	66.1	25.4	74.5	129.5	53.5	56.1	77.3	151.0	30.0
89G	28.0	170.7	41.8	42.9	231.2	43.0	59.3	52.0	19.8	58.1	103.9	44.3	51.5	67.5	141.3	25.8
90G	36.2	171.1	55.1	45.5	316.2	56.8	77.6	69.0	23.1	66.3	122.7	50.3	53.8	74.8	152.1	35.3
91G	14.0	82.3	17.6	168.8	202.4	14.9	30.9	26.5	4.6	14.6	40.4	17.2	15.7	22.8	75.6	18.2
92G	34.8	150.9	51.9	51.8	286.8	56.7	76.4	70.7	24.6	69.8	125.2	51.7	56.1	75.9	160.6	32.7
93G	33.3	207.0	45.9	51.3	372.2	41.3	64.9	54.7	17.3	49.6	95.3	34.1	43.9	61.5	145.1	36.3
94G	5.2	106.4	7.1	22.2	17.5	3.6	5.4	9.4	4.9	11.3	20.2	4.3	13.4	8.6	45.8	-0.1
95G	5.8	108.5	9.0	177.1	26.5	6.6	8.1	20.4	6.2	19.0	26.6	14.7	12.9	21.6	62.4	2.2

Trace Element analyses of surface sediments (cont'd)

SAMPLE NUMBER	Nb ppm	Zr ppm	Y ppm	Sr ppm	Rb ppm	Th ppm	Pb ppm	Zn ppm	Ni ppm	Cr ppm	Ce ppm	Nd ppm	La ppm	V ppm	Ba ppm	Sn ppm
96G	7.8	170.8	12.7	246.5	38.4	9.1	12.8	22.1	9.2	32.1	45.0	14.4	21.1	38.0	95.3	1.3
97G	9.5	173.7	13.5	240.2	46.5	10.2	13.2	29.8	11.4	51.4	55.3	23.7	26.9	53.9	110.5	4.3
98G	6.7	133.4	11.3	382.9	29.2	7.0	11.6	29.0	10.3	39.8	52.8	18.8	22.1	38.8	53.3	2.0
99G	—	—	—	—	—	—	—	—	—	—	—	—	—	—	—	5.0
100G	9.8	188.8	15.8	84.6	51.0	10.5	17.6	28.8	14.1	50.7	54.8	22.2	29.5	45.8	93.4	3.0
101G	15.6	233.3	23.9	136.3	88.2	18.3	29.7	34.9	16.7	46.4	51.4	19.9	27.1	41.4	63.6	5.5
103G	14.7	202.5	23.4	462.6	88.3	18.4	26.3	49.1	23.2	85.6	75.1	33.8	42.4	71.1	135.6	4.7
104G	12.9	204.2	19.2	138.3	69.9	14.8	23.1	35.7	16.6	60.7	65.0	29.3	33.3	53.5	122.7	4.4
105G	16.3	287.0	24.3	158.7	94.0	19.7	27.3	43.2	20.1	70.9	93.0	35.6	33.9	62.2	128.2	7.6
106G	5.5	50.0	8.7	1000.2	20.8	5.9	12.1	14.5	6.9	34.9	39.5	7.6	8.5	32.2	20.7	1.3
107G	8.4	154.1	14.8	354.9	40.2	8.3	15.5	28.7	13.8	48.2	45.0	17.3	20.1	29.7	62.1	2.4
108G	7.0	179.8	9.3	393.4	17.8	5.4	8.1	13.2	7.6	25.0	17.9	14.6	12.6	17.0	38.5	2.8
109G	5.0	155.0	7.4	240.1	15.8	2.9	6.8	10.9	5.3	15.1	17.3	8.1	4.8	8.3	30.7	2.3
111G	4.9	68.4	10.9	1433.0	18.0	4.6	13.3	10.2	10.6	38.0	27.8	9.1	16.3	36.0	57.2	2.3
112G	8.8	166.9	14.5	786.7	47.2	12.2	18.0	25.6	15.2	46.4	58.4	24.4	35.6	40.0	96.0	33.8
113G	6.5	95.5	8.4	479.5	18.9	5.5	7.7	10.9	4.5	15.5	18.2	6.8	2.5	14.8	37.9	33.8
114G	7.6	72.9	28.6	1364.8	88.1	14.4	19.9	7.0	8.0	24.8	44.5	9.8	15.0	17.4	50.5	29.5
115G	8.5	134.1	18.2	835.2	86.7	11.2	18.0	15.2	8.3	26.4	51.2	26.2	10.3	22.5	104.0	8.3
117G	5.0	71.1	9.3	1383.2	118.3	8.9	20.4	10.7	5.3	15.4	39.3	19.6	15.4	10.7	107.6	6.2
118G	1.2	100.2	1.5	4306.9	47.7	1.1	10.1	1.4	1.8	1.9	8.2	-0.5	-4.5	3.5	45.3	1.0
119G	0.8	99.4	1.1	4286.7	39.2	1.5	8.8	1.1	3.1	3.7	32.3	8.9	-0.6	4.8	26.6	0.9
120G	5.7	39.4	7.4	997.5	77.7	7.2	18.1	6.5	6.2	20.6	40.2	23.4	6.4	13.2	113.9	0.3
121G	5.8	96.8	8.6	750.9	15.3	4.7	6.4	5.7	5.2	12.8	21.6	3.7	3.4	7.9	23.9	19.4
122G	4.9	100.4	6.8	630.2	10.7	4.5	5.9	5.6	5.3	15.4	15.5	7.8	11.3	9.2	34.0	41.3
123G	5.2	90.6	7.5	784.8	16.0	5.6	6.7	10.3	6.0	16.2	25.5	11.0	12.6	13.5	34.7	4.5
124G	6.1	104.6	7.8	493.2	12.9	6.1	7.5	8.7	5.2	19.3	25.3	12.8	4.4	12.3	26.4	
125G	4.4	98.5	10.1	1033.7	9.5	4.7	7.9	16.2	8.9	24.6	28.4	6.9	7.0	22.9	14.3	15.6
126G	5.7	168.1	9.2	500.2	20.7	4.1	7.0	17.7	7.1	20.2	29.1	14.0	6.7	13.0	35.9	4.4
127G	4.2	126.9	6.2	473.3	9.2	2.0	6.0	6.9	2.9	15.0	13.3	3.7	5.9	8.9	21.0	2.8
128G	4.3	80.6	5.5	381.1	5.9	2.8	4.6	10.1	3.7	10.0	15.6	7.3	3.5	7.2	32.8	7.0
129G	5.1	133.4	8.5	330.9	13.7	3.6	6.8	12.5	5.3	21.0	30.3	14.6	9.7	9.8	27.0	5.1
130G	4.3	88.9	6.1	397.8	10.5	1.8	4.2	13.8	4.2	13.1	22.9	8.3	9.9	9.1	29.8	0.6

Trace Element analyses of surface sediments (cont'd)

SAMPLE NUMBER	Nb ppm	Zr ppm	Y ppm	Sr ppm	Rb ppm	Th ppm	Pb ppm	Zn ppm	Ni ppm	Cr ppm	Ce ppm	Nd ppm	La ppm	V ppm	Ba ppm	Sn ppm
131G	5.8	226.1	9.2	433.7	14.9	4.3	7.2	13.6	5.1	16.6	26.8	7.7	5.6	11.5	29.2	3.5
132G	2.8	134.3	5.7	2989.8	6.6	1.7	2.8	6.4	4.0	8.0	19.2	11.0	-2.0	5.0	21.3	3.0
133G	-0.2	137.0	-1.0	5092.2	1.7	1.4	2.2	2.7	2.4	1.5	24.3	-5.6	-6.2	5.8	14.1	3.0
134G	1.0	118.7	0.7	4796.6	-0.6	-0.7	3.3	2.6	2.6	0.3	8.5	-1.5	-13.7	1.8	15.6	1.8
135G	4.0	151.2	7.8	715.1	11.9	2.9	6.4	12.3	5.6	14.0	23.4	6.6	8.6	10.6	42.0	2.7
136G	5.1	146.4	7.8	515.3	11.8	3.6	6.5	10.8	5.9	14.1	19.1	8.7	11.7	11.4	34.1	14.2
137G	5.0	118.2	6.9	914.5	17.2	3.9	9.3	10.6	5.6	14.0	33.6	10.2	8.1	9.8	28.8	18.0
138G	5.7	63.9	7.4	602.2	24.3	4.0	8.8	13.6	5.6	14.8	11.5	5.3	7.9	10.9	46.2	31.5
139G	10.4	182.9	19.1	531.3	65.7	12.8	20.2	27.2	12.5	47.0	67.0	25.5	25.4	42.1	110.6	9.6
AQ-KL1	1.9	118.4	2.6	4484.3	7.2	3.3	5.9	2.5	2.6	-1.7	17.4	7.3	-2.4	4.6	-1.5	3.4
AQ-KL2	1.8	113.6	5.5	4262.9	10.7	6.2	6.8	10.1	3.3	15.6	44.7	16.8	-3.9	12.6	43.2	3.4
AQ-KL3	2.3	84.6	6.4	3540.0	9.8	4.5	6.3	7.8	4.3	17.4	40.0	11.8	12.1	15.7	31.1	3.8
AQ-KL4	3.3	71.3	9.3	2867.0	10.8	4.8	9.7	8.2	11.4	61.1	32.3	3.7	11.5	28.8	26.2	5.3
AQ-KL5	4.4	74.0	12.6	2291.7	16.9	7.1	12.7	11.7	5.2	35.3	28.5	18.0	9.4	23.2	49.5	7.3
AQ-KL6	6.8	114.1	16.3	1318.0	34.9	13.3	13.0	14.8	8.7	23.7	62.7	25.8	23.5	19.2	43.0	11.3
AQ-KL7	7.8	128.5	16.3	1270.8	44.5	16.3	14.7	12.5	4.8	12.3	41.4	18.0	16.7	15.8	36.7	9.6
AQ-KL8	9.6	171.9	19.1	1222.0	52.9	16.3	16.9	24.6	8.8	33.9	71.5	29.3	30.8	34.7	85.9	18.8
AQ-KL9	10.0	167.7	17.6	1168.9	57.4	15.5	19.2	23.9	9.0	28.8	62.1	23.9	29.9	28.6	81.8	17.5
AQ-KL10	8.4	141.9	17.9	1248.6	49.2	13.4	15.4	19.7	8.4	27.4	52.5	18.2	23.9	27.3	66.2	14.4
AQ-KL11	6.1	154.9	13.8	1423.0	32.4	12.0	11.3	12.2	4.6	17.4	35.8	15.7	19.7	11.4	30.7	10.3
AQ-KL12	9.2	165.7	16.2	1407.1	46.6	14.0	14.3	14.4	6.5	16.1	32.3	9.6	19.7	17.2	53.2	13.0
AQ-KL13	9.7	175.7	16.9	1487.9	53.6	16.1	20.5	16.9	5.7	19.0	41.3	18.8	17.6	23.3	57.2	16.3
AQ-KL14	5.3	159.7	10.6	3724.0	32.8	10.0	13.7	16.5	6.1	19.8	57.4	21.6	13.0	19.7	63.5	9.2
AQ-KL15	3.0	139.1	4.7	4627.4	13.9	4.0	7.0	9.8	3.6	11.1	33.4	11.1	7.3	11.6	23.0	5.6
AQ-KL16	3.4	69.0	3.3	2211.4	11.1	2.7	4.8	7.6	1.8	9.7	17.3	5.4	1.2	10.3	61.9	-1.1
AQ-KL17	8.9	78.8	4.4	230.9	8.1	2.7	1.9	8.1	1.7	4.4	16.5	7.1	0.0	6.3	41.7	-0.8
TK1	2.9	125.4	3.4	4388.5	17.0	5.9	17.4	7.5	4.8	5.2	29.7	7.8	4.0	11.9	24.9	16.9
TK2	3.0	88.5	2.0	3176.8	2.8	2.6	4.3	3.0	2.5	3.1	23.0	5.0	-4.8	3.2	19.0	6.5
TK3	3.9	121.4	2.8	3407.8	5.0	3.2	4.6	5.3	2.9	7.0	23.1	10.6	6.2	8.2	18.1	11.7
TK4	5.8	83.4	1.6	3294.1	2.3	1.9	6.8	9.2	2.8	7.3	26.6	4.1	2.2	7.5	27.1	8.5
TK5	2.6	125.2	5.4	4439.4	14.5	4.1	9.6	7.6	3.8	5.0	33.8	7.5	2.2	9.1	11.1	11.1
TK6	10.3	111.2	16.6	1940.4	69.3	15.4	22.5	20.0	6.6	19.1	43.1	10.7	15.9	24.0	40.4	31.5

Selected **major** and **trace elements** and **dry bulk density** of core samples (cont'd)

SAMPLE NUMBER	Ca wt %	Al wt %	Si wt %	Zr ppm	Rb ppm	Sn ppm	D.B.D. gm/cm2
44/4-5	12.73	3.93	21.15	169.20	68.00	8.20	0.80
9-10	24.05	2.14	10.98	105.20	37.10	6.60	0.93
14-16	25.57	1.61	10.28	90.50	26.60	4.60	1.03
20-22	27.54	1.67	8.14	79.80	26.90	3.40	0.99
32-34	25.30	2.20	9.73	87.80	34.60	3.20	0.91
38-40	21.93	3.20	11.75	103.00	50.00	6.20	0.91
53C/0-3	25.14	7.29	2.31	201.90	127.20	10.80	0.27
4-6	25.80	7.51	2.43	213.50	128.90	10.70	0.41
9-10	26.24	7.36	2.54	220.50	128.70	11.00	0.50
14-16	26.39	7.23	2.82	225.80	124.20	11.50	0.53
20-22	27.25	6.79	2.96	236.40	120.00	9.30	0.58
26-28	26.36	7.03	3.21	233.60	118.30	10.10	0.57
32-34	26.07	7.07	3.43	232.30	119.80	10.40	0.56
38-40	26.62	6.99	3.21	243.40	117.80	10.10	0.62
44-46	27.20	6.85	2.85	246.70	114.70	9.30	0.60
50-52	26.46	6.62	3.70	242.40	111.10	7.60	0.62
56-58	25.96	6.08	5.17	255.10	103.80	6.70	0.64
62-64	25.27	6.07	6.12	243.70	99.70	6.20	0.69
68-70	24.61	6.15	5.93	240.90	98.20	4.10	0.72
60/4-5	4.54	4.90	29.31	232.00	104.30	13.00	0.75
9-10	4.76	4.47	29.92	220.80	94.20	10.20	0.74
14-16	5.40	3.91	30.11	240.30	83.70	10.40	0.81
20-22	5.87	3.96	29.42	231.30	81.10	9.20	0.85
26-28	9.40	2.94	27.34	259.30	64.90		0.99
67C/9-10	25.47	7.30	2.87	310.20	97.60	14.80	0.52
18-20	20.29	4.70	2.84	273.90	110.50	12.30	0.71
28-30	23.31	3.20	12.88	344.00	58.10	6.80	0.93
38-40	22.26	1.64	16.47	474.80	32.90	13.10	1.20
48-50	23.80	2.63	13.61	434.10	49.60	7.00	1.07
58-60	24.52	4.49	9.46	365.00	72.80	7.50	0.91
68-70	26.94	5.58	5.87	319.70	88.00	5.30	0.83
78-80	27.38	5.39	5.66	367.50	85.90	7.20	0.80

SAMPLE NUMBER	Ca wt %	Al wt %	Si wt %	Zr ppm	Rb ppm	Sn ppm	D.B.D. gm/cm2
78C/8-10	24.62	9.96	0.21	218.10	160.90	16.90	0.61
18-20	24.63	9.85	0.20	202.60	155.30	13.20	0.61
25-30	24.01	9.60	0.22	190.10	152.10	14.60	0.60
35-40	24.23	9.64	0.20	189.20	157.50	12.40	0.54
45-50	24.61	9.08	0.24	194.40	139.70	11.20	0.63
55-60	24.32	8.81	0.24	193.40	137.60	8.30	0.66
65-70	23.99	8.86	0.25	184.60	138.30	8.50	0.60
75-80	24.35	8.77	0.25	183.60	135.20	6.90	0.62
85-90	23.91	8.78	0.29	186.50	134.70	7.40	0.62
95-100	24.24	8.94	0.28	180.60	136.80	6.70	0.63
88C/8-10	30.87	7.97	0.39	159.00	214.80	24.90	0.75
18-20	34.32	6.17	0.44	164.00	204.30	20.90	0.92
25-30	35.92	5.26	0.37	144.50	192.30	18.00	1.16
35-40	35.26	4.97	0.51	159.30	176.60	22.40	1.04
45-50	33.42	5.67	0.45	170.50	170.10	16.20	1.00
55-60	36.10	4.32	0.42	163.50	177.30	11.80	1.05
65-70	36.85	3.76	0.94	153.80	175.20	14.30	1.15
75-80	39.22	3.10	0.88	129.70	193.30	11.50	1.33
85-90	38.26	3.34	0.88	122.40	189.50	14.40	1.21
95-100	39.56	3.12	0.88	114.60	183.90	9.00	1.28
105-110	37.16	3.61	1.03	143.50	192.70	13.50	1.16
115-120	36.60	3.85	0.83	162.70	202.30	12.50	1.22
125-130	37.64	3.34	1.14	156.90	196.70	15.80	1.19
135-140	44.71	3.85	1.42	154.60	191.20	14.70	1.24
145-150	38.44	2.95	1.10	139.40	187.10	14.90	1.32
155-160	39.38	2.44	1.66	93.40	186.80	9.80	1.46
165-170	39.13	2.49	1.78	73.60	193.20	5.70	1.41
185-190	39.13	3.01	1.16	105.20	196.20	9.10	1.42
195-200	37.48	3.17	1.52	136.50	186.90	9.10	1.33
205-210	27.67	3.34	8.80	156.30	136.40	15.00	1.17
215-220	22.42	4.60	10.04	193.10	118.20	15.00	1.01
225-230	29.55	6.06	2.12	256.80	154.50	12.80	1.00

Selected **major** and **trace elements** and **dry bulk density** of core samples

SAMPLE NUMBER	Ca wt %	Al wt %	Si wt %	Zr ppm	Rb ppm	Sn ppm	D.B.D. gm/cm2
9/4-5	2.78	5.91	29.24	258.20	95.70	9.90	0.62
9/9-10	2.84	5.59	29.74	261.10	90.50	7.20	0.64
9/14-16	2.80	5.65	29.69	269.90	94.10	9.80	0.66
9/20-22	2.89	5.54	29.76	252.60	76.60	8.30	0.81
9/26-28	3.15	4.89	30.71	284.20	93.60	8.20	0.75
9/32-34	3.38	4.48	31.65	294.80	84.90	3.90	0.75
9/38-40	3.99	4.80	29.90	277.20	80.70	7.70	0.70
16/4-5	2.01	5.43	30.14	231.50	89.50	5.60	0.62
16/9-10	2.33	5.82	29.65	245.60	92.90	5.80	0.63
16/14-16	2.21	6.08	28.80	235.50	95.10	5.90	0.62
16/20-22	2.93	6.04	27.82	235.20	95.10	6.60	0.65
16/26-28	3.75	5.93	27.41	234.70	92.80	6.70	0.69
16/32-34	2.38	5.76	29.21	251.30	91.20	5.40	0.64
16/38-40	2.32	5.70	29.65	230.40	83.30	4.40	0.67
21/4-5	1.78	5.98	29.52	231.70	91.80	5.40	0.56
21/9-10	2.15	5.29	30.52	248.60	83.90	4.00	0.55
21/14-16	4.45	5.56	27.25	227.30	85.00	3.80	0.58
21/20-22	13.24	3.29	21.59	219.70	53.40	3.40	0.82
21/26-28	7.35	4.25	26.89	262.00	64.80	1.70	0.85
21/32-34	5.52	4.67	28.23	270.00	71.40	3.70	0.76
26/4-5	0.51	3.03	38.94	130.70	50.30	2.70	1.08
26/9-10	0.50	1.98	41.32	89.90	33.50	3.80	1.35
26/14-16	0.40	3.18	37.72	129.80	52.20	3.90	1.12
26/20-22	0.68	1.73	41.83	139.10	28.90	7.90	1.40
26/26-28	0.34	2.47	39.46	95.30	42.40	1.90	1.16
26/32-34	0.24	1.62	41.94	102.20	29.80	2.30	1.70
26/38-40	0.87	2.17	39.29	110.40	36.30	2.80	1.25
26/44-46	0.13	0.77	43.97	82.40	16.40	3.50	1.58

SAMPLE NUMBER	Ca wt %	Al wt %	Si wt %	Zr ppm	Rb ppm	Sn ppm	D.B.D. gm/cm2
30/4-5	2.88	6.58	27.95	239.30	130.80	14.40	0.55
30/9-10	5.63	5.88	26.25	250.00	115.10	10.60	0.71
30/14-16	7.88	5.15	24.77	255.70	99.50	11.60	0.71
30/20-22	3.44	6.44	26.89	262.10	113.70	8.20	0.60
30/26-28	2.43	6.83	27.36	260.90	111.50	7.00	0.64
30/32-34	2.24	7.06	27.05	247.60	113.40	8.90	0.63
36/4-5	0.23	6.10	32.97	255.70	163.20	19.60	0.78
36/9-10	0.33	4.63	34.05	281.30	143.10	22.60	0.82
36/14-16	0.31	5.31	33.08	238.80	149.60	19.40	0.87
36/20-22	0.38	4.86	33.94	233.70	146.70	19.90	0.93
36/26-28	0.54	4.05	35.17	232.70	137.80	19.80	0.95
36/32-34	0.44	3.82	35.80	223.00	137.90	17.50	1.07
36/38-40	0.56	3.72	35.97	235.10	137.00	20.30	0.99
36/44-46	0.77	4.39	34.89	234.30	138.20	24.10	1.02
36/50-52	0.68	3.59	36.33	235.50	128.20	17.30	1.14
38/4-5	0.36	4.99	36.18	183.80	342.80	36.40	1.18
38/9-10	0.43	5.18	35.65	186.60	326.60	33.80	1.13
38/14-16	0.67	5.09	35.19	170.80	318.90	35.60	1.08
38/20-22	0.72	4.86	35.71	174.10	313.10	33.70	1.09
38/26-28	1.58	4.02	36.53	218.20	267.90	40.90	1.24
38/32-34	1.00	4.58	36.38	203.90	275.60	35.70	1.21
38/38-40	0.88	3.28	38.11	217.00	157.30	27.90	1.24
38/44-46	1.46	2.68	38.57	239.10	130.20	27.40	1.30
38/50-52	1.48	2.23	39.10	196.90	114.30	17.80	1.33
38/56-58	1.67	2.20	38.70	238.70	110.10	27.00	1.32
38/62-64	2.44	2.15	37.99	212.80	103.00	21.30	1.29
38/68-70	1.72	2.68	37.80	237.30	115.90	27.20	1.29

Grain Size statistics and fractions for surface sediments (statistics calculated using moments method)

SAMPLE NUMBER	MEAN	SORTING	SKEWNESS	% GRAVEL	% SAND	% SILT	% CLAY	% SILT/CLAY
3G	4.2	1.9	0.8	0.2	60.6	34.0	5.2	39.2
4G	2.7	1.7	0.9	2.1	89.9	6.1	2.0	8.0
5G	3.0	1.6	0.7	1.8	88.6	7.8	1.9	9.8
6G	2.9	1.8	0.3	2.4	86.5	9.1	2.0	11.1
7G	2.5	2.1	0.3	5.9	84.3	7.4	2.4	9.8
8G	2.8	2.5	0.7	4.9	72.5	18.2	4.4	22.6
9G	5.9	1.7	-0.2	0.0	18.5	69.5	12.1	81.6
10G	5.5	1.9	-0.1	0.0	30.5	58.1	11.3	69.5
11G	3.6	2.1	0.8	1.2	76.2	17.0	5.6	22.6
12G	4.4	1.6	1.4	0.0	62.2	33.1	4.6	37.7
13G	0.5	2.4	0.6	33.6	58.1	6.3	1.9	8.2
14G	6.4	1.6	-0.5	0.0	8.9	74.4	16.7	91.1
15G	0.8	2.6	1.3	27.6	61.3	8.9	2.2	11.1
16G	5.8	1.7	0.0	0.0	19.6	69.5	10.9	80.4
17G	5.9	1.7	-0.2	0.0	16.6	71.2	12.2	83.4
18G	4.5	2.4	-0.1	0.0	50.0	42.8	7.2	50.0
19G	6.3	1.6	-0.4	0.0	9.5	76.1	14.4	90.5
20G	6.0	1.7	-0.4	0.0	16.1	69.7	14.2	83.9
21G	5.1	2.5	-0.4	5.1	28.3	56.5	10.1	66.6
22G	5.5	1.5	0.6	0.0	9.6	82.7	7.8	90.4
23G	-0.7	2.4	2.4	73.1	18.8	7.2	1.0	8.2
24G	1.9	3.7	0.5	34.6	32.1	27.0	6.4	33.4
25G	6.5	1.8	-0.6	0.4	8.8	70.6	20.1	90.8
27G	1.2	1.7	0.7	12.4	84.3	2.6	0.7	3.3
28G	2.1	2.4	0.8	10.9	76.2	9.6	3.3	12.9
29G	6.5	1.8	-0.0	0.0	10.3	68.2	21.5	89.7
30G	5.7	2.3	-0.9	2.7	17.5	65.5	14.2	79.7
31G	6.2	1.8	0.1	0.0	11.9	71.0	17.1	88.1
32G	5.8	2.2	-1.0	1.6	20.8	63.5	14.1	77.7
33G	4.8	2.8	-0.5	4.5	36.8	47.0	11.7	58.7
34G	2.5	3.1	0.8	9.2	65.2	18.8	6.9	25.6
35BG	1.3	1.7	1.0	11.9	84.3	2.9	0.9	3.8

SAMPLE NUMBER	MEAN	SORTING	SKEWNESS	% GRAVEL	% SAND	% SILT	% CLAY	% SILT/CLAY
35AG	6.5	1.8	0.3	[illegible]	[illegible]	[illegible]	[illegible]	[illegible]
36G	5.1	2.2	0.7	0.0	47.0	40.6	12.5	53.0
37G	3.8	1.7	2.4	0.0	83.8	11.3	4.9	16.2
38G	3.5	1.4	2.8	0.0	88.7	8.1	3.2	11.3
39G	3.6	3.9	-0.2	23.2	24.9	40.1	11.8	51.9
40G	3.9	2.2	0.9	1.7	73.5	17.6	7.1	24.8
41G	6.6	1.7	-0.4	0.3	7.5	71.0	21.2	92.3
42G	6.6	1.7	-0.4	0.0	10.0	69.6	20.4	90.0
43G	6.7	1.9	0.1	0.0	9.6	64.6	25.9	90.4
44AG	-1.5	0.9	5.2	81.7	17.6	0.6	0.1	0.7
44BG	2.9	3.4	0.2	16.7	48.2	27.6	7.5	35.1
45G	-0.1	2.6	1.9	53.6	37.4	7.3	1.7	9.0
46G	5.7	2.0	-0.9	0.9	22.5	65.5	11.1	76.6
47G	5.7	1.9	-0.7	0.6	18.9	69.4	11.1	80.5
48G	3.1	3.6	0.0	16.3	41.2	33.8	8.6	42.5
49G	5.3	1.9	0.6	0.0	40.7	47.8	11.5	59.3
50G	4.4	3.4	-0.5	11.0	30.2	46.7	12.0	58.8
51G	2.1	3.2	0.6	20.2	53.7	21.0	5.2	26.1
52G	6.0	1.8	0.2	0.0	15.6	70.7	13.6	84.4
53G	6.5	1.6	-0.2	0.0	6.1	76.2	17.7	93.9
54G	5.0	1.8	0.9	0.0	41.1	50.4	8.5	58.9
55G	0.2	2.6	1.8	41.7	47.7	8.6	2.0	10.7
56G	6.0	2.5	-1.5	5.0	8.5	70.1	16.5	86.6
57G	2.6	2.9	0.6	7.0	66.8	20.9	5.4	26.2
58G	2.0	2.7	0.9	13.7	69.6	12.3	4.4	16.7
59G	1.3	2.2	1.6	12.6	79.2	5.5	2.7	8.2
60G	4.7	2.2	0.3	1.6	51.9	37.1	9.4	46.5
61G	5.9	1.7	0.0	0.0	18.5	68.9	12.5	81.4
62G	1.9	2.1	1.1	6.9	83.8	7.2	2.1	9.3
63G	5.9	2.0	0.2	0.0	19.5	63.8	16.7	80.5
64G	2.1	1.9	1.3	3.9	87.5	6.3	2.3	8.6
65G	3.6	2.3	0.6	0.3	64.6	30.3	4.8	35.1

Grain Size statistics and fractions for surface sediments (cont'd)

SAMPLE NUMBER	MEAN	SORTING	SKEWNESS	% GRAVEL	% SAND	% SILT	% CLAY	% SILT/CLAY
66G	1.9	2.4	1.0	10.1	78.5	8.3	3.1	11.4
67G	6.1	1.9	-0.2	0.0	19.6	64.1	16.3	80.4
68G	1.4	2.8	0.9	21.1	64.9	11.2	2.8	14.0
69G	0.4	2.9	1.4	48.0	38.0	11.4	2.5	14.0
70G	6.0	1.8	-0.1	0.0	14.7	70.2	15.0	85.3
71G	5.5	2.0	0.4	0.2	29.7	57.0	13.1	70.1
72G	4.8	2.0	0.4	1.1	51.4	38.9	8.6	47.5
73G	2.3	1.4	1.1	1.8	93.0	4.3	0.9	5.2
74G	2.8	2.8	0.7	4.6	69.4	20.2	5.8	26.0
75G	1.2	2.9	0.9	30.3	54.1	12.7	2.9	15.6
76G	6.3	1.9	-0.8	0.0	12.6	69.0	18.4	87.4
77G	6.7	1.7	-0.0	0.0	6.3	72.5	21.2	93.7
78G	6.1	2.1	-0.0	0.0	22.5	59.2	18.3	77.5
79AG	6.6	2.1	-0.3	0.0	11.2	65.7	23.1	88.8
79BG	0.2	2.5	1.4	43.6	48.6	6.4	1.5	7.8
80G	6.4	2.1	-0.0	0.0	16.5	60.3	23.2	83.5
81G	5.4	2.1	0.2	0.0	37.0	50.8	12.2	62.9
82G	5.9	1.7	-0.3	0.0	17.1	71.1	11.8	82.9
83G	2.0	1.9	0.6	8.0	85.2	5.5	1.3	6.8
84G	1.8	2.5	0.8	16.2	71.9	9.2	2.7	11.9
85G	2.9	3.1	0.5	8.3	61.6	22.7	7.3	30.1
86G	3.6	1.3	1.6	0.0	90.8	7.4	1.9	9.2
88G	6.9	1.7	0.1	0.0	4.8	70.8	24.4	95.2
89G	4.8	2.3	0.3	0.0	44.4	46.5	9.1	55.6
90G	6.3	1.9	0.4	0.0	11.4	69.7	19.0	88.6
91G	2.3	2.4	1.0	5.4	77.0	14.1	3.5	17.6
92G	6.1	2.0	0.3	0.0	13.9	69.0	17.0	86.1
93G	5.2	2.1	0.7	0.0	43.1	45.5	11.4	56.9
94G	2.3	1.5	1.8	0.0	93.8	4.3	2.1	6.4
95G	2.3	1.9	1.7	2.7	87.6	7.0	2.6	9.7
96G	2.8	2.5	0.6	8.6	73.0	13.6	4.8	18.4
97G	3.2	2.5	0.6	5.3	71.0	18.7	5.0	23.7

SAMPLE NUMBER	MEAN	SORTING	SKEWNESS	% GRAVEL	% SAND	% SILT	% CLAY	% SILT/CLAY
98G	2.3	2.4	0.5	11.7	74.7	10.5	3.1	13.6
99G	5.4	2.3	-0.2	1.0	34.0	51.8	13.2	65.0
100G	3.9	2.1	0.7	1.7	66.0	26.9	5.4	32.3
101G	5.7	2.1	-0.4	0.6	18.9	67.3	13.2	80.5
102G	5.7	2.6	-1.2	5.0	16.9	62.6	15.4	78.0
103G	5.6	2.6	-1.2	3.7	14.6	67.8	14.0	81.7
104G	4.7	2.0	0.8	0.0	56.9	34.9	8.2	43.1
105G	5.4	2.1	0.0	0.3	36.6	51.0	12.0	63.1
106G	-0.5	2.2	2.3	54.8	39.0	5.1	1.1	6.2
107G	4.2	1.9	1.0	0.0	70.4	24.0	5.6	29.6
108G	3.2	1.6	1.0	0.9	89.4	7.1	2.6	9.7
109G	2.9	1.2	1.5	0.4	94.8	3.7	1.1	4.8
111G	0.2	2.1	1.3	38.8	57.1	3.2	0.9	4.1
112G	3.3	2.2	1.0	0.3	75.8	18.9	5.0	23.9
113G	1.7	1.8	1.1	6.5	87.4	4.9	1.2	6.2
114G	-0.3	1.8	1.0	48.5	50.3	0.9	0.2	1.2
115G	2.0	1.7	0.9	4.2	89.6	5.0	1.3	6.2
116G	-0.3	1.7	1.9	40.1	57.3	2.2	0.5	2.6
117G	1.1	1.5	1.3	6.5	90.6	2.3	0.6	2.9
118G	2.4	0.4	-0.3	0.0	100.0	0.0	0.0	0.0
119G	1.6	0.6	-1.8	0.3	99.7	0.0	0.0	0.0
120G	1.4	1.1	1.5	0.9	97.8	1.0	0.3	1.3
121G	1.7	1.6	0.9	3.8	92.0	3.3	0.9	4.2
122G	1.6	1.6	1.0	4.9	91.3	3.0	0.8	3.8
123G	2.2	1.8	1.0	2.4	90.1	6.1	1.4	7.5
124G	1.9	1.5	1.4	2.0	93.7	3.2	1.0	4.3
125G	2.0	1.5	0.2	2.5	94.9	2.0	0.5	2.6
126G	3.2	1.6	0.0	2.3	84.5	11.8	1.5	13.2
127G	2.5	1.4	0.2	1.5	94.8	3.0	0.7	3.7
128G	1.9	1.4	1.0	0.6	96.2	2.5	0.6	3.2
129G	2.5	1.6	0.6	1.8	91.7	5.2	1.2	6.5
130G	2.6	1.5	0.6	2.0	91.7	5.0	1.3	6.2

Grain Size statistics and fractions for surface sediments (cont'd)

SAMPLE NUMBER	MEAN	SORTING	SKEWNESS	% GRAVEL	% SAND	% SILT	% CLAY	% SILT/CLAY
131G	3.4	1.4	0.6	1.2	85.3	11.7	1.9	13.6
132G	3.1	1.3	1.0	0.1	81.7	17.5	0.8	18.3
133G	2.2	1.6	-0.1	4.2	91.8	3.6	0.4	4.0
134G	1.6	1.0	-0.8	2.5	97.3	0.0	0.0	0.0
135G	3.1	1.4	1.2	0.3	89.6	8.5	1.7	10.2
136G	2.6	1.6	0.4	2.7	89.9	5.9	1.4	7.4
137G	1.9	1.8	0.3	5.1	89.7	4.2	1.0	5.2
138G	1.7	1.6	0.9	2.2	92.9	3.9	1.0	4.9
139G	3.5	2.1	0.5	0.2	73.6	21.5	4.8	26.3
Tan Khen 1	0.5	2.1	0.7	25.0	69.3	4.5	1.1	5.6
Tan Khen 2	2.6	0.7	-2.8	0.5	99.2	0.3	0.0	0.4
Tan Khen 3	2.6	1.5	-0.8	4.3	94.1	1.3	0.2	1.5
Tan Khen 4	0.9	1.3	0.6	4.6	95.2	0.2	0.0	0.2
Tan Khen 5	1.3	2.0	0.0	20.2	76.7	2.4	0.7	3.1
Tan Khen 6	0.6	2.2	0.9	14.4	75.7	8.1	1.8	9.9
AOMAN RF FT	6.0	1.5	-0.1	0.0	6.9	82.8	10.3	93.1
AQ BEACH	0.5	0.7	-1.8	4.9	95.1	0.0	0.0	0.0
AQ REEF TOP	2.1	1.1	-0.0	3.5	94.5	1.7	0.4	2.0
AQ-KL 1	2.0	1.6	0.6	3.0	92.8	3.1	1.0	4.1
AQ-KL 2	2.3	1.5	0.6	2.4	92.7	3.8	1.1	5.0
AQ-KL 3	1.7	1.3	1.6	2.4	94.5	2.5	0.7	3.2
AQ-KL 4	0.9	1.4	1.6	4.9	91.6	2.9	0.6	3.5
AQ-KL 5	1.0	2.4	0.6	18.4	69.6	10.1	2.0	12.0
AQ-KL 6	2.3	2.5	0.3	2.5	75.8	18.4	3.2	21.6
AQ-KL 7	2.4	2.7	0.3	3.3	72.2	20.6	3.8	24.5
AQ-KL 8	2.8	2.4	0.2	1.8	74.1	20.6	3.5	24.2
AQ-KL 9	2.9	2.7	0.2	3.5	67.7	24.4	4.4	28.8
AQ-KL 10	2.6	2.6	0.2	1.7	71.7	23.0	3.7	26.6
AQ-KL 11	2.0	2.3	0.4	3.0	82.1	12.8	2.2	15.0
AQ-KL 12	2.8	2.6	0.2	1.0	72.1	23.3	3.6	26.9
AQ-KL 13	3.3	2.7	0.1	2.3	62.8	30.0	4.9	34.9
AQ-KL 14	3.0	2.3	0.4	1.1	73.2	21.7	3.9	25.6
AQ-KL 15	2.3	1.8	0.4	5.4	87.3	5.8	1.5	7.3
AQ-KL 16	0.8	1.5	0.4	13.5	85.0	1.3	0.2	1.6
AQ-KL 17	1.9	0.4	-2.5	0.0	100.0	0.0	0.0	0.0

Accumulation rate calculations and **logs** for cores 21, 26 and 53

CORE 21

Log	Depth (cm)	Thickness before Compaction	Dry Bulk Density (gm/cm³)	Thickness after Compaction[1]	Thickness before Compaction[2]
	0-1	1cm	0.437	0.52cm	1.0cm
	1-2	1	0.531	0.63	1.22
	2-3	1	0.564	0.67	1.29
	3-4	1	0.618	0.74	1.41
	4-5	1	0.556	0.66	1.27
	5-6	1	0.567	0.68	1.30
	6-7	1	0.547	0.65	1.25
	7-8	1	0.459	0.55	1.05
	8-9	1	0.557	0.66	1.27
	9-10	1	0.564	0.67	1.29
	10-12	2cm	0.507	1.20	2.32
	12-14	2	0.510	1.22	2.33
	14-16	2	0.582	1.39	2.66
	16-18	2	0.769	1.83	3.52
	18-20	2	0.788	1.88	3.61
	20-22	2	0.824	1.96	3.77
	22-24	2	0.878	2.09	4.02
	24-26	2	0.800	1.91	3.66
	26-28	2	0.854	2.03	3.91
	28-30	2	0.822	1.96	3.76
	30-32	2	0.839	2.00	3.83
Total Depth (cm)		32		25.9	49.7
A.A.R. (mm/year)		0.3			
C.A.R. (mm/year)				0.25	
U.A.R. (mm/year)					0.48

Mean D.B.D. (gm/cm³) = 0.646
Flux (mg/cm²/year) = 19.4

CORE 26

Log	Depth (cm)	Thickness before Compaction	Dry Bulk Density (gm/cm³)	Thickness after Compaction[1]	Thickness before Compaction[2]
	0-1	1cm	0.937	0.67cm	1.14cm
	1-2	1	1.12	0.8	1.38
	2-3	1	0.901	0.65	1.1
	3-4	1	0.819	0.59	1.0
	4-5	1	1.075	0.77	1.31
	5-6	1	1.102	0.79	1.34
	6-7	1	1.19	0.85	1.45
	7-8	1	1.21	0.43	1.47
	8-9	1	1.30	0.93	1.59
	9-10	1	1.35	0.86	1.65
	10-12	2cm	1.22	1.75	2.98
	12-14	2	1.23	1.77	3.02
	14-16	2	1.12	1.60	2.73
	16-18	2	1.13	1.62	2.78
	18-20	2	1.37	1.96	3.34
	20-22	2	1.40	2.00	3.41
	22-24	2	1.31	1.87	3.2
	24-26	2	1.24	1.78	3.02
	26-28	2	1.16	1.66	2.84
	28-30	2	1.22	1.74	2.98
Total Depth (cm)		30		26.1	43.7
A.A.R. (mm/year)		1.53			
C.A.R. (mm/year)				1.37	
U.A.R. (mm/year)					3.3

Mean D.B.D. (gm/cm³) = 1.17
Flux (mg/cm²/year) = 179

CORE 53

Log	Depth (cm)	Present Thickness of core	Dry Bulk Density (gm/cm³)	Thickness after Compaction[1]	Thickness before Compaction
	0-1	1cm	0.248	0.35cm	1.00cm
	1-2	1	0.319	0.45	1.29
	2-3	1	0.340	0.48	1.35
	3-4	1	0.403	0.56	1.62
	4-5	1	0.405	0.57	1.63
	5-6	1	0.424	0.59	1.71
	6-7	1	0.436	0.61	1.76
	7-8	1	0.466	0.65	1.88
	8-9	1	0.499	0.70	2.01
	9-10	1	0.497	0.70	2.00
	10-12	2cm	0.531	1.49cm	4.28cm
	12-14	2	0.534	1.50	4.31
	14-16	2	0.530	1.48	4.27
	16-18	2	0.525	1.47	4.23
	18-20	2	0.503	1.41	4.06
	20-22	2	0.577	1.62	4.65
	22-24	2	0.534	1.49	4.31
	24-26	2	0.557	1.56	4.49
	26-28	2	0.567	1.60	4.57
	28-30	2	0.608	1.70	4.90
	30-32	2	0.592	1.66	4.77
	32-34	2	0.561	1.57	4.52
	34-36	2	0.579	1.62	4.67
	36-38	2	0.625	1.75	5.04
	38-40	2	0.624	1.75	5.03
	40-42	2	0.617	1.73	4.98
	42-44	2	0.584	1.64	4.71
	44-46	2	0.598	1.67	4.82
	46-48	2	0.714	2.00	3.76
Total Thickness (cm)		48		36.4	103.6
A.A.R. (mm/year)		1.52			
C.A.R. (mm/year)				1.17	
U.A.R. (mm/year)					3.3

Mean D.B.D. (gm/cm³) = 0.517
Flux (mg/cm²/year) = 78.6

[1]To calculate thickness after compaction:

divide DBD of sub-sample by greatest DBD at base of core and multiply by thickness.

[2]To calculate thickness before compaction:

divide DBD of sub-sample by lowest DBD at top ofcore and multiply by thickness.

APPENDIX E

CHECKLIST OF BIVALVES AND GASTROPODS FOUND IN PHANGNGA BAY

CLASS BIVALVIA

Subclass PTERIOMORPHIA

Order NUCULOIDA
Superfamily NUCULACEA

Family NUCULIDAE

Nucula (Lionucula) semiramisensis (Preston 1916) (plate 15b)

Superfamily NUCULANACEA

Family NUCULANIDAE

Nuculana mauritania (Sowerby 1825) (plate 15c)
Yoldia tenella (Hinds 1843) (plate 16c)

Order ARCOIDA
Superfamily ARCACEA

Family ARCIDAE

Barbatia fasciata (Reeve 1845)
Scapharca (Scapharca) japonica (Reeve 1844)
Scapharca inaequivalvis (Bruguiere 1789)
Anadara granosa (Lamarck 1758) (plate 15d)
Sheldonella lateralis (Reeve 1844)
Trisidos tortuosa (Linn. 1758)
Cucullaea concamerata (Martini 1777)

Family NOETIIDAE

Striarca sp.

Superfamily LIMOPSACEA

Family LIMOPSIDAE

Limopsis cancellata (Reeve 1844)

Family GLYCYMERIDIDAE

Glycymeris sp.

Order MYTILOIDA
Superfamily MYTILACEA

Family MYTILIDAE

Modiolus auriculatus cf. (plate 16g)
Musculus senhousia (Benson 1842)

Superfamily PINNACEA

Family PINNIDAE

Pinna bicolor (Gmelin 1791)

Order PTERIOIDA
Superfamily PECTINACEA

Family PECTINIDAE

Chlamys sp.
Pecten sp.

Family SPONDYLIDAE

Spondylus sp.

Family PLACUNIDAE

Placuna placenta (Linnaeus 1758)

Superfamily **LIMACEA**

Family LIMIDAE

Lima fragilis (Chemitz 1784)

Superfamily **OSTREACEA**

Family OSTREIDAE

Ostrea sp.

Subclass **HETERODONTA**
Order **VENEROIDA**
Superfamily **LUCINACEA**

Family LUCINIDAE

Lucina edentula (Linnaeus 1758)
Lucina sp. (plate 15e)
Phacoides semperianus (Issel) (plate 15f)
Phacoides dentilfer (Jonas 1846) (plate 15g)
Loripes sp.
Divaricella sp.

Superfamily **CHAMACEA**

Family CHAMIDAE

Chama sp.

Superfamily **CARDITACEA**

Family CARDITIDAE

Carditella sp.

Superfamily **CRASSATELLACEA**

Family CRASSATELLIDAE

Crassatella radiata (Sowerby 1825) (plate 15h)

Superfamily **CARDIACEA**

Family CARDIIDAE

*Laevicardium (Vulvia) sp.*A
*Laevicardium sp.*B
Bucardium asiaticum (Keen 1980)
Cardium (Bucardium) fimbriatum (Wood 1828)
Trigoniocardia (Americardia) victor (Angus 1892)

Superfamily **MACTRACEA**

Family MACTRIDAE

Mactra reevsii (Gray 1852)

Superfamily **TELLINACEA**

Family TELLINIDAE

Clathrotellina pretium (Sowerby 1825)
Gari sp.
Pinguitellina robusta (Hanley)
Pinguitellina sp.
Leptomya sp.
Macoma praetexta (Von Markens)
*Macoma sp.*A
*Macoma sp.*B
Abra sp.

Superfamily **GLOSSACEA**

Family GLOSSIDAE

Meiocardia vulgaris (Reeve 1845)

Superfamily **VENERACEA**

Family VENERIDAE

Dosinia histrio (Gmelin 1798) (plate 16d)
Dosinia laminata (Reeve 1845) (plate 15l)
Paphia undulata (Born 1778) (plate 16f)
Paphia gallus (Gmelin 1791) (plate 16e)
Meretrix lusoria (Roding 1798) (plate 16b)
*Timoclea sp.*A (plate 15j)
*Timoclea sp.*B
Pitar belcheri (Sowerby 1853)
Clausinella sp.
Circe scripta (Linn. 1758)

Order **MYOIDA**
Superfamily **MYACEA**

Family CORBULIDAE

Anisocorbula (Aloidis) solidula (Hinds) (plate 16a)
Corbula crassa (Hinds 1843)
Corbula fortisuleata (Smith 1906)

Subclass **ANOMALODESMATA**
Order **PHOLADOMYOIDA**
Subfamily **POROMYACEA**

Family CUSPIDARIIDAE

Cuspidaria cuspidata (Olivi)

Family CLAVAGELLIDAE

Pencillus (Brechites) dichotomus (Chenu)

CLASS GASTROPODA

Subclass PROSOBRANCHIA
Order ARCHAEOGASTROPODA
Superfamily TROCHACEA

Family TROCHIDAE

Monilea biangulosa (Cuddalore) (plate 17a)
Minolea sp. (plate 17b)
Euchelus sp.

Family TURBINIDAE

Liotia sp.
Turbo spinosus (Chemnitz, 1784)
Liotina sp.

Order MESOGASTROPODA
Superfamily RISSOACEA

Family TORNIDAE

Pseudoliotia sp.
Pymaeorota cingulifera (Adams 1885) (plate 17c)

Family RISSOIDAE

Rissoina (Phosinella) sp.
Iravadia trochlearis (Gould 1850)
Alvania (Alvania) sp.

Superfamily CERITHIACEA

Family TURRITELLIDAE

Turritella sp.
Turritella cingulifera (Sowerby 1825) (plate 16h)

Family CERITHIIDAE

Cerithium sp.

Superfamily EULIMACEA

Family EULIMIDAE

Niso sp.

Family STROMBIDAE

Strombus labiosus (Wood 1828)
Strombus marginatus septimus (Duclos 1844)
Strombus vittatus vittatus (Linn. 1758)
Strombus sp. (juvenile)

Superfamily CALYPTRAEACEA

Family CREPIDULIDAE

Calyptraea pellucida (Reeve 1845) (plate 16j)

Superfamily NATICACEA

Family NATICIDAE

Polinices sp
Eunaticina papilla (Gmelin 1791)

Superfamily **TONNACEA**

Family CASSIDAE

Phalium (Semicassis) bisulcatum (Schubert and Wagner 1758)

Family TONNIDAE

Tonna dolium (Linn. 1758)

Family FICIDAE

Ficus gracilis (Sowerby)

Family CYMATIIDAE

Cymatium cordatum (Gmelin 1791)
Cymatium pfeifferianus (Reeve 1844)
Gyrineum pusilla (Broderip 1892)
Distorsio sp. (juvenile)

Family BURSIDAE

Bursa rana (Linn. 1758)

Order **NEOGASTROPODA**
Superfamily **MURICACEA**

Family MURICIDAE

Murex trapa (Roding 1798) (plate 17e)
Pterynotus pinnatus (Wood 1858)

Superfamily **BUCCINACEA**

Family BUCCINIDAE

Phos roseatus (Hinds 1844)

Family NASSARIIDAE

Nassarius castus (Gould 1850)

Family COLUMBELLIDAE

Zafra sp.

Family FASCIOLARIIDAE

Latirus nodatus,
Latirus sp.
Fusinus colus (Linn. 1758)
Fusinus longicaudus (Lamarck 1822)

Superfamily **VOLUTACEA**

Family OLIVIDAE

Ancilla cylindrica (Sowerby 1887) (plate 17f)

Family MARGINELLIDAE

Marginella angustata (Sowerby 1846)

Superfamily **CONACEA**

Family COSTELLARIDAE

Cancilla sp
Vexillum (Costellaria) amanda (Reeve 1845)

Family TURRIDAE

Turricula sp. (juvenile)
Daphnella sp.
Eucythara sp.
Tritonoturris sp.
Clathurella (Etremopa) sp.
Obesotoma sp.
Clavus sp.
Etrema sp.
Gemmula sp.
Inquisitor sp.

Family CANCELLARIIDAE

Trigonostoma bicolor (Hinds 1843)

Family CONNIDAE

Conus aculeiformis (Reeve 1844)
Conus acutangulus (Lamarck 1810)
Conus eugrammotus,
Conus sp.

Order **HETEROGASTROPODA**
Superfamily **EPITONICEA**

Family EPITONIIDAE

Epitonium scalare (Lamarck 1758) (plate 17h)
Epitonium japonica (Dunker 1847)
Eptionium pallasii (Kiener 1838)

Subclass **OPISTHOBRANCHIA**
Order **ENTOMOTAENIATA**
Superfamily **PYRAMIDELLACEA**

Family PYRAMIDELLIDAE

Leucotina adamsi (Kuroda & Habe 1971)
Chemnitzia multigyra (Dunker 1847) (plate 17g)
Amathina tricarinata

Order **CEPHALASPIDEA**
Superfamily **ACTEONACEA**

Family ACTEONIDAE

Acteocina sp.

Family RINGICULIDAE

Ringicula sp. (plate 17i)

Order **PTEROPODA**

Family CAVOLINIDAE

Cavolina longirostris (Blainville) (plate 16i)

APPENDIX F

PUBLISHED PAPER

Phuket mar. biol. Cent. Res. Bull. 55:77-96(1991)

GRAIN SIZE, CALCIUM CARBONATE CONTENT AND ACCUMULATION RATES OF RECENT SEDIMENTS IN PHANGNGA BAY, SOUTH THAILAND

By Deborah J. Carr[1], Somkiat Khokiattiwong[2], Terry P. Scoffin[1], Alexander W. Tudhope[1]
Phuket Marine Biological Centre, P.O. Box 60, Phuket 83000, Thailand

ABSTRACT

168 surface sediment samples and 46 short cores were collected from Phangnga Bay, South Thailand in January 1989 and January 1990. These samples have been analysed for grain size distributions and $CaCO_3$ content. The depositional enviroments have been distinguished on the basis of sea bed water depth, morphology and sediment grain size. The depositional environments are: mangrove channel; mangrove swamp; open intertidal; shallow marine; open marine; beach; reef and reef front. Mean grain size and sediment sorting show an overall increasing trend southwards (towards the more marine environment). $CaCO_3$ in the form of shell fragments also increases southwards as the diluting effect of terrigenous sediment decreases away from the dominant source of this sediment in the north. $CaCO_3$ also controls grain size distributions to some extent in that carbonate skeletal debris is the main component of the gravel size fraction and so high $CaCO_3$ values correspond to high gravel fraction values. Quartz sand abundance also increases towards the more open marine continental shelf environment and these samples are thought to represent relict sediments which were originally deposited in shallow marine or coastal plain environments when sea level was lower during the last glacial period. Seven wood and shell fragments from core sub-samples have been radiocarbon dated and accumulation and progradation rates calculated from these dates. Vertical apparent accumulation rates for the northern part of the bay for the last 6000 years vary between 0.3 and 1.53 mm $year^{-1}$ and mangrove swamp lateral progradation rates have been estimated at 1.5-1.67 m $year^{-1}$.

INTRODUCTION

Objectives and Scope of Study

This study describes patterns of sedimentation in Phangnga Bay which is a tropical restricted bay encompassing a spectrum of sedimentary environments from mangrove swamps at the head of the bay in the north, through to fully marine open shelf conditions in the south. The objectives of the work reported here were as follows:

1. To describe the nature, grain size and calcium carbonate content of surface sediments across the area.

2. To determine average Late Holocene sediment accumulation rates, and mangrove progradation rates in the northern part of the bay.

Study Area

Phangnga Bay is situated on the west coast of Peninsular South Thailand (Fig.1) 8°C and 98°30E' in the tropical monsoonal area of South East Asia. The dry north easterly monsoon occurs from November to March whilst the wet south westerly monsoon extends from April to October. Rainfall is highly seasonal with an average of 300 mm/month in the wet season. Coastal waters vary in temperature between 26°C and 31°C. The bay encompasses approximately 1500 km^2 and is surrounded by a relatively small catchment area of approximately 2500 km^2. The bay is elongate north-south, the southern side being open to the Andaman Sea

Present address: 1 Geol. and Geophys. Dept., Edinburgh Univ., King Buildings, Edinburgh EH9 3JW.
2 Phuket Marine Biological Centre, P.O. Box 60, Phuket 83000, Thailand.

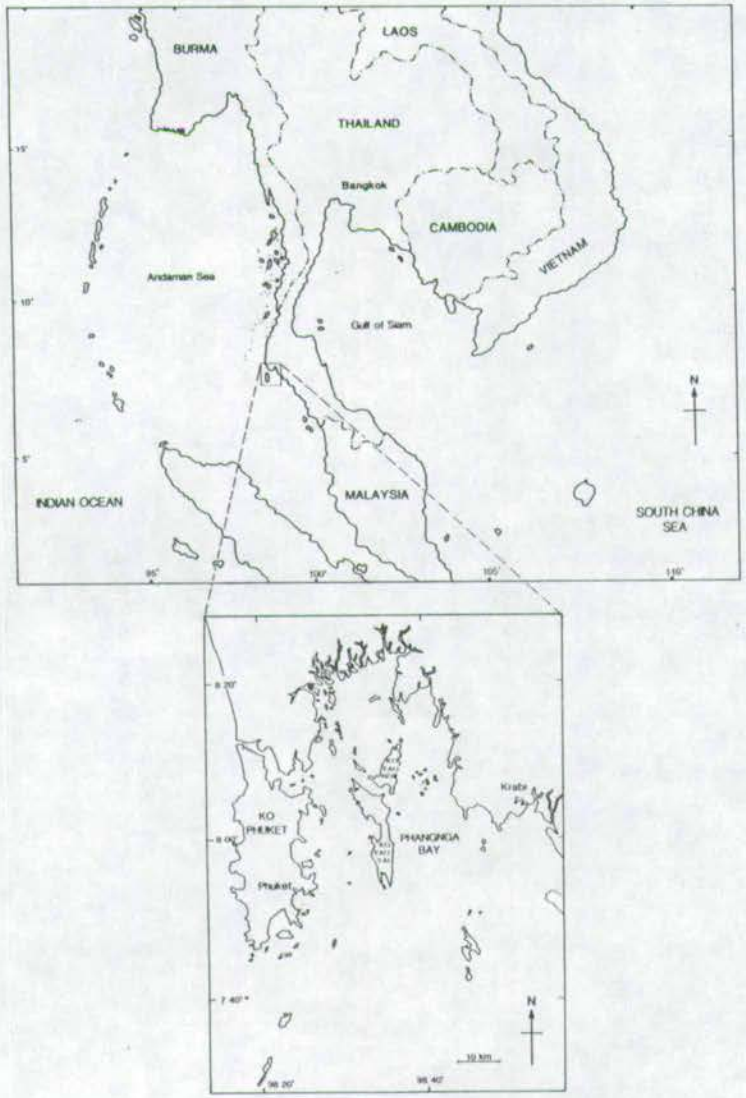

Figure 1. Location map of study area

whereas estuarine conditions prevail in the north. Much of the area north of Ko Yao Noi (Fig.1) is less than 5 m water depth, and depth increases to 65 m in the southern limit of the study area.

The estuarine environment is restricted to the northern limit of the Bay around the mangroves but its extent varies seasonally. In the rainy season the diluting effect of fresh water flow can extend up to 10 km further south into the Bay than in the dry season when lowered salinities (25-30 ppt) are restricted to mangrove areas (Limpsaichol, 1988). However, within this broad description there are a number of depositional environments which can be distinguished by the geomorphology and water depth of the deposits which result from them. Eight such environments have been distinguished; their distributions are illustrated in Fig.2

1. The **mangrove swamp** environment develops in the upper part of the intertidal zone and extends into the supratidal area (the latter area is not examined in this study). The largest development of mangrove swamps is around the northern coast of Phangnga Bay. There are smaller pockets in sheltered bays further south but these have not been sampled. The mangroves form very dense vegetation growing on soft grey-brown oxidised mud which becomes anoxic below 1-2cm (Limpsaichol, 1978).

2. The **mangrove channels** (up to 150 m wide at their mouths) are also located within the intertidal zone, dissecting the mangrove swamps and extending into the open intertidal zone. Some channels extend landward into entirely freshwater alluvial channels although most start as smaller channels within the mangroves.

3. The **open intertidal** environment extends from the mangrove swamp front to the lowest low water level although this boundary is gradational into the shallow marine environment (see below). The larger mangrove channels extend through the open intertidal zone and grade into the shallow marine environment with no exposure at low tide.

4. The **shallow marine** environment extends from the open intertidal environment and mangrove channel environment southwards and is entirely sub-tidal. The southern-most limit bounds with the open marine environment at the 20 m isobath.

5. The **open marine** environment extends seaward from the shallow marine environment at depths greater than 20 m, continuing outside of the field study area across the continental shelf.

6. The **beach** environment contains sand and gravel sediment deposited in the more exposed littoral areas which exist predominantly in bays in the southern part of the study area.

7. The **reef top** environment which consists of fringing reefs frequently with intertidal reef flats 100-200 m wide. The dominant frame-building coral is *Porites* but faviids and acroporids are also common (Brown and Holley, 1984).

8. The **reef front** environment in this area is generally a narrow (10-30 m wide) zone from 1-10 m water depth seaward of the reef where a mixture of reef-derived calcareous debris and a variable amount of terrigenous sediment accumulate on a gentle slope (Scoffin *et al.*, 1991)

Previous Work in Area

Previous investigations of Phangnga Bay have focused on aspects of water circulation (Siripong *et al.*, 1987) on resources and resource utilization (Limpsaichol, 1988) and on faunal distributions on mangrove shores (Frith *et al.*, 1976), reef flats (Nielsen, 1976, Brown and Holley, 1984 and Ditlev, 1978) and selected areas of the Peninsula west coast including southern regions of Phangnga Bay (Chatananthawej and Bussarawit, 1987 and Tantanasiriwong, 1978). On sediments, Limpsaichol

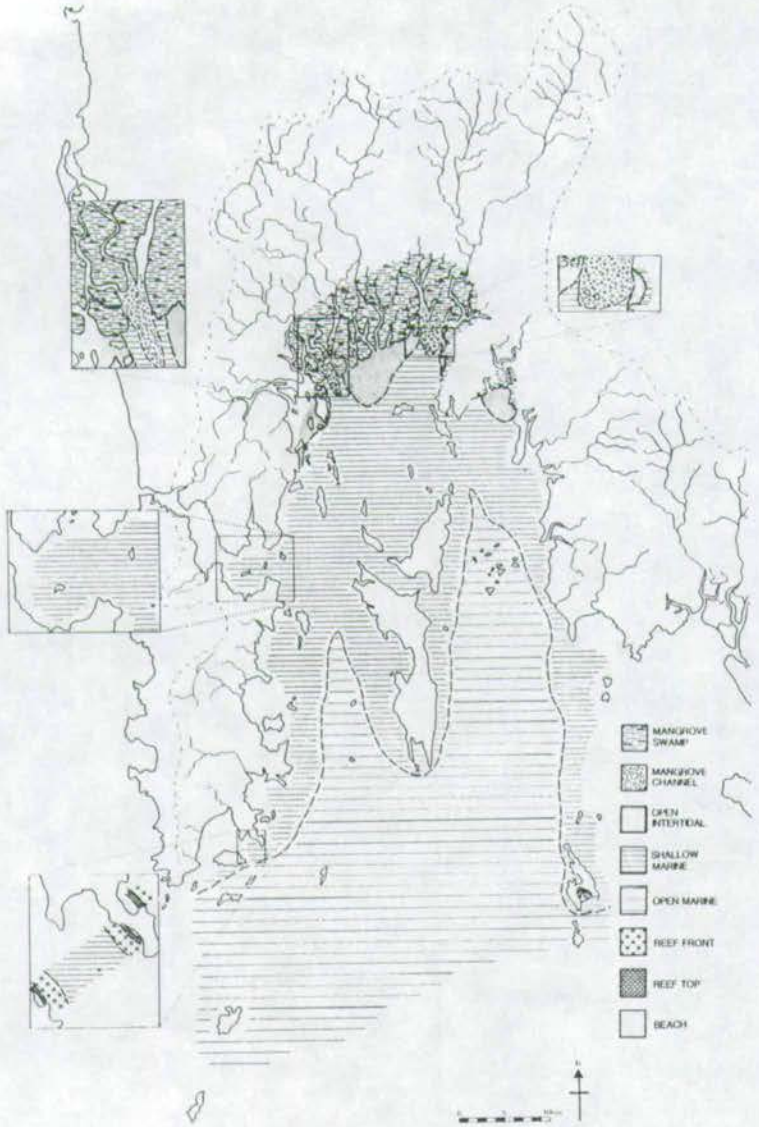

Figure 2. Distribution of depositional environments distinguished on the basis of elevation and sea bed morphology

(1978) investigated the redox potential of mangrove muds from the east coast of Phuket Island (south west Phangnga Bay) and Hylleberg *et al.*, (1985) described the effects of tin dredging on sediments on the west coast of Phuket Island. A detailed description of the geology of the catchment area of the bay is given by Garson *et al.* (1975).

METHODS

Collection and Storage

Surface sediment samples were collected from the Phuket Marine Biological Centre (PMBC) research vessel No 14 in 2 field seasons. Sites 1-63 (see Fig.3) were sampled between 17th and 20th January 1989 and sites 64-139 (including transects) were sampled between 5th and 9th January 1990. The distribution of sampling sites reflects an attempt to gain a good areal coverage of the area as well as to assess the degree of local variation at a few selected sites. In the north, 2 transects cross mangrove channel mouths and one runs from the mangrove front over the intertidal flat. In the south, one transect crosses the beach and reef at Tang Khen and another runs from the Aquarium beach across to Ko Lon (these samples are labelled T.K.1-6 and Aq-K11-17 respectively) (see Fig.3). Surface sediment samples were collected by 2 methods depending on the water depth. For water depths greater than approximately 5 m a Van Veen type grab was used from the research vessel. For shallower sites SCUBA equipment was used from a small boat to collect the surface sediment with a hand held scoop. To enable accurate grain size determination it was essential to preserve the sediments wet to prevent any aggregation of clays through drying. Immediately after collection of the top 5 cm of the sediment it was scooped into a plastic bottle, sealed and stored on ice until returning to the laboratory where the sediments were treated with 30% hydrogen peroxide (H_2O_2) to remove organic matter thus preventing deterioration of the sample during transit back to Britain. A subsample of sediment for chemical analysis was also collected from the grab sample and stored in a sealed plastic bag before oven drying at 55°C.

Cores were taken from a selection of sites (marked "C" on Fig.3) using either a gravity corer operated from the research vessel (see Fig. 4a) or with a length of 4 cm diameter plastic piping manually pushed in and retrieved from the sediment in shallow areas. The success of the gravity corer used from the research vessel depended on the sediment type - if it was of sand or gravel grain size then there was virtually no core penetration; if the sediment was muddy then recovery was good (30-60 cm). The manual method of coring was very successful and cores of up to 2.5 m in length were retrieved. The cored sediments were extruded (see Fig.4b) and sliced at 1 cm intervals for the top 10 cm and at 2 cm intervals thereafter. Each subsample was stored in a sealed plastic bag on ice before weighing, drying and reweighing in the laboratory to obtain the water content of the sediment and thus calculate the amount of compaction downcore.

Dry bulk density measurements were made on the cored sediment in order to take account of compaction when calculating sediment accumulation rates. The dry bulk density calculaltion is as follows:

$$\text{Dry Bulk Density} = \frac{\text{Mass of Dry Sediment}}{(\text{Mass of Dry Sed./2.45}) + (\text{Mass of Water}/1.02)}$$

The average density of the sediment is taken as 2.45 g cm^{-3} and the density of seawater is taken as 1.02 g cm^{-3}. A slight correction is made to account for the salt content of the sediment. The dry bulk density describes the density of the sediment in relation to the volume of the sediment and the water as a whole. As the sediment is compacted with depth, water is expelled and the dry bulk density increases. The dry bulk density varies, however, with the grain size composition of the sediment. Fine grained sediments have a greater volume of pore spaces, therefore higher water contents (hence lower dry bulk density) than coarse grained sediments.

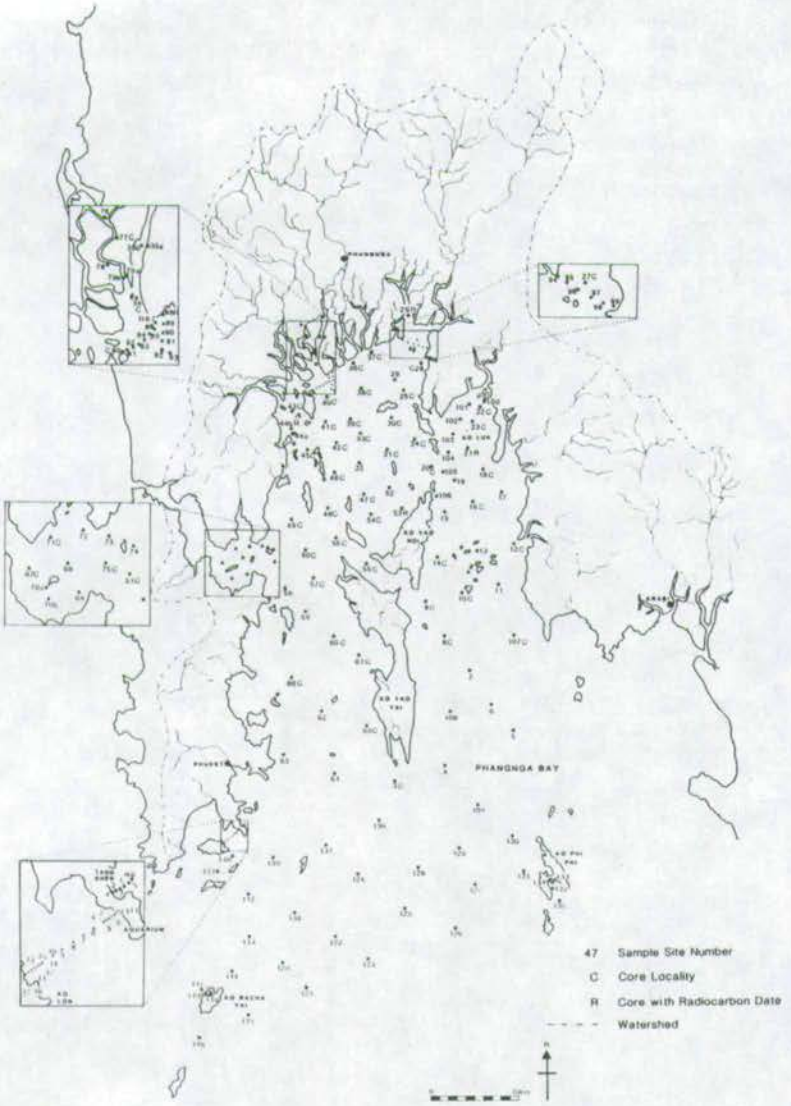

Figure 3. Distribution of sample sites throughout Phangnga Bay, Extent of watershed and main drainage system is also shown

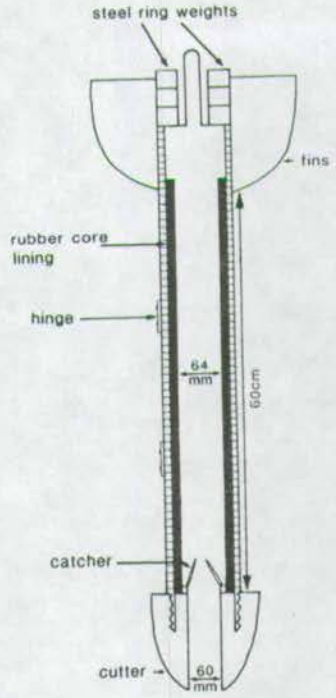

Figures 4a. Gravity corer used from research vessel.

In order to compact the column of sediment down to the degree of compaction at the base of a sequence of sediments the following formula is used for each subsample:

$$\alpha = \frac{A \times \beta}{B}$$

where:

- α = thickness of subsample after compaction correction
- β = thickness of subsample prior to compaction correction
- A = dry bulk density of subsample
- B = dry bulk density of sample at base of sequence

$CaCO_3$ Content Determination

In order to calculate the $CaCO_3$ content of the sediments, the amount of Ca in each sample was measured using X-ray fluorescence

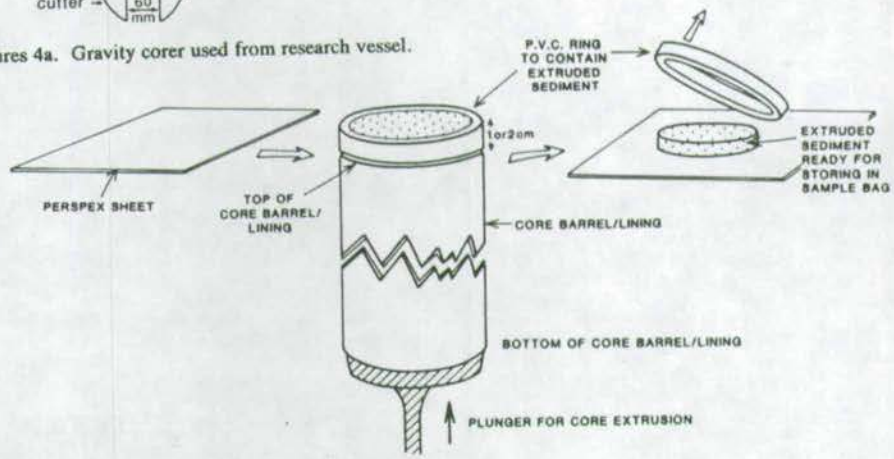

Figure 4b. Technique for extruding sediment from core.

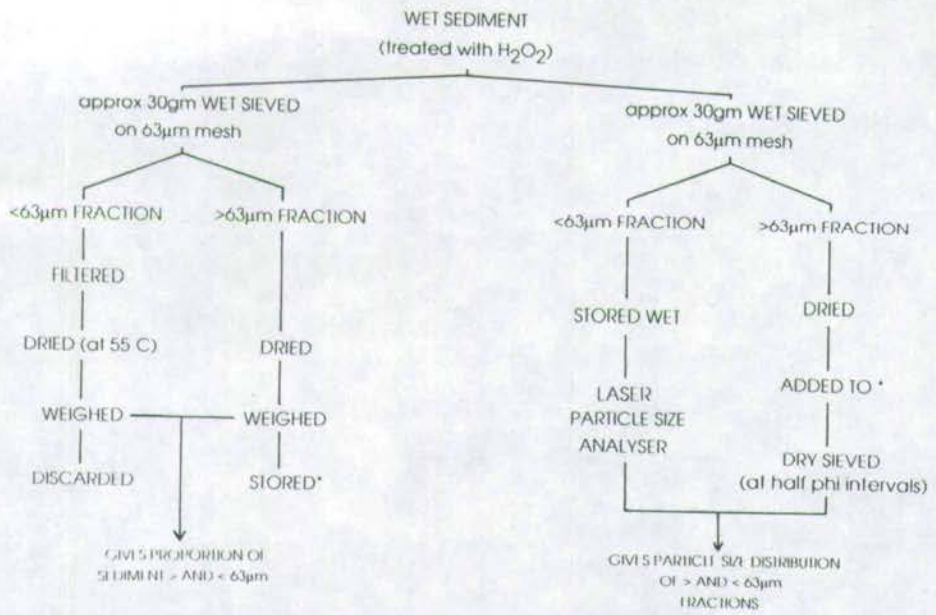

Figure 5. Flow diagram of grain size analysis technique

spectrometry. This method is considered accurate as X-ray diffraction analysis of the mineralogical content of the samples indicates that neither dolomite nor Ca-bearing clays are present in the samples and therefore all Ca measured is from $CaCO_3$. The samples were ground to less than 2 μm in an agate tema mill and then fused into glass discs following the method of Norrish and Hutton (1969) which were then run through a Philips PW1480 X-Ray Spectrometer. The analytical precision is 0.052% and the accuracy of the whole technique is 0.14% (these figures are calculated from 10 repeat analyses of one sample). Multiplying the Ca percentage by 2.5 gives the $CaCO_3$ content.

Grain Size Determination

To enable a detailed and complete measurement of the spread of grain sizes in each sample, 2 methods of analysis were used for different grain size fractions and the results combined. The >63 μm "coarse" fraction was dry sieved and the <63 μm "fine" fraction was analysed using a laser particle size analyser. A summary of the whole process is illustrated in Fig.5.

The >63 μm fraction was dry sieved using a nest of sieves at half phi mesh size intervals on a sieve shaker for 12 minutes. Each fraction was then weighed to the nearest 0.01 g. The fine fraction was analysed on a Coulter Laser LS-100 particle size analyser and the results collected in half phi intervals up to 12 phi and combined with the coarse fraction data from dry sieving.

Since this method of grain size determination provides the full size distribution of the sediment the moments method of analysing the grain size distribution was employed. This method uses the entire grain population which provides more representative parameters than the graphically derived values (McManus, 1988). The formulae for the first moment (mean) and second moment (standard deviation) are as follows:

Mean (first moment): $$\chi = \frac{\Sigma f\, m\varphi}{100}$$

Standard Deviation (second moment) $$\sigma^2 = \frac{\Sigma f\,(m\varphi - \chi)^2}{100}$$

where f is the percentage fraction in each class interval of the total weight of sediment and m is the mid-point interval of each class interval in phi units.

Radiocarbon Dating

In order to calculate accumulation rates of sediment in the Bay, 7 samples of shell and wood from cores were radiocarbon dated by accelerater mass spectrometry at the AMS Unit, Oxford, Britian. Samples were taken from a range of depths in 6 different cores distributed around the northern part of the Bay (sites labelled "R" on Fig.3)

RESULTS

Distribution of $CaCO_3$ in Surface Sediments

The areal distribution of $CaCO_3$ in the surface sediments of Phangnga Bay is illustrated in Figure 6. Most of the $CaCO_3$ in the sediments is from the whole and fragmented skeletal remains of bivalves, gastropods, barnacles, foraminifera, pteropods, arthropods, echinoids, starfish, corals, bryozoans and calcareous red and green algae. Visual inspection of the sediments whilst sieving did not reveal any evidence of limestone fragments.

In general terms there is an increase in the $CaCO_3$ content of the sediments from north to south (Fig.6). Within this general trend there are variations in $CaCO_3$ content notably in the northern area where patches of high $CaCO_3$ (>30%) are surrounded by sediments with <10% $CaCO_3$. In the southern part of the bay $CaCO_3$ contents of >30% are concentrated in the western and southern area and around beach and reef environments.

Grain Size Characteristics of Surface Sediments

The areal distribution of mean grain size is illustrated in Figure 7. It is evident that there is a general trend of increasing grain size from the north to the south. The northern area of the bay is dominated by coarse quartz silts (4-6 phi) and areas of medium to fine quartz silts (>6 phi). The central and southern area is dominated by fine quartz sand (2-4 phi) and the extreme southern area around Ko Racha is dominated by medium to coarse quartz and carbonate sands and gravels (2 to -2 phi). In the northern half of the bay there are patches of coarser sediments within the dominantly silty and muddy area. Around the northern mangroves these coarser sediments are coincident with the mangrove channels and are composed of quartz and occasional feldspar grains. The small area of coarse sediments on the northern tip of Ko Yao Noi (sampled at site 106) and other patches of coarse sediments are coincident with areas of high $CaCO_3$ content (see Fig.6). In the southern area the coarsest sediments (0 to -2 phi) are coincident with areas of strong currents around Ko Racha. The samples from beaches and reefs on Ko Racha, Ko Phi Phi and South East Phuket show a coarser mean grain size than the surrounding shallow and open marine seiment. The clay fraction is composed of kaolinite, illite and montmorillonite (from detailed X-ray Diffraction analysis).

Fig.8 illustrates the areal distribution of sorting values for the surface sediments of Phangnga Bay. Like the mean grain size distribution, a general trend can be seen. This is an increase in sorting (decrease in standard deviation phi values) from north to south.

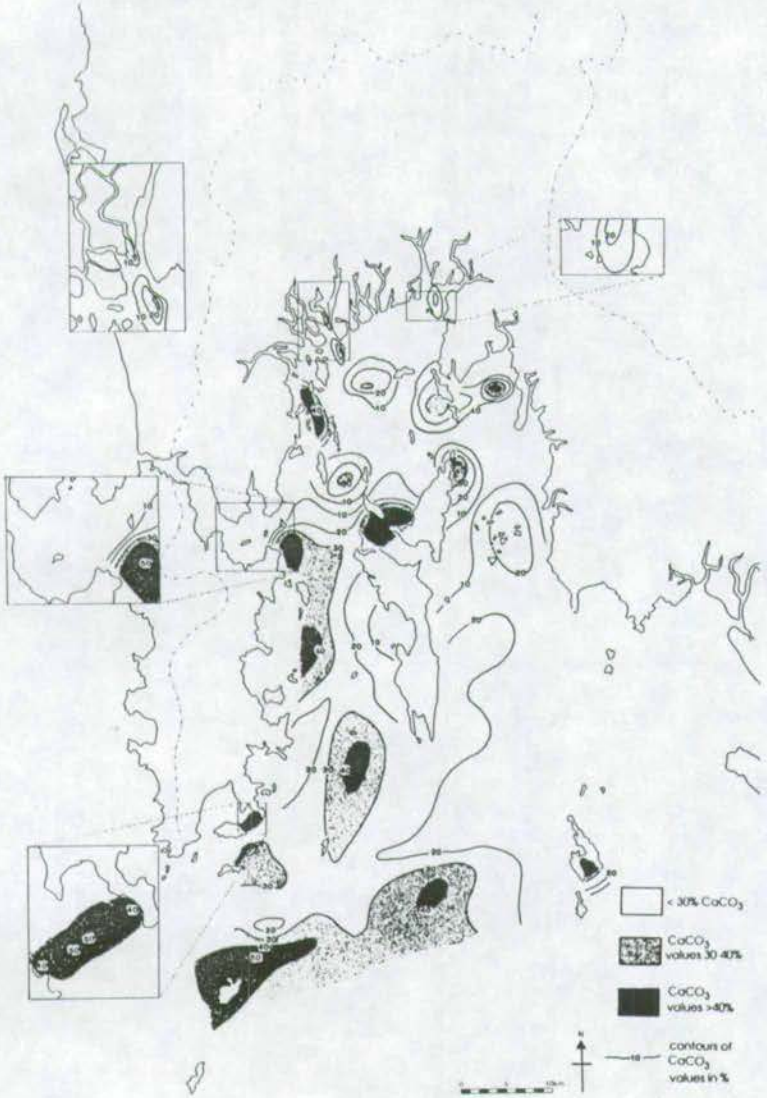

Figure 6. Distribution of calcium carbonate percent values

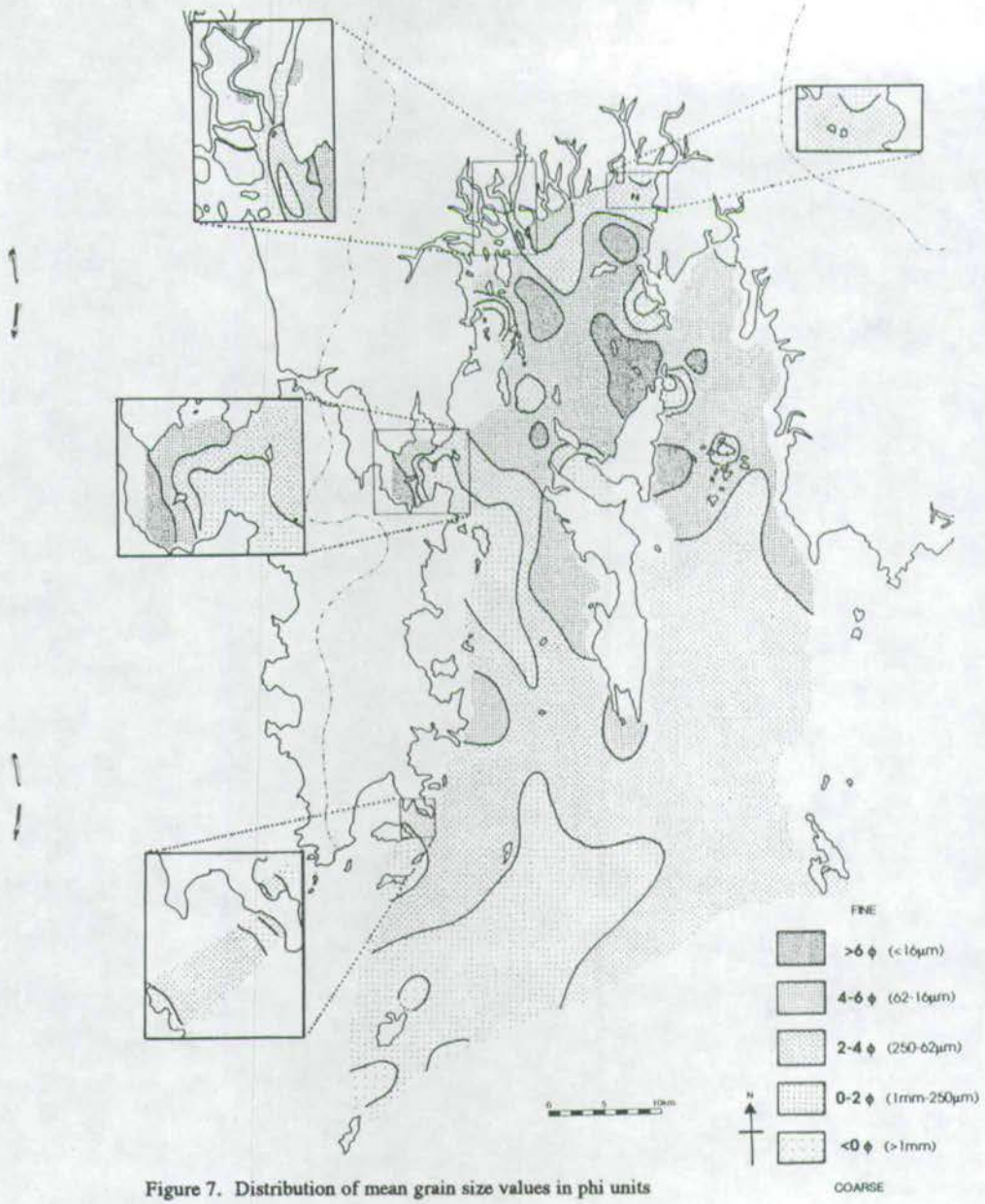

Figure 7. Distribution of mean grain size values in phi units

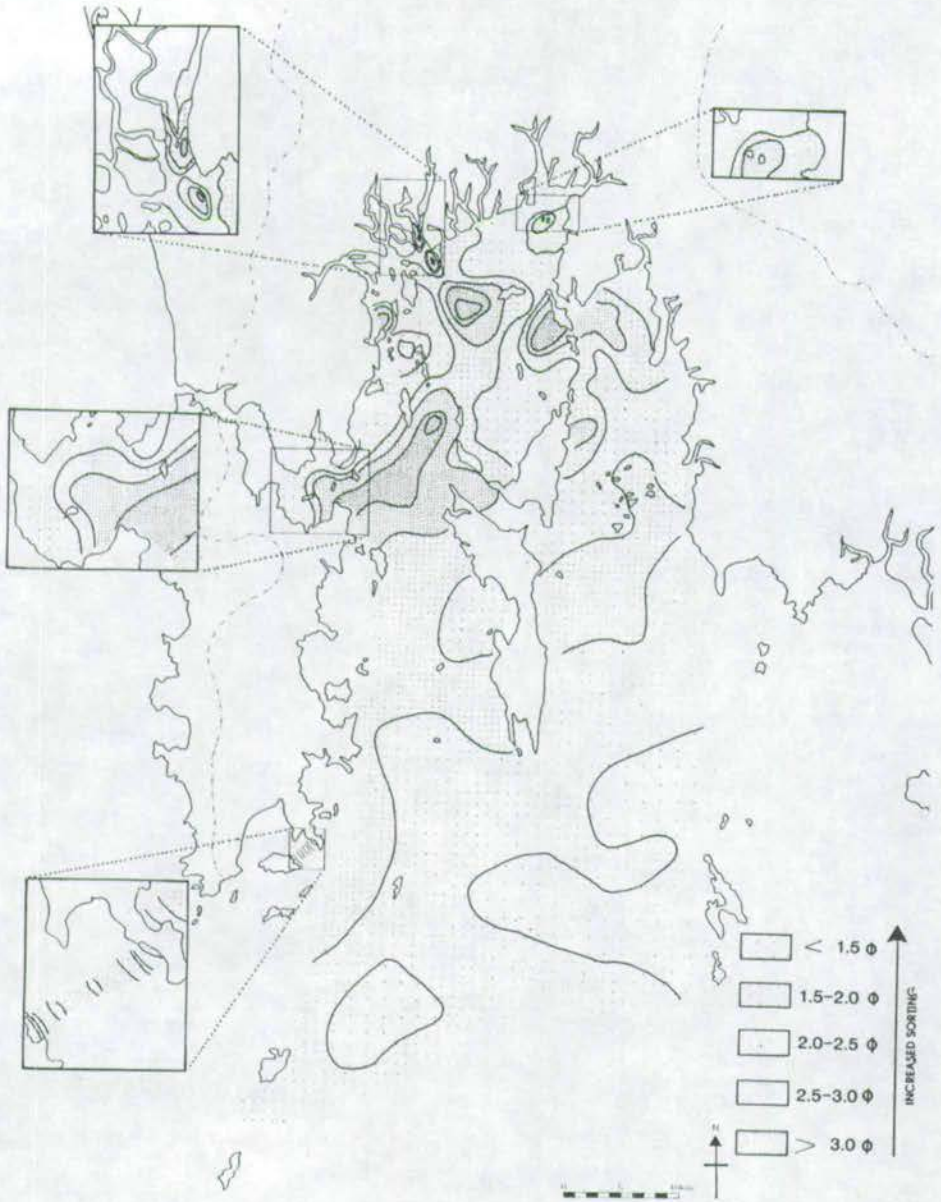

Figure 8. Distribution of standard deviation (sorting) values in phi unit

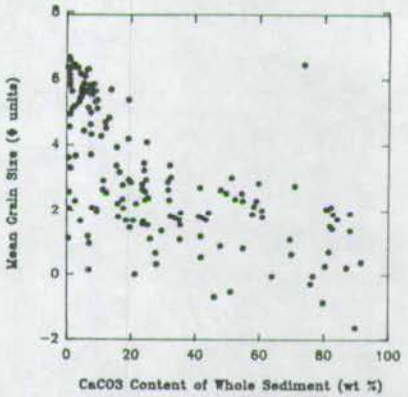

Figure 9. Graph of relationship between calcium carbonate content and mean grain size.

The pattern in the northern part of the Bay is, like mean grain size, more complicated than in the southern area. Patches of poorly sorted sediment (>2.5 phi standard deviation) coincide with the areas of coarse mean grain size and hence with areas of high $CaCO_3$ content. The exceptions to this are the mangrove channels where coarse mean grain size and poor sorting do not relate to high $CaCO_3$ content.

Fig.9 illustrates the relationship between $CaCO_3$ content and mean grain size of the sediment. In general there is a relationship of increasing $CaCO_3$ with increasing grain size (decreasing phi). This along with visual inspection of sediments shows that $CaCO_3$ occurs mainly as sand and gravel size fragments.

The relationship between mean grain size, standard deviation and depositional environments as determined by bathymetry and sea bed morphology is illustrated in Figure 10. Fig.10a illustrates the sediment differences between the intertidal, mangrove channel and mangrove swamp environments. Clearly mangrove swamps have a finer grain size and less variation between samples than the mangrove channel sediments.

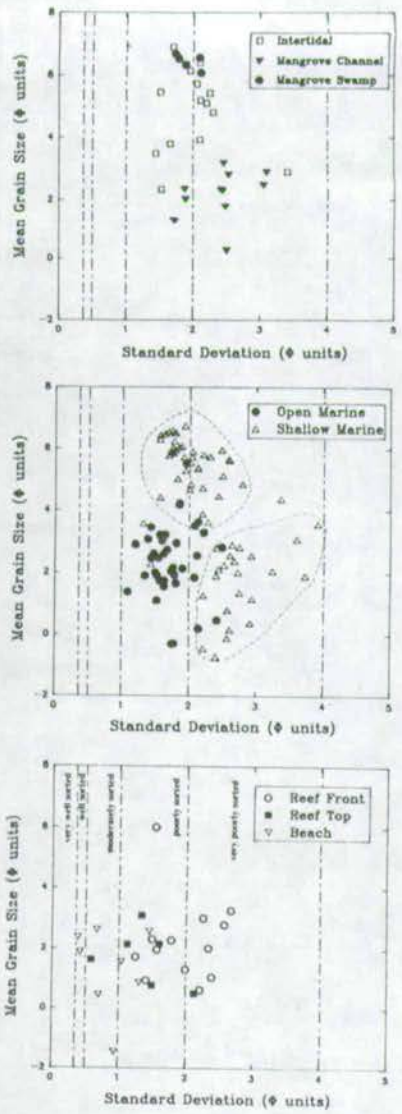

Figures 10a-c. Graphs of mean grain size versus standard deviation for individual depositional environments.

The intertidal sediments are more variable than both the mangrove environments and range from fine muds typical of the mangrove swamp sediments to poorly sorted sands typical of the mangrove channel environments. Fig.10b plots the sediment characteristics of the shallow and open marine environments. The open marine sediments are all clustered around the medium to fine sand mean and around the 1 to 2.5 phi standard deviation. Compared to the shallow marine sediments they tend to be coarser and better sorted. The shallow marine sediments show a much wider variation and may even be split into two groups (delineated by dotted lines on the graph) one of poorly sorted, coarse sediments and another of better sorted fine sediments similar to the mangrove swamp sediments. Finally, Fig.10c illustrates the sediment grain size characteristics of the beach, reef top and reef front environments. These sediments are mostly coarse grained but show varying degrees of sorting. The beach deposits are the best sorted of all the environments studied with standard deviations of 0-1.5 phi. The reef top sediments are better sorted than the reef front sediment.

Fig.11 plots typical grain size frequency distributions of the different depositional environments of Phangnga Bay. The mean and standard deviation for each example are also plotted and they summarise the characteristic sediment parameters for each environment described above.

Accumulation Rates and Progradation Rates

The radiocarbon dates obtained from AMS dating of 7 samples are listed in Table 1. Correction of -450±35 years for all shell sample dates has been applied to account for the apparent age of marine carbonate [from the age of Australian coastal water carbonate (Gillespie and Pollach, 1979) as there is no available age for Thai coastal waters] and +40 years to correct ages to the date of collection as all dates are determined as radiocarbon year B.P., *i.e* 1950.

Soft sediment cores consist of an upper part which has a high water content and therefore relatively low bulk density, above compacted and dewatered sediment of relatively high bulk density (Table 2). Consequently, sediment accumulation rates may be expressed in a variety of different ways:

1. An average accumulation rate (in mm $year^{-1}$) determined by dividing the thickness of the core by the time it took to accumulate (apparent accumulation rate, AAR).

2. An average accumulation rate of **compacted** sediment (in mm $year^{-1}$) determined by "compacting" the core to the dry bulk density of the lower part. This accumulation rate approximates that which would be determined for an equivalent sedimentary rock record (compacted accumulation rate, CAR).

3. An average accumulation rate of **uncompacted** sediment on the sea bed (in mm $year^{-1}$) determined by "decompacting" the core to the dry bulk density of the surface and then dividing the expanded thickness by the time taken for it to deposit. This approximates to the net sediment accumulation experienced by sessile benthos (uncompacted accumulation rate, UAR).

4. A net sediment accumulation rate expressed in g cm^{-2} $year^{-1}$, determined by dividing the mean dry bulk density of the cored sediment by the time it took to accumulate (flux).

These 4 values have been calculated for core 53 and are listed in Table 2. Because of the change in dry bulk density caused by a change in grain size down core these calculations cannot be made on all cores

Radiocarbon dates not only provide an indication of the vertical accumulation of sediment but also help in trying to measure the horizontal accumulation or progradation rate of the entire mangrove system. In the calculation

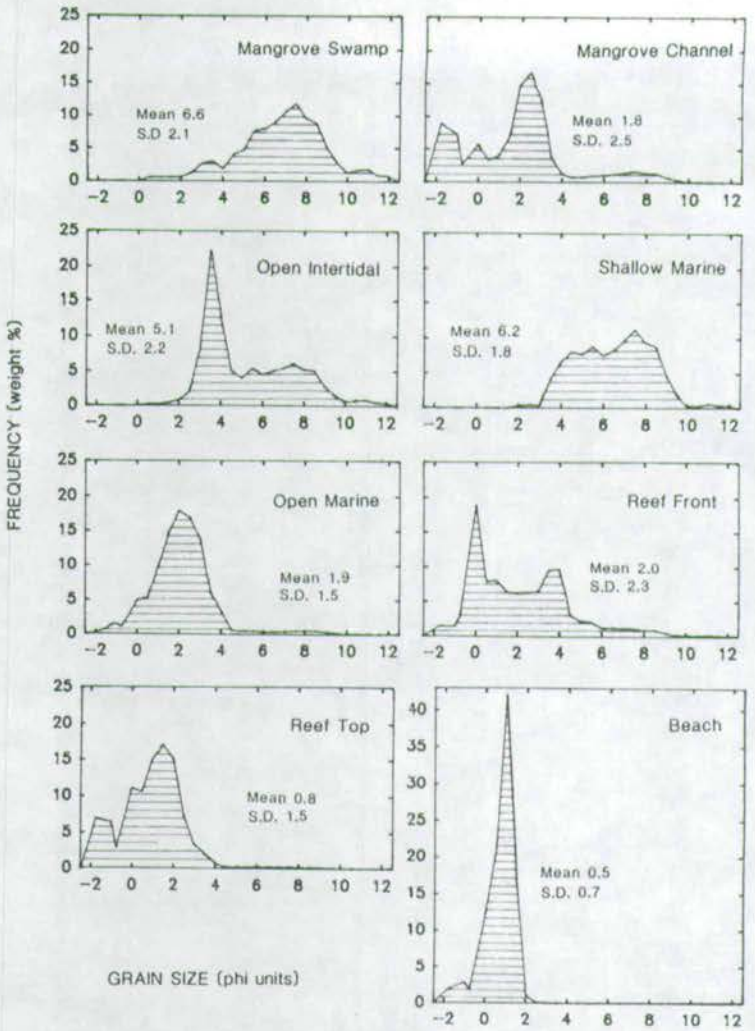

Figure 11. Grain size distribution frequency diagrams for the individual depositional environments (half phi intervals).

of the progradation rate, two methods have been used:

1. An estimate of average progradation rate of the mangrove system since 6000 years ago when the sea reached its present level fo lowing the Holocene transgression may achieved by dividing the width of intertid mangrove cover (10 km) by 6000. This yiel

Table 1. Radiocarbon dates of samples from core sub-samples obtained from Oxford University Radiocarbon Accelerator Unit) and the calculated sediment accumulation rates.

Laboratory Reference	Core No.	Depth down core (cm)	Uncorrected Sample Type	Corrected ^{14}C Age (years)*	Age (years)#	Apparent Accumulation Rate (mm/year)
OxA-2699	21	30-32	*Paphia undulata* (infaunal bivalve)	1440 ±60	1030 ±69	0.3 ±0.02
OxA-2700	26	28-30	wood fragment (?mangrove)	150 ±60	190 ±60	1.53 ±0.5
OxA-2701	44	44-46	*Ostrea sp.* (oyster)	3220 ±70	2810 ±78	0.15 ±0.006
OxA-2702	44	26-28	*Paphia gallus* (infaunal bivalve)	820 ±60	410 ±69	0.66 ±0.1
OxA-2703	53	46-48	*Paphia undulata* (infaunal bivalve)	720 ±60	310 ±69	1.52 ±0.3
OxA-2704	87	185-190	Barnacle fragment	1980 ±70	1570 ±78	1.19 ±0.06
OxA-2705	88	210-215	*Ostrea sp.* (oyster)	2170 ±70	1760 ±78	1.2 ±0.06

* the age in radiocarbon years B.P. (Before Present - AD 1950) provided by the Oxford AMS laboratory.

\# the age in radiocarbon years before year of collection (1990) and with a marine reservoir correction.

an average progradation rate of 1.67 m year^{-1} (Fig.12a). This value is a minimum, which ignores the possibility that landward alluvial deposits may have reduced the width of the mangrove swamp.

2. A second estimate of progradation rate may be made by consideration of bathymetry of the sea bed in front of the present mangroves, and applying our calculated average vertical sediment accumulation rates in this environment (Fig.12b). This method yields a projected mangrove progradation rate of about 1.5 m year^{-1}.

DISCUSSION

The north end of Phangnga Bay is dominated by muds. This is a result of a combination of factors, including the following:

1. proximity to source of the weathered products of granites (predominantly kaolinite).

2. low wave energy consequent on the shelter afforded by the enveloping landmasses.

3. low tidal energy due to the restricted, semi-enclosed setting.

4. Flocculation of colloids occurs as fresh and salt water meet, resulting in the settling out of fine grained, clay sediment.

Table 2. Dry bulk density, pre-and post-compaction calculations for Core 53. A.A.R.:apparent accumulation rate; C.A.R.:compacted accumulation rate; U.A.R.:uncompacted sedimentation rate.

CORE 53

Log	Depth (cm)	Present Thickness of core	Dry Bulk Density (gm/cm^3)	Thickness after Compaction	Thickness before Compaction
	0-1	1cm	0.248	0.35cm	1.00cm
	1-2	1	0.319	0.45	1.29
	2-3	1	0.340	0.48	1.35
	3-4	1	0.403	0.56	1.62
	4-5	1	0.405	0.57	1.63
	5-6	1	0.424	0.59	1.71
	6-7	1	0.436	0.61	1.76
	7-8	1	0.466	0.65	1.88
	8-9	1	0.499	0.70	2.01
	9-10	1	0.497	0.70	2.00
	10-12	2cm	0.531	1.49cm	4.28cm
	12-14	2	0.534	1.50	4.31
	14-16	2	0.530	1.48	4.27
	16-18	2	0.525	1.47	4.23
	18-20	2	0.503	1.41	4.06
	20-22	2	0.577	1.62	4.65
	22-24	2	0.534	1.49	4.31
	24-26	2	0.557	1.56	4.49
	26-28	2	0.567	1.60	4.57
	28-30	2	0.608	1.70	4.90
	30-32	2	0.592	1.66	4.77
	32-34	2	0.561	1.57	4.52
	34-36	2	0.579	1.62	4.67
	36-38	2	0.625	1.75	5.04
	38-40	2	0.624	1.75	5.03
	40-42	2	0.617	1.73	4.98
	42-44	2	0.584	1.64	4.71
	44-46	2	0.598	1.67	4.82
	46-48	2	0.714	2.00	3.76
Total Thickness (cm)		48		36.4	103.6
A.A.R. (mm/year)		1.52			
C.A.R. (mm/year)				1.17	
U.A.R. (mm/year)					3.3
Mean dry bulk density (gm/cm^2)			0.517		
Flux = 1.67 mg/cm^2/year					

Hylleberg, J., A. Nateewathana & B. Chatananthawej. 1985. Temporal changes in sediment characteristics on the west coast of Phuket Island *Phuket mar. biol. Cent. Res. Bull.* **37**:16 pp.

Limpsaichol, P. 1978. Reduction and oxidation properties of the mangrove sediment, Phuket Island, Southern Thailand. *Phuket mar. biol. Cent. Res. Bull.* **23**:13 pp.

Limpsaichol, P. 1988. Coastal Environment of Phangnga Bay. *Phuket Marine Biological Center Final Technical Report.*

McManus, J. 1988. Grain size determination and interpretation. *In*: M. Tucker (ed.). Techniques in Sedimentology, pp. 63-85. Blackwell Scientific Publications, Oxford.

Nielsen, C. 1976. An illustrated checklist of bivalves from PMBC beach with a reef-flat at Phuket, Thailand. *Phuket mar. biol. Cent. Res. Bull.* **9**:7 pp.

Norrish, K. & J.T. Hutton. 1969. An accurate X-ray spectrographic method for the analysis of a wide range of geological samples. *Geochim et Cosmo Acta* **33**:431-453 pp.

Scoffin, T.P., A.W. Tudhope, B.E.Brown, H. Chansang & R.F. Cheeney. 1991. Patterns and possible environmental controls of skeletongenesis of *Porites lutea,* South Thailand. *Coral Reefs* (in press).

Siripong, A. & collaborators. 1987. Estuarine Ecosystems of the Phangnga Bay - Chemical and Physical Oceanography. *Research Report to the National Research Council of Thailand.*

Tantanasiriwong, R. 1978. An illustrated checklist of marine shelled Gastropods from Phuket Island, adjacent mainland and offshore islands, western Peninsular Thailand. *Phuket mar. biol. Cent. Res. Bull.* **21**:22 pp.